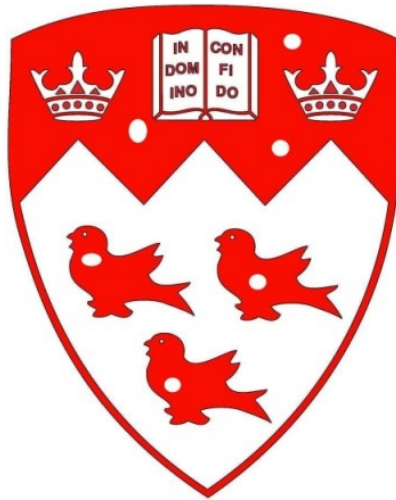


Testing of Extended Shear Tab Connections Subjected to Shear



Jacob Hertz

Civil Engineering and Applied Mechanics

McGill University, Montreal

August 2014

A thesis submitted to McGill University in partial fulfillment of the requirements
of the degree of Master of Engineering (M.Eng.) Thesis Option

© Jacob Hertz 2014

Abstract

Shear tab, or single-plate, connections are widely used as simple shear connections in the construction of steel structures. These connections take the form of a single plate shop welded to a supporting column or girder. During erection, the supported beam is moved into place and connected to the shear tab using bolts. In some cases, the eccentricity of the bolt group to the face of the supporting member must be increased due to congestion near the support face or for constructability. In this case, the shear tab connection is considered “extended” (the alternative being conventional). The Canadian Institute of Steel Construction (CISC) Handbook of Steel Construction and the American Institute for Steel Construction (AISC) Steel Construction Manual both include pre-designed conventional shear tab connections, the shear resistances of which were computed using the AISC design method [confirmed through testing by Aastha et al. (1989)]. In addition, the AISC Manual includes a design method for extended configurations.

This research aims to verify the accuracy in predicting the shear resistance of extended shear tab connections using a modified method, combining that of CSA S16-09 (2009), the CISC Handbook (2010), and the AISC Manual (2010). The shear resistances of 12 representative shear tab connections were predicted using said method and compared with the measured resistances found through full-scale testing. Four beam-to-column and eight beam-to-girder extended shear tab connections were tested in the Macdonald Engineering Jamieson Structures Laboratory at McGill University.

Two of the four beam-to-column tests were governed by flexural tearing of the weld. The welds were sized, as specified in the AISC design method, at $5/8$ ths of the plate thickness (which assumes 345MPa steel welded with E49 electrodes). This author recommends the welds be sized using a design equation that takes into account the probable yield stress of the steel. The other two beam-to-column tests resulted in plastic local buckling of the bottom edge of the shear tab. The AISC design method allows for the buckling resistance to be calculated using two models: i) lateral torsional buckling or ii) a conservative classical plate buckling. The measured buckling resistances for both tests were significantly better predicted by the latter model.

The beam-to-girder tests revealed that two limit states should be accounted for in the design method: i) biaxial buckling of full-height connections, and ii) localized deformation of the

supporting girder web and flange for partial-height connections. Design equations are proposed for both of these limit states.

Résumé

Les plaques de cisaillement sont largement utilisées en tant que connexions de cisaillement simple dans la construction de structures en acier. Ces connexions prennent la forme d'une unique plaque soudée à une colonne ou une poutre. Pendant le montage, la poutre est mise en place et reliée à la plaque de cisaillement en utilisant des boulons. Dans certains cas, l'excentricité du groupe de boulons sur la face de l'élément de support (soit la colonne soit la poutre) doit être augmentée à cause de l'encombrement à proximité de la face d'appui ou à des fins de constructibilité. Dans ce cas, la plaque de cisaillement est considérée comme «étendue» (l'alternative étant classique). Le manuel de la construction en acier par l'Institut canadien de la construction en acier (ICCA) et celui par l'Institut américain pour la construction en acier (IACA) incluent tous les deux des plaques de cisaillement conventionnelles déjà préconçues. Les résistances en cisaillement ont été établies à l'aide de la méthode de l'IACA [confirmée par les tests de Astaneh et al. (1989)]. Contrairement au Manuel de l'ICCA, le Manuel IACA comprend une méthode de conception pour les configurations étendues, qui est principalement basée sur la recherche ci-dessus.

Cette recherche vise à vérifier l'exactitude dans la prédiction de la résistance au cisaillement de connexions étendues en utilisant une méthode modifiée, combinant celle des Manuels de l'ICCA et de l'IACA. La résistance au cisaillement de 12 connexions étendues représentatives a été prédite à l'aide de cette méthode modifiée et comparée à celle mesurée par des tests à grande échelle. Quatre plaques de cisaillements étendues utilisées comme connexions poutre-colonne et huit pour des connexions poutre-poutre ont été conçues et testées dans le laboratoire de structures de génie civil Macdonald.

Deux tests poutre-colonne furent régis par flexion suivi par le déchirement de la soudure. Les soudures ont été réalisées, comme spécifié dans la méthode de conception IACA, à 5/8èmes de l'épaisseur de la plaque (ce qui suppose un acier soudable de 345MPa avec des électrodes E49). L'auteur recommande de dimensionner les soudures en utilisant une équation de conception qui prend en compte la contrainte de rendement probable de l'acier. Deux tests ont abouti à un voilement plastique sur le bord inférieur de la plaque de cisaillement. La méthode de conception de l'IACA indique que la résistance de voilement doit être calculé en utilisant deux

modèles : i) flambement par torsion latérale ou ii) un flambement classique conservateur. Les résistances au voilement local mesurées pour les deux tests ont été mieux prédites par ce dernier, et ce, de manière significative.

Les tests sur les connexions poutre-poutre ont révélés que deux états limites doivent être pris en compte dans la méthode de conception : i) un flambement biaxial sur toute la hauteur de la plaque de cisaillement étendue, et ii) une déformation localisée de l'âme et de la semelle de la poutre de support. Des équations sont proposées pour la conception dans ces deux états limites.

Acknowledgements

I would like to thank my supervisors: Professor Colin Rogers and Professor Dimitrios Lignos. Their patience, guidance, and feedback along every stage of this research program was invaluable.

I would like to thank ADF Group Inc., DPHV Structural Consultants, and NSERC, for their financial contributions. The real-world knowledge of Martin Frappier and Denis D’Aronco, of DPHV, was crucial in the design and analysis stages. I would also like to thank Augustin Silva, of ADF Group, for coordinating fabrication and delivery of the test specimens.

Rigorous lab testing would not have been possible without day-to-day help from the lab team: Harrison Moir, Farbod Pakpour, Milad Moradi, and Mohammad Motallebi. I also owe a big thank you to the lab coordinator, Dr. William Cook, and the lab staff: Marek Przykorski, John Bartczak, and Gerard Bechard. Marco D’Aronco, of DPHV, was of great assistance in teaching me the ins and outs of lab testing.

I would like to thank Heng Khoo of Carleton University for permitting the use of Carleton University’s lab facilities as well as Stanley Conley for assistance in coupon testing.

This has been no trivial task and I owe many thanks to my friends and family, especially to my parents, Debra and Blaine, for shaping me into the man I am today.

Thank you Gloria Ivanković for your unwavering support and love. This has been a journey not just for me, but for the both of us. I will always be grateful to you for standing by me.

Table of Contents

Abstract	ii
Résumé	iv
Acknowledgements	vi
Table of Contents	vii
List of Figures	ix
List of Tables	xii
Chapter 1 – Introduction	1
1.1. Overview	1
1.2. Objectives	6
1.3. Scope	7
1.4. Outline	7
Chapter 2 – Literature Review	8
2.1. Overview	8
2.2. Research	8
2.2.1. Full-Scale Testing	8
2.2.2. Numerical Finite Element Studies	34
2.2.3. Design Aids	40
2.3. Design Handbooks	42
2.3.1. Canada	42
2.3.2. USA	43
2.4. Summary	45
Chapter 3 – Testing Program	47
3.1 Overview	47
3.2 Test Specimens	47
3.3 Design Method	51
3.3.1. Definition of Extended Shear Tab Connections	51
3.3.2. Design Check 1: Bolt Shear and Bolt Bearing	52
3.3.3. Design Check 2: Plate Ductility	54
3.3.4. Design Check 3: Shear Yielding, Rupture, Block Rupture	54
3.3.5. Design Check 4: Combined Shear and Flexural Yielding	55
3.3.6. Design Check 5: Buckling	58
3.3.7. Design of Beams	59
3.3.8. Design of Girders	61
3.4. Testing Setup	63
3.4.1. Test Beams	67

3.4.2.	Reaction Frames, Stub Columns, and Girder Segments	67
3.4.3.	Compression and Tension Actuators	70
3.4.4.	Lateral Bracing System	72
3.4.5.	Installation of Test Configurations	72
3.5.	Test Procedure	73
3.5.1.	Instrumentation	73
3.5.2.	Test Procedure	77
3.6.	Summary	79
Chapter 4 – Discussion of Experimental Results		81
4.1.	Overview	81
4.2.	Coupon Testing	81
4.2.1.	Test Methodology	81
4.2.2.	Test Results	84
4.2.3.	Remarks	85
4.3.	Experimental Results and Discussion	87
4.3.1.	Predicted Resistances	87
4.3.2.	Summary of Experimental Results and Comparisons	88
4.3.4.	Beam-to-Girder Extended Shear Tab Connections	97
4.4.	Recommendations	111
4.4.1.	Weld Proportioning	111
4.4.2.	Buckling at Unsupported Edges of Shear Tab Connections	112
4.4.3.	Buckling of Full Height Beam-to-Girder Connections	113
4.4.4.	Girder Rigidity	117
4.5.	Summary	119
Chapter 5 – Conclusions and Recommendations		121
5.1.	Summary	121
5.2.	Recommendations	123
5.3.	Future Work	124
References		125
Appendix A – Design Calculations		A-1
Appendix B – Fabrication Drawings		B-1
Appendix C – Test Setup and Instrumentation		C-1
Appendix D – Specimen Test Summaries		D-1

List of Figures

Figure 1.1: Shear Tab Connection Examples	1
Figure 1.2: Rigid vs. Flexible Support Conditions for Shear Tab Connections	2
Figure 1.3: Conventional vs. Extended Shear Tab Configurations	3
Figure 1.4: Comparison of Installation Method for Beam-to-Girder Shear Connections	5
Figure 1.5: Plan View of Installation Method for Shear Tab Connection with Beam Coped at Both Ends	5
Figure 1.6: Beam-to-Column Extended Shear Tab Example (Courtesy of DPHV Structural Consultants)	6
Figure 2.1: Shear-Deflection Curves for Welded-Bolted Single Plate Connections, Lipson (1968)	9
Figure 2.2: Load-Deformation for 19mm Bolts Connecting 9.5mm Plates, Richard et al. (1980)	10
Figure 2.3: Proposed Block Shear Failure Model, Ricles (1980)	12
Figure 2.4: Test 5A, W460x39 Beam with 402mm Deep Girder (45°), Stierner et al. (1986)	13
Figure 2.5: Test 2B, W460x61 Beam with 452mm Deep Girder (0°), Stierner et al. (1986)	13
Figure 2.6: Tri-Linear Shear-Rotation Curve for Shear Tab Connections, Astaneh et al. (1989)	14
Figure 2.7: Yielding of Girder Web (Flecks Indicate Yielding), Shaw and Astaneh (1992)	16
Figure 2.8: Girder Web Deformation, Shaw and Astaneh (1992)	16
Figure 2.9: Typical Test Setup, Liu and Astaneh (2000)	17
Figure 2.10: Deformation of Bolt Hole and Fracture, Bare-Steel Test, Liu and Astaneh (2000)	18
Figure 2.11: Load-Drift Response for Specimens with and without a Slab, Liu and Astaneh (2000)	19
Figure 2.12: Load-Drift Response for Specimens with and without Angle, Liu and Astaneh (2000)	20
Figure 2.13: Specimen with Supplemental Seat Angle, End of Test, Liu and Astaneh (2000)	20
Figure 2.14: Conventional Shear Tab Connection, Sherman and Ghorbanpoor (2002)	21
Figure 2.15: Unstiffened vs. Stiffened Extended Shear Tabs, Sherman and Ghorbanpoor (2002)	22
Figure 2.16: Inflection Point Eccentricity, e , Sherman and Ghorbanpoor (2002)	24
Figure 2.17: Conventional vs. Extended Unstiffened Beam-to-Column Shear Tab Connections	27
Figure 2.18: Shear Tab Before Testing, Test 1, Goodrich (2005)	27
Figure 2.19: Buckled Shear Tab, Test 1, Goodrich (2005)	28
Figure 2.20: Weld Rupture, Test 5b, Baldwin Metzger (2006)	30
Figure 2.21: Flexible Support Beam-to-Column Test Setup, D'Aronco (2014)	33
Figure 2.22: Shear Tab Deformation, Rigid vs. Flexible Support, D'Aronco (2014)	34
Figure 2.23: Stress Distribution within Shear Tab, Ashakul (2004)	35
Figure 2.24: Twist Failure Mode in Shear Tab for Five Bolt Connection, Rahman et al. (2007)	37
Figure 2.25: Web Mechanism for Three Bolt Connection, Rahman et al. (2007)	37
Figure 2.26: Modelled Web Failure for 10 Bolt Beam-to-Girder Connection, Mahamid et al. (2007)	38
Figure 2.27: Component-Based Model of Shear Tab Connection, Koduru and Driver (2013)	39

Figure 3.1: Beam-to-Column Extended Shear Tab Configurations	48
Figure 3.2: Full Height vs. Partial Height Shear Tabs	49
Figure 3.3: Installation Method for Side Plate Connections (Configuration 8)	50
Figure 3.4: Renderings of Typical Test Setup (Arrows Indicate Actuator Locations)	64
Figure 3.5: Plan View of the Beam-to-Column Test Setup (Configuration 1 pictured); dimensions in mm	65
Figure 3.6: Plan View of the Beam-to-Girder Test Setup (Configuration 5 pictured); Dimensions in mm	66
Figure 3.7: Reaction Frame Details, Elevation and Section Views; Dimensions in mm	68
Figure 3.8: Beam-to-Column Reaction Frame with Stub Column Installed	69
Figure 3.9: Beam-to-Girder Reaction Frame	70
Figure 3.10: Compression Actuator	71
Figure 3.11: Tension Actuator	71
Figure 3.12: Lateral Bracing System	72
Figure 3.13: Welding Procedure, Shear Tab with Partial "C" Weld	73
Figure 3.14: Instrumentation Plan, Configuration 3, Dimensions in mm	74
Figure 3.15: Out-of-Plane LVDT Placement (Configuration 4 Pictured)	76
Figure 3.16: Modified Shear-Rotation Response for Shear Tab Connections, Marosi (2011)	77
Figure 3.17: Rotational and Shear Response for Beam	78
Figure 3.18: Half Cylinder and Rollers	79
Figure 4.1: Beam Coupon Locations (Image Courtesy of DPHV Structural Consultants)	82
Figure 4.2: Coupon Test Setup	83
Figure 4.3: Coupon Specimens Before (W24x94 Flange) and After (W27x84 Flange) Uniaxial Tensile Test	85
Figure 4.4: Engineering Stress vs. Strain, Coupon PL3/8 5A-3 (horizontal direction in shear tab)	86
Figure 4.5: Engineering Stress vs. Strain, Coupon PL3/8 5B-3 (vertical direction in shear tab)	86
Figure 4.6: Connection Shear vs. Rotation, Configurations 1 & 3	90
Figure 4.7: Weld Tearing and Deformed Shear Tab, Configuration 1	91
Figure 4.8: Weld Tearing and Deformed Shear Tab, Configuration 3	91
Figure 4.9: Sheared Bolt, Configuration 1	92
Figure 4.10: Eccentric Loads on Bolt Groups, Reproduction of CISC Handbook (2010)	93
Figure 4.11: Connection Shear vs. Rotation, Configuration 2	94
Figure 4.12: Bottom Edge of Shear Tab, Configuration 2	94
Figure 4.13: Connection Shear vs. Rotation, Configuration 4	96
Figure 4.14: Shear Tab Deformation at End of Test, Configuration 4	96
Figure 4.15: Buckling Failure Mode Shape (Configuration 5 Pictured)	97
Figure 4.16: Strain Gauge Layout, Full Height Beam-to-Girder Shear Tab Connections	98
Figure 4.17: Connection Shear vs. Rotation, Full Height Beam-to-Girder Shear Tab Connections	98
Figure 4.18: Buckled Shear Tab at Test End, Full Height Beam-to-Girder Shear Tab Connections	99

Figure 4.19: Buckling at Neck of Shear Tab, Full Height Beam-to-Girder Shear Tab Connections _____	99
Figure 4.20: Girder Yielding Deformation, Partial-Height Beam-to-Girder Shear Tabs _____	101
Figure 4.21: Connection Shear vs. Rotation, Configurations 6 & 7 _____	102
Figure 4.22: Girder Web Yielding at Base of Shear Tab, Configuration 6 and 7 _____	102
Figure 4.23: Computed Bolt Bearing Rotation Schematic and Sign Convention _____	103
Figure 4.24: Connection Shear vs. Computed Bolt Bearing Rotation, Configurations 6 & 7 _____	104
Figure 4.25: Beam vs. Shear Tab, Deformation Around Bolt Holes, Configuration 7 _____	104
Figure 4.26: Beam Behaviour for Load Phases, Configuration 9 and 10 _____	106
Figure 4.27: Connection Response, Configurations 9 & 10 _____	107
Figure 4.28: Girder Web Yielding at Base of Shear Tab, Configuration 9 and 10 _____	108
Figure 4.29: Bolt Bearing Failure, Configuration 8 _____	108
Figure 4.30: Connection Shear vs. Rotation, Configuration 8 _____	109
Figure 4.31: Bearing Deformation at Bolt Holes in Side Plate Connection, Configuration 8 _____	110
Figure 4.32: Moment Diagrams for Idealized vs. Experimental Zero Moment Inflection Point _____	110
Figure 4.33: Local Buckling Schematic, Reproduced from AISC Manual (2010) _____	112
Figure 4.34: Buckling of a Thin Plate Under Biaxial Compression, Modelled After Rees (2009) _____	114
Figure 4.35: Horizontal Stress for Full Height Beam-to-Girder Buckling Calculation _____	115
Figure 4.36: Torsional rigidity for partial-height beam-to-girder shear tab connections _____	118

List of Tables

Table 2.1: Stiffened Extended Beam-to-Column Shear Tab Configurations, Goodrich (2006) _____	27
Table 2.2: Extended Beam-to-Column Shear Tab Configurations, Baldwin Metzger (2006) _____	29
Table 3.1: Summary of Test Specimens _____	50
Table 3.2: Instrumentation List, Configurations 1 and 3 _____	75
Table 4.1: Coupon Test Results _____	84
Table 4.2: Factored and Predicted Connection Resistances _____	88
Table 4.3: Summary of Experimental Results _____	89
Table 4.4: Measured vs. Predicted Local Buckling Resistance, Configuration 2 and 4 _____	113
Table 4.5: Calculated vs. Measured Buckling Resistance, Full-Height Configurations _____	116
Table 4.6: Calculated vs. Measured Girder Yielding Resistances for Partial-Height Beam-to-Girder Connections _____	119

Chapter 1 – Introduction

1.1. Overview

Single plate shear connections, commonly referred to as shear tabs, are widely used in steel construction due to low cost, ease of fabrication and ease of installation. A shear tab connection consists of a beam connected to a plate which is fillet welded to a column or girder. The supported beam is connected to the shear tab using bolts. Shear tab connections require little fabrication in the shop, primarily drilling of bolt holes in the shear tab and beam and welding of the shear tab to the supporting member. On site, the beam is moved into position and bolted to the shear tab. Figures 1.1a and 1.1b illustrate examples of beam-to-column and beam-to-girder shear tab connections.

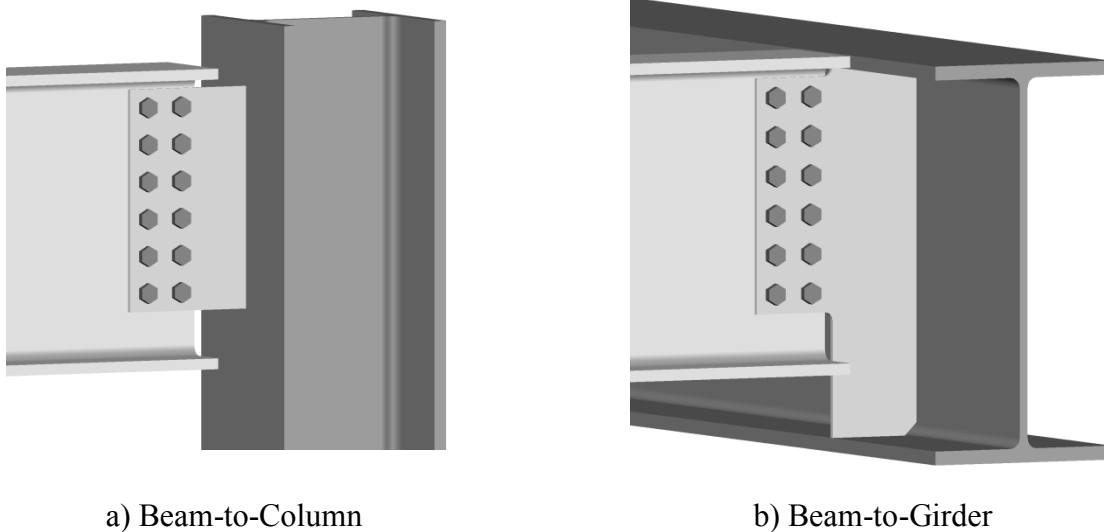
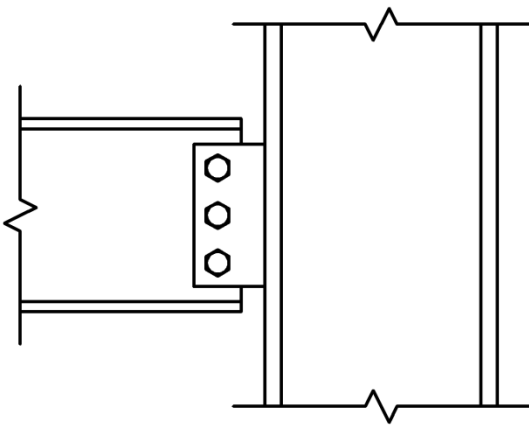


Figure 1.1: Shear Tab Connection Examples

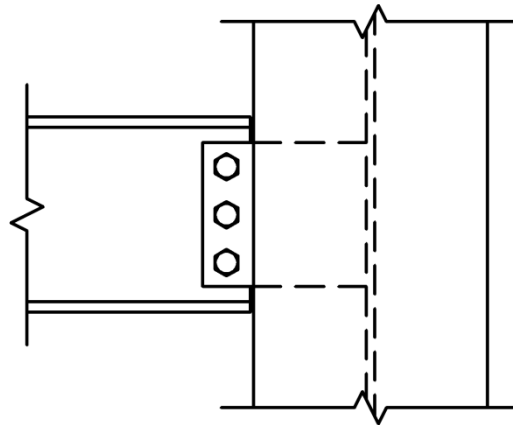
Shear tab connections can connect a supported beam to a supporting column or girder. The type of support greatly influences the rotational stiffness of the connection. In the case of a beam connected to a column flange, the support condition is referred to as “rigid”. When load is applied to the beam, the column undergoes strong axis bending and experiences relatively small rotation compared to that of the supported beam. Alternatively, when the supported beam is connected to the web of the column, the support condition is considered “flexible”. Rotation of the global beam-to-column joint is significant due to the weak axis bending in the column,

localized deformation of the column web occurring along the depth of the shear tab, or a combination of both.

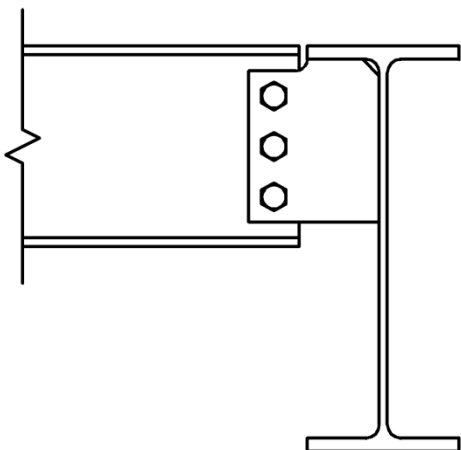
For the case of beam-to-girder shear tab connections, the support condition is dependent on whether or not beams are supported on both sides of the girder, as well as the size of the girder and its torsional stiffness. When a beam frames into a single side of a supporting girder, the support condition is considered flexible (assuming the girder is not torsionally stiff or restrained from rotating). Alternatively, the support condition is considered rigid when beams are located on both sides of the girder. This is due to the counteracting nature of opposing moments from opposite beams. Figure 1.2 illustrates both rigid and flexible support conditions.



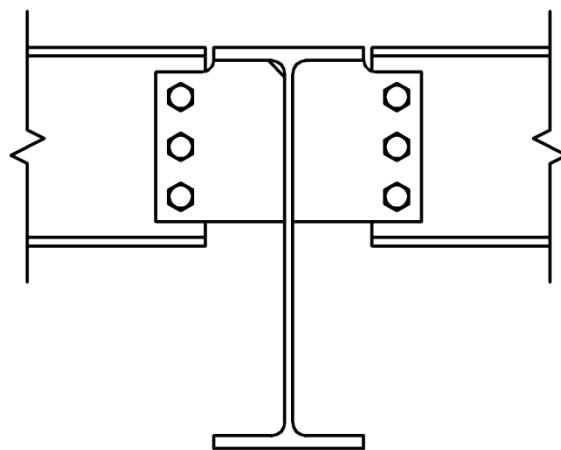
a) Rigid Support, Beam-to-Column Flange



b) Flexible Support, Beam-to-Column Web



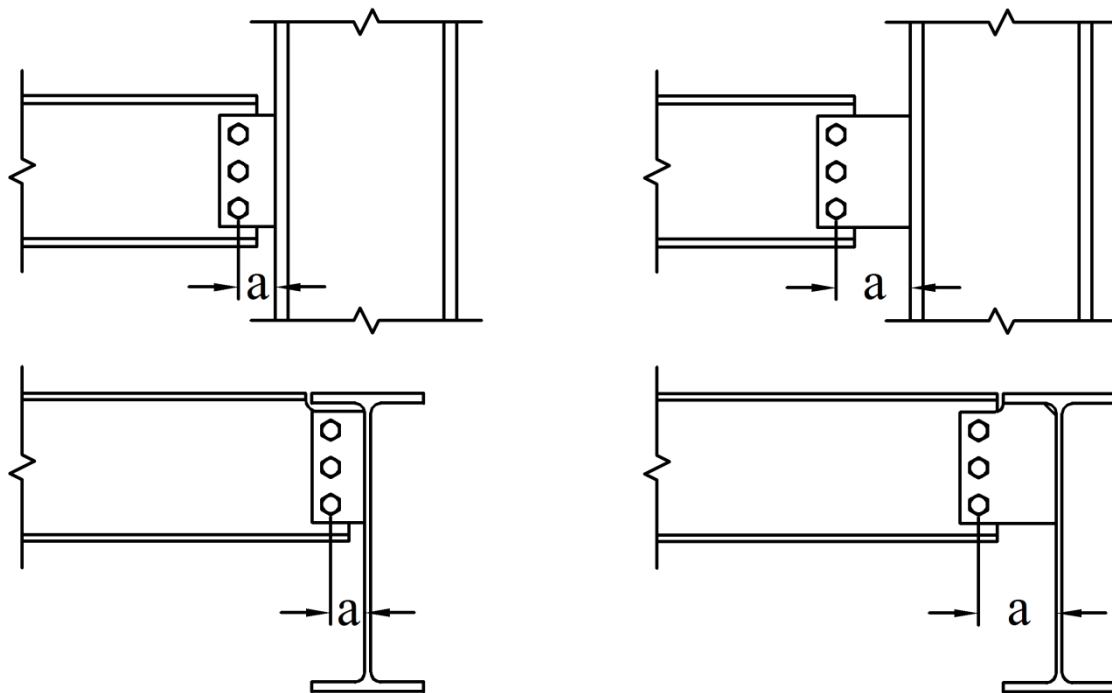
c) Flexible Support, Beam-to-Girder Web



d) Rigid Support, Beams on Both Sides of Girder

Figure 1.2: Rigid vs. Flexible Support Conditions for Shear Tab Connections

Part 10 “Single-Plate Connections” of the American Institute for Steel Construction (AISC) Steel Construction Manual (2010), hereafter referred to as the AISC Manual, divides shear tab connections into two configurations. Conventional configurations have a single vertical row of two to 12 bolts and an “a” distance less than or equal to 89mm (3½in). The “a” distance is defined as the distance between the support face and the first vertical row of bolts (Figure 1.3). A shear tab connection is considered to be of an extended configuration if either the “a” distance exceeds 89mm (3½in), or has two or more vertical row of bolts. This research concerns itself with “extended” configurations. Figure 1.3 illustrates the difference in “a” distances between conventional and extended shear tab configurations.



a) Conventional Configuration ($a \leq 89\text{mm}$)

b) Extended Configuration ($a > 89\text{mm}$)

Figure 1.3: Conventional vs. Extended Shear Tab Configurations

The anticipated failure modes for conventional shear tab connections were confirmed to be plate yielding, bearing failure at bolt holes, net section fracture, block tear-out, bolt shear fracture and weld fracture [primarily through lab testing conducted by Astaneh et al. (1989)]. The AISC Manual (2010) specifies that shear tabs meeting the conventional criteria and having certain dimensional limitations need only be checked such that the bolts and the plate have the required shear resistance. Alternatively, extended configurations must be checked for the six

limit states proposed by Astaneh et al. (1989) as well as two additional requirements. Firstly, the plate buckling resistance must be checked. Secondly, the plate thickness must be sized such that it possesses enough ductility to yield before the bolts fracture. The Canadian Institute of Steel Construction (CISC) Handbook of Steel Construction (2010), hereafter referred to as the CISC Handbook, provides tabulated pre-qualified conventional shear tab connections whose design is in accordance with the method originally proposed by Astaneh et al. (1989). Marosi (2011) proposed modifications to the AISC Manual (2010) design method for extended shear tab connections such that it would be applicable to Canadian design philosophy. Marosi proposed increasing the shear strength of the bolts when checking the limit state of bolt fracture and validated this hypothesis through testing of shear tab connections with two vertical rows of bolts. It should be noted that the shear tabs tested by Marosi had “a” distances of less than 89mm ($3\frac{1}{2}$ in) but had multiple vertical rows of bolts.

Extended shear tab connections are often preferred, compared to other shear connections, when connecting a beam to a girder due to their ease of installation. End plate, double angle, single angle, and conventional shear tab connections all require the beam to be lowered to the correct height outside of the girder flange and then moved horizontally into position. Extended shear tab connections offer an advantage. The beam is simply lowered vertically into position, moved horizontally towards the shear tab and then bolted to the shear tab without the need to turn the beam in the horizontal plane. This translates to quicker installation and safer working conditions for construction workers. Figure 1.4 provides a comparison between the installation methods for extended shear tab connections versus that of other typical shear connection types. If a similar connection is used on both ends of the beam (such as a conventional shear tab) then the beam must be rotated horizontally into position to clear the flanges of the two facing girders (see Figure 1.5). Also, for cases where a beam frames between two girders, it may sometimes be impossible to move the beam into place for end plate, single angle, and double angle connections. Furthermore, the use of extended shear tab connections eliminates the need for a coped beam. This reduces the steel material needs (a shorter member is used) as well as the fabrication time.

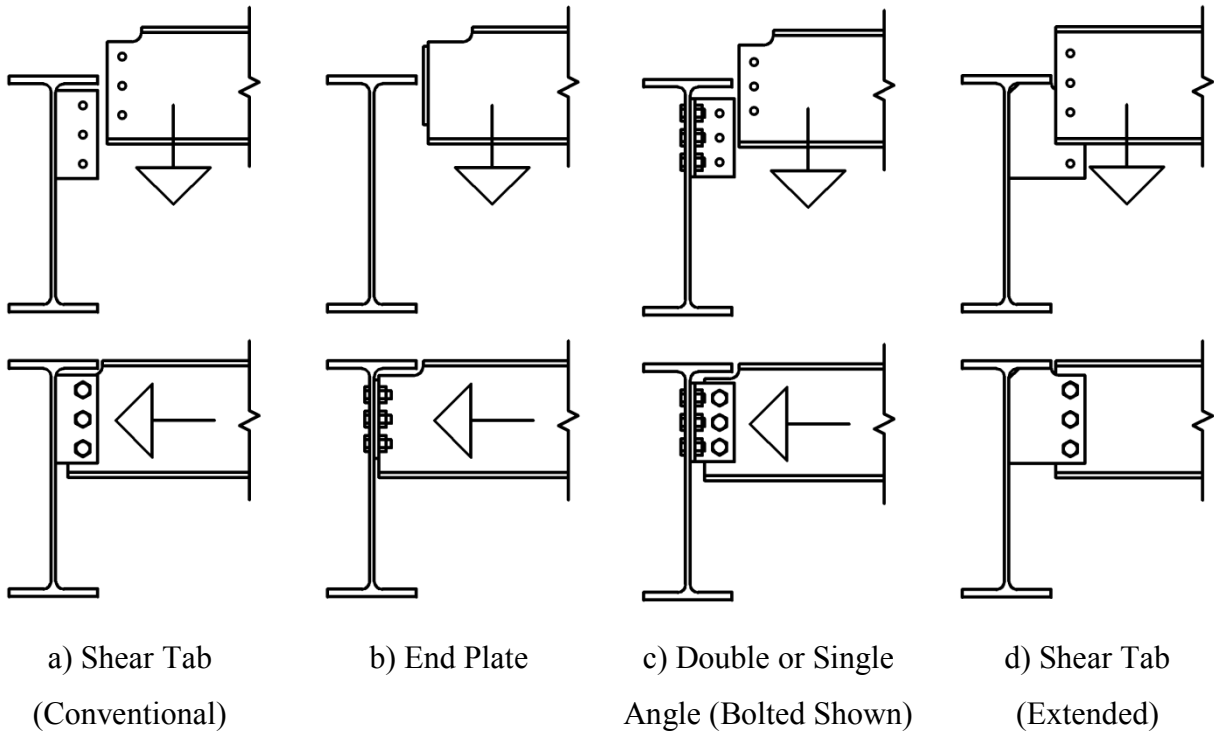


Figure 1.4: Comparison of Installation Method for Beam-to-Girder Shear Connections

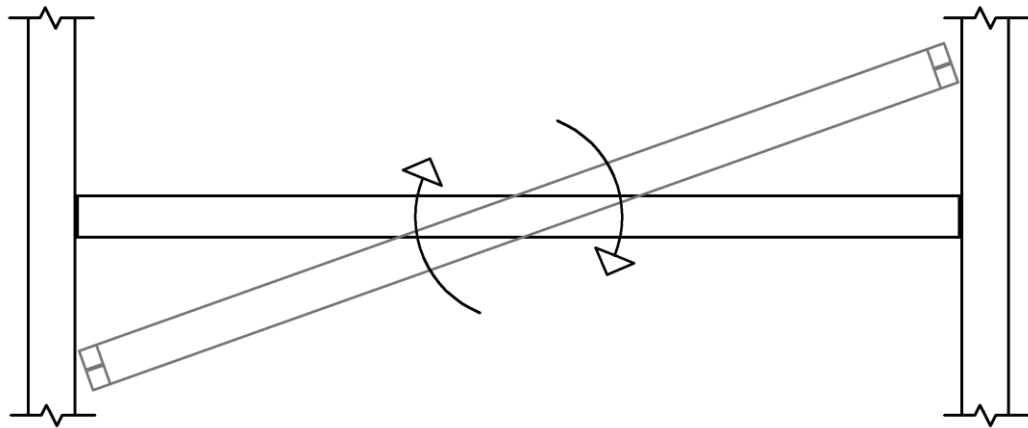


Figure 1.5: Plan View of Installation Method for Shear Tab Connection with Beam Coped at Both Ends Showing Need to Rotate the Member

Extended beam-to-column shear tab connections are typically specified when the space close to a column becomes congested due to multiple beams framing into said column. Figure 1.6 provides an in-situ example of an extended beam-to-column shear tab connection where this is the case. Because the working line of the W460x52 beam is located inside the other shear tab, its shear tab is welded to that of the W410x39 beam. In this case, both of the shear tabs are

considered extended due to corresponding “a” distances of 114mm (4½in) and 140mm (5½in), respectively.

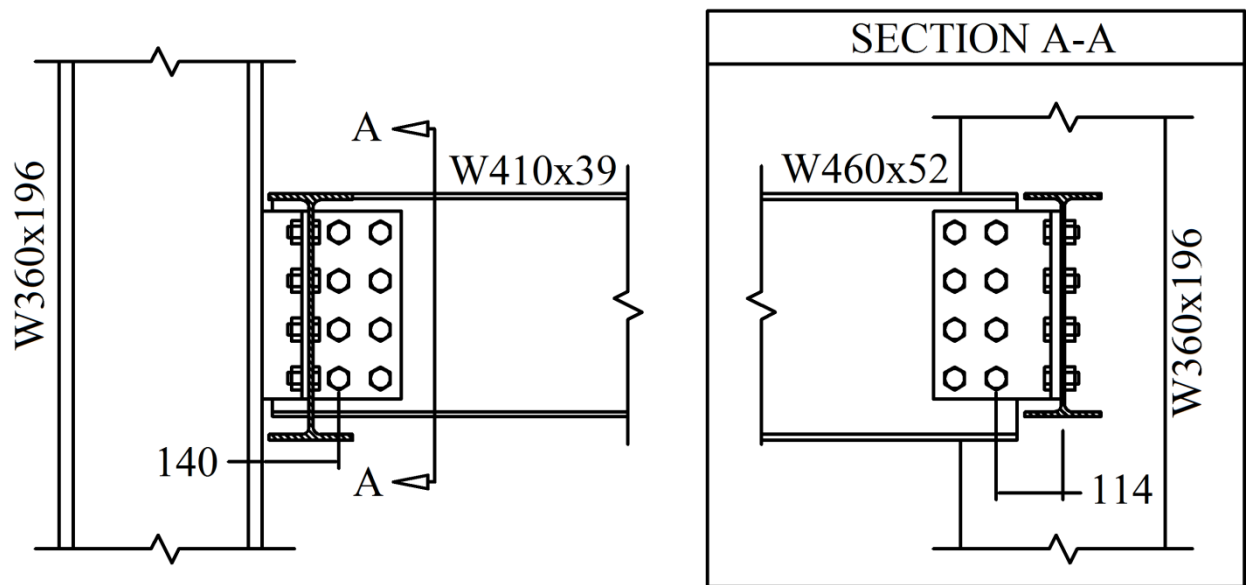


Figure 1.6: Beam-to-Column Extended Shear Tab Example (Courtesy of DPHV Structural Consultants), Dimensions in mm

1.2. Objectives

The primary objective of this research is to assess the accuracy of the combined CSA S16-09 (2009), CISC Handbook (2010), and AISC Manual (2010) extended shear tab design method in predicting the resistance and behaviour (failure mode) of extended shear tab connections having multiple vertical rows of bolts. To attain this objective, the following measures were taken:

- Design eight beam-to-girder and four beam-to-column extended shear tab connections with varying “a” distances and quantity of bolts using the combined extended shear tab design method
- Subject the twelve connections to full-scale testing until failure to observe the primary failure mode, any secondary failure modes, and rotational behaviour
- Compare the observed failure modes and corresponding loads to that predicted by the combined extended shear tab design method and comment on its validity

- Where discrepancies are seen between the design method and the test observations, make recommendations for modifications to the combined extended shear tab design method

1.3. Scope

In order to achieve the stated objectives a total of four beam-to-column and eight beam-to-girder extended shear tab connections were selected and designed in collaboration with our industry partners. These connections were tested in the Jamieson Structures Laboratory at McGill University. A set of hydraulic actuators was used to apply displacement to two points of a beam to create a specified rotation and corresponding shear force in the shear tab connection at the beam end. The applied rotation was increased until ultimate failure was seen in the connection or the maximum stroke in the tension actuator was reached. Primary and secondary failure modes were assessed using measurements from various monitoring devices. The measured connection resistances were compared with the predicted and factored resistances calculated using the combined extended shear tab design method. Where discrepancies between the observed behaviour and predicted were encountered, recommendations were made for modifications to the design method.

1.4. Outline

The details and findings of this research program are presented in the following chapters:

- Chapter 2 provides a summary of previous research on both conventional and extended shear tab connections as well as the relevant sections from the American and Canadian steel codes used in the design of these connections.
- Chapter 3 gives comprehensive descriptions of the test specimens, the combined extended shear tab design method, the test setup, and the testing procedure.
- Chapter 4 describes the experimental results and provides a comparison of these results with the current design method. The suitability of the combined extended shear tab design method in predicting the behaviour of extended shear tab connections is commented on. Proposed design equations are presented where discrepancies between the predictions and observed behaviour exist. Results from coupon tests are presented.
- Chapter 5 summarizes the findings and recommendations.

Chapter 2 – Literature Review

2.1. Overview

This chapter presents the literature related to the behaviour and design of conventional and extended shear tab connections. The first portion focuses on past research and is subdivided into full-scale testing, numerical finite element studies and design aids. The second portion provides a review of the current methods for the design of shear tab connections in North America. CSA S16-09 (2009), the CISC Handbook (2010) and the AISC Manual (2010) provide guidance for the design of shear tab connections, primarily based upon the results from full-scale testing conducted by Astaneh et al. (1989).

2.2. Research

This section gives pertinent details of the relevant testing conducted on shear tab connections, numerical modelling and design aids published within the past 45 years.

2.2.1. Full-Scale Testing

Lipson (1968) investigated the behaviour of single angle and single plate connections as an alternative to double angle connections, which were typical for beam-to-column simple shear connections at the time. Single plate and single angle connections were more economical and easier to assemble on site than double plate or angle connections. The experimental program consisted of three sets of tests: bolted-bolted angle connections, welded-bolted angle connections, and welded-bolted plate connections (also referred to as shear tabs). The aim was to examine the performance of such connections under working loads, maximum rotation, ultimate limit states and whether the connections could be classified as simply-supported (referred to as flexible) under the AISC Design Specification (1963). Twelve tests were run for the welded-bolted angle connections, each with one vertical row of three to six bolts. The connections were subjected to: i) pure moment ii) shear and moment or iii) shear, moment, and rotation. For the case of shear and moment, beams were connected to a heavy column to minimize rotation. As a result, moments at the connections were minimal. Slip loads (shown by spiking in the shear-

deflection curve in Figure 2.1) were found to be proportional to the shear force divided by the number of bolts.

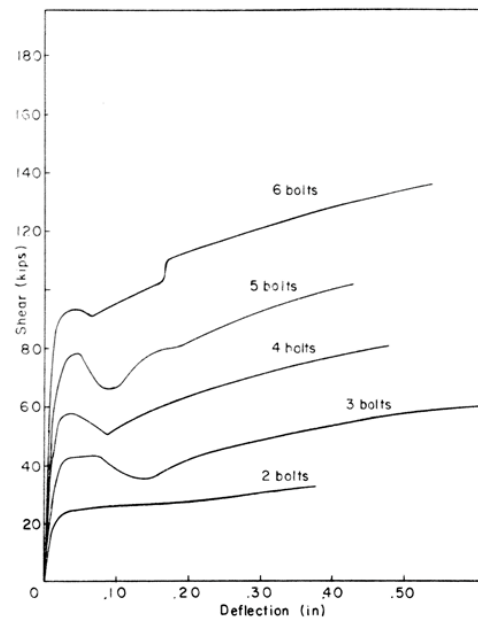


Figure 2.1: Shear-Deflection Curves for Welded-Bolted Single Plate Connections, Lipson (1968)

Lipson concluded that welded-bolted plates could be classified as “flexible” under the AISC Design Specification (1963). This specification required a minimum connection rotation capacity of 0.033rad at yielding for a connection to be considered flexible. For the welded-bolted plates, slip values for applied shear were found to exceed the acceptable value. All of the tested connections were found to develop some moment at the support due to partial restraint against bending supplied by the supporting member. The magnitude of the moments was greatly exceeded by the flexural strength of the beams. Welded-bolted single plate connections were found to be feasible when bearing type bolts were utilized.

Richard et al. (1980) conducted further research on shear tab connections to examine deformation and rotation under applied shear loading. Previously, the distribution of stresses to the bolt group was thought to be such that each bolt carried equal portions of the shear loading on the connection. Richard et al. hypothesized that this assumption was not accurate; it was postulated that the stresses were distributed to the given bolts based on connection geometry. Limited rotational ductility in shear tab connections was thought to be attributed to shear deformation of the bolts, bearing deformations of bolt holes, out-of-plane plate deformation and

bolt slippage. Lipson (1968) had stated that the end moments in the beam were a function of the bolt layout, plate thickness, beam loading and flexibility and flexibility of the support element. For the purpose of the research by Richard et al., only the effect of varying the plate geometry and bolt size and layout were examined.

Great effort was taken in developing a numerical model to simulate accurately the moment-rotation curves for shear tab connections. Single shear tests were conducted on varying plate geometries and bolt sizes to determine the load deformation relationship for the bolts. The finite element analysis method conducted by Caccavale (1975) was used in combination with the tested bolt data to model the moment rotation curves for such connections. The failure modes in these connections was observed to be: i) shear failure of the bolts ii) bearing failure of the plate and iii) transverse tension tearing of the plate (comparative to net section shear failure). Figure 2.2 illustrates the load deformation response for 19mm (3/4in) A325 bolts connecting 9.5mm (3/8in) plates to 13mm (1/2in) plates.

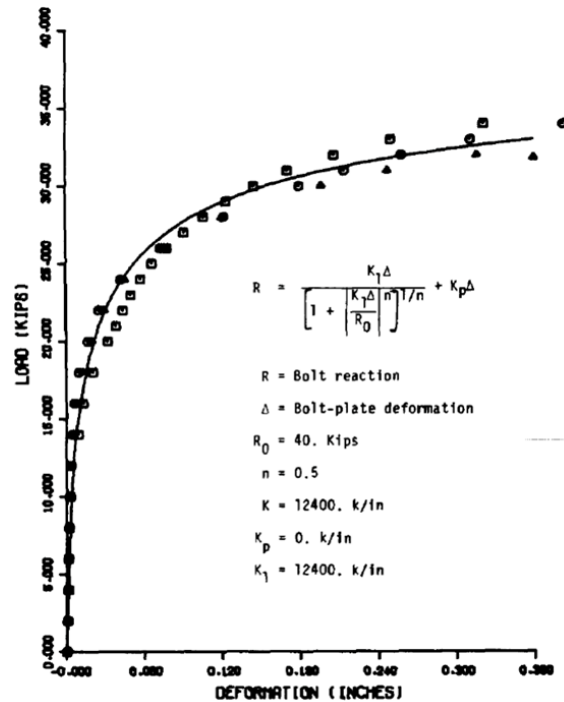


Figure 2.2: Load-Deformation for 19mm Bolts Connecting 9.5mm Plates, Richard et al. (1980)

The combination of the load deformation plots for the bolts and the finite element model was used to produce the following expression for the connection moment, M .

$$M = M^*[1 - (1 - e/h)^{3.9}]M_{ref} \quad (2.1)$$

$$M^* = \frac{60 \phi^*}{\left[1 + \left(\frac{60 \phi^*}{1.1}\right)^{2/3}\right]^{3/2}} \quad (2.2)$$

In which ϕ^* is the ratio of the free end rotation of the beam to a reference rotation. This reference rotation is a function of the number of bolts (lesser bolts, gives greater rotation) and is based on a 76mm (3in) offset between the vertical row of bolts and the weld line. This distance is referred to as the “a” distance. The eccentricity of the load and the depth of the bolts are given as e and h , respectively. The reference moment, M_{ref} , is based on the pure moment on the connection with all bolts loaded to their maximum capacity.

The two relations were used to predict the magnitude of the moment seen at the connection for a given bolt configuration (number of bolts, depth of bolt group and load eccentricity). Seven tests were conducted to confirm the moment-rotation model, which was found to be accurate.

Five full-scale tests were run to explore the eccentricity of the inflection point to the support face as a function of the applied load. Estimated eccentricity values from the finite element model were found suitable as compared to those measured experimentally.

Richard et al. (1980) established the following design procedure: i) choose a plate thickness similar to that of the beam web, ii) specify bolts based on the plate thickness to ensure rotational ductility, iii) compute the connection eccentricity, e , using the beam shear span ratio and the beam moment, and iv) use the eccentricity to compute shear stresses in the shear tab.

Ricles (1980) examined the behaviour of shear tab connections with two vertical rows of bolts used to support coped beams. Until this time, only shear tab connections with a single vertical row of bolts had been examined. Eight full-scale tests were conducted and all of them resulted in shear block failure of the beam web. This indicated that the AISC Specification (1978) under-predicted the shear block failure strength for simple shear connections. Web thicknesses were typically 11mm (7/16in) with edge and end distances varying between 25mm (1in) and 51mm (2in). A new block shear failure model was proposed, which accounted for gross yielding on the vertical plate section with a triangular stress distribution acting at the

bottom line of bolts (Figure 2.3). The then existing AISC Specification (1978) calculations assumed full shear strength along the vertical line of bolts and full tensile strength along the bottom line of bolts.

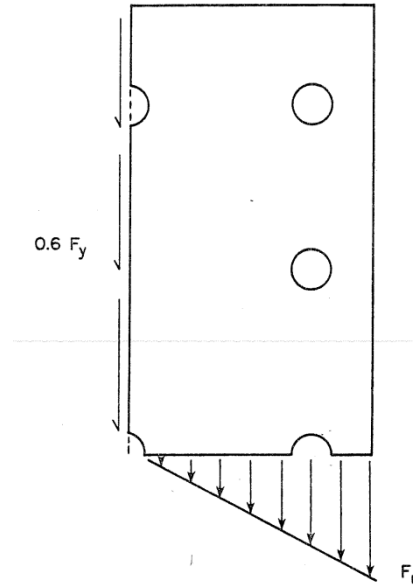


Figure 2.3: Proposed Block Shear Failure Model, Ricles (1980)

Stiemer et al. (1986) conducted full-scale testing on four beam-to-girder shear tab connections to examine the behaviour of flexible supports. Shear tabs were welded to the single side of the girder webs. The first two tests had beams that framed into the girder in a typical perpendicular fashion. This was varied over the other two tests with beams at skew angles of 30° and 45° to the centreline of the girder. This was to assess the effect of skewed beams on connection behaviour. Girder segments were 2440mm (96in) and were restrained at the ends by welding of the girder webs to end plates. Plate steel was ASTM A572 Grade A36. Connections with one vertical row of either two or three bolts were tested. The connections were bolted with 25mm (1in) ASTM A490 bolts.

It was concluded that shear tab connections with flexible supports, such as girder webs, behave very differently than that of rigid connections. Large deformations were induced in the supporting girder due to shear, torsion and bending in the shear tab (Figures 2.4 and 2.5). Connections with a shear tab depth to girder depth (d_{plt}/D) ratio of less than 60% were found to behave flexibly. For those connections with a d_{plt}/D ratio of less than 40%, the torsional moment

caused the web of the girder to buckle below the connection plate. Stierner et al. (1986) recommended that the maximum connection shear force be less than 30% of the ultimate shear resistance of the supporting girder. The design equation for a single plate connection connecting to a single side of a girder web was proposed to be:

$$[(V_{max}/\phi V_{ult})^2 + (M_t/\phi T_{ult})^2 + (M_b/\phi M_r)^2]^{1/2} \leq 1.0 \quad (2.3)$$

where V_{ult} and M_r are calculated for the girder alone and T_{ult} is calculated for the girder and single plate. The resistance factor, ϕ , is taken as 0.9.

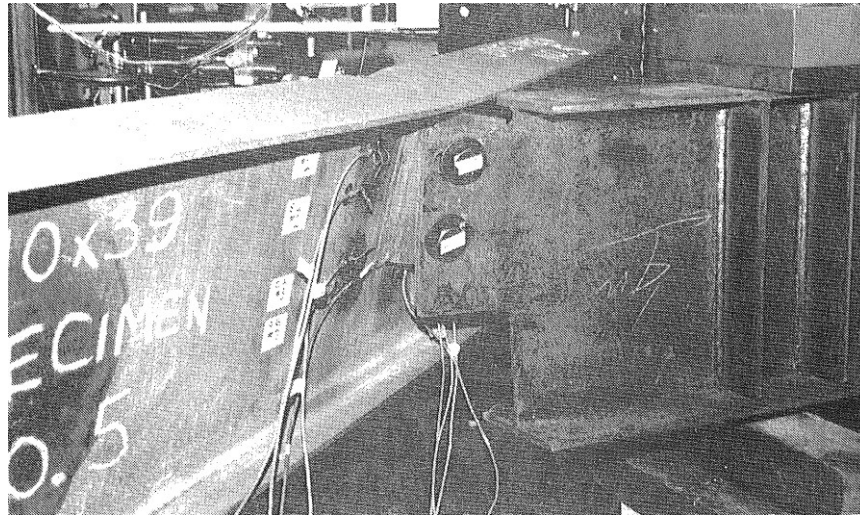
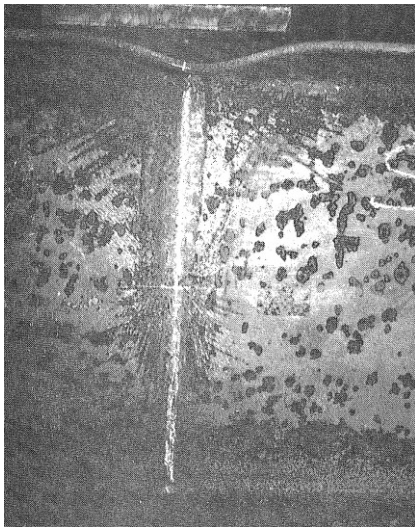


Figure 2.4: Test 5A, W460x39 Beam with 402mm Deep Girder (45°), Stierner et al. (1986)



a) Back of Girder Web and Flange



b) Front of Girder

Figure 2.5: Test 2B, W460x61 Beam with 452mm Deep Girder (0°), Stierner et al. (1986)

Astaneh et al. (1989) investigated the behaviour of shear tab connections by testing six full-scale specimens, each with an increasing number of bolts. Shear tab connections with a single vertical row of bolts were tested. The key outputs of this study were the shear resistance and the rotational ductility of the connection. Astaneh et al. wished to create a design procedure for shear tab connections to be implemented in the AISC Manual (1993). Design equations were developed for each of the applicable limit states to estimate their shear resistance. Rotational ductility was examined to ensure that the connections act as simply supported: possessing enough rotational ductility that to not attract significant moment (and therefore act as a hinge). In order to conduct the testing, a shear rotation relationship of the connection was required. Preliminary tests were conducted on beams with varying shape factors and span-to-depth ratios to produce a tri-linear curve as shown in Figure 2.6. This curve accounted for both the elastic and the nonlinear behaviour of the shear tab connection.

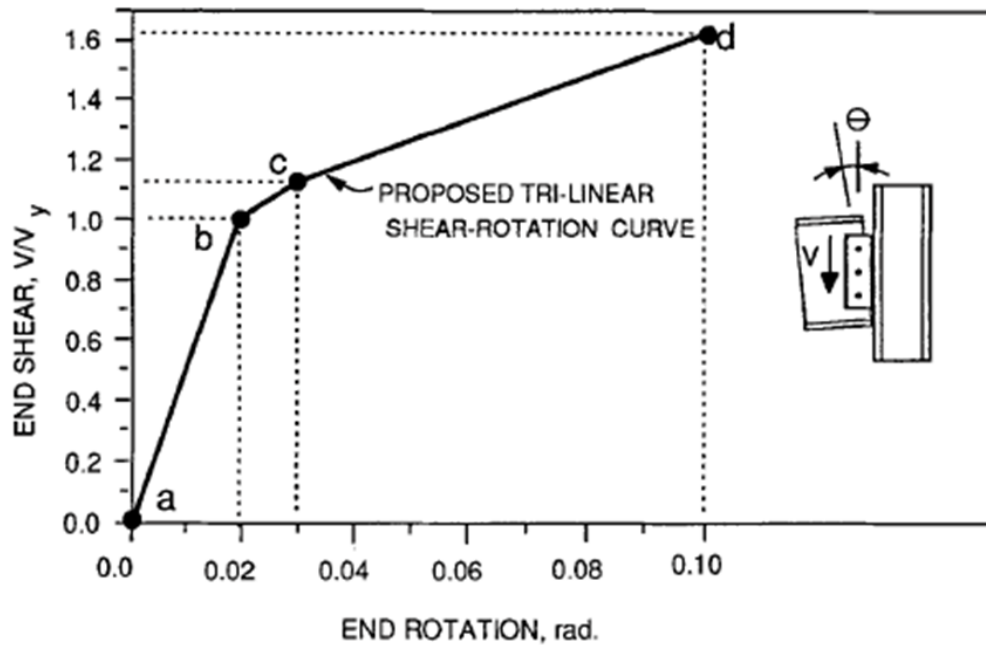


Figure 2.6: Tri-Linear Shear-Rotation Curve for Shear Tab Connections, Astaneh et al. (1989)

The test specimens were connected with ASTM A325 & A490 bolts, which were pre-tensioned to 70% of the minimum bolt tensile strength in accordance with the AISC Manual (1986). Noticeable shear yielding of the plates occurred in all of the tests, with ultimate failure taking the form of bolt shear fracture. It should be noted that a test specimen experienced weld fracture. This was the result of the weld being inadequately sized and was purposefully done to

examine the connection behaviour for the limit state of weld tearing. Design equations and procedures for the proposed limit states were developed. The limit state hierarchy was organized such that ductile failure modes such as plate yielding were developed in the connection before brittle failure modes such as bolt and weld fracture.

It was found that as the connection shear increased, the inflection point in the beam approached the column face rapidly and then remained relatively stationary. Empirical equations were developed to determine the inflection point eccentricity as a function of the number of bolts in the connection and the “a” distance.

The limit states of plate yielding, bearing at bolt holes, net fracture of the plate, edge distance fracture of the plate, bolt and weld fractures were concluded to be applicable for shear tab connections. Design equations were developed for the limit states not already addressed in the AISC Manual (1986). The interaction between flexural and shear stresses was accounted for by an expression for the available flexural stress using the Von-Mises criterion.

It was concluded by Astaneh et al. (1989) that shear tab connections undergo large amounts of shear yielding, thus releasing rotational stiffness at beam ends, which may then act similarly to a simply supported structure. Rotational ductility was found to decrease with an increasing number of bolts. It was recommended that plates should be sized such that shear yielding occurs before brittle types of failures.

Shaw and Astaneh (1992) conducted six full-scale tests to determine the applicability of Astaneh et al.’s (1989) design equations in predicting the behaviour of beam-to-girder shear tab connections. Girder sections measured 711mm (28in) in length and were fixed at each end. All steel was ASTM Grade A36. Girder depths ranged from 457mm (18in) to 610mm (24in). The shear tabs were welded to the girder flange only and the beams were coped at the top flange. Test specimens had a single vertical row of four or six 19mm (3/4in) A490 bolts with depths of 305mm (12in) or 457mm (18in), respectively.

All of the tests were characterized by yielding of the girder web (see Figures 2.7 and 2.8). The amount of yielding was influenced by the girder web thickness and the girder clear span (the distance between the bottom edge of the shear tab and the bottom girder flange). Girders with thicker webs and lesser clear spans underwent less yielding than their counterparts.

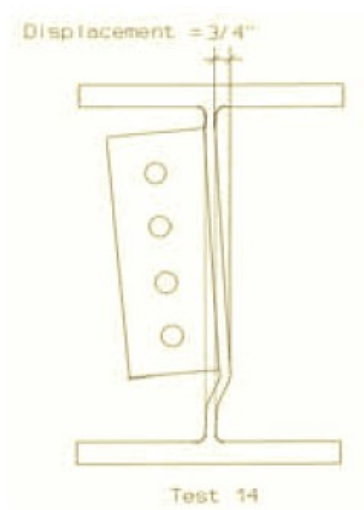
The welds fractured slightly for all tests in a ductile manner. Similar to the beam-to-column shear tab connections [(Astaneh et al. (1989)], the zero moment inflection point moved towards the connection as the shear and rotation increased. The ductility of the connections was contributed to significantly by deformation of the girder web, much different than yielding of the plate itself in beam-to-column connections.



a) Test 12

b) Test 13

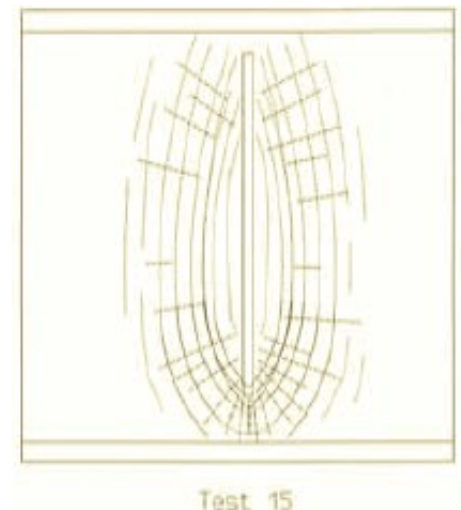
Figure 2.7: Yielding of Girder Web (Flecks Indicate Yielding), Shaw and Astaneh (1992)



a) Test 14



b) Test 14



c) Test 15

Figure 2.8: Girder Web Deformation, Shaw and Astaneh (1992)

Shaw and Astaneh (1992) concluded that the resistance of beam-to-girder shear tab connections is adequately predicted by the design method that was formulated by testing of beam-to-column connections. None of the tested connections failed at shear loads less than predicted by Astaneh et al.'s (1989) design equations. Shaw and Astaneh recommended welding additional plates to the top flange of the girder for one-sided beam-to-girder connections in situations where girder web rotation is not desired.

Liu and Astaneh (2000) investigated the seismic behaviour of shear tab connections supporting floor slabs to determine the feasibility of using shear tab connections as part of a building's lateral force resisting system (LFRS). Sixteen full-scale tests were split into two series. Series A included shear tabs designed as per the industry practice at the time. Testing of Series B was conducted after A, with shear tab connections designed to improve upon A. All of the connection configurations saw shear tabs on both sides of a supporting column, whether it be to the flange or the web. The presence of a slab was varied over the tests to examine the effect of composite action on the overall shear tab connection performance. Both light and normal weight concretes were used for the slab. The typical test setup can be seen in Figure 2.9. The W-shapes were made of ASTM A572 Grade 50 steel and the connection plates and angles were made of A36 steel. Slabs were 160 mm thick and sat on top of 20 gauge steel decking with 74mm (3in) ribs at 305mm (12in). This test setup allowed lateral drifts to be applied in combination with gravity loads.

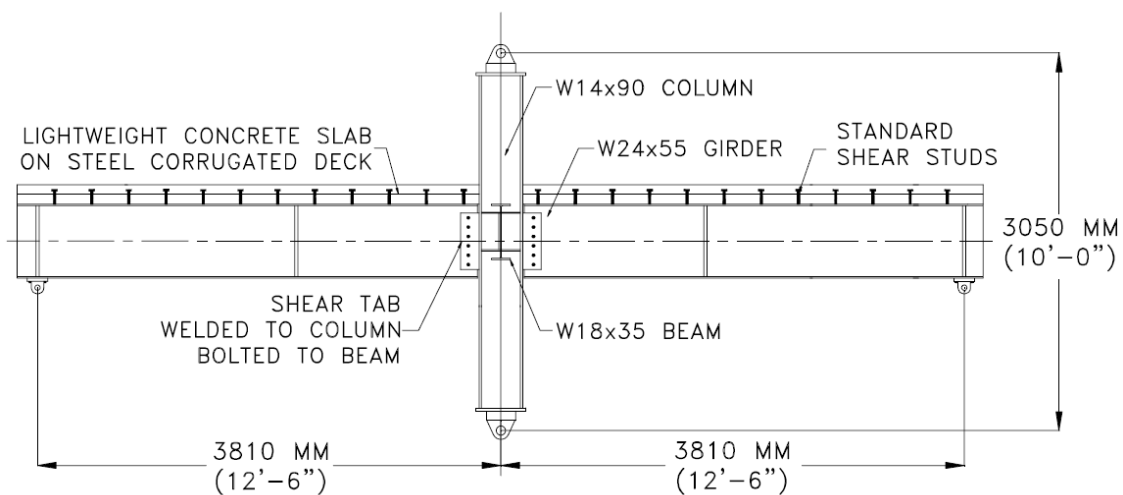


Figure 2.9: Typical Test Setup, Liu and Astaneh (2000)

Testing of the bare-steel (without a slab present) specimen revealed that the flexural capacity of the shear tab was approximately 15% to 20% of the plastic moment capacity of the beams and thus, the moment resistance was greater than assumed in design (zero moment assumption). Rotational ductility was characterized by bolt slippage, yielding of the shear tab and deformation of bolt holes. Some local buckling of the shear tabs was also observed. Eventually, fracture occurred in the shear tab underneath the bottommost bolt at 0.09rad of drift (Figure 2.10).

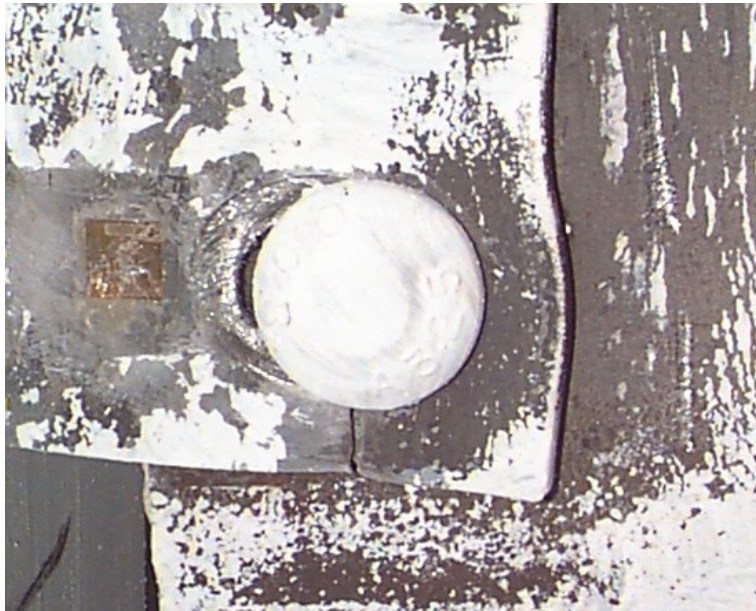


Figure 2.10: Deformation of Bolt Hole and Fracture, Bare-Steel Test, Liu and Astaneh (2000)

The inclusion of a slab was found to increase the flexural stiffness and strength of a shear tab beam-to-column connection. By including a slab, the neutral axis shifted upwards. This caused more deformation to occur in the lower portion of the shear tab. The effect of concrete density on the shear tab connection performance was not found to be significant, with similar performance from both light and normal weight slabs. Figure 2.11 shows the load-drift response for specimens with and without a slab

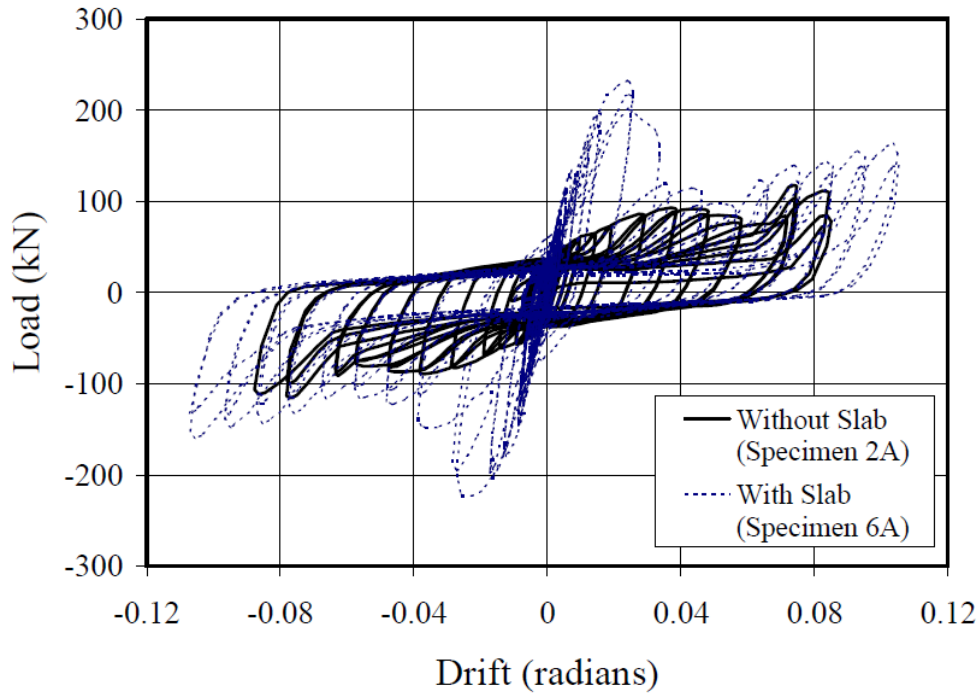


Figure 2.11: Load-Drift Response for Specimens with and without a Slab, Liu and Astaneh (2000)

The addition of a seat angle bolted to the column and bottom flange of the beams was examined as a potential retrofit option. Testing revealed a significant increase in lateral stiffness and flexural resistance of the shear tab connection, with a moment resistance of 80% (versus 50% for those without a seat angle) of the beam. When the angle retrofit was used, excessive panel zone shear distortion occurred. Figure 2.12 compares the load-drift response for specimens with and without the angle retrofit. Fracture occurred along the bolt line at 0.09 radians and the test was ended. The specimen at the end of test can be seen in Figure 2.13.

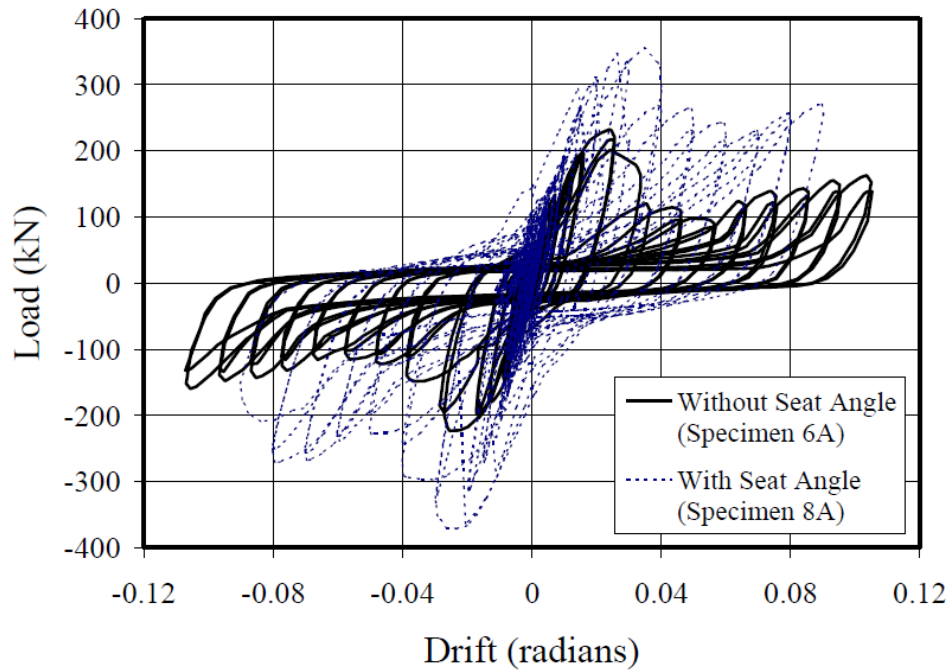


Figure 2.12: Load-Drift Response for Specimens with and without Angle, Liu and Astaneh (2000)

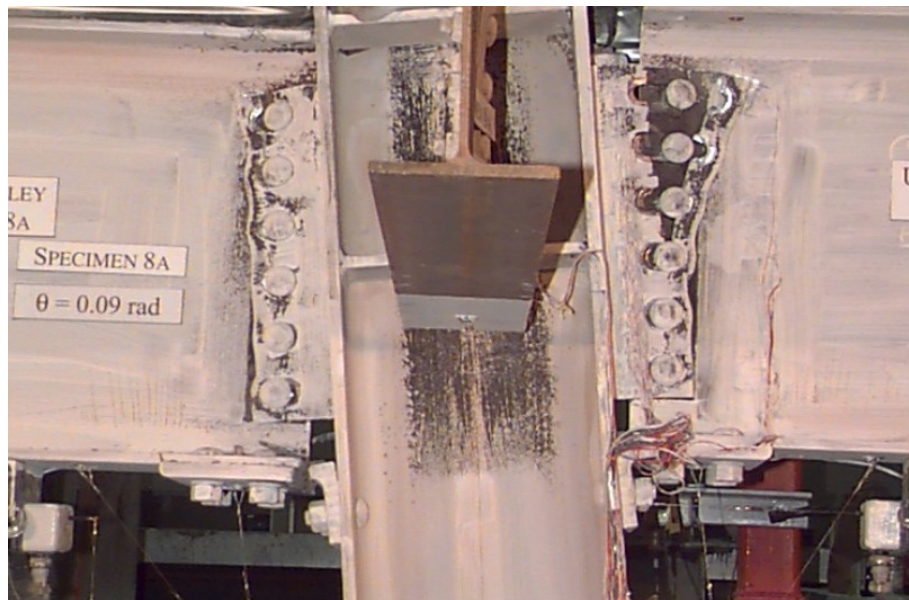


Figure 2.13: Specimen with Supplemental Seat Angle, End of Test, Liu and Astaneh (2000)

It was concluded that simple shear connections do possess more flexural resistance than assumed in design but their inclusion into the LFRS of structures needs further analysis: both experimental and analytical.

Sherman and Ghorbanpoor (2002) performed 31 full-scale tests to investigate the behaviour of extended shear tab connections. The purpose of this research was to determine the applicability of the limit states defined from the research on conventional shear tab connections performed by Astanek et al. (1989), as well as to explore any failure modes unique to extended shear tab configurations. Sherman and Ghorbanpoor (2002) considered an extended shear tab connection to be that with an “a” distance exceeding 76mm (3in). Figure 2.14 depicts a conventional (not extended) shear tab connection with a 76 mm (3in) “a” distance.

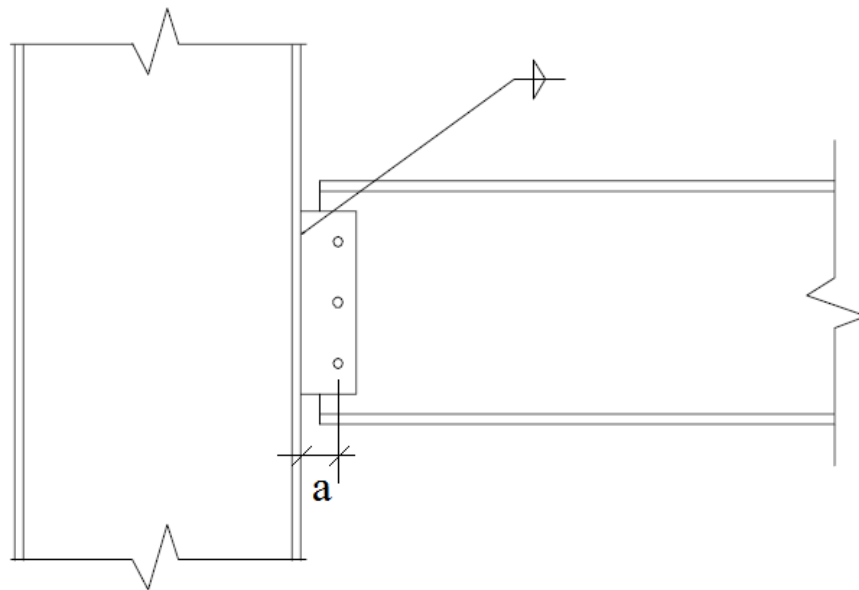


Figure 2.14: Conventional Shear Tab Connection, Sherman and Ghorbanpoor (2002)

Testing was split into three phases. Phase I examined both stiffened and unstiffened beam-to-column and beam-to-girder connections with a single vertical row of three or five bolts. The unstiffened tests consisted of two beam-to-column web tests and two beam-to-girder web tests. The unstiffened tests had shear tabs of 9.5mm (3/8in) (except a single five bolt beam-to-column test) with welds of 6.5mm (1/4in). The stiffened tests consisted of five beam-to-girder tests where the shear tab was welded to the web and top flange of the girder and eight beam-to-column web tests where a pair of stiffeners spanned between the column flanges. The stiffened tests had shear tabs that were 6.5mm (1/4in) thick and used 5mm (3/16in) welds. Figure 2.15 illustrates the difference between stiffened and unstiffened extended shear tab connections.

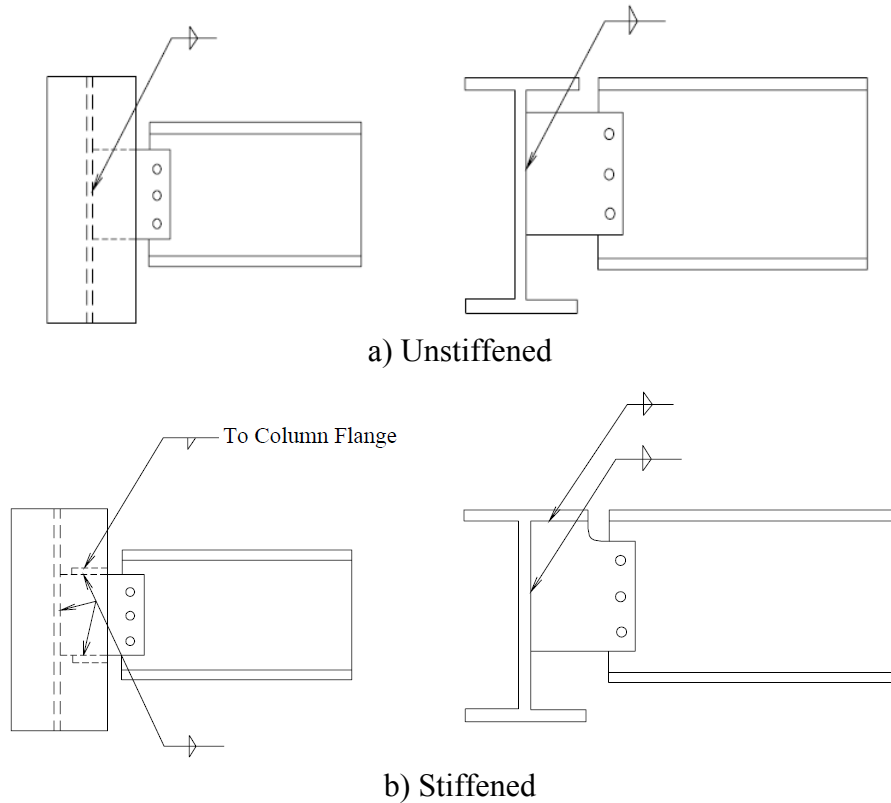


Figure 2.15: Unstiffened vs. Stiffened Extended Shear Tabs, Sherman and Ghorbanpoor (2002)

Phase II consisted of four tests and examined snug tightened bolts in short slotted holes, single stiffening plates for beam-to-column web connections, and the behaviour of stiffening plates.

Phase III examined connections with deeper shear tabs (with six and eight bolts in a vertical row). Six beam-to-column tests were run, three of which were stiffened and three unstiffened. Four beam-to-girder tests were run, two with six bolts and two with eight bolts. All beam-to-girder tests were stiffened. One of each six and eight bolt configuration used partial height shear tabs welded to the girder web and top flange and the other used a full height shear tab that extended to the bottom flange of the girder. The stiffened tabs in Phase III were sized at 8mm (5/16in), except for the eight bolt connections where the thickness was 9.5mm (3/8in). All shear tabs in Phase III had welds sized at 8 mm. All Phase I and III tests had shear tabs made of ASTM Grade A36 steel and used 19mm (3/4in) A325 bolts. The dimensions of the column-to-plate and girder-to-plate fillet welds were sized at three quarters of the plate thickness for the unstiffened tabs to ensure shear yielding of the shear tab would occur before weld failure.

The following parameters were varied over the tests to discern their impact on rotational ductility and ultimate shear resistance: i) span-to-depth ratio of supported beam ii) width to thickness ratio of supported beam web iii) shear tab size iv) the number of bolts v) type of bolt hole and vi) lateral bracing of supported beam. Since shear tab connections have partial rotational rigidity and do not act as perfect simple supports, some moment exists at the face of the support. For this research, the point of zero moment was assumed to be located at the vertical row of bolts. Lateral torsional buckling of the unsupported plate length was proposed to be a limit state particular to extended shear tab connections. It was proposed that the shear tab and supported beam could be idealized as a beam coped at both flanges. Shear yielding of the shear tab, twisting of the shear tab and bearing failure of the bolt holes were found to occur simultaneously for the majority of tests. This was expected due to the decrease in shear yielding, flexural yielding and bolt bearing resistance with increasing eccentricity. In the tests with deeper shear tabs, shear yielding of the girder web at weld locations was observed.

The limit states were calculated using two values of the inflection point eccentricity, e . The inflection point eccentricity is defined as the distance from the support face to the point of zero moment in the beam. The eccentricity was found first using the equations from the AISC Manual (2001) (Equations 2.4 to 2.7) and, secondly, using a regression analysis based on the experimental data. The AISC Manual (2001) equations were found to over-predict the eccentricity. Using the calculated eccentricity to determine the connection resistance resulted in a prediction of bolt shear and bearing failure. The eccentricity found by the regression analysis was more accurate than the code equations. When used to predict the failure method, shear and flexural yielding was found to govern.

$$\text{Rigid – Standard:} \quad e = |(n - 1) - a| \quad (2.4)$$

$$\text{Rigid – Slotted:} \quad e = |2n/3 - a| \quad (2.5)$$

$$\text{Flexible – Standard:} \quad e = |(n - 1) - 1| \geq a \quad (2.6)$$

$$\text{Flexible – Slotted:} \quad e = |2n/3 - 1| \geq a \quad (2.7)$$

where n is the number of bolts in the connection and a is the “a” distance. Rigid and flexible refer to the support condition. Standard and slotted refer to the type of bolt hole used. Figure 2.16 illustrates the inflection point eccentricity, e , and the corresponding sign convention.

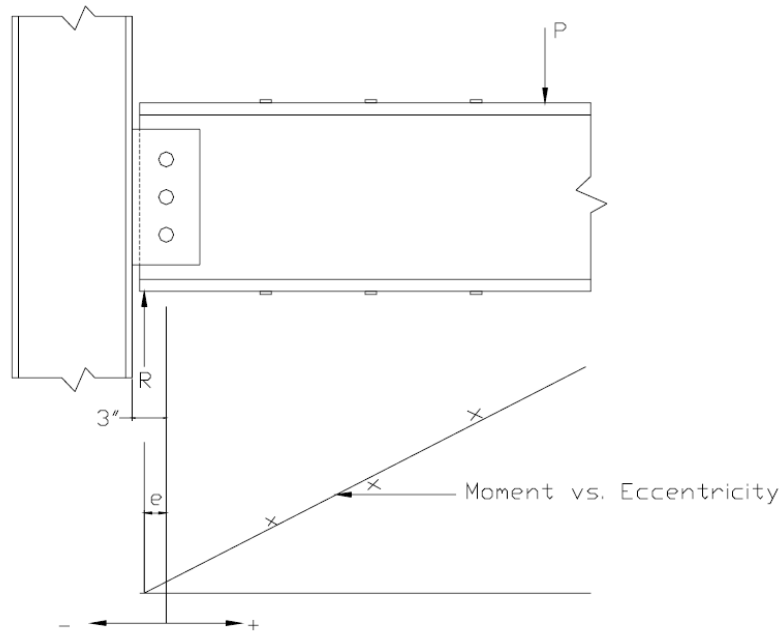


Figure 2.16: Inflection Point Eccentricity, e , Sherman and Ghorbanpoor (2002)

The proposed limit state of lateral torsional buckling did not appear to be critical for any of the tested connections. Twisting of the unsupported plate length was seen before lateral torsional buckling could occur. This was especially prevalent in deep connections [with 610mm (24in) deep beams] where separation of the top of the shear tab from the supported beam web was seen. A torsional limit state was developed with a corresponding design equation. This was attributed to the offset between the centreline of the shear tab and that of the beam. Phase III utilized lateral and rotational bracing, which minimized twisting of the beam and shear tab itself. Plate buckling occurred in two beam-to-girder tests as a secondary effect of twisting.

It was found that extending the shear tab to the bottom flange of the girder for beam-to-girder shear tab connections did not increase the rotational stiffness of the connection but instead decreased the shear capacity of the connection. This was due to the shear tab acting as a compressive strut that buckled under loading.

Sherman and Ghorbanpoor (2002) found substantial distortion of the column web in unstiffened beam-to-column web connections. They proposed the following equation based on a yield line mechanism:

$$V_{ew} = \left((2h/L) + (4L/h) + 4(3)^{1/2} \right) (F_{yw} t_w^2 / 4) (L) / e_w \quad (2.8)$$

where h is the shear tab depth, L is the shear tab length, F_{yw} is the yield strength of the column web, t_w is the column web thickness and e_w is the distance between the weld and the bolt vertical row. This yield line mechanism was not considered to be a limit state for unstiffened beam-to-girder connections. Distortion of the girder webs was not as severe as that of column webs. This was attributed to the top edge of the shear tab being located very close to the girder flange, which was thought to act as a stiffener.

Creech (2005) conducted 10 full-scale shear tab tests to assess the suitability of the limit states identified in the AISC Manual (2001). He hypothesized that the design equations were overly conservative. Behaviour examined was that of the bolts, the inflection point eccentricity and the flexural response of the shear tab itself. Creech compared his observations against that of previous research, including Astaneh et al. (1989). Three beam-to-column connections were tested and seven beam-to-girder connections. All connections had “a” distances of 76mm (3in) and used 9.5mm (3/8in) thick shear tabs made of ASTM Grade A36 steel. All connections were bolted with 19mm (3/4in) ASTM A325 bolts. The restraining effect of a slab sitting on top of the connection was simulated by welding a plate to the top of the beam and the girder for three of the beam to girder tests. Two and three bolted beam-to-girder connections used a W460x74 girder while the seven bolt beam-to-girder tests used a W760x147 girder. All tests had a single vertical row of bolts.

The design method located in “Single-Plate Shear Connections” of the AISC Manual (2001) was found to over-predict the bolt group shear resistance for flexible support conditions (i.e. beam-to-girder). However, the bolt bearing resistance of the shear tab was found to be accurately predicted when the eccentricity of loading was taken into account (by means of the instantaneous centre of rotation method). A modified design method was proposed for the limit state of flexural yielding, which allowed for the full plastic section modulus of the plate to be used to calculate the flexural resistance. This resistance would then be compared to the applied moment which is calculated using the eccentricity of the bolt group from the support.

The location of the inflection point was examined throughout the tests. For rigid connections, the inflection point started and remained opposite the bolt group from the support

face for the duration of loading. For flexible connections, the inflection point began between the support face and the bolt group and moved toward the centre of the beam as loading was increased. This was concluded to be due to the flexible connections acting as simple supports. The ductility in the connection releases flexural demands.

Creech (2005) completed a thorough literature review on shear tab connections. A review of the following studies can be found in Creech's thesis:

- White (1965) *Framing Connections for Square and Rectangular Structural Tubing*
- Becker and Richard (1985) *Design of Single Plate Framing Connections with A307 Bolts*
- Hormby et al. (1984) *Single-Plate Framing Connections with Grade-50 Steel and Composite Construction*
- Sarkar and Wallace (1992) *Design of Single Plate Framing Connections*
- Duggal and Wallace (1996) *Behavior and Applications of Slotted Hole Connections*
- Forcier (2002) *Shear Tab Connection Primer*
- Crocker and Chambers (2004) *Single Plate Shear Connection Response to Rotation Demands Imposed by Frames Undergoing Cyclic Lateral Displacements*

Creech (2005) also reviewed the design of shear tab connections in the British and Australian/ New Zealand handbooks:

- The British Constructional Steelwork Association Ltd. (2002) *Joints in Steel Construction: Simple Connections*
- New Zealand Heavy Engineering Research Association (1999), *Structural Steelwork Connections Guide*
- OneSteel Market Mills (2000) *Composite Structures Design Manual – Design Booklet DB5.1, Design of the Web-Side-Plate Steel Connection*

Goodrich (2005) investigated the behaviour of stiffened beam-to-column web shear tab connections. These types of shear tab connections are considered extended (see Figure 2.17) due to the beam being outside of the column flanges. The shear tab geometry was such that the plate extended further to the bottom stiffener than to the top (Figure 2.18).

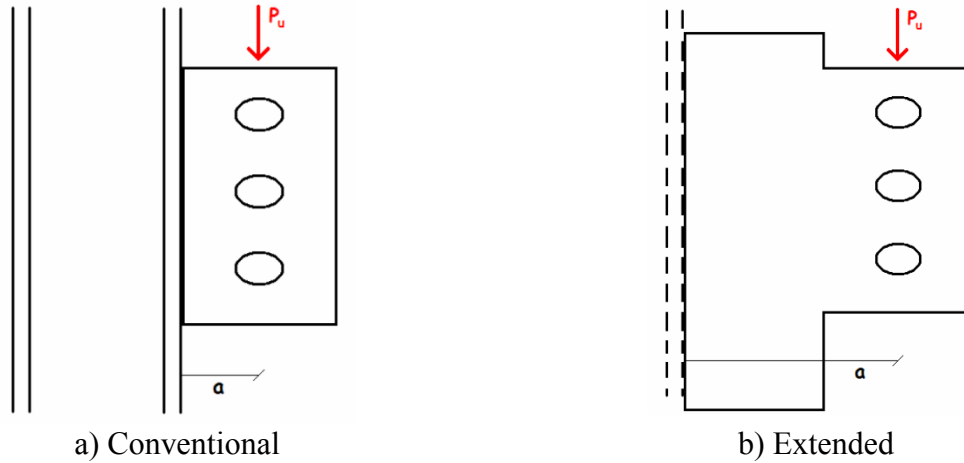


Figure 2.17: Conventional vs. Extended Unstiffened Beam-to-Column Shear Tab Connections, Goodrich (2005)

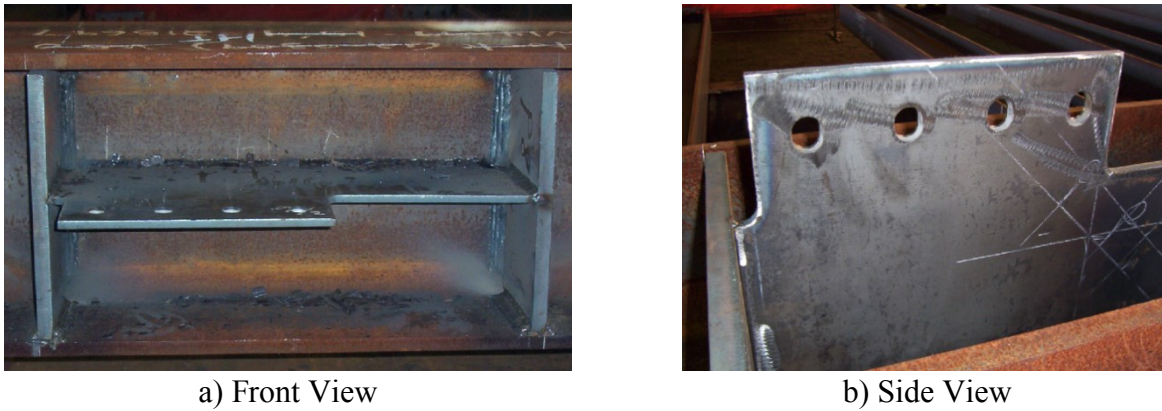


Figure 2.18: Shear Tab Before Testing, Test 1, Goodrich (2005)

Six tests were conducted and split into three sessions. Each session had two tests with identical connection parameters to account for any experimental variation. A W690x125 beam and W360x147 column were used for all sessions. ASTM A572 Grade A36 steel was used for the shear tabs. All bolts were 19mm (3/4in) ASTM A325 in short slotted holes. Table 2.1 presents the three test configurations.

Table 2.1: Stiffened Extended Beam-to-Column Shear Tab Configurations, Goodrich (2006)

Session	Bolts (c x r)	Plate Thickness (mm)	Plate Depth (mm)	Stiffener Depth (mm)	Load (kN)	Failure Type
1	1 x 4	9.5	305	573	400	Buckling
2	1 x 3	6.5	229	380	294	Buckling
3	1 x 3	13	229	380	454	Buckling

Buckling of the shear tab within the column flange was found to be the governing failure mode for all tests. Figure 2.19 shows the buckled plate for the first test. This was attributed to the compressive stresses in the plate.



Figure 2.19: Buckled Shear Tab, Test 1, Goodrich (2005)

Baldwin Metzger (2006) conducted eight full-scale tests on beam-to-column shear tab connections with single and multiple vertical rows of bolts. The experimental results were compared with the behaviour predicted by use of the design equations found in the 13th Edition AISC Manual (2005). All of the configurations were considered to have rigid support conditions due to the shear tab being welded to the column flange. Extended shear tabs accounted for four of those tested [with “a” distances of 114, 114, 229 and 267 mm (4.5, 4.5, 9, and 10.5 in)]. As specified in the AISC Manual for extended shear tab connections, a bolt group action factor of 0.8 was applied to the bolt group strength. A bolt shear strength reduction factor of 0.75 was also applied to the bolt strength due to the shear plane intercepting the threaded portion of the bolts. The length of all bolts was specified such that their threads were intercepted by the shear plane. All shear tabs were made of ASTM A572 Grade 50 steel and connected with ASTM A325 bolts. The test setup consisted of a pin support at the beam far end with two actuators placed between this support and the connection. Lateral bracing was provided along the top and bottom flanges of the beam to eliminate twisting.

Test 5a was run until the onset of plastic deformation in the beam. At this point, the test was stopped and the two bottom bolts were removed. After which, the test was resumed and

referred to as Test 5b. A summary of the extended shear tab test configurations by Baldwin Metzger is provided in Table 2.2. Tests 6 and 8 had the same bolt group geometry (two vertical rows of five bolts) but with varying “a” distances [114mm (4.5in) and 267 mm (10.5in)]. Test 7 used a single vertical row of seven bolts.

Table 2.2: Extended Beam-to-Column Shear Tab Configurations, Baldwin Metzger (2006)

Test	Bolts (c x r)	“a” Distance (mm)	Plate Thickness (mm)	Beam Size	Plate Depth (mm)	Load (kN)	Rotation (rad)	Failure Type
5a	2 x 3	114	13	W460x82	216	400	0.03	None
5b	2 x 2					391	0.036	Weld fracture
6	2 x 5	114	13	W760x161	368	890	0.025	Weld fracture
7	1 x 7	229	9.5	W610x91	521	431	0.034	None
8	2 x 5	267	13	W610x91	368	431	0.035	None

The bolt strength reduction factors were concluded to be overly conservative. In fact, all connections were expected to fail in bolt shear but failed either in weld rupture (Figure 2.20) or failure of the beam itself. Note, the welds were sized at $1/2 t$ versus $5/8 t$, where t is the plate thickness, as recommended in the AISC Manual (2005). The shear tabs were welded with lower amperage than typically used by the steel fabricator, which led to weaker nominal strength. This modification of weld thickness and amperage was to assess the suitability of single pass welds. Rotational ductility was provided by yielding of the plate for the 229mm (9in) and 267mm (10.5in) test specimens. There was no observed distortion of the bolt holes for any of the tests. This lack of distortion of the bolt holes is contrasted to previous research by Richard et al. (1980) and Astaneh (1989) in which 250MPa steel was used for the plates (as opposed to 345MPa steel). It was recommended to proportion the plate thickness such that the moment capacity of the bolt group exceeded the flexural strength of the plate. This design check appears in “Single-Plate Connections”, Part 10 of the 14th Edition AISC Manual (2010).



Figure 2.20: Weld Rupture, Test 5b, Baldwin Metzger (2006)

Gong (2010) investigated the behaviour of shear tabs welded to hollow structural section (HSS) columns subjected to shear loading. Gong noted that the web failure mechanism was a limit state for columns with slender webs [as seen in testing conducted by Sherman and Ghorbanpoor (2002)]. Gong tested six configurations under monotonically increasing shear loads. All shear tabs had a nominal thickness of 9.5mm (3/8in) and were of CSA-G40.21 300W steel. Welds were sized at $5/8 t$, where t is the plate thickness. ASTM A325 22mm (7/8in) bolts were used and sized such that the threads were excluded from the shear plane. Horizontal and vertical edge distances were 45mm (1 3/4in) and 38mm (1 1/2in) respectively. One vertical row of bolts was used for each test with a pitch of 76mm (3in). The six tests were split into three groups, each with a three and five bolt shear tab connection. Between the three groups, the HSS size was varied.

All of the tested shear tab connections behaved similarly. Yielding was seen to occur at the mid height of the shear tab and then spread to the top and bottom as shear loading increased. Loading was ceased when cracking occurred near the weld at the top of the shear tab. Permanent shear deformation in the plates and bearing deformation on the bolt holes was seen while the welds and bolts remained undamaged. Punching shear failure of the HSS column was observed in all tests at the base of the shear tabs.

Marosi (2011) investigated the behaviour of deep [with beams up to 920mm (36in) in depth] beam-to-column shear tab connections with one and two vertical rows of up to 10 bolts. Three beam sizes were used: W310x60, W610x140, and W920x233. The design method detailed in the CISC Handbook (2010) was based on tests of connections with one vertical row of less than eight bolts, and hence the need for tests of connections with two vertical rows of bolts. In addition, the applicability of existing design methods for deeper shear tab connections was to be verified. "Single Plate Connections", Part 10 of the AISC Manual (2010) defines an extended configuration as those with more than one vertical row of bolts, even if the "a" distance is 89mm (3½in) or less. The majority of Marosi's (2010) tests were therefore done on extended configurations.

Sixteen full-scale tests were conducted with three different test beams and with connection sizes ranging between one vertical row of three bolts to two vertical rows of 10 bolts. Six tests were bolted and 10 tests were retrofit welded to simulate the case of onsite welding due to misalignment of bolt holes. The welds were designed using the Instantaneous Centre of Rotation (ICR) method (CISC 2010) with their factored resistance being the same as the equivalent bolted connections. The ratio of weld strength to bolt group strength was seen to be larger in connections with two vertical rows of bolts when compared to those with a single vertical row of bolts. The weld retrofits were either a "Full C" (the full perimeter around the shear tab edge), a "Partial C" (terminating at the closest vertical row of bolts to the column), or "L Shape" (similar to Partial C but not having a weld on the top of the shear tab).

It was concluded that the predictions based on the CISC Handbook (2010) design approach were overly conservative, when they could be applied. This was thought to be due to out-dated resistance factors used in the calculation of the tabulated shear tab connections. The CISC Handbook (2010) design approach was not applicable for connections with more than a single vertical row of bolts or more than seven bolts in a single vertical row. A new design method was proposed which was based on the design procedure for extended shear tab connections in the AISC Manual (2005): for calculation of the bolt shear resistance the factor accounting for uneven stress distribution in the bolts is omitted. Marosi concluded this design method was applicable for single or double vertical row connections. The shear tabs were made from ASTM A572 Grade 50 (i.e., the nominal yield stress is 345MPa) steel. They were seen to

have sufficient ductility to meet rotational demands. All bolted connections underwent shear yielding prior to flexural yielding. Connection rotations were generally higher for connections comprising a single vertical row of bolts.

For the bolted connections, deformation in the shear tab primarily occurred between the column face and the first row of bolts. Alternatively, in the weld retrofit connections, deformation occurred between the column face and the far edge of the shear tab. This allowed the weld retrofit connections to have higher ductility and greater resistance. This was more significant in connections with more than one vertical row of bolts as deformation could occur between the vertical rows of bolts. The areas around the empty bolt holes were able to deform significantly, further increasing the ductility in the welded connections. On average, the Partial C weld retrofits had greater ductility and resistance than the Full C weld retrofits.

D'Aronco (2014) conducted ten full-scale tests on beam-to-column shear tab connections with two and three vertical rows of bolts. The support conditions were considered rigid for four tests and flexible for the other six. The test setup for the flexible support tests consisted of a column segment pinned at the top and bottom to mimic inter-storey column segments (Figure 2.21). Two of the rigid tests were weld-retrofit connections with partial “C” welds that terminated at the vertical row of bolts closest to the support face. The welds were designed using the Instantaneous Centre of Rotation (ICR) method (CISC 2010) with their factored resistance being the same as the equivalent bolted connections. Two beam sizes were used: sizes W310 and W610. Shear tab thicknesses ranged from 8mm (5/16in) to 16mm (5/8in). D'Aronco used the method proposed by Marosi (2011) to design the connections.

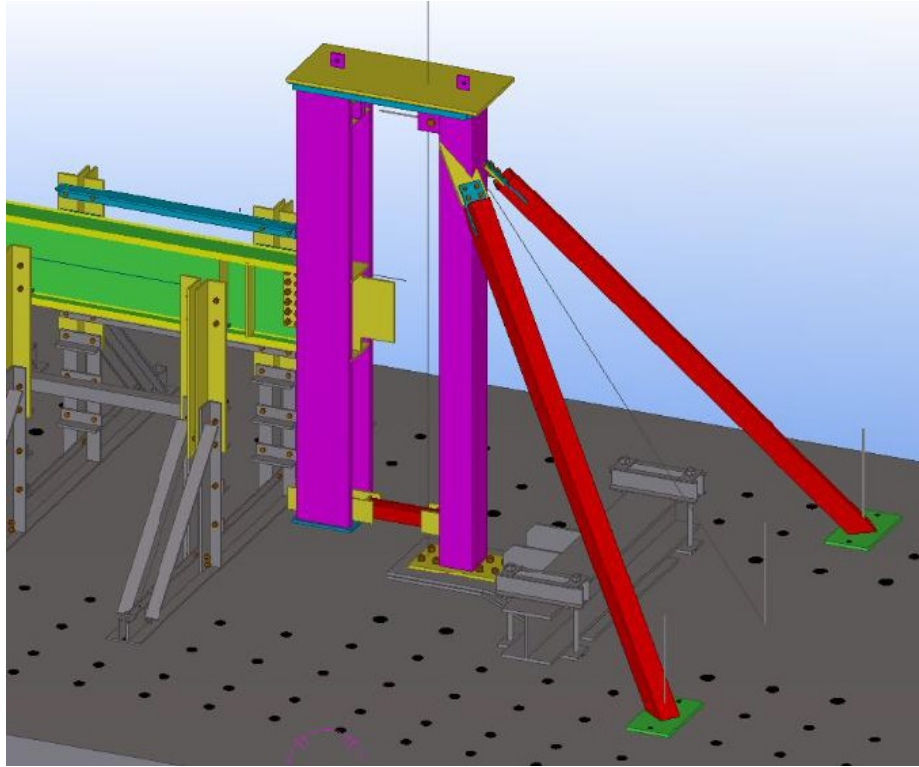
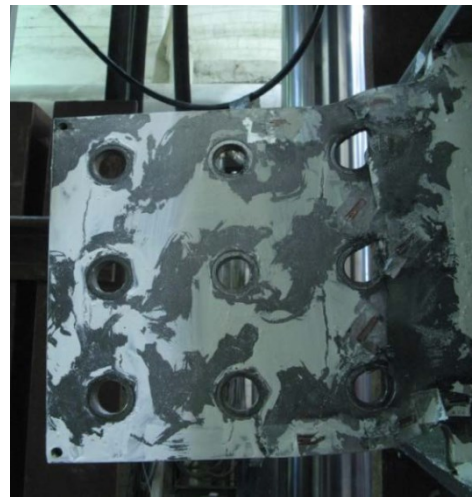


Figure 2.21: Flexible Support Beam-to-Column Test Setup, D'Aronco (2014)

The weld retrofit connections possessed adequate ductility to meet rotational demands. It was seen that the welded connections reached higher resistances than the bolted counterparts. D'Aronco confirmed that Marosi's (2011) design procedure was also applicable for connections with three vertical rows of bolts. Measured resistances were found to be greater than predicted for both flexible and rigid support conditions. Target rotation values were met for all tests except one, where significant yielding occurred in the column. This indicates that double and triple vertical row shear tab connections possess adequate rotational ductility. It was found that the addition of a third vertical row of bolts had little effect on the connection resistance. However, the double vertical row connections possessed more ductility than the single vertical row connections. ASTM A572 Grade 50 steel was used for all shear tabs and was concluded to be a suitable grade for shear tabs. Figure 2.22 illustrates the difference in deformation between rigid and flexible support conditions.



a) Rigid Support



b) Flexible Support

Figure 2.22: Shear Tab Deformation, Rigid vs. Flexible Support, D'Aronco (2014)

2.2.2. Numerical Finite Element Studies

Caccavale (1975) used the results of Lipson's (1968) laboratory based study to perform finite element modelling of steel plate connections. By performing numerous tests on bolts to determine the load-deformation response, Caccavale (1975) was able to accurately model the interaction between the bolts and the shear tab. Comparison to several tests conducted by Lipson (1968) confirmed the validity of the model. It was concluded that the ductility of shear tab connections could be attributed primarily to the bearing distortion of the plate adjacent to the bolt holes.

Ashakul (2004) modelled single plate shear connections using the finite element program ABAQUS. The goal was to produce a realistic model that accurately simulated the distribution of shear stresses among the bolt group as well as the distribution of shear and flexural stresses in the shear tab itself for shear tab connections with two vertical rows of bolts. The design method for shear tab connections in the AISC Manual (2001) specifies the bolt shear capacity as a function of the "a" distance. Ashakul found that horizontal forces acting on the bolts were a function of the "a" distance and that the horizontal forces decreased the bolts' ability to resist vertical forces. The horizontal forces were not uniform but, rather, were larger for bolts further away from the bolt group centroid. Modelling of connections with two vertical rows of bolts indicated force redistribution, thus putting large stresses on the bolt line furthest from the support.

When the shear tab underwent strain hardening, the stress distribution was not constant over the cross section. An equation for the limit state of shear yielding was proposed taking into account the increased shear stress over the cross section bounded by bolt holes. Zero shear stress was assumed at the top and bottom portions of the plate. The force redistribution in connections with two vertical rows of bolts was accounted for by assuming a triangular distribution of normal stresses with a maximum amount occurring at the topmost and bottommost bolts. Figure 2.23 illustrates the idealized flexural and shear stress distribution in shear tab connections. Beam rotation was found to be a function of the beam's stiffness and not a function of the connection geometry.

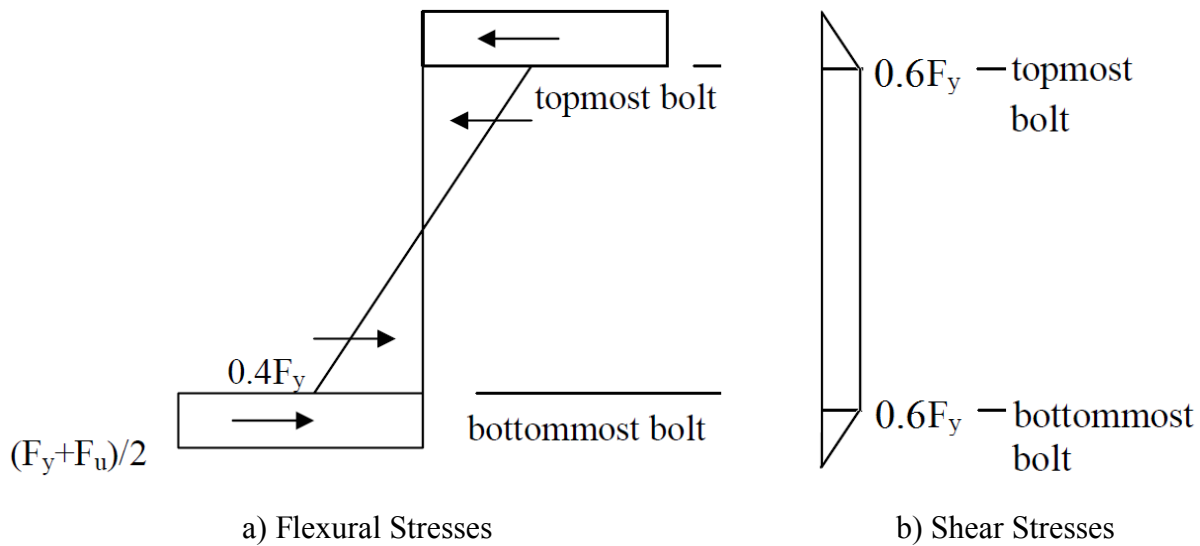


Figure 2.23: Stress Distribution within Shear Tab, Ashakul (2004)

Rahman et al. (2007) composed a finite element model for use with extended unstiffened shear tab connections. Experimental results from testing done by Sherman and Ghorbanpoor (2002) were compared with finite element models constructed for two extended unstiffened connections with three and five bolts. A W310x129 beam was connected to the web of a W200x46 column and a W460x106 beam was connected to the web of a W360x134 column, respectively. The finite element program ANSYS was used to create a model accounting for both elastic and inelastic behaviour as well as considering several failure modes. This model was intended to be applicable for a wide range of connection types, configurations, materials and loading scenarios. The model predicted the three bolt configuration to fail by column web

punching followed by bolt shear and out-of-plane twist. The model predicted the five bolt configuration to fail in twist followed by column web punching and bolt shear. This was consistent with testing results. Weld tearing was not considered to be a critical failure mode. Thus, the weld was modelled such that weld tearing would not occur.

Key outputs from the model included vertical connection displacement along the bolt line, shear load eccentricity relative to the bolt line, and out of plane twisting of the shear tab. Connection shear versus vertical connection displacement was accurately predicted by the model for both configurations with a precise global yield point (stiffness decrease). Linear regression analysis was used to determine the point of zero strain from the experimental results. The model and experimental inflection point converged with small deviations. Both the experimental and modelled eccentricities were similar to flexible standard shear tab connections as detailed in the AISC Manual (2005).

Out-of-plane twisting of the shear tab was significant in the testing of extended shear tab connections conducted by Sherman and Ghorbanpoor (2002). When the test values were compared with the model, the difference in displacements at the top and bottom of the shear tabs differed by 15mm for the three bolt connections and 16mm for the five bolt connection (Figure 2.24). This confirmed that the model accurately predicted the twisting failure mode observed in testing. Good agreement between the test results and the model showed the model to be accurate in predicting shear yielding in both connections. The model revealed high stresses and plastic deformation in bolts in both connections, which was consistent with the observed bolt deformation in the tests. Attention was paid to modelling the plasticity of the shear tab and column at top and bottom tips of the shear tab, which caused plastic deformation of the web. This punching mechanism resulted in high plastic deformation and permanent deformation of the web in testing. These stresses were seen to be significant with values reaching 485MPa in both tension and compression in the five bolt connection (Figure 2.25). This model was seen to accurately address failure in the plastic region and accounted for tension of bolts and nonlinear contact stresses between elements.

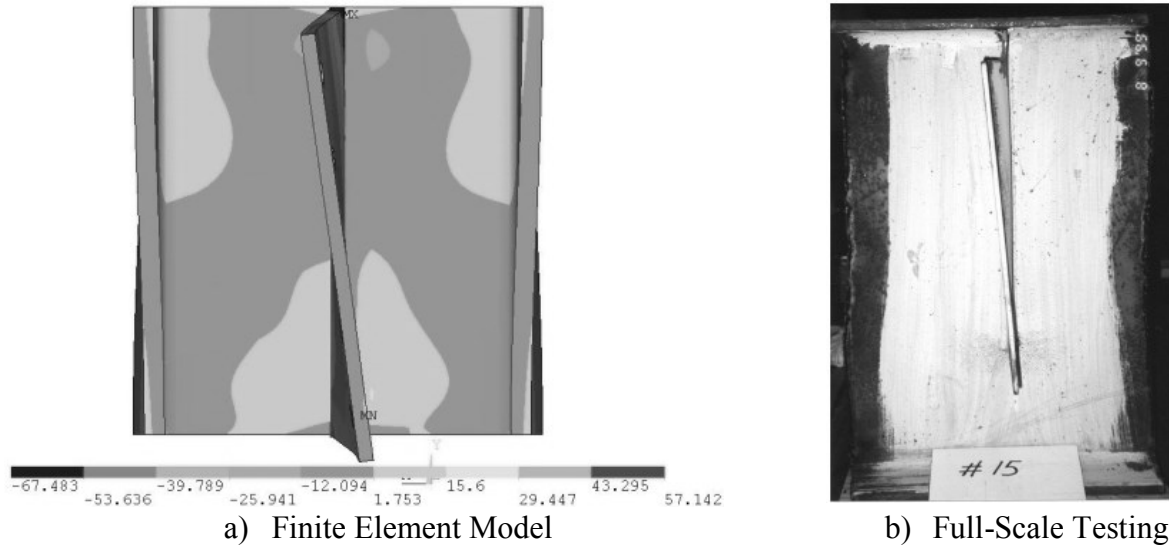


Figure 2.24: Twist Failure Mode in Shear Tab for Five Bolt Connection, Rahman et al. (2007)

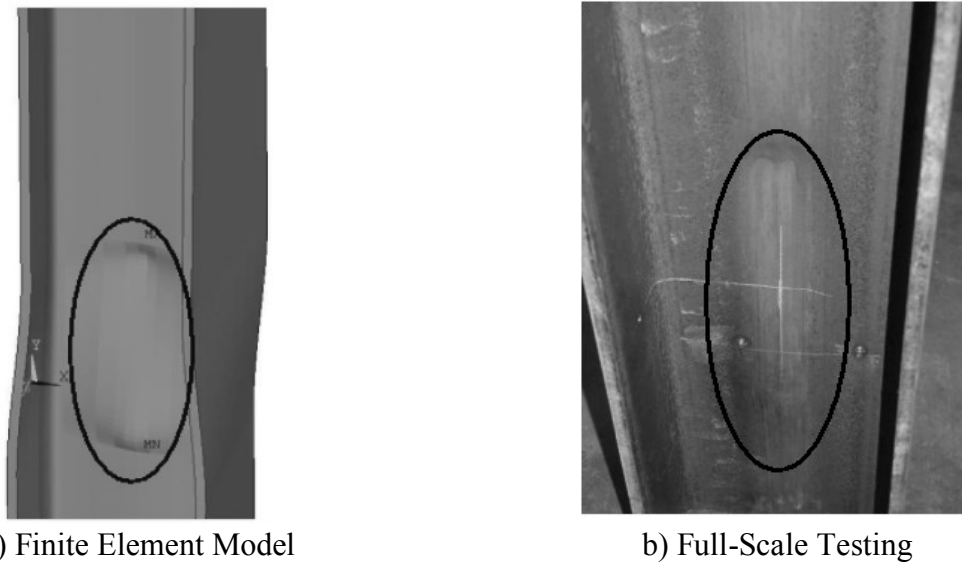


Figure 2.25: Web Mechanism for Three Bolt Connection, Rahman et al. (2007)

Mahamid et al. (2007) continued the work of Rahman et al. (2007) by modelling stiffened extended shear tab connections using finite element analysis. The behaviour of three configurations was modelled and compared to experimental results (Sherman and Ghorbanpoor 2002). The configurations were as follows: i) three bolt beam-to-girder [$a=165$ mm (6.5in)] ii) six bolt beam-to-girder [$a=228$ mm (9in)] and iii) eight bolt beam-to-column [$a=228$ mm (9in)]. An additional five models were created and analysed in the plastic range: i) two bolt beam-to-column ii) 10 bolt beam-to-girder iii) ten bolt beam-to-column iv) 12 bolt beam-to-column and v) two bolt beam-to-girder. The shallower connections (three and five bolt) were seen to fail

primarily in shear yielding, bearing and bolt shear with secondary failures of girder web mechanism and out-of-plane twisting of the shear tab. The eight bolt connection failed in bolt shear and bearing. Use of the model accurately predicted these failure modes as well as locations of plastic strain, bearing failure, plate twisting, and web punching mechanism.

Computation of the location of the inflection point from the model revealed that deep extended shear tabs behaved similarly to rigid connections. Twisting failure was observed for stiffened beam-to-girder connections and in deep beam-to-column connections. Twisting failure was seen in both testing and the modelled behaviour for the eight bolt configuration. In testing, this was followed by buckling at the bottom edge of the shear tab. This was not accounted for in the finite element model. Plasticity was seen in the supporting girder at the lower tip of the shear tab. Stresses exceeded the yield stress of the girder material and significant plastic deformation occurred (Figure 2.26).

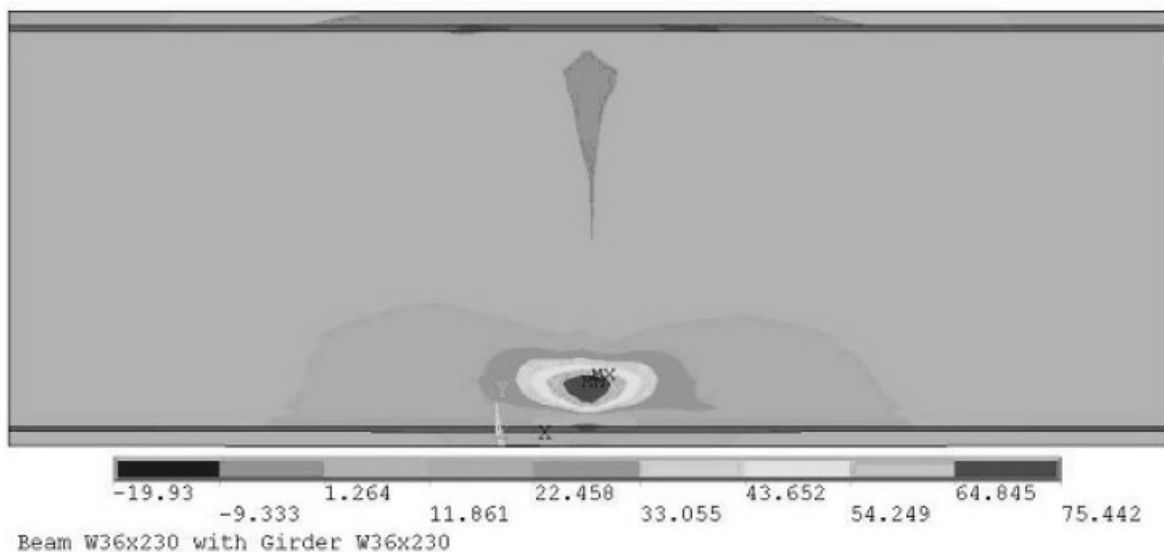


Figure 2.26: Modelled Web Failure for 10 Bolt Beam-to-Girder Connection, Mahamid et al. (2007)

Comparison with results from the stiffened finite element model (Rahman et al. 2007) shows the vulnerability of unstiffened plate connections to twisting failure and consequentially: lowered capacity. For this reason, Mahamid et al. (2007) decided that stiffened connections were preferred. The failure modes encountered in testing [Sherman and Ghorbanpoor (2002)] are in

agreement with those predicted by the model as well as the location of plastic strain, bearing failure, web deterioration and twisting.

Koduru and Driver (2013) developed and validated a component based mechanical shear tab model. A component based model was preferred to finite element modelling due to difficulty in accounting for the contact between bolts and the plate or beam web. A component based model was also preferred when modelling an entire structure due to the finite element modelling of individual connections being computationally demanding.

This model accounted for the interaction between shear, axial and flexural demands. The connection was broken into parts with individual force versus deformation responses. When combined, the global connection behaviour was accurately modelled. The shear tab was represented by a group of parallel springs. Each of these springs was comprised of several springs representing weld deformation, plate yielding, bolt shear, plate fracture and edge tear-out due to bolt bearing (Figure 2.27). The monotonic load deformation responses for all of these components were derived from previous studies.

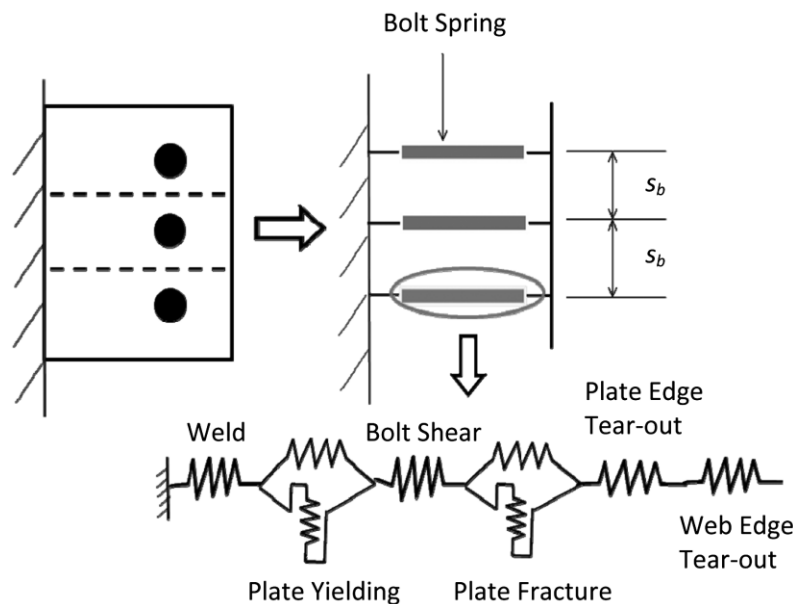


Figure 2.27: Component-Based Model of Shear Tab Connection, Koduru and Driver (2013)

This model was intended for use with both monotonic and cyclic loading. The model was compared with numerous test findings including that of Astanteh et al. (1989). Specifically two 9.5mm (3/8in) thick tabs with “a” distances of 78mm (3in) and plate depths of 229mm (9in) and

362mm (14 1/4in) were modelled and compared with the results from testing. The model predicted failure shear loads of 368kN and 534kN compared with the test values of 418kN and 578kN, respectively.

2.2.3. Design Aids

Young and Disque (1981) developed a guide to assist in the design of shear tab connections based on findings from previous research. The design method is as follows:

- The eccentricity of the inflection point from the column face, e , is computed as: $e(S)^{0.4}/S^{0.4}$. The eccentricity coefficient, $e(S)^{0.4}$ is tabulated as a function of beam shear span ratio, L/d , the number of bolts per vertical row and bolt diameter. $S^{0.4}$ is tabulated for various W shapes and is based upon member cross section.
- Using this eccentricity, the moment at the bolt line and support face can be calculated and used to calculate stresses in the plate.

For convenience, a list of pre-designed shear tab connections is included in the design guide as an Appendix. Minimum values for plate thickness are tabulated for various typical bolt patterns and standard steel grades. The tables are variable in number of bolts (2 to 10) and weld size. Note, the design aid produced by Young and Disque (1981) is only applicable for connections composed of a single vertical row of bolts at typical distances from the support face.

Muir and Hewitt (2009) established a comprehensive design guide for unstiffened extended shear tab connections. This guide summarizes the AISC (2005) extended shear tab design method. Muir and Hewitt (2009) recommended that the design equation to check the interaction between shear and flexural yielding (Design Check 4) be replaced by a less cumbersome equation:

$$\left(\frac{f_v}{\phi 0.6 F_y}\right)^2 + \left(\frac{f_a}{\phi F_y}\right)^2 \leq 1.0 \quad (2.9)$$

where ϕ is the resistance factor (taken as 0.9), F_y is the yield stress, f_v is the shear stress, and f_a is the flexural stress. This equation was included in the 14th Edition AISC Manual (2010). Details for both the 13th and 14th Edition AISC Manual equations are found in Section 3.4.5 of this thesis

Muir and Hewitt (2009) confirmed the requirement for weld sizing of $5/8 t$, where t is the plate thickness, through a derivation based on the interaction between shear and flexural stresses in the weld. The minimum weld size such that the plate yields before the weld fractures is given by:

$$w \geq \frac{t_p F_y \sqrt{3}}{2 F_{EXX}} \quad (2.10)$$

where t_p is the plate thickness and F_{EXX} is the electrode strength. For ASTM A572 Grade 50 (345MPa) steel with E70 (490MPa) electrodes, Equation 2.9 simplifies to:

$$w \geq 0.619 t_p \cong \frac{5}{8} t_p \quad (2.11)$$

2.3. Design Handbooks

In Canada, conventional shear tab connections can quickly be selected from Table 3-41 of the CISC Manual (2010). The tabulated connections have been designed in accordance with the design method proposed by Astanteh et al. (1989). In the United States, both conventional and extended shear tabs can be designed in accordance with Part 10, “single plate connections”, from the AISC Manual (2010).

Canadian industry practice for the design of extended shear tab connections uses a combined design method: based on the AISC (2010) method with design equations from the CISC Handbook (2010) and CSA S16-09 (2009) substituted where applicable. The AISC method addresses both extended and conventional configurations, whereas the CISC method is applicable only for conventional shear tab connections.

The CISC (2010) method for conventional shear tabs and the AISC (2010) methods for conventional and extended shear tabs will be described in this section. A detailed description of the combined design method can be found in Section 3.3 of this thesis.

2.3.1. Canada

Table 3-41 of the CISC Handbook (2010) provides connection capacities for typical conventional shear tab connections. All configurations listed use an 89mm (3.5in) “a” distance with the number of bolts varying between two and seven. Support conditions can be either flexible or rigid and typical A325 bolts are to be used. The bolts are sized under the assumption that the bolt threads are intercepted by the shear plane. This table was formulated with the following design method [established by Astanteh et al. (1989)].

Step 1: Bolt shear

Calculate the bolt shear resistance using the effective bolt eccentricity and the single shear strength of an individual bolt (with threads included in the shear plane).

The effective bolt eccentricity is calculated using one of the following equations:

Rigid:
$$e_b = |2.5(n - 1) - a| \quad (cm) \quad (2.12)$$

$$\text{Flexible: } e_b = \max_a \left| 2.5(n-1) - a \right| \quad (cm) \quad (2.13)$$

Step 2: Shear Yielding

Calculate the plate thickness to ensure adequate shear resistance.

Step 3: Weld Fracture

Size the weld to develop the plate in shear. The values in the table are formulated using $\frac{3}{4}$ of the plate thickness, which was concluded as adequate by Astanek et al. (1989).

Requirements

- Tab thickness is to be greater than 6mm and no more than the bolt diameter plus 2mm to ensure ductile plate behaviour.
- Edge distances should not be less than 38 mm.
- Welds should be proportioned to $\frac{3}{4}$ of the shear tab thickness in order for the plate to reach full capacity. Note that the AISC Manual (2010) gives this ratio to be $\frac{5}{8}$, which is currently the accepted value in practice.

2.3.2. USA

Part 10 of the 14th Edition AISC Manual (2010) includes detailed provisions for the design of shear tab connections (referred to as “single plate connections”). Two methods are provided: i) conventional shear tab connections [with an “a” distance less than or equal to 89mm (3.5in)] and ii) extended shear tab connections. For both of these methods, fillet welds are to be sized at $\frac{5}{8}$ of the plate thickness.

i) Conventional Shear Tab Configurations

The conventional method requires only the limit states of bolt shear, bearing and plate shear rupture to be checked. Bolt shear and bearing are checked at an eccentricity, e , which is chosen based on the number of bolts and the type of bolt holes (short slotted or standard). Only a single vertical row of two to 12 bolts is permitted.

ii) Extended Shear Tab Configurations

The extended configuration method is applicable for larger than typical “a” distances and for multiple vertical rows of bolts. The steps are as follows:

- Design the bolt group for the limit states of bearing and bolt shear accounting for the eccentricity of the bolt group centroid to the weld line,
- Determine the maximum plate thickness such that the moment strength of the plate does not exceed that of the bolt group,
- Check the limit states of shear yielding, rupture and block rupture,
- Check the limit state of combined shear and flexural failure,
- Check the limit state of plate buckling of the shear tab over the unsupported length,
- Ensure the supported beam is laterally braced.

This procedure differs slightly from the 13th Edition Manual (2005) for the limit state of combined shear and flexural failure. Muir and Hewitt (2009) established a less cumbersome design equation which was implemented in the 14th Edition AISC Manual (2010) (See Section 2.2.3 of this thesis).

2.4. Summary

The behaviour of conventional shear tab connections is well understood. Early work by Lipson (1968) showed that conventional shear tab connections possessed enough rotational ductility to be classified as simply-supported connections. Richard et al. (1980) built upon Lipson's testing by establishing a design procedure concerned with ensuring rotational ductility. Astaneh (1989) conducted a comprehensive testing program on conventional shear tabs and formed the design method seen in "Single-Plate Connections" of the AISC Manual (1993). Shaw and Astaneh (1992) found that the AISC (1993) design method was applicable for beam-to-girder shear tab connections. Creech (2005) proposed modifications to Astaneh et al.'s (1989) design method. The suitability of these modifications was confirmed through 10 full-scale tests in addition to finite element modelling. The modifications were for calculation of the following :

- i) bolt group eccentricity for bolt shear, ii) shear yielding capacity, iii) flexural yielding capacity, iv) the eccentricity used to calculate the bearing and tear out resistance, and v) the weld strength taking into account the combination of shear and moment in the weld.

The effect of increasing the "a" distance from 89mm (3.5in) was first examined by Sherman and Ghorbanpoor (2002). They conducted 31 tests on shear tabs with single vertical rows of bolts and "a" distances greater than 89mm (3.5in). Plate buckling was proposed as a limit state unique to shear tab connections with large eccentricities. A design equation was proposed addressing the observed distortion of the column web was seen in unstiffened beam-to-column web connections. It was found that extending the shear tab to the bottom girder flange in beam-to-girder connections changed the governing failure mode to plate buckling of the shear tab segment spanning the girder flanges. Goodrich (2005) observed that this buckling failure mode was also applicable to stiffened beam-to-column web connections where the bottom portion of the shear tab was extended towards the bottom flange of the beam.

Increasing the number of vertical rows of bolts from one to two in connections with coped beams was explored by Ricles (1980). It was found that block shear failure of the beam itself was under predicted by the AISC Manual (1978), and thus was updated in the next edition. Marosi (2011) proposed and validated a more accurate design method for deep shear tab connections with multiple vertical rows of bolts based on the AISC Manual (2010) procedure.

D'Aronco (2014) confirmed that Marosi's design approach was accurate when extended to connections with three vertical rows of bolts for both flexible and rigid beam-to-column connections.

Baldwin Metzger (2006) conducted tests on extended shear tab connections with: i) "a" distances exceeding 89mm (3.5in) and ii) more than a single vertical row of bolts. This study investigated beam-to-column connections and it was concluded that the reduction factors (0.75 for the bolt threads intercepting the shear plane and 0.80 for uncertainty of the bolt group behaviour) for bolt shear strength were overly conservative.

Liu and Astaneh (2000) explored the feasibility of using shear tab connections as part of a building's lateral force resisting system. Full-scale cyclic testing revealed that bare-steel (without a slab present) shear tab connections possessed approximately 20% of the plastic moment capacity of the bare beam cross section. In the presence of a slab, the flexural capacity of the shear tab connection increased to nearly 50% of that of the bare beam cross section. This further increased to 80% when a supplementary seat angle was bolted to the bottom flange of the beam and to the flange of the column.

The behaviour of extended beam-to-girder connections with multiple vertical rows of bolts has not yet been explored to date. Also, the effect of including stiffeners on the side of the girder opposite the shear tab has not yet been examined. Baldwin Metzger's (2006) tests resulted in weld rupture as the primary failure mode and this was most likely due to sizing of welds at $\frac{1}{2}$ the plate thickness. The accuracy of the design method in predicting failures when the weld is sized at $\frac{5}{8}$ of the plate thickness is yet to be addressed for beam-to-column connections with "a" distances exceeding 89mm (3.5in) and with multiple vertical rows of bolts. This is true both for full-scale testing and numerical finite element studies.

Chapter 3 – Testing Program

3.1 Overview

This chapter describes the 12 connection configurations that were tested as part of this thesis, the method used in their design, the testing setup and the testing procedure. Four beam-to-column and eight beam-to-girder extended shear tab connections were designed and tested in the Jamieson Structures Laboratory at McGill University.

The rationale as to why the given configurations were chosen is explained: the key parameters being the plate thickness, “a” distance (distance between the support face and the first vertical row of bolts), number of vertical rows of bolts, number of bolts in each row, bolt size and the girder rigidity (for beam-to-girder only). The design method, which uses a combination of the approaches found in CSA S16-09 (2009), the CISC Handbook (2010), and the AISC Manual (2010), is discussed in detail. Design calculations for the 12 test configurations can be found in Appendix B. The same test setup that was designed by Marosi (2011) was used for the four beam-to-column connections. In order to test the beam-to-girder connections, a new reaction frame and a girder segment were designed.

3.2 Test Specimens

Twelve shear tab connection configurations were first selected in collaboration with our industry research partners, and then designed and tested as part of this research program (Table 3.1). All 12 configurations had “a” distances exceeding 89mm (3.5in) [with a maximum “a” distance of 203mm (8in) for beam-to-column and 241mm (9.5in) for beam-to-girder] and thus were considered “extended” by Part 10 of the AISC (2010) Manual. All shear tabs were fabricated from ASTM A572 Grade 50 (345MPa) plates with a thickness of 9.5mm (3/8in). The supported beams, supporting beams and supporting girders were fabricated from ASTM A992 Grade 50 (345MPa) steel.

The presence of a concrete slab attached to the upper flange of the beam and girder was not accounted for in any of the tests. Shear tab connections may be utilized in industrial buildings where steel grating is often used instead of slabs. The test setup was designed to emulate a situation where the steel grating is not capable of providing significant rotational

stiffness or grating is placed directly on the supporting girder. Therefore, rotational restraint was not provided in testing other than at the girder ends. The test setup for the beam-to-girder configurations provided fixity at the ends of the supporting girder, allowing out-of-plane bending of the girder along its length.

The beam-to-column tests were all considered to have rigid support. Configurations 1, 2 and 3 used small beams (W310x74) with 229mm (9in) deep shear tabs (Figure 3.1). Configurations 1 and 2 both used two vertical rows of three bolts with “a” distances of 152mm (6in) and 203mm (8in), respectively. Configuration 3 was included to simulate the situation in which the shear tab cannot be bolted to the beam on site due to misalignment of bolt holes. In this case the shear tab would have to be site welded to the beam. This configuration had identical parameters as configuration 1 but with a partial “C” weld replacing the bolts. Configuration 4 used a deep beam (W610x140) with a 457mm (18in) deep shear tab. A 152mm (6in) “a” distance (similar to Configurations 1 and 3) and two vertical rows of six bolts were specified for this configuration. A W360x196 column was chosen for all beam-to-column configurations. The shallow shear tabs (Configurations 1 and 2) were bolted with 19mm (3/4in) diameter A325 bolts. The bolt threads were intersected by the shear plane for these configurations. The deep shear tab (Configuration 4) used 22mm (7/8in) diameter A325 bolts. The bolt threads were excluded from the shear plane for Configuration 4.

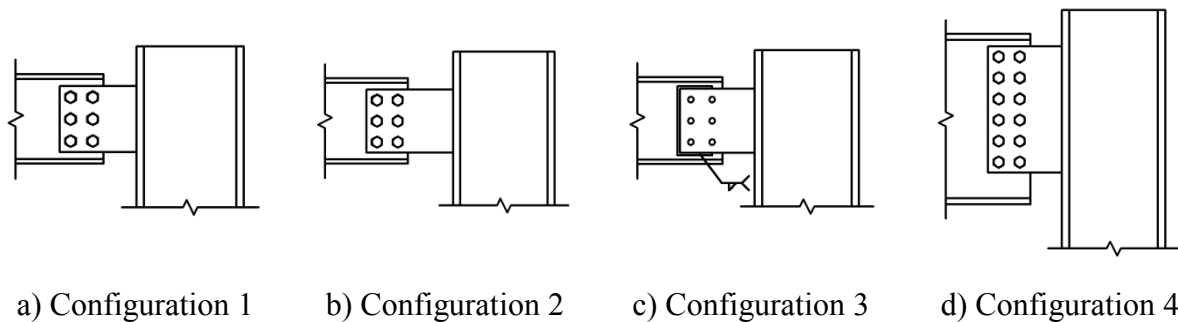


Figure 3.1: Beam-to-Column Extended Shear Tab Configurations

Flexible support conditions were assumed for the entirety of the beam-to-girder connections due to the shear tab being located on one side of the supporting girder. Configurations 5 through 10 used small beams (W310x60) with 229mm (9in) deep shear tabs. Configurations 11 and 12 used deep beams (W610x140 and W690x125) with 457mm (18in) and 533mm (21in) shear tabs, respectively. Both full-height shear tabs (welded to the girder web and

flanges) and partial-height shear tabs (welded to part of the girder web and only the top flange) were tested. For partial-height shear tabs, the effect of including a stiffener on the opposite side of the girder was examined. Figure 3.2 illustrates full-height, partial-height and partial-height with stiffener shear tab configurations. Configurations 5, 11 and 12 used full-height shear tabs. Configurations 6 and 9 used partial-height shear tabs and configurations 7 and 10 were identical to 6 and 9 but had stiffeners opposite the shear tab. Configurations 5 through 8 used a W610x125 supporting girder versus a W760x257 for 9 through 12 to examine the effects of increasing girder size.

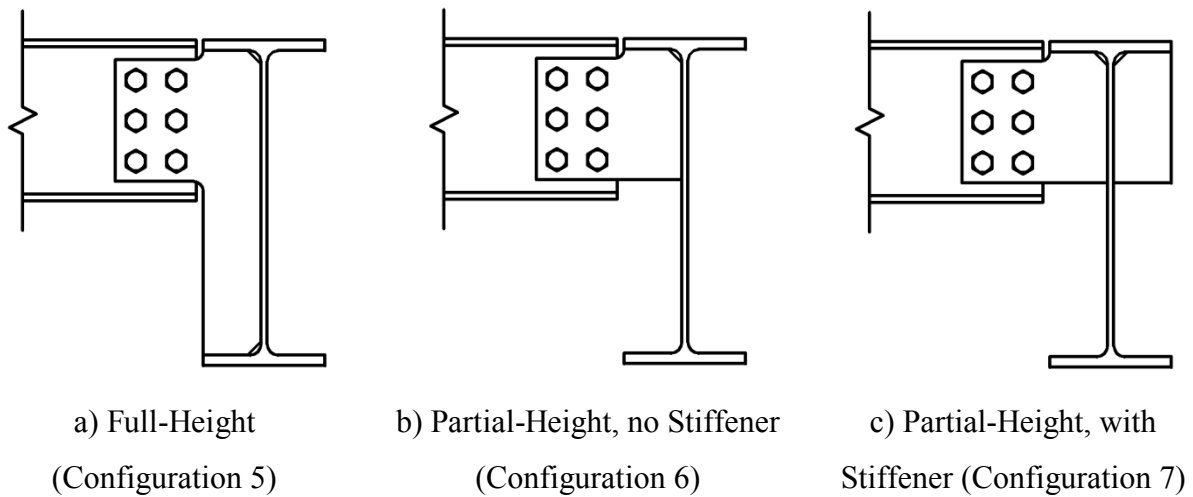


Figure 3.2: Full Height vs. Partial Height Shear Tabs

Configuration 8 featured two side plates to connect the beam to a stiffener located inside the girder. One vertical row of three bolts in both the beam and stiffener was used. Side plate connections are very efficient in terms of construction and this configuration was included to assess their behaviour. The installation method consists of lowering the beam into position and then bolting the side plates to the beam web and stiffener. Figure 3.3 illustrates the installation method for side plate connections.

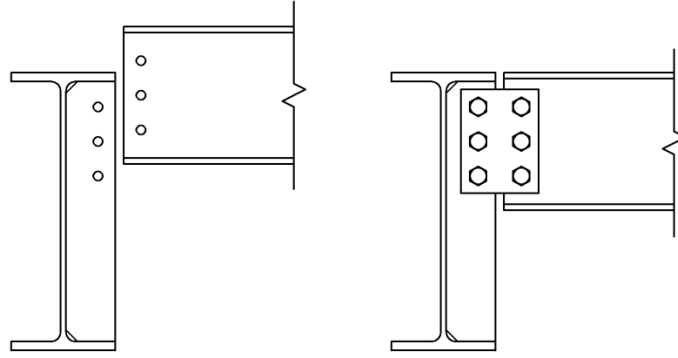


Figure 3.3: Installation Method for Side Plate Connections (Configuration 8)

Similar to the beam-to-column tests, the small beams (5 through 10) were bolted with 19mm (3/4in) diameter A325 bolts. The bolt threads were intercepted by the shear plane for Configurations 5, 6, 7, 9 and 10. Configurations 11 and 12 featured 22mm (7/8in) and 25mm (1in) diameter A325 bolts, respectively. A summary of the test configurations can be seen in Table 3.1. The number of bolts is expressed in “number of vertical rows” x “number of bolts per row”.

All configurations were designed with 9.5mm (3/8in) thick plates. This thickness was chosen to ensure that all configurations would undergo yielding failure and, thus, assess the accuracy of the AISC (2010) extended shear tab design method in predicting this failure type.

Table 3.1: Summary of Test Specimens

Config.	Beam	Column or Girder	"a" Distance (mm)	Number of Bolts	Bolt Size (mm)	Comments
Beam-to-Column						
1	W310x74	W360x196	152	2 x 3	19	-
2	W310x74	W360x196	203	2 x 3	19	-
3	W310x74	W360x196	152	-	-	Partial "C" weld
4	W610x140	W360x196	152	2 x 6	22	-
Beam-to-Girder						
5	W310x60	W610x125	165	2 x 3	19	Full height shear tab
6	W310x60	W610x125	165	2 x 3	19	Partial height shear tab
7	W310x60	W610x125	165	2 x 3	19	Partial height with stiffener
8	W310x60	W610x125	171	1 x 3	19	Side plate
9	W310x60	W760x257	241	2 x 3	19	Partial height shear tab
10	W310x60	W760x257	241	2 x 3	19	Partial height with stiffener
11	W610x140	W760x257	241	2 x 6	22	Full height shear tab
12	W690x125	W760x257	241	3 x 7	25	Full height shear tab

3.3 Design Method

The shear tab connections were designed primarily using the procedure “Single-Plate Connections” (Part 10) from the 14th Edition AISC (2010) Manual. However, for the limit states of block shear, bolt shear and bolt bearing, design equations from the Canadian Standards Association (CSA) S16-09: Design of Steel Structures (2009) Standard were substituted. Detailed design calculations for all 12 test configurations are provided in “Appendix A: Design Calculations”. The supported beams and supporting girders were designed in accordance with CSA S16-09 (2009). The supporting girders were designed to resist the connection shear and torsion due to the connection shear at the eccentricity of the “a” distance in accordance with AISC Design Guide 9: Torsional Analysis of Structural Steel Members (2003).

Factored connection resistances were calculated using the applicable resistance factors and nominal material properties. Predicted connection resistances were calculated by omitting the resistance factors and assuming a yield stress of 110% of the nominal yield stress for the W-sections and plate elements as specified in Clause 27.1.7 of CSA S16-09 (2009). These predictions were revised with measured material properties once coupon tests had been conducted (see Chapter 4). In the calculation of connection resistance the tensile stress of the welds and bolts was not increased from the nominal values due to the potential variability of the material properties and the possible brittle nature of fracture.

3.3.1. Definition of Extended Shear Tab Connections

Part 10 of the 14th Edition AISC (2010) Manual, entitled “Single-Plate Connections”, defines a “conventional” configuration as a shear tab connection meeting the following criteria:

1. Those with a single vertical row of between two and 12 bolts.
2. Those with an “a” distance less than or equal to 89mm (3.5in).
3. Those with standard or short-slotted holes perpendicular to the direction of shear.
4. Those with vertical edge distances meeting the requirements of Table J3.4 (AISC 2010) and with horizontal edge distances must meeting or exceeding twice the bolt diameter.
5. Those with the beam web thickness and plate thicknesses not exceeding those found in Table 10-9 (AISC 2010).

Alternatively, an extended configuration is defined as those not meeting the requirements for a conventional configuration. All shear tab connections tested were of extended configuration due to having more than one vertical row of bolts and having “a” distances exceeding 89 mm (3.5in).

The following design checks are required for extended configurations. Where possible, the design checks were substituted by applicable CSA S16-09 (2009) design equations.

3.3.2. Design Check 1: Bolt Shear and Bolt Bearing

The bolt group is checked for the limit states of bolt bearing and bolt shear. Bolt group shear resistance and plate bearing resistance is checked in accordance with CSA S16-09 (2009). The Instantaneous Centre of Rotation (ICR) method was used to account for eccentricity of loading as detailed in Part 3, “Eccentric Loads on Bolt Groups”, of the CISC Handbook (2010).

The ICR method is suitable for bearing type connections where the line of action of the applied force does not coincide with the centroid of the bolt group. The ICR is located such that the moment created by the bolt forces balance the moment generated by the applied loading. Bolts furthest from the ICR are assumed to reach failure first. The line of action of a bolt's force is assumed to be located perpendicular to the chord between bolt centres and the ICR. Tables 3-14 through 3-20 of the CISC Handbook of Steel Construction (CISC 2010) provide tabulated values of the unitless coefficient, C , which accounts for the reduction in bolt shear and bearing capacity of the entire bolt group. The shear resistance of an individual bolt is multiplied by this coefficient in order to compute the capacity of the bolt group. The tables are based on the number of vertical rows of bolts, column pitch, row pitch, number of rows and the moment arm to the reaction support.

Clause 13.12.1.2 of CSA S16-09 (2009) was used to compute the resistance per individual bolt for shear and bearing. The number of bolts, n , has been left out of these equations to give values per bolt. The factored resistance is taken as the lesser of the:

$$\text{Bearing resistance of plate, } B_r = 3\phi_{br}tdF_uC \quad (3.1)$$

$$\text{Shear resistance of the bolt group, } V_r = 0.60\phi_bmA_bF_uC \quad (3.2)$$

where t is the thickness of the base metal (the lesser of the plate thickness and the beam web thickness), d is the bolt diameter, F_u is the tensile stress of the least thick section (plate or beam), m is the number of shear planes (1 for single plate shear tabs) and A_b is the area of an individual bolt. The resistance factor for bearing and bolt shear, ϕ_{br} and ϕ_b , are taken both as 0.8. Note, for cases where the bolt threads are intercepted by the shear plane, only 70% of the bolt group shear resistance can be taken.

Configuration 3 was designed with a partial “C” weld instead of bolts. The weld was designed such that the factored resistance of the weld group matched that of the bolt group used for the corresponding bolted connection (Configuration 1). The ICR method was used for this reason as it is also applicable to weld groups. In this case, the moment resistance is provided by finite weld elements as opposed to that of finite bolts [CISC Handbook (2010) Part 3, “Eccentric Loads on Weld Groups”]. Tables 3-26 through 3-33 (CISC 2010) provide tabulated values of C for different weld configurations. This C is used differently than for bolts. The resistance of the weld group is given by:

$$V_r = CDL \quad (3.3)$$

where C is the weld ICR coefficient, D is the weld throat size, and L is the characteristic length of the weld group in the direction of loading.

The tabulated values are calculated based on the following assumptions:

- Electrode tensile stress, $X_u = 490\text{MPa}$
- Base metal tensile stress, $F_u = 450\text{MPa}$
- Resistance factor for weld, $\phi_w = 0.67$

The electrode and base metal tensile stress are applicable for the materials used in this testing. The resistance factor, however, is not used when calculating predicted resistance. Thus, ϕ_w was left out when computing the predicted resistance of the partial “C” weld group.

3.3.3. Design Check 2: Plate Ductility

The plate thickness is checked to ensure that the flexural resistance of the plate does not exceed that of the bolt group. The maximum plate thickness is given by Equation 10-3 (AISC 2010) as:

$$t_{max} = \frac{6M_{max}}{F_y d^2} \quad (3.4)$$

where F_y is the yield stress of the plate and d is the depth of the plate. M_{max} is the moment capacity of the bolt group, which is given by Equation 10-4 (AISC 2010) as:

$$M_{max} = \frac{F_v}{0.90} (A_b C') \quad (3.5)$$

where F_v is the shear stress of an individual bolt, as found in Table J3.2 of the AISC Manual (2010). The shear stress, F_v , is taken as 414MPa (60ksi) for A325 bolts with threads excluded from the shear plane and 330MPa (48ksi) when the threads are not excluded, A_b is the area of an individual bolt, and C' is a factor to account for eccentric loading as defined in Part 7 of the AISC Manual (2010). This is done in a similar manner as the CISC Handbook (2010) (see Design Check 1), except that C' is for pure moment (the ICR is at the centroid of the bolt group). Tables 7-8 and 7-11 of the AISC Manual (2010) tabulate values of C' for 76mm (3in) column pitch with perpendicular applied loading (load at an angle 90° to the beam span).

3.3.4. Design Check 3: Shear Yielding, Rupture, Block Rupture

The shear tab is checked for the limit states of shear yielding, shear rupture, and block rupture. Section J4 of the AISC Manual (2010) is used to compute the resistance of connecting elements such as plates. Equation J4-3 gives the shear yielding resistance of such an element as:

$$\phi R_n = \phi 0.60 F_y A_g \quad (3.6)$$

where ϕ is the resistance factor for yielding (given as 1.0 in the AISC Manual (2010)) but will be taken as 0.9 to conform to CSA S16-09 (2009), F_y is the yield stress of the plate, and A_g is the gross plate area.

The shear rupture resistance of an element is given by Equation J4-4 (AISC 2010) as:

$$\phi R_n = \phi 0.60 F_u A_{nv} \quad (3.7)$$

where ϕ is the resistance factor for ultimate resistance of the section (given as 0.75), F_u is the ultimate stress of the plate material, and A_{nv} is the net plate area. The net area is taken at the bolt column.

The CSA S16-09 (2009) provisions (see Clause 13.11) define the factored resistance for a block shear failure in a plate connection as:

$$V_r = \phi_u \left[U_t A_n F_u + 0.6 A_{gv} \frac{(F_y + F_u)}{2} \right] \quad (3.8)$$

where ϕ_u is the ultimate resistance factor (taken as 0.75 as defined in Clause 13.1), U_t is an efficiency factor which varies based on connection type (0.3 for coped beams with two vertical rows of bolts), A_n is the net area of the plate in tension, F_u is the ultimate stress of the plate, A_{gv} is the gross plate area in shear and F_y is the yield stress of the plate.

For Configuration 12, which featured three vertical rows of bolts, no tabulated efficiency factor, U_t , was applicable. In this case, the AISC Manual (2010) was used. Equation J4-5 (AISC 2010) defines the block shear resistance as:

$$\phi R_n = \phi \left[\min(0.6 F_u A_{nv}, 0.6 F_y A_{gv}) + U_{bs} F_u A_{nt} \right] \quad (3.9)$$

where ϕ is the resistance factor (taken as 0.75), F_u is the tensile stress, A_{nv} is the net area in shear, F_y is the yield stress, A_{gv} is the gross area in shear, U_{bs} is an efficiency factor related to shear lag (taken as 0.5 for a non-uniform stress distribution), and A_{nt} is the net area in tension.

3.3.5. Design Check 4: Combined Shear and Flexural Yielding

The shear tab is checked for the limit state of combined shear and flexural yielding. This check differs between the 13th and 14th Editions of the AISC Manual. The 14th Edition (AISC 2010) formulation is based on the interaction between shear and moment. The 13th Edition (AISC 2005) formulation uses a reduction in allowable flexural stress due to applied shear stress (Von-Mises reduction).

The 14th Edition of the AISC Manual (2010) accounts for the combined effects of flexure and shear by Equation 10-5 (AISC 2010):

$$\left(\frac{V_r}{V_c}\right)^2 + \left(\frac{M_r}{M_c}\right)^2 \leq 1.0 \quad (3.10)$$

where V_r and M_r are the applied shear and moment and V_c and M_c are the shear and flexural yielding resistances.

The applied moment, M_r , is given as:

$$M_r = V_r e \quad (3.11)$$

The shear and flexural yielding resistances, V_c and M_c are given as:

$$V_c = \phi_v 0.60 F_y A_g \quad (3.12)$$

and

$$M_c = \phi_b F_y Z_{pl} \quad (3.13)$$

where ϕ_v and ϕ_b are resistance factors for shear and bending (both taken as 0.9 to comply with CSA S16-09 (2009)), F_y is the yield stress of the plate, A_g is the gross plate area in shear and Z_{pl} is the plastic section modulus of the plate.

Rearranging Equation 3.10 in terms of the applied shear, V_r , gives:

$$V_r \leq \frac{1}{\sqrt{\left(\frac{1}{V_c}\right)^2 + \left(\frac{M_r}{M_c V_r}\right)^2}} \quad (3.14)$$

Substituting M_r from Equation 3.11 gives a final expression for the shear resistance:

$$V_r = \frac{1}{\sqrt{\left(\frac{1}{V_c}\right)^2 + \left(\frac{e}{M_c}\right)^2}} \quad (3.15)$$

The 13th Edition of the AISC Manual (2005) addresses the interaction between shear and flexural stresses by computing a critical flexural stress. This critical stress is given as:

$$F_{cr} = \sqrt{F_y^2 - 3f_v^2} \quad (3.16)$$

where F_{cr} is the critical flexural stress, F_y is the plate yield stress and f_v is shear stress due to applied loading, which can be calculated as:

$$f_v = V/A_g \quad (3.17)$$

where V is the applied shear and A_g is the gross cross sectional area of the plate. Substituting Equation 3.17 into Equation 3.16 gives:

$$F_{cr} = \sqrt{F_y^2 - 3(V/A_g)^2} \quad (3.18)$$

The flexural yielding resistance of the plate accounting for the reduction in flexural capacity due to applied shear stress is given by:

$$M_r = \phi F_{cr} Z_{pl} \quad (3.19)$$

where ϕ is the flexural resistance factor (taken as 0.9) and Z_{pl} is the plastic section modulus of the plate.

It is assumed that the support face is the location of zero moment in the beam. This means that the moment can be expressed in terms of the connection shear and the bolt group eccentricity. The flexural yielding resistance can be expressed as:

$$M_r = V_r e \quad (3.20)$$

where V_r is the shear yielding resistance and e is the bolt group eccentricity. Substituting Equation 3.18 and Equation 3.20 into Equation 3.19 gives the shear yielding resistance accounting for Von-Mises reduction as:

$$V_r = \frac{F_y}{\sqrt{\left(\frac{e}{\phi Z_{pl}}\right)^2 + 3\left(\frac{1}{A_g}\right)^2}} \quad (3.21)$$

3.3.6. Design Check 5: Buckling

The shear tab is treated as a doubly coped-beam (one with both top and bottom flanges removed at the beam tip) and checked for the limit state of buckling as specified in Part 9 of the AISC Manual (2010). The flexural buckling resistance of the coped section is given by:

$$M_r = \phi_b F_{cr} S_{net} \quad (3.22)$$

where ϕ_b is the resistance factor for buckling (taken as 0.9), F_{cr} is the available buckling stress, and S_{net} is the net section modulus of the shear tab.

The moment resistance, M_r , is a function of the shear resistance, V_r , and the bolt group eccentricity, e , and can be taken as:

$$M_r = V_r e \quad (3.23)$$

Substituting Equation 3.23 into Equation 3.22 and expressing in terms of shear resistance gives:

$$V_r = \phi_b F_{cr} S_{net} / e \quad (3.24)$$

For a doubly-coped beam, the available buckling stress is calculated in one of two ways. If the ratio of the compression flange cope depth, d_c , to the beam depth, d , is less than or equal to 0.2 ($d_c/d \leq 0.2$) and the length of the coped section, c , is less than twice the beam depth ($c/d \leq 2$), then the Lateral-Torsional Buckling formulation can be used. Otherwise, the Classical Plate Buckling formulation is used.

i) Lateral-Torsional Buckling (f_d equation)

The available buckling stress is given by:

$$F_{cr} = 0.62\pi E \frac{t_w^2}{ch_o} f_d \quad (3.25)$$

where E is the elastic modulus of the plate steel, t_w is the plate thickness, c is the length of the coped section (taken as the “a” distance to be conservative), h_o is the depth of the plate, and f_d is the lateral-torsional buckling factor. This factor is given as:

$$f_d = 3.7 - 7.5 \left(\frac{d_c}{d} \right) \quad (3.26)$$

ii) Classical Plate Buckling (Q Equation)

The conservative value for available buckling stress is given as:

$$F_{cr} = F_y Q \quad (3.27)$$

where F_y is the yield stress of the plate and Q is a factor for the slenderness of the coped section. Q is given as:

$$\begin{aligned} Q &= 1 & \text{for } \lambda &\leq 0.7 \\ Q &= (1.34 - 0.486\lambda) & \text{for } 0.7 < \lambda &\leq 1.41 \\ Q &= (1.30/\lambda^2) & \text{for } \lambda &> 1.41 \end{aligned} \quad (3.28)$$

where the slenderness, λ , is given as:

$$\lambda = \frac{h_o \sqrt{F_y}}{10t_w \sqrt{475 + 280 \left(\frac{h_o}{c} \right)^2}} \quad (3.29)$$

3.3.7. Design of Beams

The beams were proportioned such that their shear and moment resistance exceeded that of the connection being tested. This allowed the structural damage to be concentrated on the shear tab itself rather than the beams. The required factor of safety for the beam shear and bending resistance to the expected shear tab resistance was 2.

The expected yield stress was taken as 110% of the nominal yield stress for the beams. For cases where this would result in an expected yield stress of less than 385MPa, this value was taken as specified in Clause 27.1.7 of CSA S16-09 (2009).

Factored Shear Resistance

The shear resistance of a flexural member is defined in Clause 13.4.1.1 of CSA S16-09 (2009) as:

$$V_r = \phi A_w F_s \quad (3.30)$$

where F_s is the ultimate shear stress, ϕ is the resistance factor (taken as 0.9), and A_w is the shear area (d_w for rolled shapes).

For beams with unstiffened webs, F_s is given as:

$$\begin{aligned} F_s &= 0.66F_y & \text{for} & \quad \frac{h}{w} \leq \frac{1014}{\sqrt{F_y}} \\ F_s &= \frac{670\sqrt{F_y}}{(h/w)} & \text{for} & \quad \frac{1014}{\sqrt{F_y}} < \frac{h}{w} \leq \frac{1435}{\sqrt{F_y}} \\ F_s &= \frac{961\,200}{(h/w)^2} & \text{for} & \quad \frac{h}{w} > \frac{1435}{\sqrt{F_y}} \end{aligned} \quad (3.31)$$

Where h/w is the height to width ratio of the web and F_y is the yield stress of the beam.

Factored Moment Resistance

The factored moment resistance for a Class 1 or 2 member that is laterally supported is given in Clause 13.5 of CSA S16-09 (2009) as:

$$M_r = \phi M_p = \phi Z F_y \quad (3.32)$$

where M_p is the plastic moment capacity, ϕ is the resistance factor (taken as 0.9), Z is the plastic section modulus and F_y is the yield stress. Table 2 of CSA S16-09 (2009) defines the limits for a Class 2 section with no axial load as follows:

$$\begin{aligned} \frac{b}{2t} &\leq \frac{170}{\sqrt{F_y}} \\ \frac{h}{w} &\leq \frac{1700}{\sqrt{F_y}} \end{aligned} \quad (3.33)$$

The maximum unbraced length below which a member will reach its plastic moment capacity, L_u , was obtained for the test configurations. Lateral bracing was provided in the test such that the distance between braces did not exceed L_u .

Bearing Stiffeners

Pairs of stiffeners were provided on both sides of the beam at the location of the compression actuator for all test configurations. This was done to minimize any local bearing deformation of the beam flange and web.

The bearing resistance of the web alone was first checked. CSA S16-09 (2009) defines the factored resistance of beam to crippling and yielding as the lesser of:

$$B_r = \phi_{bi} w (N + 10t) F_y \quad (3.34)$$

$$B_r = 1.45 \phi_{be} w^2 \sqrt{F_y E} \quad (3.35)$$

where ϕ_{bi} is the bearing resistance factor (taken as 0.80), w is the web thickness, N is the length of bearing (taken as the length of the bottom bearing plate used to connect the beam to the actuator), t is the flange thickness, F_y is the beam yield stress, and E is the modulus of elasticity.

The stiffeners were then designed in accordance with Clause 14.4 of CSA S16-09 (2009). This clause specifies that the central strip of the web and the stiffeners themselves are treated as a column and the compressive resistance is calculated using Clause 13.3.

3.3.8. Design of Girders

Girders were designed for the connection shear, moment due to the connection shear and torsion due to the connection moment. The ends of the girders were considered fixed due to the stiffness of the supporting girder reaction frame (see Section 3.4.2).

Section 4.1 of AISC Design Guide 9: Torsional Analysis of Structural Steel Members (2003) provides expressions for shear and axial stresses acting on an I-shaped section due to torsion. The shear and normal stresses due to torsion on a member are given as:

$$\text{Pure torsional shear stress (flange and web):} \quad \tau_t = Gt\theta' \quad (3.36)$$

$$\text{Warping shear stress (flange only):} \quad \tau_{ws} = \frac{-ES_{ws}\theta'''}{t} \quad (3.37)$$

$$\text{Warping normal stress:} \quad \sigma_{ws} = EW_{ns}\theta'' \quad (3.38)$$

where G is the shear modulus, E is the elastic modulus, and t is the flange or web thickness. S_{ws} and W_{ns} are provided for given steel sections in Appendix A (AISC 2003). The first, second and third derivatives of angle of rotation are given by θ' , θ'' , and θ''' . These values are found in Appendix B (AISC 2003), specifically Case 6. This case is for beams fixed at both ends with torsion applied at a point along the beam.

The axial stresses at the top and bottom of the beam cross section due to flexure are taken as:

$$\sigma_b = M_u/S_x \quad (3.39)$$

where M_u is the applied moment and S_x is the elastic section modulus.

The shear stress acting over the cross beam cross section is taken as:

$$\tau_s = \frac{V_u Q}{I_x t} \quad (3.40)$$

where V_u is the applied shear, Q is the first moment of area about the neutral axis, I_x is the moment of inertia and t is the section thickness.

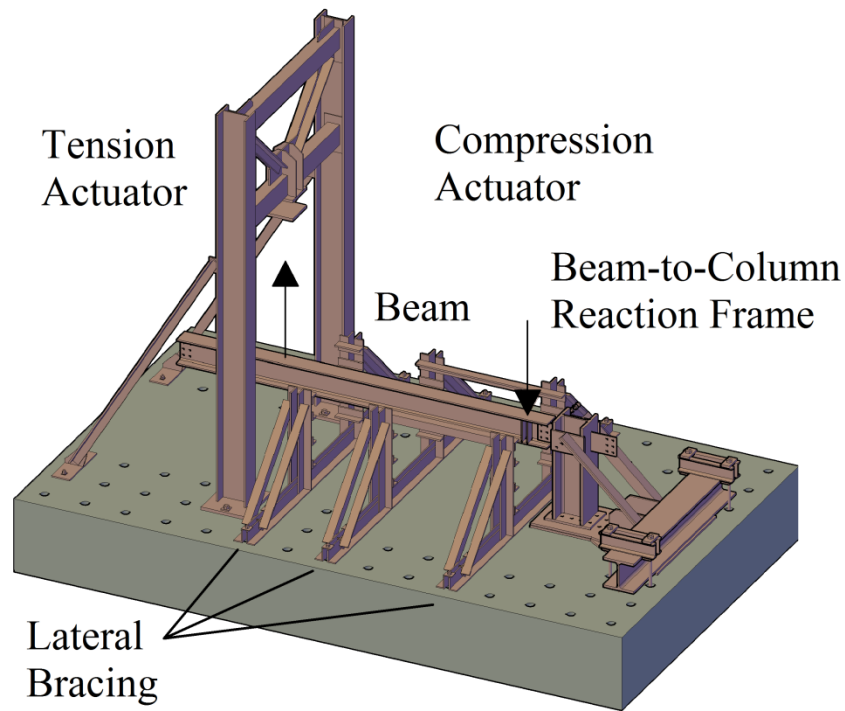
The stresses from torsion were combined with the axial and shear stresses from flexure and the net stresses were compared to the yield stress of the beam material. A factor of safety of 2.0 or more was provided for all beam-to-girder test configurations.

3.4. Testing Setup

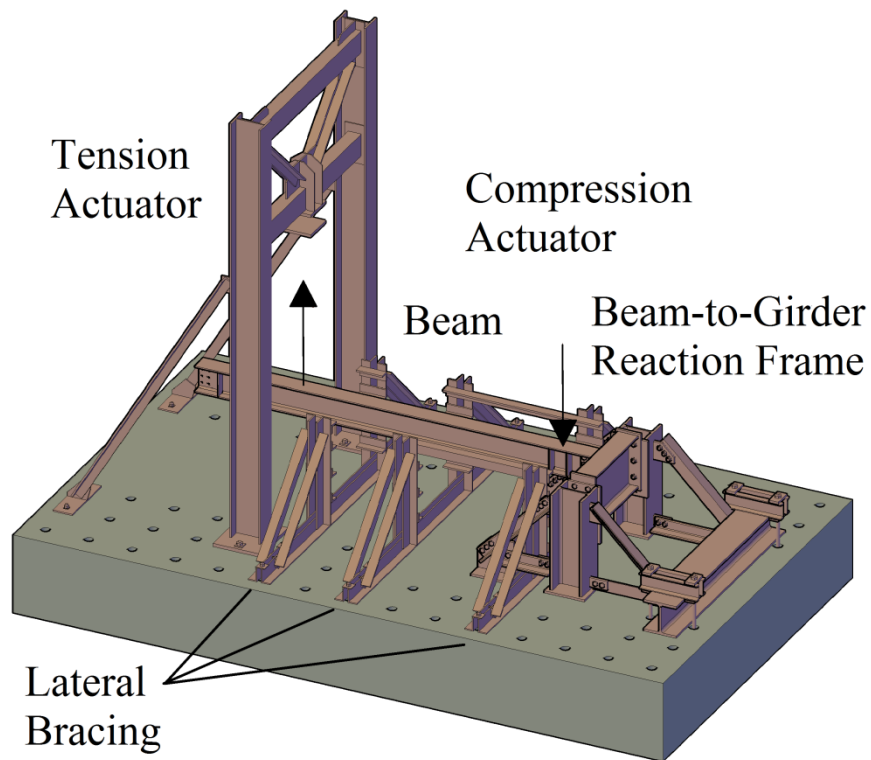
The testing setup (Figures 3.4 to 3.6) consisted of the following major components:

- Test beam
- Beam-to-column reaction frame (or beam-to-girder reaction frame)
- Stub column (or girder segment)
- Compression actuator
- Tension actuator (attached to tension actuator frame)
- Lateral bracing system

This setup was similar to that used by Marosi (2011) and D'Aronco (2014), the only difference being the requirement for a beam-to-girder reaction frame. The beam-to-girder reaction frame was designed and built as part of the testing program discussed in this study.

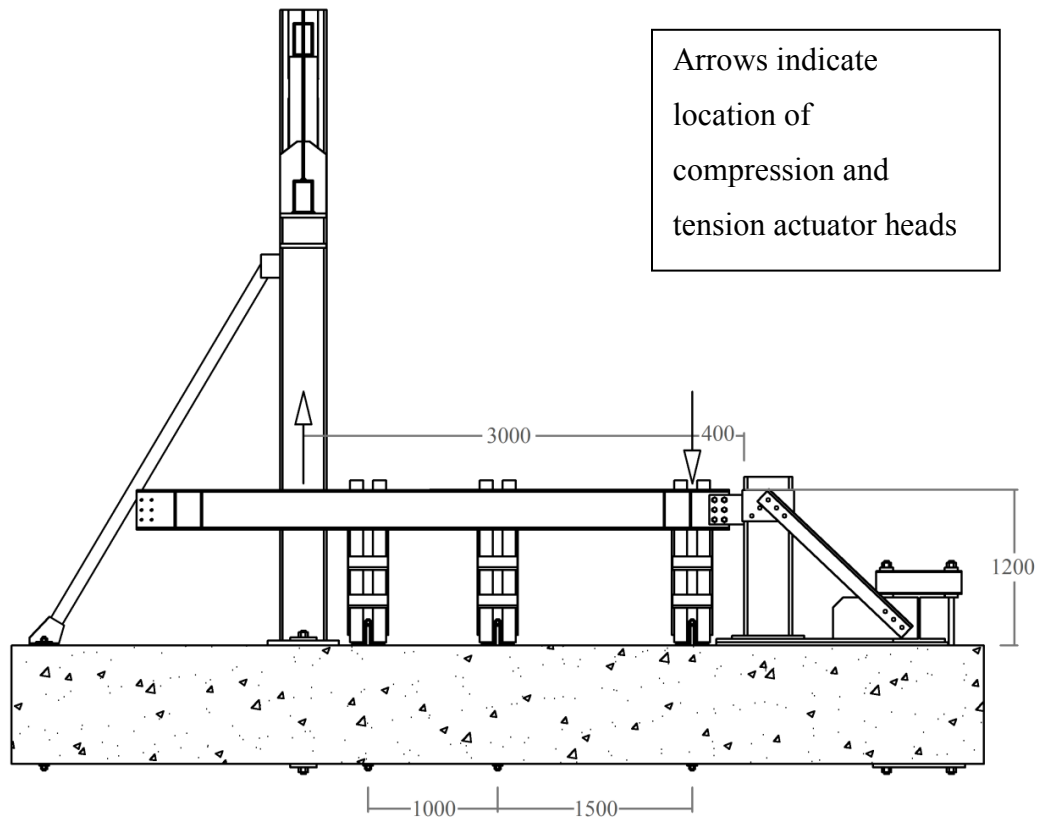


a) Beam-to-Column (Configuration 1)

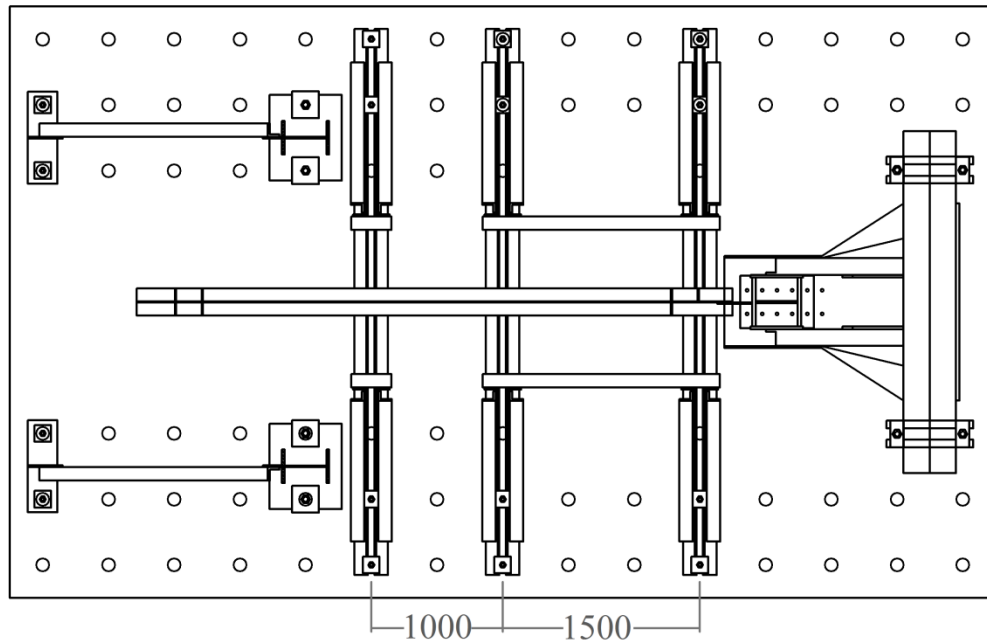


b) Beam-to-Girder (Configuration 5)

Figure 3.4: Renderings of Typical Test Setup (Arrows Indicate Actuator Locations)

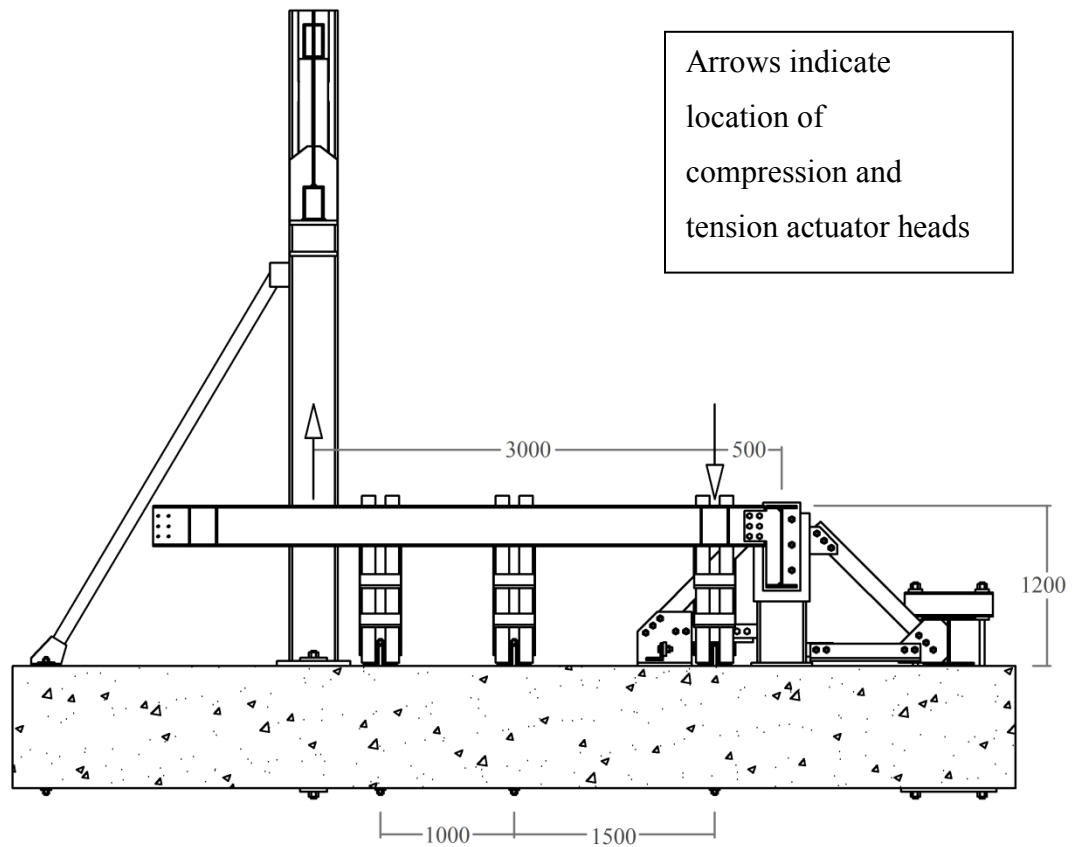


a) Elevation View

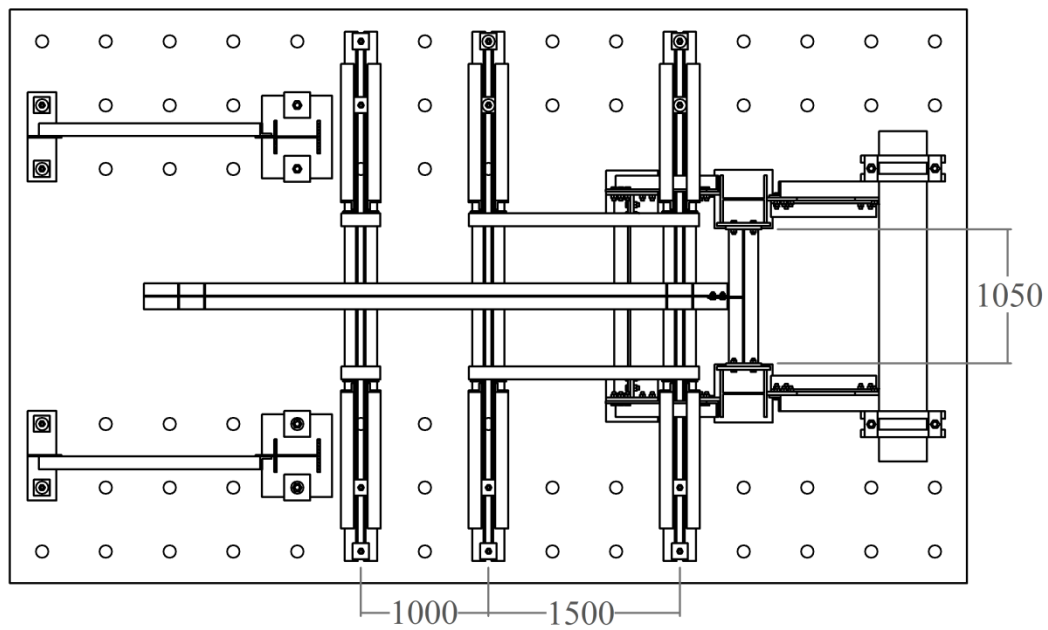


b) Plan View

Figure 3.5: Plan View of the Beam-to-Column Test Setup (Configuration 1 pictured); dimensions in mm



a) Elevation View



b) Plan View

Figure 3.6: Plan View of the Beam-to-Girder Test Setup (Configuration 5 pictured); Dimensions in mm

3.4.1. Test Beams

The test beams were bolted to the shear tab connection at one end and attached to the tension actuator at the other, with the compression actuator located between the two. The beams were laterally braced between the compression and tension actuators (Figure 3.4, 3.5, and 3.6). The tested beams were designed such that, where possible, they could be used for two tests. Since an odd number of test configurations (three) required W310x74 beams, the beam used for Configuration 3 could only be used once. Both ends of the W310x74 beams, W310x60 beams, and W610x140 beam were drilled with holes and fabricated with stiffeners. This allowed the beams to be used for one test, then rotated and used for a second test. The W690x125 beam was only required for one test. Stiffeners were located on each beam underneath the compression actuator to resist web buckling and crippling.

3.4.2. Reaction Frames, Stub Columns, and Girder Segments

The beam-to-column reaction frame and stub column format (Figure 3.7a, Figure 3.8) were designed by Marosi (2011) and used by D'Aronco (2014) and Mirzaei (2014) for testing of shear tab connections. The beam-to-girder reaction frame and girder segment format were designed as part of this study (Figure 3.7b, Figure 3.9).

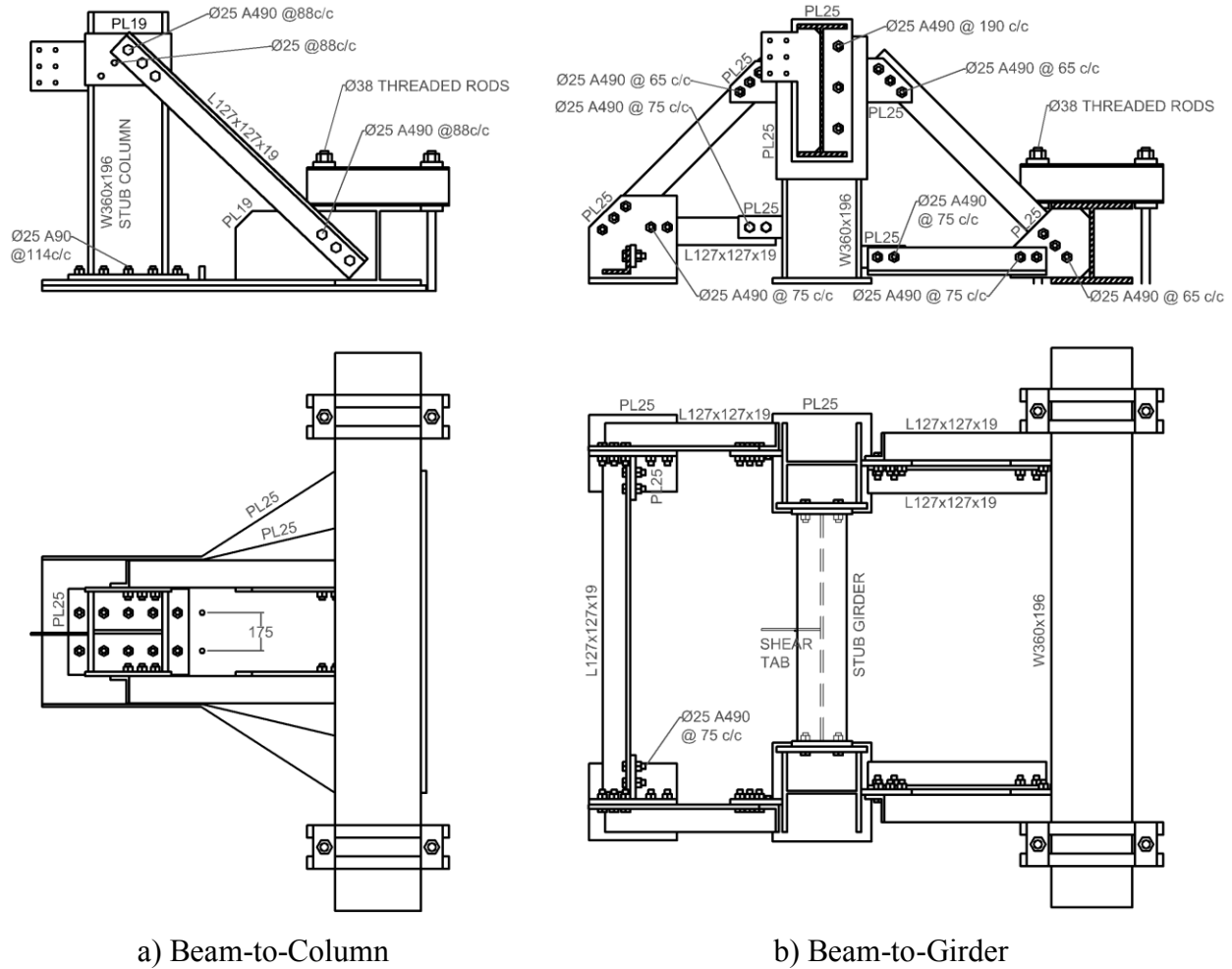


Figure 3.7: Reaction Frame Details, Elevation and Section Views; Dimensions in mm

The beam-to-column reaction frame consisted of two layers of 25mm (1in) thick plates. The lower plate rested on the strong floor. A W360x196 beam was welded to the top of this plate and pre-tensioned to the strong floor at each end. The upper plate was welded to the lower plate and threaded with two rows of 25mm (1in) A325 bolts, which were used to fix the stub column to the reaction frame. Two L127x127x19 inclined members were used to brace the stub columns. These bracing angles were connected to two 25mm (1in) plates, which were welded between the flanges of the W360x196 ground beam.

The 1220mm (48in) tall W360x196 columns were welded to 25mm (1in) base plates to create the stub columns. These base plates were drilled with holes, which lined up with the protruding bolts from the reaction frame. Side plates [25mm (1in)] were welded to the flange tips of the stub columns at the height of the shear tab. Holes were provided in these side plates to

attach the bracing angles. Shear tabs were welded to both flanges of the stub columns such that each stub column could be used for two tests. The column size was chosen such that shear and moment from the connection resulted in only elastic deformation.

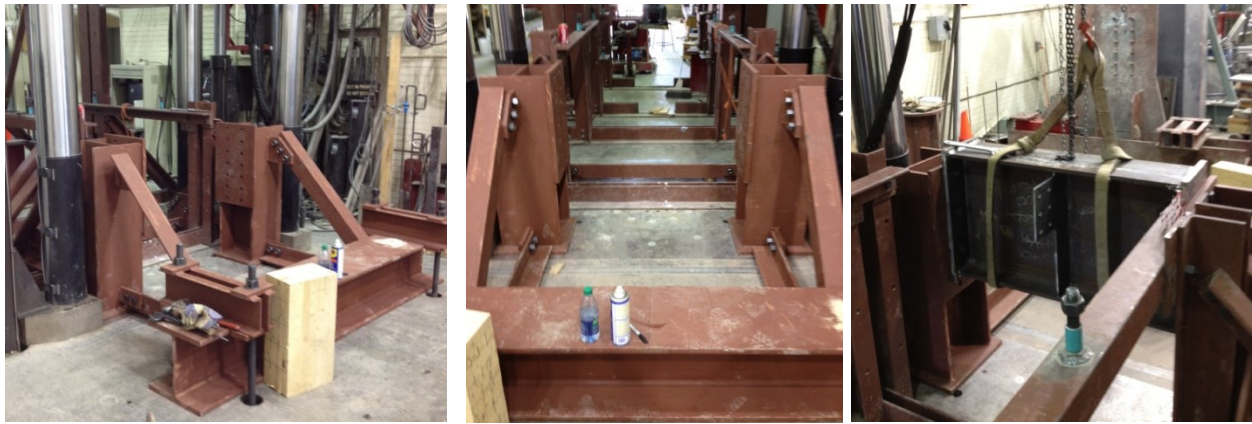


Figure 3.8: Beam-to-Column Reaction Frame with Stub Column Installed

The beam-to-girder reaction frame and girder segments were designed as part of this testing program. Two W360x162 columns at 1525mm (60in) centre-to-centre were used to support the girder. These columns were welded to 25mm (1in) base plates, which sat directly on the strong floor. Side plates [25mm (1in)] were welded to the inside flanges of the columns and were drilled with bolt holes to attach the girder. To minimize deflection and rotation of the top of the columns, bracing was supplied by two pairs of L127x127x19 angles. The rear bracing angles (tension) were connected to a W360x196 ground beam, which was pre-tensioned to the strong floor. The front bracing angles (compression) framed into two base plates which were connected to each other by another L127x127x19 angle. This connecting angle was included such that the base plates would not slide apart from each other due to compression in the bracing angles.

Girder segments [1050mm (41.3in)] were welded on both ends to 25mm (1in) plates. The end plates were drilled with bolt holes for 25mm (1in) A490 bolts which were used to bolt the stub girder to the reaction frame. This connection was required to be slip critical to minimize rotation and thus the bolts were pre-tensioned in the lab. Each girder was only used for one test.

The shear tabs were welded to the girder such that the middle of the supported beam was in line with the middle of the supporting girder.



a) Side View

b) Rear View

c) Front View, Girder Segment

Figure 3.9: Beam-to-Girder Reaction Frame

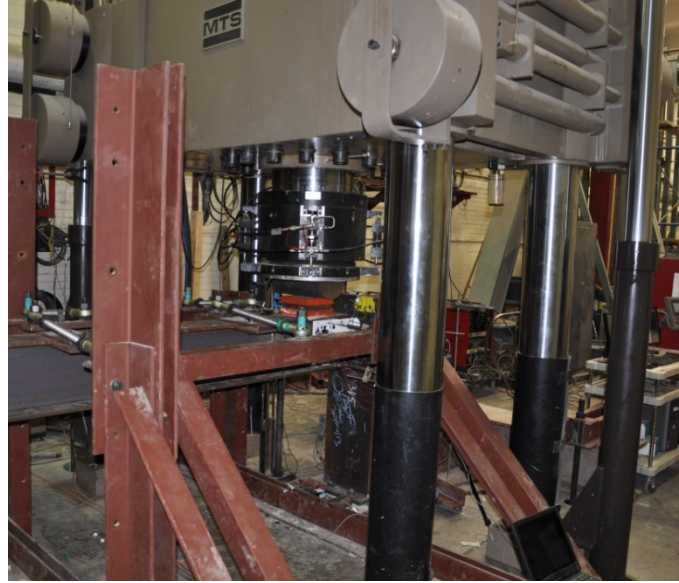
For both the beam-to-column and beam-to-girder test setups, the ground beam was required to be sufficiently anchored to the strong floor such that slippage did not occur. Two sets of two threaded rods were attached to a set of channels located at each end of the ground beam. Each set of channels was fixed with two threaded rods into the strong floor. Threaded rods of 38mm (1.5in) diameter were pre-tensioned to a pressure of 21MPa (3000psi) to the strong floor to meet this requirement.

3.4.3. Compression and Tension Actuators

The compression actuator had a capacity of 12,000kN and was used to apply compression force to the top flange of the beam at the end closest to the connection. This compressive force created shear in the beam which was balanced by the tension actuator at the end opposite the connection. This tension actuator had a capacity of 269kN and was supported by the frame designed by Marosi (2011). This frame was designed to support the 269kN maximum tension load while minimizing vertical deflection. Figures 3.10 and 3.11 illustrate the compression and tension actuators, respectively.



a) Before Test, Actuator Body Retracted



b) During Test, Actuator Crosshead Lowered

Figure 3.10: Compression Actuator



a) Tension Actuator Frame



b) Tension Actuator Head

Figure 3.11: Tension Actuator

3.4.4. Lateral Bracing System

The lateral bracing system, inspired by that of Yarimci et al. (1967), was used to secure the top flange of the supported beam at a maximum spacing of 1500mm (59in). The bottom flange of the beam was also braced at the brace closest to the tension actuator. A pair of threaded rods connected the top flange of the beam to the bracing system using ball joints. This allowed bracing to be maintained while the beam deflected vertically while loading and connection rotation was increased during testing. The bracing frame was anchored to the strong floor using a pair of 25mm (1in) threaded rods. Figure 3.12 illustrates the lateral bracing system securing the top flange of the beam.



Figure 3.12: Lateral Bracing System

3.4.5. Installation of Test Configurations

The installation procedure for each test consisted of the following steps: i) installing the stub column or girder segment into its corresponding reaction frame, ii) moving the supported beam into place, iii) bolting (or welding) the supported beam to the shear tab, iv) attaching the lateral bracing to the top and bottom flanges of the supported beam, v) lowering the tension

actuator head such that it rested on the beam, vi) fastening the bottom plate to the top plate of the actuator head using threaded rods, and vii) placing blocking under the beam end opposite the connection to ensure the supported beam was level in both parallel and transverse planes.

All test configurations except for 3 were bolted. Configuration 3 was required to be welded in the lab. This represented cases in which a weld retrofit needs to be done on a construction site due to bolt hole misalignment. The aforementioned installation procedure was followed except that after installation, a certified welder came to the laboratory and welded the shear tab to the supported beam using a partial “C” shape weld. Figure 3.13 depicts the welding procedure and the finished welded shear tab.



a) Welder, Beam View



b) Welder, Column View



c) Welded Shear Tab

Figure 3.13: Welding Procedure, Shear Tab with Partial "C" Weld

3.5. Test Procedure

3.5.1. Instrumentation

Detailed instrumentation plans for each of the 12 test configurations can be found in Appendix C. The instrumentation plan and list for Configurations 1 and 3 have been included in this chapter for illustration purposes (Figure 3.14 and Table 3.2).

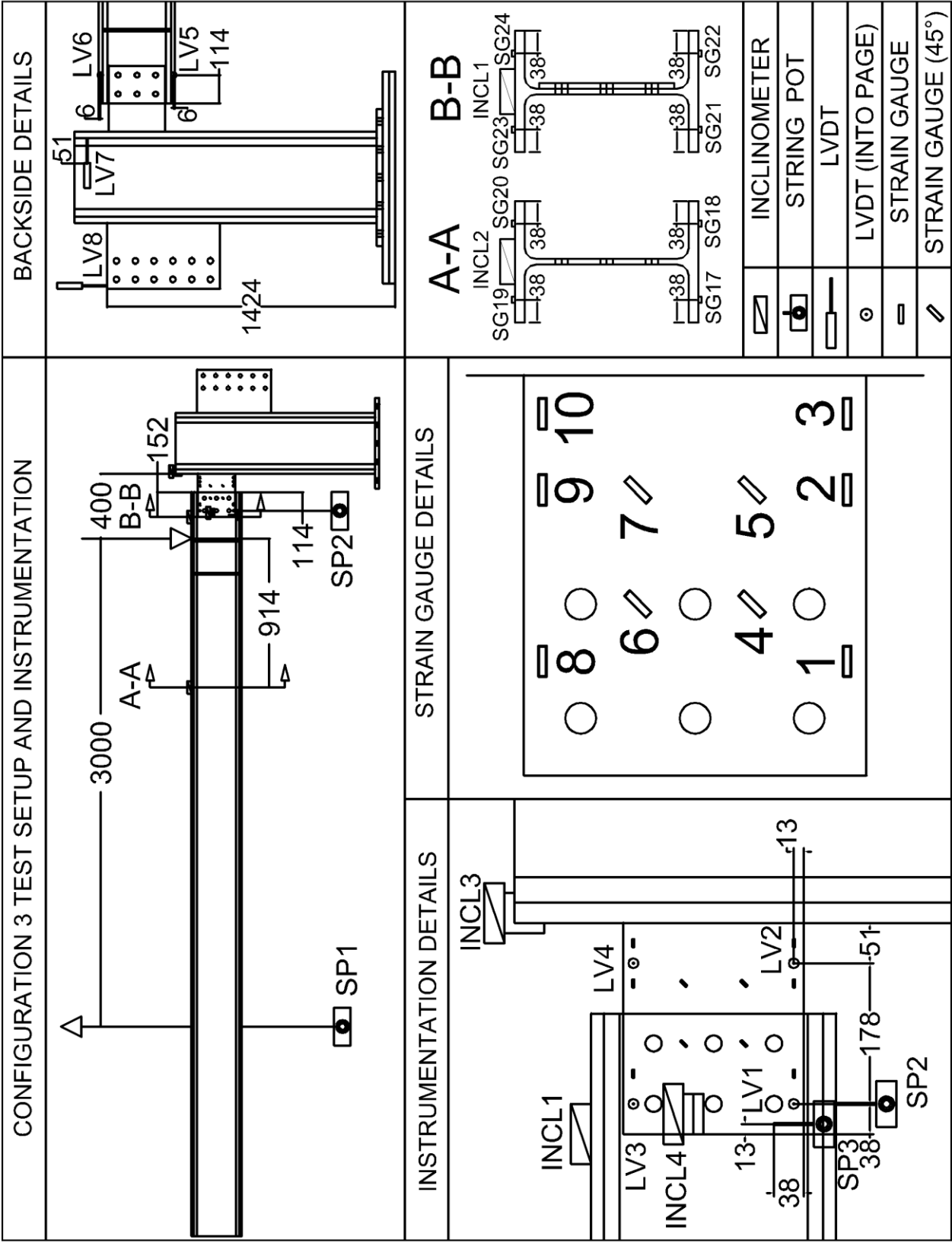


Figure 3.14: Instrumentation Plan, Configuration 3, Dimensions in mm

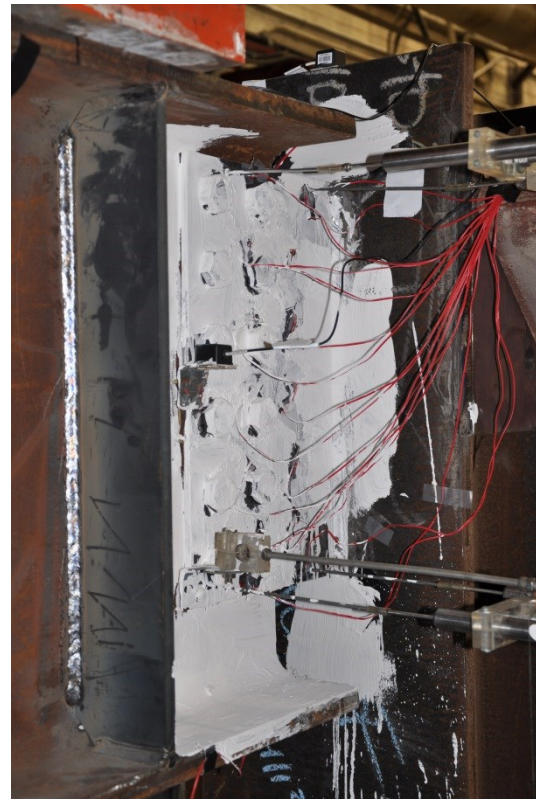
Table 3.2: Instrumentation List, Configurations 1 and 3

#	Type	direction	units	description
SP1	string potentiometer	Z	mm	beam deflection at tension actuator
SP2	string potentiometer	Z	mm	beam deflection at bolt line
SP3	string potentiometer	Z	mm	tab deflection
LV1	LVDT (25 mm)	Y	mm	out of plane deflection of tab, BOTTOM LEFT
LV2	LVDT (25 mm)	Y	mm	out of plane deflection of tab, BOTTOM RIGHT
LV3	LVDT (25 mm)	Y	mm	out of plane deflection of tab, TOP LEFT
LV4	LVDT (25 mm)	Y	mm	out of plane deflection of tab, TOP RIGHT
LV5	LVDT (25 mm)	Y	mm	out of plane deflection of beam end, BOTTOM
LV6	LVDT (25 mm)	Y	mm	out of plane deflection of beam end, TOP
LV7	LVDT (15 mm)	X	mm	deflection at top of column
LV8	LVDT (15 mm)	Z	mm	column vertical deflection w.r.t. ground
INCL1	inclinometer	XZ	deg	beam rotation at beam end
INCL2	inclinometer	XZ	deg	beam rotation, intermediate point
INCL3	inclinometer	XZ	deg	column top rotation
INCL4	inclinometer	XZ	deg	shear tab rotation, in plane
INCL4	inclinometer	YZ	deg	shear tab rotation, out of plane
SG1	strain gauge	X	ϵ	shear tab strain, bottom horizontal
SG2	strain gauge	X	ϵ	shear tab strain, bottom horizontal
SG3	strain gauge	X	ϵ	shear tab strain, bottom horizontal
SG4	strain gauge	XZ(45°)	ϵ	shear tab strain, intermediate 45
SG5	strain gauge	XZ(45°)	ϵ	shear tab strain, intermediate 45
SG6	strain gauge	XZ(45°)	ϵ	shear tab strain, intermediate 45
SG7	strain gauge	XZ(45°)	ϵ	shear tab strain, intermediate 45
SG8	strain gauge	X	ϵ	shear tab strain, top horizontal
SG9	strain gauge	X	ϵ	shear tab strain, top horizontal
SG10	strain gauge	X	ϵ	shear tab strain, top horizontal
SG17	strain gauge	X	ϵ	flange strain, bottom flange, at INCL1
SG18	strain gauge	X	ϵ	flange strain, bottom flange, at INCL1
SG19	strain gauge	X	ϵ	flange strain, top flange, at INCL1
SG20	strain gauge	X	ϵ	flange strain, top flange, at INCL1
SG21	strain gauge	X	ϵ	flange strain, bottom flange, at INCL2
SG22	strain gauge	X	ϵ	flange strain, bottom flange, at INCL2
SG23	strain gauge	X	ϵ	flange strain, top flange, at INCL2
SG24	strain gauge	X	ϵ	flange strain, top flange, at INCL2

Elastic and plastic deformation in the shear tabs and supporting girders (for the beam-to-girder tests) was monitored using 10mm strain gauges (120 Ohm resistance). Horizontal strain gauges were placed on the top and bottom edges of the shear tabs to capture flexural strains while strain gauges inclined to 45° were placed along the mid height of the shear tabs to record shear strains. At two points of the beam pairs of strain gauges were attached to the bottom and top flanges to record flexural strains. These strain values were used to compute the moment in the beam at the given locations. This was done at a point 114mm (4.5in) from the beam tip and at

920 mm from the compression load cell. Flexural strain gauges were attached to the tips of the girder flange in line with the supported beam and on the girder web opposite the bottom edge of the shear tab. These were used to monitor longitudinal yielding of the girder web and transverse yielding in the girder top flange for the beam-to-girder tests.

Out-of-plane shear tab and beam displacement was measured using 6 linear variable differential transformers (referred to as LVDTs). Two were attached to the beam, at the bottom and top flanges, to measure beam twist. Two were attached to the top edge of the shear tab and two were attached to the bottom edge. These were spaced such that the twist of the shear tab could be computed. Figure 3.15 illustrates the placement of these LVDTs.



a) Back-Side of Shear Tab (LVDT 5 & 6)

b) Front-Side of Shear Tab (LVDT 1, 2, 3 & 4)

Figure 3.15: Out-of-Plane LVDT Placement (Configuration 4 Pictured)

Vertical deflections of the shear tab, the beam at the location of the tension actuator and the beam end at the connection were measured using string potentiometers. For the beam to girder tests, a fourth string potentiometer was fixed at the middle of the supporting girder to measure its vertical deflection.

The rotations of the shear tab, the beam end at the connection, the beam at 920 mm from the compressive actuator and the supporting element (column or girder) were measured using inclinometers. Both the rotation in the longitudinal axis of the beam as well as out-of-plane twisting was recorded for the shear tab itself. The rotation of the connection was computed as the difference between the absolute beam rotation and the support rotation.

3.5.2. Test Procedure

The loading regime was the same used by Marosi (2011). The loading was adjusted such that the expected yielding shear for the shear tab was reached at a rotation of 0.015rad. Afterwards, the connections were expected to undergo plastic deformation. This regime was based on that created by Astaneh et al. (1989), the difference being the target rotation for yielding in the shear tab. Astaneh proposed that 0.02rad marked the rotation at which typical beams underwent yielding. Since the test beams were required to behave elastically, the target rotation was reduced from 0.02 to 0.015 rad. This loading regime can be seen in Figure 3.16.

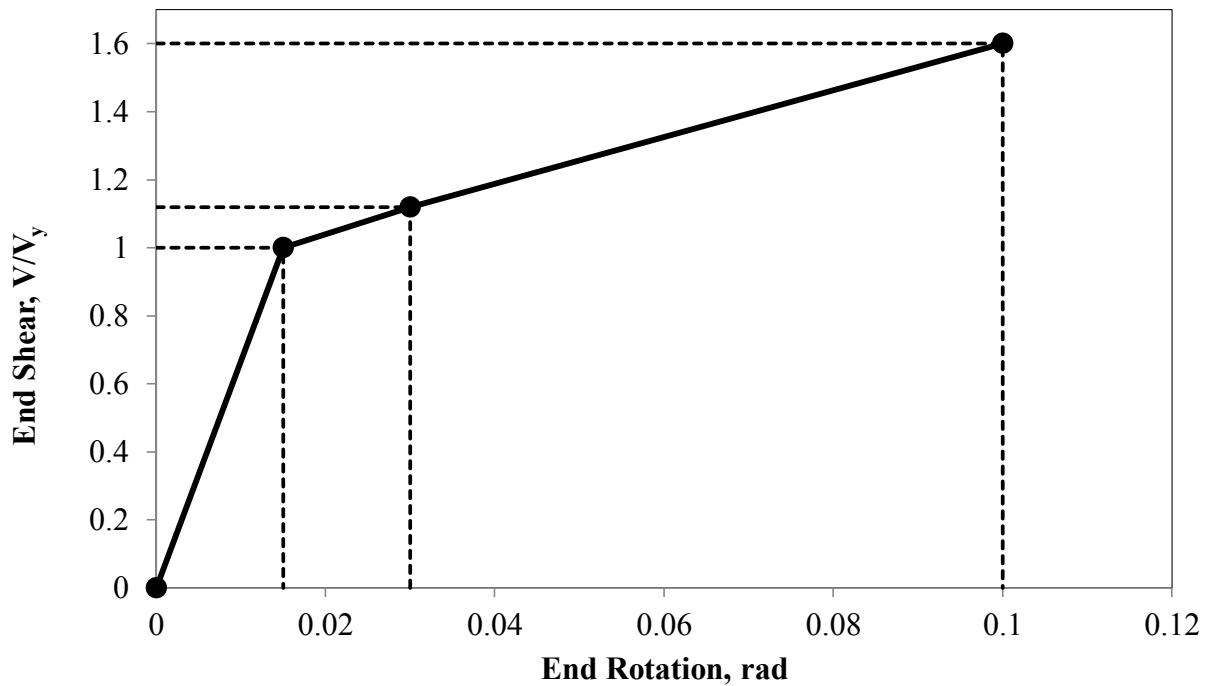


Figure 3.16: Modified Shear-Rotation Response for Shear Tab Connections, Marosi (2011)

The rotation and shear in the connection was modified during the test by adjusting the displacement rates of the tension and compression actuators. The shear in the connection, V , was

deduced as the algebraic sum of the compressive and tension actuator loads, C and T . The rotation in the connection was dependent on the displacement of the beam at the compressive actuator with respect to that at the tension actuator. Figure 3.17 depicts the relationship between the connection shear, V , and the connection rotation, θ .

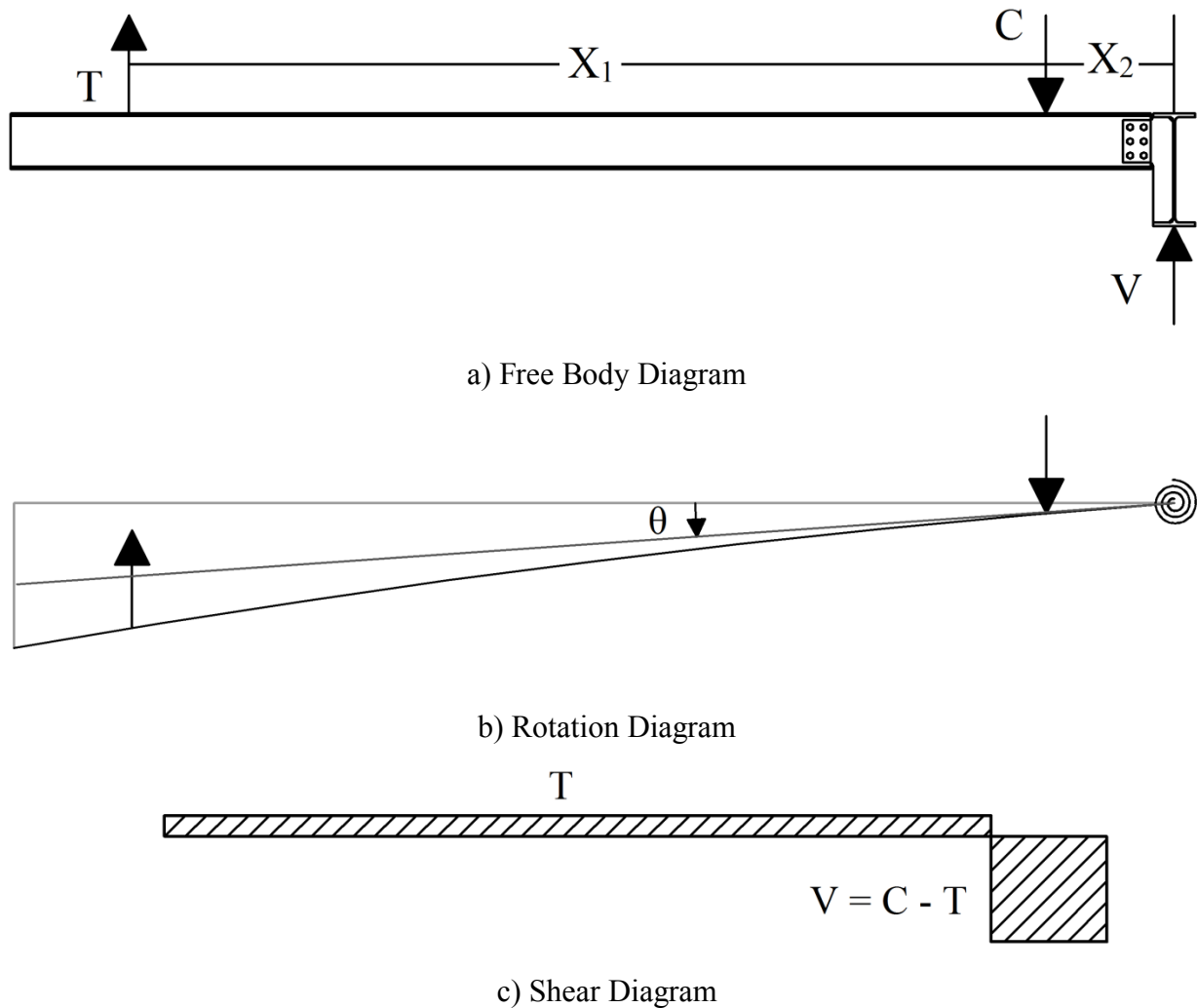


Figure 3.17: Rotational and Shear Response for Beam

The load from the compressive actuator was required only to act vertically on the beam. This was ensured by the use of a half cylinder and rollers. The rollers were sandwiched by two heavy steel plates which were milled on the inside face. One plate sat directly on the beam with the rollers placed on top and then the second plate on top of the rollers. This ensured the load was applied at the same point in the beam while it rotated. Compound (Ultracal 30 gypsum

cement) was placed between the bottom plate and the beam in cases where the top of the beam was uneven. The half cylinder was placed on top of the sandwich plates such that the load was vertical. Figure 3.18 illustrates the half cylinder and rollers for one of the deep beam tests. A smaller set of plates and rollers was used for the shallow beam tests.



Figure 3.18: Half Cylinder and Rollers

3.6. Summary

Twelve extended shear tab configurations were selected to be representative of typical in-situ shear tabs and designed using a combination of the CISC Handbook (2010), CSA S16-09 (2009), and the AISC Manual (2010). Four tests were run on beam-to-column connections: three of which used shallow (W310) beams and one with a deep beam (W610). All four beam-to-column tests had two vertical rows of bolts and “a” distances of 152mm (6in) or more. Eight tests were run on beam-to-girder connections. Six of these tests had shallow beams (W310) and two were with deeper beams (W610, W690). Two support girder sizes, W610 and W760, were

used with corresponding “a” distances of 165mm (6.5in) and 241mm (9.5in). The form of shear tab (partial-height, partial-height with stiffener and full-height) was varied for the shallow beam tests, except Configuration 8 which was a side plate connection. The deep beam tests used full-height shear tabs.

The configurations underwent full-scale laboratory testing with the test setup being comprised of: a tension actuator frame, compression actuator, lateral bracing system and reaction frame. The beam-to-column reaction frame was designed in previous testing done by Marosi (2011) whereas the beam-to-girder reaction frame was designed as part of this study. A combination of strain gauges, LVDTs, string potentiometers and inclinometers were used. The testing procedure was established based on the modified method by Marosi (2011), which was based on that of Astaneh et al. (1989).

Chapter 4 – Discussion of Experimental Results

4.1. Overview

This chapter presents the results from the full-scale testing of the 12 extended shear tab configurations as described in Chapter 3. Firstly, the results from coupon testing are presented. Coupon testing was conducted on the shear tab plate as well as the web and flange of the test beams to determine the actual material properties (yield stress, tensile stress, elongation, and modulus of elasticity). The observed behaviour of the connection test specimens is described in terms of failure modes and their corresponding resistances. The measured resistance values are compared with the theoretical values calculated using the combined CISC Handbook (2010), CSA S16-09 (2009), and AISC Manual (2010) extended shear tab design method. Where discrepancies between the measured and predicted resistances arise, recommendations are made to modify the combined AISC and CISC design method. The theoretical resistances were calculated in two manners: i) with inclusion of resistance factors and using the nominal material properties and ii) omitting the resistance factors and using the measured material properties.

4.2. Coupon Testing

4.2.1. Test Methodology

Coupons were cut from the shear tab plate, beam webs and beam flanges and tested under tension to determine the mechanical properties. A 500kN capacity hydraulic actuator (Figure 4.2a) was used to apply tension to the coupons until fracture occurred. The coupons were fabricated and tested to meet the requirements outlined in the ASTM A370 Standard (ASTM 2012). Figure 4.1 illustrates the specification for cutting of coupons from beams. The same parent plate was used for all shear tabs used in the 12 extended shear tab test configurations, and hence only three coupons were taken from the shear tab plate in the horizontal (5A) direction and three from the vertical (5B) direction.

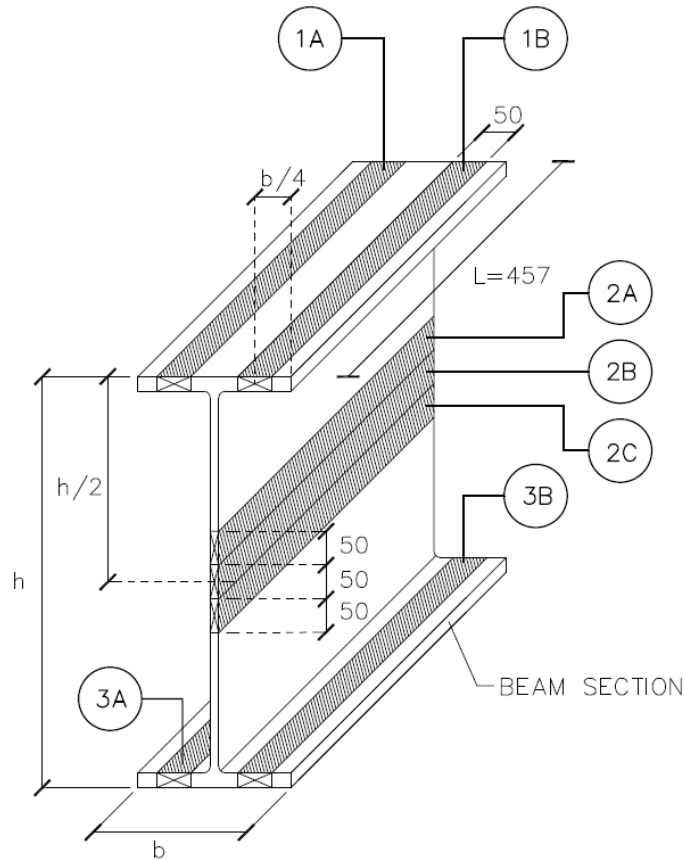
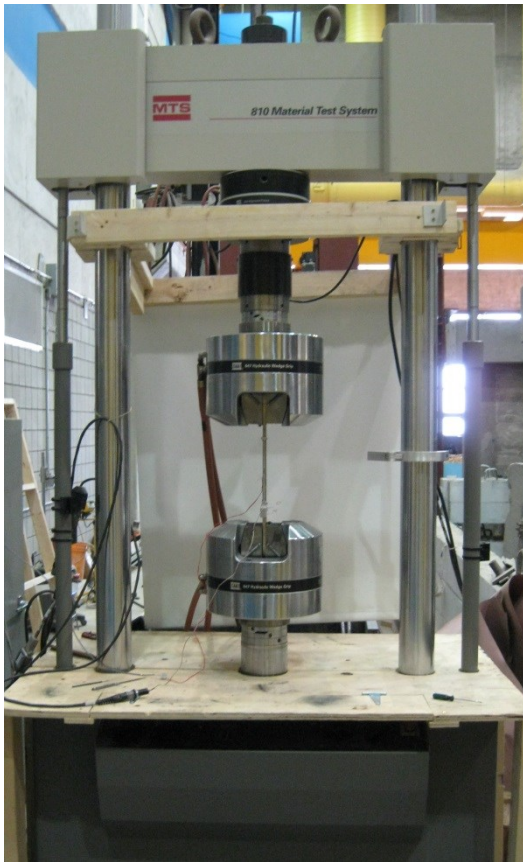


Figure 4.1: Beam Coupon Locations (Image Courtesy of DPHV Structural Consultants)

To obtain engineering stress-strain curves, three displacement rates of the actuator head were used: i) 0.0026mm/s in the elastic region ii) 0.026mm/s in the yield plateau and iii) 0.26mm/s in the strain hardening region. A 203mm (8in) extensometer was attached to the coupon to measure the longitudinal deformation. The maximum extensometer stroke was 12.7mm ($\frac{1}{2}$ in). Since final coupon deformations were in the range of 50mm (2in), the tests had to be paused when the extensometer had reached maximum stroke and the extensometer adjusted back to zero. An LVDT located in the actuator head was used to record deformation of the coupons. These values, however, are thought to be inaccurate for a number of reasons: mainly movement between the actuator grips and the coupon grips. Therefore, these readings were used only to confirm accuracy in the extensometer readings. It was seen that the values of LVDT strain did not match the stress-strain curve when compared to the extensometer strain. The correlation between the LVDT and extensometer strain was calculated and used to obtain accurate strain values for the tests where the extensometer was only used at the beginning of the test. Strain gauges were attached to some of the coupons to obtain a direct measure of Young's

modulus and to verify the extensometer readings in the elastic region. Comparison of the two values confirmed accuracy in the extensometer Young's modulus. Beam coupons 1A, 2A and 3A were all equipped with strain gauges as well as one from the plate coupons 5A and 5B. The strain gauges were oriented along the long axis of the coupons and placed on the middle of one face (Figure 4.2b).



a) Tension Actuator



b) Extensometer and Strain Gauge Details

Figure 4.2: Coupon Test Setup

The engineering strain was calculated using the extensometer displacement over the 203mm (8in) length. For some of the tests, the extensometer was not reset to zero once maximum stroke of 12.7mm (1/2in) had been reached. In these cases, the engineering strain was calculated using the LVDT displacement over the length between actuator grips once the maximum extensometer stroke had been reached. The Percent Elongation was computed as the LVDT strain multiplied by a conversion factor (the average ratio between the extensometer strain and LVDT strain at fracture, taken as 1.12). These cases are indicated in Table 4.1. The engineering stress was calculated as the actuator force over the original cross sectional area of

the coupon. Engineering stress-strain curves were plotted for all 27 tests. The ultimate stress, F_U , was taken as the maximum stress in the strain hardening region. The modulus of elasticity, E , was found by linear fitting in the elastic region. For coupons with strain gauges the strain gauge strain was used, otherwise the extensometer strain was used to calculate the elastic modulus. The yield stress, F_Y , was obtained by finding the intercept of the stress-strain curve and a line with slope, E , located at a 0.2% offset from the origin. The Percent Elongation was taken as the strain at failure. The ratios R_Y and R_T were computed as the ratio of actual yield and tensile stress to the specified minimum yield and tensile stresses.

4.2.2. Test Results

The coupon test results are presented in Table 4.1. For the beams, the flange values are averaged from four tests (two from the top flange and two from the bottom) and web values are averaged from three tests. For the shear tab plate, both the horizontal and vertical values are averaged from three tests. Coupon specimens before and after testing are pictured in Figure 4.3.

Table 4.1: Coupon Test Results

Section	Region	Cross Section mm x mm	F_Y MPa	F_U MPa	% Elongation	E GPa	F_U/F_Y	R_Y	R_T
W310x60 (W12x40)	Flange	37.5 x 12.7	376	492	23	210	1.31	1.08	1.09
	Web	37.5 x 7.1	414	511	24*	214	1.23	1.18	1.14
W610x140 (W24x94)	Flange	37.5 x 21.2	390	513	25	198	1.32	1.11	1.14
	Web	37.7 x 12.5	448	539	22	205	1.20	1.28	1.20
W690x125 (W27x84)	Flange	34.7 x 15.8	371	503	24	212	1.36	1.06	1.12
	Web	34.6 x 11.0	405	511	23	211	1.26	1.16	1.13
PL9.5 (PL3/8)	Horizontal	37.5 x 9.5	480	541	16*	215	1.13	1.39	1.20
	Vertical	37.5 x 9.5	433	509	18*	201	1.18	1.26	1.13

*Elongation values based on LVDT displacement with conversion factor (1.12)



Figure 4.3: Coupon Specimens Before (W24x94 Flange) and After (W27x84 Flange) Uniaxial Tensile Test

4.2.3. Remarks

Test results from the beams show good agreement between the assumptions made in design versus the actual material properties. The ratios of R_Y and R_T were both assumed to be 1.10 in design. The measured values are within 6% of this assumption, except for the flange web of the W610x140 beam.

In contrast, the R_Y value for the shear tab plates is much larger in the horizontal direction. This is more critical than that of the beam due to the desirable failure mode for the shear tab connections being yielding of the shear tab plate. Typical engineering stress-strain curves for the shear tab plate are provided in Figures 4.4 and 4.5. The jumps in stress on the curves at 0.03mm/mm and 0.04mm/mm are due to adjustment of the cross-head displacement rate. It should be noted that the behaviour in the horizontal and vertical directions is very different. The horizontal is characterized by a linear elastic region and defined yield plateau. The vertical is characterized by a curving elastic region and a small yield plateau. There is also variation in the yield stress with the horizontal direction having significantly larger yield stress than the vertical.

This variation in material properties between the vertical and horizontal directions can be attributed to the hot and cold rolling processes needed to achieve the desired plate thickness and flatness (Keeler 1986). Both of these processes influence the grain structure of the steel as the grain structure aligns itself with the direction of rolling.

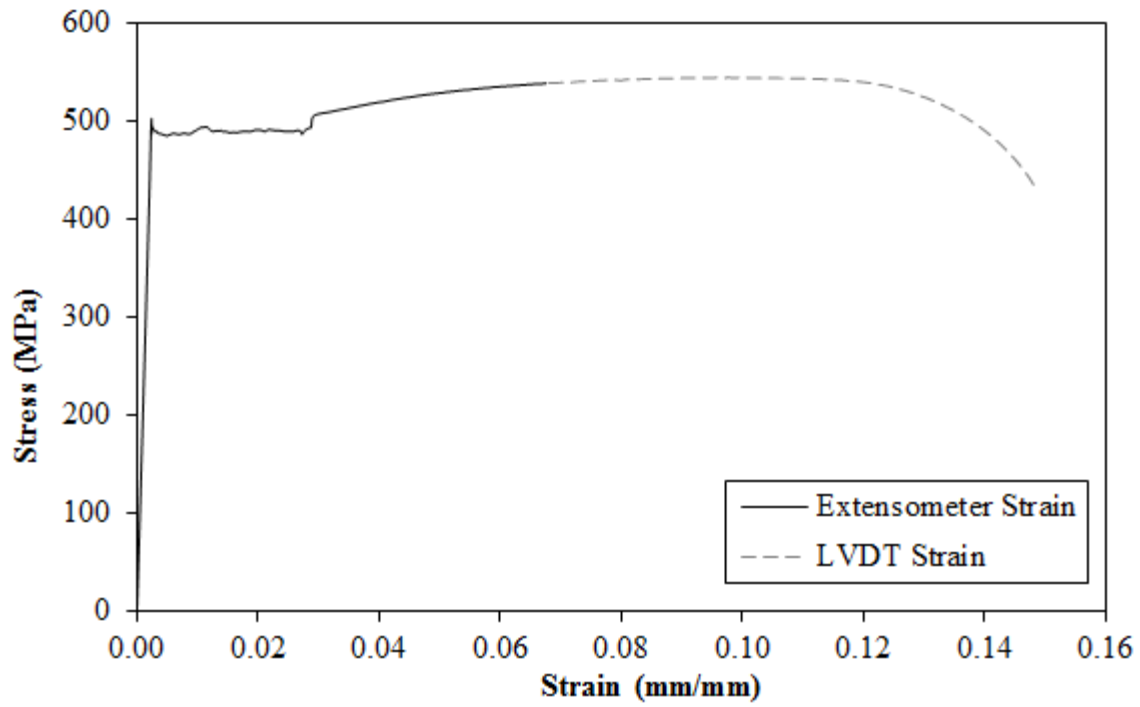


Figure 4.4: Engineering Stress vs. Strain, Coupon PL3/8 5A-3 (horizontal direction in shear tab)

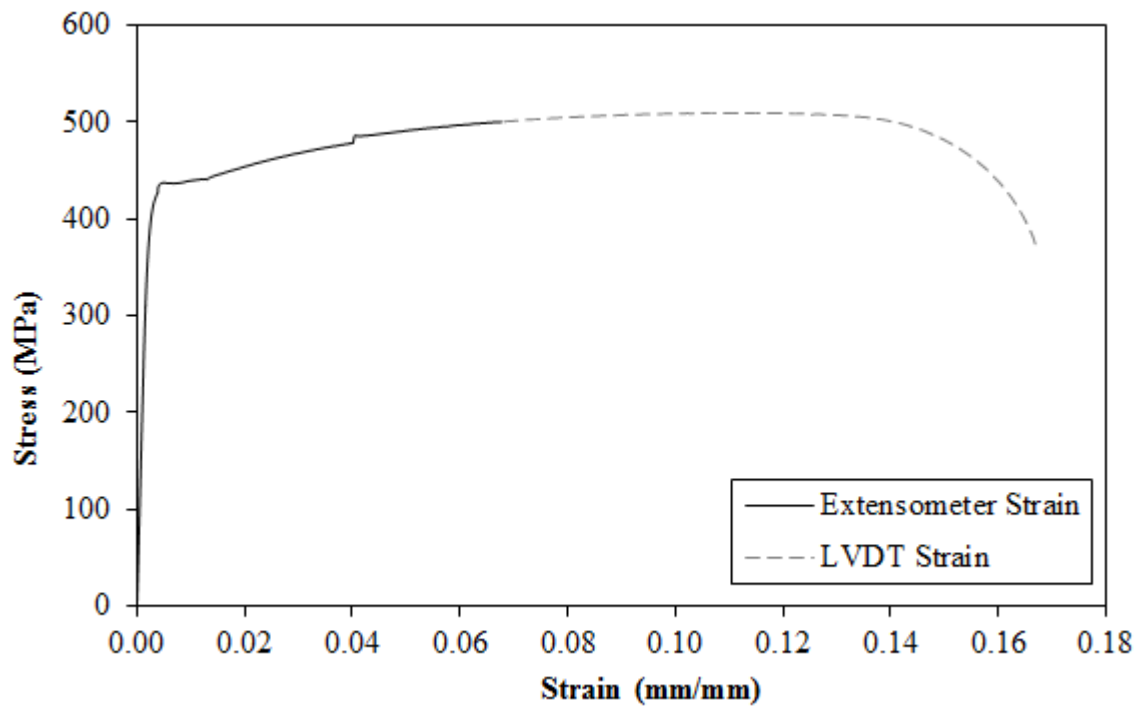


Figure 4.5: Engineering Stress vs. Strain, Coupon PL3/8 5B-3 (vertical direction in shear tab)

4.3. Experimental Results and Discussion

4.3.1. Predicted Resistances

Table 4.2 presents the factored and predicted resistances for the 12 test configurations along with the corresponding failure mode. The AISC extended shear tab design method (AISC 2010) modified with provisions from CSA S16-09 (2009) and the CISC Handbook (2010) was used to calculate these resistances (Section 3.3.1). The factored resistances were calculated using reduction factors and the nominal material properties. The measured material properties were used to compute the predicted resistances (Section 4.2 – Coupon Testing). The nominal bolt and electrode strengths were used. All design calculations can be seen in Appendix A: Design Calculations.

All 12 configurations were originally designed under the assumption that the bolt threads would be excluded from the shear plane. However, the bolts received for use in configurations 1, 2, 5, 6, 7, 9 and 10 were fully threaded. Thus, the critical limit state for configurations shifted from combined shear and flexural yielding to bolt shear when the 30% reduction in bolt strength was accounted for. In addition, the resistance of the partial “C” weld for configuration 3 was designed to have the same strength as the corresponding bolt group in configuration 1. Based on the assumption that the threads were excluded from the shear plane, the partial “C” weld was sized at 9.5mm (3/8in). If the 30% reduction had been applied to the bolt group shear strength, the weld should have been sized at 6.5mm (1/4in).

In addition, coupon testing revealed that the measured yield stress and tensile stress of the shear tab parent plate was much greater than expected. When calculating the predicted connection resistances, the measured values for the yield and tensile stress were assumed to be 110% of the nominal (i.e. 385MPa and 495MPa). The measured values were found to be 457MPa and 525MPa (132% and 117% of the nominal). These values were averaged from the vertical and horizontal oriented coupons and show good agreement with the mill test results (452MPa and 531MPa). This shifted the expected failure mode for the majority of the connections from combined shear and flexural yielding to other failure modes such as bolt shear and weld tearing. All shear tabs were sized at 9.5mm (3/8in) thickness and were fabricated from the same parent plate.

Table 4.2: Factored and Predicted Connection Resistances

Test	Factored Resistance based on Nominal Material Properties kN	Predicted Failure Mode	Predicted Resistance Based on Measured Material Properties kN	Predicted Failure Mode
1	157	BS	197	BS
2	129	BS	161	BS
3	191	CT	285	CT
4	588	SR	922	FS
5, 6, 7	149	BS	186	BS
8	142	BB	178	BB
9 & 10	114	BS	142	BS
11	510	FS	732	FS
12	643	SR	933	FS

Failure Modes

BS = Bolt Shear

CT = Weld Tearing (Partial “C” Weld)

SR = Shear Rupture

BB = Bolt Bearing

FS = Flexural and Shear Yielding

4.3.2. Summary of Experimental Results and Comparisons

Table 4.3 presents the maximum connection shear and connection rotation (computed as the difference between the beam end and the support rotations as measured using inclinometers) for the twelve tests. The tests were terminated when the connection was expected to fail abruptly, the shear-rotation stiffness had decreased significantly or when the equipment limit (actuator displacement) had been reached.

As detailed in Section 4.2.1, all predicted resistances were computed with a resistance factor (ϕ) of 1.0 and measured material properties (or nominal for bolts and electrodes).

Table 4.3: Summary of Experimental Results

Test	Maximum Connection Shear kN	Maximum Connection Rotation rad	Failure Mode: Primary (and Secondary)	Remarks
1	317	0.031	WT (BS)	-
2	240	0.065	PB	-
3	390	0.055	WT	-
4	1040	0.033	SR (PB, FS)	-
5	266	0.021	FB	-
6	108	0.009	GY	Equipment malfunction
7	445	0.127	BB	Max tension actuator stroke
8	410	0.036	BB	-
9	433	0.024	-	Max tension actuator stroke
10	501	0.024	-	Max tension actuator stroke
11	455	0.014	FB	-
12	415	0.011	FB	-

Failure Modes

WT = Weld Tearing

PB = Plate Buckling

SR = Shear Rupture

FB = Full Height Buckling

GY = Girder Yielding

BB = Bolt Bearing

4.3.3. Beam-to-Column Extended Shear Tab Connections

Six-bolt Configurations (1, 2 and 3)

Configurations 1 and 3 were designed with nominally identical geometries, with Configuration 1 being bolted and Configuration 3 being welded with a partial “C” weld. The observed behaviour was similar for both. Flexural yielding of the shear tab initiated at a connection shear of 215kN for the bolted connection and 135kN for the welded one (see Figure 4.6). Flexural yielding occurred when the strain at the locations of SG3 and SG10 exceeded the yield strain. The delay in yielding in the bolted versus the welded connection was most likely due to the partial “C” weld having greater rigidity than the corresponding bolt group. Since the portion of plate enclosed by the partial “C” weld was fixed, deformation primarily occurred in

the unsupported length of shear tab. In the bolted connection, deformation was able to occur in the area of plate around the bolt group and by means of bolt slip. No stiffness decrease was associated with flexural yielding in either the bolted or welded connection.

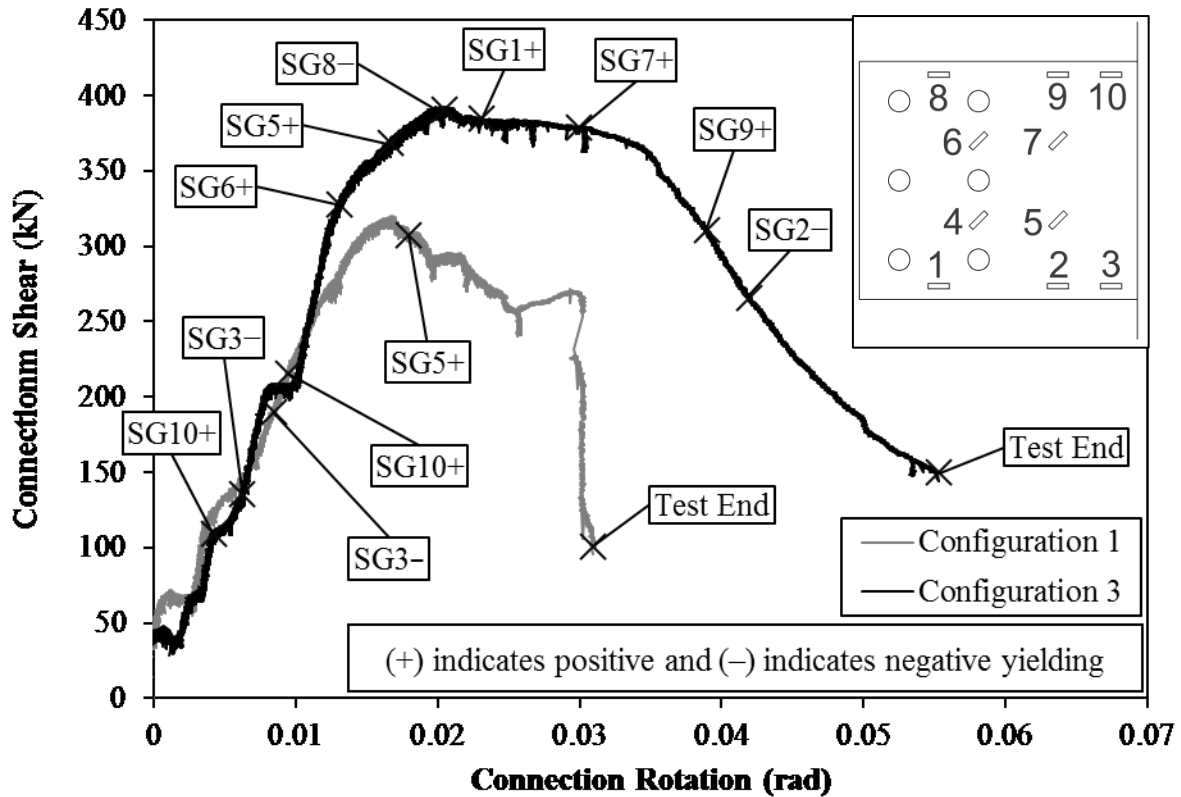


Figure 4.6: Connection Shear vs. Rotation, Configurations 1 & 3

Significant flexural tearing of the weld ultimately controlled the shear resistance in both tests. The maximum connection shear loads were 317kN and 390kN for the bolted and welded connection, respectively. The extent of weld tearing at the end of each experiment (greater than half the plate height for the bolted and mid-height for the bolted and welded connection, respectively) can be seen in Figures 4.7 and 4.8.



a) Deformed Shear Tab

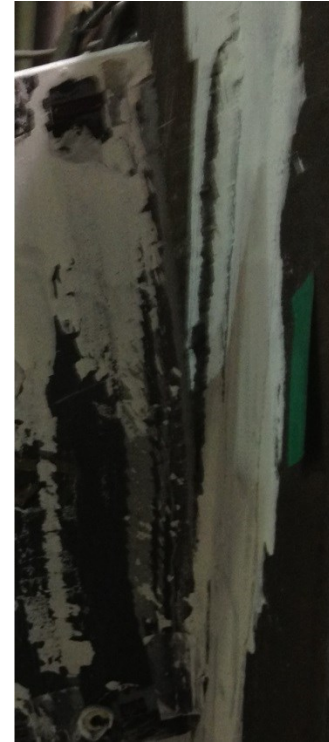


b) Weld Fracture Detail

Figure 4.7: Weld Tearing and Deformed Shear Tab, Configuration 1



a) Deformed Shear Tab



b) Weld Fracture Detail

Figure 4.8: Weld Tearing and Deformed Shear Tab, Configuration 3

In the bolted connection, a steep decline in the connection shear can be seen after 0.03radians of rotation (Figure 4.6). This is attributed to the shearing of bolts, which occurred at a higher rotation than that of the ultimate load (0.03radians). Thus, this is not thought to be the governing ultimate limit state for the connection. Figure 4.9 shows one of the three bolts, which had sheared after it had been removed from the bolt hole at the end of the test. The shear plane intercepted the bolt threads.



Figure 4.9: Sheared Bolt, Configuration 1

The predicted bolt shear resistance for Configuration 1 was 197kN. In testing, bolt shear was seen to occur at approximately 270kN. The AISC extended shear tab design method (AISC 2010) specifies that the bolt shear resistance is calculated under the assumption that rotation occurs about the support face. In reality, the support does provide some moment restraint which means that rotation actually occurs outside the support face. For Configuration 1, the bolt group eccentricity was assumed in design as 190mm (7.5in). However, the experimental eccentricity, L , was calculated as 128mm (5in) using the measured bolt shear resistance. Figure 4.10 illustrates the experimental eccentricity of a bolt group with an eccentric load applied to it.

$$C_{experimental} = \frac{V_{r,experimental}}{0.6\phi_b m A_b F_u} = \frac{(270 \text{ kN})}{(0.70)0.6(1.0)(1)(285 \text{ mm}^2)(825 \text{ MPa})} = 2.72$$

$$\frac{125 - L}{125 - 150} = \frac{2.77 - (2.72)}{2.77 - 2.41} \rightarrow L = 128 \text{ mm}$$

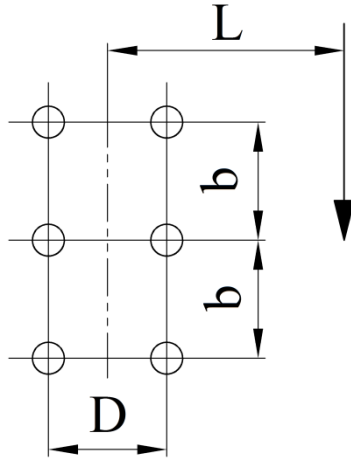


Figure 4.10: Eccentric Loads on Bolt Groups, Reproduction of CISC Handbook (2010)

In the welded connection, shear yielding occurred at the location of SG5 before the ultimate resistance had been reached. The initiation of combined shear and flexural yielding would require yielding to occur at the location of SG7 as well but this occurred at a greater rotation than that of the ultimate load. Yielding at the location of SG6 was most likely due to the partial “C” weld geometry, which created high stresses at the line of bolts. Combined shear and flexural yielding was expected to occur at 313kN. The extent of flexural and shear yielding in the lower half of the shear tab indicates that this is a good assumption. Tearing of the plate-to-column weld inhibited yielding in the top half of the shear tab.

The resistance of Configuration 2, which was detailed with a larger 'a' distance than Configurations 1 and 3, was ultimately controlled by local plastic buckling of the bottom edge of the shear tab. The connection stiffness (shear-rotation) remained constant until a connection shear of 215kN, where the stiffness began to decrease rapidly until an ultimate load of 240kN (Figure 4.11). Afterwards, the local buckling mechanism had fully formed and the stiffness became negative, i.e. the resistance decreased. Figure 4.12 (taken from the underside of the shear tab) shows the extent of plate deformation at the end of the test. The predicted local buckling resistance was calculated to be 185kN using the conservative classical plate buckling (applicable for both elastic and plastic) (Q) formulation [(AISC extended shear tab design check 5 (AISC 2010)]. Flexural yielding [signalled by yielding at the top (SG12) and bottom (SG3) edges of the shear tab] occurred at a load of 185kN with no corresponding stiffness decrease.

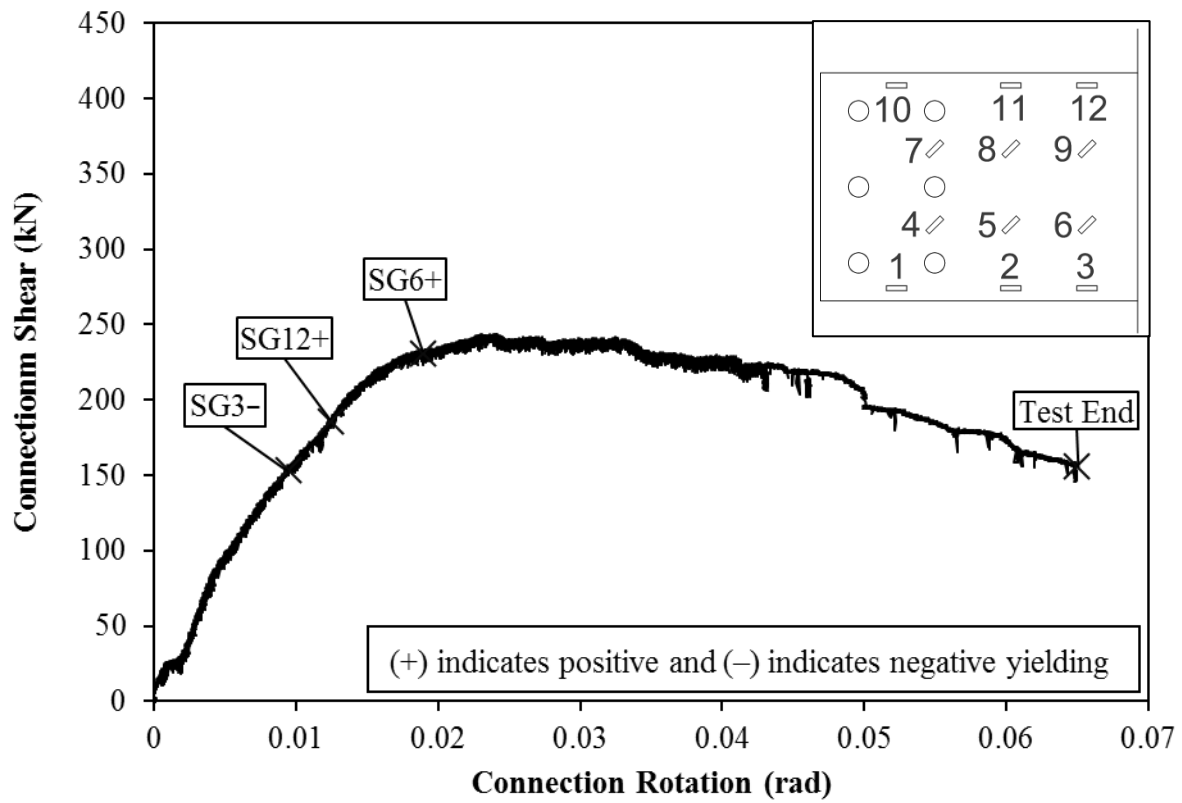


Figure 4.11: Connection Shear vs. Rotation, Configuration 2

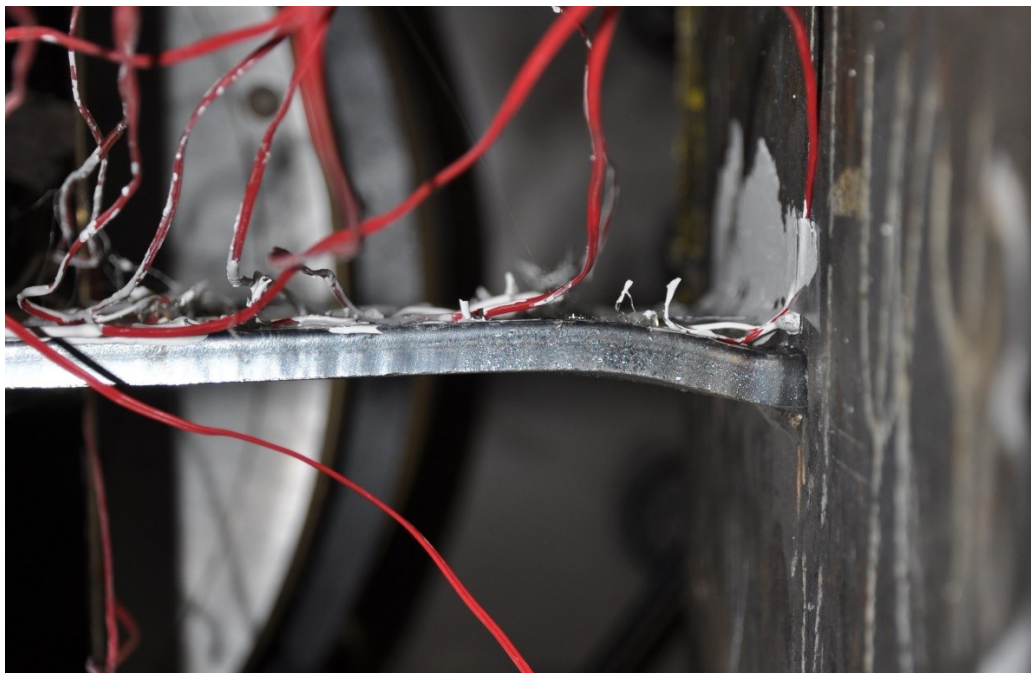


Figure 4.12: Bottom Edge of Shear Tab, Configuration 2

Twelve-bolt Configuration (4)

Configuration 4 experienced a combination of failure modes of the shear tab. Flexural yielding of the shear tab initiated at a connection shear of 440kN (SG3 and SG16, Figure 4.13). The entire height of the shear tab began to yield in shear after 780kN. Yielding could be seen visually as the majority of white wash peeled off along the unsupported length of shear tab (Figure 4.14a). It should be noted that tearing of the weld at the top of the shear tab reduced strains at the location of SG13, and thus no yielding occurred at this location. The expected combined shear and flexural yielding resistance was calculated as 643kN.

At a connection shear of 838kN, significant plastic local buckling of the shear tab bottom edge initiated [predicted by AISC (2010) design method as 984kN]. After which, the connection stiffness temporarily stayed at zero before increasing again. Figure 4.14b shows the extent of local buckling at the bottom of the shear tab. The connection shear resistance was ultimately controlled by net section fracture through the vertical row of bolt holes nearest to the weld (Figure 4.14c). An ultimate resistance of 1040kN was reached, after which, the connection shear dropped rapidly and the test was ended. The predicted net section shear resistance was calculated as 925kN.

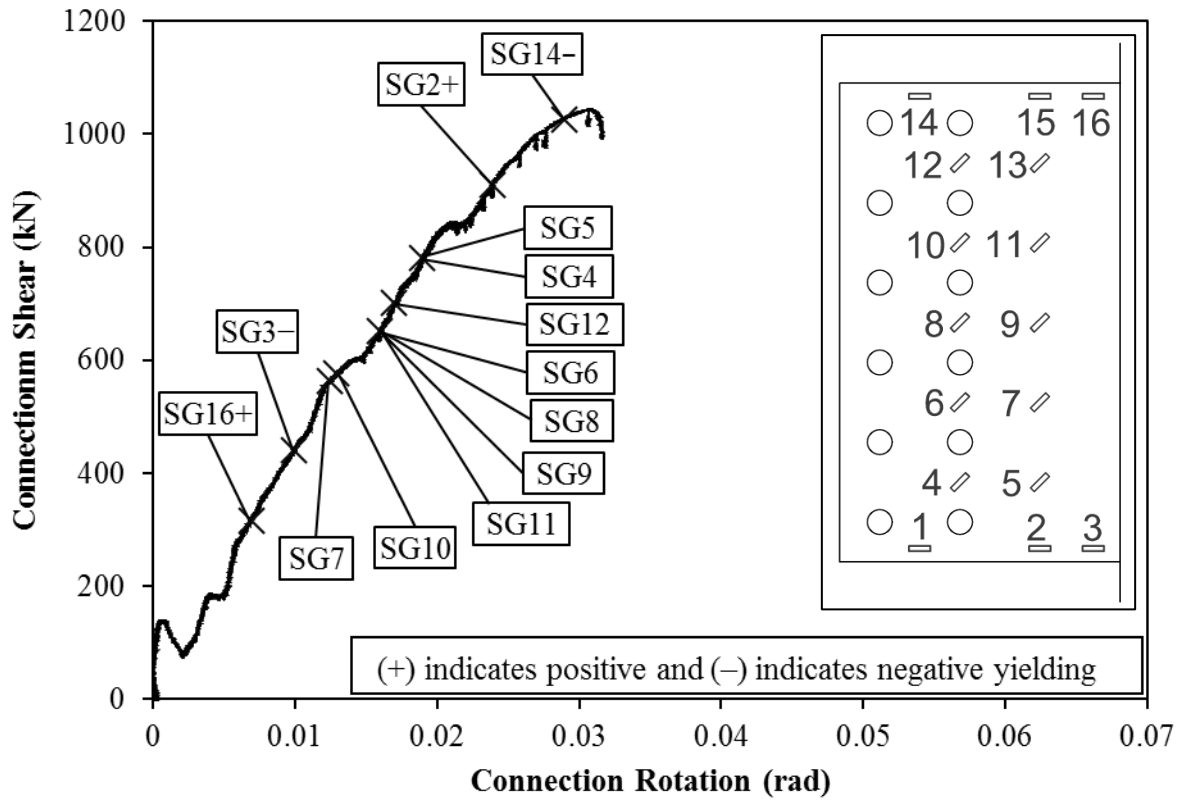
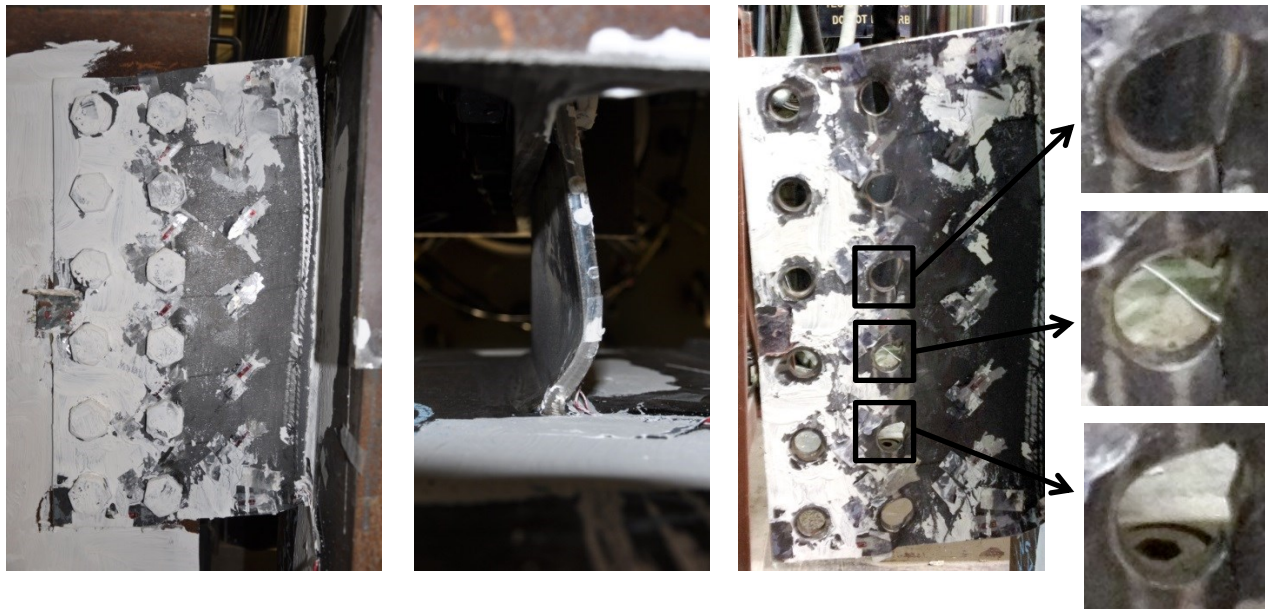


Figure 4.13: Connection Shear vs. Rotation, Configuration 4



a) Yielding b) Plate Buckling c) Net Section Rupture

Figure 4.14: Shear Tab Deformation at End of Test, Configuration 4

4.3.4. Beam-to-Girder Extended Shear Tab Connections

Full Height Beam-to-Girder Connections (5, 11, 12)

The full height beam-to-girder connections underwent the same failure type. Once the buckling resistance had been reached, the edge of the shear tab closest to the bottom right bolt buckled out-of-plane in a plastic manner (see Figure 4.15). After the initiation of buckling, the shear-rotation stiffness decreased substantially. Eventually, the bottom flange of the supported beam began to bear on the stiffener portion of the shear tab. This caused an increase in connection stiffness due to beam binding. This has been observed in numerous tests documented in prior studies [see Liu and Astanah (2000)]. As depicted in Figure 4.15, the portion of shear tab within the girder will be hereafter referred to as the stiffener.

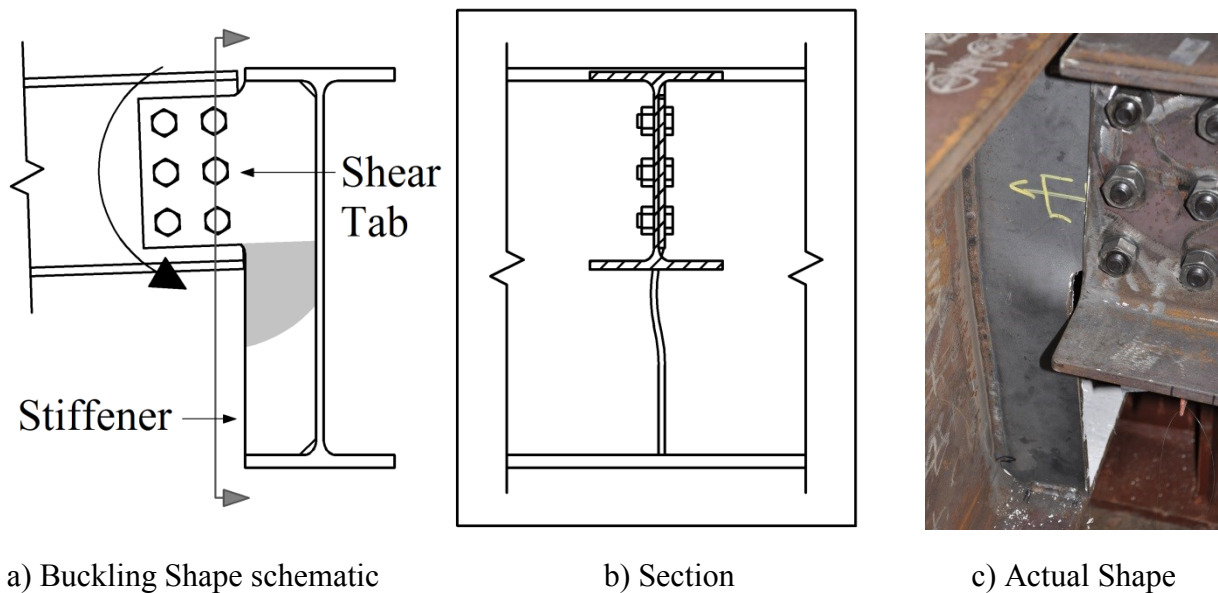


Figure 4.15: Buckling Failure Mode Shape (Configuration 5 Pictured)

This failure mode was consistent for all three full-height beam-to-girder test configurations (5, 11 and 12). All three tests were ended shortly after the beam bottom flange began to bear on the stiffener. The shear tab of each of the three configurations (5, 11 and 12) buckled at loads of 221kN, 490kN, and 389kN, respectively (Figure 4.16 and 4.17). Yielding was seen prior to buckling for Configuration 5 at the top of the shear tab (SG8). The extent of buckling can be seen in Figures 4.18 and 4.19.

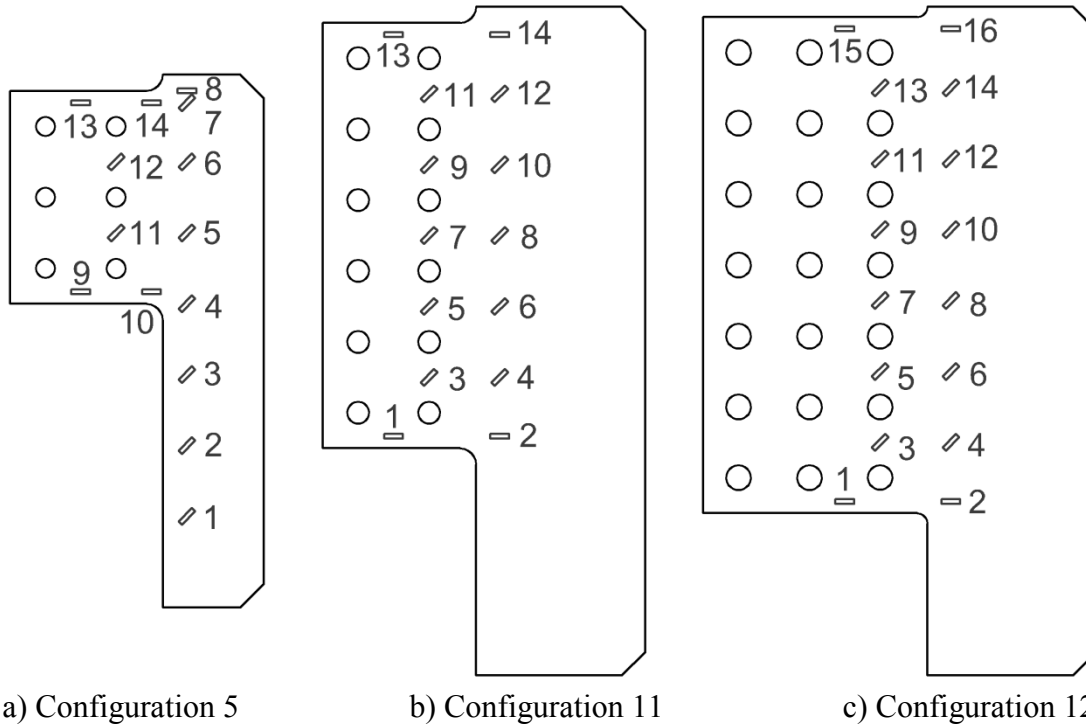


Figure 4.16: Strain Gauge Layout, Full Height Beam-to-Girder Shear Tab Connections

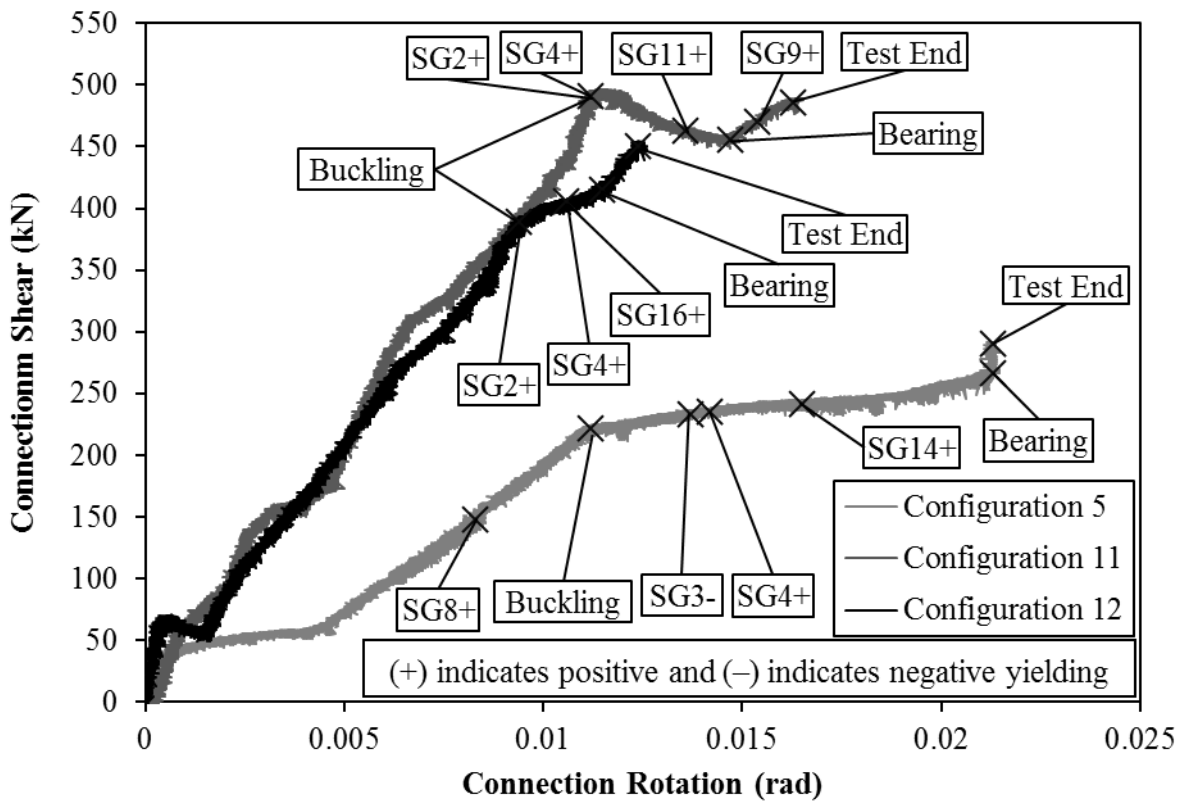


Figure 4.17: Connection Shear vs. Rotation, Full Height Beam-to-Girder Shear Tab Connections



a) Configuration 5

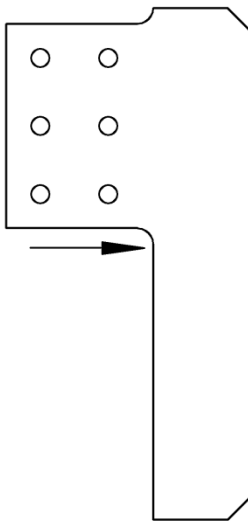


b) Configuration 11



c) Configuration 12

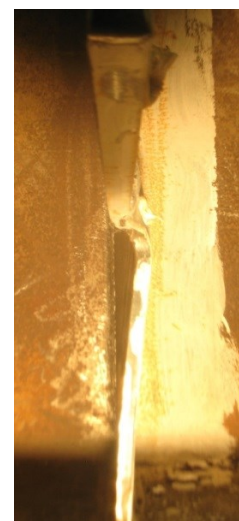
Figure 4.18: Buckled Shear Tab at Test End, Full Height Beam-to-Girder Shear Tab Connections



b) Configuration 5



c) Configuration 11



d) Configuration 12

Figure 4.19: Buckling at Neck of Shear Tab, Full Height Beam-to-Girder Shear Tab Connections

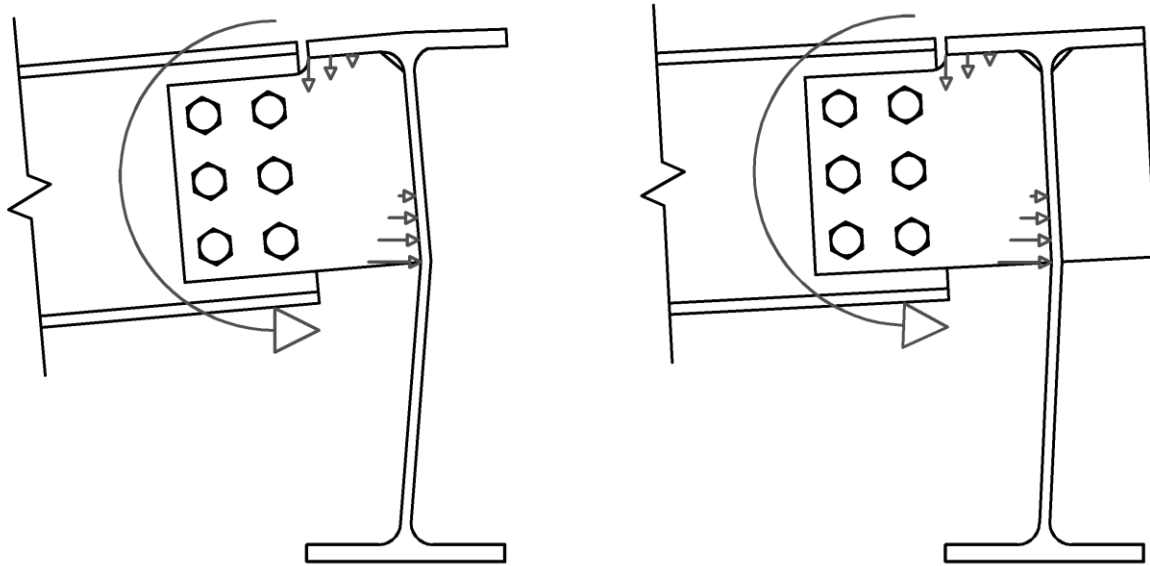
It should be noted that Configuration 12 buckled at a lesser load than Configuration 11 even though the expected resistance was thought to be higher. This could be attributed to the fact that the buckling of full height shear tab connections is due to a combination of: i) vertical compressive stresses from transfer of shear into the girder and ii) horizontal compressive stresses

from the flexural action of the beam. Since the beam used for Configuration 12 (W690) was deeper than that for Configuration 11 (W610), the horizontal stresses would be larger for the same shear load and thus buckling of the stiffeners would occur at a lower connection shear force. The shear-rotation stiffness for Configuration 11 and 12 is similar for two reasons. Firstly, the target resistance for the two configurations (based off the predicted flexural yielding resistance) is similar. Secondly, the difference in rotational stiffness between connections with two and three vertical rows of bolts was found to be very small in previous testing of shear tabs done by D'Aronco (2014).

The slenderness ratios (h/t) for the two stiffeners (W610 for Configuration 5 and W760 for Configurations 11 and 12) are calculated to be 60.1 and 75.5, respectively. Considering only axial compression, Configurations 11 and 12 would be predicted to have the same resistance since they have the same slenderness ratio. The stiffener for Configuration 12 was seen to buckle at a lesser connection shear than Configuration 11. This difference is due to increased compression in the horizontal direction from flexural action of the deeper beam (Configuration 12).

Partial Height Beam-to-Girder Connections (6, 7, 9, 10)

Configurations 6, 7, 9 and 10 were designed with partial height shear tabs. Configurations 7 and 10 had additional stiffeners on the opposite side of the girder web. Deformation in the supporting girder was seen for all four configurations. This deformation primarily affected the girder top flange and girder web due to the flexural action of the beam imparting: i) concentrated horizontal compressive stresses to the girder web at the base of the shear tab and ii) vertical tension stresses on the underside of the girder top flange. Figure 4.20 illustrates the manner in which the supporting girder deformed in these tests.



a) Without Stiffener (Configuration 6)

b) With Stiffener (Configuration 7)

Figure 4.20: Girder Yielding Deformation, Partial-Height Beam-to-Girder Shear Tabs

Comparing Configuration 6 (stiffened) with 7 (unstiffened), it was found that the inclusion of an additional stiffener for Configuration 7 delayed yielding of the girder web and top flange significantly. Yielding was monitored by strain gauges attached to the girder flange and web. The side of the girder web opposite the shear tab (SG15) yielded at a connection shear of 26kN and the top edge of the girder flange (SG13) yielded at 80kN for the unstiffened connection (see Figure 4.21). In contrast, web yielding (SG15) occurred at a connection shear of 210kN and flange yielding (SG13) occurred at 297kN for the stiffened connection. Compressive yielding in the girder web at the base of the shear tab can be seen in Figure 4.21.

It should be noted that the maximum connection rotation for the unstiffened connection (0.009radians) is much less than the stiffened (0.127radians). This is due to the unstiffened girder rotation being essentially the same as the beam rotation. The connection rotation is computed as the difference between the girder rotation and the beam rotation. Thus, the maximum actuator stroke was reached very early in the unstiffened test, with the majority of deformation occurring solely in the girder. Figure 4.20 illustrates this. Even though both beams have rotated the same amount, there is much more deformation in the girder of the unstiffened connection versus the stiffened.

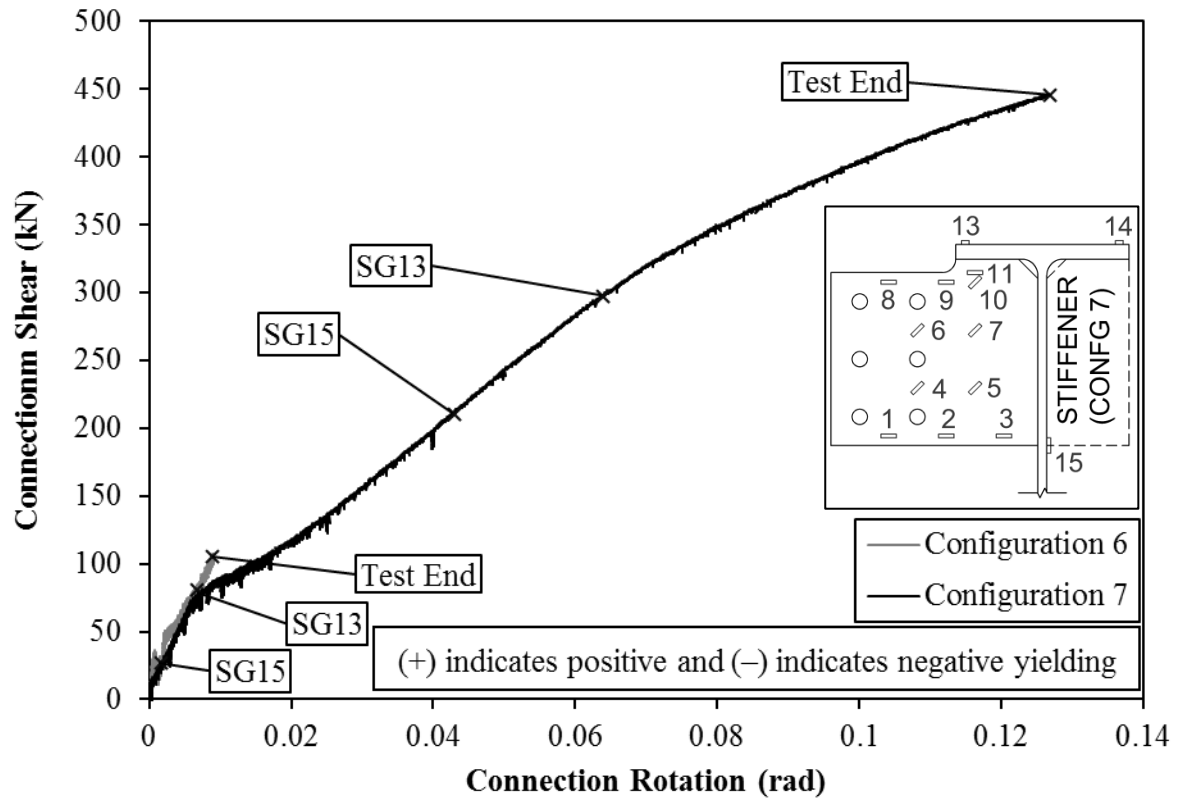


Figure 4.21: Connection Shear vs. Rotation, Configurations 6 & 7

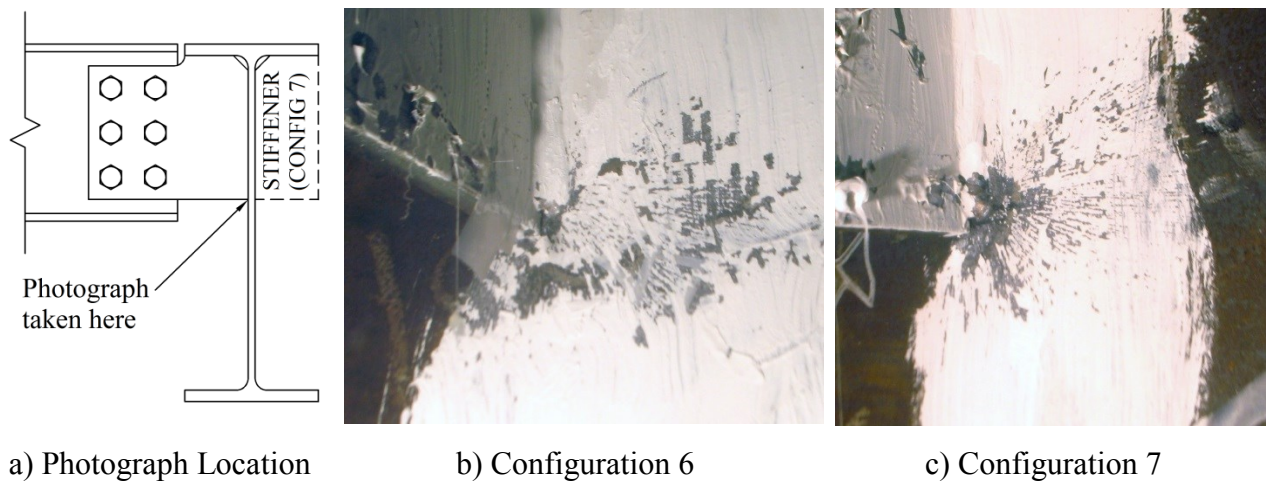


Figure 4.22: Girder Web Yielding at Base of Shear Tab, Configuration 6 and 7

The stiffened connection (Configuration 7) was subject to significant bearing deformation at the steel around the bolt holes. At a connection shear of 75kN, there was a sudden decrease in shear-rotation stiffness due this deformation controlling the overall connection response (Figure 4.21). This can be seen clearly when the relation between the connection shear

and the computed bolt hole bearing rotation is examined. This rotation is estimated as the difference between the beam rotation and the shear tab rotation (see Figure 4.23). These rotations were measured using inclinometers placed on the shear tab and beam end. The bolt hole bearing rotation is seen to be negligible up until a connection shear of 75kN, after which it increases rapidly (Figure 4.24). The expected bolt bearing resistance was calculated to be 364kN using the I.C.R. Method (CISC 2010). Figure 4.25a illustrates the extent of bearing deformation within the beam web. Figure 4.25b illustrates the lack of deformation in the bolt holes in the shear tab.

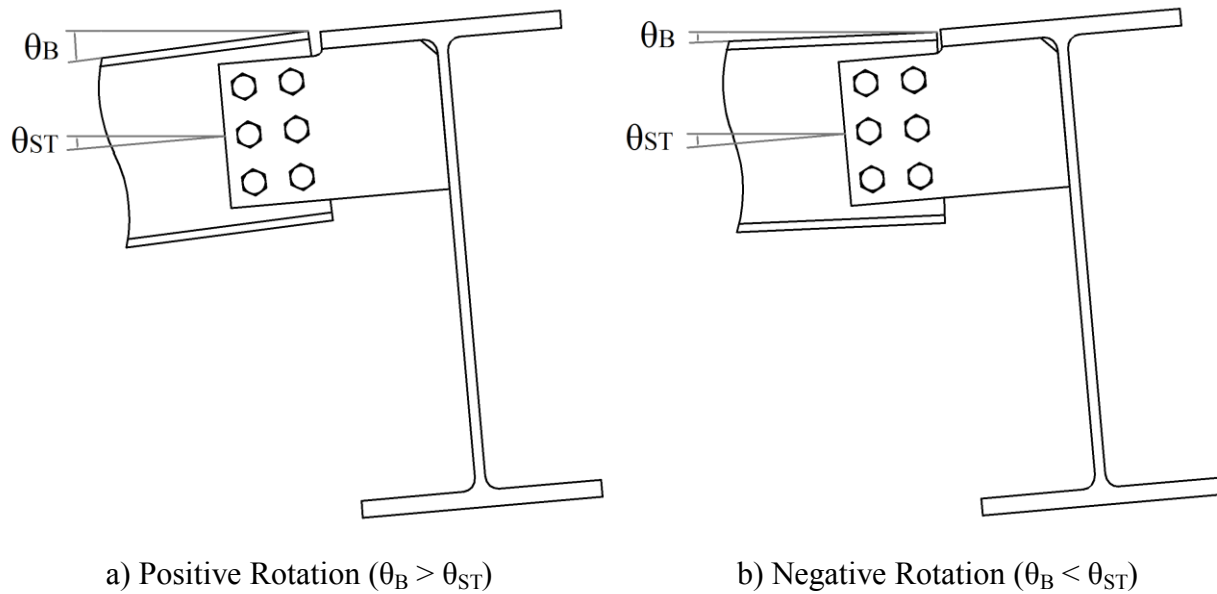


Figure 4.23: Computed Bolt Bearing Rotation Schematic and Sign Convention

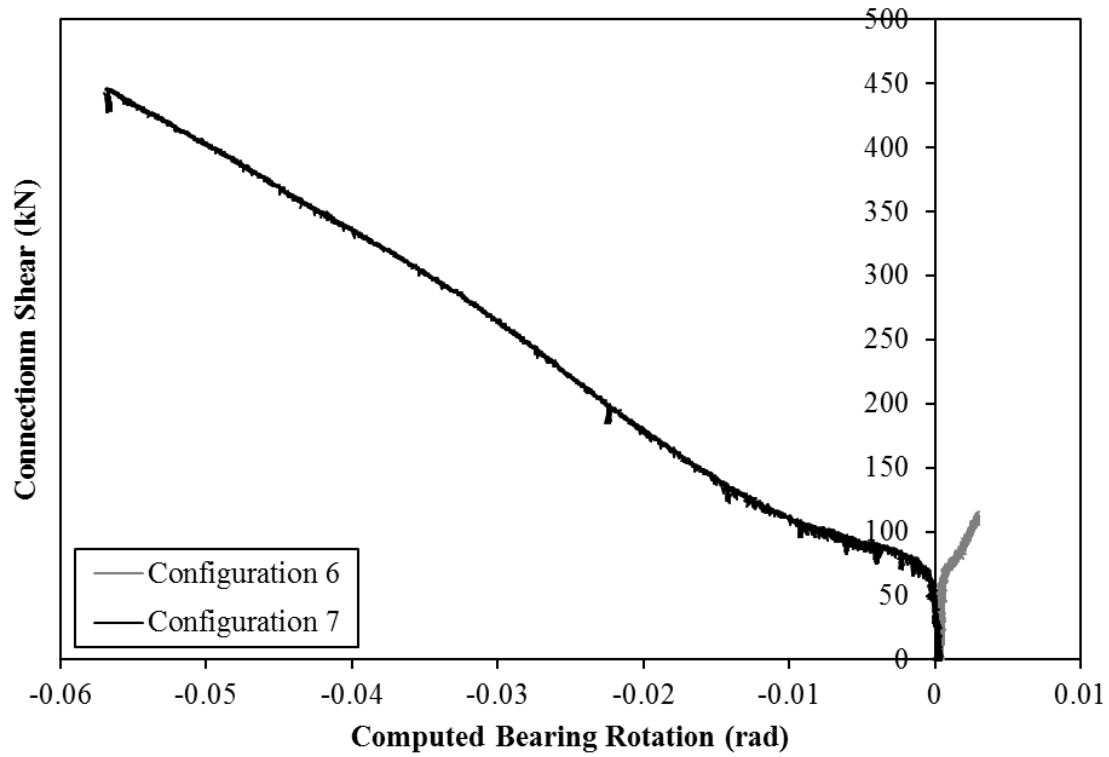


Figure 4.24: Connection Shear vs. Computed Bolt Bearing Rotation, Configurations 6 & 7



a) Beam Web

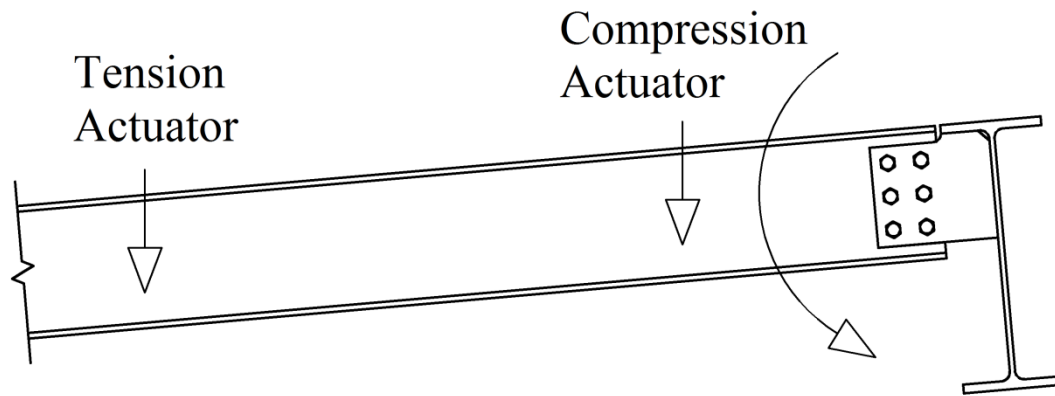
b) Shear Tab

Figure 4.25: Beam vs. Shear Tab, Deformation Around Bolt Holes, Configuration 7

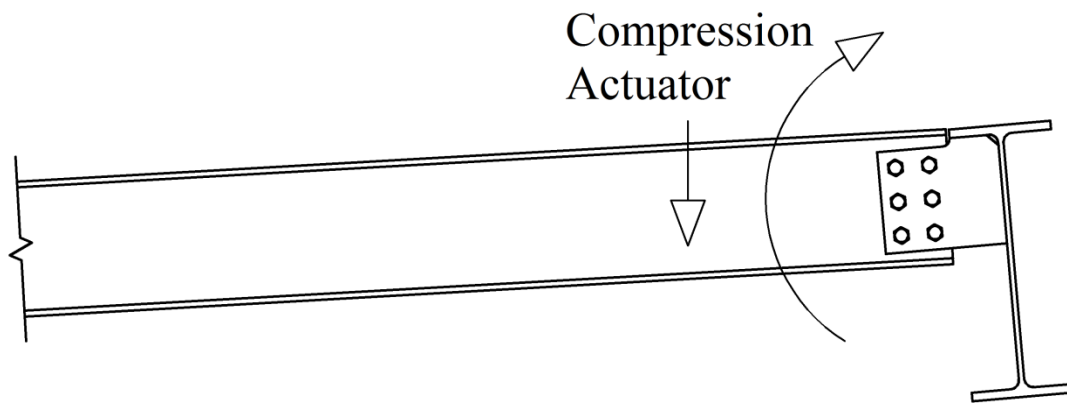
It should be noted that the unstiffened connection was seen to have “positive” bolt bearing rotation (Figure 4.23a) whereas the stiffened was seen to have “negative” (Figure 4.23b). For the stiffened connection, looking at the deformation of steel around the beam bolt holes (Figure 4.25) reveals that the rotation is in a counter clockwise direction. This confirms that the shear tab is rotating more than the beam end, thus creating negative bolt bearing rotation. The difference in sign in the bolt bearing rotation between the unstiffened and stiffened connections can be attributed to the fact that the bolt bearing failure did not initiate for the unstiffened connection. Stiffening of the beam web allowed for yielding to occur in the shear tab itself, delaying deformation in the bolt holes.

The response of Configurations 9 and 10 were seen to be very similar to each other, indicating that the effect of the additional stiffener on the back side of the web for larger girders was not as significant as for the smaller girders (Figure 4.19 and 4.20). This is due to the larger girder having thicker webs and wider flanges, which greater resist localized stresses. For the stiffened connection (Configuration 10), tension yielding on the back side of the girder web (SG27) was measured at a connection shear of 127kN. For the unstiffened connection (Configuration 9), SG27 did not record yielding and it is likely that it malfunctioned given the extent of damage observed to the web. Compressive yielding in the opposite side of the girder web was evident for both configurations (Figure 4.21). Yielding of the girder top flange (SG25) occurred at a connection shear of 183kN for the unstiffened connection and 188kN for the stiffened.

In testing of both the unstiffened and stiffened connections, the tension actuator reached its maximum stroke before any significant change in rotational stiffness was seen. At this point, the tension actuator was held at maximum stroke while the displacement on the compression actuator was increased. This caused the connection rotation to decrease and the connection shear to increase. Figure 4.26 illustrates the behaviour of the beam and shear tab in the two phases of loading. Figures 4.27a and 4.27b show the connection shear vs. rotation and connection shear vs. deflection, respectively. The deflection was computed as the difference in vertical deflection of the beam end and the girder.



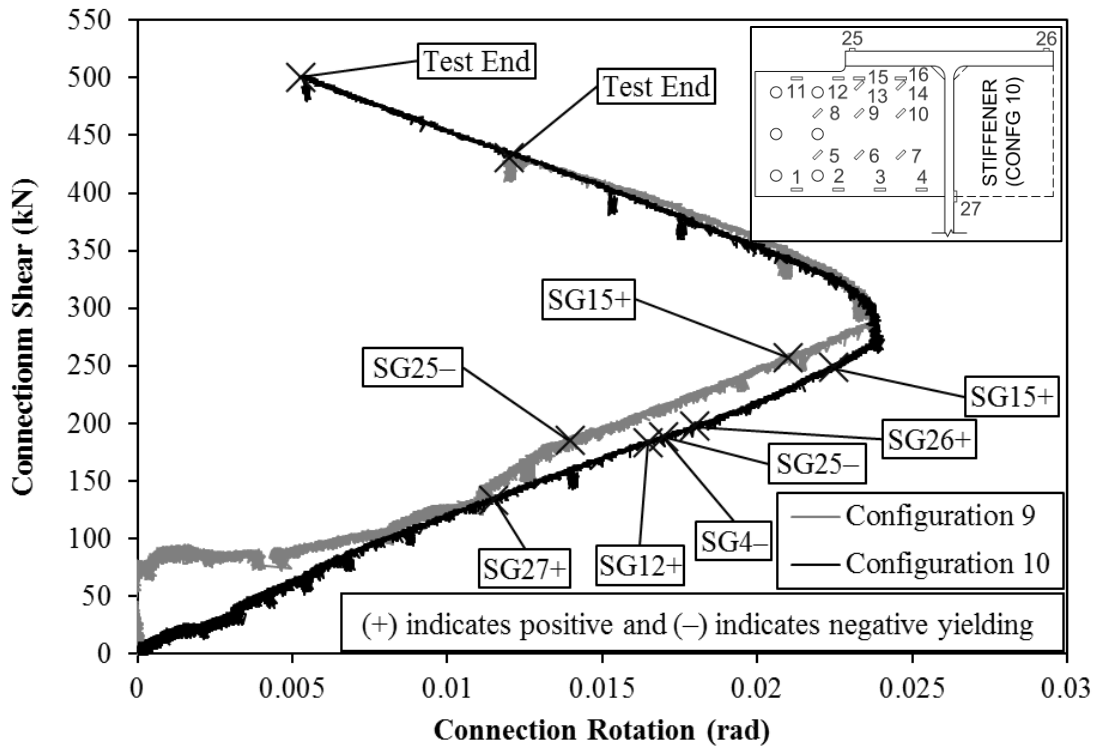
a) Phase I – Tension and Compression Actuator Displacement Increasing



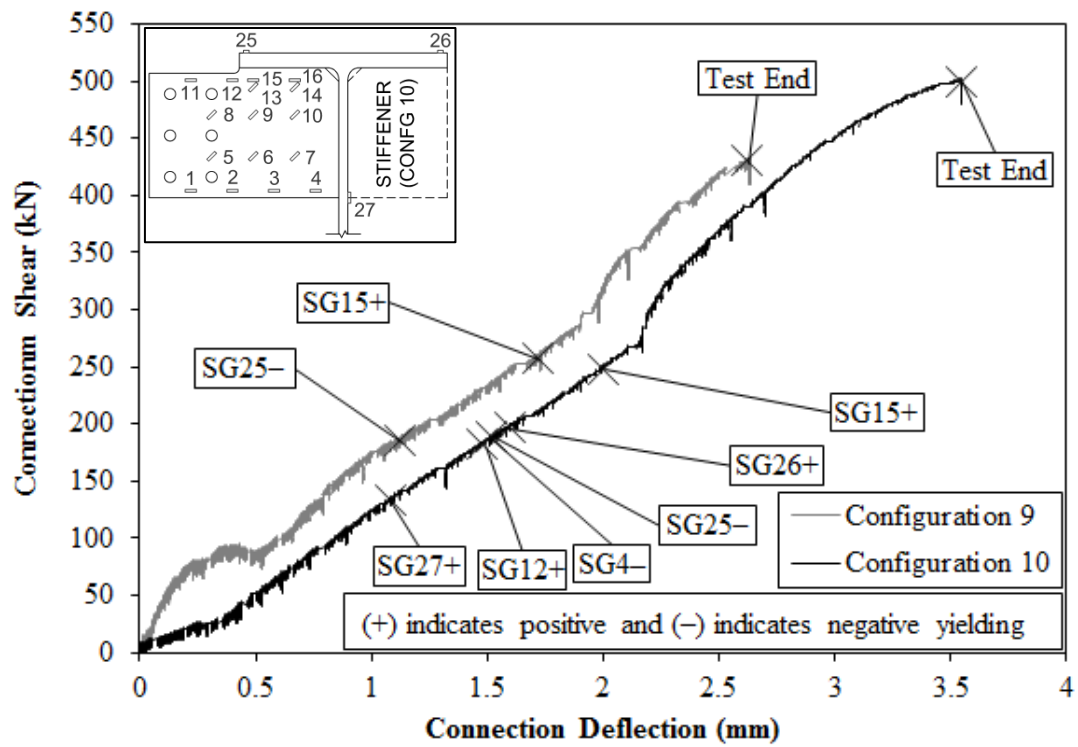
b) Phase II – Tension Actuator Stopped and Compression Actuator Displacement Increasing

Figure 4.26: Beam Behaviour for Load Phases, Configuration 9 and 10

Flexural yielding in the shear tab occurred at a connection shear of 150kN (at SG4 and SG12) for the stiffened connection. A corresponding stiffness decrease of the connection was not observed. Flexural yielding of the shear tab was not seen for the unstiffened connection. This is most likely due to the deformation of the unstiffened connection occurring primarily in the supporting girder.



a) Connection Shear vs. Rotation



b) Connection Shear vs. Deflection

Figure 4.27: Connection Response, Configurations 9 & 10

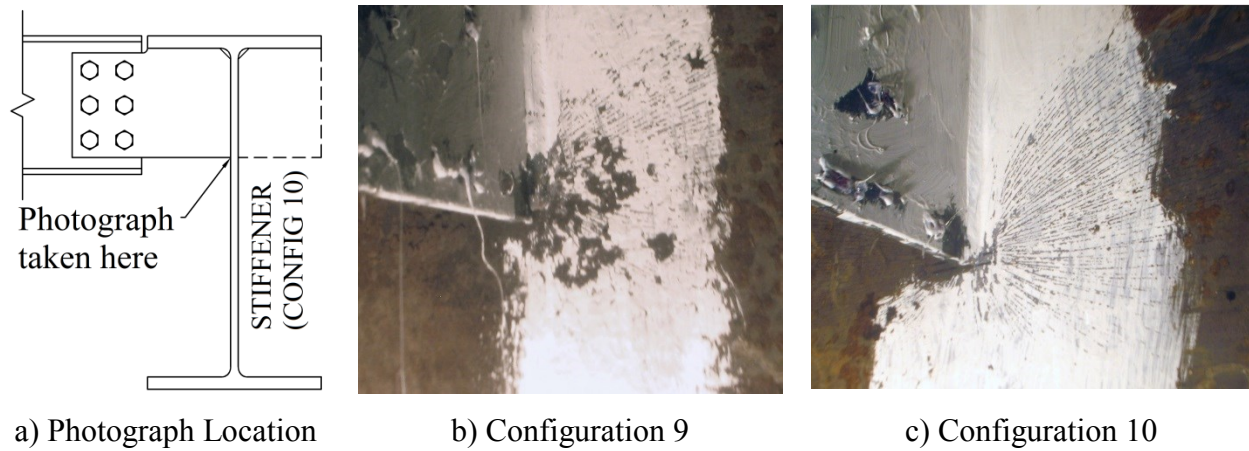


Figure 4.28: Girder Web Yielding at Base of Shear Tab, Configuration 9 and 10

Side Plate Beam-to-Girder Connection (8)

The side plate connection (Configuration 8) was expected to fail by bolt bearing on the beam web. Bearing failure was observed in the form of rotational bolt bearing deformation within the stiffener and combined rotational and vertical bolt bearing deformation in the beam web (Figure 4.29).

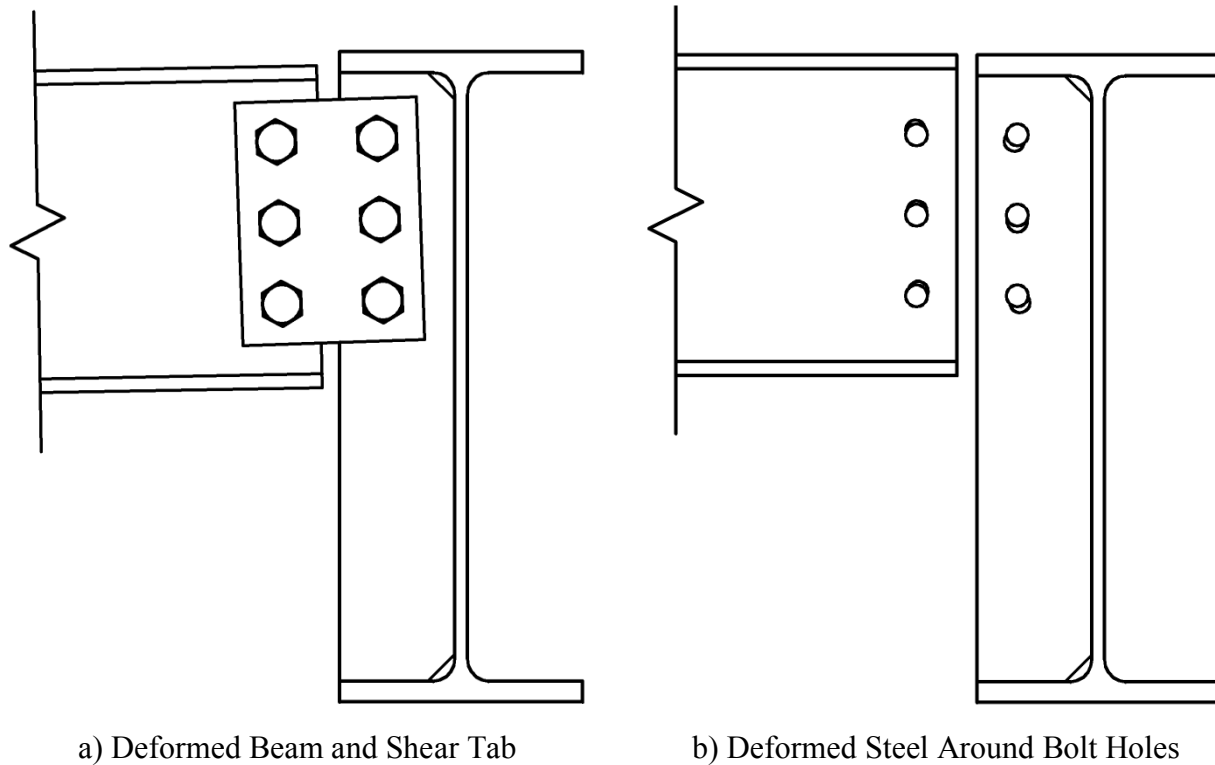


Figure 4.29: Bolt Bearing Failure, Configuration 8

The stiffness remained relatively constant up until a connection shear of 360kN (Figure 4.30). After which the stiffness decreased due to significant bolt bearing deformation in both the beam web and the stiffener. Figure 4.31 illustrates the bearing deformation in the steel around the bolt holes in the beam web, stiffener and one of the two side plates. Vertical and rotational deformation can be seen in the beam web whereas only slight rotation is seen in the stiffener. No deformation is seen in the side plates themselves. This is expected as bearing resistance is directly proportional to the thickness of the bearing element. The two 9.5mm (3/8in) plates have a total bearing thickness of 19mm (3/4in). This is much greater (2.5x) than the beam web thickness of 7.5mm (0.295in).

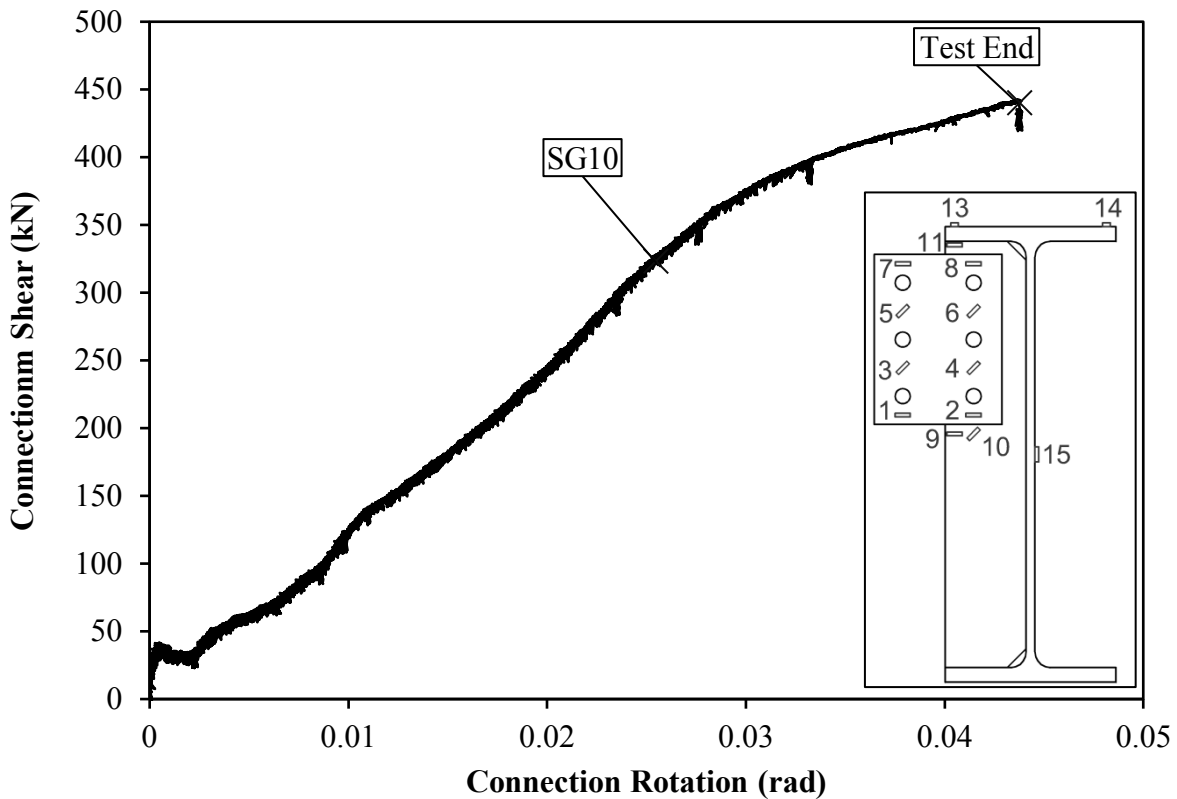
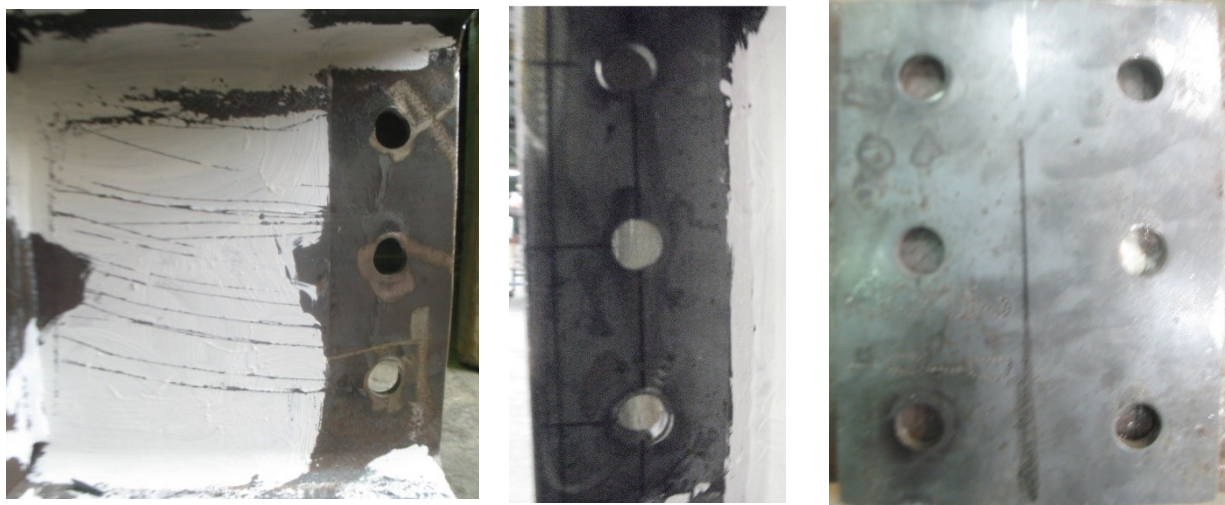


Figure 4.30: Connection Shear vs. Rotation, Configuration 8



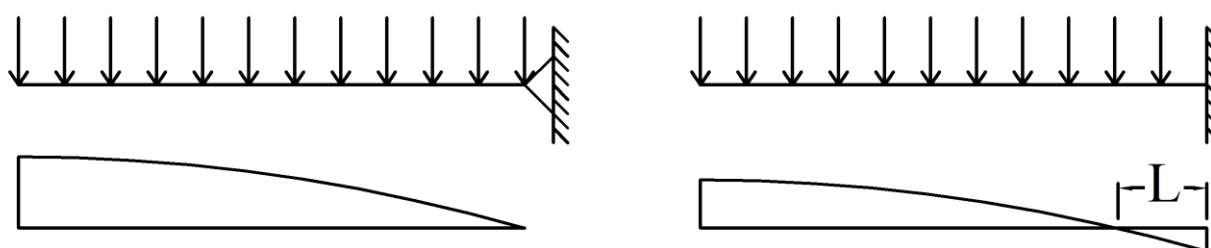
a) Beam Web

b) Stiffener

c) Side Plate

Figure 4.31: Bearing Deformation at Bolt Holes in Side Plate Connection, Configuration 8

The side plate connection failed in bearing as predicted. Failure was expected to occur at a connection shear of 178kN, approximately 50% of the measured resistance. This discrepancy is most likely due to assuming the zero moment inflection point is at the centre of the supporting girder. In actuality, the inflection point would likely be outside the girder centroid and thus, the bearing resistance would be much larger. Figure 4.32 illustrates the difference in bending moment diagrams for an idealized simple support versus a realistic simple support which resists some moment.



a) Idealized Simple Support

b) Actual Support (Moment Restraint)

Figure 4.32: Moment Diagrams for Idealized vs. Experimental Zero Moment Inflection Point

The experimental eccentricity, L , can be calculated for a three bolt connection with bolt pitch of 80 mm using the experimental bolt bearing resistance. The measured bearing resistance is taken as the connection shear at which the rotational stiffness of the connection began to decrease.

$$C_{experimental} = \frac{B_{r,experimental}}{3\phi_{br}d_b t_{web} F_{u,web}} = \frac{(360 \text{ kN})}{3(1.0)\left(\frac{3}{4}in \times 25.4 \text{ mm/in}\right)(7.5 \text{ mm})(485 \text{ MPa})} = 1.73$$

$$\frac{75 - L}{75 - 100} = \frac{1.87 - (1.73)}{1.87 - 1.5} \rightarrow L = 85 \text{ mm}$$

Thus, the experimental inflection point is solved for as $(170 \text{ mm} - 85 \text{ mm}) = 85 \text{ mm}$. Therefore, the girder provides some moment restraint. If the girder provided zero moment restraint, the moment at the support face would be zero. This would mean that the connection acted as an idealized pin connection. Since the moment is not zero, the connection provides some flexural resistance.

4.4. Recommendations

4.4.1. Weld Proportioning

The shear-tab-to-column weld fractured to approximately half of the shear tab height for configurations 1 and 3. For both configurations, the welds were sized at 5/8ths of the plate thickness to develop yielding in the shear tab as specified in the AISC Manual (2010). Muir and Hewitt (2009) derived the required weld thickness to develop yielding in shear tabs of ASTM A572 Grade 50 (345 MPa yield stress) steel welded with E70 (490 MPa) electrodes such that:

$$w \geq \frac{t_p F_y \sqrt{3}}{2F_{EXX}} = \frac{(345 \text{ MPa})\sqrt{3}}{2(490 \text{ MPa})} t_p = 0.61 t_p \cong \frac{5}{8} t_p \quad (4.1)$$

The shear tab plate material used in this testing program had a measured yield stress of 456 MPa. This value for yield stress can be substituted into Equation 4.1 as seen below.

$$w \geq \frac{t_p F_y \sqrt{3}}{2F_{EXX}} = \frac{(456 \text{ MPa})\sqrt{3}}{2(490 \text{ MPa})} t_p = 0.8 t_p$$

Thus, the welds should have been sized at approximately 80% of the plate thickness as opposed to 5/8ths (62%). This explains the severity of weld tearing in Configurations 1 and 3. Since the designer does not know the actual plate yield stress when designing a shear tab connection, an assumption has to be made. In Canada, the probable yield stress is typically assumed to be 110% of the minimum specified yield stress as stated in CSA S16-09 (2009) Clause 27.1.7. This is consistent with AISC's Seismic Provision for Structural Steel Buildings

(2005). Table I-6-1 9 (AISC 2005) specifies that for Grade 50 steel, R_y and R_t are taken as 1.1. Thus, this author recommends replacing the 5/8ths requirement with a modified Equation 4.1 that takes into account the probable plate yield stress.

$$w \geq \frac{t_p(1.1F_y)\sqrt{3}}{2F_{EXX}} \quad (4.2)$$

For ASTM A572 Grade 50 steel welded with E70 electrodes, the required weld thickness by Equation 4.2 becomes 11/16ths of the plate thickness.

4.4.2. Buckling at Unsupported Edges of Shear Tab Connections

Configurations 2 and 4 were subject to plastic local buckling failures. The bottom (compression) edge of the shear tab buckled outwards near the weld once the buckling resistance had been reached. When calculating the local buckling resistance using the AISC (2010) extended shear tab design method, the designer is instructed to treat the shear tab as a doubly coped beam. There are two ways that the local buckling resistance of the shear tab can be calculated: i) lateral torsional buckling (f_d) model and ii) classical plate buckling (Q) model. The first model assumes that the top of the shear tab will laterally-torsional buckle outwards at the edge of the beam (see Figure 4.33). The second model assumes that the unsupported length of shear tab (between the support face and the bolts) will buckle outwards. Design equations can be found in Section 3.3.1 under “Design Check 5 – Local Buckling” (AISC 2010).

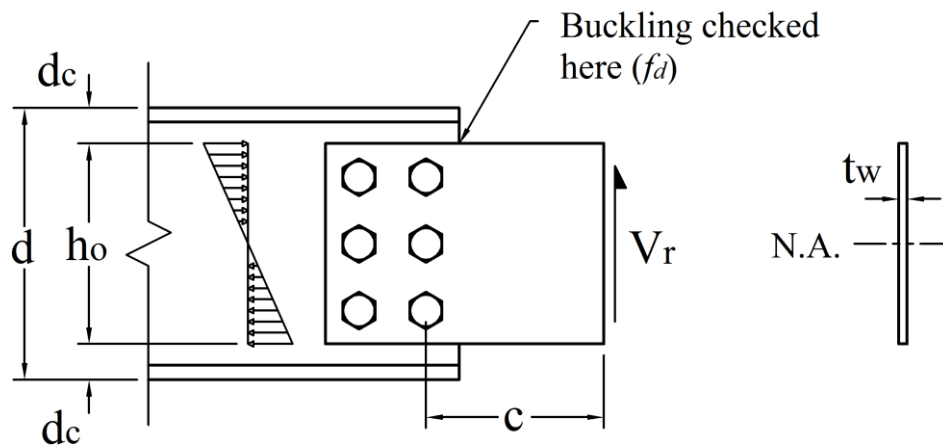


Figure 4.33: Local Buckling Schematic, Reproduced from AISC Manual (2010)

Table 4.4 compares the measured buckling loads for these two configurations with the calculated buckling resistances. For both of these configurations, the lateral torsional buckling (f_d) formulation can be used to calculate the buckling resistance of the shear tab due to dimensional limitations being met. This formulation, however, significantly over predicts the buckling resistance in both cases. The conservative classical plate buckling (Q) formulation is seen to give more accurate results. It appears that for relatively short cope lengths (such as for shear tab connections), lateral torsional buckling at the top edge of the unsupported length of the shear tab is not an applicable limit state.

Table 4.4: Measured vs. Predicted Local Buckling Resistance, Configuration 2 and 4

#	V_{test} kN	$D_c < 0.2d?$	$C < 2d?$	f_d or Q	$V_{calc}(f_d)$ kN	Measured/ Predicted	$V_{calc}(Q)$ kN	Measured/ Predicted
2	215	$41 < 62$	$203 < 610$	f_d	781	0.28	185	1.16
4	838	$115 < 123$	$152 < 1234$	f_d	3352	0.25	984	0.85

This author recommends using the classical plate buckling (Q) formulation for calculation of the buckling resistance since: i) the predicted resistances calculated using the classic plate buckling model are much more accurate than those obtained by using the lateral torsional buckling model, and ii) the buckled shape of both test configurations are characteristic of the classical plate buckling model.

4.4.3. Buckling of Full Height Beam-to-Girder Connections

All three full-height extended beam-to-girder shear tab configurations (5, 11 and 12) underwent the same characteristic buckling failure. Once the buckling resistance of the connection had been reached, significant out-of-plane deformation occurred at the neck of the shear tab (shaded region in Figure 4.15a). This was accompanied with a significant shear-rotation stiffness decrease and eventually the bottom flange of the beam began to bear on the stiffener itself.

The limit state of buckling as observed in the connections with full height stiffeners is not explicitly addressed in the AISC extended shear tab design method (AISC 2010). This author

recommends an additional design check be included in the AISC design method for cases where a full height shear tab is specified.

For a thin plate in biaxial compression (Figure 4.35), the critical stress in the primary direction, σ_1 , is given by [Rees (2009)]:

$$(\sigma_1)_{cr} = \frac{\pi^2 E t^2 [(m/a)^2 + (n/b)^2]^2}{12(1 - \nu^2) [(m/a)^2 + \beta(n/b)^2]} \quad (4.3)$$

where t is the plate thickness, a and b are the height and width of the plate, m and n are the number of buckling half-waves in either direction and β is the ratio of stresses ($\beta = \sigma_2/\sigma_1$), as illustrated in Figure 4.34.

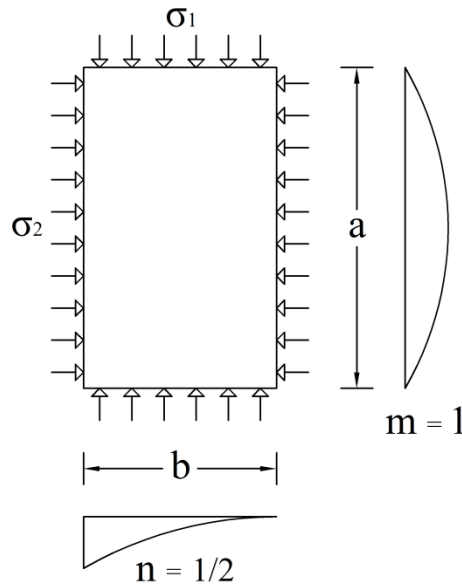


Figure 4.34: Buckling of a Thin Plate Under Biaxial Compression, Modelled After Rees (2009)

The portion of the shear tab connection within the bottom and top flanges of the supporting girder will be referred to as the stiffener and the bolted portion as the shear tab (Figure 4.15a). The stiffener is assumed to act as simply supported in the vertical direction ($m=1$) and as fixed-free in the horizontal direction ($n=1/2$). The height of the plate, a , is taken as the height of the girder web (h_w). The width of the plate, b , is taken as the half of the girder flange width ($b_f/2$). Substituting these values into Equation 4.3 gives the following:

$$(\sigma_1)_{cr} = \frac{\pi^2 E t^2 \left[\left(\frac{1}{h} \right)^2 + \left(\frac{1}{b_f} \right)^2 \right]^2}{12(1 - \nu^2) \left[\left(\frac{1}{h} \right)^2 + \beta \left(\frac{1}{b_f} \right)^2 \right]} \quad (4.4)$$

The vertical stress, σ_1 , is assumed to be a function of the connection shear, V , and acts over the area of the stiffener.

$$\sigma_1 = \frac{V}{\frac{1}{2} b_f t} = \frac{2V}{b_f t} \quad (4.5)$$

The horizontal stress, σ_2 , is taken as the maximum compressive stress acting horizontally on the stiffener. Flexural stresses are assumed to act upon the face of the stiffener in a linear elastic fashion (Figure 4.35). These stresses are assumed to act differently depending on how deep the shear tab is with respect to the height of the stiffener. For shear tabs with depths less than half the stiffener height [$d < \frac{1}{2}h$] the neutral axis is taken as mid-height of the shear tab [$X_1 = X_2$]. For shear tabs with depth of greater than half the stiffener height [$d > \frac{1}{2}h$] the neutral axis is taken as mid-height of the stiffener [$X_1 > X_2$]. These two classifications are referred to as shallow and deep shear tabs, respectively.

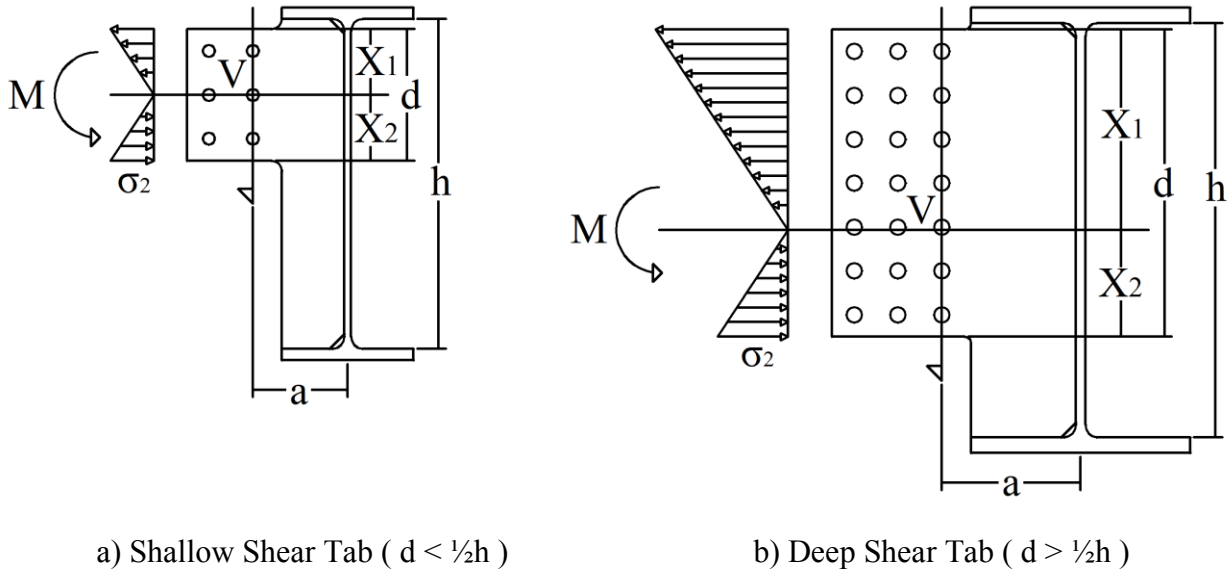


Figure 4.35: Horizontal Stress for Full Height Beam-to-Girder Buckling Calculation

The connection moment, M , is assumed to be the product of the connection shear, V , and the “a” distance, a , (such that $M = Va$). Summation of the moments about the neutral axis gives:

$$\Sigma M_{@N.A.} = M - \frac{1}{3}\sigma_2 t \left(\frac{X_1^3}{X_2} + X_2^2 \right) = 0 \rightarrow \sigma_2 = \frac{3Va}{t \left(\frac{X_1^3}{X_2} + X_2^2 \right)} \quad (4.6)$$

The stress above the neutral axis acts away from the stiffener and thus does not apply compression to the stiffener. Since tension does not decrease the buckling resistance of the plate, these stresses are ignored. Now the stress ratio, β , can be calculated as:

$$\beta = \frac{\sigma_2}{\sigma_1} = \frac{3Va}{t \left(\frac{X_1^3}{X_2} + X_2^2 \right)} \times \frac{b_f t}{2V} = \frac{3b_f a}{2 \left(\frac{X_1^3}{X_2} + X_2^2 \right)} \quad (4.7)$$

For computation of the biaxial buckling resistance of the connection, the critical vertical stress, $(\sigma_I)_{cr}$, is set equal to the applied vertical stress, σ_I , and rearranged in terms of the shear resistance, V .

$$V = \frac{\pi^2 E b_f t^3 \left[\left(\frac{1}{h} \right)^2 + \left(\frac{1}{b_f} \right)^2 \right]^2}{24(1 - \nu^2) \left[\left(\frac{1}{h} \right)^2 + \beta \left(\frac{1}{b_f} \right)^2 \right]} \quad \text{with} \quad \beta = \frac{3b_f a}{2 \left(\frac{X_1^3}{X_2} + X_2^2 \right)} \quad (4.8)$$

Table 4.5 gives the calculated buckling resistance, V_{calc} , for the full height beam-to-girder configurations based on Equation 4.6 and 4.7, in addition to the measured shear resistance of the connection, V_{test} . The value for the measured resistance is taken as the connection shear at which buckling became significant and there was a significant decrease in shear-rotation stiffness. Configuration 5 is classified as shallow [case i)] because the shear tab height, d , is less than half the stiffener height, h . Configurations 11 and 12 are both classified as deep [case ii)]. The calculated values appear to be accurate and thus this formulation provides a good estimate for the buckling resistance. Increasing the plate thickness is a suitable way to increase the buckling resistance, given that this results in a cubic increase in buckling resistance.

Table 4.5: Calculated vs. Measured Buckling Resistance, Full-Height Configurations

#	b_f mm	t mm	h mm	a mm	Case	X_1 mm	X_2 mm	β	V_{calc} kN	V_{test} kN	Measured/ Predicted
5	229	9.5	572	165	i) Shallow	114	114	2.17	198	221	1.12
11	381	9.5	719	241	ii) Deep	343	114	0.38	511	490	0.96
12	381	9.5	719	241	ii) Deep	349	184	0.52	420	389	0.93

4.4.4. Girder Rigidity

All of the tests on partial-height beam-to-girder configurations (6, 7, 9 and 10) were characterized by significant localized deformation in the supporting girder. The top of flange of the supporting girder was not restrained in this testing program. In typical construction, a slab resting on the top flange would stiffen the girder significantly, and thus would likely influence the behaviour. Nonetheless, construction may exist in which the girders are not restrained; in such cases the findings of this research are applicable.

There is currently no design check in the AISC Manual (2010) that addresses the ability of the supporting girder to resist these localized deformations. This author recommends a torsional strength check for partial-height beam-to-girder shear tab connections that are considered to have flexible support conditions. As stated in Chapter 1: for beam-to-girder connections, the support condition is considered flexible when a beam frames into a single side of a girder. A reinforced concrete slab resting on the top flange of the supporting girder was not present in these tests. The inclusion of a slab would most likely prevent girder deformation by resisting the upwards movement of the flange tip away from the connection, which would limit downwards movement of the flange tip close to the connection. Since the flange tip close the connection is directly connected to the web through the shear tab itself, web deformation would be minimized.

For an unstiffened connection, only the portion of the top girder flange above the shear tab and the top segment of the web are assumed to resist the applied torsion. For a stiffened connection, the entire top flange as well as the top segment of the girder web is assumed to resist the same torsion. Thus, the stiffened connection would have a higher strength. This is consistent with the test results. Figure 4.37 illustrates the difference between a stiffened and an unstiffened connection.

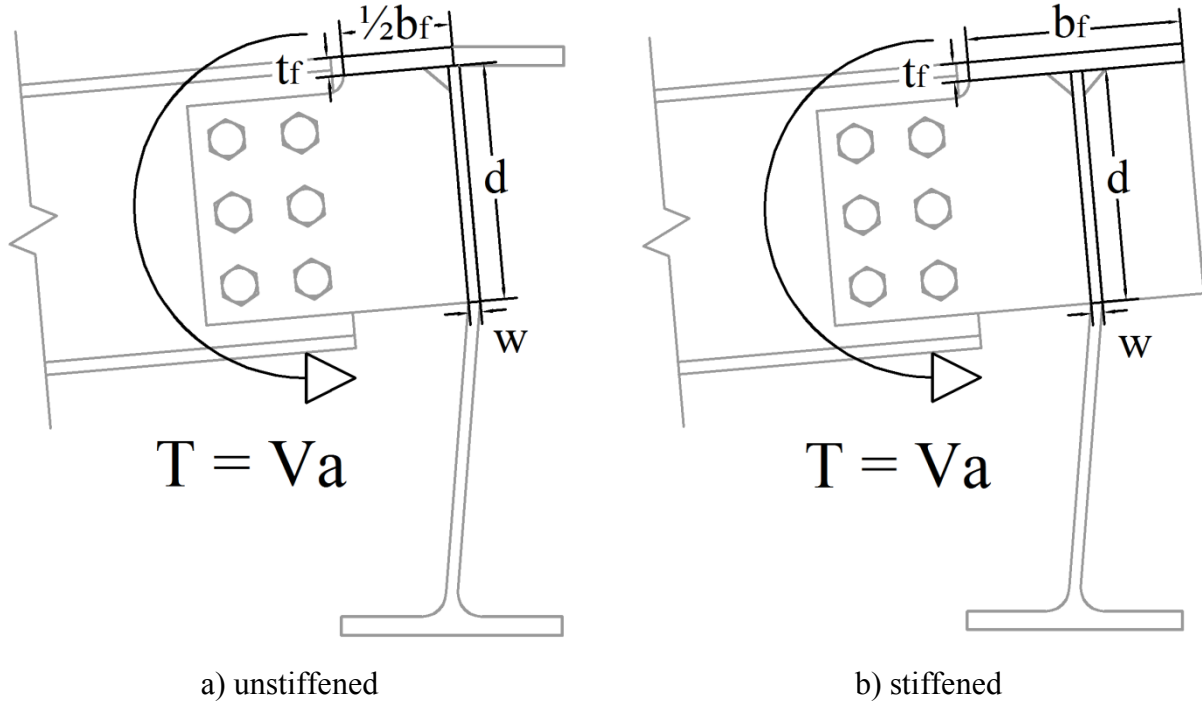


Figure 4.36: Torsional rigidity for partial-height beam-to-girder shear tab connections

The torsional rigidity, J , can be calculated for both unstiffened and stiffened:

$$J_{unst} = \frac{1}{3} \left(\frac{1}{2} b_f \right) (t_f)^2 + \frac{1}{3} (d)(w)^2 \quad (4.9)$$

$$J_{stif} = \frac{1}{3} (b_f) (t_f)^2 + \frac{1}{3} (d)(w)^2 \quad (4.10)$$

where b_f is the flange width, t_f is the flange thickness, d is the shear tab depth and w is the web thickness.

The maximum shear stress in the girder web, $\tau_{max,w}$, can be expressed in terms of the applied torsion, T , the web thickness, w , and the modulus of rigidity.

$$\tau_{max,w} = \frac{Tw}{J} \quad (4.11)$$

The applied torsion is assumed to be the connection moment ($T = Va$ where V is the connection shear and a is the “a” distance). The shear stress is taken as the shear yield stress of steel ($\tau_y = 0.6F_y$) such that the shear causing yielding of the web can be solved for.

$$\tau_y = \frac{Vaw}{J} \rightarrow V = \frac{0.6F_y J}{aw} \quad (4.12)$$

Table 4.6 compares the calculated girder yielding resistances using Equations 4.12, 4.9 and 4.10 with the measured resistances from testing. The values aren't very accurate but they give a good indication of whether or not girder yielding will be present. The most effective way to minimize girder yielding would be to provide a full height stiffener opposite of the shear tab. This would significantly stiffen the girder web and eliminate yielding.

Table 4.6: Calculated vs. Measured Girder Yielding Resistances for Partial-Height Beam-to-Girder Connections

#	Stiffened or Unstiffened	J mm ³	w mm	a mm	V _{calc} kN	V _{test} kN	Measured / Predicted
6	Unstiffened	416×10 ³	11.9	165	44.4	26	0.59
7	Stiffened	703×10 ³	11.9	165	84.5	210	2.79
9	Unstiffened	1610×10 ³	16.6	241	75.2	-	-
10	Stiffened	2880×10 ³	16.6	241	150.8	127	0.84

4.5. Summary

Twelve extended shear tab connections were subjected shear and rotational loading. The measured resistances were compared to those predicted by the combined AISC Manual (2005), CSA S16-09 (2009), and CISC Handbook (2010) extended shear tab design method. In design, these predicted resistances were computed with 110% of the nominal material properties. Coupon testing was conducted to determine the actual material properties of the plate steel and test beams.

The beam-to-column tests showed good agreement between the predicted and measured resistances. Plastic local buckling was accurately predicted by the classical plate buckling formulation (as opposed to the lateral torsional buckling model). All of the beam-to-column tests were characterized by some tearing of the plate-to-column welds. This was due to under sizing of the welds. The AISC (2010) design method specifies sizing the welds 5/8ths of the plate thickness. This ratio is based on experimental observation [Astaneh et al. (1989)] as well as theory [(Muir and Hewitt (2009))]. It is recommended that this ratio be replaced by Muir and Hewitt's design equation with the plate yield stress taken as 110% of the nominal.

The full-height beam-to-girder tests were characterized by plastic buckling of the stiffener portion of the shear tab. A design check is proposed taking into account the vertical stresses due to the connection shear and the horizontal stresses due to flexural action of the beam.

The partial-height beam-to-girder shear tab tests revealed that girder web and flange deformation is significant when the top flange of the supporting girder is unrestrained. In these cases, including a stiffener opposite the shear tab for flexible connections can reduce the deformation.

The side-plate connection failed in bearing as predicted, although, at a much higher resistance than anticipated. The bearing resistance is calculated under the assumption that the inflection point of the beam is at the support face. The increased measured resistance is attributed to the fact that the inflection point is closer to the bolt group.

Chapter 5 – Conclusions and Recommendations

5.1. Summary

Shear tab connections are a simple and cost effective simple shear connection for steel construction. There are two classifications of shear tab connections: conventional and extended. Those with “a” distances (distance between support face and first vertical row of bolts) exceeding 89mm (3½in) or those with more than one vertical row of are considered extended [as defined in the AISC Manual (2010)]. The others, considered conventional, can be designed using either the CISC Handbook (2010) or AISC Manual (2010). These design methods have been confirmed to accurately predict the behaviour of conventional shear tab connections through previous testing. The behaviour of extended shear tab connections, however, has not been thoroughly explored: specifically those with “a” distances greater than 89mm (3½in) and with more than one vertical row of bolts.

In Canada, extended shear tabs have typically been designed using the AISC Manual (2010) design method for extended shear tabs, substituting CISC Handbook (2010) and CSA S16-09 (2009) provisions where possible.

Full-scale testing was conducted on 12 representative extended shear tab connections to assess the accuracy of current industry design practice in predicting their behaviour and resistance. Four tests were conducted on beam-to-column flange (rigid support) and eight on beam-to-girder (flexible support). All of the test configurations had “a” distances exceeding 89mm (3½in) and two or more vertical rows of bolts.

The test configurations were designed in accordance with the AISC Manual (2010) extended shear tab design method, substituting design equations from the CISC Handbook (2010) and CSA S16-09 (2009) where possible. All configurations were detailed with 9.5mm (3/8in) thick shear tabs.

Three beam-to-column tests were detailed with 229mm (9in) shear tabs supporting W310x74 beams. Two of these tests were conducted on geometrically identical connections with “a” distances of 152mm (6in) and two vertical rows of three bolts, one of which was bolted and the other welded with a partial “C” shape weld. The shear resistance of both connections was

ultimately governed by the capacity of the weld to the support face. The weld underwent flexural tearing to an extent greater than half the plate height for the bolted connection and approximately half the plate height for the welded connection. The geometry for the third small beam test configuration was very similar to the welded-bolted pair but with an increased “a” distance of 203mm (8in). Plastic buckling of the bottom edge of the shear tab was found to be the governing limit state. The fourth beam-to-column test was conducted on a 457mm (18in) shear tab supporting a W610x140 beam. This connection had two vertical rows of six bolts and underwent flexural yielding and buckling of the shear tab while the ultimate resistance was governed by net section rupture of the shear tab along the vertical row of bolts closest to the column.

The beam-to-girder test setup was designed as part of this research program. No rotational restraint of the girders was provided directly above the connections. This boundary condition is consistent with light industrial buildings where grating or steel deck (that does not provide rotational restraint) sit upon the girders and beams.

Three tests were conducted on beam-to-girder connections with shear tabs extending to the bottom flange of the supporting girder (full-height). All of the tests resulted in buckling at the neck of the shear tab (where the bottom edge of the shear tab meets the edge of the stiffener portion) which was accompanied with a sudden rotational stiffness decrease. Test beam sizes were W310x60, W610x140 and W690x125 with shear tab depths of 229mm (9in), 457mm (18in) and 533mm (21in), respectively. The buckling resistance of the W610x140 connection was found to be greater than the W690x125 connection even though the shear tab for the W610x140 was 76mm (3in) shallower. This is a particularly important observation because it illustrates that buckling for full-height shear tabs is due to a combination of vertical and horizontal stresses arising from flexural action of the beam and shear transfer.

Four tests were conducted on partial-height beam-to-girder connections (those with shear tabs welded to the underside of the top girder flange and part of the girder web). Significant localized deformation within the supporting girder was seen in all of the tests. This deformation was characterized by extensive yielding in the girder web at the base of the shear tab as well as in the portion of girder flange above the shear tab. All test configurations supported shallow beams (W310x60) and were designed with 229mm (9in) deep shear tabs with two vertical rows of three 19mm (3/4in) bolts. Two tests were run for each girder size: one without a partial-height

stiffener opposite the girder web and one with. For the shallow girder (W610x125), the inclusion of a stiffener delayed girder yielding by a significant amount. For the deeper girder (W760x257), the stiffener was not seen to make a difference.

A single test was run on a side-plate beam-to-girder connection. This connection took the form of two plates which were bolted through a single vertical row of three bolt holes in both the beam web and a full-height stiffener within the supporting girder. Bearing failure was predicted to be the governing limit state and this was proved correct by testing, although at a much larger resistance than anticipated. Thus, the assumption of the zero moment inflection point being located at the support face is conservative when calculating the bolt bearing and bolt shear resistances.

5.2. Recommendations

Two beam-to-column tests resulted in flexural tearing of the weld as the failure mode. Currently, the AISC (2010) design method recommends sizing the weld at 5/8ths of the plate thickness. This has been formulated by Muir and Hewitt (2009) and is applicable for 345MPa (50ksi) yield stress steel welded with E49 (E70) electrodes. The parent plate for the tested shear tab connections had a yield stress of 456MPa. Thus, the welds should have been sized at 4/5ths of the plate thickness using Muir and Hewitt's formulation (Equation 4.1) and accounting for the actual material strength. This author recommends calculating the required weld size using a formulation that accounts for the probable material properties of the shear tab (Equation 4.2) instead of using the current 5/8 t design rule. In this formulation, the probable value for the yield stress would be taken as 110% of the minimum specified yield stress.

Plastic buckling occurred in the two other beam-to-column tests. The design check for buckling in the AISC (2010) design method specifies that the designer treat the shear tab as a doubly coped beam to check the resistance. There are two methods specified for calculating this resistance: i) a lateral torsional buckling model and ii) a conservative classical plate buckling model. The latter was found to be more accurate in predicting the buckling resistance (with measured/predicted values of 1.16 and 0.85 for the W310x74 and W610x140 beams, respectively). This author recommends that the buckling resistance of the shear tab be calculated

by using the conservative classical plate-buckling model. This model assumes that the bottom edge of the plate (unsupported) buckles outwards in a plastic manner.

Biaxial buckling failure was consistent for all three full-height beam-to-girder connections. The current buckling design check assumes the length of shear tab between the beam and the support face is unsupported on the top and bottom. For full-height beam-to-girder shear tabs, the plate extends to the top and bottom girder flanges, thus, buckling is not thought to be applicable. Classical plate buckling theory was used to develop an equation for the biaxial plate buckling resistance (Equation 4.7). Calculated values show good agreement with the measured values (measured/predicted ratios of 1.12, 0.96 and 0.93 for the W310x60, W610x140 and W690x125 beams, respectively). The values calculated using the proposed design equation confirm that the W690x125 beam had a lower measured resistance than that of the W610x140.

This author recommends checking the ability of the supporting girder to resist localized deformations for partial-height beam-to-girder connections without slabs resting on the top girder flange. The proposed design equation (Equation 4.11) is a torsional stress check taking a reduced section of the girder. For connections without a stiffener, the reduced section includes the top portion of the girder web and the half of the flange above the shear tab (Equation 4.8). For connections with a stiffener opposite the shear tab, the reduced section includes the top portion of the girder web and the top flange (Equation 4.9).

5.3. Future Work

Biaxial buckling for full-height shear tabs should be investigated further. The stiffener portion for the three full-height shear tabs tested had very high slenderness ratios. Thus, buckling failure was probable. It is unclear if biaxial buckling would govern the connection resistance for those full-height connections having lower slenderness ratios.

More tests should be conducted on partial-height shear tabs that have the top flange of the supporting girder fully restrained. This is consistent with girders and beams supporting concrete slabs. Buckling of the bottom edge of the shear tab may be an applicable limit state for these connections as they most likely would behave with rigid support conditions.

References

- AISC (1963). *Manual of Steel Construction, 6th Edition*. American Institute of Steel Construction. Chicago, IL.
- AISC (1978). *Specification for the Design, Fabrication and Erection of Structural Steel for Buildings, 8th Edition*. American Institute of Steel Construction. Chicago, IL.
- AISC (1986). *Steel Construction Manual, Load and Resistance Factor Design, 1st Edition*. American Institute of Steel Construction. Chicago, IL.
- AISC (1993). *Steel Construction Manual, Load and Resistance Factor Design, 2nd Edition*. American Institute of Steel Construction. Chicago, IL.
- AISC (2001). *Steel Construction Manual, Load and Resistance Factor Design, 3rd Edition*. American Institute of Steel Construction. Chicago, IL.
- AISC (2005). *Steel Construction Manual, 13th Edition*. American Institute of Steel Construction. Chicago, IL.
- AISC (2005). *Seismic Provisions for Structural Steel Buildings*. American Institute of Steel Construction. Chicago, IL.
- AISC (2010). *Steel Construction Manual, 14th Edition*. American Institute of Steel Construction. Chicago, IL.
- ASTM (2013). *ASTM A370 – 13 Standard Test Methods and Definitions for Mechanical Testing of Steel Products*. American Society for Testing and Materials. Philadelphia, PA.
- Astaneh, A., McMullin, K.M., and Call, S.M. (1989). *Behaviour and Design of Steel Single Plate Shear Connections*. American Society of Civil Engineers – Journal of Structural Engineering, Volume 119, Issue 8, 2421-2440.
- Ashakul, Aphinat (2004). *Finite Element Analysis of Single Plate Shear Connections*. PhD Thesis, Dept. of Civil and Environmental Engineering, Virginia Polytechnic Institute. Blacksburg, VA.
- Baldwin Metzger, K.A. (2006). *Experimental Verification of a New Single Plate Shear Connection Design Model*. MSc. Thesis, Dept. of Civil and Environmental Engineering, Virginia Polytechnic Institute. Blacksburg, VA.
- Becker, E.P. and Richard, R.M. (1985). *DISCUSSION: Design of Single Plate Framing Connections with A307 Bolts*. American Institute of Steel Construction – Engineering Journal, Vol. 22, No. 1, First Quarter, 50-51.
- The British Constructional Steelwork Association Ltd. (2002). *Joints in Steel Construction: Simple Connections*. The Steel Construction Institute.

- Caccavale, S.E. (1975). *Ductility of Single Plate Framing Connections*. MSc Thesis, The University of Arizona. Tucson.
- CSA (2009). *S16-09 – Design of Steel Structures*. Canadian Standards Association. Mississauga, ON.
- CISC (2010). *Handbook of Steel Construction, 10th Edition*. Canadian Institute of Steel Construction. Markham, ON.
- Creech, D.D. (2005). *Behaviour of Single Plate Shear Connections with Rigid and Flexible Supports*. MSc Thesis, North Carolina State University. Raleigh, NC.
- Crocker J.P. and Chambers, J.J. (2004). *Single Plate Shear Connection Response to Rotation Demands Imposed by Frames Undergoing Cyclic Lateral Displacements*. American Society of Civil Engineers – Journal of Structural Engineering, Vol. 130, No. 6, 934-941.
- D’Aronco, M. (2014). *Behaviour of Double and Triple Vertical Rows of Bolts Shear Tab Connections and Weld Retrofits*. MAsc Thesis, Dept. of Civil Engineering, Ecole Polytechnique. Montreal, Quebec.
- Duggal, S. and Wallace, B. (1996). *Behavior and Applications of Slotted Hole Connections*. MSc Thesis, School of Civil Engineering and Environmental Science, University of Oklahoma. Norman, OK.
- Forcier, G. (2002). *Shear Tab Connection Primer*. Proceedings, American Institute of Steel Construction National Steel Conference, Seattle, 1-10.
- Gong, Y. (2010). *Plastic Behavior of Shear Tabs Welded to Flexible Wall Support*. American Society of Civil Engineers – Journal of Structural Engineering, Issue 136(10), 1197-1204.
- Goodrich, W. S. (2005). *Behavior of Extended Shear Tabs in Stiffened Beam-to-Column Web Connections*. MSc Thesis, Vanderbilt University. Nashville, TN.
- Hornby, D. E., Richard, R. M. , and Kreigh, J. D. (1984). *Single-Plate Framing Connections with Grade-50 Steel and Composite Construction*. American Institute of Steel Construction – Engineering Journal, Vol. 21, No. 3, Third Quarter, 125-138.
- Keeler, S. P. (1968). *Ductility of Anisotropic Sheet Metal*. Papers Presented at a Seminar of the American Society for Metals, 1968, 227-254.
- Koduru, S. D., and Driver, R.G. (2013). *Generalized Component-Based Model for Shear Tab Connections*. American Society of Civil Engineers – Journal of Structural Engineering, Issue 140, No. 2.
- Lipson, S. L. (1968). *Single Angle and Single Plate Framing Connections*. Canadian Structural Engineering Conference Proceedings, 1968, 139-162.

- Liu, J. and Astanteh, A. (2000). *Seismic Behavior and Design of Steel Shear Connections with Floor Slabs*. Proceedings, 12th World Conference on Earthquake Engineering, Auckland, New Zealand, January.
- Mahamid, M., Rahman, A., Ghorbanpoor, A. (2007). *Analyses of the Shear-Tab Steel Connections Part II: Stiffened Connections*. American Institute of Steel Construction – Engineering Journal, Volume 44, Issue 2, 133-146.
- Marosi, M. (2011). *Behaviour of Single and Double Row Bolted Shear Tab Connections and Weld Retrofits*. MEng Thesis, Dept. of Civil Engineering, McGill University Montreal, Quebec.
- Mirzaei, A. (2014). *Steel Shear Tab Connections Subjected to Combined Shear and Axial Forces*. PhD Thesis, Dept. of Civil Engineering, McGill University. Montreal, QC.
- Muir, L. S., and Hewitt, C. M. (2009). *Design of Unstiffened Extended Single-Plate Shear Connections*. American Institute of Steel Construction – Engineering Journal, Volume 46, No. 2, 2nd Quarter, 67-79.
- New Zealand Heavy Engineering Research Association (1999). *Structural Steelwork Connections Guide*. HERA Report R4-100:1999, June 1999.
- OneSteel Market Mills (2000). *Composite Structures Design Manual – Design Booklet DB5.1, Design of the Web-Side-Plate Steel Connection*. November, 2000.
- Rahman, A., Mahamid, M., Amro, A. Ghorbanpoor, A. (2007). *Analyses of the Shear-Tab Steel Connections Part I: Unstiffened Connections*. American Institute of Steel Construction – Engineering Journal, Volume 44, Issue 2, 117-132.
- Rees, D.W.A. (2009). *Appendix C: Plate Buckling Under Biaxial Compression and Shear*. Mechanics of Optimal Structural Design: Minimum Weight Structures, 537-541.
- Richard, R., Gillett, P., Kriegh, J., and Lewis, A. (1980). *The Analysis and Design of Single Plate Framing Connections*. American Institute of Steel Construction – Engineering Journal, 2nd Quarter, 38-52.
- Ricles, J.M. (1980). *The Behaviour and Analysis of Bolted Double Row Shear Web Connections*. MSc Thesis, University of Texas. Austin, TX.
- Sarkar, D. and Wallace, B. (1992). *Design of Single Plate Framing Connections*. Draft Research Report, Report No. FSEL/AISC 92-01, University of Oklahoma. Norman, OK.
- Seaburg, P.A. and Carter, C.J. (1997). *Design Guide 9: Torsional Analysis of Structural Steel Members*. American Institute of Steel Construction. Chicago, IL.
- Shaw, A.L., and Astanteh, A. (1992). *Experimental Study of Single-Plate Steel Beam-to-Girder Connections*. Report, Dept. of Civil Engineering, University of California. Berkeley, California.

- Sherman, D. R., and Ghorbanpoor, A. (2002). *Design of Extended Shear Tabs*. American Institute of Steel Construction Final Report, University of Wisconsin. Milwaukee, WI.
- Stiemer, S.F., Wong, H.H., and Ho, A. (1986). *Ultimate Capacity of Single Plate Connectors*. Proceedings of the Pacific Structural Steel Conference, 117-132. Auckland, NZ.
- White, R. N., (1965). *Framing Connections for Square and Rectangular Structural Tubing*. American Institute of Steel Construction – Engineering Journal, Vol. 2, No. 3, Third Quarter, 94-102.
- Yarimci, E., Yura, J.A., and Lu, L.W. (1967). *Techniques for Testing Structures Permitted to Sway*. Experimental Mechanics, Volume 7, Number 8, 321-331.
- Young, N. W. and Disque, R. O. (1981). *Design Aids for Single Plate Framing Connections*. American Institute of Steel Construction – Engineering Journal, 4th Quarter, 129-148.

Appendix A – Design Calculations

Configuration 1

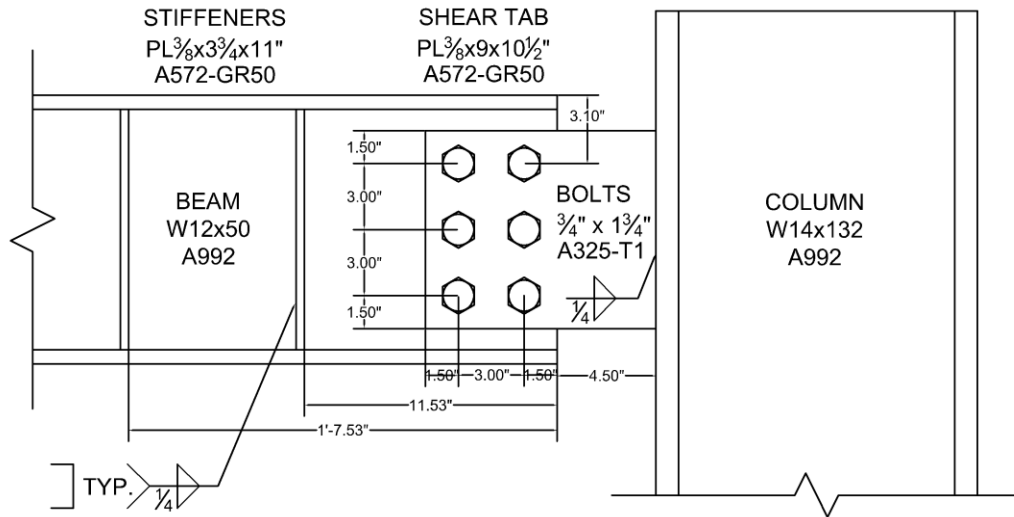


Figure A-1: Connection Details, Configuration 1

Configuration Parameters

Supporting Column		W360x196
Supported Beam		W310x74
Offset of Bolt Group, a	=	152 mm 6 in
Bolt Diameter, d_b	=	19.1 mm 3/4 in
Number of Bolt Lines, m	=	2 2
Number of Bolts Rows, n	=	3 3
Plate Depth, d	=	228.6 mm 9 in

1) Bolt Shear & Bearing

AISC 14th Ed Extended Config Design Check 1 (10-5)

Compute ICR Coefficient, C

Number of Bolt Lines, m	=	2	2
Moment Arm, L	=	190.50 mm	7.5 in
gage, D	=	76.2 mm	3 in
Pitch, b	=	76.2 mm	3 in
Number of Bolt Rows, n	=	3	3
L1	=	175 mm	-
C1	=	2.13	-
L2	=	200 mm	-
C2	=	1.91	-
Eccentric Loading Coefficient, C	=	1.99	1.99

interpolating CISC Handbook Table 3-15

Bearing

$B_r = 3\phi_{br}d_b \min[(tF_u)_{plate}, (tF_u)_{web}] \times C$				*S16-09 C13.12.1.2a)*
Modification factor, ϕ_{br}	=	0.8	0.8	
Plate Thickness, t_p	=	9.53 mm	3/8 in	
Beam Web Thickness, t_w	=	9.40 mm	0.370 in	
Bolt Diameter, d_b	=	19.05 in	3/4 in	
Specified Tensile Stress of Plate, $F_{u,plate}$	=	450 MPa	65 ksi	
Specified Tensile Stress of Beam $F_{u,beam}$	=	450 MPa	65 ksi	
Factored Bearing Resistance, B_r	=	386 kN	86 kip	<-----
Measured Tensile Stress of Plate, $R_y F_{u,plate}$	=	525 MPa	76.1 ksi	
Measured Tensile Stress of Beam, $R_y F_{u,beam}$	=	501 MPa	72.7 ksi	*Mill Test Value*
Predicted Bearing Resistance B_r ($\phi=1.0, R_y F_u$)	=	537 kN	121 kip	<-----

Bolt Shear

$V_r = 0.6\phi_b n m A_b F_u \times C$					*S16-09 C13.12.1.2c)*
Modification factor, ϕ_b	=	0.8		0.8	*S16-09 C13.12.1.1*
Number of Shear Planes, m	=	1		1	
Bolt Area, A_b	=	285 mm ²		0.442 in ²	
Specified Tensile Stress of Bolts, F_u	=	825 MPa		120 ksi	
Reduction factor for thread intercept	=	0.7		0.7	
Factored Bolt Shear Resistance, V_r	=	157 kN		35 kip	<-----
Nominal Bolt Shear Resistance, V_r ($\phi=1.0$)	=	197 kN		44 kip	<-----

2) Plate Ductility

AISC 14th Ed Extended Config Design Check 2 (10-5)

$t_{pmax} = 6M_{max}/F_y d^2$					
$M_{max} = F_{NV}/0.90(A_b C')$					
Bolt Shear Strength, F_{NV} (threads not excl)	=	331 MPa		48 ksi	*AISC 13th Ed, Table J3.2*
Bolt Area, A_b	=	285 mm ²		0.442 in ²	
Compute ICR Coefficient, C', for Moment Only					
Case					
Number of Bolt Lines, m	=	2		2	
Column Spacing	=	76.2 mm		3 in	
Row Spacing, s	=	76.2 mm		3 in	
Number of Bolts Rows, n	=	3		3	
ICR Coefficient, C'	=	401.32 mm		15.8 in	*AISC 13th Ed, Table 7-8*
M_{max}	=	42 kNm		372 kipin	
Specified Yield Stress of Plate, F_y	=	345 MPa		51 ksi	
Plate Depth, d	=	228.6 mm		9.0 in	
Maximum Plate Thickness, t_{pmax}	=	14.0 mm		0.540 in	
Is this requirement satisfied? ($t_p < t_{pmax}$)		YES			<-----

3) Shear Yielding, Shear Rupture and Block Shear Rupture

AISC 14th Ed Extended Config Design Check 3 (10-5)

Shear Yielding

$V_G = 0.60\phi F_y A_g$					*AISC 13th Ed Equation J4-3*
Resistance Factor, ϕ	=	0.9		0.9	*taken as 0.9 from S16-09*
Specified Yield Stress, F_y	=	345 MPa		51 ksi	
$A_g = t_p d_p$					
Plate Thickness, t_p	=	9.53 mm		3/8 in	
Plate Depth, d_p	=	228.6 mm		9 in	
Gross Plate Area, A_g	=	2177 mm ²		3.375 in ²	
Shear Yielding Resistance, V_G	=	406 kN		93 kip	<-----
Measured Yield Stress, $R_y F_y$	=	457 MPa		66 ksi	
Predicted Yielding Resistance, V_G ($\phi=1.0, R_y F_y$)	=	596 kN		134 kip	<-----

Shear Rupture

$V_N = 0.60\phi F_u A_{NV}$					*AISC 13th Ed Equation J4-4*
Resistance Factor, ϕ	=	0.75		0.75	
Specified Tensile Stress, F_u	=	450 MPa		65 ksi	
$A_{NV} = t_p d_{pN}$					
Plate Thickness, t_p	=	9.53 mm		3/8 in	
Net Depth, d_{pN}	=	161.9 mm		6.38 in	
Net Plate Area, A_{NV}	=	1542 mm ²		2.391 in ²	
Factored Shear Rupture Resistance, V_N	=	312 kN		70 kip	<-----
Measured Tensile Stress, $R_y F_u$	=	525 MPa		76.1449 ksi	
Predicted Rupture Resistance V_N ($\phi=1.0, R_y F_u$)	=	486 kN		109 kip	<-----

Block Shear Rupture

$V_{BS} = \phi U_t A_n F_u + 0.6 A_{gV} (F_y + F_u) / 2$					*S16-09 C13.11*
Resistance Factor, ϕ_U	=	0.75		0.75	*S16-09 13.1a)*
Efficiency Factor, U_t	=	0.3		0.3	*coped beam w 2 bolt lines*
Net Area in Tension, A_n	=	771 mm ²		1.195 in ²	

Specified Tensile Stress, F_U	=	450	MPa	65	ksi	
Gross Area in Shear, A_{gV}	=	1815	mm ²	2.813	in ²	
Specified Yield Stress, F_Y	=	345	MPa	51	ksi	
Factored Block Shear Resistance, V_{BS}	=	403	kN	91	kip	<-----
Measured Tensile Stress, $R_Y F_U$	=	525	MPa	76.1449	ksi	
Measured Yield Stress, $R_Y F_Y$	=	457	MPa	66	ksi	
Predicted Block Resistance $V_{BS} (\phi=1.0, R_Y F_Y \& F_U)$	=	656	kN	147	kip	<-----

4) Flexural Shear Yielding, Shear Buckling, and Yielding

AISC 14th Ed Extended Config Design Check 4 (10-5)

AISC 14th Ed LFRD Approach

$$V_r = (1/V_c^2 + (e/M_c)^2)^{-1/2} \quad \text{*AISC Handbook Eqn 10-5, modified*}$$

$V_c = \phi_v V_n$						
Resistance Factor, ϕ_v	=	0.90		0.90		*use 0.9 as in S16-09 versus 1.0*
$V_n = 0.6 F_Y A_g$						
Specified Yield Stress, F_Y	=	345	MPa	51	ksi	
Gross Area of Plate, A_g	=	2177	mm ²	3.375	in ²	
Nominal Shear Capacity, V_n	=	451	kN	103	kip	
Factored Shear Capacity, V_c	=	406	kN	93	kip	
Eccentricity to first bolt column, e	=	152	mm	6	in	
$M_c = \phi_b M_n$						
Resistance Factor, ϕ_b	=	0.90		0.90		
$M_n = F_Y Z_{pl}$						
Plastic Section Modulus, Z_{pl}	=	124	x10 ³ mm ³	7.594	in ³	
Nominal Moment Capacity, M_n	=	43	kNm	387	kipin	
Factored Moment Capacity, M_c	=	39	kNm	349	kipin	
Factored Combined Yielding Resistance, V_r	=	215	kN	49	kip	<-----
Measured Yield Stress, $R_Y F_Y$	=	457	MPa	66	ksi	
Predicted Yielding Resistance, $V_r (\phi=1.0, R_Y F_Y)$	=	316	kN	71	kip	<-----

AISC 13th Ed Approach

$$V_r = F_Y / \sqrt{[(e/\phi Z_{pl})^2 + 3(1/t_p d_p)^2]} \quad \text{*AISC Handbook Eqn 10-4, modified*}$$

Resistance Factor, ϕ	=	0.90		0.90		
Specified Yield Stress, F_Y	=	345	MPa	51	ksi	
Eccentricity to first bolt column, e	=	152	mm	6	in	
Plate Thickness, t_p	=	9.53	mm	3/8	in	
Plate Depth, d_p	=	228.6	mm	9	in	
Plastic Section Modulus, Z_{pl}	=	124	x10 ³ mm ³	7.594	in ³	
Shear and Flexural Yielding Resistance, V_r	=	219	kN	50	kip	<-----
Measured Yield Stress, $R_Y F_Y$	=	457	MPa	66	ksi	
Predicted Yielding Resistance, $V_r (\phi=1.0, R_Y F_Y)$	=	313	kN	70	kip	<-----

5) Plate Buckling

AISC 14th Ed Extended Config Design Check 5 (10-5)

$V_r = \phi_b F_{cr} S_{net} / e$						*AISC 13th Ed Part 9, coped beams*
Resistance Factor, ϕ_b	=	0.90		0.90		
$S_{net} = 1/6 t_w h_o^2$	=	83	x10 ³ mm ³	5.06	in ³	
Cope Depth at Compression Flange, d_c	=	41	mm	1.6	in	
Beam Depth, d	=	310	mm	12.2	in	
Eccentricity to first bolt column, e	=	152.4	mm	6	in	*conservative, take to first row of bolts*
Unsupported Length of Plate, c	=	152.4	mm	6	in	
$d_c < 0.2d$ & $c < 2d$?			YES, fd equation valid			

fd equation (Cheng et al. 1984)

$F_{cr} = 0.62 \pi E t_w^2 / ch_o f_d$						
Modulus of Elasticity, E	=	200000	MPa	29000	ksi	
Thickness of Plate, t_w	=	9.53	mm	3/8	in	
Reduced Beam Depth, h_o	=	228.6	mm	9	in	
$f_d = 3.5 - 7.5 (d_c / d)$						
Adjustment Factor, f_d	=	2.52		2.52		

Critical Stress, F_{cr}	=	2550	MPa	369.8	ksi	
Plate Buckling Resistance, V_r	=	1250	kN	281	kip	<-----
Predicted Buckling Resistance, $V_r(\phi=1.0)$	=	1388	kN	312	kip	<-----

Q equation (classical plate buckling)

($d_c > 0.2d$)

$$F_{cr} = F_y Q$$

$$\lambda = h_o \sqrt{F_y} / 10 t_w \sqrt{475 + 280(h_o/c)^2}$$

Specified Yield Stress, F_y	=	345	MPa	51	ksi
-------------------------------	---	-----	-----	----	-----

Measured Yield Stress, $R_y F_y$	=	457	MPa	66	ksi
----------------------------------	---	-----	-----	----	-----

Slenderness of Coped Section, λ	=			0.52	
---	---	--	--	------	--

Slenderness of Coped Section, $\lambda_{EXPECTED}$	=			0.59	
--	---	--	--	------	--

Strength Reduction Factor, Q	=	1.00		1.00	
--------------------------------	---	------	--	------	--

Strength Reduction Factor, $Q_{EXPECTED}$	=	1.00		1.00	
---	---	------	--	------	--

Critical Stress, F_{cr}	=	345	MPa	51	ksi
---------------------------	---	-----	-----	----	-----

Critical Stress, $F_{cr,EXPECTED}$	=	456.5	MPa	66.2098	ksi
------------------------------------	---	-------	-----	---------	-----

Plate Buckling Resistance, V_r	=	169	kN	39	kip	<-----
----------------------------------	---	-----	----	----	-----	--------

Predicted Buckling Resistance $V_r(\phi=1.0, R_y F_y)$	=	248	kN	56	kip	<-----
--	---	-----	----	----	-----	--------

6) Flexural Limit States

Gross Area Resistance Factor, ϕ_G	=	0.9		0.9	
--	---	-----	--	-----	--

Net Area Resistance Factor, ϕ_N	=	0.75		0.75	
--------------------------------------	---	------	--	------	--

Specified Yield Stress, F_y	=	345	MPa	51	ksi
-------------------------------	---	-----	-----	----	-----

Specified Tensile Stress, F_u	=	450	MPa	65	ksi
---------------------------------	---	-----	-----	----	-----

Measured Yield Stress, $R_y F_y$	=	457	MPa	66	ksi
----------------------------------	---	-----	-----	----	-----

Measured Tensile Stress, $R_y F_u$	=	525	MPa	76.1449	ksi
------------------------------------	---	-----	-----	---------	-----

Thickness of Plate, t_p	=	9.53	mm	3/8	in
---------------------------	---	------	----	-----	----

Plate Depth, d_p	=	228.6	mm	9	in
--------------------	---	-------	----	---	----

Gauge, s	=	76.2	mm	3	in
------------	---	------	----	---	----

Number of Bolt Rows, n	=	3		3	
--------------------------	---	---	--	---	--

Diameter of Bolt Holes, d_h	=	22.2	mm	7/8	in
-------------------------------	---	------	----	-----	----

Section Modulus, S	=	82960	mm ³	5.06	in ³
----------------------	---	-------	-----------------	------	-----------------

Plastic Section Modulus, Z	=	124439	mm ³	7.59	in ³
------------------------------	---	--------	-----------------	------	-----------------

$$S_{net} = t_p / 6 [d_p^2 - s^2 n (n^2 - 1) d_h / d_p]$$

Net Section Modulus, S_{net}	=	61451	mm ³	3.75	in ³
--------------------------------	---	-------	-----------------	------	-----------------

$$Z_{net} = 1/4 t_p (s - d_h) (n^2 s + d_h)$$

$$Z_{net} = 1/4 t_p (s - d_h) n^2 s$$

Net Plastic Section Modulus, Z_{net}	=	91001	mm ³	5.55	in ³
--	---	-------	-----------------	------	-----------------

Eccentricity to first bolt column, e	=	152	mm	6	in
--	---	-----	----	---	----

Engineering Journal 2008 / 2nd quarter, p102

Engineering Journal 2008 / 2nd quarter, p103

AISC 3rd Edition

Bending on Gross Area

$$V_r = \phi_G F_y S / e$$

Factored Gross Bending Resistance, V_r	=	169	kN	39	kip	<-----
--	---	-----	----	----	-----	--------

Predicted Bending Resistance $V_r(\phi=1.0, R_y F_y)$	=	248	kN	56	kip	<-----
---	---	-----	----	----	-----	--------

Bending on Net Area

$$V_r = \phi_N F_u S_{net} / e$$

Factored Net Bending Resistance, V_r	=	136	kN	30	kip	<-----
--	---	-----	----	----	-----	--------

Predicted Bending Resistance $V_r(\phi=1.0, R_y F_y)$	=	212	kN	48	kip	<-----
---	---	-----	----	----	-----	--------

AISC 13th & 14th Edition

Bending on Gross Area

$$V_r = \phi_G F_y Z / e$$

Factored Gross Bending Resistance, V_r	=	254	kN	58	kip	<-----
--	---	-----	----	----	-----	--------

Predicted Bending Resistance $V_r(\phi=1.0, R_y F_y)$	=	373	kN	84	kip	<-----
---	---	-----	----	----	-----	--------

Bending on Net Area

$$V_r = \phi_N F_u Z_{net} / e$$

Factored Net Bending Resistance, V_r	=	202	kN	45	kip	<-----
--	---	-----	----	----	-----	--------

Predicted Bending Resistance $V_r(\phi=1.0, R_y F_y)$	=	313	kN	70	kip	<-----
---	---	-----	----	----	-----	--------

Configuration 2

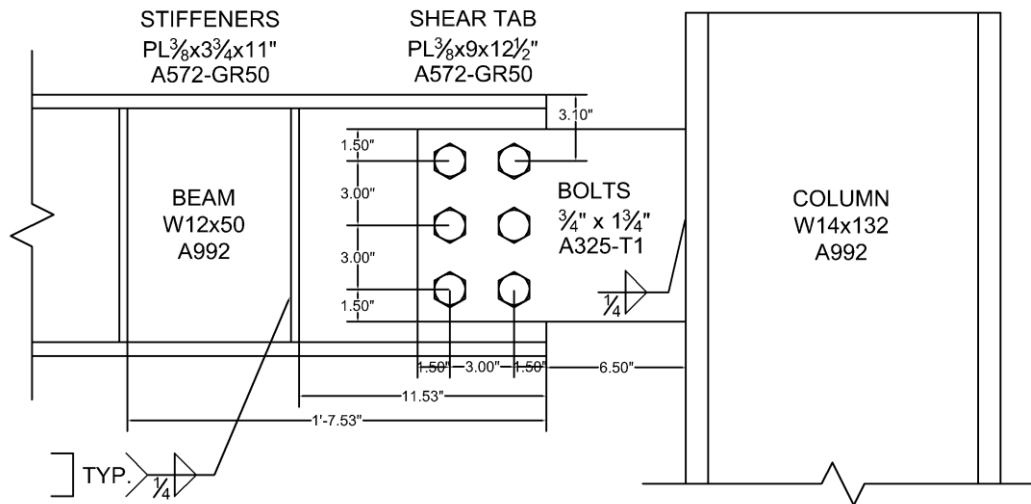


Figure A-2: Connection Details, Configuration 2

Configuration Parameters

Supporting Column		W360x196	
Supported Beam		W310x74	
Offset of Bolt Group, a	=	203 mm	8 in
Bolt Diameter, d_b	=	19.1 mm	3/4 in
Number of Bolt Lines, m	=	2	2
Number of Bolts Rows, n	=	3	3
Plate Depth, d	=	228.6 mm	9 in

1) Bolt Shear & Bearing

AISC 14th Ed Extended Config Design Check 1 (10-5)

Compute ICR Coefficient, C

Number of Bolt Lines, m	=	2	2	
Moment Arm, L	=	241.30 mm	9.5 in	
gage, D	=	76.2 mm	3 in	
Pitch, b	=	76.2 mm	3 in	
Number of Bolt Rows, n	=	3	3	
L1	=	225 mm	-	
C1	=	1.73	-	
L2	=	250 mm	-	
C2	=	1.58	-	
Eccentric Loading Coefficient, C	=	1.63	1.63	*interpolating CISC Handbook Table 3-15*

Bearing

$B_r = 3\phi_{br}d_b \min[(tF_u)_{plate}, (tF_u)_{web}] \times C$				*S16-09 C13.12.1.2a)*
Modification factor, ϕ_{br}	=	0.8	0.8	
Plate Thickness, t_p	=	9.53 mm	3/8 in	
Beam Web Thickness, t_w	=	9.40 mm	0.370 in	
Bolt Diameter, d_b	=	19.05 in	3/4 in	
Specified Tensile Stress of Plate, $F_{u,plate}$	=	450 MPa	65 ksi	
Specified Tensile Stress of Beam $F_{u,beam}$	=	450 MPa	65 ksi	
Factored Bearing Resistance, B_r	=	316 kN	71 kip	<-----
Measured Tensile Stress of Plate, $R_y F_{U,plate}$	=	525 MPa	76.14489 ksi	
Measured Tensile Stress of Beam, $R_y F_{U,beam}$	=	501 MPa	71.5 ksi	*Mill Test Value*
Predicted Bearing Resistance B_r ($\phi=1.0, R_y F_U$)	=	439 kN	97 kip	<-----

Bolt Shear

$V_r = 0.6\phi_b n m A_b F_u \times C$					*S16-09 C13.12.1.2c)*
Modification factor, ϕ_b	=	0.8		0.8	*S16-09 C13.12.1.1*
Number of Shear Planes, m	=	1		1	
Bolt Area, A_b	=	285 mm ²		0.442 in ²	
Specified Tensile Stress of Bolts, F_u	=	825 MPa		120 ksi	
Reduction factor for thread intercept	=	0.7		0.7	
Factored Bolt Shear Resistance, V_r	=	129 kN		29 kip	<-----
Nominal Bolt Shear Resistance, $V_r (\phi=1.0)$	=	161 kN		36 kip	<-----

2) Plate Ductility

AISC 14th Ed Extended Config Design Check 2 (10-5)

$t_{pmax} = 6M_{max}/F_y d^2$					
$M_{max} = F_{nv}/0.90(A_b C')$					
Bolt Shear Strength, F_{nv} (threads not excl)	=	331 MPa		48 ksi	*AISC 13th Ed, Table J3.2*
Bolt Area, A_b	=	285 mm ²		0.442 in ²	
Compute ICR Coefficient, C', for Moment Only Case					
Number of Bolt Lines, m	=	2		2	
Column Spacing	=	76.2 mm		3 in	
Row Spacing, s	=	76.2 mm		3 in	
Number of Bolts Rows, n	=	3		3	
ICR Coefficient, C'	=	401.32 mm		15.8 in	*AISC 13th Ed, Table 7-8*
M_{max}	=	42 kNm		372 kipin	
Specified Yield Stress of Plate, F_y	=	345 MPa		51 ksi	
Plate Depth, d	=	228.6 mm		9.0 in	
Maximum Plate Thickness, t_{pmax}	=	14.0 mm		0.540 in	
Is this requirement satisfied? ($t_p < t_{pmax}$)		YES			<-----

3) Shear Yielding, Shear Rupture and Block Shear Rupture

AISC 14th Ed Extended Config Design Check 3 (10-5)

Shear Yielding

$V_G = 0.60\phi F_y A_g$					*AISC 13th Ed Equation J4-3*
Resistance Factor, ϕ	=	0.9		0.9	
Specified Yield Stress, F_y	=	345 MPa		51 ksi	
$A_g = t_p d_p$					
Plate Thickness, t_p	=	9.53 mm		3/8 in	
Plate Depth, d_p	=	228.6 mm		9 in	
Gross Plate Area, A_g	=	2177 mm ²		3.375 in ²	
Shear Yielding Resistance, V_G	=	406 kN		93 kip	<-----
Measured Yield Stress, $R_y F_y$	=	457 MPa		66 ksi	
Predicted Yielding Resistance, $V_G (\phi=1.0, R_y F_y)$	=	596 kN		134 kip	<-----

Shear Rupture

$V_N = 0.60\phi F_u A_{NV}$					*AISC 13th Ed Equation J4-4*
Resistance Factor, ϕ	=	0.75		0.75	
Specified Tensile Stress, F_u	=	450 MPa		65 ksi	
$A_{NV} = t_p d_{pN}$					
Plate Thickness, t_p	=	9.53 mm		3/8 in	
Net Depth, d_{pN}	=	161.9 mm		6.38 in	
Net Plate Area, A_{NV}	=	1542 mm ²		2.391 in ²	
Factored Shear Rupture Resistance, V_N	=	312 kN		70 kip	<-----
Measured Tensile Stress, $R_y F_u$	=	525 MPa		76.14489 ksi	
Predicted Rupture Resistance $V_N (\phi=1.0, R_y F_u)$	=	486 kN		109 kip	<-----

Block Shear Rupture

$V_{BS} = \phi U_t [A_t F_u + 0.6 A_{gV} (F_y + F_u)] / 2$					*S16-09 C13.11*
Resistance Factor, ϕ	=	0.75		0.75	*S16-09 13.1a)*
Efficiency Factor, U_t	=	0.3		0.3	*coped beam w 2 bolt lines*
Net Area in Tension, A_t	=	771 mm ²		1.195 in ²	
Specified Tensile Stress, F_u	=	450 MPa		65 ksi	

Gross Area in Shear, A_{gV}	=	1815	mm ²	2.813	in ²	
Specified Yield Stress, F_Y	=	345	MPa	51	ksi	
Factored Block Shear Resistance, V_{BS}	=	403	kN	91	kip	<-----
Measured Tensile Stress, $R_Y F_U$	=	525	MPa	76.14489	ksi	
Measured Yield Stress, $R_Y F_Y$	=	457	MPa	66	ksi	
Predicted Block Resistance $V_{BS} (\phi=1.0, R_Y F_Y \& F_U)$	=	656	kN	147	kip	<-----

4) Flexural Shear Yielding, Shear Buckling, and Yielding

AISC 14th Ed Extended Config Design Check 4 (10-5)

AISC 14th Ed LFRD Approach

$$V_r = (1/V_c^2 + (e/M_c)^2)^{-1/2}$$

AISC Handbook Eqn 10-5, modified

$$V_c = \phi_V V_n$$

$$\text{Resistance Factor, } \phi_V$$

$$= 0.90$$

$$0.90$$

use 0.9 as in S16-09 versus 1.0

$$V_n = 0.6 F_Y A_g$$

$$\text{Specified Yield Stress, } F_Y$$

$$= 345$$

$$\text{MPa}$$

$$51$$

$$\text{ksi}$$

$$\text{Gross Area of Plate, } A_g$$

$$= 2177$$

$$\text{mm}^2$$

$$3.375$$

$$\text{in}^2$$

$$\text{Nominal Shear Capacity, } V_n$$

$$= 451$$

$$\text{kN}$$

$$103$$

$$\text{kip}$$

$$\text{Factored Shear Capacity, } V_c$$

$$= 406$$

$$\text{kN}$$

$$93$$

$$\text{kip}$$

$$\text{Eccentricity to first bolt column, } e$$

$$= 203$$

$$\text{mm}$$

$$8$$

$$\text{in}$$

$$M_c = \phi_b M_n$$

$$\text{Resistance Factor, } \phi_b$$

$$= 0.90$$

$$0.90$$

$$M_n = F_Y Z_{pl}$$

$$\text{Plastic Section Modulus, } Z_{pl}$$

$$= 124$$

$$\times 10^3 \text{ mm}^3$$

$$7.594$$

$$\text{in}^3$$

$$\text{Nominal Moment Capacity, } M_n$$

$$= 43$$

$$\text{kNm}$$

$$387$$

$$\text{kipin}$$

$$\text{Factored Moment Capacity, } M_c$$

$$= 39$$

$$\text{kipin}$$

$$349$$

$$\text{kNm}$$

$$\text{Factored Combined Yielding Resistance, } V_r$$

$$= 172$$

$$\text{kN}$$

$$39$$

$$\text{kip}$$

<-----

$$\text{Measured Yield Stress, } R_Y F_Y$$

$$= 457$$

$$\text{MPa}$$

$$66$$

$$\text{ksi}$$

$$\text{Predicted Yielding Resistance, } V_r (\phi=1.0, R_Y F_Y)$$

$$= 253$$

$$\text{kN}$$

$$57$$

$$\text{kip}$$

<-----

AISC 13th Ed Approach

$$V_r = F_Y / \sqrt{[(e/\phi Z_{pl})^2 + 3(1/t_p d_p)^2]}$$

AISC Handbook Eqn 10-4, modified

$$\text{Resistance Factor, } \phi$$

$$= 0.90$$

$$0.90$$

$$\text{Specified Yield Stress, } F_Y$$

$$= 345$$

$$\text{MPa}$$

$$51$$

$$\text{ksi}$$

$$\text{Eccentricity to first bolt column, } e$$

$$= 203$$

$$\text{mm}$$

$$8$$

$$\text{in}$$

$$\text{Plate Thickness, } t_p$$

$$= 9.53$$

$$\text{mm}$$

$$3/8$$

$$\text{in}$$

$$\text{Plate Depth, } d_p$$

$$= 228.6$$

$$\text{mm}$$

$$9$$

$$\text{in}$$

$$\text{Plastic Section Modulus, } Z_{pl}$$

$$= 124$$

$$\times 10^3 \text{ mm}^3$$

$$7.594$$

$$\text{in}^3$$

$$\text{Shear and Flexural Yielding Resistance, } V_r$$

$$= 174$$

$$\text{kN}$$

$$40$$

$$\text{kip}$$

<-----

$$\text{Measured Yield Stress, } R_Y F_Y$$

$$= 457$$

$$\text{MPa}$$

$$66$$

$$\text{ksi}$$

$$\text{Predicted Yielding Resistance, } V_r (\phi=1.0, R_Y F_Y)$$

$$= 251$$

$$\text{kN}$$

$$57$$

$$\text{kip}$$

<-----

5) Plate Buckling

AISC 14th Ed Extended Config Design Check 5 (10-5)

$$V_r = \phi_b F_{cr} S_{net} / e$$

AISC 13th Ed Part 9, coped beams

$$\text{Resistance Factor, } \phi_b$$

$$= 0.90$$

$$0.90$$

$$S_{net} = 1/6 t_w h_o^2$$

$$= 83$$

$$\times 10^3 \text{ mm}^3$$

$$5.06$$

$$\text{in}^3$$

$$\text{Cope Depth at Compression Flange, } d_c$$

$$= 41$$

$$\text{mm}$$

$$1.6$$

$$\text{in}$$

$$\text{Beam Depth, } d$$

$$= 310$$

$$\text{mm}$$

$$12.2$$

$$\text{in}$$

$$\text{Eccentricity to first bolt column, } e$$

$$= 203.2$$

$$\text{mm}$$

$$8$$

$$\text{in}$$

*conservative, take to first

$$\text{Unsupported Length of Plate, } c$$

$$= 203.2$$

$$\text{mm}$$

$$8$$

$$\text{in}$$

row of bolts*

$$d_c < 0.2d \& c < 2d?$$

YES, fd equation valid

fd equation (Cheng et al. 1984)

$$F_{cr} = 0.62 \pi E t_w^2 / (ch_o f_d)$$

$$\text{Modulus of Elasticity, } E$$

$$= 200000$$

$$\text{MPa}$$

$$29000$$

$$\text{ksi}$$

$$\text{Thickness of Plate, } t_w$$

$$= 9.53$$

$$\text{mm}$$

$$3/8$$

$$\text{in}$$

$$\text{Reduced Beam Depth, } h_o$$

$$= 228.6$$

$$\text{mm}$$

$$9$$

$$\text{in}$$

$$f_d = 3.5 - 7.5 (d_c / d)$$

$$\text{Adjustment Factor, } f_d$$

$$= 2.52$$

$$2.52$$

$$\text{Critical Stress, } F_{cr}$$

$$= 1913$$

$$\text{MPa}$$

$$277.4$$

$$\text{ksi}$$

Plate Buckling Resistance, V_r	=	703	kN	158	kip	<-----
Predicted Buckling Resistance, $V_r(\phi=1.0)$	=	781	kN	176	kip	<-----

Q equation (classical plate buckling)

$$F_{cr} = F_y Q$$

$$\lambda = h_o \sqrt{F_y} / 10 t_w \sqrt{(475 + 280(h_o/c)^2)}$$

Specified Yield Stress, F_y	=	345	MPa	51	ksi
-------------------------------	---	-----	-----	----	-----

Measured Yield Stress, $R_y F_y$	=	457	MPa	66	ksi
----------------------------------	---	-----	-----	----	-----

Slenderness of Coped Section, λ	=			0.60	
---	---	--	--	------	--

Slenderness of Coped Section, $\lambda_{EXPECTED}$	=			0.68	
--	---	--	--	------	--

Strength Reduction Factor, Q	=	1.00		1.00	
--------------------------------	---	------	--	------	--

Strength Reduction Factor, $Q_{EXPECTED}$	=	1.00		1.00	
---	---	------	--	------	--

Critical Stress, F_{cr}	=	345	MPa	51	ksi
---------------------------	---	-----	-----	----	-----

Critical Stress, $F_{cr,EXPECTED}$	=	456.5	MPa	66.2098	ksi
------------------------------------	---	-------	-----	---------	-----

Plate Buckling Resistance, V_r	=	127	kN	29	kip	<-----
----------------------------------	---	-----	----	----	-----	--------

Predicted Buckling Resistance $V_r(\phi=1.0, R_y F_y)$	=	186	kN	42	kip	<-----
--	---	-----	----	----	-----	--------

6) Flexural Limit States

Gross Area Resistance Factor, ϕ_G	=	0.9		0.9	
--	---	-----	--	-----	--

Net Area Resistance Factor, ϕ_N	=	0.75		0.75	
--------------------------------------	---	------	--	------	--

Specified Yield Stress, F_y	=	345	MPa	51	ksi
-------------------------------	---	-----	-----	----	-----

Specified Tensile Stress, F_u	=	450	MPa	65	ksi
---------------------------------	---	-----	-----	----	-----

Measured Yield Stress, $R_y F_y$	=	457	MPa	66	ksi
----------------------------------	---	-----	-----	----	-----

Measured Tensile Stress, $R_y F_u$	=	525	MPa	76.14489	ksi
------------------------------------	---	-----	-----	----------	-----

Thickness of Plate, t_p	=	9.53	mm	3/8	in
---------------------------	---	------	----	-----	----

Plate Depth, d_p	=	228.6	mm	9	in
--------------------	---	-------	----	---	----

Gauge, s	=	76.2	mm	3	in
------------	---	------	----	---	----

Number of Bolt Rows, n	=	3		3	
--------------------------	---	---	--	---	--

Diameter of Bolt Holes, d_h	=	22.2	mm	7/8	in
-------------------------------	---	------	----	-----	----

Section Modulus, S	=	82960	mm ³	5.06	in ³
----------------------	---	-------	-----------------	------	-----------------

Plastic Section Modulus, Z	=	124439	mm ³	7.59	in ³
------------------------------	---	--------	-----------------	------	-----------------

$S_{net} = t_p / 6 [d_p^2 - s^2 n (n^2 - 1) d_h / d_p]$	=	61451.5	mm ³	3.75	in ³
---	---	---------	-----------------	------	-----------------

Net Section Modulus, S_{net}	=	61451.5	mm ³	3.75	in ³
--------------------------------	---	---------	-----------------	------	-----------------

$Z_{net} = 1/4 t_p (s - d_h) (n^2 s + d_h)$	=	91001	mm ³	5.55	in ³
---	---	-------	-----------------	------	-----------------

$Z_{net} = 1/4 t_p (s - d_h) n^2 s$	=	91001	mm ³	5.55	in ³
-------------------------------------	---	-------	-----------------	------	-----------------

Net Plastic Section Modulus, Z_{net}	=	91001	mm ³	5.55	in ³
--	---	-------	-----------------	------	-----------------

Eccentricity to first bolt column, e	=	203	mm	8	in
--	---	-----	----	---	----

*Engineering Journal 2008 /
2nd quarter, p102*

*Engineering Journal 2008 /
2nd quarter, p103*

AISC 3rd Edition

Bending on Gross Area

$$V_r = \phi_G F_y S / e$$

Factored Gross Bending Resistance, V_r	=	127	kN	29	kip	<-----
--	---	-----	----	----	-----	--------

Predicted Bending Resistance $V_r(\phi=1.0, R_y F_y)$	=	186	kN	42	kip	<-----
---	---	-----	----	----	-----	--------

Bending on Net Area

$$V_r = \phi_N F_u S_{net} / e$$

Factored Net Bending Resistance, V_r	=	102	kN	23	kip	<-----
--	---	-----	----	----	-----	--------

Predicted Bending Resistance $V_r(\phi=1.0, R_y F_y)$	=	159	kN	36	kip	<-----
---	---	-----	----	----	-----	--------

AISC 13th & 14th Edition

Bending on Gross Area

$$V_r = \phi_G F_y Z / e$$

Factored Gross Bending Resistance, V_r	=	190	kN	44	kip	<-----
--	---	-----	----	----	-----	--------

Predicted Bending Resistance $V_r(\phi=1.0, R_y F_y)$	=	280	kN	63	kip	<-----
---	---	-----	----	----	-----	--------

Bending on Net Area

$$V_r = \phi_N F_u Z_{net} / e$$

Factored Net Bending Resistance, V_r	=	151	kN	34	kip	<-----
--	---	-----	----	----	-----	--------

Predicted Bending Resistance $V_r(\phi=1.0, R_y F_y)$	=	235	kN	53	kip	<-----
---	---	-----	----	----	-----	--------

Configuration 3 (Partial "C" Weld Retrofit)

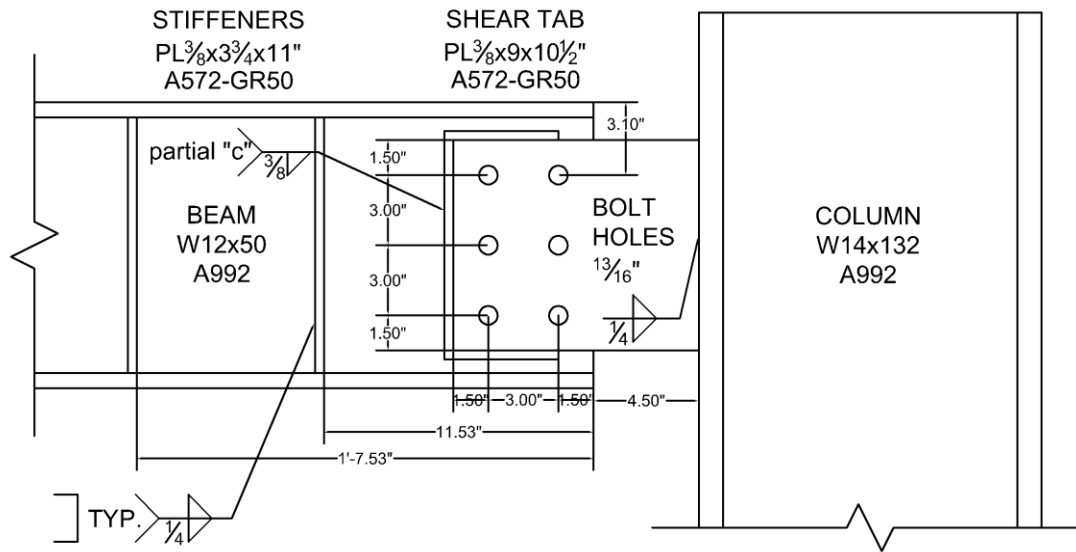


Figure A-3: Connection Details, Configuration 3

Configuration Parameters

Supporting Column		W360x196	
Supported Beam		W310x74	
Offset of Bolt Group, a	=	152 mm	6 in
Bolt Diameter, d_b	=	19.1 mm	3/4 in
Number of Bolt Lines, m	=	2	2
Number of Bolts Rows, n	=	3	3
Plate Depth, d	=	228.6 mm	9 in
Longitudinal Weld Length, L_t	=	114.3 mm	4 1/2 in
Transverse Weld Length, L	=	228.6 mm	9 in

1) Partial "C" Weld

Modified AISC 14th Ed Extended Config Design Check 1 (10-5)

$V_r = C D L$			
Characteristic Length of Weld, L	=	229 mm	9 in
Aspect Ratio, k	=	0.50	0.50
C.G. ratio, x	=	0.125	0.125
Centroid Distance, xL	=	29 mm	1.125 in
Distance from weld to column face, aL + xL	=	267 mm	10.50 in
Moment Arm Ratio, $a = [(aL + xL) - xL] / L$	=	1.042	1.042
a1	=	1.00	
C1	=	0.136 kN/mm ²	
a2	=	1.20	
C2	=	0.115 kN/mm ²	
Eccentric Loading Coefficient, C	=	0.132 kN/mm ²	19.1 kip/in ²
Minimum Factored Resistance, $V_{r,min}$	=	157 kN	35 kip
$D_{w,min} = V_{r,min} / C L$			
Minimum Weld Throat Size, $D_{w,min}$	=	5.23 mm	0.206 in
Weld Throat Size, D	=	6.35 mm	1/4 in
Factored Weld Resistance, V_r	=	191 kN	43 kip
Modification factor, ϕ_w	=	0.67	0.67
Predicted Weld Resistance V_r / ϕ_w	=	285 kN	64 kip

* S16-09 Table 3-28*

capacity of equivalent bolted connection

*Table 3-28 with $\phi_w = 0.67$ *

2) Plate Ductility

NOT APPLICABLE

AISC 14th Ed Extended Config Design Check 2 (10-5)

3) Shear Yielding and Shear Rupture

Modified AISC 14th Ed Extended Config Design Check 3 (10-5)

Shear Yielding

$$V_G = 0.60\phi F_Y A_g$$

AISC 13th Ed Equation J4-3

Resistance Factor, ϕ	=	0.9	0.9	
Specified Yield Stress, F_Y	=	345 MPa	51 ksi	
$A_g = t_p d_p$				
Plate Thickness, t_p	=	9.53 mm	3/8 in	
Plate Depth, d_p	=	228.6 mm	9 in	
Gross Plate Area, A_g	=	2177 mm ²	3.375 in ²	
Shear Yielding Resistance, V_G	=	406 kN	93 kip	<-----
Measured Yield Stress, $R_Y F_Y$	=	457 MPa	66 ksi	
Predicted Yielding Resistance, $V_G (\phi=1.0, R_Y F_Y)$	=	596 kN	134 kip	<-----

Shear Rupture

$$V_N = 0.60\phi F_U A_{NV}$$

AISC 13th Ed Equation J4-4

Resistance Factor, ϕ	=	0.75	0.75	
Specified Tensile Stress, F_U	=	450 MPa	65 ksi	
$A_{NV} = t_p d_{pN}$				
Plate Thickness, t_p	=	9.53 mm	3/8 in	
Net Depth, d_{pN}	=	161.9 mm	6.38 in	
Net Plate Area, A_{NV}	=	1542 mm ²	2.391 in ²	
Factored Shear Rupture Resistance, V_N	=	312 kN	70 kip	<-----
Measured Tensile Stress, $R_Y F_U$	=	525 MPa	76.14489 ksi	
Predicted Rupture Resistance $V_N (\phi=1.0, R_Y F_U)$	=	486 kN	109 kip	<-----

Block Shear Rupture

NOT APPLICABLE

4) Flexural Shear Yielding, Shear Buckling, and Yielding

AISC 14th Ed Extended Config Design Check 4 (10-5)

AISC 14th Ed LFRD Approach

$$V_r = (1/V_c^2 + (e/M_c)^2)^{-1/2}$$

AISC Handbook Eqn 10-5, modified

$$V_c = \phi_v V_n$$

Resistance Factor, ϕ_v = 0.90 0.90 *use 0.9 as in S16-09 versus 1.0*

$$V_n = 0.6F_Y A_g$$

Specified Yield Stress, F_Y	=	345 MPa	51 ksi	
Gross Area of Plate, A_g	=	2177 mm ²	3.375 in ²	
Nominal Shear Capacity, V_n	=	451 kN	103 kip	
Factored Shear Capacity, V_c	=	406 kN	93 kip	
Eccentricity to first bolt column, e	=	152 mm	6 in	
$M_c = \phi_b M_n$				
Resistance Factor, ϕ_b	=	0.90	0.90	
$M_n = F_Y Z_{pl}$				
Plastic Section Modulus, Z_{pl}	=	124 x10 ³ mm ³	7.594 in ³	
Nominal Moment Capacity, M_n	=	43 kNm	387 kipin	
Factored Moment Capacity, M_c	=	39 kipin	349 kNm	
Factored Combined Yielding Resistance, V_r	=	215 kN	49 kip	<-----
Measured Yield Stress, $R_Y F_Y$	=	457 MPa	66 ksi	
Predicted Yielding Resistance, $V_r (\phi=1.0, R_Y F_Y)$	=	316 kN	71 kip	<-----

AISC 13th Ed Approach

$$V_r = F_Y / \sqrt{[(e/\phi Z_{pl})^2 + 3(1/t_p d_p)^2]}$$

AISC Handbook Eqn 10-4, modified

Resistance Factor, ϕ	=	0.90	0.90	
Specified Yield Stress, F_Y	=	345 MPa	51 ksi	
Eccentricity to first bolt column, e	=	152 mm	6 in	
Plate Thickness, t_p	=	9.53 mm	3/8 in	
Plate Depth, d_p	=	228.6 mm	9 in	

Plastic Section Modulus, Z_{pl}	=	124	$\times 10^3 \text{ mm}^3$	7.594	in^3	
Shear and Flexural Yielding Resistance, V_r	=	219	kN	50	kip	<-----
Measured Yield Stress, $R_y F_y$	=	457	MPa	66	ksi	
Predicted Yielding Resistance, $V_r (\phi=1.0, R_y F_y)$	=	313	kN	70	kip	<-----

5) Plate Buckling

AISC 14th Ed Extended Config Design Check 5 (10-5)

AISC 13th Ed Part 9, coped beams

$V_r = \phi_b F_{cr} S_{net} / e$						
Resistance Factor, ϕ_b	=	0.90		0.90		
$S_{net} = 1/6 t_w h_o^2$	=	83	$\times 10^3 \text{ mm}^3$	5.06	in^3	
Cope Depth at Compression Flange, d_c	=	41	mm	1.6	in	
Beam Depth, d	=	310	mm	12.2	in	
Eccentricity to first bolt column, e	=	152.4	mm	6	in	*conservative, take to first
Unsupported Length of Plate, c	=	152.4	mm	6	in	row of bolts*
$d_c < 0.2d$ & $c < 2d$?			YES, fd equation valid			

fd equation (Cheng et al. 1984)

$F_{cr} = 0.62 \pi E t_w^2 / (ch_o f_d)$						
Modulus of Elasticity, E	=	200000	MPa	29000	ksi	
Thickness of Plate, t_w	=	9.53	mm	3/8	in	
Reduced Beam Depth, h_o	=	228.6	mm	9	in	
$f_d = 3.5 - 7.5 (d_c / d)$						
Adjustment Factor, f_d	=	2.52		2.52		
Critical Stress, F_{cr}	=	2550	MPa	369.8	ksi	
Plate Buckling Resistance, V_r	=	1250	kN	281	kip	<-----
Predicted Buckling Resistance, $V_r (\phi=1.0)$	=	1388	kN	312	kip	<-----

Q equation (classical plate buckling)

$F_{cr} = F_y Q$						
$\lambda = h_o \sqrt{F_y} / 10 t_w \sqrt{(475 + 280(h_o/c)^2)}$						
Specified Yield Stress, F_y	=	345	MPa	51	ksi	
Measured Yield Stress, $R_y F_y$	=	457	MPa	66	ksi	
Slenderness of Coped Section, λ	=			0.52		
Slenderness of Coped Section, $\lambda_{EXPECTED}$	=			0.59		
Strength Reduction Factor, Q	=	1.00		1.00		
Strength Reduction Factor, $Q_{EXPECTED}$	=	1.00		1.00		
Critical Stress, F_{cr}	=	345	MPa	51	ksi	
Critical Stress, $F_{cr, EXPECTED}$	=	456.5	MPa	66.2098	ksi	
Plate Buckling Resistance, V_r	=	169	kN	39	kip	<-----
Predicted Buckling Resistance $V_r (\phi=1.0, R_y F_y)$	=	248	kN	56	kip	<-----

6) Flexural Limit States

Gross Area Resistance Factor, ϕ_G	=	0.9		0.9		
Net Area Resistance Factor, ϕ_N	=	0.75		0.75		
Specified Yield Stress, F_y	=	345	MPa	51	ksi	
Specified Tensile Stress, F_u	=	450	MPa	65	ksi	
Measured Yield Stress, $R_y F_y$	=	457	MPa	66	ksi	
Measured Tensile Stress, $R_y F_u$	=	525	MPa	76.14489	ksi	
Thickness of Plate, t_p	=	9.53	mm	3/8	in	
Plate Depth, d_p	=	228.6	mm	9	in	
Gauge, s	=	76.2	mm	3	in	
Number of Bolt Rows, n	=	3		3		
Diameter of Bolt Holes, d_h	=	22.2	mm	7/8	in	
Section Modulus, S	=	82960	mm^3	5.06	in^3	
Plastic Section Modulus, Z	=	124439	mm^3	7.59	in^3	
$S_{net} = t_p / 6 [d_p^2 - s^2 n (n^2 - 1) d_h / d_p]$						
Net Section Modulus, S_{net}	=	61451.5	mm^3	3.75	in^3	*Engineering Journal 2008 / 2nd quarter, p102*
$Z_{net} = 1/4 t_p (s - d_h) (n^2 s + d_h)$						
$Z_{net} = 1/4 t_p (s - d_h) n^2 s$						
Net Plastic Section Modulus, Z_{net}	=	91001	mm^3	5.55	in^3	*Engineering Journal 2008 / 2nd quarter, p103*

Eccentricity to first bolt column, e = 152 mm 6 in

AISC 3rd Edition

Bending on Gross Area

$$V_r = \phi_G F_y S / e$$

Factored Gross Bending Resistance, V_r	=	169	kN	39	kip	<-----
--	---	-----	----	----	-----	--------

Predicted Bending Resistance $V_r(\phi=1.0, R_y F_y)$	=	248	kN	56	kip	<-----
---	---	-----	----	----	-----	--------

Bending on Net Area

$$V_r = \phi_N F_u S_{net} / e$$

Factored Net Bending Resistance, V_r	=	136	kN	30	kip	<-----
--	---	-----	----	----	-----	--------

Predicted Bending Resistance $V_r(\phi=1.0, R_y F_y)$	=	212	kN	48	kip	<-----
---	---	-----	----	----	-----	--------

AISC 13th & 14th Edition

Bending on Gross Area

$$V_r = \phi_G F_y Z / e$$

Factored Gross Bending Resistance, V_r	=	254	kN	58	kip	<-----
--	---	-----	----	----	-----	--------

Predicted Bending Resistance $V_r(\phi=1.0, R_y F_y)$	=	373	kN	84	kip	<-----
---	---	-----	----	----	-----	--------

Bending on Net Area

$$V_r = \phi_N F_u Z_{net} / e$$

Factored Net Bending Resistance, V_r	=	202	kN	45	kip	<-----
--	---	-----	----	----	-----	--------

Predicted Bending Resistance $V_r(\phi=1.0, R_y F_y)$	=	313	kN	70	kip	<-----
---	---	-----	----	----	-----	--------

Configuration 4

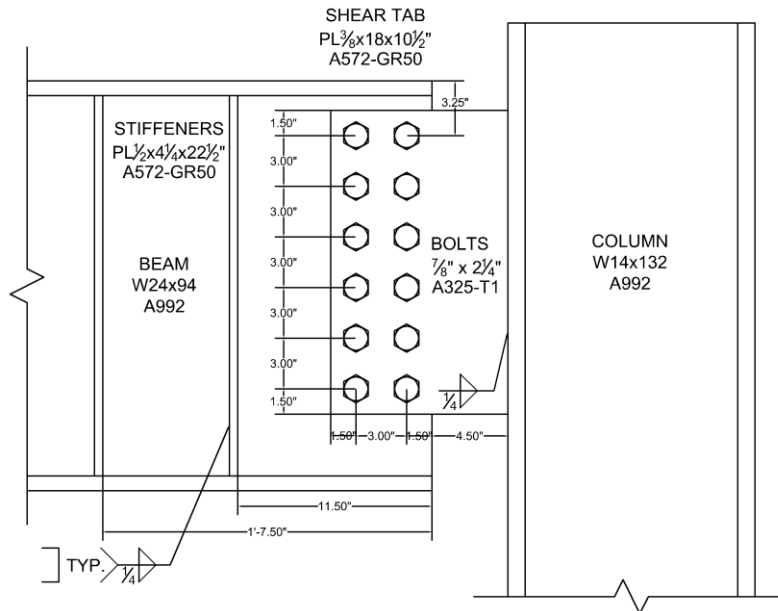


Figure A-4: Connection Details, Configuration 4

Configuration Parameters

Supporting Column		W360x196	
Supported Beam		W610x140	
Offset of Bolt Group, a	=	152 mm	6 in
Bolt Diameter, d_b	=	22.2 mm	7/8 in
Number of Bolt Lines, m	=	2	2
Number of Bolts Rows, n	=	6	6
Plate Depth, d	=	457.2 mm	18 in

1) Bolt Shear & Bearing

AISC 14th Ed Extended Config Design Check 1 (10-5)

Compute ICR Coefficient, C

Number of Bolt Lines, m	=	2	2	
Moment Arm, L	=	190.50 mm	7.5 in	
gage, D	=	76.2 mm	3 in	
Pitch, b	=	76.2 mm	3 in	
Number of Bolt Rows, n	=	6	6	
L1	=	175 mm	-	
C1	=	6.87	-	
L2	=	200 mm	-	
C2	=	6.25	-	
Eccentric Loading Coefficient, C	=	6.49	6.49	*interpolating CISC Handbook Table 3-15*

Bearing

$B_r = 3\phi_{br}d_b \min[(tF_u)_{plate}, (tF_u)_{web}] \times C$				*S16-09 C13.12.1.2a)*
Modification factor, ϕ_{br}	=	0.8	0.8	
Plate Thickness, t_p	=	9.53 mm	3/8 in	
Beam Web Thickness, t_w	=	13.10 mm	0.516 in	
Bolt Diameter, d_b	=	22.23 in	7/8 in	
Specified Tensile Stress of Plate, $F_{u,plate}$	=	450 MPa	65 ksi	
Specified Tensile Stress of Beam $F_{u,beam}$	=	450 MPa	65 ksi	
Factored Bearing Resistance, B_r	=	1483 kN	332 kip	<-----
Measured Tensile Stress of Plate, $R_y F_{u,plate}$	=	525 MPa	76.1 ksi	

Measured Tensile Stress of Beam, $R_y F_{U,beam}$	=	539	MPa	78.2	ksi	
Predicted Bearing Resistance $B_r (\phi=1.0, R_y F_U)$	=	2162	kN	486	kip	<-----

Bolt Shear

$V_r = 0.6 \phi_b n m A_b F_u \times C$						*S16-09 C13.12.1.2c)*
Modification factor, ϕ_b	=	0.8		0.8		*S16-09 C13.12.1.1*
Number of Shear Planes, m	=	1		1		
Bolt Area, A_b	=	388	mm ²	0.601	in ²	
Specified Tensile Stress of Bolts, F_u	=	825	MPa	120	ksi	
Factored Bolt Shear Resistance, V_r	=	996	kN	225	kip	<-----
Nominal Bolt Shear Resistance, $V_r (\phi=1.0)$	=	1245	kN	281	kip	<-----

2) Plate Ductility

AISC 14th Ed Extended Config Design Check 2 (10-5)

$t_{pmax} = 6M_{max} / F_y d^2$						
$M_{max} = F_{NV} / 0.90 (A_b C')$						
Bolt Shear Strength, F_{NV}	=	496.422	MPa	72	ksi	*AISC 13th Ed, Table J3.2*
Bolt Area, A_b	=	388	mm ²	0.601	in ²	
Compute ICR Coefficient, C', for Moment Only Case						
Number of Bolt Lines, m	=	2		2		
Column Spacing	=	76.2	mm	3	in	
Row Spacing, s	=	76.2	mm	3	in	
Number of Bolts Rows, n	=	6		6		
ICR Coefficient, C'	=	1376.68	mm	54.2	in	*AISC 13th Ed, Table 7-8*
M_{max}	=	294	kNm	2606	kipin	
Yield Stress of Plate, F_y	=	345	MPa	51	ksi	
Plate Depth, d	=	457.2	mm	18.0	in	
Maximum Plate Thickness, t_{pmax}	=	24.5	mm	0.946	in	
Is this requirement satisfied? ($t_p < t_{pmax}$)			YES			<-----

3) Shear Yielding, Shear Rupture and Block Shear Rupture

AISC 14th Ed Extended Config Design Check 3 (10-5)

Shear Yielding

$V_G = 0.60 \phi F_y A_g$						*AISC 13th Ed Equation J4-3*
Resistance Factor, ϕ	=	0.9		0.9		
Specified Yield Stress, F_y	=	345	MPa	51	ksi	
$A_g = t_p d_p$						
Plate Thickness, t_p	=	9.53	mm	3/8	in	
Plate Depth, d_p	=	457.2	mm	18	in	
Gross Plate Area, A_g	=	4355	mm ²	6.750	in ²	
Shear Yielding Resistance, V_G	=	811	kN	186	kip	<-----
Measured Yield Stress, $R_y F_y$	=	457	MPa	66	ksi	
Predicted Yielding Resistance, $V_G (\phi=1.0, R_y F_y)$	=	1193	kN	268	kip	<-----

Shear Rupture

$V_N = 0.60 \phi F_u A_{NV}$						*AISC 13th Ed Equation J4-4*
Resistance Factor, ϕ	=	0.75		0.75		
Specified Tensile Stress, F_u	=	450	MPa	65	ksi	
$A_{NV} = t_p d_{pN}$						
Plate Thickness, t_p	=	9.53	mm	3/8	in	
Net Depth, d_{pN}	=	304.8	mm	12.00	in	
Net Plate Area, A_{NV}	=	2903	mm ²	4.500	in ²	
Factored Shear Rupture Resistance, V_N	=	588	kN	132	kip	<-----
Measured Tensile Stress, $R_y F_u$	=	525	MPa	76.14489	ksi	
Predicted Rupture Resistance $V_N (\phi=1.0, R_y F_u)$	=	915	kN	206	kip	<-----

Block Shear Rupture

$V_{BS} = \phi [U_t A_n F_u + 0.6 A_{gv} (F_y + F_u) / 2]$						*S16-09 C13.11*
Resistance Factor, ϕ	=	0.75		0.75		*S16-09 13.1a)*
Efficiency Factor, U_t	=	0.3		0.3		*coped beam w 2 bolt lines*

Net Area in Tension, A_n	=	726	mm ²	1.125	in ²	
Specified Tensile Stress, F_u	=	450	MPa	65	ksi	
Gross Area in Shear, A_{gv}	=	3992	mm ²	6.188	in ²	
Specified Yield Stress, F_y	=	345	MPa	51	ksi	
Factored Block Shear Resistance, V_{BS}	=	788	kN	178	kip	<-----
Measured Tensile Stress, $R_y F_u$	=	525	MPa	76.14489	ksi	
Measured Yield Stress, $R_y F_y$	=	457	MPa	66	ksi	
Predicted Block Resistance $V_{BS} (\phi=1.0, R_y F_y \& F_u)$	=	1290	kN	290	kip	<-----

4) Flexural Shear Yielding, Shear Buckling, and Yielding

AISC 14th Ed Extended Config Design Check 4 (10-5)

AISC 14th Ed LFRD Approach

$$V_r = (1 / V_c^2 + (e / M_c)^2)^{-1/2} \quad \text{*AISC Handbook Eqn 10-5, modified*}$$

$$V_c = \phi_v V_n$$

$$\text{Resistance Factor, } \phi_v = 0.90 \quad 0.90 \quad \text{*use 0.9 as in S16-09 versus 1.0*}$$

$$V_n = 0.6 F_y A_g$$

$$\text{Specified Yield Stress, } F_y = 345 \text{ MPa} \quad 51 \text{ ksi}$$

$$\text{Gross Area of Plate, } A_g = 4355 \text{ mm}^2 \quad 6.750 \text{ in}^2$$

$$\text{Nominal Shear Capacity, } V_n = 901 \text{ kN} \quad 207 \text{ kip}$$

$$\text{Factored Shear Capacity, } V_c = 811 \text{ kN} \quad 186 \text{ kip}$$

$$\text{Eccentricity to first bolt column, } e = 152 \text{ mm} \quad 6 \text{ in}$$

$$M_c = \phi_b M_n$$

$$\text{Resistance Factor, } \phi_b = 0.90 \quad 0.90$$

$$M_n = F_y Z_{pl}$$

$$\text{Plastic Section Modulus, } Z_{pl} = 498 \text{ x}10^3 \text{ mm}^3 \quad 30.375 \text{ in}^3$$

$$\text{Nominal Moment Capacity, } M_n = 172 \text{ kNm} \quad 1549 \text{ kipin}$$

$$\text{Factored Moment Capacity, } M_c = 155 \text{ kNm} \quad 1394 \text{ kipin}$$

$$\text{Factored Combined Yielding Resistance, } V_r = 634 \text{ kN} \quad 145 \text{ kip} \quad <-----$$

$$\text{Measured Yield Stress, } R_y F_y = 457 \text{ MPa} \quad 66 \text{ ksi}$$

$$\text{Predicted Yielding Resistance, } V_r (\phi=1.0, R_y F_y) = 931 \text{ kN} \quad 209 \text{ kip} \quad <-----$$

AISC 13th Ed Approach

$$V_r = F_y / \sqrt{[(e/\phi Z_{pl})^2 + 3(1/t_p d_p)^2]} \quad \text{*AISC Handbook Eqn 10-4, modified*}$$

$$\text{Resistance Factor, } \phi = 0.90 \quad 0.90$$

$$\text{Specified Yield Stress, } F_y = 345 \text{ MPa} \quad 51 \text{ ksi}$$

$$\text{Eccentricity to first bolt column, } e = 152 \text{ mm} \quad 6 \text{ in}$$

$$\text{Plate Thickness, } t_p = 9.53 \text{ mm} \quad 3/8 \text{ in}$$

$$\text{Plate Depth, } d_p = 457.2 \text{ mm} \quad 18 \text{ in}$$

$$\text{Plastic Section Modulus, } Z_{pl} = 498 \text{ x}10^3 \text{ mm}^3 \quad 30.375 \text{ in}^3$$

$$\text{Shear and Flexural Yielding Resistance, } V_r = 659 \text{ kN} \quad 151 \text{ kip} \quad <-----$$

$$\text{Measured Yield Stress, } R_y F_y = 457 \text{ MPa} \quad 66 \text{ ksi}$$

$$\text{Predicted Yielding Resistance, } V_r (\phi=1.0, R_y F_y) = 909 \text{ kN} \quad 204 \text{ kip} \quad <-----$$

5) Plate Buckling

AISC 14th Ed Extended Config Design Check 5 (10-5)

$$V_r = \phi_b F_{cr} S_{net} / e$$

$$\text{Resistance Factor, } \phi_b = 0.90 \quad 0.90 \quad \text{*AISC 13th Ed Part 9, coped beams*}$$

$$S_{net} = 1/6 t_w h_o^2 = 332 \text{ x}10^3 \text{ mm}^3 \quad 20.25 \text{ in}^3$$

$$\text{Cope Depth at Compression Flange, } d_c = 38 \text{ mm} \quad 1.5 \text{ in}$$

$$\text{Beam Depth, } d = 617 \text{ mm} \quad 24.3 \text{ in}$$

$$\text{Eccentricity to first bolt column, } e = 152.4 \text{ mm} \quad 6 \text{ in}$$

$$\text{Unsupported Length of Plate, } c = 152.4 \text{ mm} \quad 6 \text{ in} \quad \text{*conservative, take to first row of bolts*}$$

$$d_c < 0.2d \& c < 2d? \quad \text{YES, fd equation valid}$$

fd equation (Cheng et al. 1984)

$$F_{cr} = 0.62 \pi E t_w^2 / (ch_o f_d)$$

$$\text{Modulus of Elasticity, } E = 200000 \text{ MPa} \quad 29000 \text{ ksi}$$

$$\text{Thickness of Plate, } t_w = 9.53 \text{ mm} \quad 3/8 \text{ in}$$

$$\text{Reduced Beam Depth, } h_o = 457.2 \text{ mm} \quad 18 \text{ in}$$

$$f_d = 3.5 - 7.5 (d_c / d)$$

Adjustment Factor, f_d	=	3.04		3.04	
Critical Stress, F_{cr}	=	1540	MPa	223.2	ksi
Plate Buckling Resistance, V_r	=	3017	kN	678	kip
Predicted Buckling Resistance, $V_r(\phi=1.0)$	=	3352	kN	753	kip

Q equation (classical plate buckling)

$F_{cr} = F_y Q$					
$\lambda = h_o \sqrt{F_y} / 10 t_w \sqrt{(475 + 280(h_o/c)^2)}$					
Specified Yield Stress, F_y	=	345	MPa	51	ksi
Measured Yield Stress, $R_y F_y$	=	457	MPa	66	ksi
Slenderness of Coped Section, λ	=			0.63	
Slenderness of Coped Section, $\lambda_{EXPECTED}$	=			0.71	
Strength Reduction Factor, Q	=	1.00		1.00	
Strength Reduction Factor, $Q_{EXPECTED}$	=	0.99		0.99	
Critical Stress, F_{cr}	=	345	MPa	51	ksi
Critical Stress, $F_{cr,EXPECTED}$	=	453.374	MPa	65.75634	ksi
Plate Buckling Resistance, V_r	=	676	kN	155	kip
Predicted Buckling Resistance $V_r(\phi=1.0, R_y F_y)$	=	987	kN	222	kip

6) Flexural Limit States

Gross Area Resistance Factor, ϕ_G	=	0.9		0.9	
Net Area Resistance Factor, ϕ_N	=	0.75		0.75	
Specified Yield Stress, F_y	=	345	MPa	51	ksi
Specified Tensile Stress, F_u	=	450	MPa	65	ksi
Measured Yield Stress, $R_y F_y$	=	457	MPa	66	ksi
Measured Tensile Stress, $R_y F_u$	=	525	MPa	76.14489	ksi
Thickness of Plate, t_p	=	9.53	mm	3/8	in
Plate Depth, d_p	=	457.2	mm	18	in
Gauge, s	=	76.2	mm	3	in
Number of Bolt Rows, n	=	6		6	
Diameter of Bolt Holes, d_h	=	25.4	mm	1	in
Section Modulus, S	=	331838	mm ³	20.25	in ³
Plastic Section Modulus, Z	=	497757	mm ³	30.38	in ³
$S_{net} = t_p / 6 [d_p^2 - s^2 n(n^2 - 1) d_h / d_p]$					
Net Section Modulus, S_{net}	=	224298	mm ³	13.69	in ³
$Z_{net} = 1/4 t_p (s - d_h) (n^2 s + d_h)$					
$Z_{net} = 1/4 t_p (s - d_h) n^2 s$					
Net Plastic Section Modulus, Z_{net}	=	331838	mm ³	20.25	in ³
Eccentricity to first bolt column, e	=	152	mm	6	in

*Engineering Journal 2008 /
2nd quarter, p102*

*Engineering Journal 2008 /
2nd quarter, p103*

AISC 3rd Edition

Bending on Gross Area

$V_r = \phi_G F_y S / e$					
Factored Gross Bending Resistance, V_r	=	676	kN	155	kip
Predicted Bending Resistance $V_r(\phi=1.0, R_y F_y)$	=	994	kN	223	kip

Bending on Net Area

$V_r = \phi_N F_u S_{net} / e$					
Factored Net Bending Resistance, V_r	=	497	kN	111	kip
Predicted Bending Resistance $V_r(\phi=1.0, R_y F_y)$	=	773	kN	174	kip

AISC 13th & 14th Edition

Bending on Gross Area

$V_r = \phi_G F_y Z / e$					
Factored Gross Bending Resistance, V_r	=	1014	kN	232	kip
Predicted Bending Resistance $V_r(\phi=1.0, R_y F_y)$	=	1491	kN	335	kip

Bending on Net Area

$V_r = \phi_N F_u Z_{net} / e$					
Factored Net Bending Resistance, V_r	=	735	kN	165	kip
Predicted Bending Resistance $V_r(\phi=1.0, R_y F_y)$	=	1143	kN	257	kip

Configuration 5, 6, 7

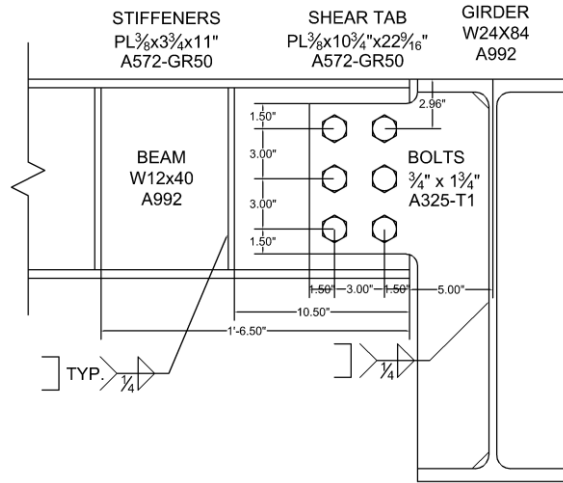


Figure A-5: Connection Details, Configuration 5

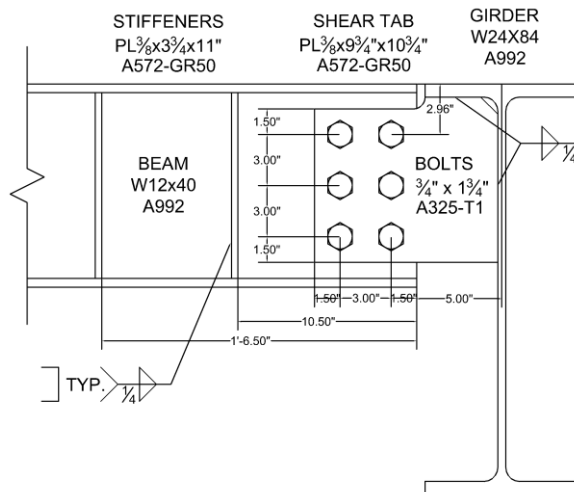


Figure A-6: Connection Details, Configuration 6

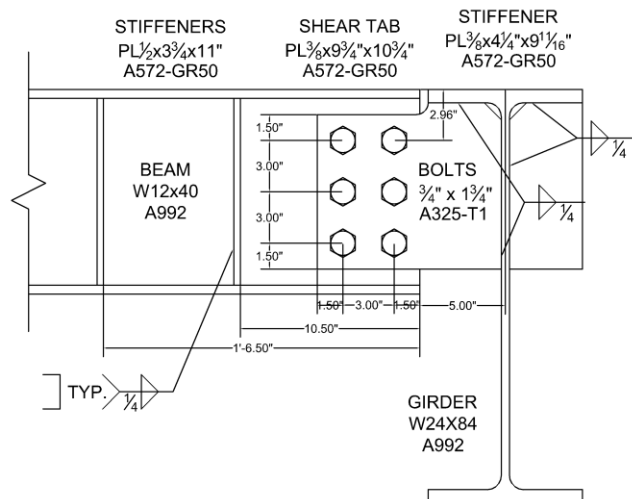


Figure A-7: Connection Details, Configuration 7

Configuration Parameters

Supporting Girder			W24x84	
Supported Beam			W12x40	
Offset of Bolt Group, a	=	165	mm	6 1/2 in
Bolt Diameter, d _b	=	19.1	mm	3/4 in
Number of Bolt Lines, m	=	2		2
Number of Bolts Rows, n	=	3		3
Plate Depth, d	=	229	mm	9 in
Plate Depth in Girder, d _g	=	573	mm	22.6 in

1) Bolt Shear & Bearing

AISC 14th Ed Extended Config Design Check 1 (10-5)

Compute ICR Coefficient, C

Number of Bolt Lines, m	=	2		2	
Moment Arm, L	=	203.20	mm	8	in
gage, D	=	76.2	mm	3	in
Pitch, b	=	76.2	mm	3	in
Number of Bolt Rows, n	=	3		3	
L1	=	200	mm	-	
C1	=	1.91		-	
L2	=	225	mm	-	
C2	=	1.73		-	
Eccentric Loading Coefficient, C	=	1.89		1.89	

interpolating CISC Handbook Table 3-15

Bearing

$B_r = 3\phi_b d_b \min[(tF_u)_{plate}, (tF_u)_{web}] \times C$					*S16-09 C13.12.1.2a)*
Modification factor, ϕ_b	=	0.8		0.8	
Plate Thickness, t_p	=	9.53	mm	3/8	in
Beam Web Thickness, t_w	=	7.50	mm	0.295	in
Bolt Diameter, d _b	=	19.05	in	3/4	in
Specified Tensile Stress of Plate, $F_{u,plate}$	=	450	MPa	65	ksi
Specified Tensile Stress of Beam $F_{u,beam}$	=	450	MPa	65	ksi
Factored Bearing Resistance, B_r	=	291	kN	65	kip
Measured Tensile Stress of Plate, $R_y F_{u,plate}$	=	525	MPa	76.144893	ksi
Measured Tensile Stress of Beam, $R_y F_{u,beam}$	=	485	MPa	70.3	ksi
Predicted Bearing Resistance $B_r (\phi=1.0, R_y F_u)$	=	392	kN	88	kip

Bolt Shear

$V_r = 0.6\phi_b n m A_b F_u \times C$					*S16-09 C13.12.1.2c)*
Modification factor, ϕ_b	=	0.8		0.8	
Number of Shear Planes, m	=	1		1	
Bolt Area, A_b	=	285	mm ²	0.442	in ²
Specified Tensile Stress of Bolts, F_u	=	825	MPa	120	ksi
Reduction factor for thread intercept	=	0.7		0.7	
Factored Bolt Shear Resistance, V_r	=	149	kN	34	kip
Nominal Bolt Shear Resistance, $V_r (\phi=1.0)$	=	186	kN	42	kip

2) Plate Ductility

AISC 14th Ed Extended Config Design Check 2 (10-5)

$t_{pmax} = 6M_{max}/F_y d^2$					
$M_{max} = F_{nv}/0.90(A_b C')$					
Bolt Shear Strength, F_{nv} (threads not excl)	=	330	MPa	48	ksi
Bolt Area, A_b	=	285	mm ²	0.442	in ²
Compute ICR Coefficient, C', for Moment Only Case					
Number of Bolt Lines, m	=	2		2	
Column Spacing	=	76.2	mm	3	in
Row Spacing, s	=	76.2	mm	3	in
Number of Bolts Rows, n	=	3		3	
ICR Coefficient, C'	=	401.32	mm	15.8	in
M_{max}	=	42	kNm	372	kipin

AISC 13th Ed, Table J3.2

AISC 13th Ed, Table 7-8

Specified Yield Stress of Plate, F_Y	=	345	MPa	51	ksi	
Plate Depth, d	=	228.6	mm	9.0	in	
Maximum Plate Thickness, t_{pmax}	=	14.0	mm	0.540	in	
Is this requirement satisfied? ($t_p < t_{pmax}$)		YES			<-----	

3) Shear Yielding, Shear Rupture and Block Shear Rupture

AISC 14th Ed Extended Config Design Check 3 (10-5)

Shear Yielding

$V_G = 0.60\phi F_Y A_g$						*AISC 13th Ed Equation J4-3*
Resistance Factor, ϕ	=	0.9		0.9		
Specified Yield Stress, F_Y	=	345	MPa	51	ksi	
$A_g = t_p d_p$						
Plate Thickness, t_p	=	9.53	mm	3/8	in	
Plate Depth, d_p	=	228.6	mm	9	in	
Gross Plate Area, A_g	=	2177	mm ²	3.375	in ²	
Shear Yielding Resistance, V_G	=	406	kN	93	kip	<-----
Measured Yield Stress, $R_Y F_Y$	=	457	MPa	66	ksi	
Predicted Yielding Resistance, $V_G (\phi=1.0, R_Y F_Y)$	=	596	kN	134	kip	<-----

Shear Rupture

$V_N = 0.60\phi F_U A_{NV}$						*AISC 13th Ed Equation J4-4*
Resistance Factor, ϕ	=	0.75		0.75		
Specified Tensile Stress, F_U	=	450	MPa	65	ksi	
$A_{NV} = t_p d_{pN}$						
Plate Thickness, t_p	=	9.53	mm	3/8	in	
Net Depth, d_{pN}	=	161.9	mm	6.38	in	
Net Plate Area, A_{NV}	=	1542	mm ²	2.391	in ²	
Factored Shear Rupture Resistance, V_N	=	312	kN	70	kip	<-----
Measured Tensile Stress, $R_Y F_U$	=	525	MPa	76.144893	ksi	
Predicted Rupture Resistance $V_N (\phi=1.0, R_Y F_U)$	=	486	kN	109	kip	<-----

Block Shear Rupture

$V_{BS} = \phi [U_t A_n F_U + 0.6 A_{gV} (F_Y + F_U)] / 2$						*S16-09 C13.11*
Resistance Factor, ϕ	=	0.75		0.75		*S16-09 13.1a)*
Efficiency Factor, U_t	=	0.3		0.3		*coped beam w 2 bolt lines*
Net Area in Tension, A_n	=	771	mm ²	1.195	in ²	
Specified Tensile Stress, F_U	=	450	MPa	65	ksi	
Gross Area in Shear, A_{gV}	=	1815	mm ²	2.813	in ²	
Specified Yield Stress, F_Y	=	345	MPa	51	ksi	
Factored Block Shear Resistance, V_{BS}	=	403	kN	91	kip	<-----
Measured Tensile Stress, $R_Y F_U$	=	525	MPa	76.144893	ksi	
Measured Yield Stress, $R_Y F_Y$	=	457	MPa	66	ksi	
Predicted Block Resistance $V_{BS} (\phi=1.0, R_Y F_Y \& F_U)$	=	656	kN	147	kip	<-----

4) Flexural Shear Yielding, Shear Buckling, and Yielding

AISC 14th Ed Extended Config Design Check 4 (10-5)

AISC 14th Ed LFRD Approach

$V_r = (1 / V_c^2 + (e / M_c)^2)^{-1/2}$						*AISC Handbook Eqn 10-5, modified*
$V_c = \phi_v V_n$						
Resistance Factor, ϕ_v	=	0.90		0.90		*use 0.9 as in S16-09 versus 1.0*
$V_n = 0.6 F_Y A_g$						
Specified Yield Stress, F_Y	=	345	MPa	51	ksi	
Gross Area of Plate, A_g	=	2177	mm ²	3.375	in ²	
Nominal Shear Capacity, V_n	=	451	kN	103	kip	
Factored Shear Capacity, V_c	=	406	kN	93	kip	
Eccentricity to first bolt column, e	=	165	mm	7	in	
$M_c = \phi_b M_n$						
Resistance Factor, ϕ_b	=	0.90		0.90		
$M_n = F_Y Z_{pl}$						

Plastic Section Modulus, Z_{pl}	=	124	$\times 10^3 \text{ mm}^3$	7.594	in^3	
Nominal Moment Capacity, M_n	=	43	kNm	387	kipin	
Factored Moment Capacity, M_c	=	39	kipin	349	kNm	
Factored Combined Yielding Resistance, V_r	=	203	kN	46	kip	<-----
Measured Yield Stress, $R_y F_y$	=	457	MPa	66	ksi	
Predicted Yielding Resistance, $V_r (\phi=1.0, R_y F_y)$	=	298	kN	67	kip	<-----

AISC 13th Ed Approach

$V_r = F_y / \sqrt{[(e/\phi Z_{pl})^2 + 3(1/t_p d_p)^2]}$						*AISC Handbook Eqn 10-4, modified*
Resistance Factor, ϕ	=	0.90		0.90		
Specified Yield Stress, F_y	=	345	MPa	51	ksi	
Eccentricity to first bolt column, e	=	165	mm	7	in	
Plate Thickness, t_p	=	9.53	mm	3/8	in	
Plate Depth, d_p	=	228.6	mm	9	in	
Plastic Section Modulus, Z_{pl}	=	124	$\times 10^3 \text{ mm}^3$	7.594	in^3	
Shear and Flexural Yielding Resistance, V_r	=	206	kN	47	kip	<-----
Measured Yield Stress, $R_y F_y$	=	457	MPa	66	ksi	
Predicted Yielding Resistance, $V_r (\phi=1.0, R_y F_y)$	=	295	kN	66	kip	<-----

5) Plate Buckling

AISC 14th Ed Extended Config Design Check 5 (10-5)

$V_r = \phi_b F_{cr} S_{net} / e$						*AISC 13th Ed Part 9, coped beams*
Resistance Factor, ϕ_b	=	0.90		0.90		
$S_{net} = 1/6 t_w h_o^2$	=	83	$\times 10^3 \text{ mm}^3$	5.06	in^3	
Cope Depth at Compression Flange, d_c	=	41	mm	1.6	in	
Beam Depth, d	=	310	mm	12.2	in	
Eccentricity to first bolt column, e	=	165.1	mm	6 1/2	in	*conservative, take to first row
Unsupported Length of Plate, c	=	165.1	mm	6 1/2	in	of bolts*
$d_c < 0.2d$ & $c < 2d$?						YES, fd equation valid

fd equation (Cheng et al. 1984)

$F_{cr} = 0.62 \pi E t_w^2 / (ch_o f_d)$						
Modulus of Elasticity, E	=	200000	MPa	29000	ksi	
Thickness of Plate, t_w	=	9.53	mm	3/8	in	
Reduced Beam Depth, h_o	=	228.6	mm	9	in	
$f_d = 3.5 - 7.5 (d_c / d)$						
Adjustment Factor, f_d	=	2.52		2.52		
Critical Stress, F_{cr}	=	2354	MPa	341.4	ksi	
Plate Buckling Resistance, V_r	=	1065	kN	239	kip	<-----
Predicted Buckling Resistance, $V_r (\phi=1.0)$	=	1183	kN	266	kip	<-----

Q equation (classical plate buckling)

$F_{cr} = F_y Q$						
$\lambda = h_o \sqrt{F_y} / 10 t_w \sqrt{(475 + 280(h_o/c)^2)}$						
Specified Yield Stress, F_y	=	345	MPa	51	ksi	
Measured Yield Stress, $R_y F_y$	=	457	MPa	66	ksi	
Slenderness of Coped Section, λ	=			0.54		
Slenderness of Coped Section, $\lambda_{EXPECTED}$	=			0.61		
Strength Reduction Factor, Q	=	1.00		1.00		
Strength Reduction Factor, $Q_{EXPECTED}$	=	1.00		1.00		
Critical Stress, F_{cr}	=	345	MPa	51	ksi	
Critical Stress, $F_{cr, EXPECTED}$	=	456.5	MPa	66.209797	ksi	
Plate Buckling Resistance, V_r	=	156	kN	36	kip	<-----
Predicted Buckling Resistance $V_r (\phi=1.0, R_y F_y)$	=	229	kN	52	kip	<-----

6) Flexural Limit States

Gross Area Resistance Factor, ϕ_G	=	0.9		0.9		
Net Area Resistance Factor, ϕ_N	=	0.75		0.75		
Specified Yield Stress, F_y	=	345	MPa	51	ksi	

Specified Tensile Stress, F_U	=	450	MPa	65	ksi	
Measured Yield Stress, $R_Y F_Y$	=	457	MPa	66	ksi	
Measured Tensile Stress, $R_Y F_U$	=	525	MPa	76.144893	ksi	
Thickness of Plate, t_p	=	9.53	mm	3/8	in	
Plate Depth, d_p	=	228.6	mm	9	in	
Gauge, s	=	76.2	mm	3	in	
Number of Bolt Rows, n	=	3		3		
Diameter of Bolt Holes, d_h	=	22.2	mm	7/8	in	
Section Modulus, S	=	82960	mm ³	5.06	in ³	
Plastic Section Modulus, Z	=	124439	mm ³	7.59	in ³	
$S_{net} = t_p / 6 [d_p^2 - s^2 n (n^2 - 1) d_h / d_p]$						*Engineering Journal 2008 /
Net Section Modulus, S_{net}	=	61451.5	mm ³	3.75	in ³	2nd quarter, p102*
$Z_{net} = 1/4 t_p (s - d_h) (n^2 s + d_h)$						
$Z_{net} = 1/4 t_p (s - d_h) n^2 s$						*Engineering Journal 2008 /
Net Plastic Section Modulus, Z_{net}	=	91001	mm ³	5.55	in ³	2nd quarter, p103*
Eccentricity to first bolt column, e	=	165	mm	7	in	

AISC 3rd Edition

Bending on Gross Area

$$V_r = \phi_G F_Y S / e$$

Factored Gross Bending Resistance, V_r	=	156	kN	36	kip	<-----
Predicted Bending Resistance $V_r (\phi=1.0, R_Y F_Y)$	=	229	kN	52	kip	<-----

Bending on Net Area

$$V_r = \phi_N F_U S_{net} / e$$

Factored Net Bending Resistance, V_r	=	126	kN	28	kip	<-----
Predicted Bending Resistance $V_r (\phi=1.0, R_Y F_Y)$	=	195	kN	44	kip	<-----

AISC 13th & 14th Edition

Bending on Gross Area

$$V_r = \phi_G F_Y Z / e$$

Factored Gross Bending Resistance, V_r	=	234	kN	54	kip	<-----
Predicted Bending Resistance $V_r (\phi=1.0, R_Y F_Y)$	=	344	kN	77	kip	<-----

Bending on Net Area

$$V_r = \phi_N F_U Z_{net} / e$$

Factored Net Bending Resistance, V_r	=	186	kN	42	kip	<-----
Predicted Bending Resistance $V_r (\phi=1.0, R_Y F_Y)$	=	289	kN	65	kip	<-----

Configuration 8

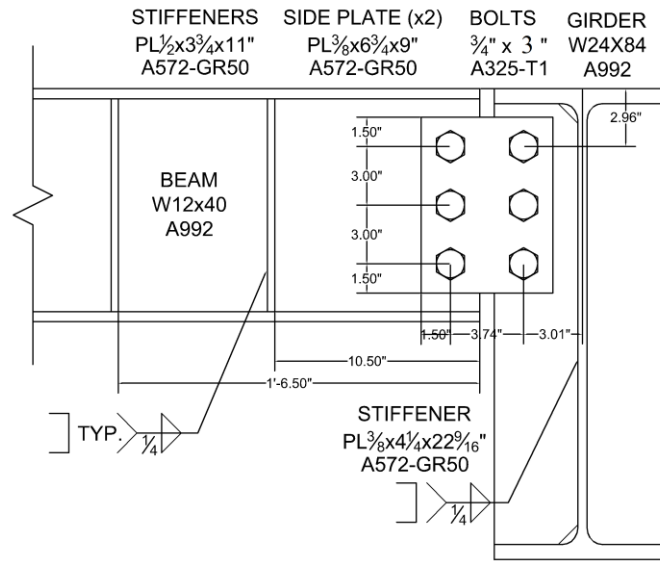


Figure A-8: Connection Details, Configuration 8

Configuration Parameters

Supporting Girder		W24x84
Supported Beam		W12x40
Offset of Bolt Group, a	=	171 mm 6 3/4 in
Bolt Diameter, d_b	=	19.1 mm 3/4 in
Number of Bolt Lines, m	=	1 1
Number of Bolts Rows, n	=	3 3
Plate Depth, d	=	229 mm 9 in
Plate Depth in Girder, d_g	=	573 mm 22.6 in
Total Plate Thickness, $t_{pT} = 2t_p$	=	19.1 mm 3/4 in

1) Bolt Shear & Bearing

AISC 14th Ed Extended Config Design Check 1 (10-5)

Compute ICR Coefficient, C

Number of Bolt Lines, m	=	1	1	
Moment Arm, L	=	171.45 mm	6.75 in	*Bolts in Beam are critical,
Pitch, b	=	76.2 mm	3 in	bolts in girder will have higher
Number of Bolt Rows, n	=	3	3	C factor"
L1	=	150 mm	-	
C1	=	1.05	-	
L2	=	175 mm	-	*interpolating CISC Handbook
C2	=	0.9	-	Table 3-14*
Eccentric Loading Coefficient, C	=	0.92	0.92	

Bearing

$$B_r = 3\phi_{br}d_b \min[(tF_u)_{plate}, (tF_u)_{web}] \times C$$

Modification factor, ϕ_{br}	=	0.8	0.8	*S16-09 C13.12.1.2a)*
Plate Thickness, t_p	=	9.53 mm	3/8 in	*take stiffener thickness*
Beam Web Thickness, t_w	=	7.50 mm	0.295 in	
Bolt Diameter, d_b	=	19.05 in	3/4 in	
Specified Tensile Stress of Plate, $F_{u,plate}$	=	450 MPa	65 ksi	
Specified Tensile Stress of Beam $F_{u,beam}$	=	450 MPa	65 ksi	
Factored Bearing Resistance, B_r	=	142 kN	32 kip	<-----
Measured Tensile Stress of Plate, $R_y F_{u,plate}$	=	525 MPa	76.144893 ksi	
Measured Tensile Stress of Beam, $R_y F_{u,beam}$	=	511 MPa	74.1 ksi	

Predicted Bearing Resistance $B_r (\phi=1.0, R_y F_U)$	=	202	kN	45	kip	<-----
--	---	-----	----	----	-----	--------

Bolt Shear

$V_r = 0.6 \phi_b n m A_b F_u \times C$						*S16-09 C13.12.1.2c)*
Modification factor, ϕ_b	=	0.8		0.8		*S16-09 C13.12.1.1*
Number of Shear Planes, m	=	2		2		
Bolt Area, A_b	=	285	mm ²	0.442	in ²	
Specified Tensile Stress of Bolts, F_U	=	825	MPa	120	ksi	
Factored Bolt Shear Resistance, V_r	=	208	kN	47	kip	<-----
Nominal Bolt Shear Resistance, $V_r (\phi=1.0)$	=	260	kN	59	kip	<-----

2) Plate Ductility

AISC 14th Ed Extended Config Design Check 2 (10-5)

$t_{pmax} = 6M_{max} / F_y d^2$						
$M_{max} = F_{nv} / 0.90 (A_b C')$						
Bolt Shear Strength, F_{nv} (threads not excl)	=	496.4	MPa	72	ksi	*AISC 13th Ed, Table J3.2*
Bolt Area, A_b	=	285	mm ²	0.442	in ²	
Compute ICR Coefficient, C', for Moment Only Case						
Number of Bolt Lines, m	=	1		1		
Column Spacing	=	76.2	mm	3	in	
Row Spacing, s	=	76.2	mm	3	in	
Number of Bolts Rows, n	=	3		3		
ICR Coefficient, C'	=	149.606	mm	5.9	in	*AISC 13th Ed, Table 7-8*
M_{max}	=	24	kNm	208	kipin	
Specified Yield Stress of Plate, F_y	=	345	MPa	51	ksi	
Plate Depth, d	=	228.6	mm	9.0	in	
Maximum Plate Thickness, t_{pmax}	=	7.8	mm	0.302	in	
Is this requirement satisfied? ($t_p < t_{pmax}$)		NO				<-----

3) Shear Yielding, Shear Rupture and Block Shear Rupture

AISC 14th Ed Extended Config Design Check 3 (10-5)

Shear Yielding

$V_G = 0.60 \phi F_y A_g$						*AISC 13th Ed Equation J4-3*
Resistance Factor, ϕ	=	0.9		0.9		
Specified Yield Stress, F_y	=	345	MPa	51	ksi	
$A_g = t_p d_p$						
Plate Thickness, t_p	=	19	mm	3/4	in	
Plate Depth, d_p	=	228.6	mm	9	in	
Gross Plate Area, A_g	=	4355	mm ²	6.750	in ²	
Shear Yielding Resistance, V_G	=	811	kN	186	kip	<-----
Measured Yield Stress, $R_y F_y$	=	457	MPa	66	ksi	
Predicted Yielding Resistance, $V_G (\phi=1.0, R_y F_y)$	=	1193	kN	268	kip	<-----

Shear Rupture

$V_N = 0.60 \phi F_u A_{NV}$						*AISC 13th Ed Equation J4-4*
Resistance Factor, ϕ	=	0.75		0.75		
Specified Tensile Stress, F_U	=	450	MPa	65	ksi	
$A_{NV} = t_p d_{pN}$						
Plate Thickness, t_p	=	19	mm	3/4	in	
Net Depth, d_{pN}	=	161.9	mm	6.38	in	
Net Plate Area, A_{NV}	=	3085	mm ²	4.781	in ²	
Factored Shear Rupture Resistance, V_N	=	625	kN	140	kip	<-----
Measured Tensile Stress, $R_y F_U$	=	525	MPa	76.144893	ksi	
Predicted Rupture Resistance $V_N (\phi=1.0, R_y F_U)$	=	972	kN	218	kip	<-----

Block Shear Rupture

$V_{BS} = \phi_U [U_t A_n F_U + 0.6 A_{gv} (F_y + F_U)] / 2$						*S16-09 C13.11*
Resistance Factor, ϕ_U	=	0.75		0.75		*S16-09 13.1a)*
Efficiency Factor, U_t	=	0.3		0.3		*coped beam w 2 bolt lines*
Net Area in Tension, A_n	=	514	mm ²	0.797	in ²	

Specified Tensile Stress, F_U	=	450	MPa	65	ksi	
Gross Area in Shear, A_{gV}	=	3629	mm ²	5.625	in ²	
Specified Yield Stress, F_Y	=	345	MPa	51	ksi	
Factored Block Shear Resistance, V_{BS}	=	701	kN	158	kip	<-----
Measured Tensile Stress, $R_Y F_U$	=	525	MPa	76.144893	ksi	
Measured Yield Stress, $R_Y F_Y$	=	457	MPa	66	ksi	
Predicted Block Resistance $V_{BS} (\phi=1.0, R_Y F_Y \& F_U)$	=	1150	kN	258	kip	<-----

4) Flexural Shear Yielding, Shear Buckling, and Yielding

AISC 14th Ed Extended Config Design Check 4 (10-5)

AISC 14th Ed LFRD Approach

$$V_r = (1/V_c^2 + (e/M_c)^2)^{-1/2} \quad \text{*AISC Handbook Eqn 10-5, modified*}$$

$$V_c = \phi_v V_n$$

$$\text{Resistance Factor, } \phi_v = 0.90 \quad 0.90 \quad \text{*use 0.9 as in S16-09 versus 1.0*}$$

$$V_n = 0.6 F_Y A_g$$

$$\text{Specified Yield Stress, } F_Y = 345 \text{ MPa} \quad 51 \text{ ksi}$$

$$\text{Gross Area of Plate, } A_g = 4355 \text{ mm}^2 \quad 6.750 \text{ in}^2$$

$$\text{Nominal Shear Capacity, } V_n = 901 \text{ kN} \quad 207 \text{ kip}$$

$$\text{Factored Shear Capacity, } V_c = 811 \text{ kN} \quad 186 \text{ kip}$$

$$\text{Eccentricity to first bolt column, } e = 171 \text{ mm} \quad 7 \text{ in}$$

$$M_c = \phi_b M_n$$

$$\text{Resistance Factor, } \phi_b = 0.90 \quad 0.90$$

$$M_n = F_Y Z_{pl}$$

$$\text{Plastic Section Modulus, } Z_{pl} = 249 \text{ x}10^3 \text{ mm}^3 \quad 15.188 \text{ in}^3$$

$$\text{Nominal Moment Capacity, } M_n = 86 \text{ kNm} \quad 775 \text{ kipin}$$

$$\text{Factored Moment Capacity, } M_c = 77 \text{ kipin} \quad 697 \text{ kNm}$$

$$\text{Factored Combined Yielding Resistance, } V_r = 394 \text{ kN} \quad 90 \text{ kip} \quad <-----$$

$$\text{Measured Yield Stress, } R_Y F_Y = 457 \text{ MPa} \quad 66 \text{ ksi}$$

$$\text{Predicted Yielding Resistance, } V_r (\phi=1.0, R_Y F_Y) = 579 \text{ kN} \quad 130 \text{ kip} \quad <-----$$

AISC 13th Ed Approach

$$V_r = F_Y / \sqrt{[(e/\phi Z_{pl})^2 + 3(1/t_p d_p)^2]} \quad \text{*AISC Handbook Eqn 10-4, modified*}$$

$$\text{Resistance Factor, } \phi = 0.90 \quad 0.90$$

$$\text{Specified Yield Stress, } F_Y = 345 \text{ MPa} \quad 51 \text{ ksi}$$

$$\text{Eccentricity to first bolt column, } e = 171 \text{ mm} \quad 7 \text{ in}$$

$$\text{Plate Thickness, } t_p = 19.05 \text{ mm} \quad 3/4 \text{ in}$$

$$\text{Plate Depth, } d_p = 228.6 \text{ mm} \quad 9 \text{ in}$$

$$\text{Plastic Section Modulus, } Z_{pl} = 249 \text{ x}10^3 \text{ mm}^3 \quad 15.188 \text{ in}^3$$

$$\text{Shear and Flexural Yielding Resistance, } V_r = 400 \text{ kN} \quad 92 \text{ kip} \quad <-----$$

$$\text{Measured Yield Stress, } R_Y F_Y = 457 \text{ MPa} \quad 66 \text{ ksi}$$

$$\text{Predicted Yielding Resistance, } V_r (\phi=1.0, R_Y F_Y) = 574 \text{ kN} \quad 129 \text{ kip} \quad <-----$$

5) Plate Buckling

AISC 14th Ed Extended Config Design Check 5 (10-5)

$$V_r = \phi_b F_{cr} S_{net} / e$$

AISC 13th Ed Part 9, coped beams

$$\text{Resistance Factor, } \phi_b = 0.90 \quad 0.90$$

$$S_{net} = 1/6 t_w h_o^2 = 166 \text{ x}10^3 \text{ mm}^3 \quad 10.13 \text{ in}^3$$

$$\text{Cope Depth at Compression Flange, } d_c = 41 \text{ mm} \quad 1.6 \text{ in}$$

$$\text{Beam Depth, } d = 310 \text{ mm} \quad 12.2 \text{ in}$$

$$\text{Eccentricity to first bolt column, } e = 171.5 \text{ mm} \quad 6 \text{ } 3/4 \text{ in}$$

$$\text{Unsupported Length of Plate, } c = 76.2 \text{ mm} \quad 3 \text{ in} \quad \text{*conservative, take to first row of bolts*}$$

$$d_c < 0.2d \& c < 2d?$$

YES, fd equation valid

NOT APPLICABLE

fd equation (Cheng et al. 1984)

$$F_{cr} = 0.62 \pi E t_w^2 / ch_o f_d$$

$$\text{Modulus of Elasticity, } E = 200000 \text{ MPa} \quad 29000 \text{ ksi}$$

$$\text{Thickness of Plate, } t_w = 19.05 \text{ mm} \quad 3/4 \text{ in}$$

$$\text{Reduced Beam Depth, } h_o = 228.6 \text{ mm} \quad 9 \text{ in}$$

$$f_d = 3.5 - 7.5 (d_c / d)$$

$$\text{Adjustment Factor, } f_d = 2.52 \quad 2.52$$

Critical Stress, F_{cr}	=	9068	MPa	1314.9	ksi	
Plate Buckling Resistance, $V_{r,84}$	=	7898	kN	1775	kip	<-----
Plate Buckling Strength, $V_r(\phi=1.0)$	=	8776	kN	1972	kip	<-----

Q equation (classical plate buckling)

$$F_{cr} = F_y Q$$

$$\lambda = h_o \sqrt{F_y} / 10 t_w \sqrt{(475 + 280(h_o/c)^2)}$$

Yield Stress of Plate, F_y	=	345	MPa	51	ksi	
Probable Yield Stress, $R_y F_y$	=	457	MPa	66	ksi	
Slenderness of Coped Section, λ	=			0.27		
Slenderness of Coped Section, $\lambda_{EXPECTED}$	=			0.31		
Strength Reduction Factor, Q	=	1.00		1.00		
Strength Reduction Factor, $Q_{EXPECTED}$	=	1.00		1.00		
Critical Stress, F_{cr}	=	345	MPa	51	ksi	
Critical Stress, $F_{cr,EXPECTED}$	=	456.5	MPa	66.209797	ksi	
Plate Buckling Resistance, V_r	=	300	kN	69	kip	<-----
Plate Buckling Strength, $V_r(\phi=1.0, R_y F_y)$	=	442	kN	99	kip	<-----

6) Flexural Limit States

Gross Area Resistance Factor, ϕ_G	=	0.9		0.9		
Net Area Resistance Factor, ϕ_N	=	0.75		0.75		
Specified Yield Stress, F_y	=	345	MPa	51	ksi	
Specified Tensile Stress, F_u	=	450	MPa	65	ksi	
Measured Yield Stress, $R_y F_y$	=	457	MPa	66	ksi	
Measured Tensile Stress, $R_y F_u$	=	525	MPa	76.144893	ksi	
Thickness of Plate, t_p	=	9.53	mm	3/8	in	
Plate Depth, d_p	=	228.6	mm	9	in	
Gauge, s	=	76.2	mm	3	in	
Number of Bolt Rows, n	=	3		3		
Diameter of Bolt Holes, d_h	=	22.2	mm	7/8	in	
Section Modulus, S	=	82960	mm ³	5.06	in ³	
Plastic Section Modulus, Z	=	124439	mm ³	7.59	in ³	
$S_{net} = t_p / 6 [d_p^2 - s^2 n (n^2 - 1) d_h / d_p]$						*Engineering Journal 2008 / 2nd quarter, p102*
Net Section Modulus, S_{net}	=	61451.5	mm ³	3.75	in ³	
$Z_{net} = 1/4 t_p (s - d_h) (n^2 s + d_h)$						
$Z_{net} = 1/4 t_p (s - d_h) n^2 s$						*Engineering Journal 2008 / 2nd quarter, p103*
Net Plastic Section Modulus, Z_{net}	=	91001	mm ³	5.55	in ³	
Eccentricity to first bolt column, e	=	171	mm	7	in	

AISC 3rd Edition

Bending on Gross Area

$$V_r = \phi_G F_y S / e$$

Factored Gross Bending Resistance, V_r	=	150	kN	34	kip	<-----
Predicted Bending Resistance $V_r(\phi=1.0, R_y F_y)$	=	221	kN	50	kip	<-----

Bending on Net Area

$$V_r = \phi_N F_u S_{net} / e$$

Factored Net Bending Resistance, V_r	=	121	kN	27	kip	<-----
Predicted Bending Resistance $V_r(\phi=1.0, R_y F_y)$	=	188	kN	42	kip	<-----

AISC 13th & 14th Edition

Bending on Gross Area

$$V_r = \phi_G F_y Z / e$$

Factored Gross Bending Resistance, V_r	=	225	kN	52	kip	<-----
Predicted Bending Resistance $V_r(\phi=1.0, R_y F_y)$	=	331	kN	74	kip	<-----

Bending on Net Area

$$V_r = \phi_N F_u Z_{net} / e$$

Factored Net Bending Resistance, V_r	=	179	kN	40	kip	<-----
Predicted Bending Resistance $V_r(\phi=1.0, R_y F_y)$	=	279	kN	63	kip	<-----

Configuration 9, 10

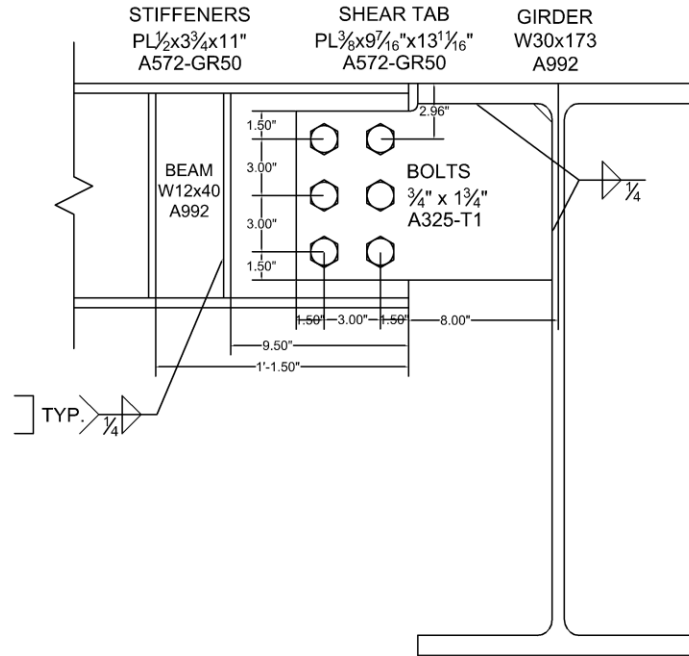


Figure A-9: Connection Details, Configuration 9

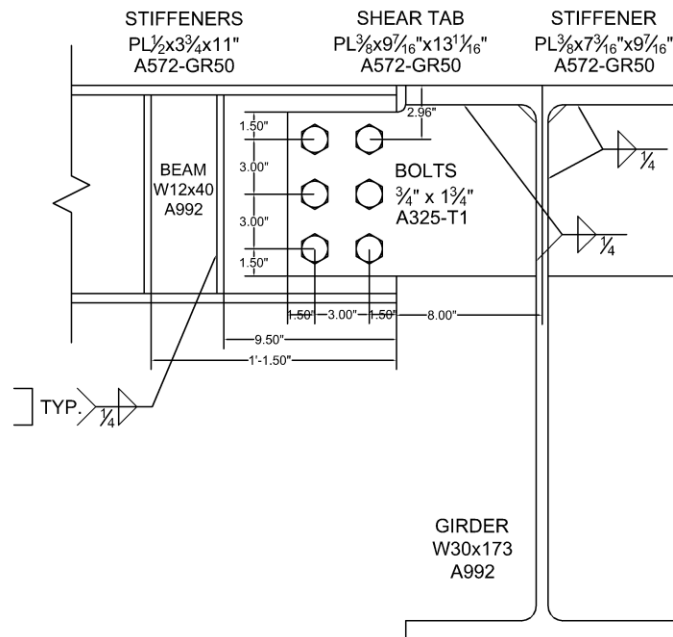


Figure A-10: Connection Details, Configuration 10

Configuration Parameters

Supporting Girder			W30x173	
Supported Beam			W12x40	
Offset of Bolt Group, a	=	241	mm	9 1/2 in
Bolt Diameter, d_b	=	19.1	mm	3/4 in
Number of Bolt Lines, m	=	2		2
Number of Bolts Rows, n	=	3		3
Plate Depth, d	=	229	mm	9 in
Plate Depth in Girder, d_g	=	229	mm	9.0 in

1) Bolt Shear & Bearing

AISC 14th Ed Extended Config Design Check 1 (10-5)

Compute ICR Coefficient, C

Number of Bolt Lines, m	=	2		2	
Moment Arm, L	=	279.40	mm	11	in
gage, D	=	76.2	mm	3	in
Pitch, b	=	76.2	mm	3	in
Number of Bolt Rows, n	=	3		3	
L1	=	250	mm	-	
C1	=	1.58		-	
L2	=	300	mm	-	
C2	=	1.34		-	
Eccentric Loading Coefficient, C	=	1.44		1.44	

interpolating CISC Handbook Table 3-15

Bearing

$B_r = 3\phi_b d_b \min[(tF_u)_{plate}, (tF_u)_{web}] \times C$					
Modification factor, ϕ_b	=	0.8		0.8	
Plate Thickness, t_p	=	9.53	mm	3/8	in
Beam Web Thickness, t_w	=	7.50	mm	0.295	in
Bolt Diameter, d_b	=	19.05	in	3/4	in
Specified Tensile Stress of Plate, $F_{u,plate}$	=	450	MPa	65	ksi
Specified Tensile Stress of Beam $F_{u,beam}$	=	450	MPa	65	ksi
Factored Bearing Resistance, B_r	=	222	kN	50	kip
Measured Tensile Stress of Plate, $R_y F_{u,plate}$	=	525	MPa	76.14489	ksi
Measured Tensile Stress of Beam, $R_y F_{u,beam}$	=	511	MPa	74.1	ksi
Predicted Bearing Resistance $B_r (\phi=1.0, R_y F_u)$	=	315	kN	71	kip

S16-09 C13.12.1.2a)

Bolt Shear

$V_r = 0.6\phi_b n m A_b F_u \times C$					
Modification factor, ϕ_b	=	0.8		0.8	
Number of Shear Planes, m	=	1		1	
Bolt Area, A_b	=	285	mm ²	0.442	in ²
Specified Tensile Stress of Bolts, F_u	=	825	MPa	120	ksi
Reduction factor for thread intercept	=	0.7		0.7	
Factored Bolt Shear Resistance, V_r	=	114	kN	26	kip
Nominal Bolt Shear Resistance, $V_r (\phi=1.0)$	=	142	kN	32	kip

S16-09 C13.12.1.2c)

S16-09 C13.12.1.1

2) Plate Ductility

AISC 14th Ed Extended Config Design Check 2 (10-5)

$t_{pmax} = 6M_{max}/F_y d^2$					
$M_{max} = F_{nv}/0.90(A_b C')$					
Bolt Shear Strength, F_{nv} (threads not excl)	=	330	MPa	48	ksi
Bolt Area, A_b	=	285	mm ²	0.442	in ²
Compute ICR Coefficient, C', for Moment Only Case					
Number of Bolt Lines, m	=	2		2	
Column Spacing	=	76.2	mm	3	in
Row Spacing, s	=	76.2	mm	3	in
Number of Bolts Rows, n	=	3		3	
ICR Coefficient, C'	=	401.32	mm	15.8	in
M_{max}	=	42	kNm	372	kipin

AISC 13th Ed, Table J3.2

AISC 13th Ed, Table 7-8

Specified Yield Stress of Plate, F_Y	=	345	MPa	51	ksi	
Plate Depth, d	=	228.6	mm	9.0	in	
Maximum Plate Thickness, t_{pmax}	=	14.0	mm	0.540	in	
<i>Is this requirement satisfied? ($t_p < t_{pmax}$)</i>						YES <-----

3) Shear Yielding, Shear Rupture and Block Shear Rupture

AISC 14th Ed Extended Config Design Check 3 (10-5)

Shear Yielding

$V_G = 0.60\phi F_Y A_g$						*AISC 13th Ed Equation J4-3*
Resistance Factor, ϕ	=	0.9		0.9		
Specified Yield Stress, F_Y	=	345	MPa	51	ksi	
$A_g = t_p d_p$						
Plate Thickness, t_p	=	9.53	mm	3/8	in	
Plate Depth, d_p	=	228.6	mm	9	in	
Gross Plate Area, A_g	=	2177	mm ²	3.375	in ²	
Shear Yielding Resistance, V_G	=	406	kN	93	kip	<-----
Measured Yield Stress, $R_Y F_Y$	=	457	MPa	66	ksi	
Predicted Yielding Resistance, $V_G (\phi=1.0, R_Y F_Y)$	=	596	kN	134	kip	<-----

Shear Rupture

$V_N = 0.60\phi F_U A_{NV}$						*AISC 13th Ed Equation J4-4*
Resistance Factor, ϕ	=	0.75		0.75		
Specified Tensile Stress, F_U	=	450	MPa	65	ksi	
$A_{NV} = t_p d_{pN}$						
Plate Thickness, t_p	=	9.53	mm	3/8	in	
Net Depth, d_{pN}	=	161.9	mm	6.38	in	
Net Plate Area, A_{NV}	=	1542	mm ²	2.391	in ²	
Factored Shear Rupture Resistance, V_N	=	312	kN	70	kip	<-----
Measured Tensile Stress, $R_Y F_U$	=	525	MPa	76.14489	ksi	
Predicted Rupture Resistance $V_N (\phi=1.0, R_Y F_U)$	=	486	kN	109	kip	<-----

Block Shear Rupture

$V_{BS} = \phi [U_t A_n F_U + 0.6 A_{gV} (F_Y + F_U)] / 2$						*S16-09 C13.11*
Resistance Factor, ϕ_U	=	0.75		0.75		*S16-09 13.1a)*
Efficiency Factor, U_t	=	0.3		0.3		*coped beam w 2 bolt lines*
Net Area in Tension, A_n	=	771	mm ²	1.195	in ²	
Specified Tensile Stress, F_U	=	450	MPa	65	ksi	
Gross Area in Shear, A_{gV}	=	1815	mm ²	2.813	in ²	
Specified Yield Stress, F_Y	=	345	MPa	51	ksi	
Factored Block Shear Resistance, V_{BS}	=	403	kN	91	kip	<-----
Measured Tensile Stress, $R_Y F_U$	=	525	MPa	76.14489	ksi	
Measured Yield Stress, $R_Y F_Y$	=	457	MPa	66	ksi	
Predicted Block Resistance $V_{BS} (\phi=1.0, R_Y F_Y \& F_U)$	=	656	kN	147	kip	<-----

4) Flexural Shear Yielding, Shear Buckling, and Yielding

AISC 14th Ed Extended Config Design Check 4 (10-5)

AISC 14th Ed LFRD Approach

$V_r = (1 / V_c^2 + (e / M_c)^2)^{-1/2}$						*AISC Handbook Eqn 10-5, modified*
$V_c = \phi_v V_n$						
Resistance Factor, ϕ_v	=	0.90		0.90		*use 0.9 as in S16-09 versus 1.0*
$V_n = 0.6 F_Y A_g$						
Specified Yield Stress, F_Y	=	345	MPa	51	ksi	
Gross Area of Plate, A_g	=	2177	mm ²	3.375	in ²	
Nominal Shear Capacity, V_n	=	451	kN	103	kip	
Factored Shear Capacity, V_c	=	406	kN	93	kip	
Eccentricity to first bolt column, e	=	241	mm	10	in	
$M_c = \phi_b M_n$						
Resistance Factor, ϕ_b	=	0.90		0.90		
$M_n = F_Y Z_{pl}$						

Plastic Section Modulus, Z_{pl}	=	124	$\times 10^3 \text{ mm}^3$	7.594	in^3	
Nominal Moment Capacity, M_n	=	43	kNm	387	kipin	
Factored Moment Capacity, M_c	=	39	kipin	349	kNm	
Factored Combined Yielding Resistance, V_r	=	149	kN	34	kip	<-----
Measured Yield Stress, $R_y F_y$	=	457	MPa	66	ksi	
Predicted Yielding Resistance, $V_r (\phi=1.0, R_y F_y)$	=	219	kN	49	kip	<-----

AISC 13th Ed Approach

$V_r = F_y / \sqrt{[(e/\phi Z_{pl})^2 + 3(1/t_p d_p)^2]}$						*AISC Handbook Eqn 10-4, modified*
Resistance Factor, ϕ	=	0.90		0.90		
Specified Yield Stress, F_y	=	345	MPa	51	ksi	
Eccentricity to first bolt column, e	=	241	mm	10	in	
Plate Thickness, t_p	=	9.53	mm	3/8	in	
Plate Depth, d_p	=	228.6	mm	9	in	
Plastic Section Modulus, Z_{pl}	=	124	$\times 10^3 \text{ mm}^3$	7.594	in^3	
Shear and Flexural Yielding Resistance, V_r	=	150	kN	34	kip	<-----
Measured Yield Stress, $R_y F_y$	=	457	MPa	66	ksi	
Predicted Yielding Resistance, $V_r (\phi=1.0, R_y F_y)$	=	218	kN	49	kip	<-----

5) Plate Buckling

AISC 14th Ed Extended Config Design Check 5 (10-5)

$V_r = \phi_b F_{cr} S_{net} / e$						*AISC 13th Ed Part 9, coped beams*
Resistance Factor, ϕ_b	=	0.90		0.90		
$S_{net} = 1/6 t_w h_o^2$	=	83	$\times 10^3 \text{ mm}^3$	5.06	in^3	
Cope Depth at Compression Flange, d_c	=	41	mm	1.6	in	
Beam Depth, d	=	310	mm	12.2	in	
Eccentricity to first bolt column, e	=	241.3	mm	9 1/2	in	*conservative, take to first row of bolts*
Unsupported Length of Plate, c	=	241.3	mm	9 1/2	in	
$d_c < 0.2d$ & $c < 2d$?			YES, fd equation valid			

fd equation (Cheng et al. 1984)

$F_{cr} = 0.62 \pi E t_w^2 / (c h_o f_d)$						
Modulus of Elasticity, E	=	200000	MPa	29000	ksi	
Thickness of Plate, t_w	=	9.53	mm	3/8	in	
Reduced Beam Depth, h_o	=	228.6	mm	9	in	
$f_d = 3.5 - 7.5 (d_c / d)$						
Adjustment Factor, f_d	=	2.52		2.52		
Critical Stress, F_{cr}	=	1611	MPa	233.6	ksi	
Plate Buckling Resistance, V_r	=	498	kN	112	kip	<-----
Predicted Buckling Resistance, $V_r (\phi=1.0)$	=	554	kN	124	kip	<-----

Q equation (classical plate buckling)

$F_{cr} = F_y Q$						
$\lambda = h_o \sqrt{F_y} / 10 t_w \sqrt{(475 + 280(h_o/c)^2)}$						
Specified Yield Stress, F_y	=	345	MPa	51	ksi	
Measured Yield Stress, $R_y F_y$	=	457	MPa	66	ksi	
Slenderness of Coped Section, λ	=			0.64		
Slenderness of Coped Section, $\lambda_{EXPECTED}$	=			0.72		
Strength Reduction Factor, Q	=	1.00		1.00		
Strength Reduction Factor, $Q_{EXPECTED}$	=	0.99		0.99		
Critical Stress, F_{cr}	=	345	MPa	51	ksi	
Critical Stress, $F_{cr, EXPECTED}$	=	450.95	MPa	65.40415	ksi	
Plate Buckling Resistance, V_r	=	107	kN	24	kip	<-----
Predicted Buckling Resistance $V_r (\phi=1.0, R_y F_y)$	=	155	kN	35	kip	<-----

6) Flexural Limit States

Gross Area Resistance Factor, ϕ_G	=	0.9		0.9		
Net Area Resistance Factor, ϕ_N	=	0.75		0.75		
Specified Yield Stress, F_y	=	345	MPa	51	ksi	
Specified Tensile Stress, F_u	=	450	MPa	65	ksi	

Measured Yield Stress, $R_y F_y$	=	457	MPa	66	ksi	
Measured Tensile Stress, $R_y F_u$	=	525	MPa	76.14489	ksi	
Thickness of Plate, t_p	=	9.53	mm	3/8	in	
Plate Depth, d_p	=	228.6	mm	9	in	
Gauge, s	=	76.2	mm	3	in	
Number of Bolt Rows, n	=	3		3		
Diameter of Bolt Holes, d_h	=	22.2	mm	7/8	in	
Section Modulus, S	=	82960	mm ³	5.06	in ³	
Plastic Section Modulus, Z	=	124439	mm ³	7.59	in ³	
$S_{net} = t_p / 6 [d_p^2 - s^2 n (n^2 - 1) d_h / d_p]$						*Engineering Journal 2008 / 2nd quarter, p102*
Net Section Modulus, S_{net}	=	61451	mm ³	3.75	in ³	
$Z_{net} = 1/4 t_p (s - d_h) (n^2 s + d_h)$						
$Z_{net} = 1/4 t_p (s - d_h) n^2 s$						*Engineering Journal 2008 / 2nd quarter, p103*
Net Plastic Section Modulus, Z_{net}	=	91001	mm ³	5.55	in ³	
Eccentricity to first bolt column, e	=	241	mm	10	in	

AISC 3rd Edition

Bending on Gross Area

$$V_r = \phi_G F_y S / e$$

Factored Gross Bending Resistance, V_r	=	107	kN	24	kip	<-----
Predicted Bending Resistance $V_r (\phi=1.0, R_y F_y)$	=	157	kN	35	kip	<-----

Bending on Net Area

$$V_r = \phi_N F_u S_{net} / e$$

Factored Net Bending Resistance, V_r	=	86	kN	19	kip	<-----
Predicted Bending Resistance $V_r (\phi=1.0, R_y F_y)$	=	134	kN	30	kip	<-----

AISC 13th & 14th Edition

Bending on Gross Area

$$V_r = \phi_G F_y Z / e$$

Factored Gross Bending Resistance, V_r	=	160	kN	37	kip	<-----
Predicted Bending Resistance $V_r (\phi=1.0, R_y F_y)$	=	235	kN	53	kip	<-----

Bending on Net Area

$$V_r = \phi_N F_u Z_{net} / e$$

Factored Net Bending Resistance, V_r	=	127	kN	28	kip	<-----
Predicted Bending Resistance $V_r (\phi=1.0, R_y F_y)$	=	198	kN	45	kip	<-----

Configuration 11

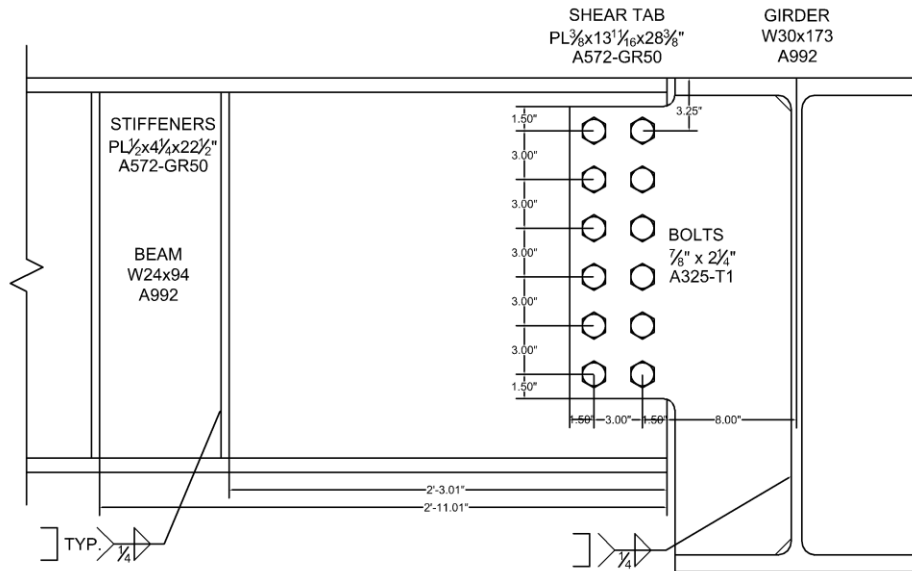


Figure A-11: Connection Details, Configuration 11

Configuration Parameters

Supporting Girder		W30x173
Supported Beam		W24x94
Offset of Bolt Group, a	=	241 mm 9 1/2 in
Bolt Diameter, d _b	=	22.2 mm 7/8 in
Number of Bolt Lines, m	=	2 2
Number of Bolts Rows, n	=	6 6
Plate Depth, d	=	457 mm 18 in
Plate Depth in Girder, d _g	=	719 mm 28.3 in

1) Bolt Shear & Bearing

AISC 14th Ed Extended Config Design Check 1 (10-5)

Compute ICR Coefficient, C

Number of Bolt Lines, m	=	2	2
Moment Arm, L	=	279.40 mm	11 in
gage, D	=	76.2 mm	3 in
Pitch, b	=	76.2 mm	3 in
Number of Bolt Rows, n	=	6	6
L1	=	250 mm	-
C1	=	5.25	-
L2	=	300 mm	-
C2	=	4.51	-
Eccentric Loading Coefficient, C	=	4.81	4.81

interpolating CISC Handbook Table 3-15

Bearing

$B_r = 3\phi_{br}d_b \min[(tF_u)_{plate}, (tF_u)_{web}] \times C$				*S16-09 C13.12.1.2a)*
Modification factor, ϕ_{br}	=	0.8	0.8	
Plate Thickness, t_p	=	9.53 mm	3/8 in	
Beam Web Thickness, t_w	=	16.60 mm	0.654 in	
Bolt Diameter, d_b	=	22.23 in	7/8 in	
Specified Tensile Stress of Plate, $F_{u,plate}$	=	450 MPa	65 ksi	
Specified Tensile Stress of Beam $F_{u,beam}$	=	450 MPa	65 ksi	
Factored Bearing Resistance, B_r	=	1101 kN	246 kip	←-----
Measured Tensile Stress of Plate, $R_y F_{u,plate}$	=	525 MPa	76.14489 ksi	

Measured Tensile Stress of Beam, $R_y F_{U,beam}$	=	539	MPa	78.2	ksi	
Predicted Bearing Resistance $B_r (\phi=1.0, R_y F_U)$	=	1605	kN	361	kip	<-----

Bolt Shear

$V_r = 0.6 \phi_b n m A_b F_u \times C$						*S16-09 C13.12.1.2c)*
Modification factor, ϕ_b	=	0.8		0.8		*S16-09 C13.12.1.1*
Number of Shear Planes, m	=	1		1		
Bolt Area, A_b	=	388	mm ²	0.601	in ²	
Specified Tensile Stress of Bolts, F_u	=	825	MPa	120	ksi	
Factored Bolt Shear Resistance, V_r	=	739	kN	167	kip	<-----
Nominal Bolt Shear Resistance, $V_r (\phi=1.0)$	=	924	kN	208	kip	<-----

2) Plate Ductility

AISC 14th Ed Extended Config Design Check 2 (10-5)

$t_{pmax} = 6M_{max} / F_y d^2$						
$M_{max} = F_{nv} / 0.90 (A_b C')$						
Bolt Shear Strength, F_{nv} (threads not excl)	=	496.42	MPa	72	ksi	*AISC 13th Ed, Table J3.2*
Bolt Area, A_b	=	388	mm ²	0.601	in ²	
Compute ICR Coefficient, C', for Moment Only Case						
Number of Bolt Lines, m	=	2		2		
Column Spacing	=	76.2	mm	3	in	
Row Spacing, s	=	76.2	mm	3	in	
Number of Bolts Rows, n	=	6		6		
ICR Coefficient, C'	=	1376.7	mm	54.2	in	*AISC 13th Ed, Table 7-8*
M_{max}	=	294	kNm	2606	kipin	
Specified Yield Stress of Plate, F_y	=	345	MPa	51	ksi	
Plate Depth, d	=	457.2	mm	18.0	in	
Maximum Plate Thickness, t_{pmax}	=	24.5	mm	0.946	in	
Is this requirement satisfied? ($t_p < t_{pmax}$)			YES			<-----

3) Shear Yielding, Shear Rupture and Block Shear Rupture

AISC 14th Ed Extended Config Design Check 3 (10-5)

Shear Yielding

$V_G = 0.60 \phi F_y A_g$						*AISC 13th Ed Equation J4-3*
Resistance Factor, ϕ	=	0.9		0.9		
Specified Yield Stress, F_y	=	345	MPa	51	ksi	
$A_g = t_p d_p$						
Plate Thickness, t_p	=	9.53	mm	3/8	in	
Plate Depth, d_p	=	457.2	mm	18	in	
Gross Plate Area, A_g	=	4355	mm ²	6.750	in ²	
Shear Yielding Resistance, V_G	=	811	kN	186	kip	<-----
Measured Yield Stress, $R_y F_y$	=	457	MPa	66	ksi	
Predicted Yielding Resistance, $V_G (\phi=1.0, R_y F_y)$	=	1193	kN	268	kip	<-----

Shear Rupture

$V_N = 0.60 \phi F_u A_{NV}$						*AISC 13th Ed Equation J4-4*
Resistance Factor, ϕ	=	0.75		0.75		
Specified Tensile Stress, F_u	=	450	MPa	65	ksi	
$A_{NV} = t_p d_{pN}$						
Plate Thickness, t_p	=	9.53	mm	3/8	in	
Net Depth, d_{pN}	=	304.8	mm	12.00	in	
Net Plate Area, A_{NV}	=	2903	mm ²	4.500	in ²	
Factored Shear Rupture Resistance, V_N	=	588	kN	132	kip	<-----
Measured Tensile Stress, $R_y F_U$	=	525	MPa	76.14489	ksi	
Predicted Rupture Resistance $V_N (\phi=1.0, R_y F_U)$	=	915	kN	206	kip	<-----

Block Shear Rupture

$V_{BS} = \phi U_t [U_t A_n F_u + 0.6 A_{gv} (F_y + F_u)] / 2$						*S16-09 C13.11*
Resistance Factor, ϕ_U	=	0.75		0.75		*S16-09 13.1a)*
Efficiency Factor, U_t	=	0.3		0.3		*coped beam w 2 bolt lines*

Net Area in Tension, A_n	=	726	mm ²	1.125	in ²	
Specified Tensile Stress, F_u	=	450	MPa	65	ksi	
Gross Area in Shear, A_{gv}	=	3992	mm ²	6.188	in ²	
Specified Yield Stress, F_y	=	345	MPa	51	ksi	
Factored Block Shear Resistance, V_{BS}	=	788	kN	178	kip	<-----
Measured Tensile Stress, $R_y F_u$	=	525	MPa	76.14489	ksi	
Measured Yield Stress, $R_y F_y$	=	457	MPa	66	ksi	
Predicted Block Resistance $V_{BS} (\phi=1.0, R_y F_y \& F_u)$	=	1290	kN	290	kip	<-----

4) Flexural Shear Yielding, Shear Buckling, and Yielding

AISC 14th Ed Extended Config Design Check 4 (10-5)

AISC 14th Ed LFRD Approach

$$V_r = (1 / V_c^2 + (e / M_c)^2)^{-1/2} \quad \text{*AISC Handbook Eqn 10-5, modified*}$$

$$V_c = \phi_v V_n$$

$$\text{Resistance Factor, } \phi_v = 0.90 \quad 0.90 \quad \text{*use 0.9 as in S16-09 versus 1.0*}$$

$$V_n = 0.6 F_y A_g$$

$$\text{Specified Yield Stress, } F_y = 345 \text{ MPa} \quad 51 \text{ ksi}$$

$$\text{Gross Area of Plate, } A_g = 4355 \text{ mm}^2 \quad 6.750 \text{ in}^2$$

$$\text{Nominal Shear Capacity, } V_n = 901 \text{ kN} \quad 207 \text{ kip}$$

$$\text{Factored Shear Capacity, } V_c = 811 \text{ kN} \quad 186 \text{ kip}$$

$$\text{Eccentricity to first bolt column, } e = 241 \text{ mm} \quad 10 \text{ in}$$

$$M_c = \phi_b M_n$$

$$\text{Resistance Factor, } \phi_b = 0.90 \quad 0.90$$

$$M_n = F_y Z_{pl}$$

$$\text{Plastic Section Modulus, } Z_{pl} = 498 \text{ x}10^3 \text{ mm}^3 \quad 30.375 \text{ in}^3$$

$$\text{Nominal Moment Capacity, } M_n = 172 \text{ kNm} \quad 1549 \text{ kipin}$$

$$\text{Factored Moment Capacity, } M_c = 155 \text{ kipin} \quad 1394 \text{ kNm}$$

$$\text{Factored Combined Yielding Resistance, } V_r = 503 \text{ kN} \quad 115 \text{ kip} \quad <-----$$

$$\text{Measured Yield Stress, } R_y F_y = 457 \text{ MPa} \quad 66 \text{ ksi}$$

$$\text{Predicted Yielding Resistance, } V_r (\phi=1.0, R_y F_y) = 739 \text{ kN} \quad 166 \text{ kip} \quad <-----$$

AISC 13th Ed Approach

$$V_r = F_y / \sqrt{[(e/\phi Z_{pl})^2 + 3(1/t_p d_p)^2]} \quad \text{*AISC Handbook Eqn 10-4, modified*}$$

$$\text{Resistance Factor, } \phi = 0.90 \quad 0.90$$

$$\text{Specified Yield Stress, } F_y = 345 \text{ MPa} \quad 51 \text{ ksi}$$

$$\text{Eccentricity to first bolt column, } e = 241 \text{ mm} \quad 10 \text{ in}$$

$$\text{Plate Thickness, } t_p = 9.53 \text{ mm} \quad 3/8 \text{ in}$$

$$\text{Plate Depth, } d_p = 457.2 \text{ mm} \quad 18 \text{ in}$$

$$\text{Plastic Section Modulus, } Z_{pl} = 498 \text{ x}10^3 \text{ mm}^3 \quad 30.375 \text{ in}^3$$

$$\text{Shear and Flexural Yielding Resistance, } V_r = 515 \text{ kN} \quad 118 \text{ kip} \quad <-----$$

$$\text{Measured Yield Stress, } R_y F_y = 457 \text{ MPa} \quad 66 \text{ ksi}$$

$$\text{Predicted Yielding Resistance, } V_r (\phi=1.0, R_y F_y) = 728 \text{ kN} \quad 164 \text{ kip} \quad <-----$$

5) Plate Buckling

AISC 14th Ed Extended Config Design Check 5 (10-5)

$$V_r = \phi_b F_{cr} S_{net} / e$$

AISC 13th Ed Part 9, coped beams

$$\text{Resistance Factor, } \phi_b = 0.90 \quad 0.90$$

$$S_{net} = 1/6 t_w h_o^2 = 332 \text{ x}10^3 \text{ mm}^3 \quad 20.25 \text{ in}^3$$

$$\text{Cope Depth at Compression Flange, } d_c = 158 \text{ mm} \quad 6.2 \text{ in}$$

$$\text{Beam Depth, } d = 773 \text{ mm} \quad 30.4 \text{ in}$$

$$\text{Eccentricity to first bolt column, } e = 241.3 \text{ mm} \quad 9 \text{ 1/2 in}$$

$$\text{Unsupported Length of Plate, } c = 241.3 \text{ mm} \quad 9 \text{ 1/2 in}$$

$$d_c < 0.2d \& c < 2d?$$

NO, conservative Q equation valid

conservative, take to first row of bolts

fd equation (Cheng et al. 1984)

$$F_{cr} = 0.62 \pi E t_w^2 / (ch_o f_d)$$

$$\text{Modulus of Elasticity, } E = 200000 \text{ MPa} \quad 29000 \text{ ksi}$$

$$\text{Thickness of Plate, } t_w = 9.53 \text{ mm} \quad 3/8 \text{ in}$$

$$\text{Reduced Beam Depth, } h_o = 457.2 \text{ mm} \quad 18 \text{ in}$$

$$f_d = 3.5 - 7.5 (d_c / d)$$

Adjustment Factor, f_d	=	1.97	1.97	
Critical Stress, F_{cr}	=	630 MPa	91.4 ksi	
Plate Buckling Resistance, V_r	=	780 kN	175 kip	<-----
Predicted Buckling Resistance, $V_r(\phi=1.0)$	=	867 kN	195 kip	<-----

Q equation (classical plate buckling)

$F_{cr} = F_y Q$				
$\lambda = h_o \sqrt{F_y} / 10 t_w \sqrt{(475 + 280(h_o/c)^2)}$				
Specified Yield Stress, F_y	=	345 MPa	51 ksi	
Measured Yield Stress, $R_y F_y$	=	457 MPa	66 ksi	
Slenderness of Coped Section, λ	=		0.89	
Slenderness of Coped Section, $\lambda_{EXPECTED}$	=		1.02	
Strength Reduction Factor, Q	=	0.91	0.91	
Strength Reduction Factor, $Q_{EXPECTED}$	=	0.85	0.85	
Critical Stress, F_{cr}	=	312.91 MPa	46.25632 ksi	
Critical Stress, $F_{cr, EXPECTED}$	=	386.48 MPa	56.05486 ksi	
Plate Buckling Resistance, V_r	=	387 kN	89 kip	<-----
Predicted Buckling Resistance $V_r(\phi=1.0, R_y F_y)$	=	531 kN	119 kip	<-----

6) Flexural Limit States

Gross Area Resistance Factor, ϕ_G	=	0.9	0.9	
Net Area Resistance Factor, ϕ_N	=	0.75	0.75	
Specified Yield Stress, F_y	=	345 MPa	51 ksi	
Specified Tensile Stress, F_u	=	450 MPa	65 ksi	
Measured Yield Stress, $R_y F_y$	=	457 MPa	66 ksi	
Measured Tensile Stress, $R_y F_u$	=	525 MPa	76.14489 ksi	
Thickness of Plate, t_p	=	9.53 mm	3/8 in	
Plate Depth, d_p	=	457.2 mm	18 in	
Gauge, s	=	76.2 mm	3 in	
Number of Bolt Rows, n	=	6	6	
Diameter of Bolt Holes, d_h	=	25.4 mm	1 in	
Section Modulus, S	=	331838 mm ³	20.25 in ³	
Plastic Section Modulus, Z	=	497757 mm ³	30.38 in ³	
$S_{net} = t_p/6 [d_p^2 - s^2 n (n^2 - 1) d_h/d_p]$				*Engineering Journal 2008 / 2nd quarter, p102*
Net Section Modulus, S_{net}	=	224298 mm ³	13.69 in ³	
$Z_{net} = 1/4 t_p (s - d_h) (n^2 s + d_h)$				*Engineering Journal 2008 / 2nd quarter, p103*
$Z_{net} = 1/4 t_p (s - d_h) n^2 s$				
Net Plastic Section Modulus, Z_{net}	=	331838 mm ³	20.25 in ³	
Eccentricity to first bolt column, e	=	241 mm	10 in	

AISC 3rd Edition

Bending on Gross Area

$V_r = \phi_G F_y S / e$				
Factored Gross Bending Resistance, V_r	=	427 kN	98 kip	<-----
Predicted Bending Resistance $V_r(\phi=1.0, R_y F_y)$	=	628 kN	141 kip	<-----

Bending on Net Area

$V_r = \phi_N F_u S_{net} / e$				
Factored Net Bending Resistance, V_r	=	314 kN	70 kip	<-----
Predicted Bending Resistance $V_r(\phi=1.0, R_y F_y)$	=	488 kN	110 kip	<-----

AISC 13th & 14th Edition

Bending on Gross Area

$V_r = \phi_G F_y Z / e$				
Factored Gross Bending Resistance, V_r	=	641 kN	147 kip	<-----
Predicted Bending Resistance $V_r(\phi=1.0, R_y F_y)$	=	942 kN	212 kip	<-----

Bending on Net Area

$V_r = \phi_N F_u Z_{net} / e$				
Factored Net Bending Resistance, V_r	=	464 kN	104 kip	<-----
Predicted Bending Resistance $V_r(\phi=1.0, R_y F_y)$	=	722 kN	162 kip	<-----

Configuration 12

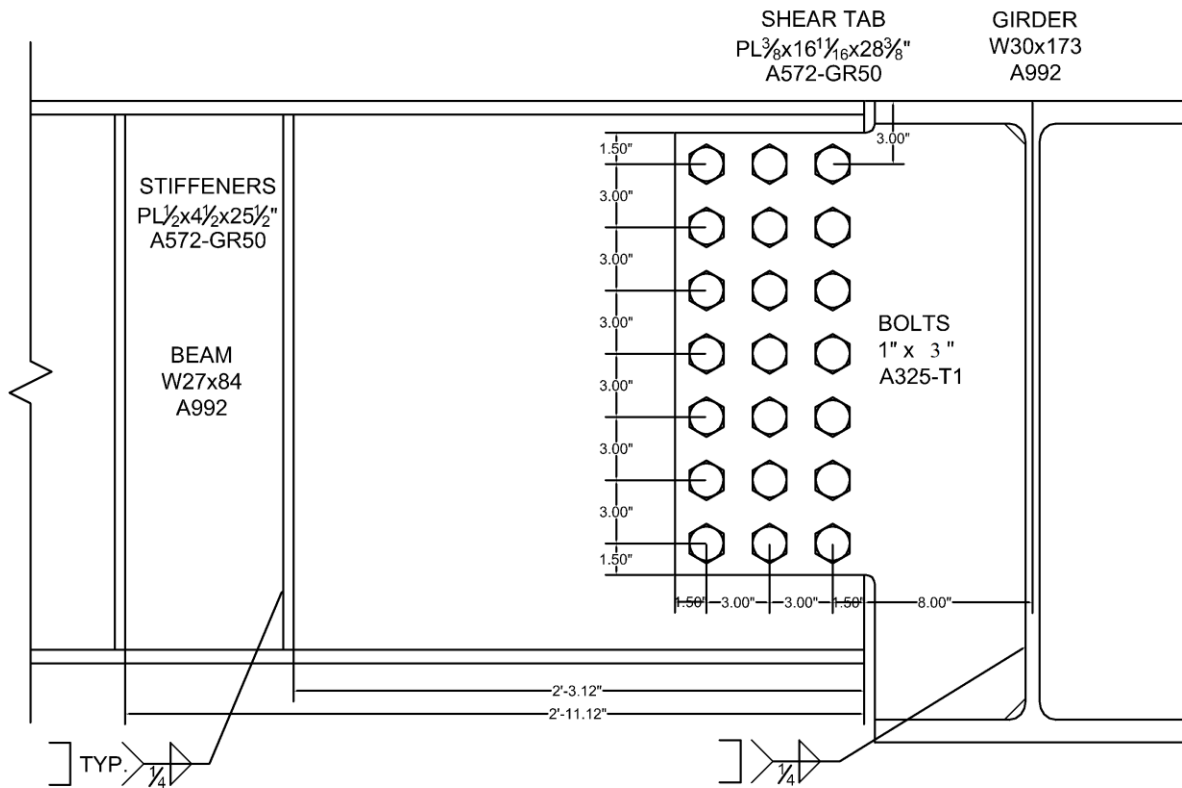


Figure A-12: Connection Details, Configuration 12

Configuration Parameters

Supporting Girder		W30x173
Supported Beam		W27x84
Offset of Bolt Group, a	= 241 mm	9 1/2 in
Bolt Diameter, d _b	= 25.4 mm	1 in
Number of Bolt Lines, m	= 3	3
Number of Bolts Rows, n	= 7	7
Plate Depth, d	= 533 mm	21 in
Plate Depth in Girder, d _g	= 719 mm	28.3 in

1) Bolt Shear & Bearing

AISC 14th Ed Extended Config Design Check 1 (10-5)

Compute ICR Coefficient, C

Number of Bolt Lines, m	= 3	3	
Moment Arm, L	= 317.50 mm	12.5 in	
gage, D	= 76.2 mm	3 in	
Pitch, b	= 76.2 mm	3 in	
Number of Bolt Rows, n	= 7	7	
L1	= 300 mm	-	*interpolating CISC Handbook Table 3-17*
C1	= 9.2	-	
L2	= 400 mm	-	
C2	= 7.26	-	
Eccentric Loading Coefficient, C	= 8.86	8.86	

Bearing

$$B_r = 3\phi_b d_b \min[(tF_u)_{plate}, (tF_u)_{web}] \times C$$

S16-09 C13.12.1.2a)

Modification factor, ϕ_{br}	=	0.8	0.8	
Plate Thickness, t_p	=	9.53 mm	3/8 in	
Beam Web Thickness, t_w	=	11.70 mm	0.461 in	
Bolt Diameter, d_b	=	25.40 in	1 in	
Specified Tensile Stress of Plate, $F_{u,plate}$	=	450 MPa	65 ksi	
Specified Tensile Stress of Beam $F_{u,beam}$	=	450 MPa	65 ksi	
Factored Bearing Resistance, B_r	=	2315 kN	518 kip	<-----
Measured Tensile Stress of Plate, $R_y F_{u,plate}$	=	525 MPa	76.144893 ksi	
Measured Tensile Stress of Beam, $R_y F_{u,beam}$	=	511 MPa	71.5 ksi	
Predicted Bearing Resistance $B_r (\phi=1.0, R_y F_u)$	=	3376 kN	759 kip	<-----

Bolt Shear

$$V_r = 0.6\phi_b n m A_b F_u \times C$$

S16-09 C13.12.1.2c)

Modification factor, ϕ_b	=	0.8	0.8	
Number of Shear Planes, m	=	1	1	
Bolt Area, A_b	=	506 mm ²	0.785 in ²	
Specified Tensile Stress of Bolts, F_u	=	825 MPa	120 ksi	
Factored Bolt Shear Resistance, V_r	=	1777 kN	401 kip	<-----
Nominal Bolt Shear Resistance, $V_r (\phi=1.0)$	=	2221 kN	501 kip	<-----

2) Plate Ductility

AISC 14th Ed Extended Config Design Check 2 (10-5)

$$t_{pmax} = 6M_{max} / F_y d^2$$

$$M_{max} = F_{NV} / 0.90 (A_b C')$$

Bolt Shear Strength, F_{NV} (threads not excl)	=	496.422 MPa	72 ksi	*AISC 13th Ed, Table J3.2*
Bolt Area, A_b	=	506 mm ²	0.785 in ²	

Compute ICR Coefficient, C', for Moment Only Case

Number of Bolt Lines, m	=	3	3	
Column Spacing	=	76.2 mm	3 in	
Row Spacing, s	=	76.2 mm	3 in	
Number of Bolts Rows, n	=	7	7	
ICR Coefficient, C'	=	2946.4 mm	116.0 in	*AISC 13th Ed, Table 7-11*
M_{max}	=	823 kNm	7285 kipin	
Specified Yield Stress of Plate, F_y	=	345 MPa	51 ksi	
Plate Depth, d	=	533.4 mm	21.0 in	
Maximum Plate Thickness, t_{pmax}	=	50.3 mm	1.943 in	
Is this requirement satisfied? ($t_p < t_{pmax}$)		YES		<-----

3) Shear Yielding, Shear Rupture and Block Shear Rupture

AISC 14th Ed Extended Config Design Check 3 (10-5)

Shear Yielding

$$V_G = 0.60\phi F_y A_g$$

AISC 13th Ed Equation J4-3

Resistance Factor, ϕ	=	0.9	0.9	
Specified Yield Stress, F_y	=	345 MPa	51 ksi	
$A_g = t_p d_p$				
Plate Thickness, t_p	=	9.53 mm	3/8 in	
Plate Depth, d_p	=	533.4 mm	21 in	
Gross Plate Area, A_g	=	5081 mm ²	7.875 in ²	
Shear Yielding Resistance, V_G	=	947 kN	217 kip	<-----
Measured Yield Stress, $R_y F_y$	=	457 MPa	66 ksi	
Predicted Yielding Resistance, $V_G (\phi=1.0, R_y F_y)$	=	1392 kN	313 kip	<-----

Shear Rupture

$$V_N = 0.60\phi F_u A_{NV}$$

AISC 13th Ed Equation J4-4

Resistance Factor, ϕ	=	0.75	0.75	
Specified Tensile Stress, F_u	=	450 MPa	65 ksi	
$A_{NV} = t_p d_{pN}$				
Plate Thickness, t_p	=	9.53 mm	3/8 in	

Net Depth, d_{pN}	=	333.4	mm	13.13	in	
Net Plate Area, A_{NV}	=	3175	mm ²	4.922	in ²	
Factored Shear Rupture Resistance, V_N	=	643	kN	144	kip	<-----
Measured Tensile Stress, $R_y F_U$	=	525	MPa	76.144893	ksi	
Predicted Rupture Resistance $V_N (\phi=1.0, R_y F_U)$	=	1000	kN	225	kip	<-----

Block Shear Rupture

$$V_{BS,AISC} = \phi [\min(0.6 F_U A_{NV}, 0.6 F_y A_{gV}) + U_{bs} F_U A_{nT}]$$

AISC Equation J4-5

Resistance Factor, ϕ	=	0.75		0.75		
Specified Tensile Stress, F_U	=	450	MPa	65	ksi	
Net Area in Shear, A_{NV}	=	2949	mm ²	4.570	in ²	
Specified Yield Stress, F_y	=	345	MPa	51	ksi	
Gross Area in Shear, A_{gV}	=	4718	mm ²	7.313	in ²	
Efficiency Factor, U_{bs}	=	0.5		0.5		*0.5 for non-uniform stress distribution*
Net Area in Tension, A_{nT}	=	1134	mm ²	1.758	in ²	
Factored Block Shear Resistance, V_{BS}	=	788	kN	177	kip	<-----
Measured Tensile Stress, $R_y F_U$	=	525	MPa	76.144893	ksi	
Measured Yield Stress, $R_y F_y$	=	457	MPa	66	ksi	
Predicted Block Resistance, $V_{BS} (\phi=1.0, R_y F_y \& F_U)$	=	1226	kN	276	kip	<-----

4) Flexural Shear Yielding, Shear Buckling, and Yielding

AISC 14th Ed Extended Config Design Check 4 (10-5)

AISC 14th Ed LFRD Approach

$$V_r = (1 / V_c^2 + (e / M_c)^2)^{-1/2}$$

AISC Handbook Eqn 10-5, modified

$$V_c = \phi_v V_n$$

Resistance Factor, ϕ_v	=	0.90		0.90		*use 0.9 as in S16-09 versus 1.0*
$V_n = 0.6 F_y A_g$						
Specified Yield Stress, F_y	=	345	MPa	51	ksi	
Gross Area of Plate, A_g	=	5081	mm ²	7.875	in ²	
Nominal Shear Capacity, V_n	=	1052	kN	241	kip	
Factored Shear Capacity, V_c	=	947	kN	217	kip	
Eccentricity to first bolt column, e	=	241	mm	10	in	
$M_c = \phi_b M_n$						
Resistance Factor, ϕ_b	=	0.90		0.90		
$M_n = F_y Z_{pl}$						
Plastic Section Modulus, Z_{pl}	=	678	x10 ³ mm ³	41.344	in ³	
Nominal Moment Capacity, M_n	=	234	kNm	2109	kipin	
Factored Moment Capacity, M_c	=	210	kipin	1898	kNm	
Factored Combined Yielding Resistance, V_r	=	641	kN	147	kip	<-----
Measured Yield Stress, $R_y F_y$	=	457	MPa	66	ksi	
Predicted Yielding Resistance, $V_r (\phi=1.0, R_y F_y)$	=	943	kN	212	kip	<-----

AISC 13th Ed Approach

$$V_r = F_y / \sqrt{[(e / \phi Z_{pl})^2 + 3(1 / t_p d_p)^2]}$$

AISC Handbook Eqn 10-4, modified

Resistance Factor, ϕ	=	0.90		0.90		
Specified Yield Stress, F_y	=	345	MPa	51	ksi	
Eccentricity to first bolt column, e	=	241	mm	10	in	
Plate Thickness, t_p	=	9.53	mm	3/8	in	
Plate Depth, d_p	=	533.4	mm	21	in	
Plastic Section Modulus, Z_{pl}	=	678	x10 ³ mm ³	41.344	in ³	
Shear and Flexural Yielding Resistance, V_r	=	661	kN	151	kip	<-----
Measured Yield Stress, $R_y F_y$	=	457	MPa	66	ksi	
Predicted Yielding Resistance, $V_r (\phi=1.0, R_y F_y)$	=	926	kN	208	kip	<-----

5) Plate Buckling

AISC 14th Ed Extended Config Design Check 5 (10-5)

$$V_r = \phi_b F_{cr} S_{net} / e$$

AISC 13th Ed Part 9, coped beams

Resistance Factor, ϕ_b	=	0.90		0.90		
$S_{net} = 1/6 t_w h^2 o$	=	452	x10 ³ mm ³	27.56	in ³	

Cope Depth at Compression Flange, d_c	=	72	mm	2.8	in	
Beam Depth, d	=	678	mm	26.7	in	
Eccentricity to first bolt column, e	=	241.3	mm	9 1/2	in	*conservative, take to first row of bolts*
Unsupported Length of Plate, c	=	241.3	mm	9 1/2	in	
$d_c < 0.2d$ & $c < 2d$?		YES, fd equation valid				

fd equation (Cheng et al. 1984)

$F_{cr} = 0.62 \pi E t_w^2 / ch_o f_d$						
Modulus of Elasticity, E	=	200000	MPa	29000	ksi	
Thickness of Plate, t_w	=	9.53	mm	3/8	in	
Reduced Beam Depth, h_o	=	533.4	mm	21	in	
$f_d = 3.5 - 7.5 (d_c / d)$						
Adjustment Factor, f_d	=	2.70		2.70		
Critical Stress, F_{cr}	=	741	MPa	107.5	ksi	
Plate Buckling Resistance, V_r	=	1248	kN	281	kip	<-----
Predicted Buckling Resistance, $V_r(\phi=1.0)$	=	1387	kN	312	kip	<-----

Q equation (classical plate buckling)

$F_{cr} = F_y Q$						
$\lambda = h_o \sqrt{F_y} / 10 t_w \sqrt{(475 + 280(h_o/c)^2)}$						
Specified Yield Stress, F_y	=	345	MPa	51	ksi	
Measured Yield Stress, $R_y F_y$	=	457	MPa	66	ksi	
Slenderness of Coped Section, λ	=			0.93		
Slenderness of Coped Section, $\lambda_{EXPECTED}$	=			1.06		
Strength Reduction Factor, Q	=	0.89		0.89		
Strength Reduction Factor, $Q_{EXPECTED}$	=	0.82		0.82		
Critical Stress, F_{cr}	=	306.1	MPa	45.3	ksi	
Critical Stress, $F_{cr,EXPECTED}$	=	376.2	MPa	54.6	ksi	
Plate Buckling Resistance, V_r	=	516	kN	118	kip	<-----
Predicted Buckling Resistance $V_r(\phi=1.0, R_y F_y)$	=	704	kN	158	kip	<-----

6) Flexural Limit States

Gross Area Resistance Factor, ϕ_G	=	0.9		0.9		
Net Area Resistance Factor, ϕ_N	=	0.75		0.75		
Specified Yield Stress, F_y	=	345	MPa	51	ksi	
Specified Tensile Stress, F_u	=	450	MPa	65	ksi	
Measured Yield Stress, $R_y F_y$	=	457	MPa	66	ksi	
Measured Tensile Stress, $R_y F_u$	=	525	MPa	76.144893	ksi	
Thickness of Plate, t_p	=	9.53	mm	3/8	in	
Plate Depth, d_p	=	533.4	mm	21	in	
Gauge, s	=	76.2	mm	3	in	
Number of Bolt Rows, n	=	7		7		
Diameter of Bolt Holes, d_h	=	28.6	mm	1 1/8	in	
Section Modulus, S	=	451668	mm ³	27.56	in ³	
Plastic Section Modulus, Z	=	677503	mm ³	41.34	in ³	
$S_{net} = t_p / 6 [d_p^2 - s^2 n (n^2 - 1) d_h / d_p]$						*Engineering Journal 2008 / 2nd quarter, p102*
Net Section Modulus, S_{net}	=	285749	mm ³	17.44	in ³	
$Z_{net} = 1/4 t_p (s - d_h) (n^2 s + d_h)$						*Engineering Journal 2008 / 2nd quarter, p103*
$Z_{net} = 1/4 t_p (s - d_h) n^2 s$						
Net Plastic Section Modulus, Z_{net}	=	426680	mm ³	26.04	in ³	
Eccentricity to first bolt column, e	=	241	mm	10	in	

AISC 3rd Edition

Bending on Gross Area

$V_r = \phi_G F_y S / e$						
Factored Gross Bending Resistance, V_r	=	581	kN	133	kip	<-----
Predicted Bending Resistance $V_r(\phi=1.0, R_y F_y)$	=	854	kN	192	kip	<-----

Bending on Net Area

$$V_r = \phi_N F_u S_{net} / e$$

Factored Net Bending Resistance, V_r	=	400	kN	89	kip	<-----
Predicted Bending Resistance $V_r (\phi=1.0, R_y F_y)$	=	622	kN	140	kip	<-----

AISC 13th & 14th Edition

Bending on Gross Area

$$V_r = \phi_G F_y Z / e$$

Factored Gross Bending Resistance, V_r	=	872	kN	200	kip	<-----
Predicted Bending Resistance $V_r (\phi=1.0, R_y F_y)$	=	1282	kN	288	kip	<-----

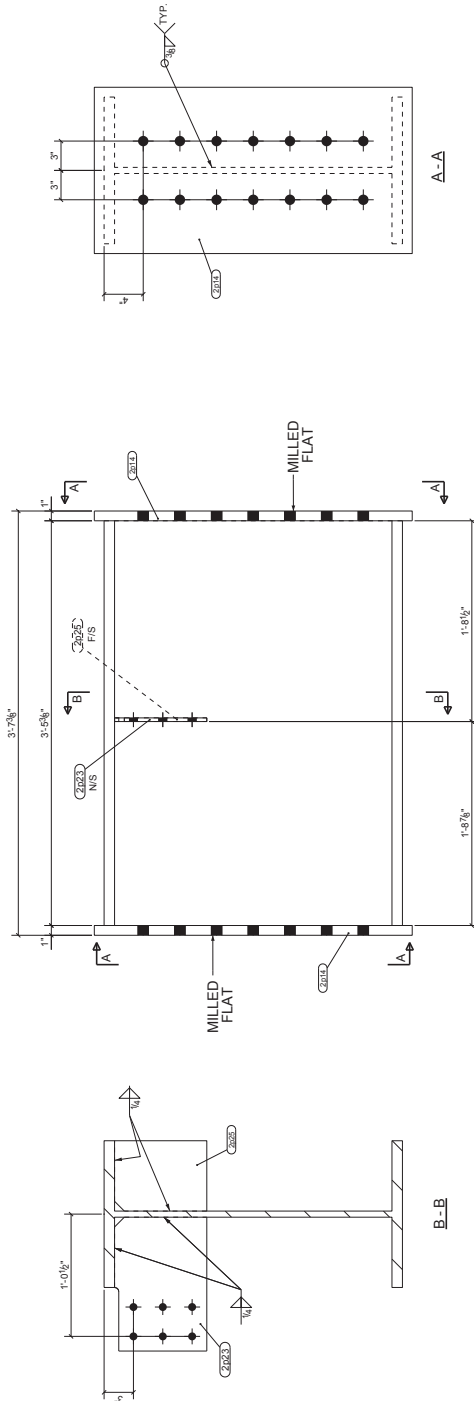
Bending on Net Area

$$V_r = \phi_N F_u Z_{net} / e$$

Factored Net Bending Resistance, V_r	=	597	kN	134	kip	<-----
Predicted Bending Resistance $V_r (\phi=1.0, R_y F_y)$	=	928	kN	209	kip	<-----

Appendix B – Fabrication Drawings

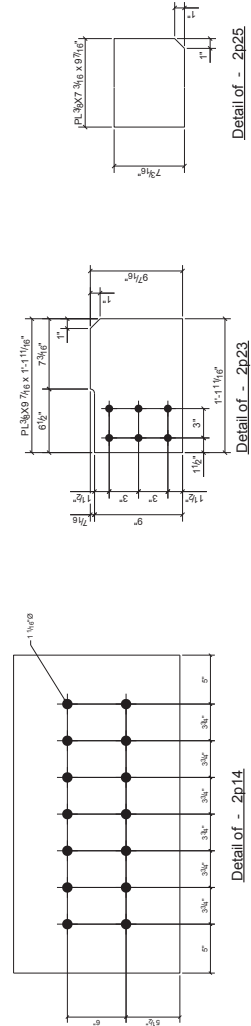
BILL OF MATERIAL					
MARK	QTY	DESCRIPTION	LENGTH	GRADE	REMARKS
1 - B1012					
B1012	1	W30X173	3'-5 3/8"	A992	917
2p44	2	PL1"x17"	2'-8 1/2"	A572-68-50	584
2p43	1	PL3/8"x97 7/16"	1'-1 11/16"	A572-68-50	157
2p45	1	PL3/8"x7 3/16"	0'-57 7/16"	A572-68-50	13
2p45	1	PL3/8"x7 3/16"	0'-57 7/16"	A572-68-50	7
Shop bolts					



A-A

B-B

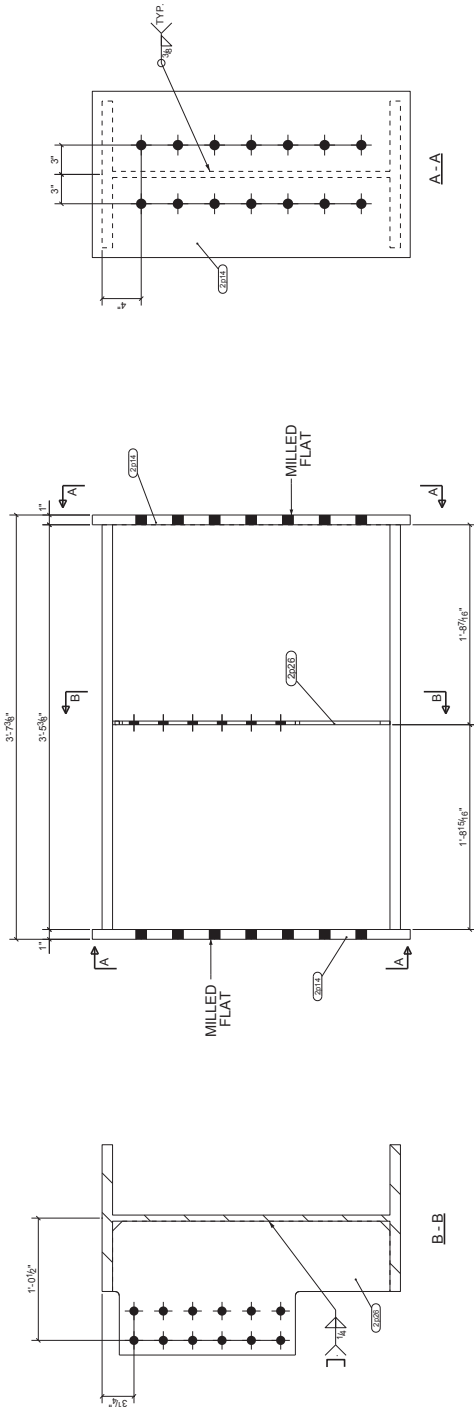
ONE BEAM B1012 (McGill drawing reference G6)



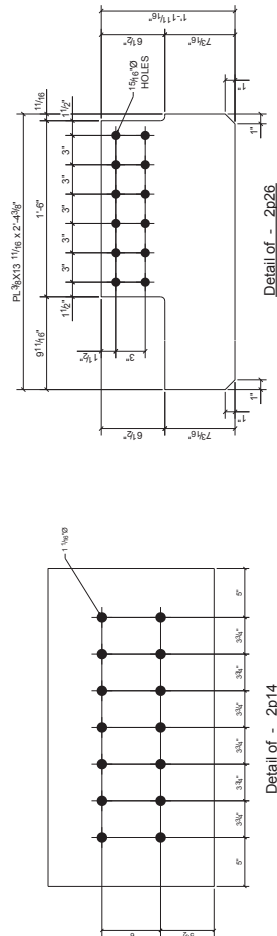
Detail of - 2p25

REVISIONS		PROJECT	McGill University Project No.1	PROJECT #1	1012
DATE		SITE	Montreal	REDUCE	1
DESCRIPTION		CLIENT	McGill University	REVISION	
DRAWING TITLE		DRAWING TITLE	BEAM	DRAWING NO.	2013-001
NO. OF SHEETS		DRAWING NO.	2013-001	PROJECT NO.	1012
DATE		DATE	2013-03-25	DATE	2013-03-25

BILL OF MATERIAL					
MARK	QTY	DESCRIPTION	LENGTH	GRADE	REMARKS
1 - B1013					
B1013	1	W30X173	3'-5 3/8"	A572-50	930
2x4	2	PL1"x17"	2'-8 1/2"	A572-50	157
2x4	1	PL3/8"x13 11/16"	2'-4 3/8"	A572-50	33
Shop bolts					



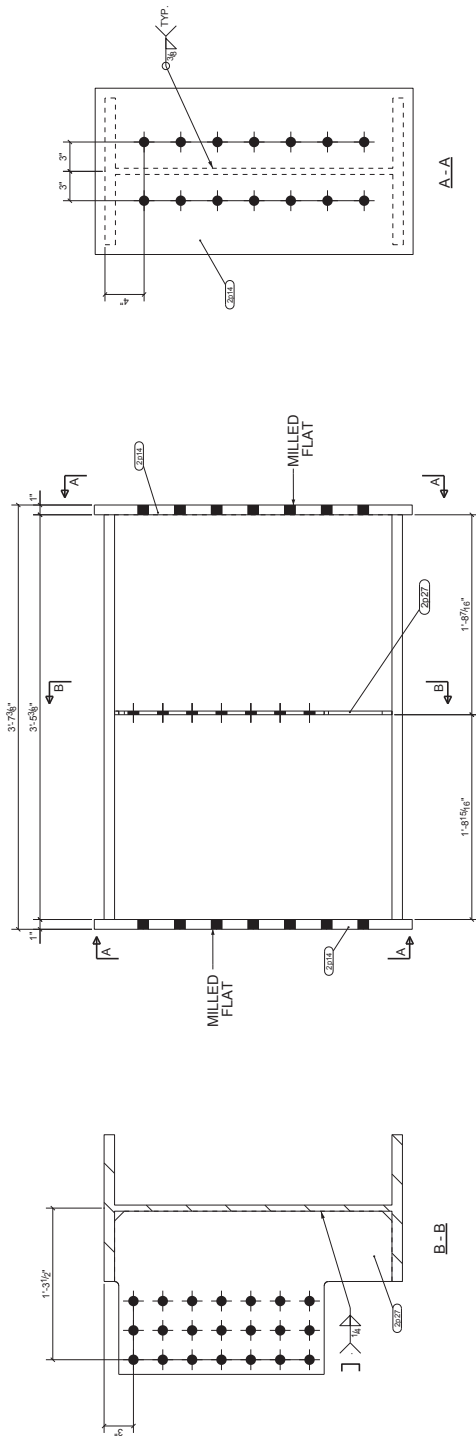
ONE BEAM B1013 (McGill drawing reference G7)



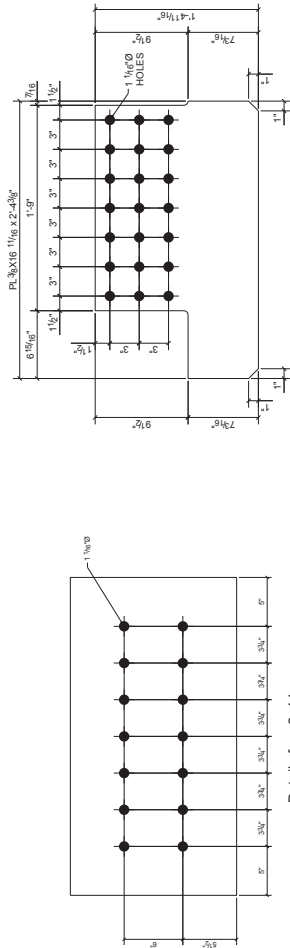
REVISIONS		PROJECT	McGill University Project No.1	PROJECT #1
INTERNAL NOTCHES TO BE PAINTED		SITE	Montreal	1
FROM		CLIENT	McGill University	
DRAWING TITLE		BEAM		
NOTES		SEAWOOD / JML		
DRAWING NO.		2013-001		
DATE		2013-03-25		

Figure B-14: Fabrication Drawing, Girder, Configuration 11

BILL OF MATERIAL					REMARKS		BILLING	
MAKE	QTY	DESCRIPTION	LENGTH	GRADE	WEIGHT			
1 - B1014								
B1014	1	W30X173	3'-4 3/8"	A572	584			
2p14	2	PL1"x17"	2'-8 1/2"	A572-66-50	157			
2p27	1	PL3/8"x16 11/16"	2'-4 3/8"	A572-66-50	42			
Shop bolts								



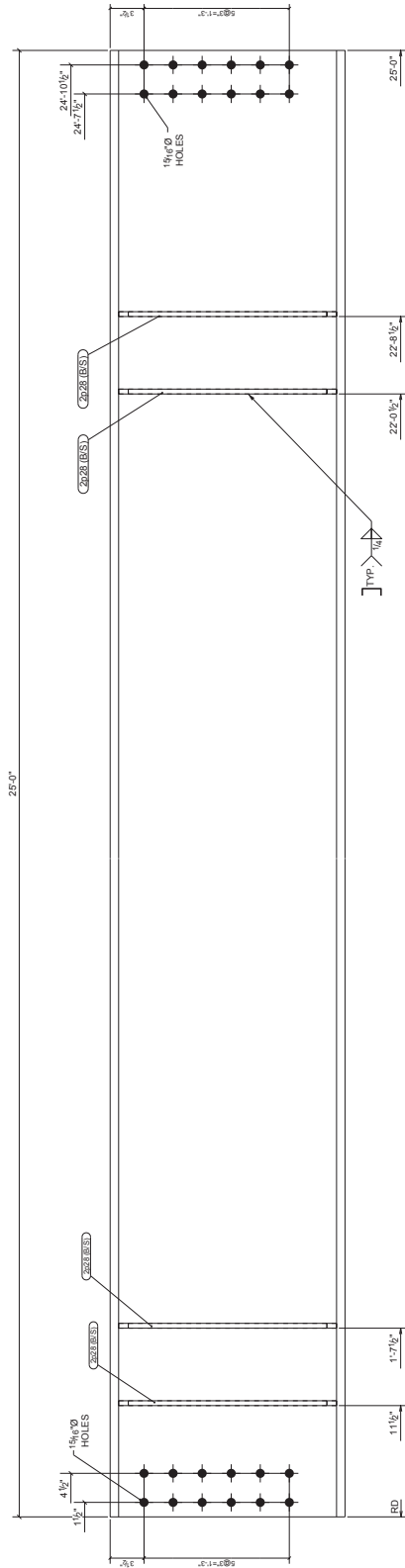
ONE BEAM B1014 (McGill drawing reference G8)



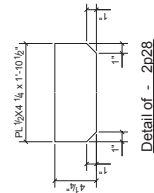
REVISIONS		PROJECT	McGill University Project No.1	PROJECT #1	1
INTERNAL NOTCHES TO BEAP RADIUS (R40)		SITE	Montreal	REDUCE	1
NO PAINT		CLIENT	McGill University	REVISION	
DRAWING TITLE		DRAWING TITLE	BEAM	PROJECT No.	1014
NO. OF SHEETS		DRAWING No.	2013-001	DRAWING No.	2013-001
DATE		DATE	2013-03-25	DATE	2013-03-25
REV		DATE		REV	
DESCRIPTION		DATE		DESCRIPTION	
0 03/27/2013 ISSUED FOR FABRICATION		DATE		0 03/27/2013 ISSUED FOR FABRICATION	
JML		DATE		JML	
MADE BY (C.N.O.B.)		DATE		MADE BY (C.N.O.B.)	

Figure B-15: Fabrication Drawing, Girder, Configuration 12

BILL OF MATERIAL					REMARKS	
MAKE	QTY	DESCRIPTION	LENGTH	GRADE	WEIGHT (lb)	BILLING
	1	- B1015			2423	
B1015	1	W24X94	25'-0"	A572	2315	
2p28	8	PL1/2"x4 1/4"	1'-10 1/2"	A572-60	13	
Shape bolts						



ONE BEAM B1015 (McGill drawing reference B3)

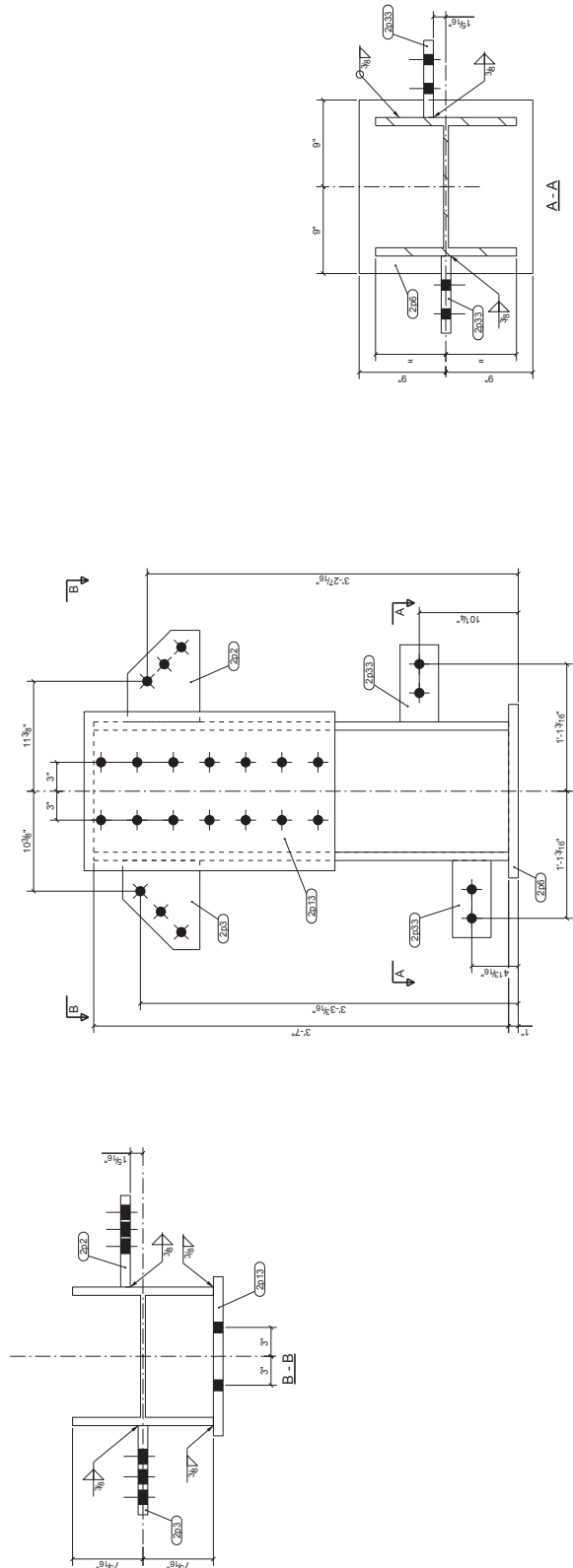


REV	DATE	DESCRIPTION	MADE BY	CHECKED BY
0	03/27/2013	ISSUED FOR FABRICATION	JML	

REVISIONS		PROJECT		PROJECT #1	
NO.	DATE	DESCRIPTION	MADE BY	PROJECT NO.	PROJECT NAME
1	03/27/2013	ISSUED FOR FABRICATION	JML	1015	2013-001

Figure B-16: Fabrication Drawing, Test Beam, Configurations 4 & 11

BILL OF MATERIAL					REMARKS	BILLING
MARK	QTY	DESCRIPTION	LENGTH	GRADE	WEIGHT (LBS)	
1 - C100						
C100	1	W4X10.9	3'-7"	A992	381	648
Zp2	1	PL1X7 1/2"	0'-9 1/2"	A572-60.50	15	
Zp3	1	PL1X8"	0'-9 1/4"	A572-60.50	15	
Zp6	1	PL1X18"	1'-5"	A572-60.50	90	
Zp13	1	PL1X16 1/2"	2'-2"	A572-60.50	121	
Zp33	2	PL1X4"	0'-8"	A572-60.50	9	
Shop bolts						



ONE COLUMN C1100

(McGill drawing reference T2)

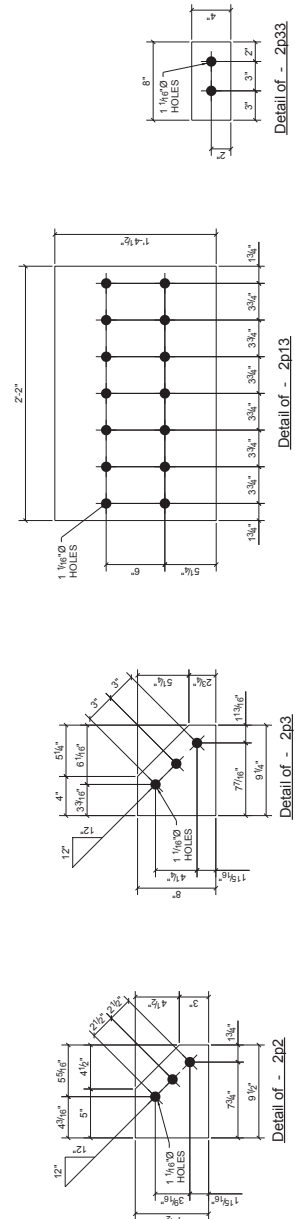
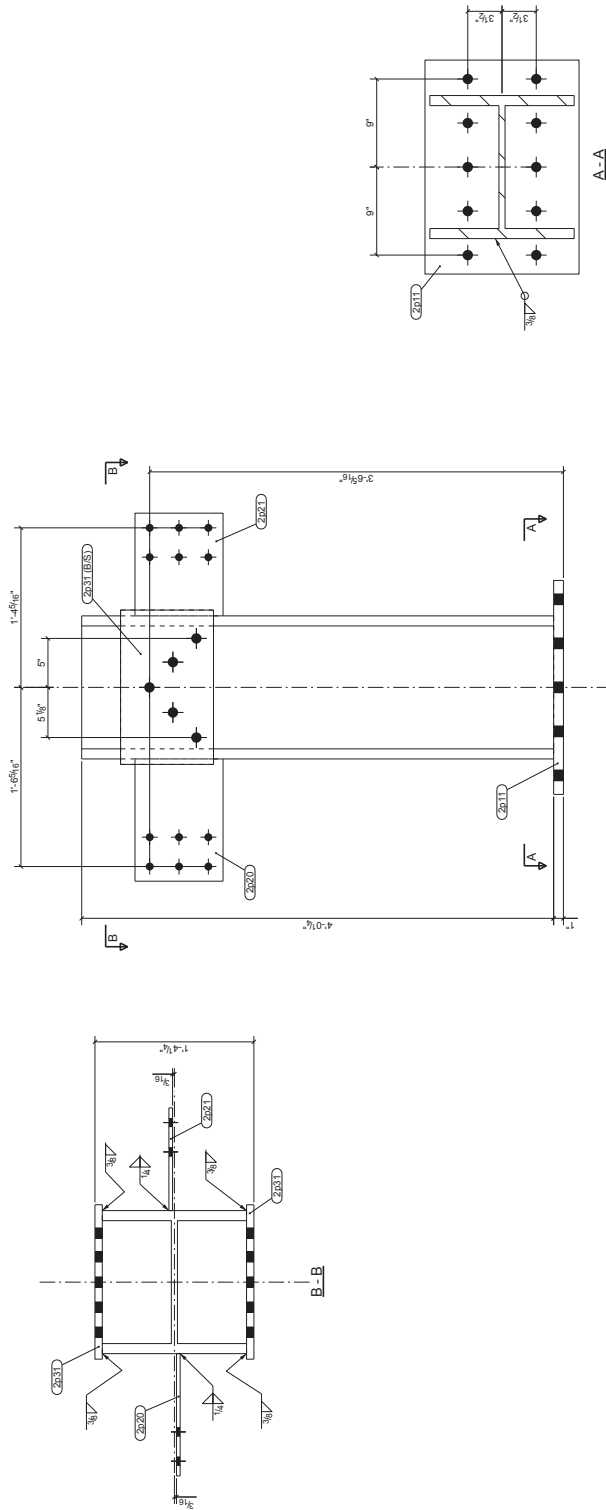


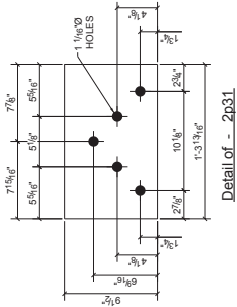
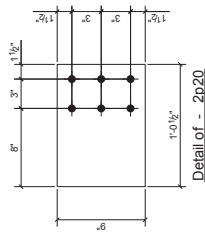
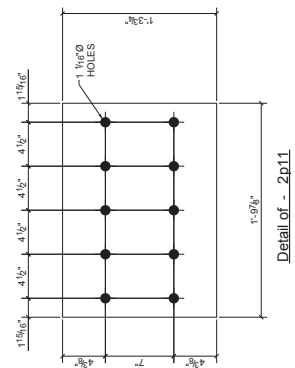
Figure B-17: Fabrication Drawing, Girder Reaction Frame, Right Column

BILL OF MATERIAL					
MARK	QTY	DESCRIPTION	LENGTH	GRADE	REMARKS
1 - C102					
C102	1	W4X132	4'-0 1/4"	A572	705
2p11	1	PL17X5 3/4"	1'-9 7/8"	A572-66-50	522
2p20	1	PL3/8"X9"	1'-0 1/2"	A572-66-50	97
2p21	1	PL3/8"X9"	0'-10 1/2"	A572-66-50	11
2p31	2	PL3/4"X9 1/2"	1'-3 3/4"	A572-66-50	9
Shop bolts					
31					



ONE COLUMN C1102

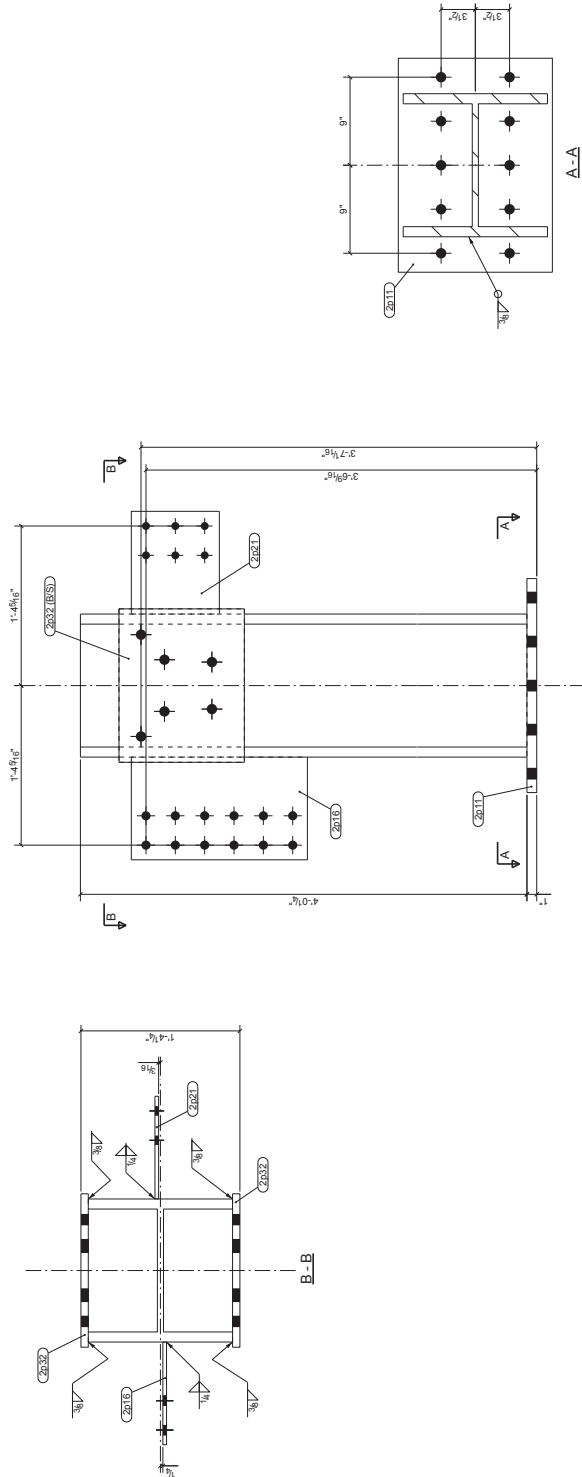
(McGill drawing reference C1)



PROJECT: McGill University Project No. 1		PROJECT #1
SITE: Montréal		REDUCE: 1
CLIENT: McGill University		REVISION: 1
DRAWING TITLE: COLUMN		PROJECT No. 1102
NO. 157-001 / 2013-03-26		DRAWING No. 2013-001
DATE: 2013-03-26		PROJECT No. 1102
PROJECT: McGill University Project No. 1		PROJECT #1
SITE: Montréal		REDUCE: 1
CLIENT: McGill University		REVISION: 1
DRAWING TITLE: COLUMN		PROJECT No. 1102
NO. 157-001 / 2013-03-26		DRAWING No. 2013-001
DATE: 2013-03-26		PROJECT No. 1102

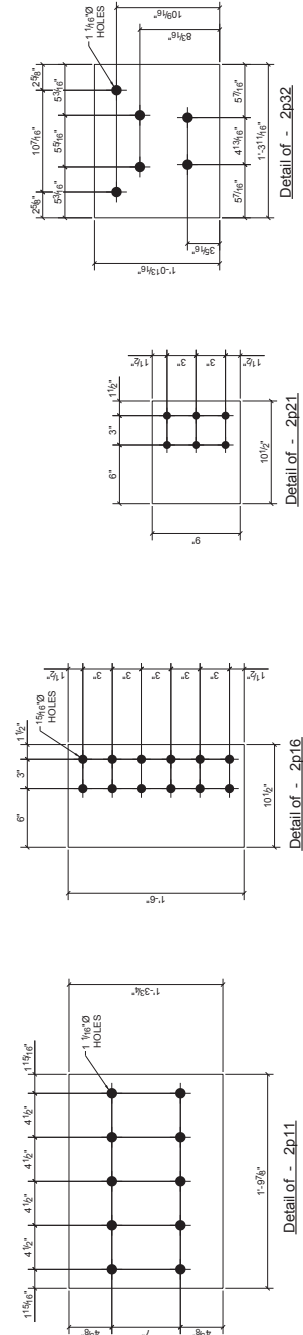
Figure B-19: Fabrication Drawing, Column, Configurations 1 & 2

BILL OF MATERIAL					
MARK	QTY	DESCRIPTION	LENGTH	GRADE	REMARKS
1 - C103					
C103	1	W4X132	4'-0 1/4"	A572	736
2p1	1	PL17X5 3/4"	1'-9 7/8"	A572-66-50	522
2p6	1	PL3/8"X8"	0'-50 1/2"	A572-66-50	97
2p8	1	PL3/8"X9"	0'-50 1/2"	A572-66-50	20
2p12	2	PL3/4"X12 13/16"	1'-3 11/16"	A572-66-50	9
Shop bolts					
					42



ONE COLUMN C1103

(McGill drawing reference C2)



PROJECT	McGill University Project No. 1	PROJECT #1
SITE	Montreal	1
CLIENT	McGill University	
DRAWING TITLE	COLUMN	
NO. OF SHEETS	1	
DATE	2013/03/26	
DESIGNED BY	JML	
CHECKED BY	JML	
DATE	2013/03/26	
PROJECT NO.	2013-001	
DRAWING NO.	2013-001	
PROJECT NO.	2013-001	
DRAWING NO.	2013-001	

Figure B-20: Fabrication Drawing, Column, Configurations 3 & 4

[illegible]

[illegible]

[illegible]

[illegible]

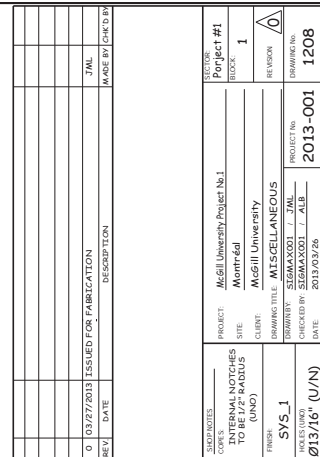
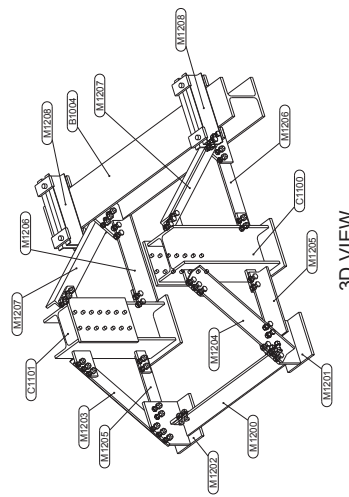


Figure B-29: Fabrication Drawing, Girder Reaction Frame, Tension Brackets



3D VIEW

[illegible]


PROJECT	McGill University Project No.1			SECTION	Project #1
SITE	Montréal			REVISION	1
CLIENT	McGill University				
DRAWING TITLE	BRECTION			REVISION	
DRAWN BY	SIGMA0001 J. JMAL			DRAWING No.	
CHECKED BY	SIGMA0001 J. ALB			E1	
DATE	2013/03/25				

Figure B-30: Fabrication Drawing, Girder Reaction Frame

Appendix C – Test Setup and Instrumentation

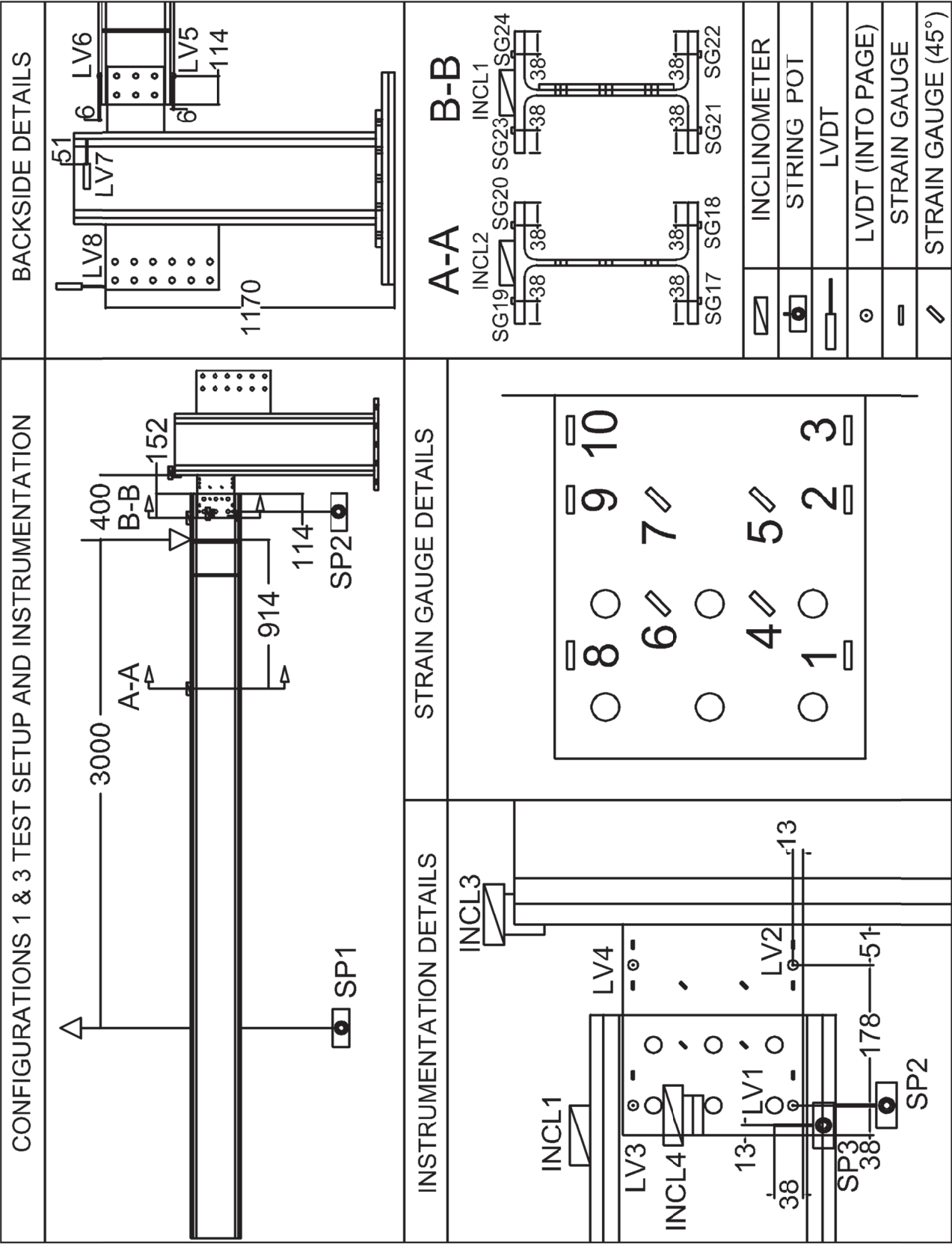


Figure C-1: Test Setup and Instrumentation, Configurations 1 & 3

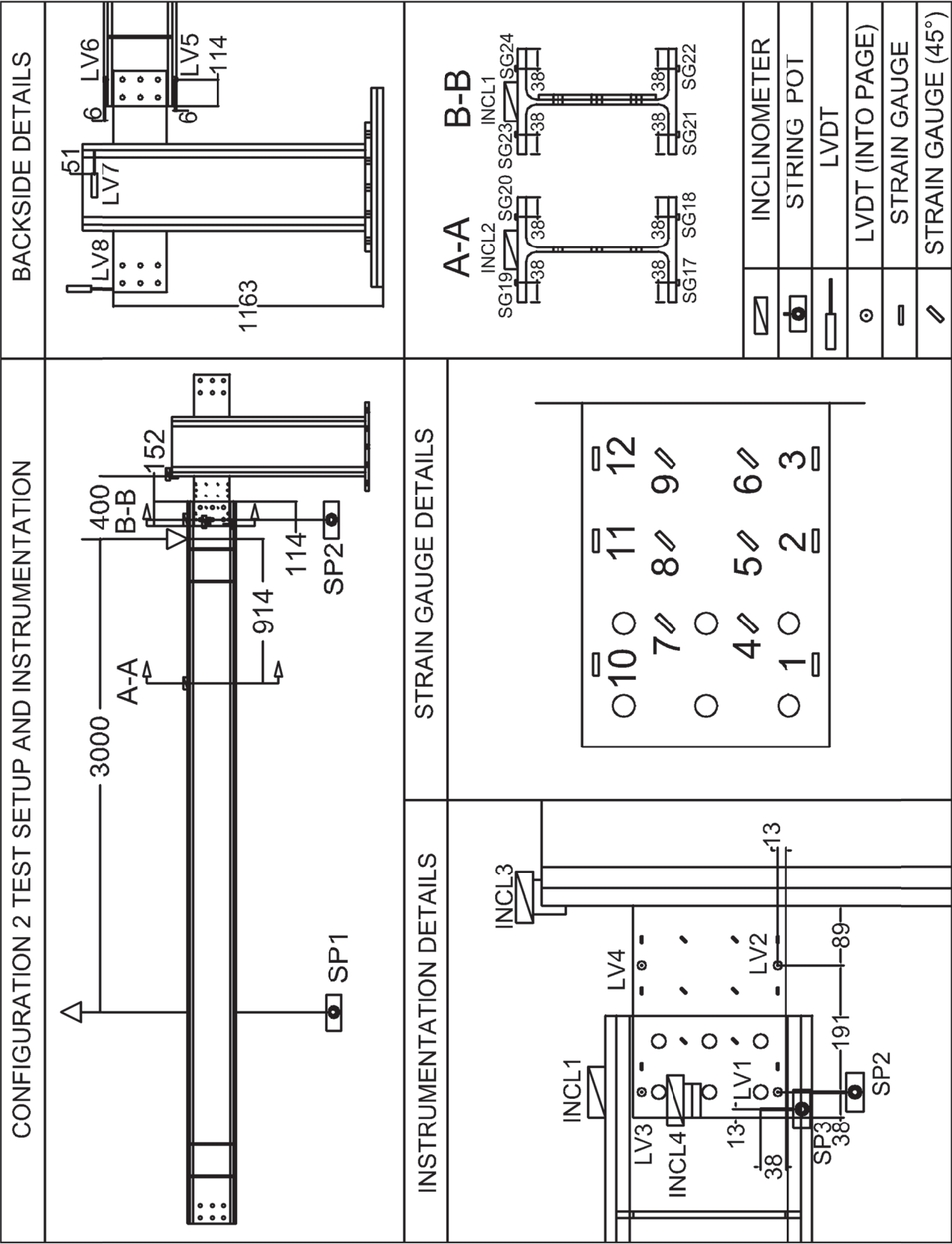


Figure C-2: Test Setup and Instrumentation, Configuration 2

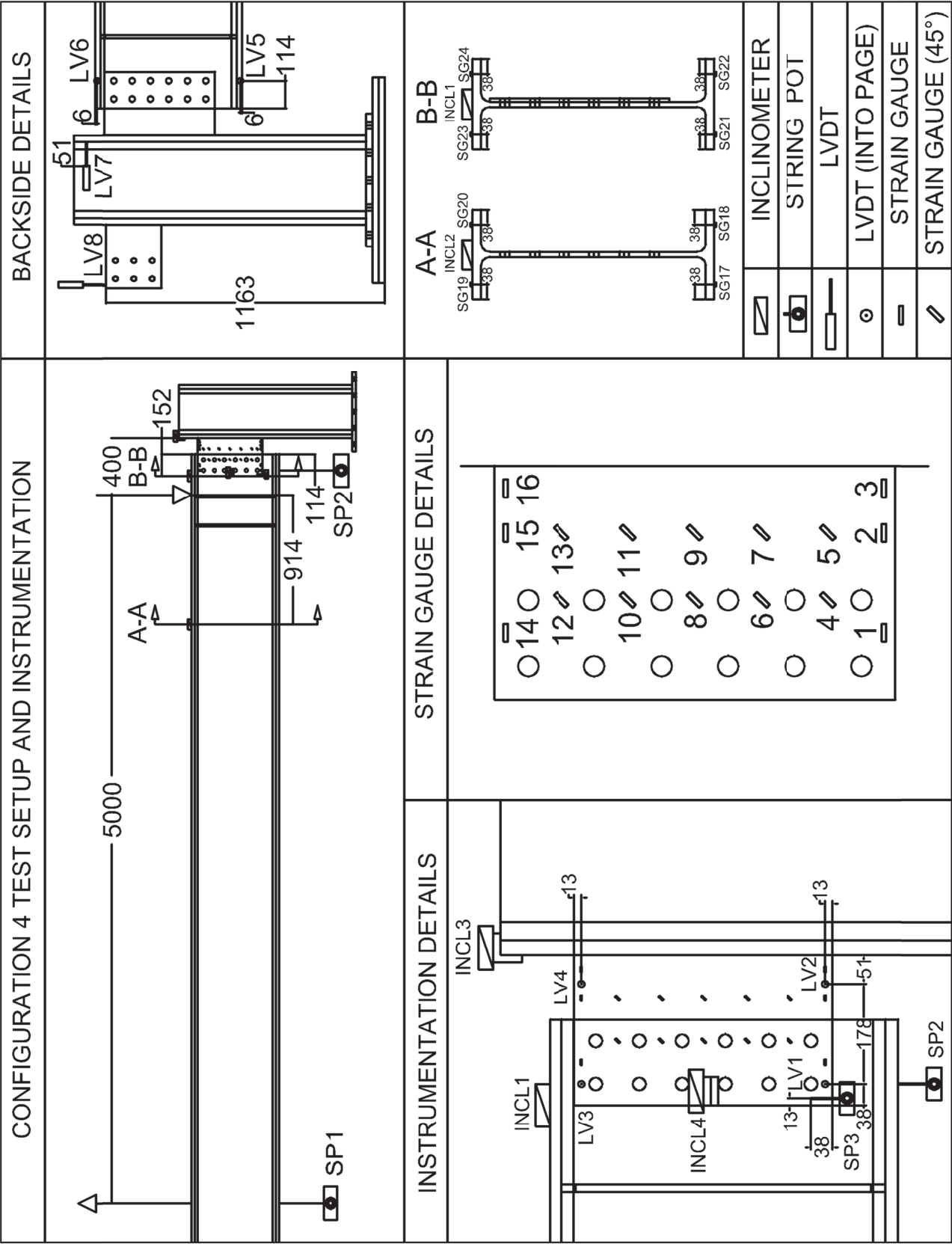


Figure C-3: Test Setup and Instrumentation, Configuration 4

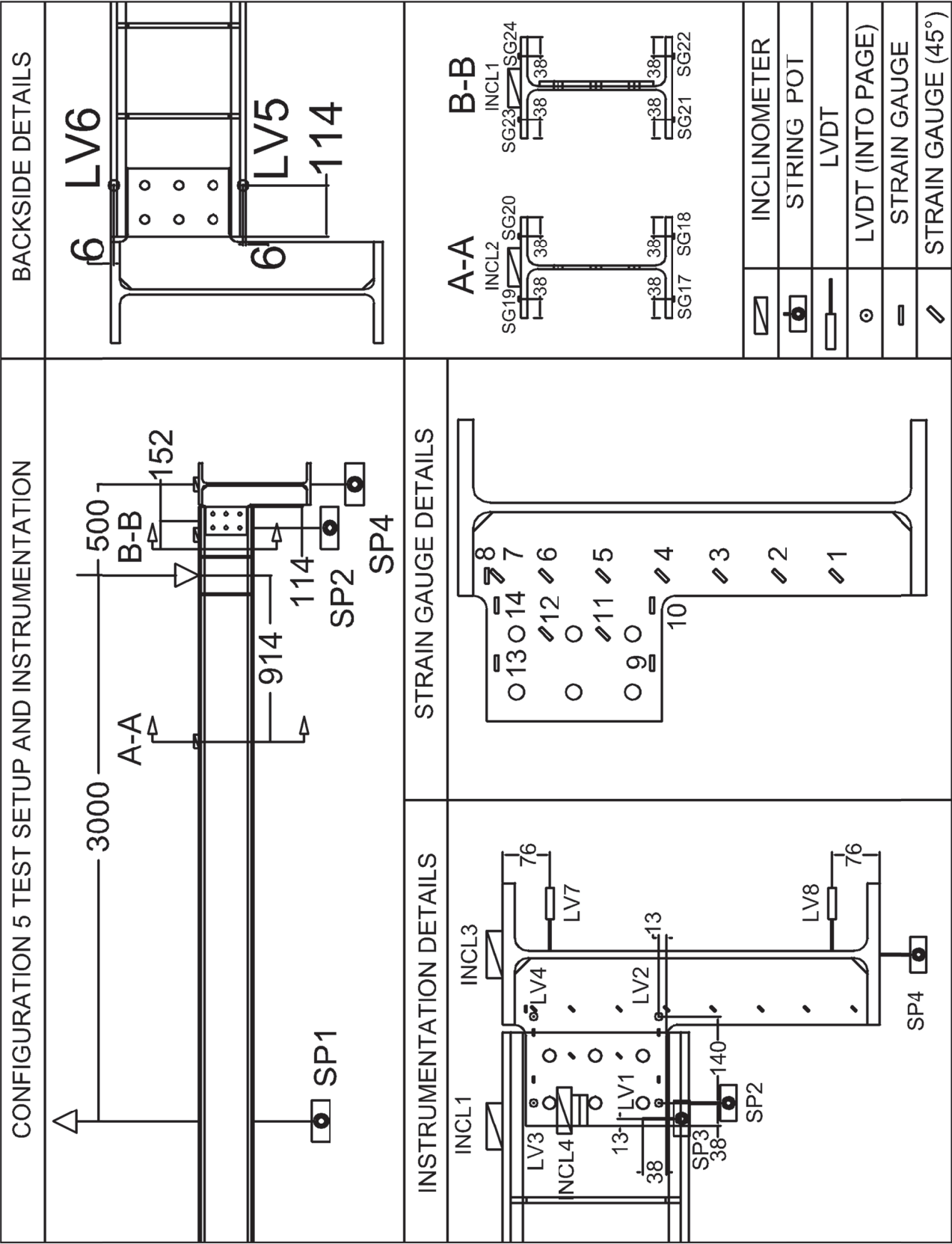


Figure C-4: Test Setup and Instrumentation, Configuration 5

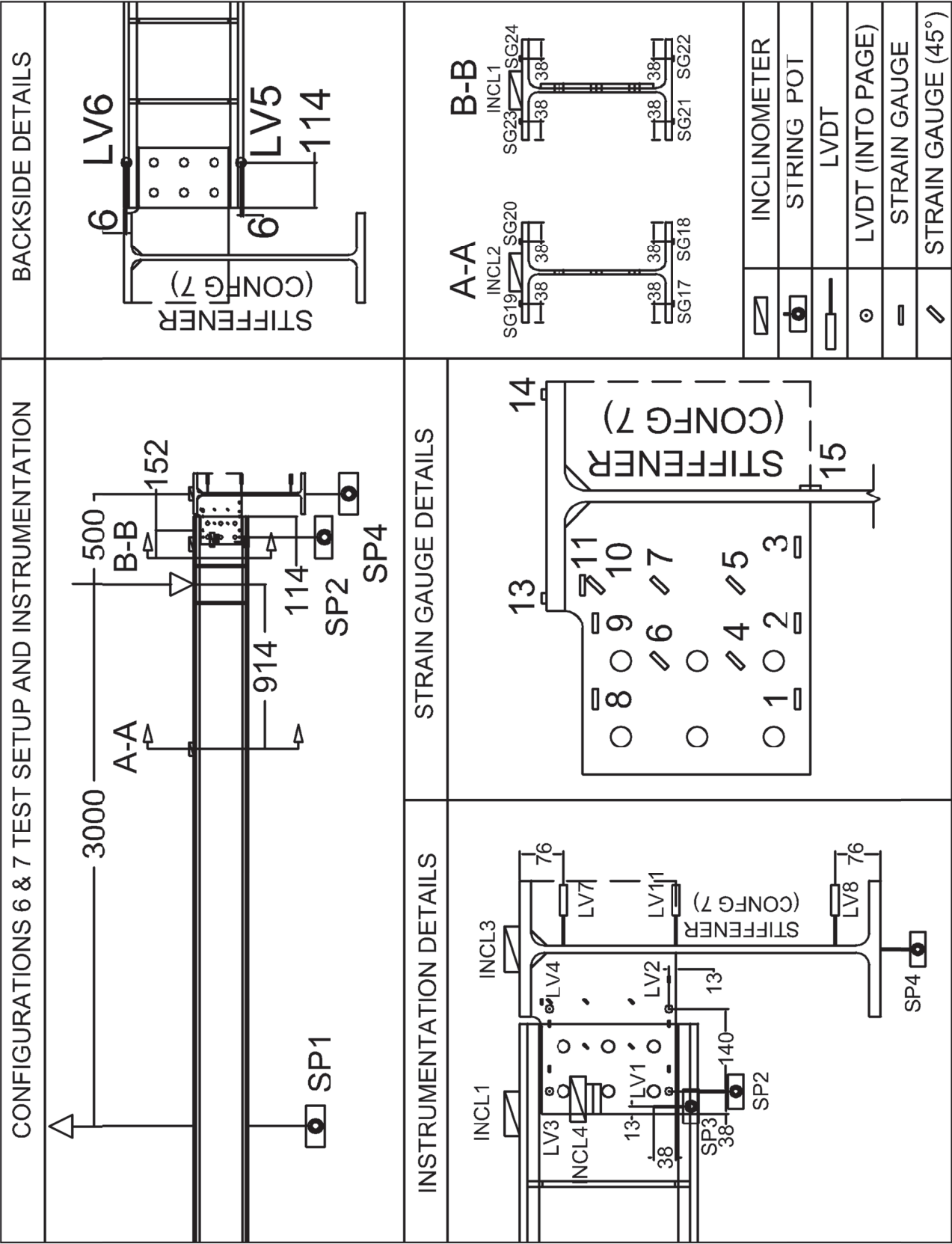


Figure C-5: Test Setup and Instrumentation, Configurations 6 & 7

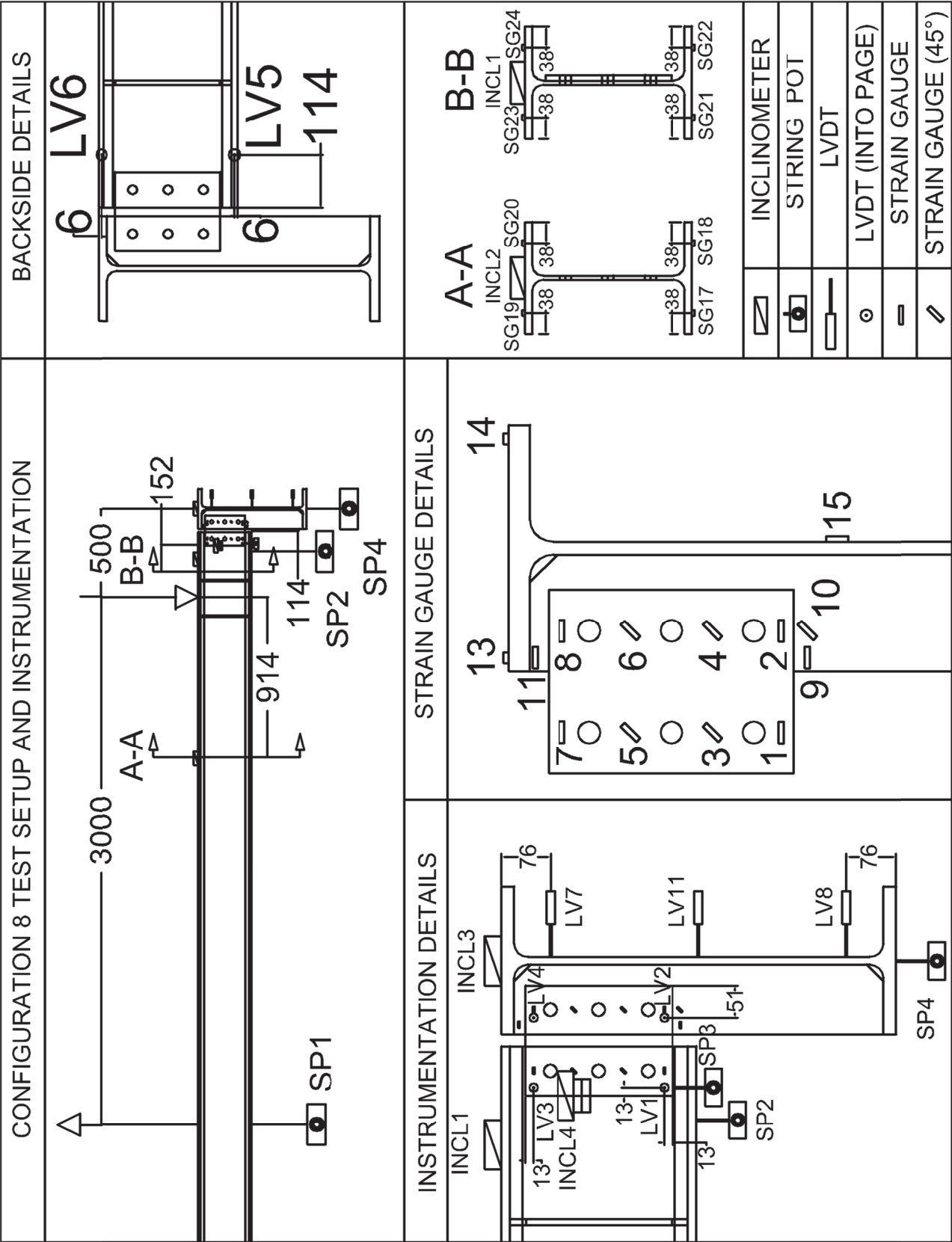


Figure C-6: Test Setup and Instrumentation, Configuration 8

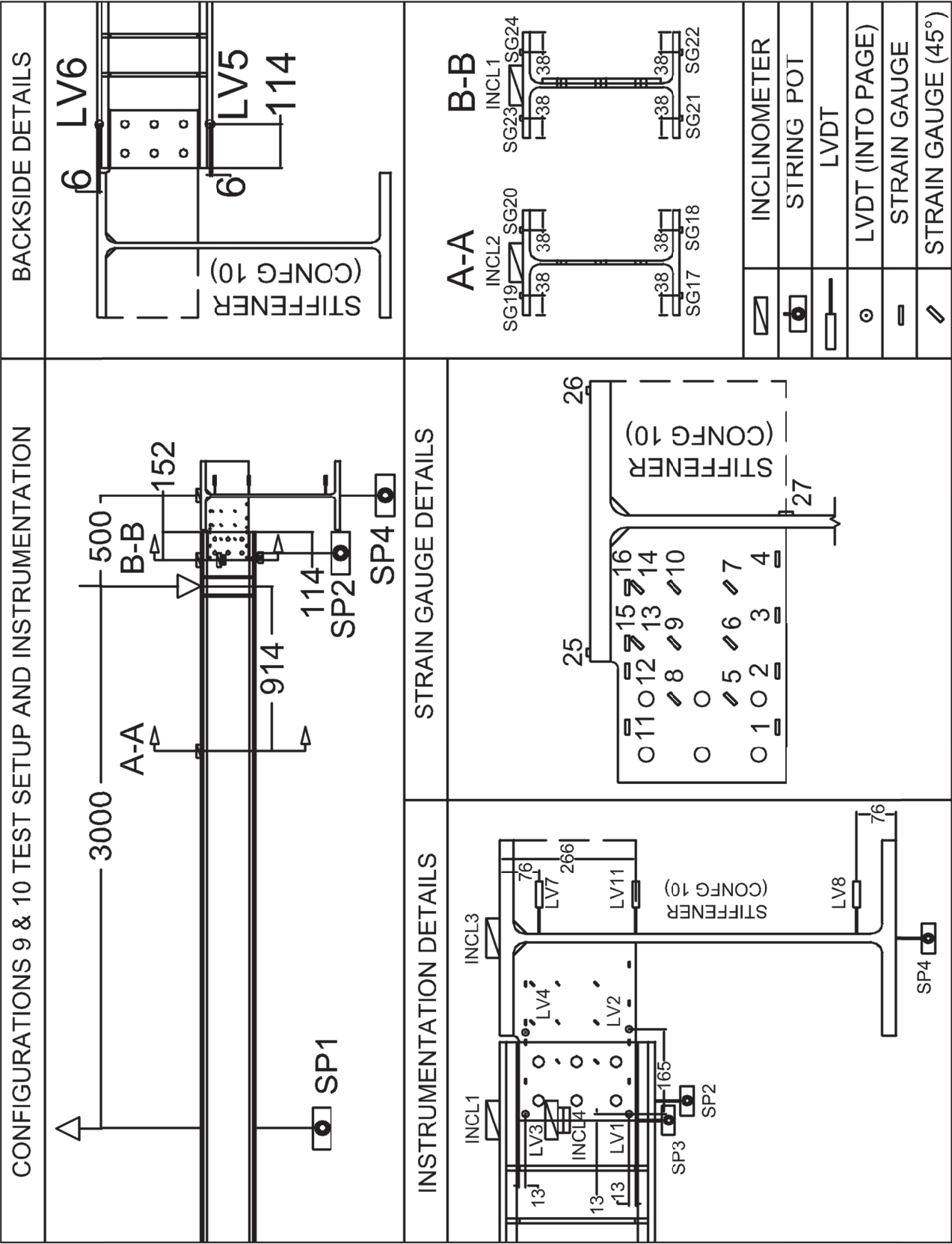


Figure C-7: Test Setup and Instrumentation, Configurations 9 & 10

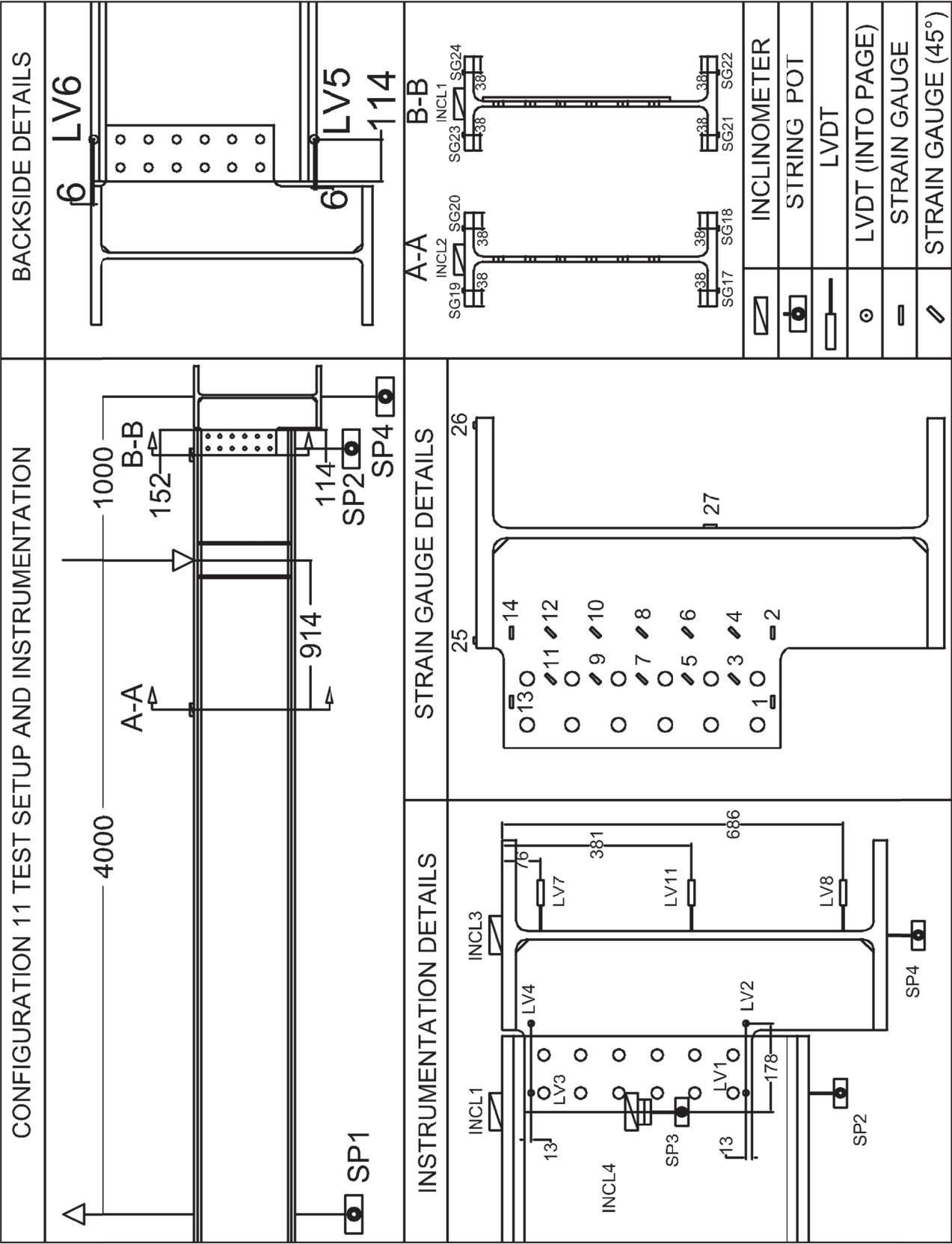


Figure C-8: Test Setup and Instrumentation, Configuration 11

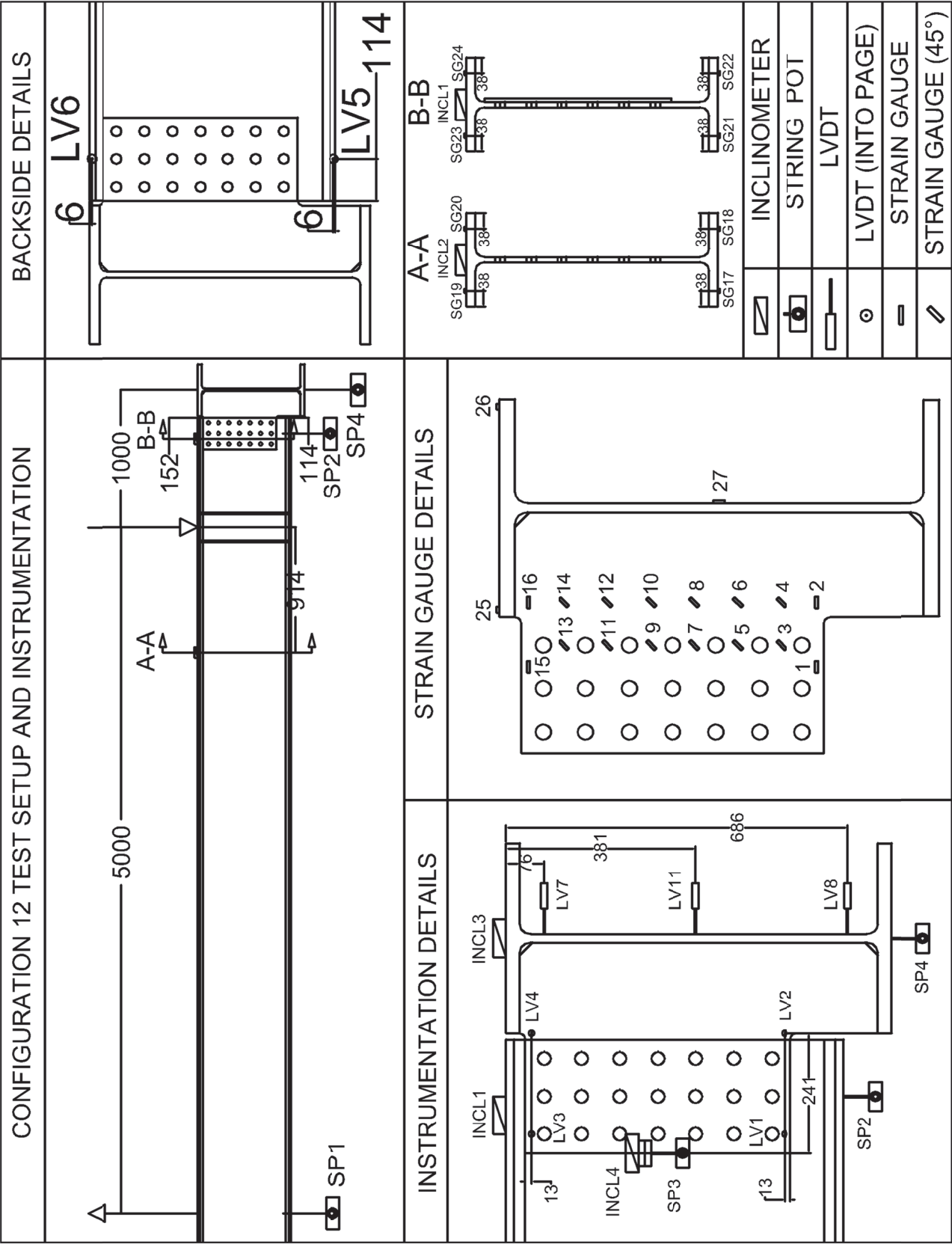


Figure C-9: Test Setup and Instrumentation, Configuration 12

Appendix D –Specimen Test Summaries

EXTENDED SHEAR TAB CONNECTION EXPERIMENTAL STUDY

TEST SUMMARY OF CONFIGURATION 1

Specimen ID	CONFIGURATION 1
Key Words	Shear Tab, Extended Configuration; Rigid Support Condition; Beam to Column;
Test Location	Structures Lab, Macdonald Engineering Building, McGill University
Test Date	May 22, 2013
Investigators	Colin A. Rogers, Dimitrios G. Lignos, Jacob W. Hertz
Main References	AISC Steel Construction Manual, 13th & 14th Editions; CISC Handbook of Steel Construction, 10th Edition
Sponsors	ADF Group Inc., DPHV and NSERC

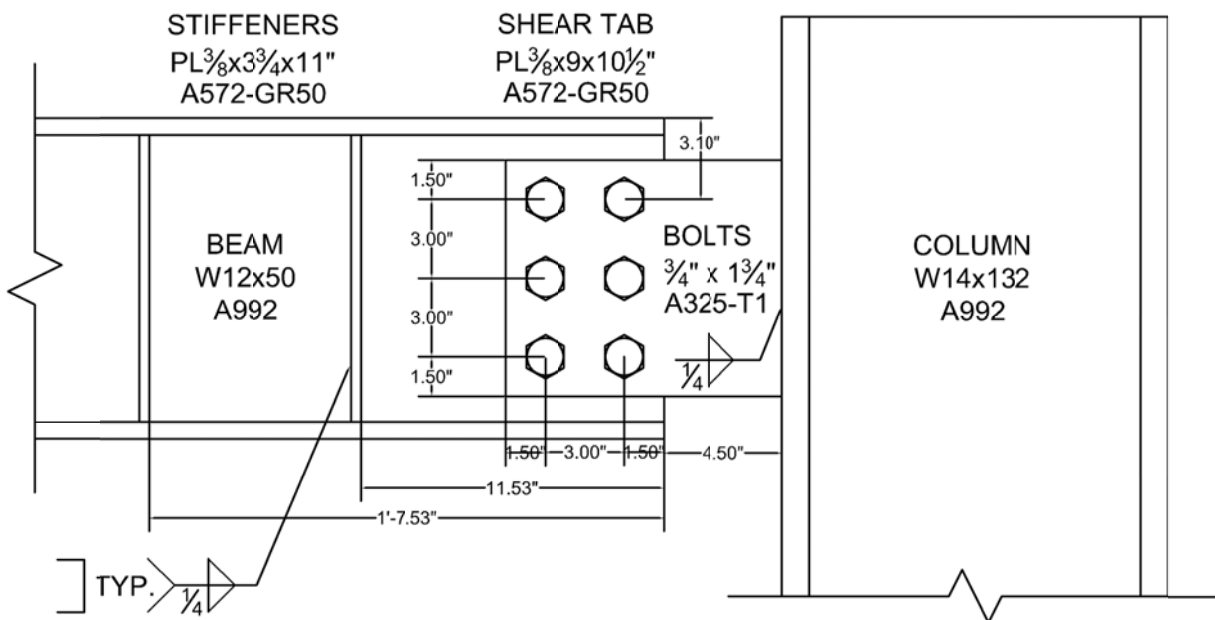


Figure D-1: Connection Details, Configuration 1

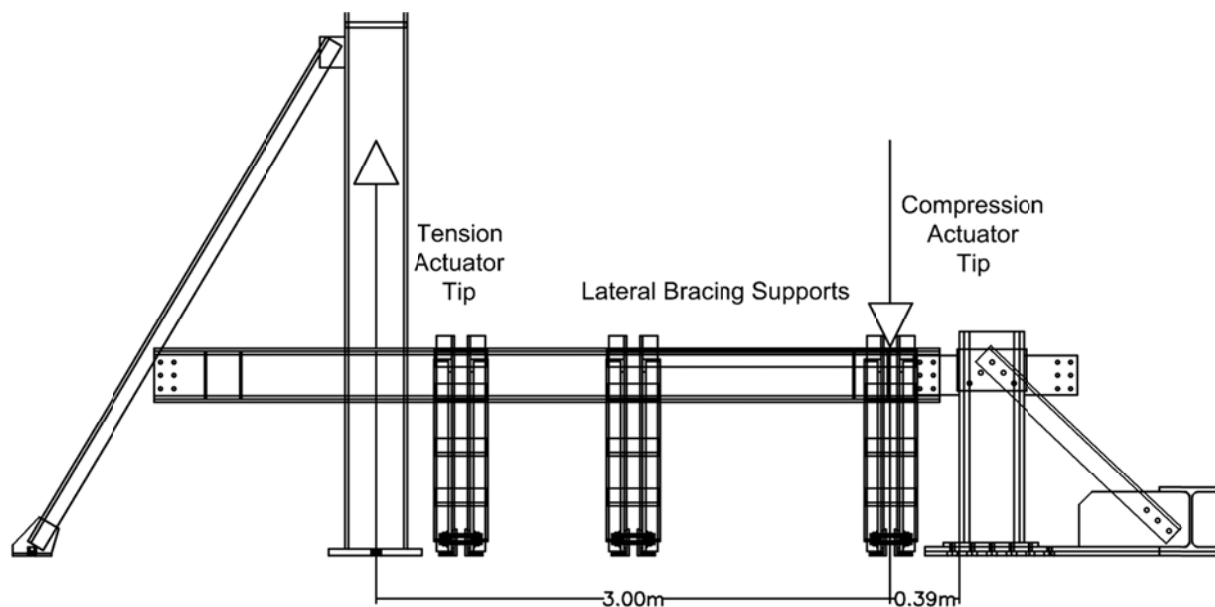
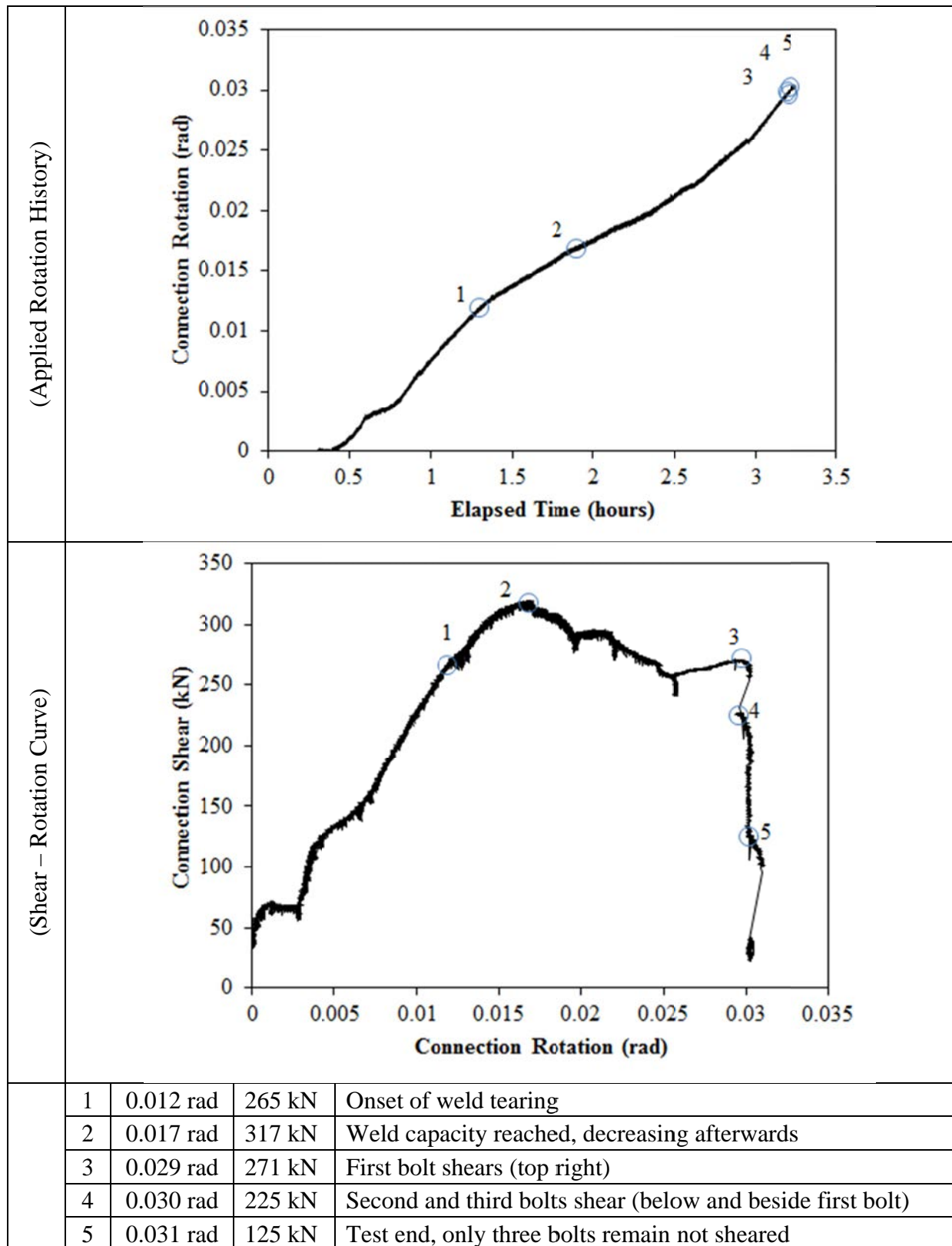


Figure D-2: Test Setup, Configuration 1

MATERIAL PROPERTIES AND SPECIMEN DETAILS

Member	Size	Grade	Yield Stress (MPa)		Ultimate Stress (MPa)	
			Mill Cert.	Coupon	Mill Cert.	Coupon
Beam	W12x50	A992	379	-	501	-
Beam Stiffeners	PL3/8"x3 3/4"	A572-GR50	-	-	-	-
Column	W14x132	A992	398	-	519	-
Shear Tab	PL3/8"x9"	A572-GR50	452	456	531	525
Bolts	3/4" x 1 3/4"	A325-T1	3 rows of 2 bolts; 3" spacing, 1 1/2" end distance; snug tight; one washer per bolt; 13/16" bolt holes;			
Welding Procedure Specification	Electrode Classification E70					
	Welding Procedure <i>Shop Welding:</i> FCAW-G (flux-cored arc welding with gas shielding) <ul style="list-style-type: none">Fillet Weld, Shear Tab to Column"C" Weld, Beam Stiffeners					
Boundary Condition	Tension Actuator Capacity: 268kN tension, 495kN compression; Stroke: 254mm; Displacement controlled					
	Compressive Actuator Capacity: 8018 kN tension, 11414kN compression; Stroke: 305mm; Displacement controlled					
	Lateral Bracing System Top and bottom flange out of plane movement restrained by ball and socket rods fixed to frame tensioned to strong floor					

ROTATION HISTORY AND KEY EXPERIMENTAL OBSERVATIONS



Note: The stiffness variation seen during the first 0.007 radians of rotation is due to adjustment of the displacement rates of both tension and compression actuators to achieve the desired stiffness. Once this stiffness value was reached, the ratio of rates was held constant for the remainder of the test.

RESISTANCE SUMMARY

Limit State	Design Check	Predicted	Observed
Bolt Shear	AISC Manual, 14 th Ed; Section J4; Equation J4-4	197 kN	271 kN
Combined Shear and Flexural Yielding	AISC Manual, 14 th Ed; Part 10; Equation 10-5	316 kN	317 kN

TEST OBSERVATIONS

Combined Shear and Flexural Yielding

Deformation within the tab was monitored using a combination of horizontal and inclined strain gauges organized as seen in Figure D-3. White wash was applied to the tab such that the yielding pattern could be observed. The face of the shear tab at the end of test can be seen in Figure D-4.

Horizontal strain gauges were placed on the top and bottom edges of the tab to record flexural strains and the results can be seen in Figures D-5 and D-6. Note, SG2 malfunctioned during the test. Compression yielding was observed in the bottom of the shear tab, closest to the weld (SG3), at 0.0085 radian rotation. Similarly, tension yielding was observed at 0.0095 radians on the top edge of the tab (SG10). After 0.012 radians of rotation, tension strain values began to decrease in magnitude due to the onset of weld tearing. The onset of flexural yielding (where the whole plate begins to undergo flexural plastic deformation at the extreme fibres) occurred at 0.0095 radians.

Strain gauges oriented to 45° were placed along the height of the tab and the results can be seen in Figures D-7 and D-8. Shear yielding can be seen first at 0.018 radians (SG5). SG4 is seen to be approach yielding in the same manor but stabilizes briefly after 0.019 radians before eventually yielding at 0.03 radians. This is due to elastic recovery while energy dissipation from bolt shear and weld tearing. SG6 and SG7 were located on the top half of the shear tab. After 0.014 radians the strains decrease due to the weld tearing.

Combined flexural and shear yielding was seen at 0.018 radian rotation. Since this is occurred after the capping due to weld tearing, the resistance is estimated to be greater than 320 kN.

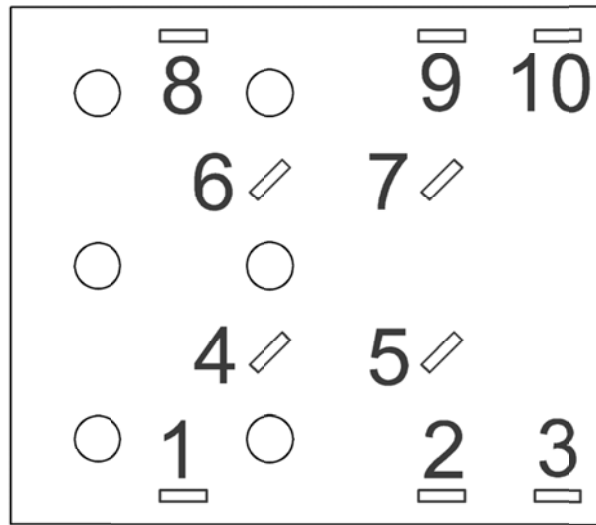


Figure D-3: Strain Gauge Layout, Configuration 1



Figure D-4: Yielded Shear Tab, Configuration 1

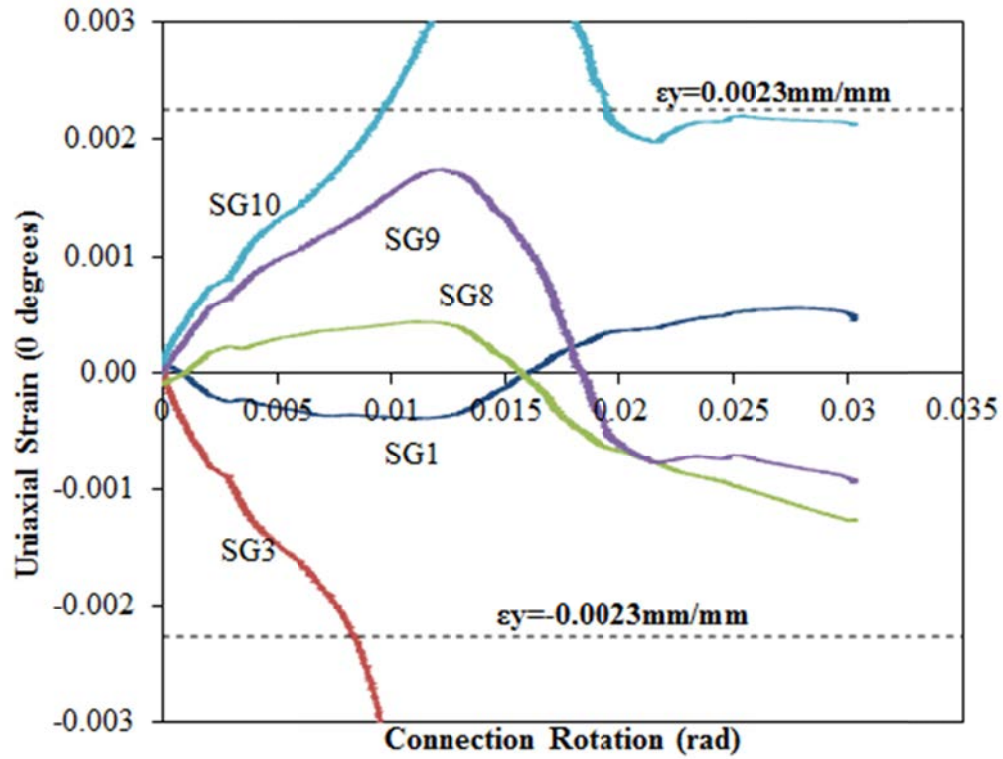


Figure D-5: Uniaxial Strain (0°) vs. Connection Rotation, Configuration 1

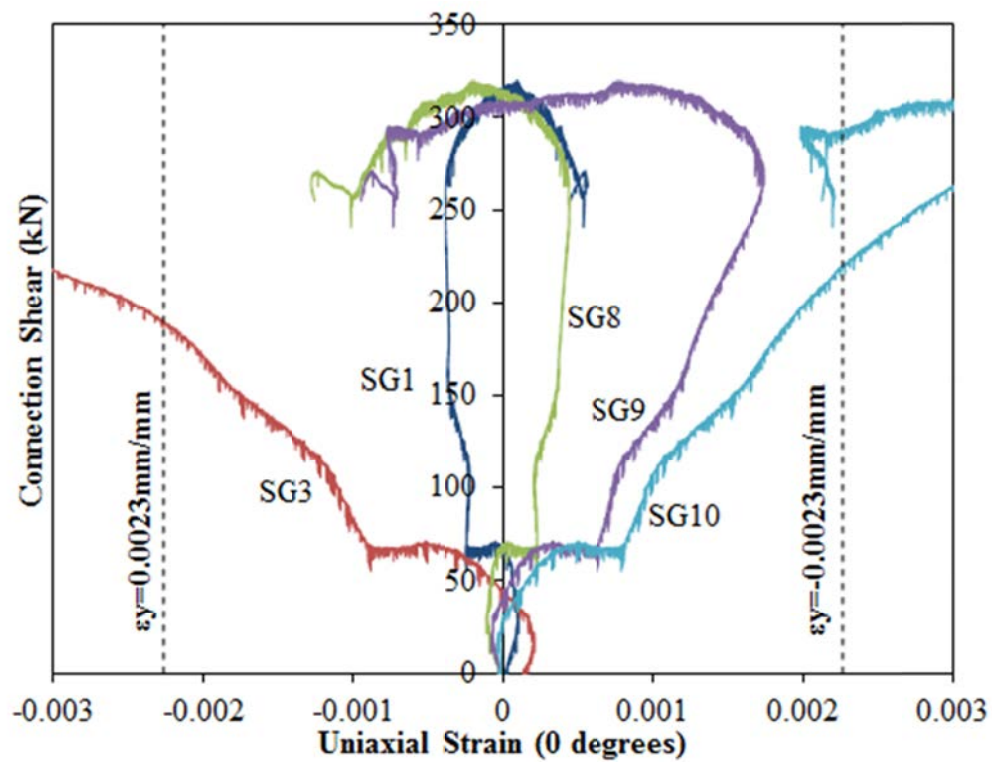


Figure D-6: Connection Shear vs. Uniaxial Strain (0°), Configuration 1

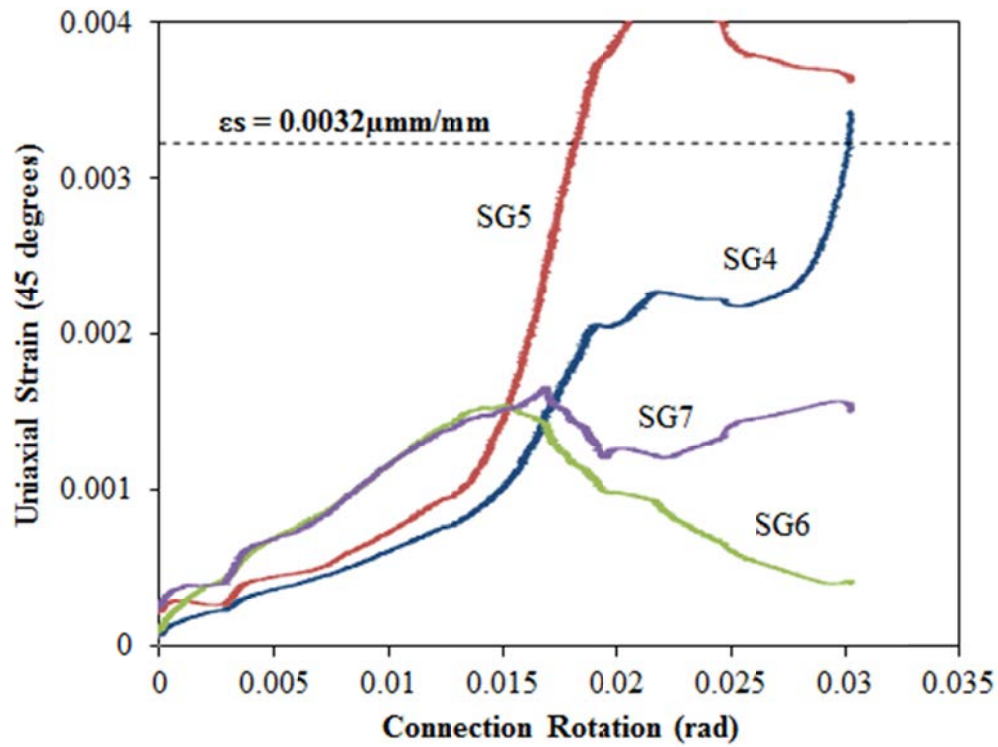


Figure D-7: Uniaxial Strain (45°) vs. Connection Rotation, Configuration 1

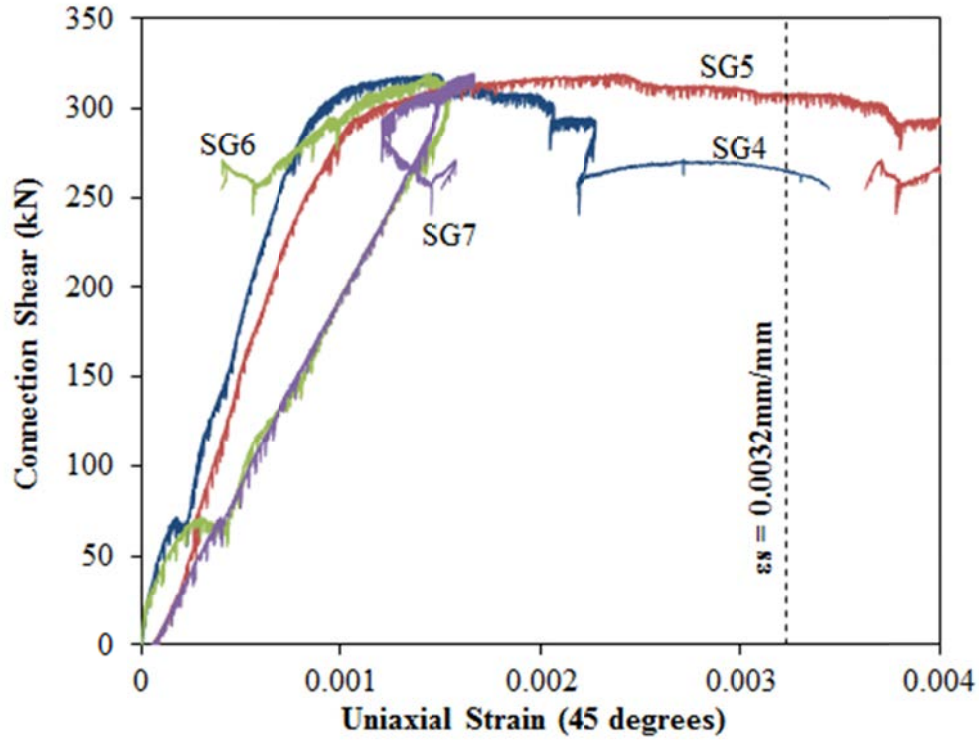


Figure D-8: Connection Shear vs. Uniaxial Strain (45°), Configuration 1

Weld Tearing

Weld tearing initiated at 0.012 radians or 265 kN. A sudden stiffness decrease can be seen on the shear-rotation curve (see Rotation History). This stiffness continued to decrease until load capped at 317 kN at 0.017 radians. After this point, the weld capacity continued to decrease as the weld continued to tear. Eventually the weld tore to half of the tab height. Figure D-9 shows the weld tear at the end of test.



Figure D-9: Weld Tear at End of Test, Configuration 1

Bolt Shear

Three bolts sheared through during the test but remained inside their respective holes. A sudden decrease in connection shear can be seen on the Shear-Rotation curve (see Rotation History) at 0.030 radians rotation or 270 kN. This decrease can be divided into two portions. The first decrease is to approximately 225 kN (45 kN decrease), then to 125 kN (100 kN decrease). The test was terminated after this due to fear of damaging equipment. The first drop is assumed to be the top right bolt and the second is for the bolts to the left and below (see Figure D-10). A representative sheared bolt can be seen in Figure D-11.



Figure D-10: Shear Tab with Sheared Bolts Removed, Configuration 1

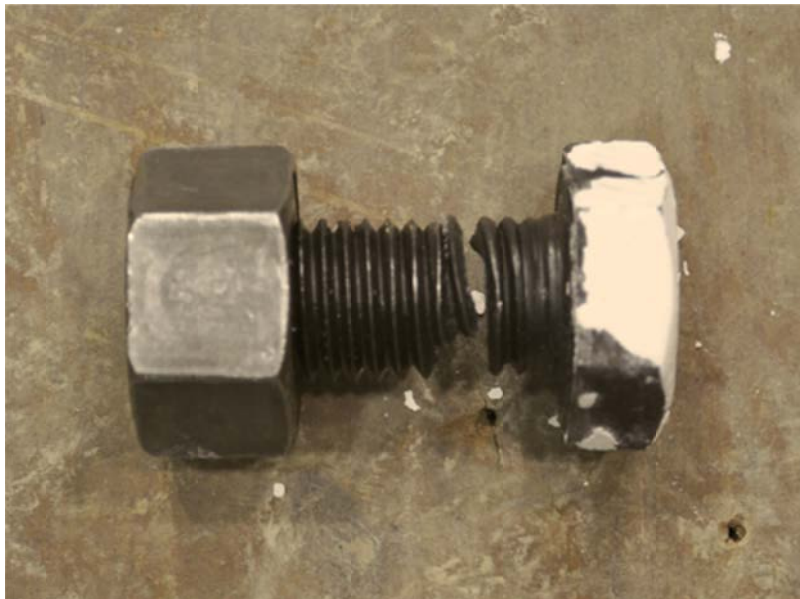


Figure D-11: Sheared Bolt, Top Right, Configuration 1

EXTENDED SHEAR TAB CONNECTION EXPERIMENTAL STUDY

TEST SUMMARY OF CONFIGURATION 2

Specimen ID	CONFIGURATION 2
Key Words	Shear Tab, Extended Configuration; Rigid Support Condition; Beam to Column;
Test Location	Structures Lab, Macdonald Engineering Building, McGill University
Test Date	May 22, 2013
Investigators	Colin A. Rogers, Dimitrios G. Lignos, Jacob W. Hertz
Main References	AISC Steel Construction Manual, 13th & 14th Editions; CISC Handbook of Steel Construction, 10th Edition
Sponsors	ADF Group Inc., DPHV and NSERC

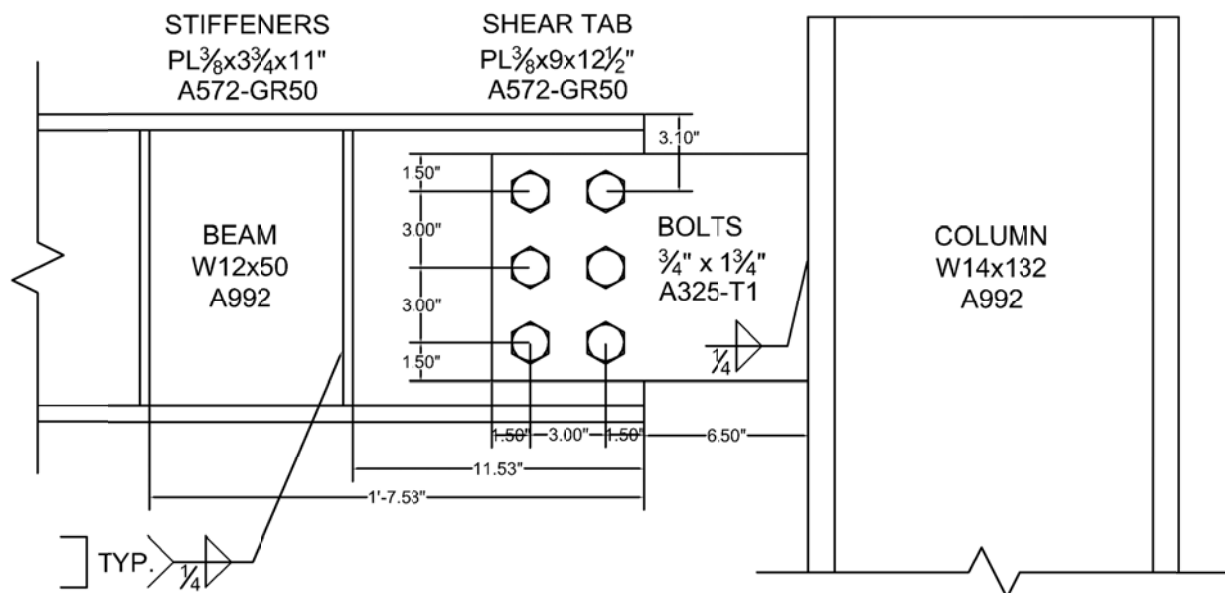


Figure D-12: Connection Details, Configuration 2

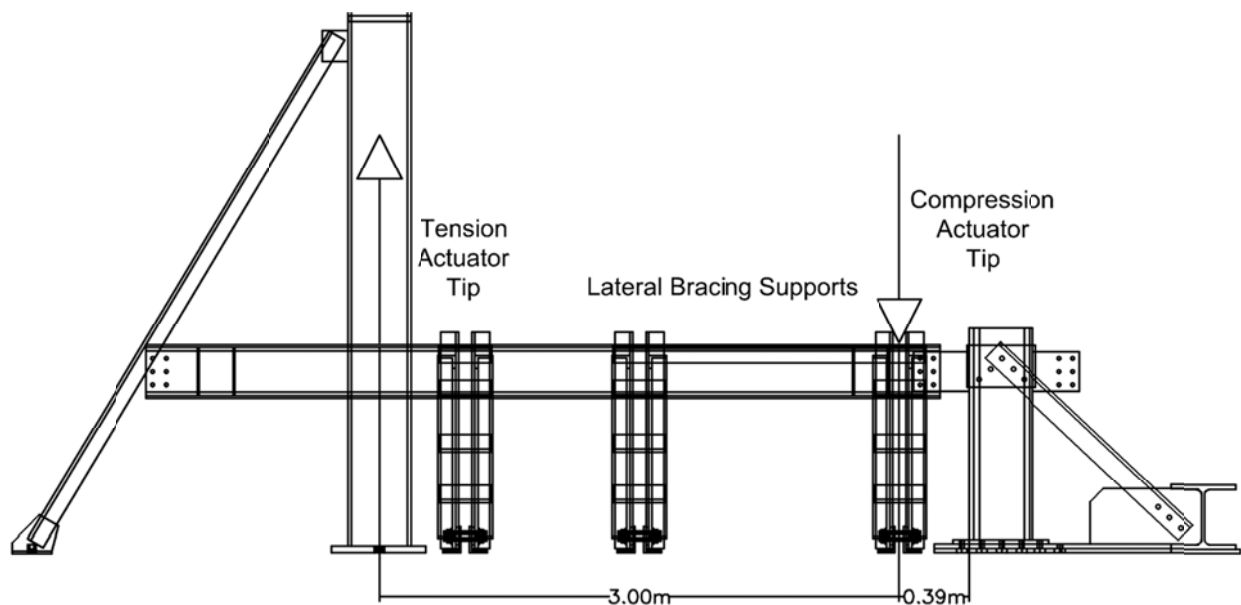
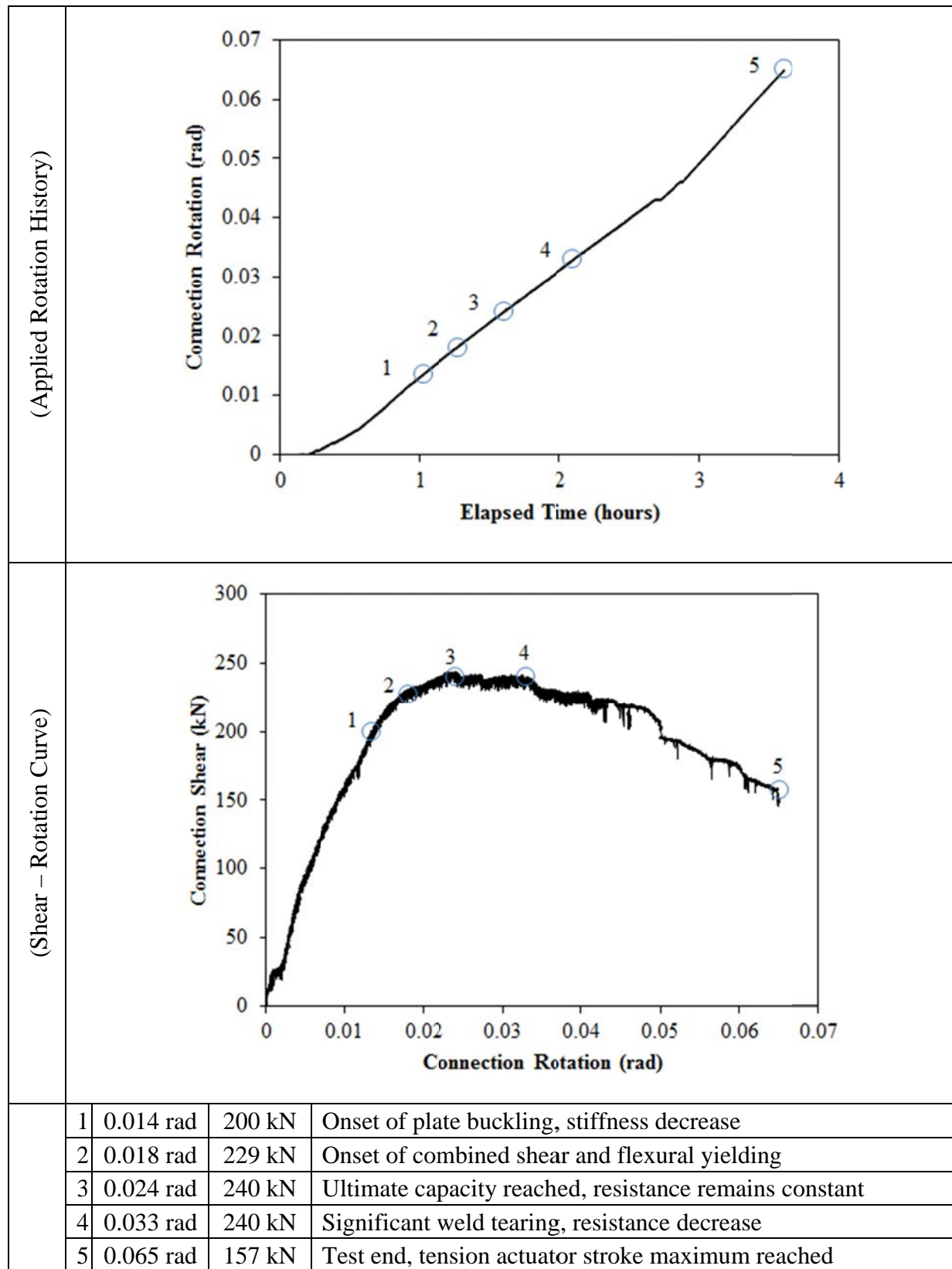


Figure D-13: Test Setup, Configuration 2

MATERIAL PROPERTIES AND SPECIMEN DETAILS

Member	Size	Grade	Yield Stress (MPa)		Ultimate Stress (MPa)	
			Mill Cert.	Coupon	Mill Cert.	Coupon
Beam	W12x50	A992	379	-	501	-
Beam Stiffeners	PL3/8"x3 3/4"	A572-GR50	-	-	-	-
Column	W14x132	A992	398	-	519	-
Shear Tab	PL3/8"x9"	A572-GR50	452	456	531	525
Bolts	3/4" x 1 3/4"	A325-T1	3 rows of 2 bolts; 3" spacing, 1 1/2" end distance; snug tight; one washer per bolt; 13/16" bolt holes;			
Welding Procedure Specification	Electrode Classification E70					
	Welding Procedure <i>Shop Welding:</i> FCAW-G (flux-cored arc welding with gas shielding) <ul style="list-style-type: none">Fillet Weld, Shear Tab to Column"C" Weld, Beam Stiffeners					
Boundary Condition	Tension Actuator Capacity: 268kN tension, 495kN compression; Stroke: 254mm; Displacement controlled					
	Compressive Actuator Capacity: 8018 kN tension, 11414kN compression; Stroke: 305mm; Displacement controlled					
	Lateral Bracing System Top and bottom flange out of plane movement restrained by ball and socket rods fixed to frame tensioned to strong floor					

ROTATION HISTORY AND KEY EXPERIMENTAL OBSERVATIONS



Note: The variation in stiffness during the first 0.012 radians of rotation is due to adjustment of the displacement rates of both tension and compression actuators to achieve the desired stiffness. Once this stiffness value was reached, the ratio of rates was held constant for the remainder of the test.

RESISTANCE SUMMARY

Limit State	Design Check	Predicted	Observed
Plate Buckling	AISC Manual, 14 th Ed; Part 9; Q Equation	186 kN	240 kN
Combined Shear and Flexural Yielding	AISC Manual, 14 th Ed; Part 10; Equation 10-5	253 kN	229 kN

TEST OBSERVATIONS

Plate Buckling

LVDTs were placed along the bottom and top edges of the shear tab to measure out of plane movement. The locations of LVDT2 and LVDT4 can be seen on Figure D-14. Out of plane shear tab movement versus rotation can be seen in Figure D-15 for these two LVDTs. Plate buckling is seen to begin at approximately 0.005 radians but becomes significant at 0.0135 radians. At 0.0135 radians, the stiffness decreased suddenly (see Shear-Rotation curve in Rotation History). At 0.024 radians, the rate of buckling became constant. The stabilizing of connection shear on the Shear-Rotation curve indicates that this mechanism had fully formed and reached its ultimate resistance of 240kN. Figure D-16 shows the buckled location from underneath the shear tab.

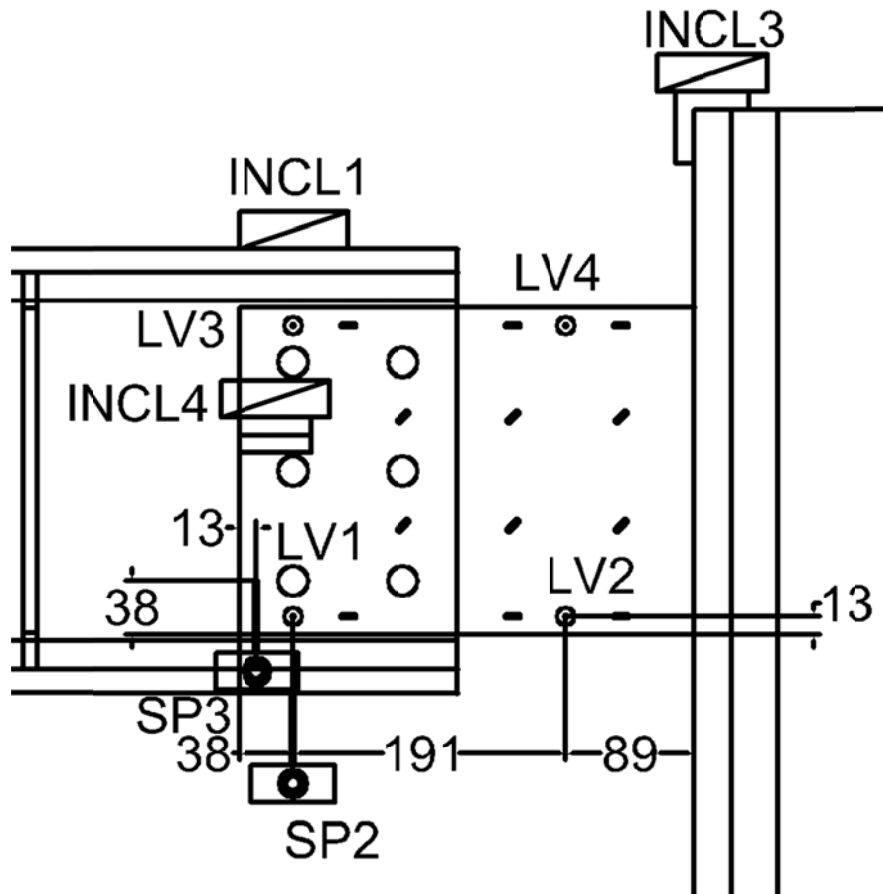


Figure D-14: Instrumentation Details, Configuration 2

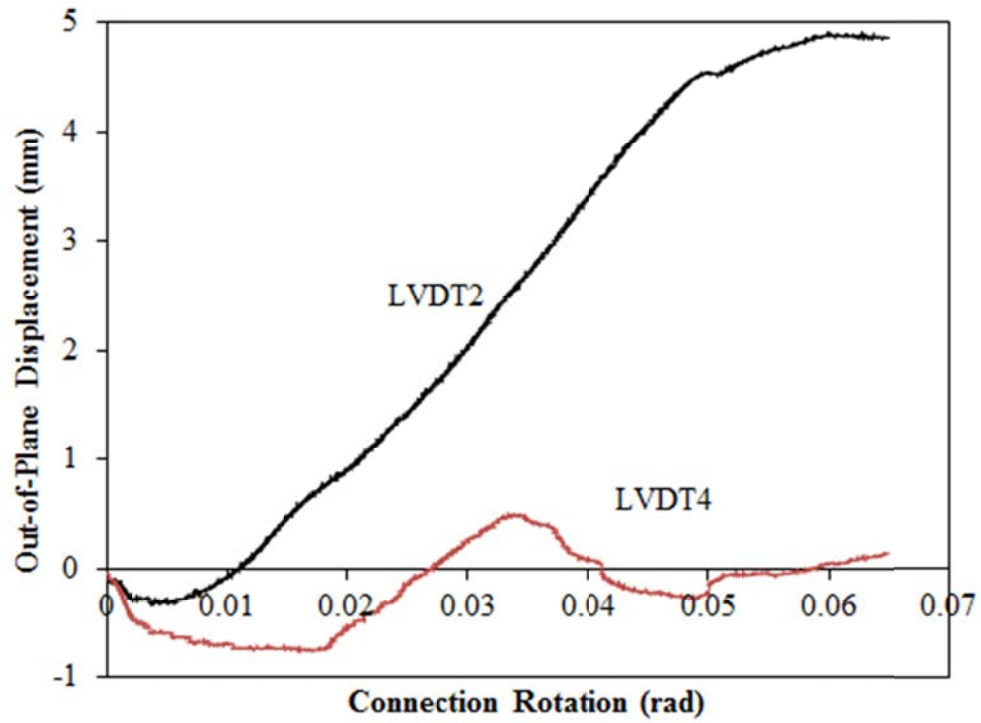


Figure D-15: Out of Plane Displacement vs. Rotation, Configuration 2

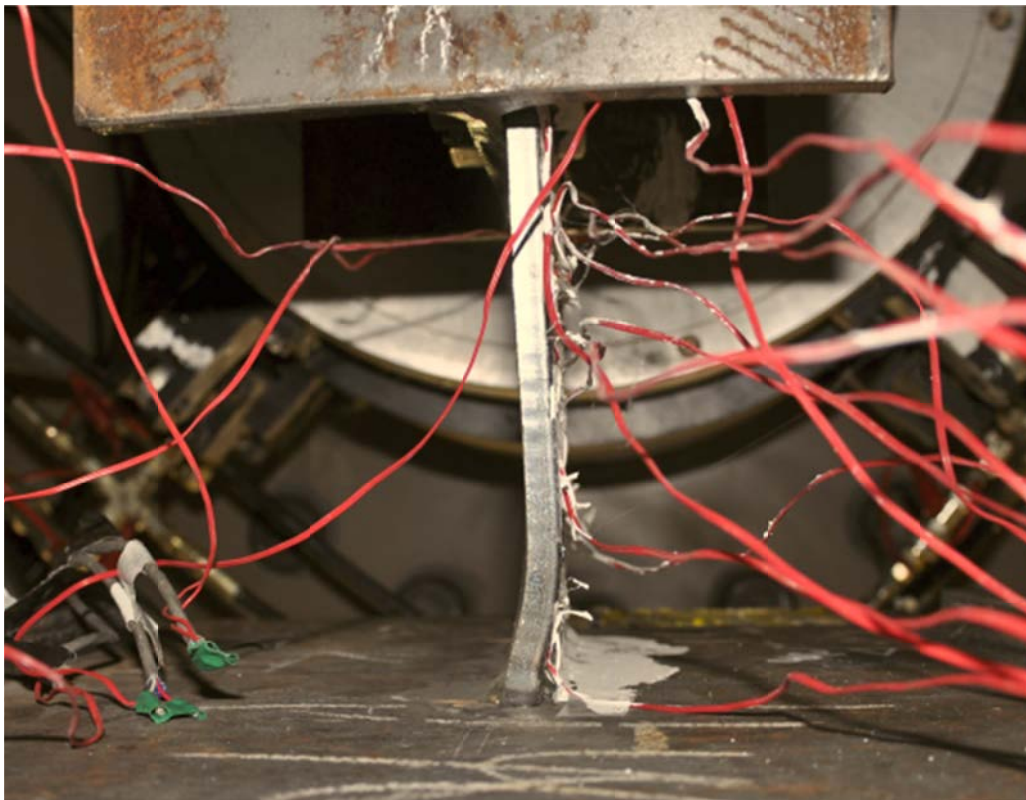


Figure D-16: Buckled Shear Tab, from Underneath Beam, Configuration 2

Combined Shear and Flexural Yielding

Deformation within the tab was monitored using a combination of horizontal and inclined strain gauges organized as seen in Figure D-17. White wash was applied to the tab such that the yielding pattern could be observed. The face of the shear tab at the end of test can be seen in Figure D-18.

Horizontal strain gauges were placed on the top and bottom edges of the tab to record flexural strains and the results can be seen in Figure D-19 and D-20. Compression yielding was observed in the bottom of the shear tab, closest to the weld (SG3) at 0.0095 radian rotation. Similarly, tension yielding was observed at 0.012 radians on the bottom edge of the tab (SG12). The onset of flexural yielding (where the whole plate begins to undergo flexural plastic deformation at the extreme fibres) occurred at 0.012 radians.

Strain gauges oriented to 45° were placed along the height of the tab and the results can be seen in Figure D-21 and D-22. Shear yielding can be seen at 0.018 radians in the locations of SG6 and SG9. These are the locations closest to the support and are in line with SG3 and SG12. This area experienced substantial yielding whereas the rest of the shear tab underwent elastic deformation.

Combined flexural and shear yielding was seen at 0.018 radian rotation and 229 kN connection shear.

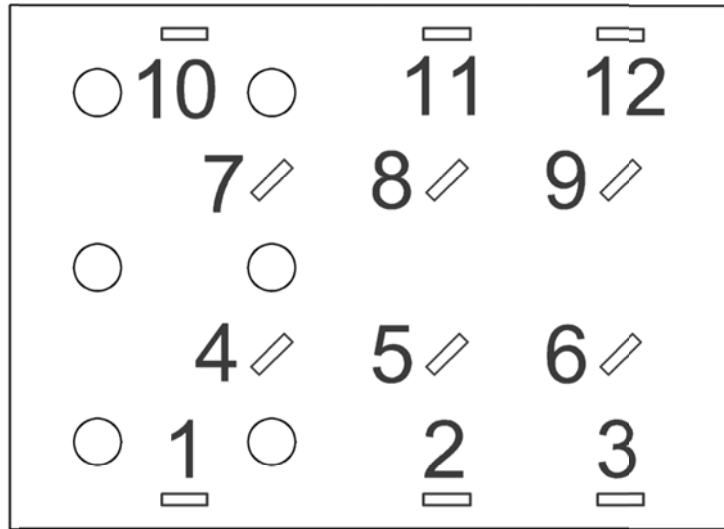


Figure D-17: Strain Gauge Layout, Configuration 2

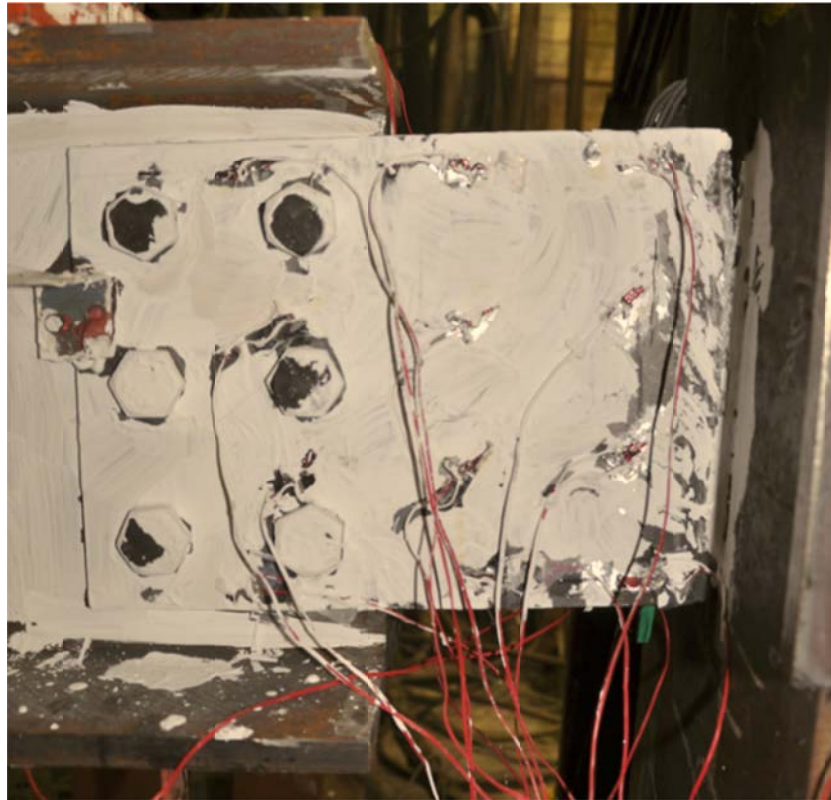


Figure D-18: Yielded Shear Tab, Configuration 2

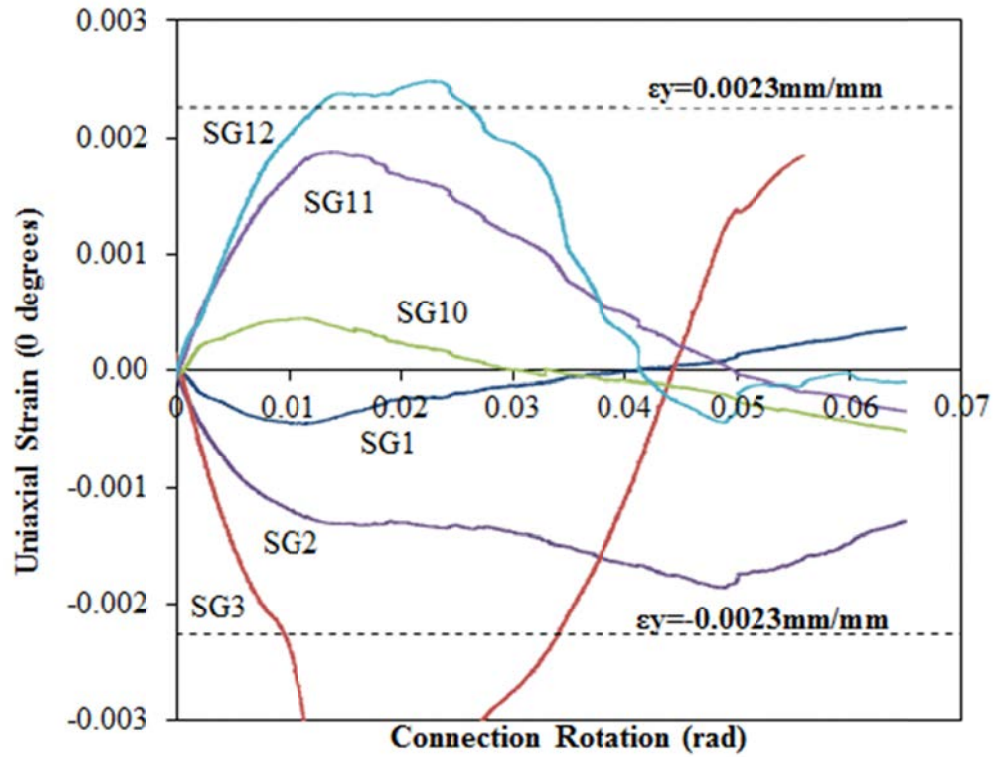


Figure D-19: Uniaxial Strain (0°) vs. Connection Rotation, Configuration 2

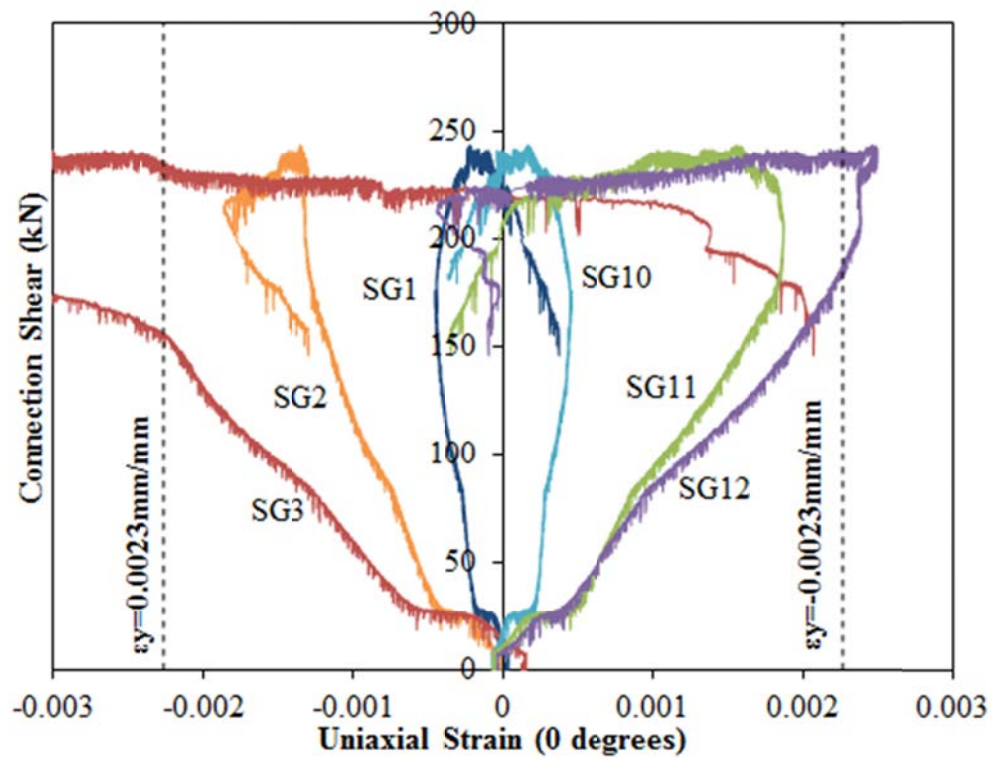


Figure D-20: Connection Shear vs. Uniaxial Strain (0°), Configuration 2

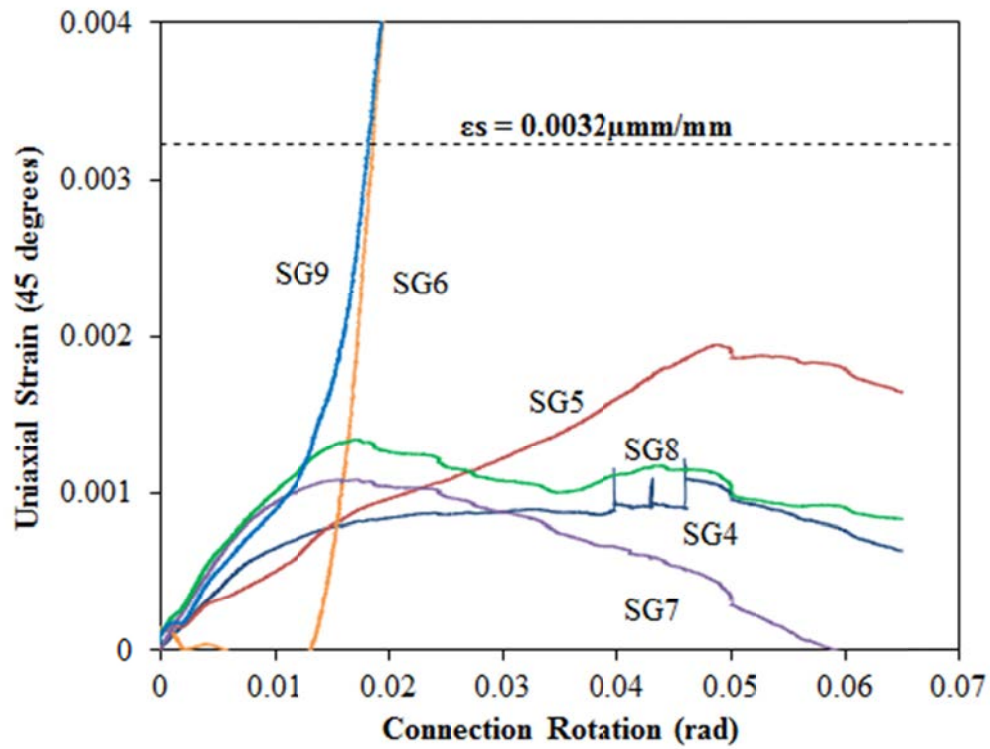


Figure D-21: Uniaxial Strain (45°) vs. Connection Rotation, Configuration 2

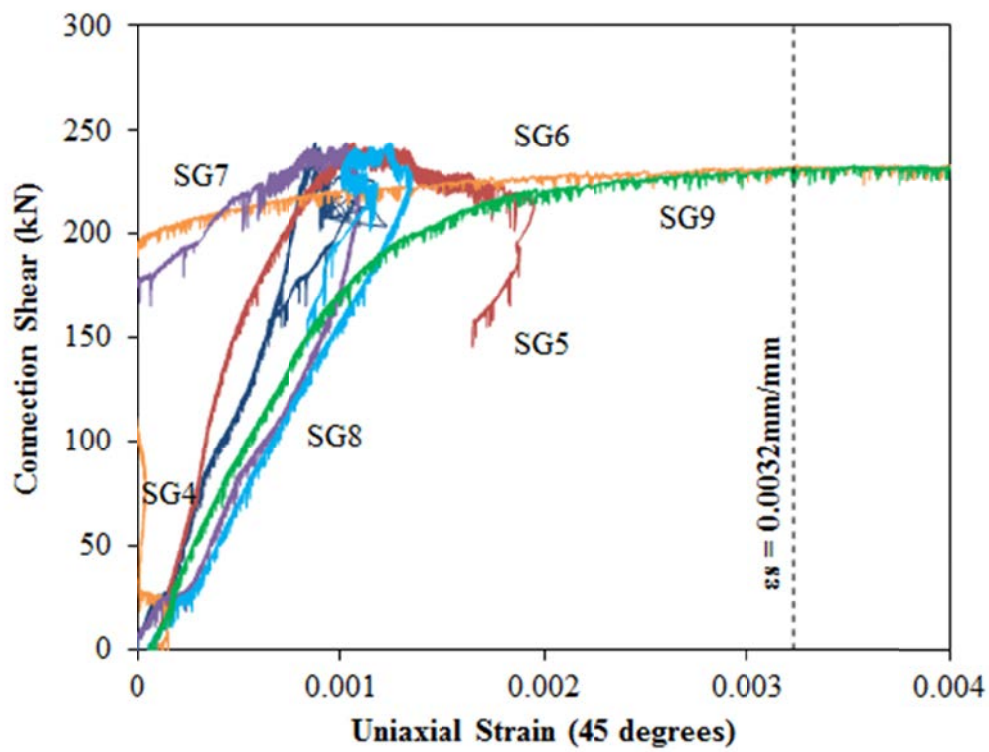


Figure D-22: Connection Shear vs. Uniaxial Strain (45°), Configuration 2

Weld Tearing

After the connection shear stabilized due to the plate buckling mechanism fully forming, the extent of weld tearing began to limit the resistance of the connection. The decreasing connection shear can be seen on the Shear-Rotation curve (see Rotation History). This occurred at 0.033 radians and 240 kN. The test was eventually ended due to the tension actuator stroke being reached. Figure D-23 shows the torn weld at the end of the test.



Figure D-23: Weld Tearing, End of Test, Configuration 2

EXTENDED SHEAR TAB CONNECTION EXPERIMENTAL STUDY

TEST SUMMARY OF CONFIGURATION 3

Specimen ID	CONFIGURATION 3
Key Words	Shear Tab, Extended Configuration; Rigid Support Condition; Beam to Column;
Test Location	Structures Lab, Macdonald Engineering Building, McGill University
Test Date	May 17, 2013
Investigators	Colin A. Rogers, Dimitrios G. Lignos, Jacob W. Hertz
Main References	AISC Steel Construction Manual, 13th & 14th Editions; CISC Handbook of Steel Construction, 10th Edition
Sponsors	ADF Group Inc., DPHV and NSERC

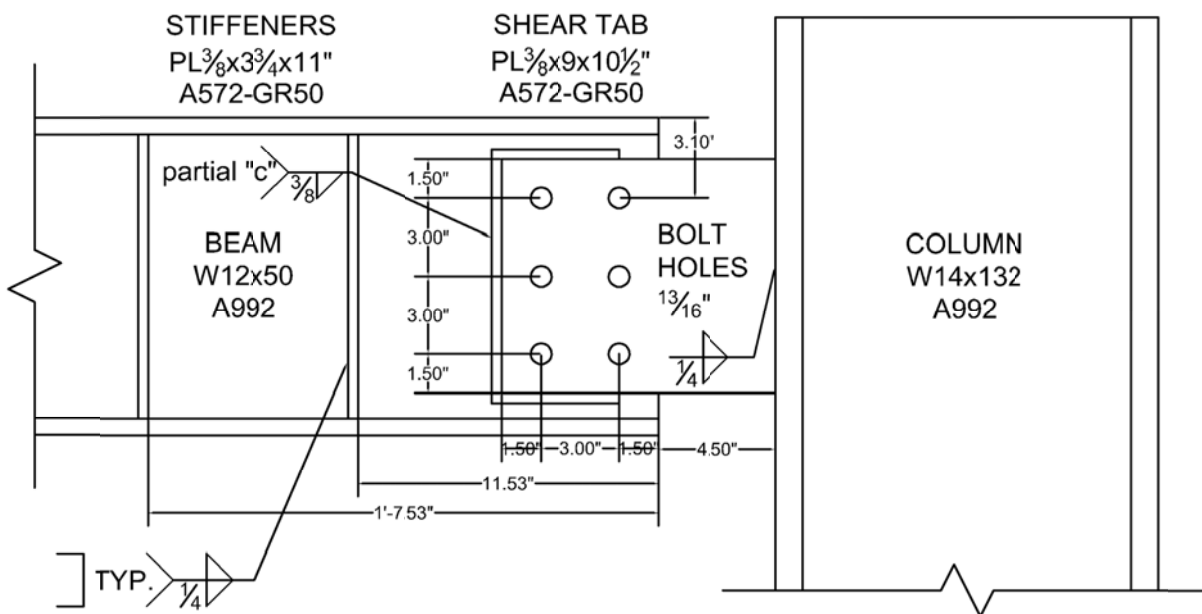


Figure D-24: Connection Details, Configuration 3

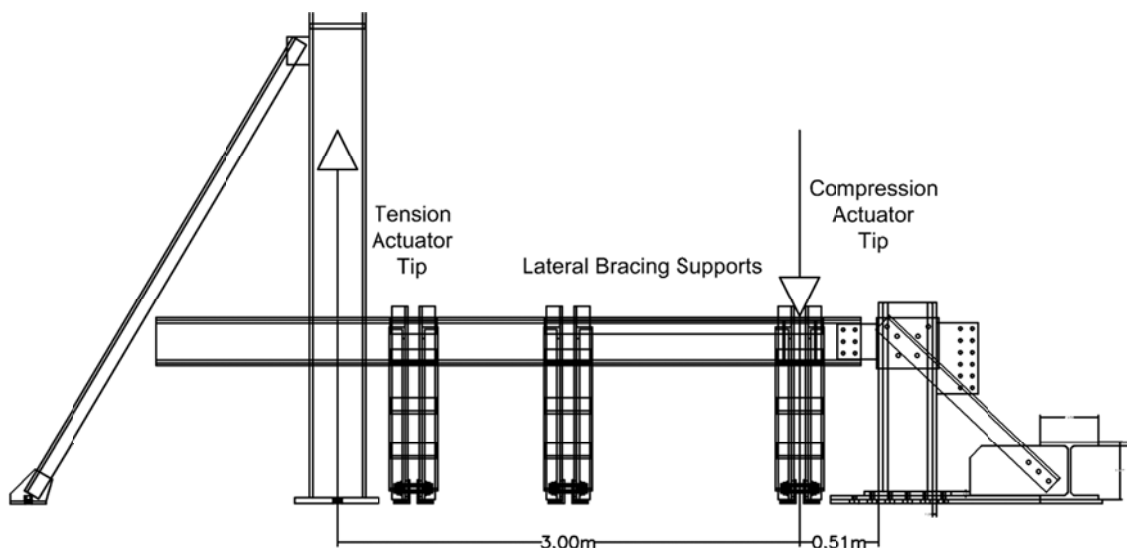
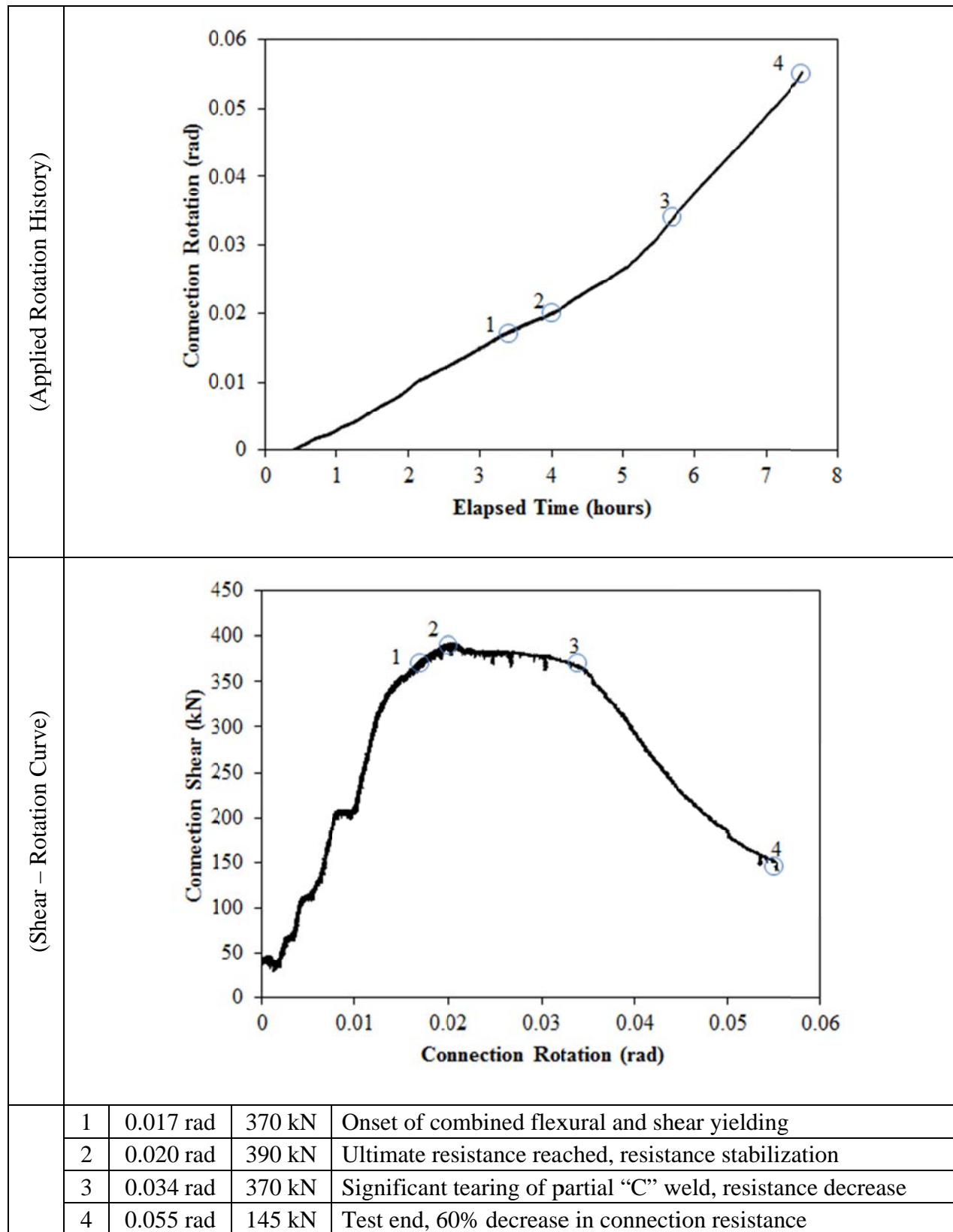


Figure D-25: Test Setup, Configuration 3

MATERIAL PROPERTIES AND SPECIMEN DETAILS

Member	Size	Grade	Yield Stress (MPa)		Ultimate Stress (MPa)	
			Mill Cert.	Coupon	Mill Cert.	Coupon
Beam	W12x50	A992	379	-	501	-
Beam Stiffeners	PL3/8"x3 3/4"	A572-GR50	-	-	-	-
Column	W14x132	A992	398	-	519	-
Shear Tab	PL3/8"x9"	A572-GR50	452	456	531	525
Bolt Holes	3 rows of 2 bolt holes; 3" spacing, 1 1/2" end distance; 13/16" bolt holes;					
Weld	3/8" thick; partial "C" weld; weld terminates at line of bolts closest to column face					
Welding Procedure Specification	Electrode Classification E70					
	Welding Procedure <i>Shop Welding:</i> FCAW-G (flux-cored arc welding with gas shielding) <ul style="list-style-type: none"> Fillet Weld, Shear Tab to Column "C" Weld, Beam Stiffeners <i>Site Welding:</i> SMAW (shielded metal arc welding) <ul style="list-style-type: none"> Partial "C" Weld, Shear Tab to Beam Web 					
Boundary Condition	Tension Actuator Capacity: 268kN tension, 495kN compression; Stroke: 254mm; Displacement controlled					
	Compressive Actuator Capacity: 8018 kN tension, 11414kN compression; Stroke: 305mm; Displacement controlled					
	Lateral Bracing System Top and bottom flange out of plane movement restrained by ball and socket rods fixed to frame tensioned to strong floor					

ROTATION HISTORY AND KEY EXPERIMENTAL OBSERVATIONS



Note: The stiffness variation seen during the first 0.013 radians of rotation is due to adjustment of the displacement rates of both tension and compression actuators to achieve the desired stiffness. Once this stiffness value was reached, the ratio of rates was held constant for the remainder of the test.

RESISTANCE SUMMARY

Limit State	Design Check	Predicted	Observed
Combined Shear and Flexural Yielding	AISC Manual, 14 th Ed; Part 10; Equation 10-5	316 kN	370 kN
Weld Tearing: Partial "C"	CISC Handbook, 2010; Chapter 3; ICR method for welds	285 kN	390 kN



Figure D-26: Partial "C" Weld, Before Test, Configuration 3

TEST OBSERVATIONS

Combined Shear and Flexural Yielding

Deformation within the tab was monitored using a combination of horizontal and inclined strain gauges organized as seen in Figure D-27. White wash was applied to the tab such that the yielding pattern could be observed. The face of the shear tab at the end of test can be seen in Figure D-28.

Horizontal strain gauges were placed on the top and bottom edges of the tab to record flexural strains and the results can be seen in Figure D-29 and D-30. The top edge of the shear tab, closest to the column weld, began to undergo tension yielding at 0.004 radians of rotation (SG10). This was followed by further tension yielding at SG9 at 0.009 radians. Similarly, SG3 underwent compressive yielding at 0.006 radians. The strain at SG8 began positive but became negative after 0.013 radians rotation and eventually yielded in compression at 0.07 radians.

Strain gauges oriented to 45° were placed along the height of the tab to measure shear strain and the results can be seen in Figure D-31 and D-32. The shear tab first experienced shear yielding at 0.013 radians (SG6) and fully underwent shear yielding after 0.017 radians (SG 4 and SG5). There was no yielding at SG7 until later. This is most likely due to tearing of the weld causing stress redistribution.

Combined shear and flexural yielding is concluded to occur at a rotation of 0.017 radians. The stiffness can be seen to decrease at approximately 0.014 radians on the Shear-Rotation curve (see Rotation History) and eventually reaches zero at 0.02 radians. This is consistent with the shear strain measurements (plastification between 0.013 and 0.018 radians). From this point onwards the shear tab underwent plastic deformation. This can be seen in Figure D-28 as there is no whitewash left on the mid-height portion of the tab between the first line of bolts and the plate-to-column weld.

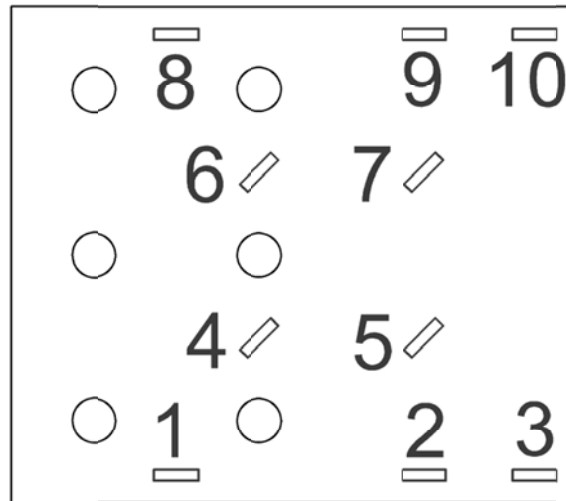


Figure D-27: Strain Gauge Layout, Configuration 3



Figure D-28: Yielded Shear Tab, Configuration 3

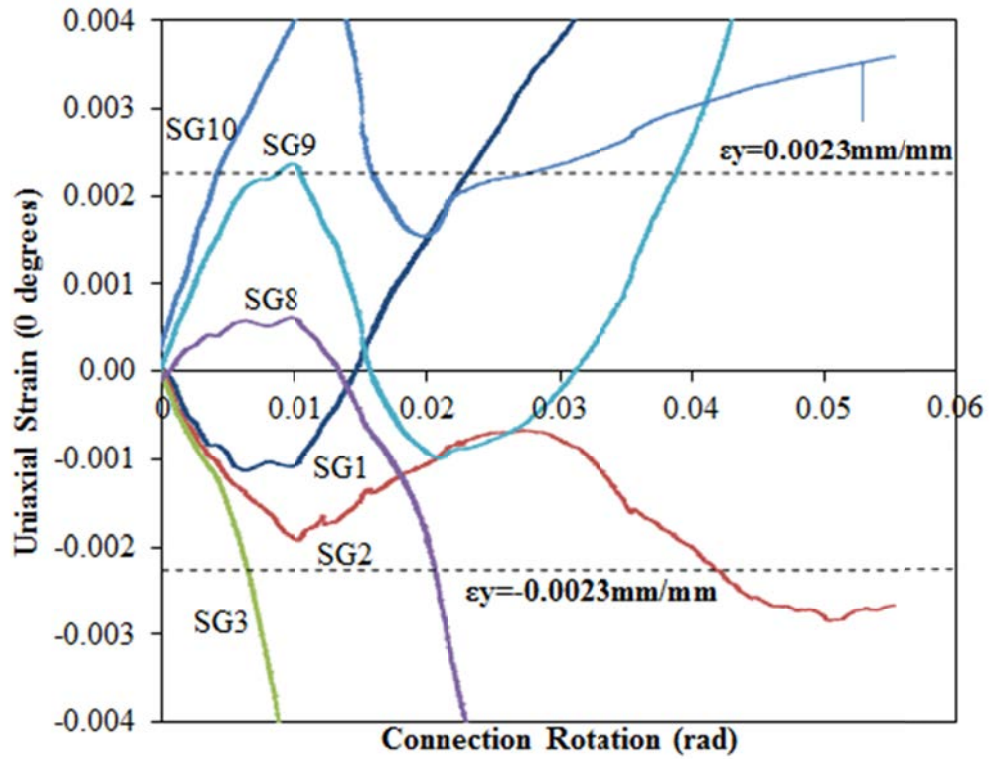


Figure D-29: Uniaxial Strain (0°) vs. Connection Rotation, Configuration 3

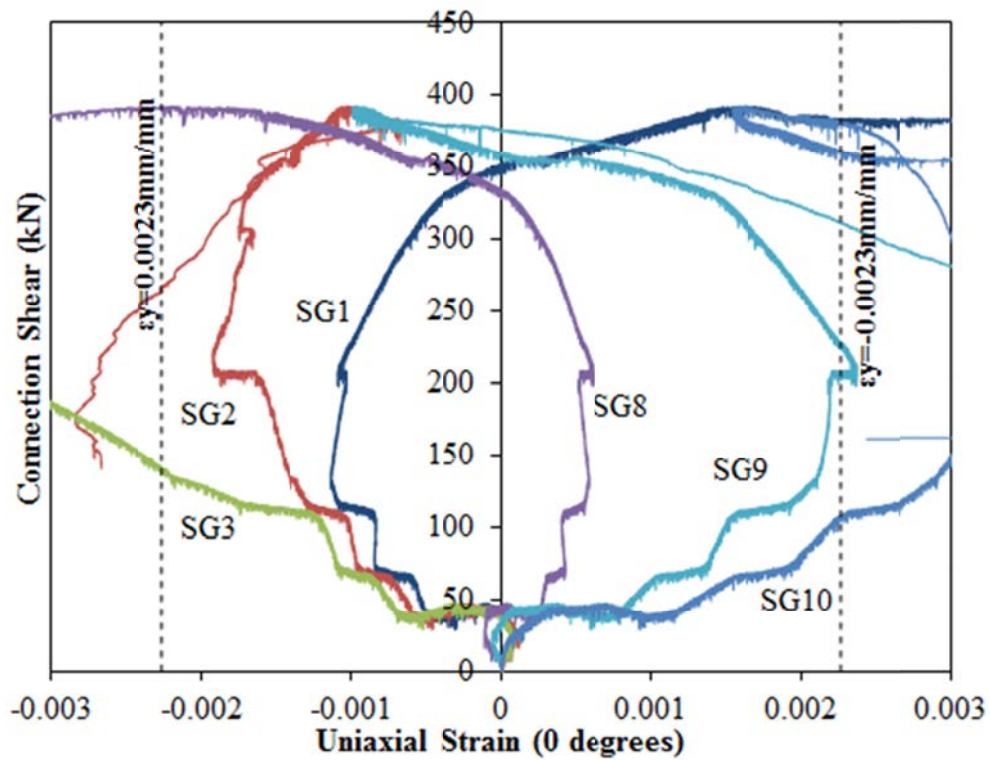


Figure D-30: Connection Shear vs. Uniaxial Strain (0°), Configuration 3

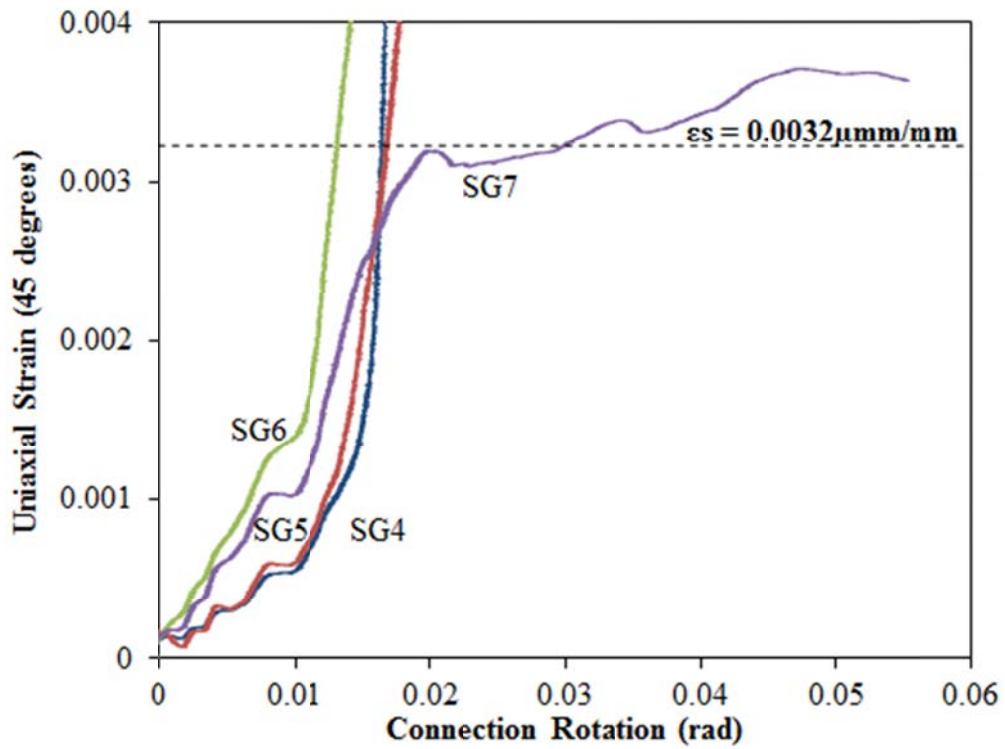


Figure D-31: Uniaxial Strain (45°) vs. Connection Rotation, Configuration 3

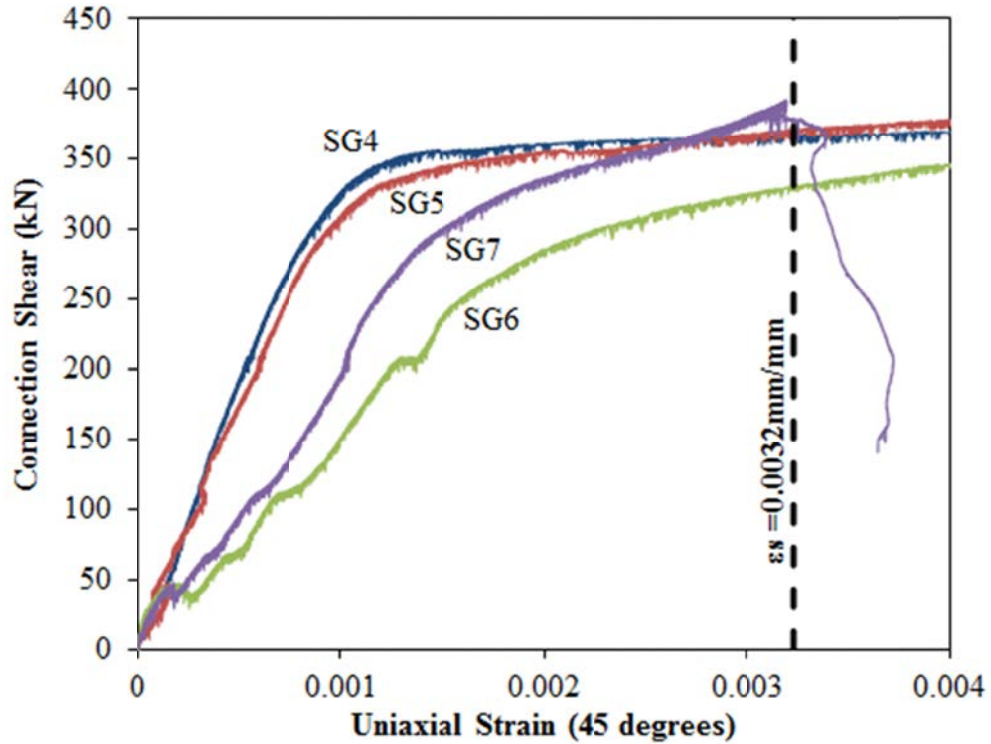


Figure D-32: Connection Shear vs. Uniaxial Strain (45°), Configuration 3

Weld Tearing: Partial “C” Weld

The connection resistance decreased rapidly after 0.034 radians (as seen on the Shear-Rotation curve; Rotation History). This could be due to the outward bending of the top edge of the tab causing the partial “C” weld to tear. LDVTs were placed along the unsupported top edge of the shear tab as seen in Figure D-33. The out of plane displacement versus rotation can be seen in Figure D-34 for LVDT2 and LVDT4. Between 0.03 and 0.04 radians there is a dramatic increase in displacement rate and this is explained by this out of plane bending of the shear tab. Figure D-35 shows this gap at the end of the test.

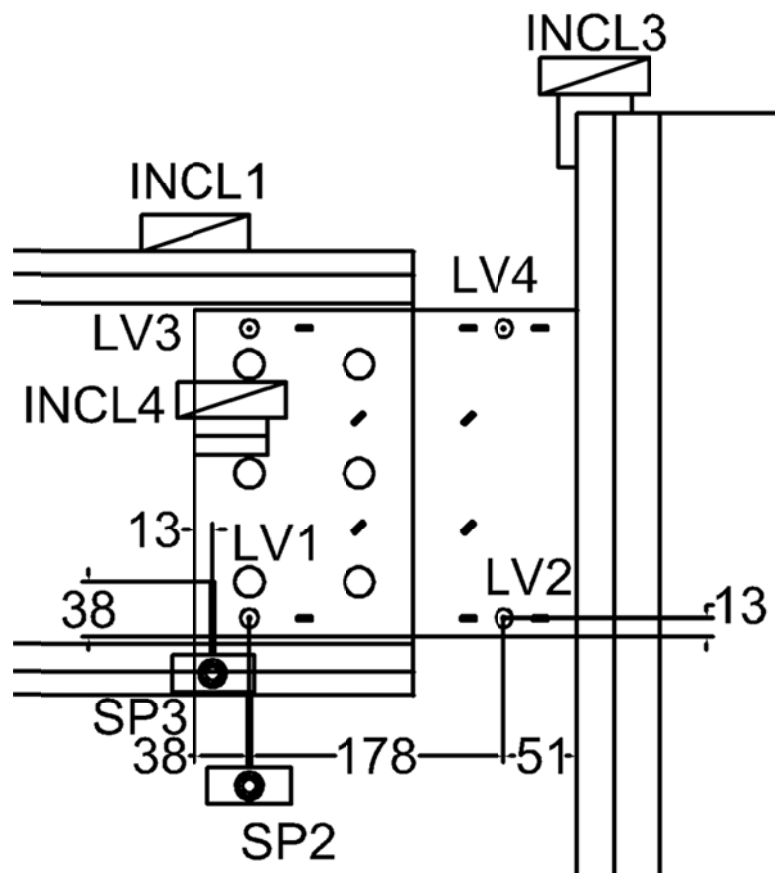


Figure D-33: Out of Plane LVDT Details, Configuration 3

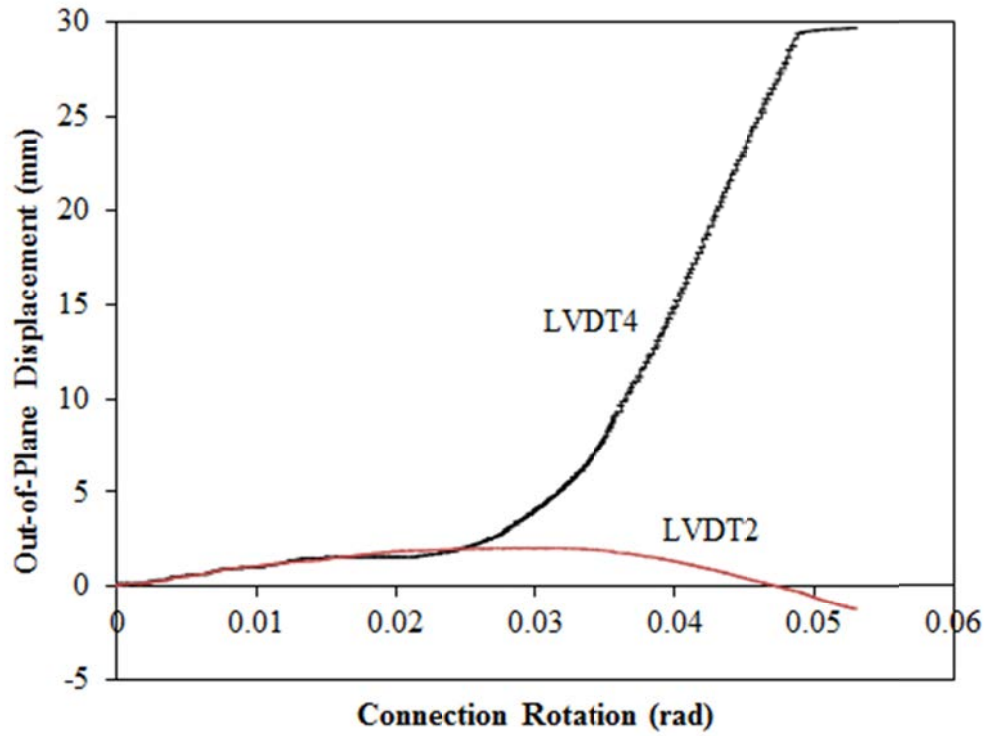


Figure 34: Out of Plane Shear Tab Movement vs. Rotation, Configuration 3



Figure D-35: Separation of Shear Tab from Beam Web, End of Test, Configuration 3

Weld Tearing: Shear Tab to Column

Significant weld tearing was observed over the course of the test and eventually tore by approximately half of the plate height. The decrease in connection shear after 0.02 radians is could be due to the extent of weld tearing limiting the connection resistance. Figure D-36 shows the extent of the tear at the end of the test.

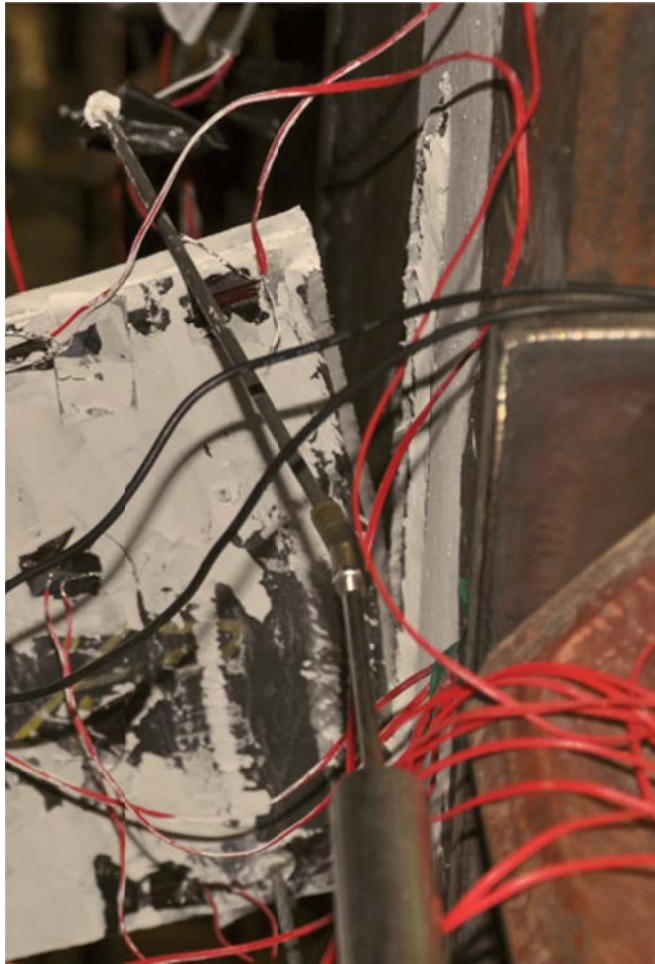


Figure D-36: Weld Tearing at End of Test, Configuration 3

EXTENDED SHEAR TAB CONNECTION EXPERIMENTAL STUDY

TEST SUMMARY OF CONFIGURATION 4

Specimen ID	CONFIGURATION 4
Key Words	Shear Tab, Extended Configuration; Rigid Support Condition; Beam to Column;
Test Location	Structures Lab, Macdonald Engineering Building, McGill University
Test Date	May 14, 2013
Investigators	Colin A. Rogers, Dimitrios G. Lignos, Jacob W. Hertz
Main References	AISC Steel Construction Manual, 13th & 14th Editions; CISC Handbook of Steel Construction, 10th Edition
Sponsors	ADF Group Inc., DPHV and NSERC

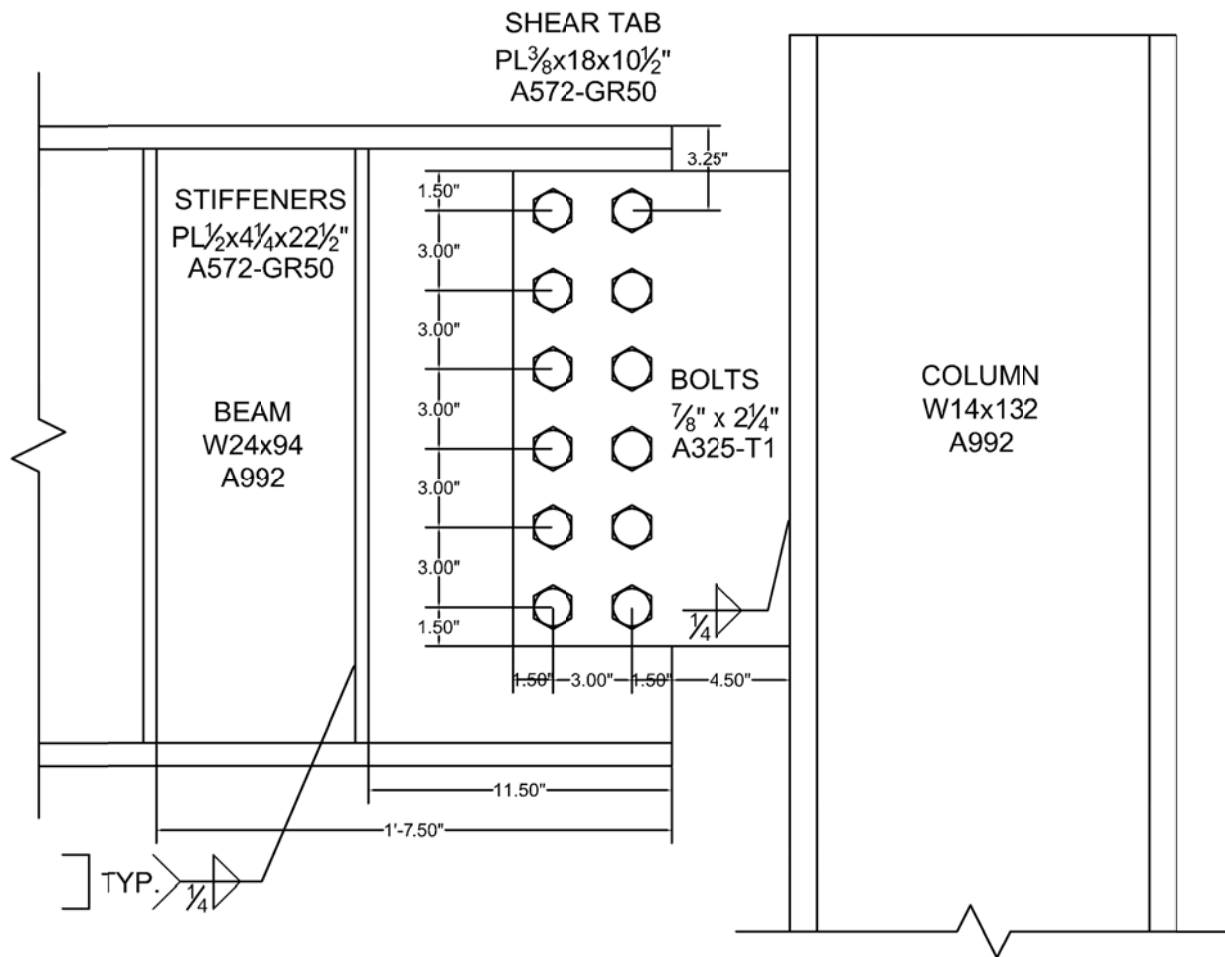


Figure D-37: Connection Details, Configuration 4

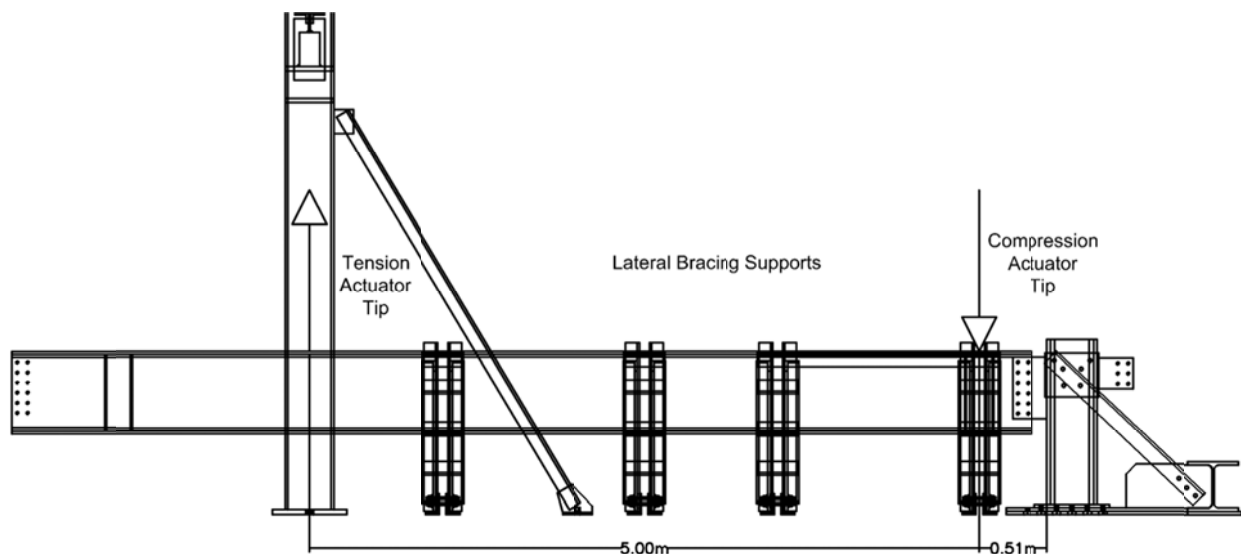
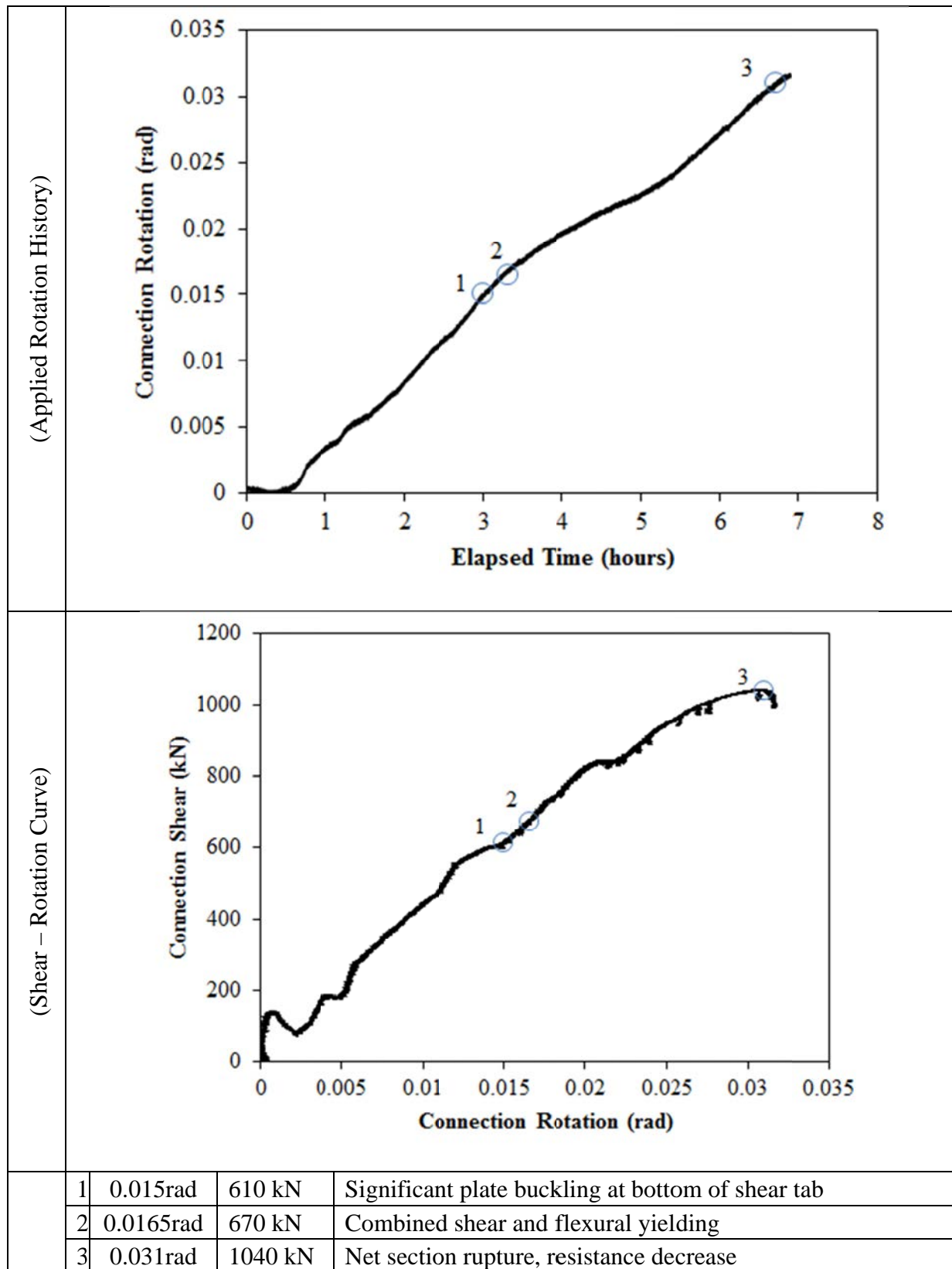


Figure D-38: Test Setup, Configuration 4

MATERIAL PROPERTIES AND SPECIMEN DETAILS

Member	Size	Grade	Yield Stress (MPa)		Ultimate Stress (MPa)	
			Mill Cert.	Coupon	Mill Cert.	Coupon
Beam	W24x94	A992	383	Flange:390 Web:448	507	Flange:513 Web:539
Beam Stiffeners	PL1/2"x4 1/4"	A572-GR50	-	-	-	-
Column	W14x132	A992	398	-	519	-
Shear Tab	PL3/8"x18"	A572-GR50	452	456	531	525
Bolts	7/8" x 2 1/4"	A325-T1	6 rows of 2 bolts; 3" spacing, 1 1/2" end distance; snug tight; one washer per bolt; 15/16" bolt holes;			
Welding Procedure Specification	Electrode Classification E70					
	Welding Procedure <i>Shop Welding:</i> FCAW-G (flux-cored arc welding with gas shielding) <ul style="list-style-type: none">Fillet Weld, Shear Tab to Column"C" Weld, Beam Stiffeners					
Boundary Condition	Tension Actuator Capacity: 268kN tension, 495kN compression; Stroke: 254mm; Displacement controlled					
	Compressive Actuator Capacity: 8018 kN tension, 11414kN compression; Stroke: 305mm; Displacement controlled					
	Lateral Bracing System Top and bottom flange out of plane movement restrained by ball and socket rods fixed to frame tensioned to strong floor					

ROTATION HISTORY AND KEY EXPERIMENTAL OBSERVATIONS



Note: The stiffness variation seen during the first 0.005 radians of rotation is due to adjustment of the displacement rates of both tension and compression actuators to achieve the desired stiffness. Once this stiffness value was reached, the ratio of rates was held constant for the remainder of the test.

RESISTANCE SUMMARY

Limit State	Design Check	Predicted	Observed
Net Section Rupture	AISC Manual, 14 th Ed; Section J4; Equation J4-4	915 kN	1040 kN
Plate Buckling	AISC Manual, 14 th Ed; Part 9; Q Equation	987 kN	610 kN
Combined Shear and Flexural Yielding	AISC Manual, 14 th Ed; Part 10; Equation 10-5	931 kN	670 kN

TEST OBSERVATIONS

Combined Shear and Flexural Yielding

Deformation within the tab was monitored using a combination of horizontal and inclined strain gauges organized as seen in Figure D-39. White wash was applied to the tab such that the yielding pattern could be observed. The face of the shear tab at the end of test can be seen in Figure D-40.

Horizontal strain gauges were placed on the top and bottom edges of the tab to record flexural strains and the results can be seen in Figure D-40 and D-41. Tension yielding was observed in the top of the tab, closest to the weld (SG16) at 0.007 radian rotation. Similarly, compressive yielding was observed at 0.01 radians on the bottom edge of the tab (SG3). Strain gauges outside the first line of bolts (SG14 and SG1) saw small flexural stresses. This was due to deformation primarily occurring between the bolts and weld line. Note, SG14 yielded in compression at 0.028 radians as a result of the weld failure quickly propagating and a compressive field forming between the top two rows of bolts. SG15 fluctuated between compression and tension due to weld tearing, ultimately yielding in tension. SG2 was located on the portion of the shear tab that buckled locally. Once buckling occurred, these strain values rapidly increased and became meaningless. The onset of flexural yielding (where the whole plate begins to undergo flexural plastic deformation at the extreme fibres) occurred at 0.01 radians.

Strain gauges oriented to 45° were placed along the height of the tab to measure shear strains and the results can be seen in Figure D-42 and D-43. Shear yielding can be seen first at 0.012 radians (SG7). The whole plate experiences shear yielding after 0.0165 radians (yielding of SG12). Note, SG13 is not seen to be consistent with the other gauges. SG13 is seen to stabilize after 0.005 and 0.02 radians. This is due to reduction in deformation at the top corner of the tab while the weld failure propagates.

Combined shear and flexural yielding is assumed to occur at a rotation of 0.0165 radians

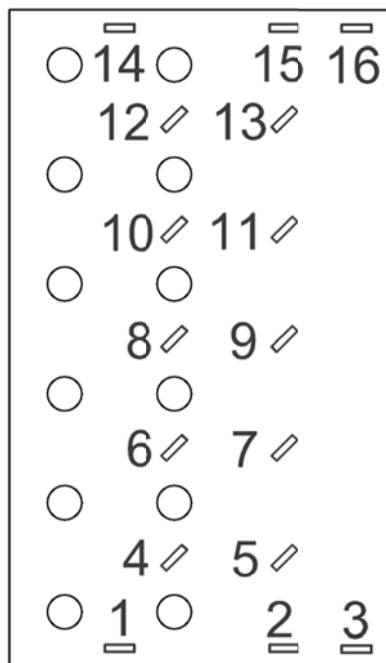


Figure D-39: Strain Gauge Layout, Configuration 4



Figure D-40: Yielded Shear Tab, Configuration 4

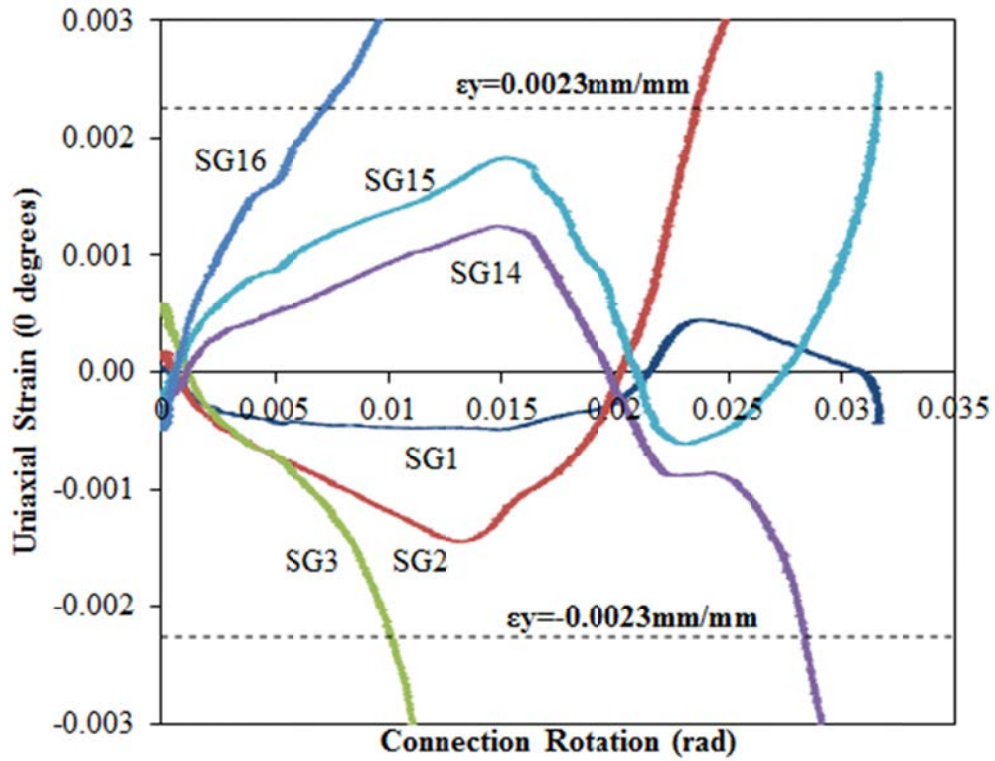


Figure D-41: Uniaxial Strain (0°) vs. Connection Rotation, Configuration 4

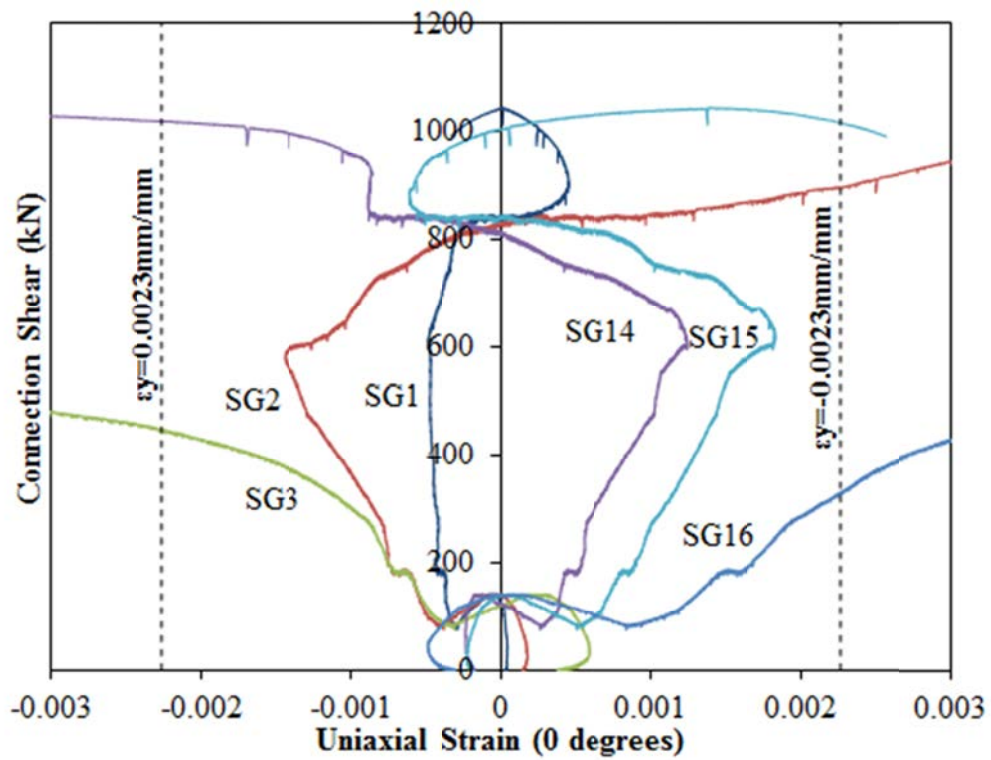


Figure D-42: Connection Shear vs. Uniaxial Strain (0°), Configuration 4

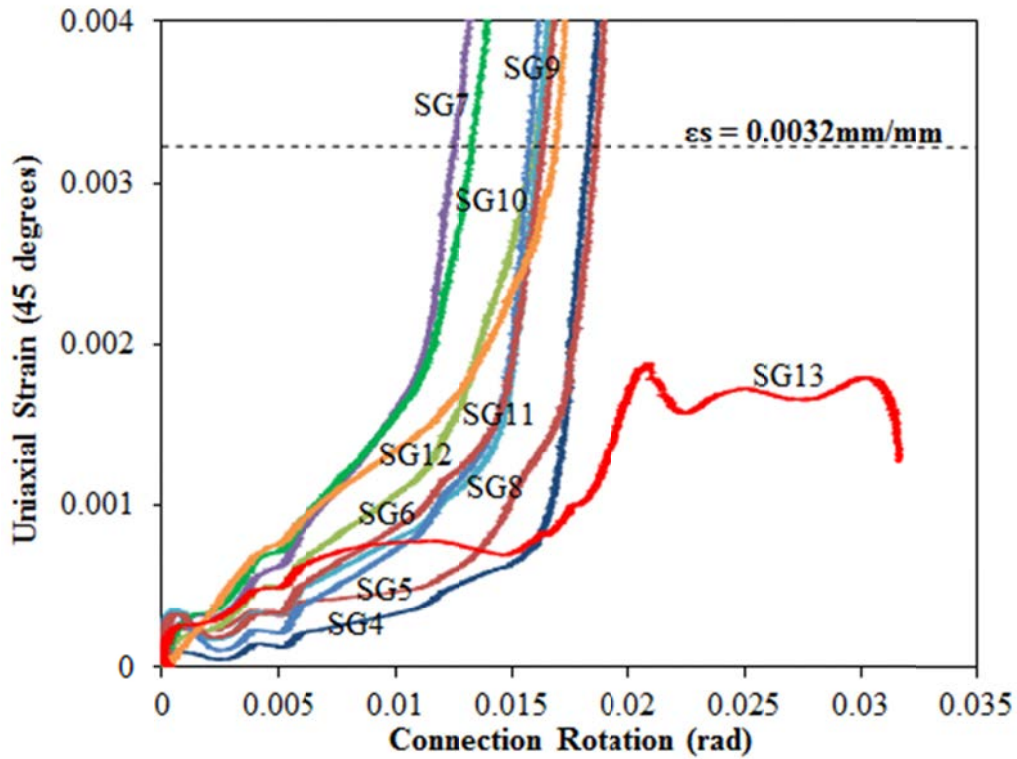


Figure D-43: Uniaxial Strain (45°) vs. Connection Rotation, Configuration 4

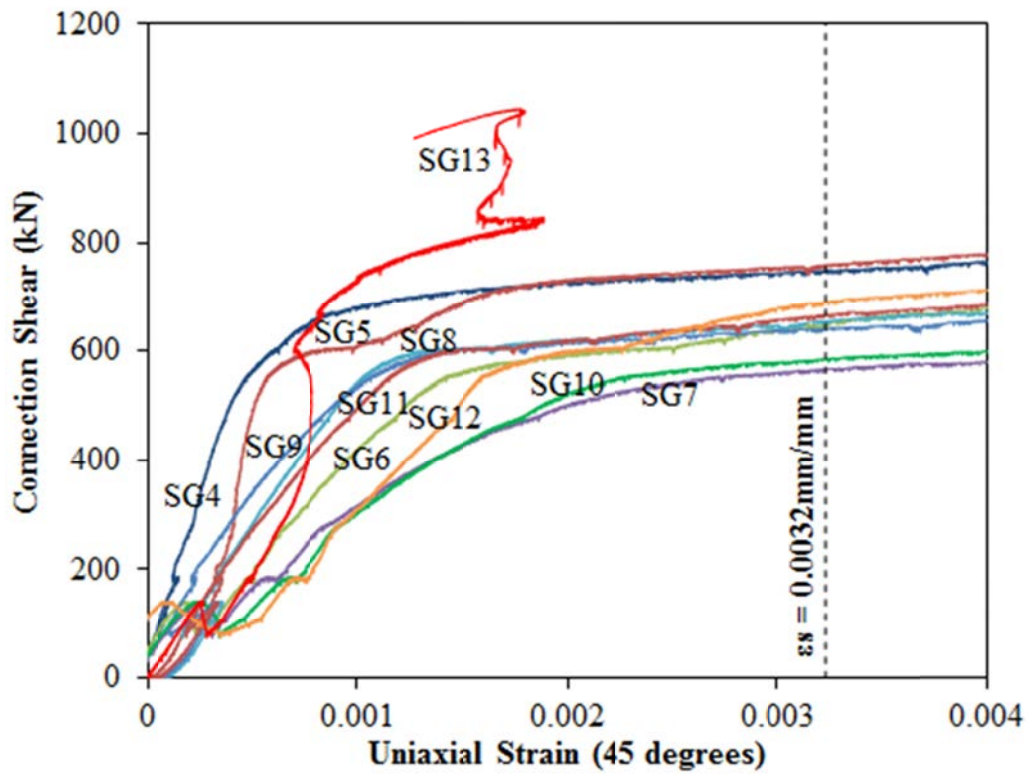


Figure D-44: Connection Shear vs. Uniaxial Strain (45°), Configuration 4

Plate Buckling

The unsupported edge of the shear tab plate between the bottommost bolts and the weld line was seen to buckle out of plane. This failure is due to high compressive stresses resulting from flexure along the plate. LVDTs were placed along the top and bottom edges of the tab to measure out of plane deformation as seen in Figure D-45. The onset of buckling can be seen between 0.01 and 0.015 radians in Figure D-46. On the Shear Rotation curve (see Rotation History), a sudden increase in stiffness can be seen and this is most likely due to the sharp increase in strength required to begin buckling of the plate. Once buckling occurred, the stiffness decreased temporarily and then resumed to the initial rate.

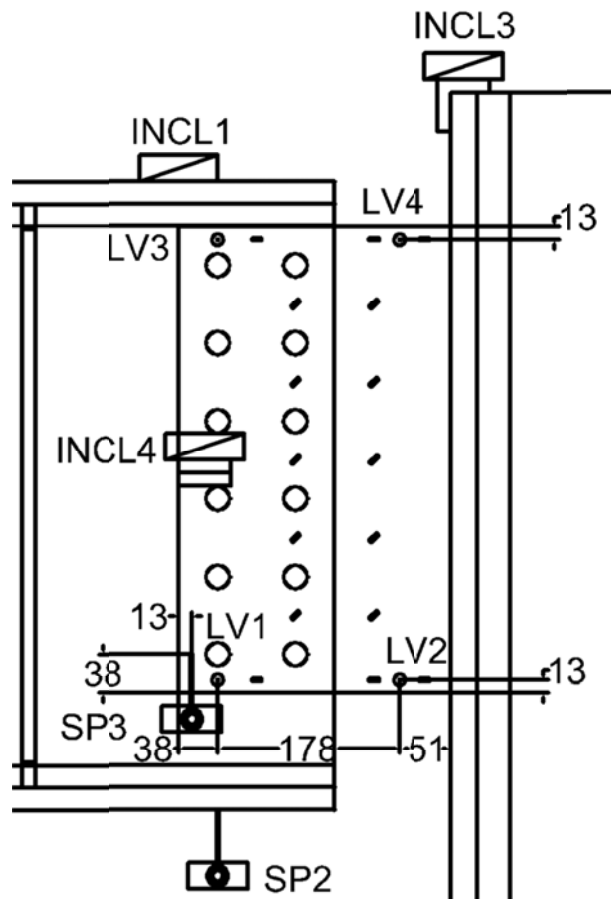


Figure D-45: Out of Plane LVDT Layout, Configuration 4

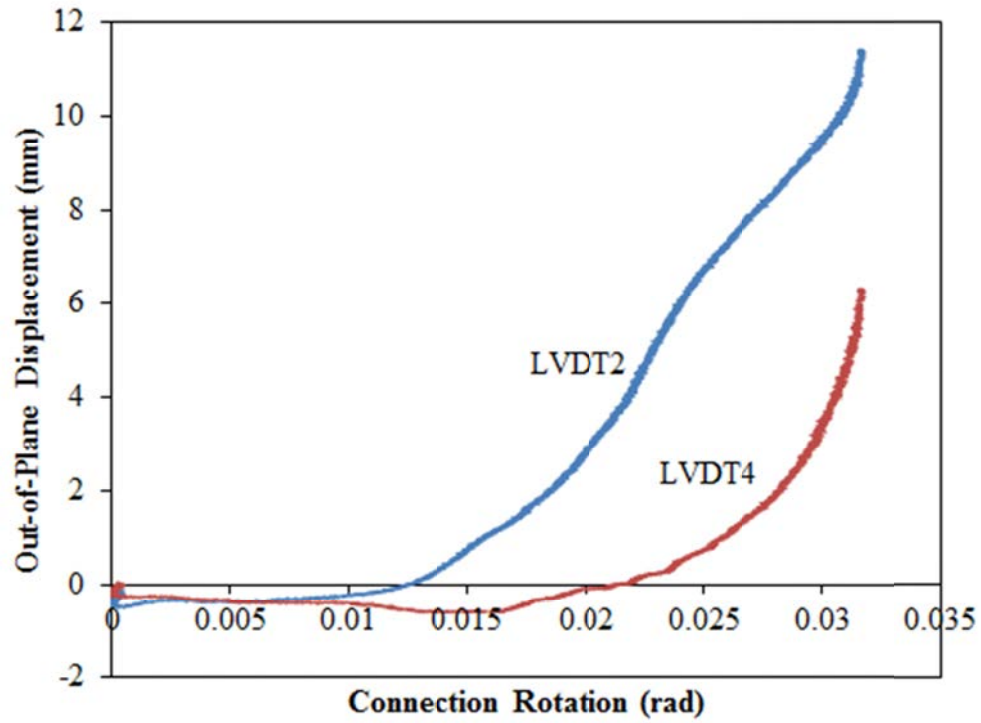


Figure D-46: Out of Plane Displacement of Shear Tab vs. Rotation, Configuration 4



Figure D-47: Buckled Shear Tab, End of Test (photo from below beam), Configuration 4

Weld Tearing

Flexural tearing of the weld was seen during the test. The final extent of weld tearing can be seen in Figure D-48.



Figure D-48: Weld Tearing, End of Test, Configuration 4

Net Section Rupture

The test was stopped when rapid strength loss was observed. After removing the bolts, it was clear that a shear plane had formed along the line of bolts closest to the weldment. The measured ultimate resistance was 1040kN at a rotation. Figure D-49 illustrates shear cracking under the bolt holes with a full fracture between the lowest bolt and the tab edge. Note, large bearing type deformations can be seen on the bolt holes.

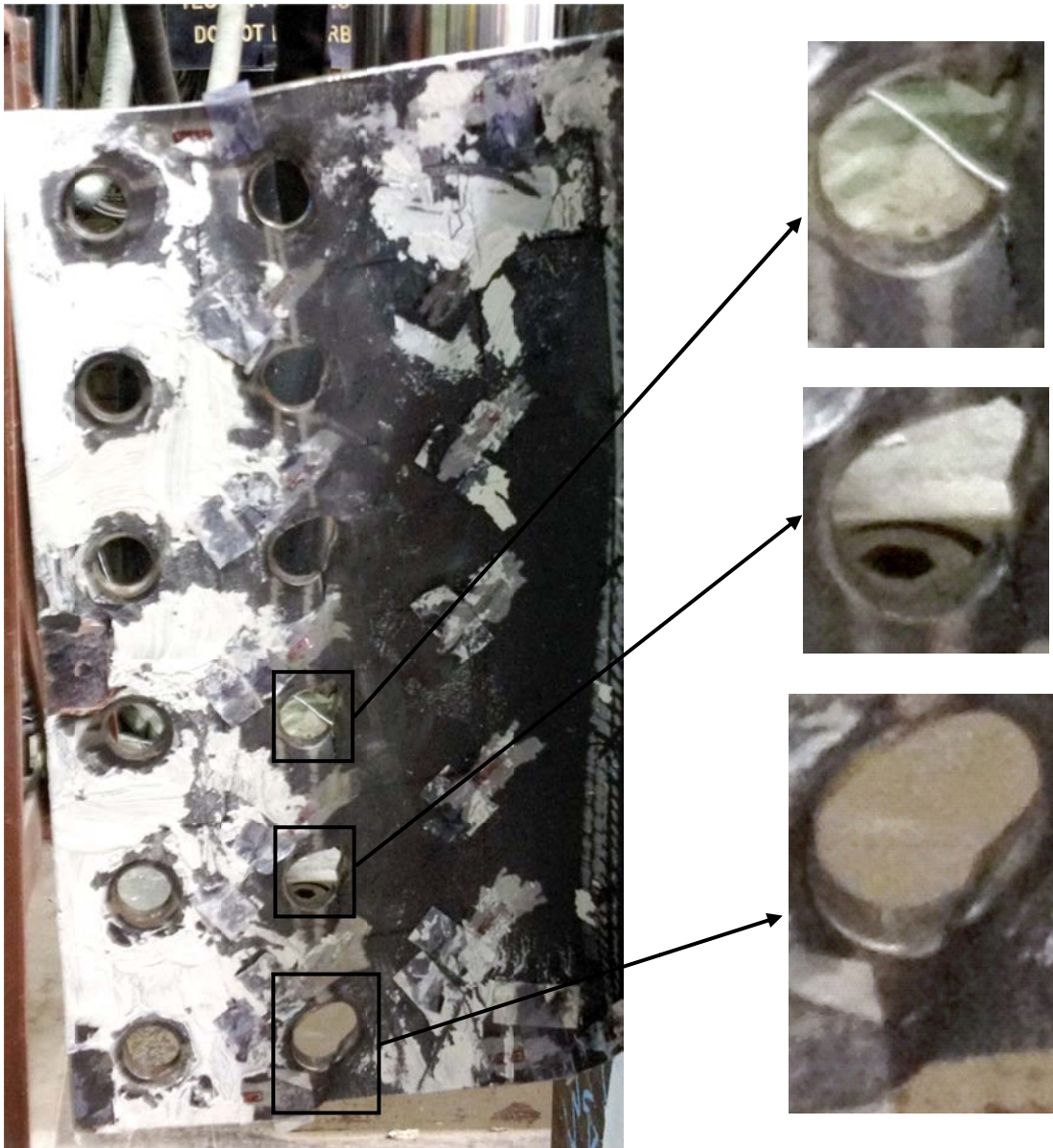


Figure D-49: Net Section Rupture Details, Configuration 4

EXTENDED SHEAR TAB CONNECTION EXPERIMENTAL STUDY

TEST SUMMARY OF CONFIGURATION 5

Specimen ID	CONFIGURATION 5
Key Words	Shear Tab, Extended Configuration; Flexible Support Condition; Beam to Girder;
Test Location	Structures Lab, Macdonald Engineering Building, McGill University
Test Date	May 31, 2013
Investigators	Colin A. Rogers, Dimitrios G. Lignos, Jacob W. Hertz
Main References	AISC Steel Construction Manual, 13th & 14th Editions; CISC Handbook of Steel Construction, 10th Edition
Sponsors	ADF Group Inc., DPHV and NSERC

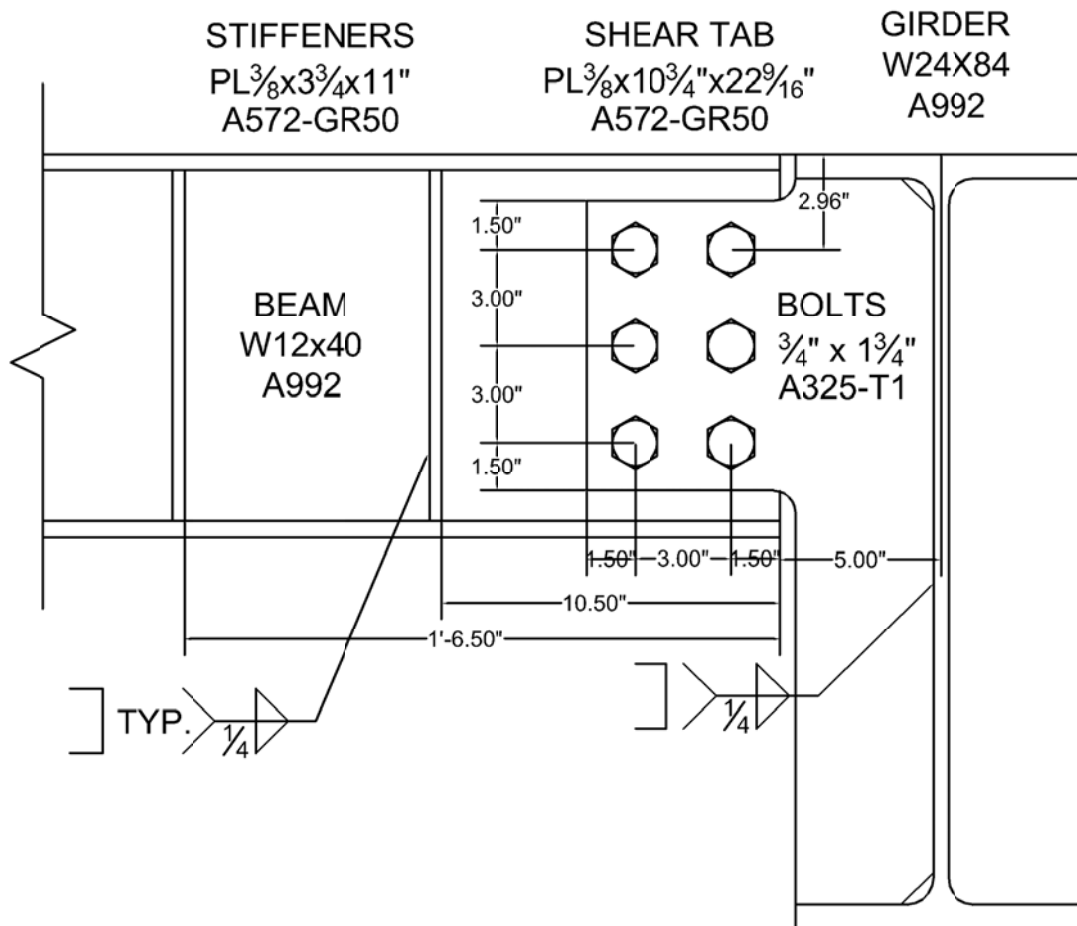


Figure D-50: Connection Details, Configuration 5

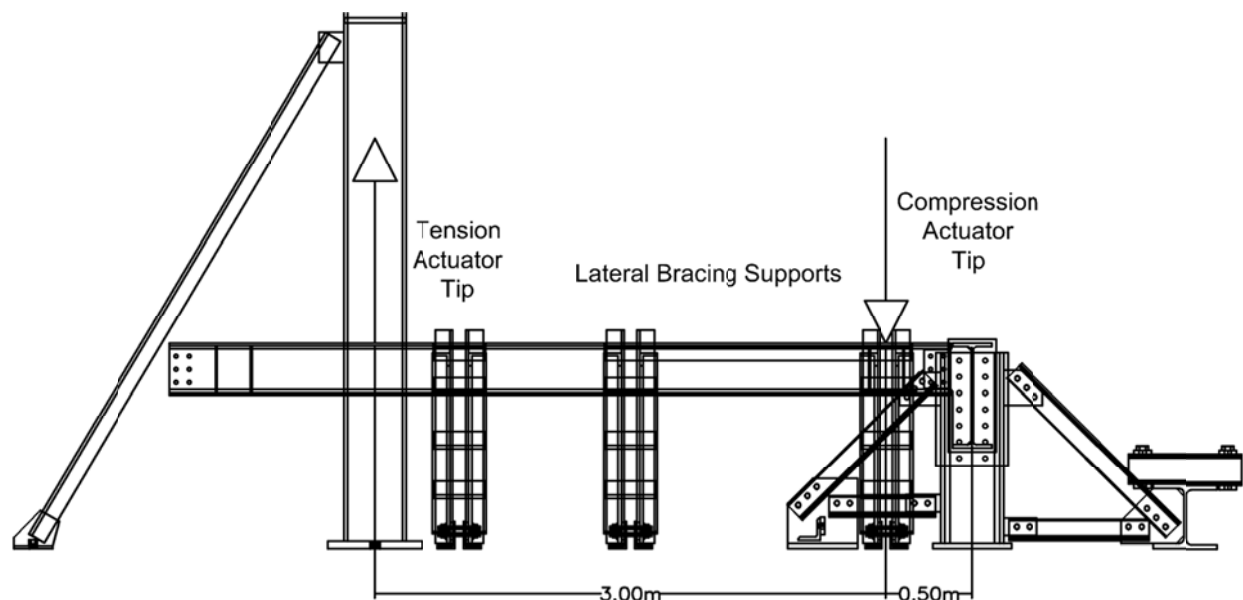
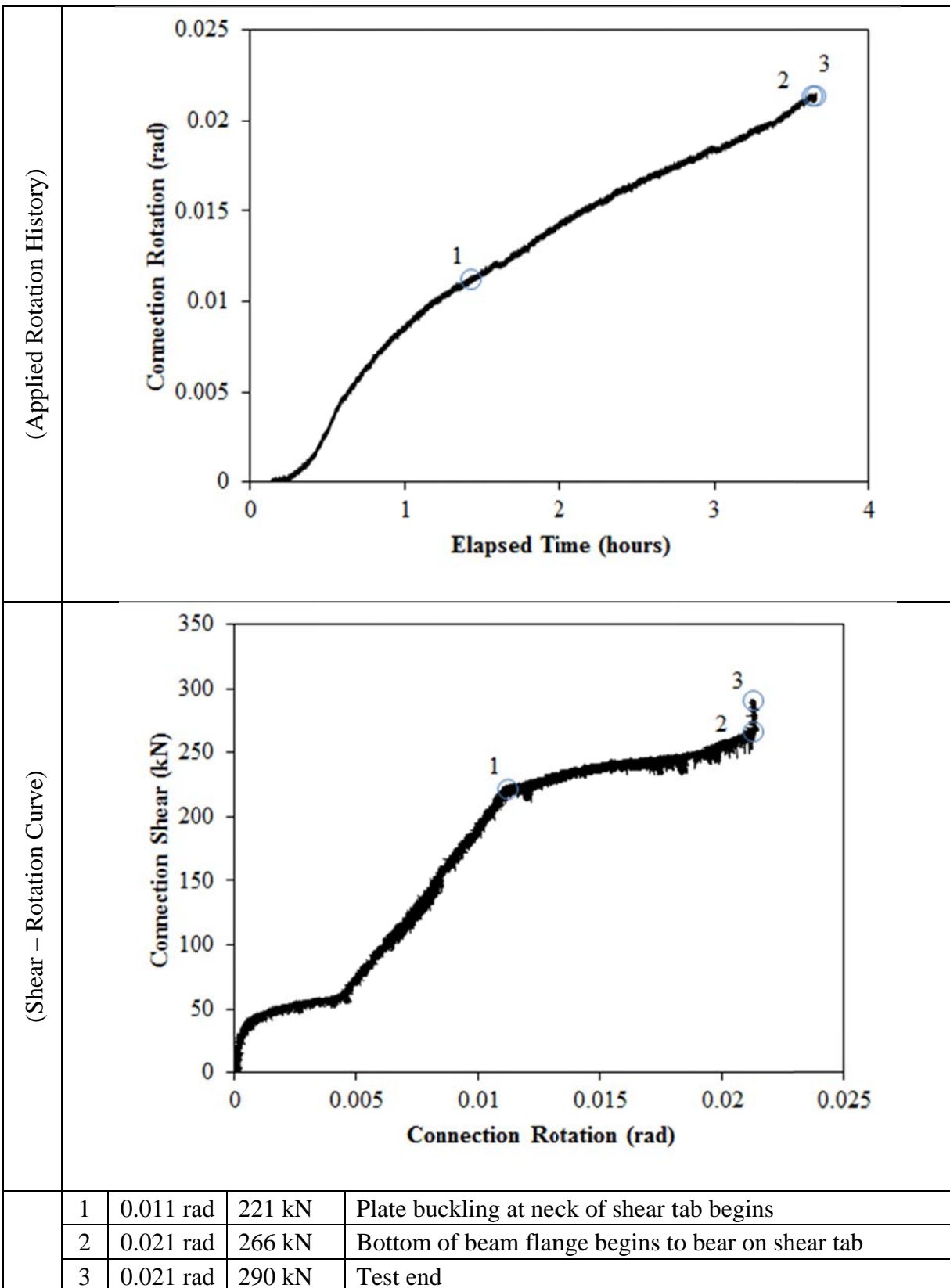


Figure D-51: Test Setup, Configuration 5

MATERIAL PROPERTIES AND SPECIMEN DETAILS

Member	Size	Grade	Yield Stress (MPa)		Ultimate Stress (MPa)	
			Mill Cert.	Coupon	Mill Cert.	Coupon
Beam	W12x40	A992	367	Flange:376 Web:414	485	Flange:492 Web:511
Beam Stiffeners	PL3/8"x3 3/4"	A572-GR50	-	-	-	-
Girder	W24x84	A992	387	-	498	-
Shear Tab	PL3/8"x10 3/4"	A572-GR50	452	456	531	525
Bolts	3/4" x 1 3/4"	A325-T1	3 rows of 2 bolts; 3" spacing, 1 1/2" end distance; snug tight; one washer per bolt; 13/16" bolt holes;			
Welding Procedure Specification	Electrode Classification E70					
	Welding Procedure <i>Shop Welding:</i> FCAW-G (flux-cored arc welding with gas shielding) <ul style="list-style-type: none">Fillet Weld, Shear Tab to Girder"C" Weld, Beam Stiffeners					
Boundary Condition	Tension Actuator Capacity: 268kN tension, 495kN compression; Stroke: 254mm; Displacement controlled					
	Compressive Actuator Capacity: 8018 kN tension, 11414kN compression; Stroke: 305mm; Displacement controlled					
	Lateral Bracing System Top and bottom flange out of plane movement restrained by ball and socket rods fixed to frame tensioned to strong floor					

ROTATION HISTORY AND KEY EXPERIMENTAL OBSERVATIONS



Note: The variation in stiffness seen during the first 0.01 radians of rotation is due to adjustment of the displacement rates of both tension and compression actuators to achieve the desired stiffness. Once this stiffness value was reached, the ratio of rates was held constant for the remainder of the test.

RESISTANCE SUMMARY

Limit State	Design Check	Predicted	Observed
Plate Buckling (Biaxial)	-	-	266 kN
Combined Shear and Flexural Yielding	AISC Manual, 14 th Ed; Part 10; Equation 10-5	298 kN	-

TEST OBSERVATIONS

Plate Buckling (Biaxial)

The portion on the shear tab to the bottom right of the bolt group (see Figure D-50) buckled outwards during the test. An LVDT (see Figure D-52) placed at this region measured a sharp increase in the out-of-plane displacement rate at approximately 0.01 radians (see Figure D-53). The stiffness dropped dramatically after 0.011 radians (see Shear Rotation Curve, Rotation History) and this can be attributed to this plate buckling mechanism. Figure D-54 shows the buckled shear tab neck after the test.

The AISC Manual includes provisions for one-directional plate buckling of the unsupported shear tab length. For this configuration, this length would be less than 76mm so this limit state was ignored. The failure mode encountered is most likely the result of buckling along the bottom edge of the shear tab due to compressive forces from flexure on the tab in addition to shear forces acting thru the vertical edge of the tab under the neck.

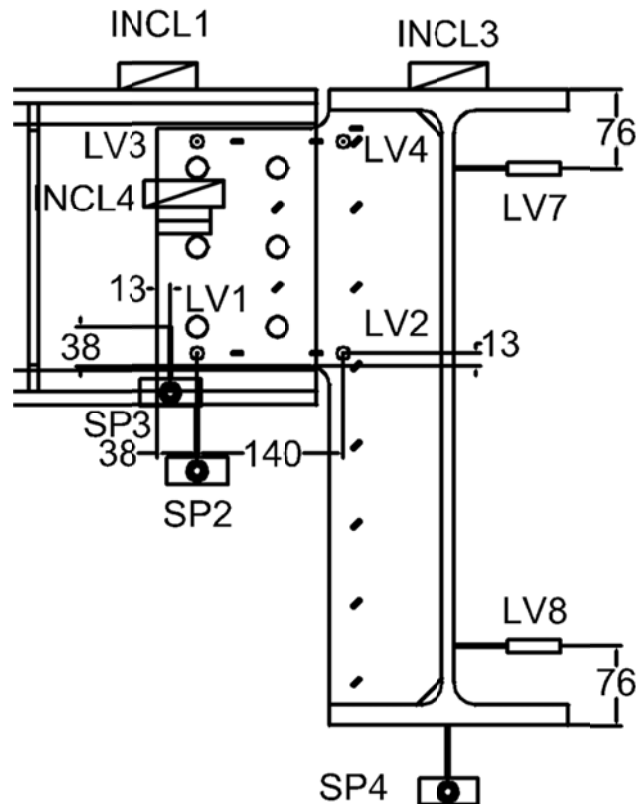


Figure D-52: Out of Plane LVDT Layout, Configuration 5

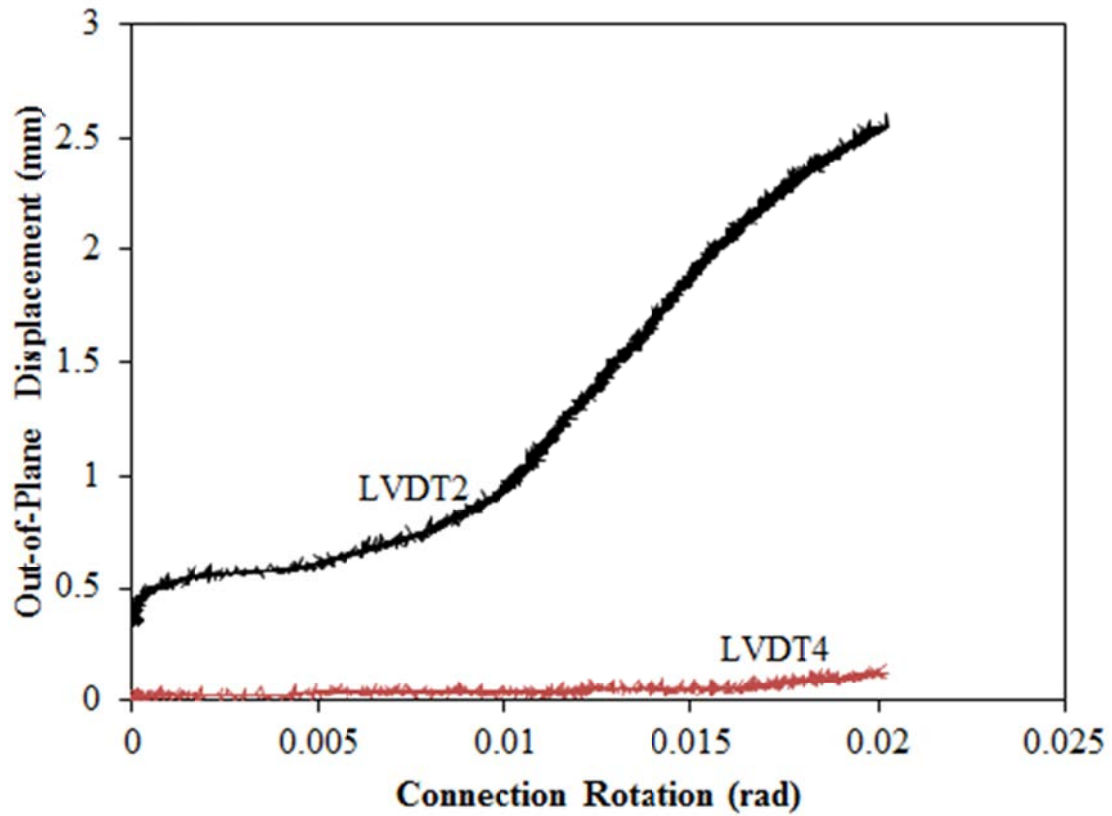


Figure D-53: Out-of-Plane Buckling Displacement vs. Rotation, Configuration 5



Figure D-54: Buckled Shear Tab Neck, Various Angles, Configuration 5

Combined Shear and Flexural Yielding

Deformation within the tab was monitored using a combination of horizontal and inclined strain gauges organized as seen in Figure D-55. White wash was applied to the tab such that the yielding pattern could be observed. The face of the shear tab at the end of test can be seen in Figure D-56.

Horizontal strain gauges were placed on the top and bottom edges of the tab to record flexural strains and the results can be seen in Figure D-57 and D-58. Tension yielding was seen in the top of the shear tab at SG8 and SG14 at 0.008 and 0.0165 radians rotation. Compressive yielding was not seen at the bottom of the shear tab due to the plate buckling mechanism forming.

Strain gauges oriented to 45° were placed along the height of the tab to measure shear strains and the results can be seen in Figure D-59 and D-60. Shear yielding was seen at the locations of SG3 and SG4 at 0.014 radians. In Figure D-53, the rate of out-of-plane displacement decreases after approximately 0.014 radians. In the Shear-Rotation curve (see Rotation History), the stiffness decreases slightly after 0.015 radians. These two observations are most likely due to a combination of plate buckling and shear yielding in the neck region of the shear tab.

The predicted shear and flexural yielding is calculated under the assumption that the entire cross section of the shear tab ($3/8'' \times 9''$) undergoes shear and flexural yielding. For this case, the shear yielding is located solely in the shear tab neck and flexural yielding in the top of the tab. Therefore, this limit state does not govern for the connection resistance. A tension field formed in the web of the beam during the test and can clearly be seen in Figure D-62.

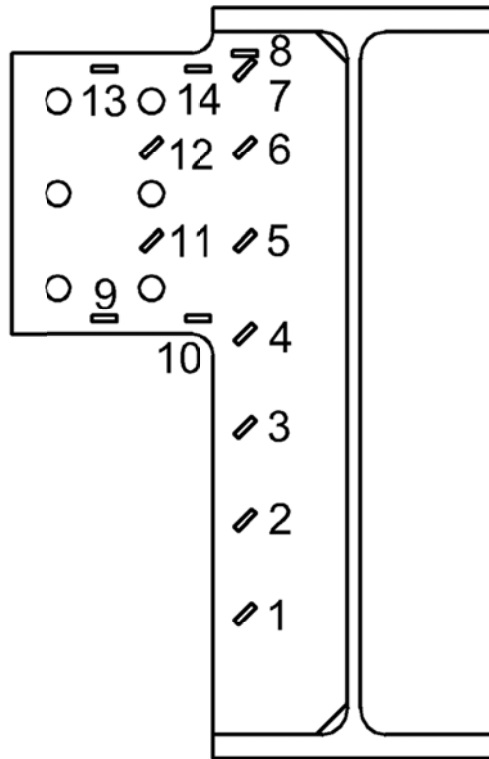


Figure D-55: Strain Gauge Layout, Configuration 5



Figure D-56: Deformed Shear Tab, End of Test, Configuration 5

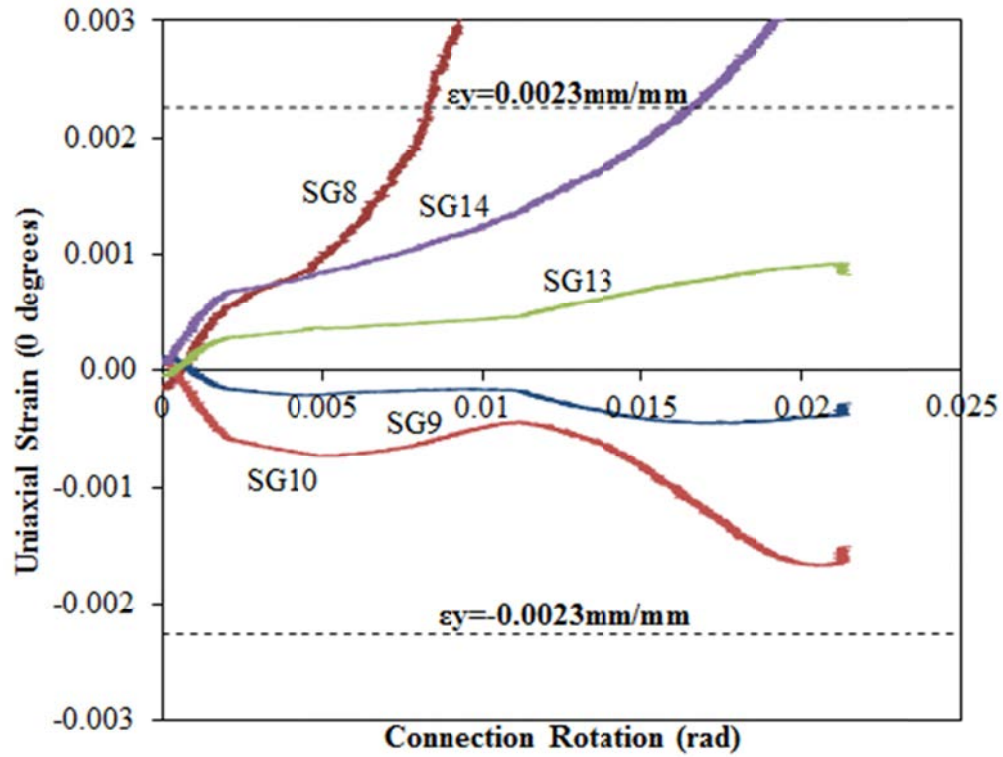


Figure D-57: Uniaxial Strain (0°) vs. Connection Rotation, Configuration 5

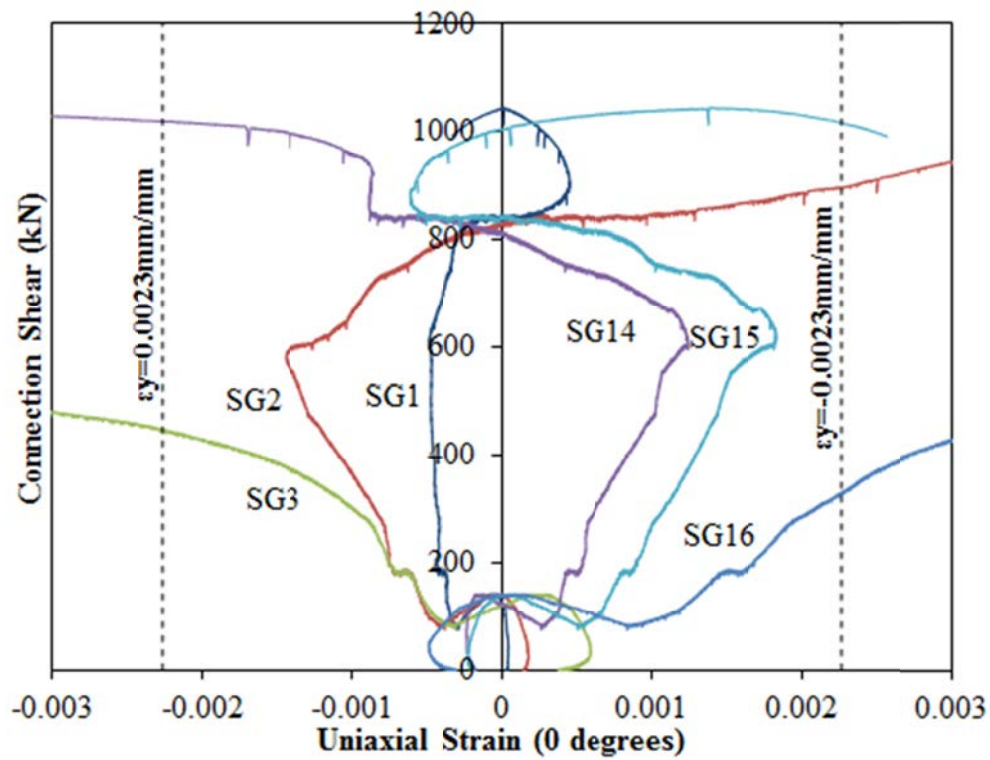


Figure D-58: Connection Shear vs. Uniaxial Strain (0°), Configuration 5

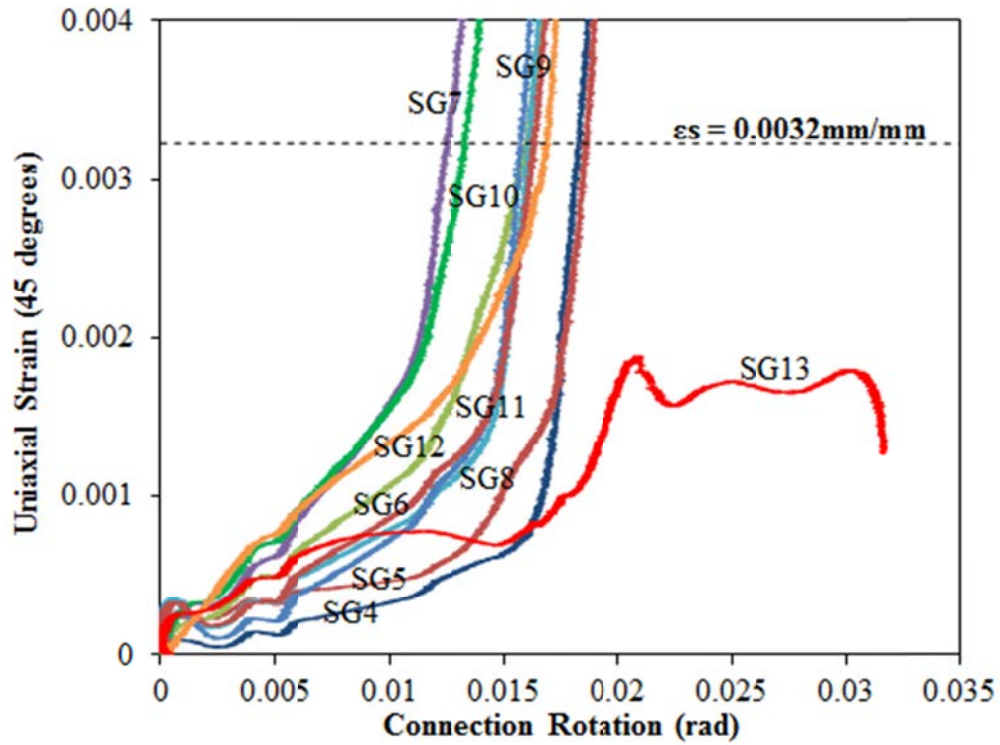


Figure D-59: Uniaxial Strain (45°) vs. Connection Rotation, Configuration 5

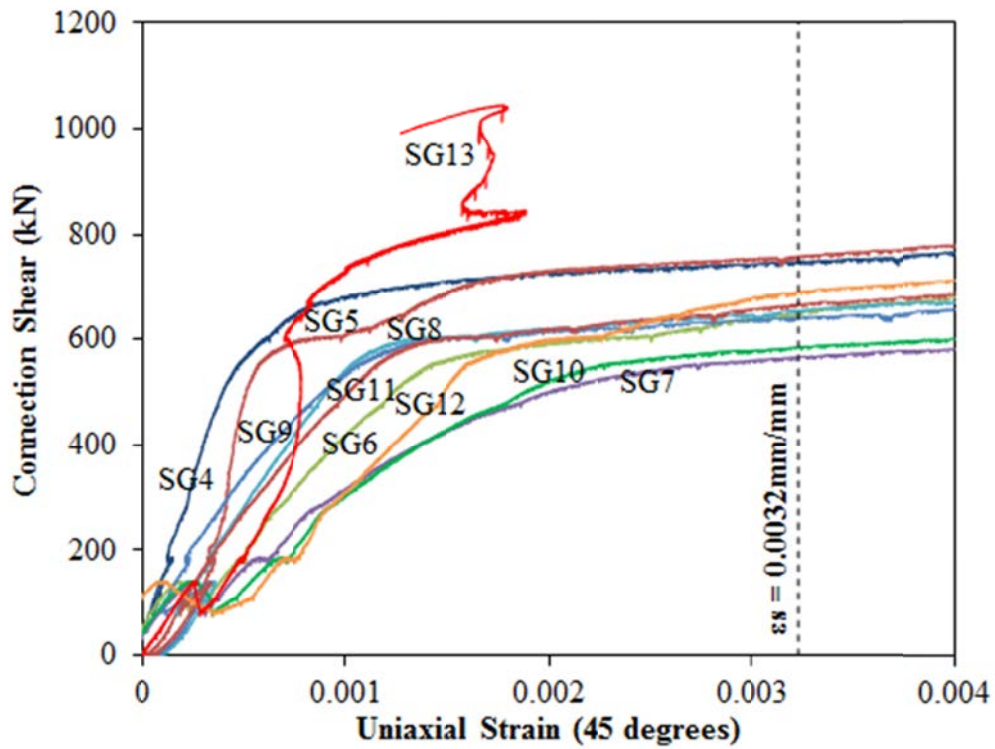


Figure D-60: Connection Shear vs. Uniaxial Strain (45°), Configuration 5

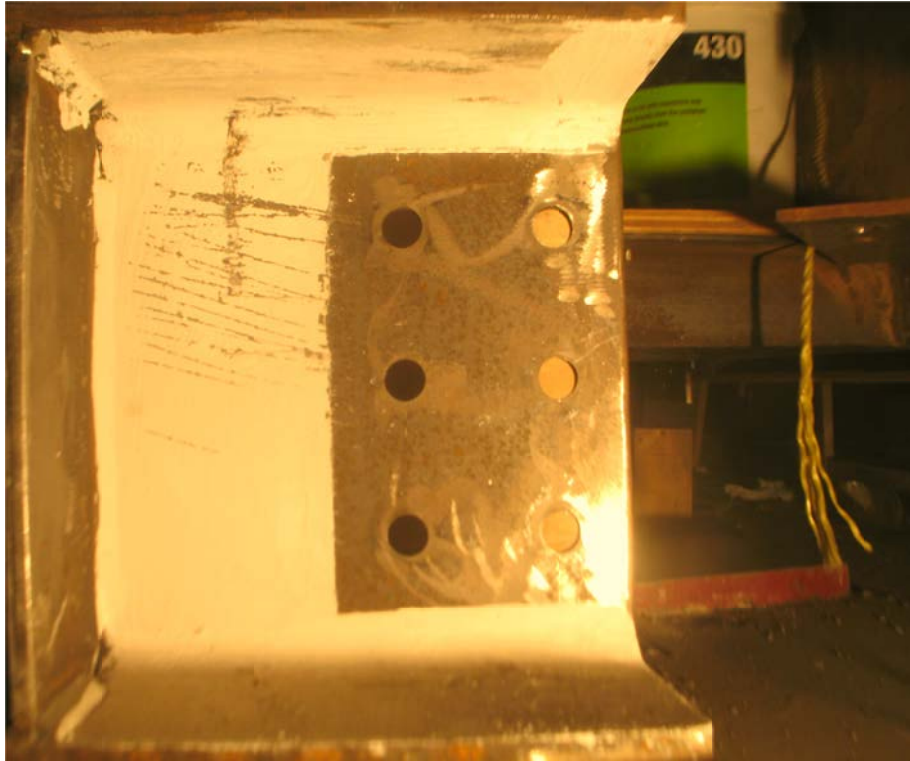


Figure D-61: Tension Field on Beam Web, End of Test, Configuration 5

EXTENDED SHEAR TAB CONNECTION EXPERIMENTAL STUDY

TEST SUMMARY OF CONFIGURATION 6

Specimen ID	CONFIGURATION 6
Key Words	Shear Tab, Extended Configuration; Flexible Support Condition; Beam to Girder;
Test Location	Structures Lab, Macdonald Engineering Building, McGill University
Test Date	June 5, 2013
Investigators	Colin A. Rogers, Dimitrios G. Lignos, Jacob W. Hertz
Main References	AISC Steel Construction Manual, 13th & 14th Editions; CISC Handbook of Steel Construction, 10th Edition
Sponsors	ADF Group Inc., DPHV and NSERC

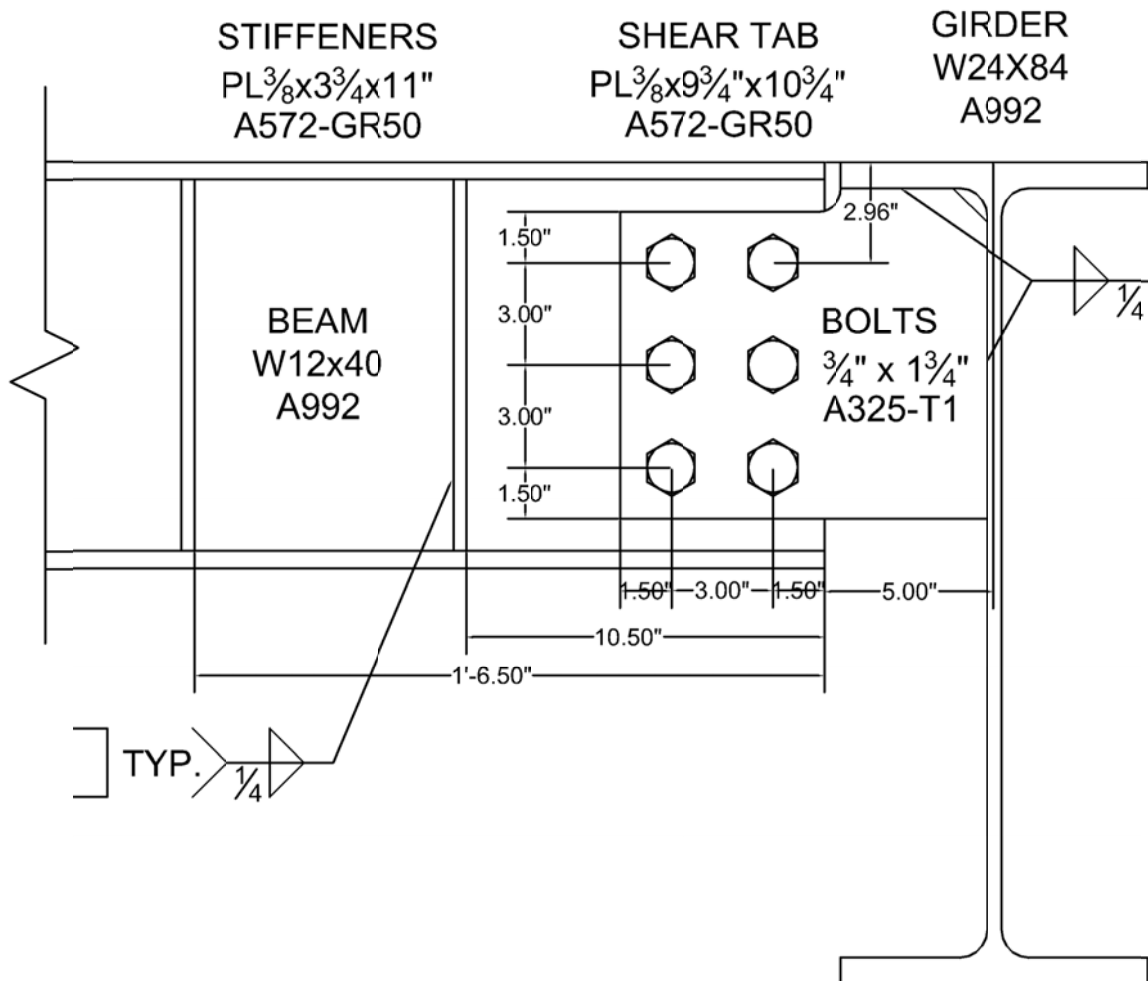


Figure D-62: Connection Details, Configuration 6

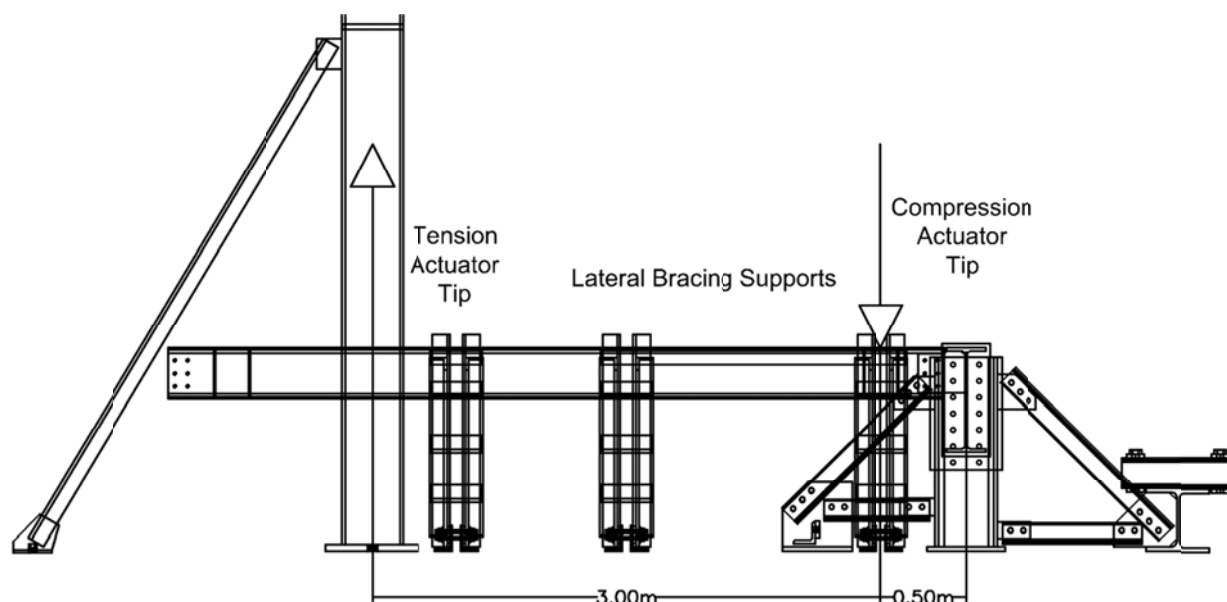
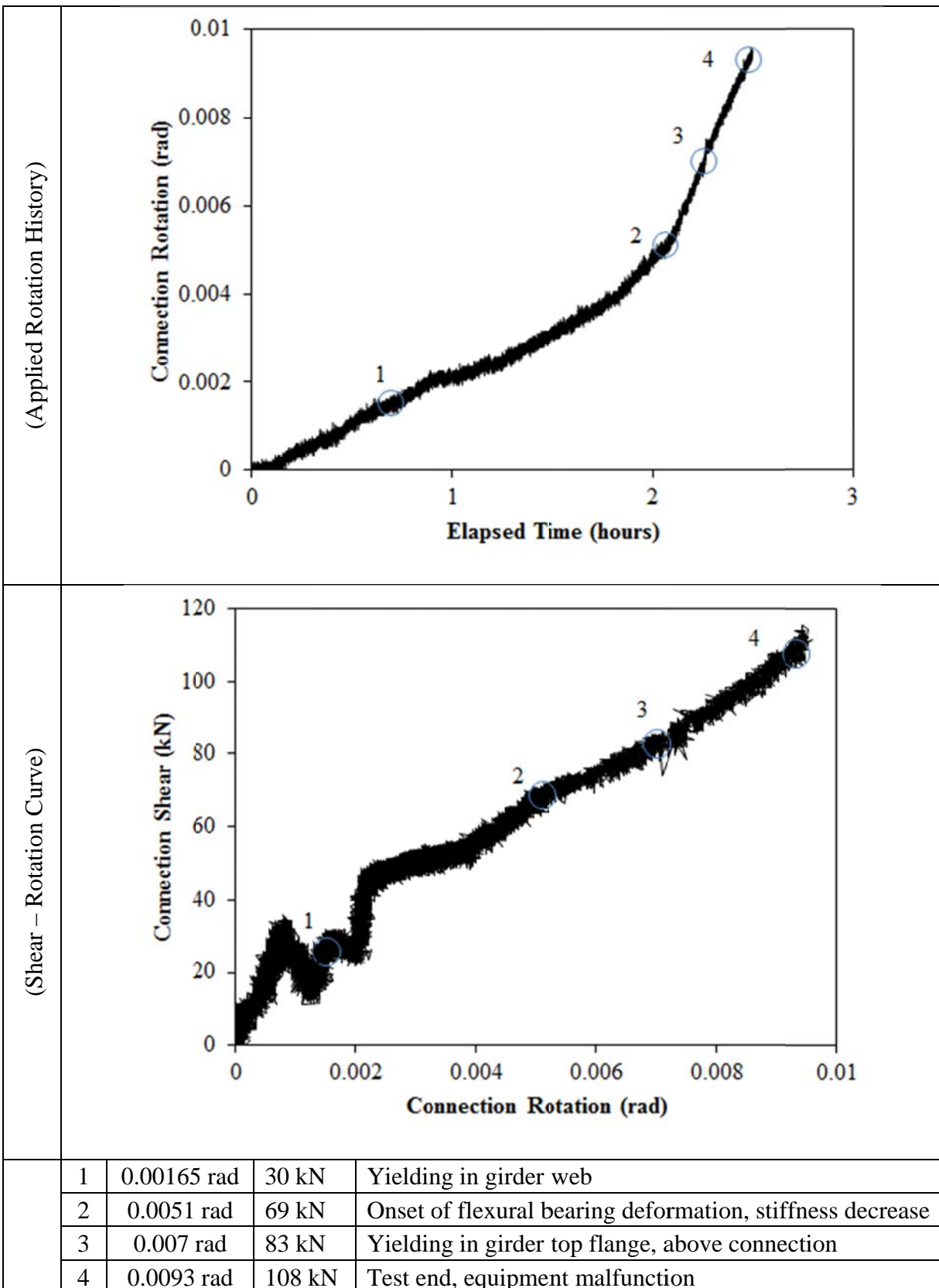


Figure D-63: Test Setup, Configuration 6

MATERIAL PROPERTIES AND SPECIMEN DETAILS

Member	Size	Grade	Yield Stress (MPa)		Ultimate Stress (MPa)	
			Mill Cert.	Coupon	Mill Cert.	Coupon
Beam	W12x40	A992	367	Flange:376 Web:414	485	Flange:492 Web:511
Beam Stiffeners	PL3/8"x3 3/4"	A572-GR50	-	-	-	-
Girder	W24x84	A992	387	-	498	-
Shear Tab	PL3/8"x9 3/4"	A572-GR50	452	456	531	525
Bolts	3/4" x 1 3/4"	A325-T1	3 rows of 2 bolts; 3" spacing, 1 1/2" end distance; snug tight; one washer per bolt; 13/16" bolt holes;			
Welding Procedure Specification	Electrode Classification E70					
	Welding Procedure <i>Shop Welding:</i> FCAW-G (flux-cored arc welding with gas shielding) <ul style="list-style-type: none">Fillet Weld, Shear Tab to Girder"C" Weld, Beam Stiffeners					
Boundary Condition	Tension Actuator Capacity: 268kN tension, 495kN compression; Stroke: 254mm; Displacement controlled					
	Compressive Actuator Capacity: 8018 kN tension, 11414kN compression; Stroke: 305mm; Displacement controlled					
	Lateral Bracing System Top and bottom flange out of plane movement restrained by ball and socket rods fixed to frame tensioned to strong floor					

ROTATION HISTORY AND KEY EXPERIMENTAL OBSERVATIONS



Note: The variation in stiffness seen during the first 0.004 radians of rotation is due to adjustment of the displacement rates of both tension and compression actuators to achieve the desired stiffness. Once this stiffness value was reached, the ratio of rates was held constant for the remainder of the test.

Note: The pump supplying both actuators malfunctioned during the test and the test had to be ended at that point due to safety of the equipment.

RESISTANCE SUMMARY

Limit State	Design Check	Predicted	Observed
Girder Yielding	-	-	26 kN
Combined Shear and Flexural Yielding	AISC Manual, 14 th Ed; Part 10; Equation 10-5	298 kN	-
Bearing	AISC 14 th Ed, Part 10, Extended Shear Tabs, Design Check 1 & S16-09 Clause 13.12.1.2	392 kN	-

TEST OBSERVATIONS

Combined Shear and Flexural Yielding

Deformation within the tab was monitored using a combination of horizontal and inclined strain gauges organized as seen in Figure D-64. White wash was applied to the tab such that the yielding pattern could be observed. The face of the shear tab at the end of test can be seen in Figure D-65.

Horizontal strain gauges were placed on the top and bottom edges of the tab to record flexural strains and the results can be seen in Figure D-66 and D-67. Strain gauges oriented to 45° were placed along the height of the tab to measure shear strains and the results can be seen in Figure D-68 and D-69.

The entire plate behaved elastically for the test. Plastic deformation occurred solely in the supporting girder.

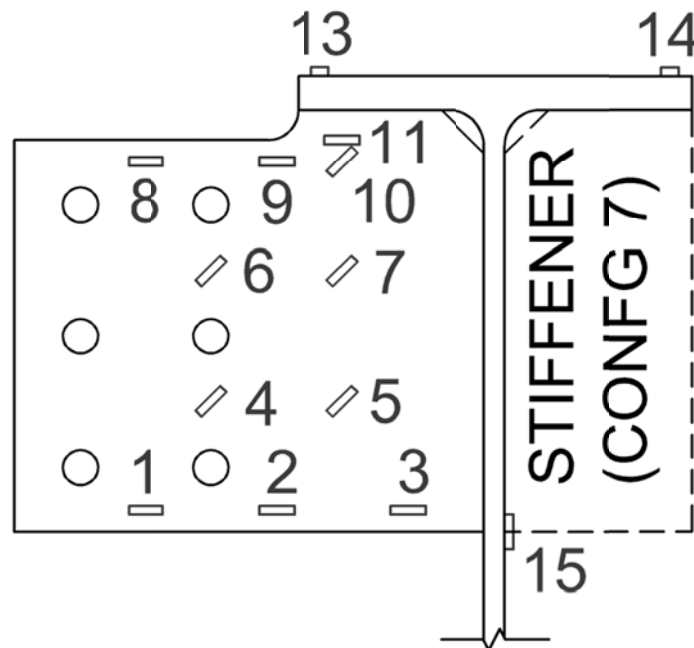


Figure D-64: Strain Gauge Layout, Configuration 6



Figure D-65: Unyielded Shear Tab, End of Test, Configuration 6

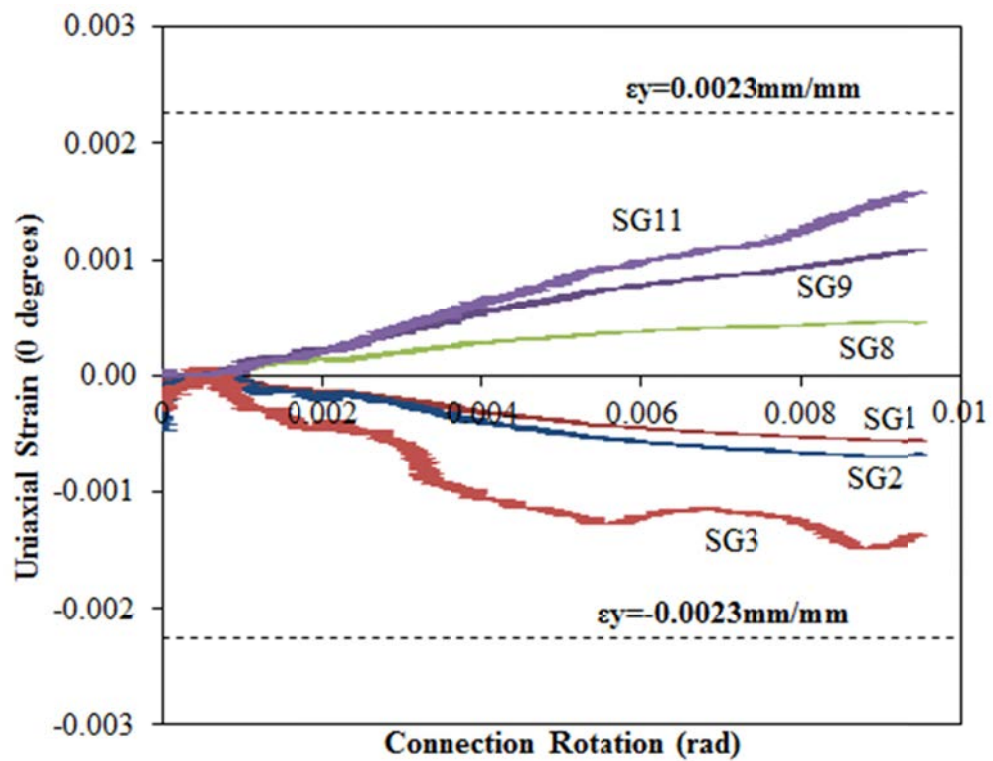


Figure D-66: Uniaxial Strain (0°) vs. Connection Rotation, Configuration 6

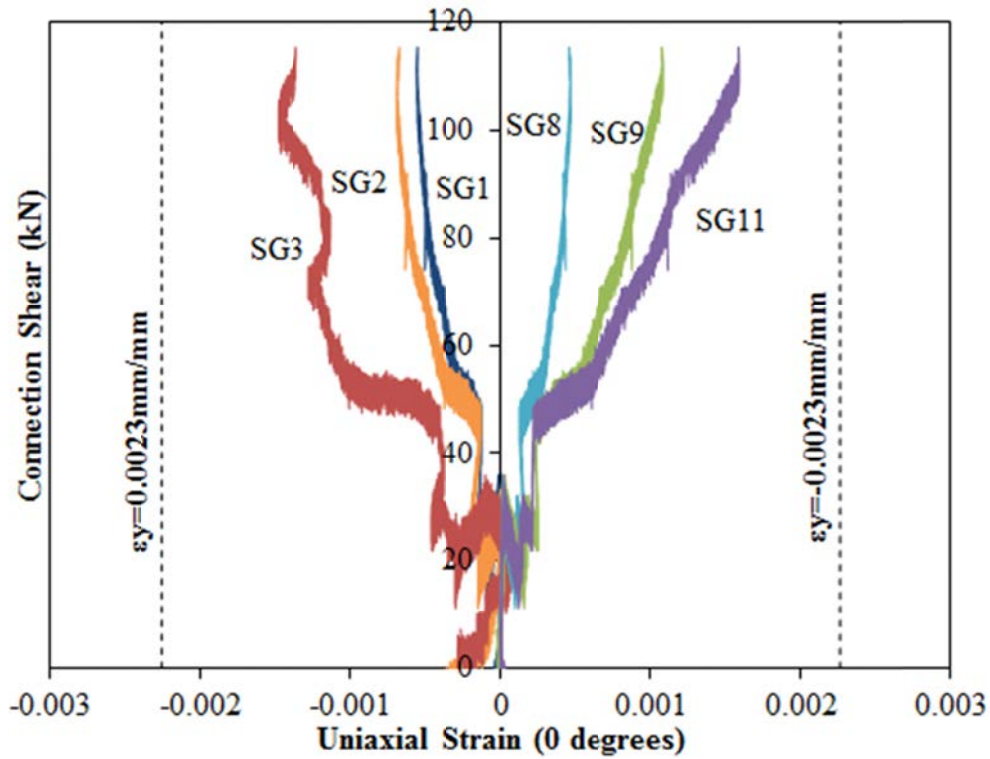


Figure D-67: Connection Shear vs. Uniaxial Strain (0°), Configuration 6

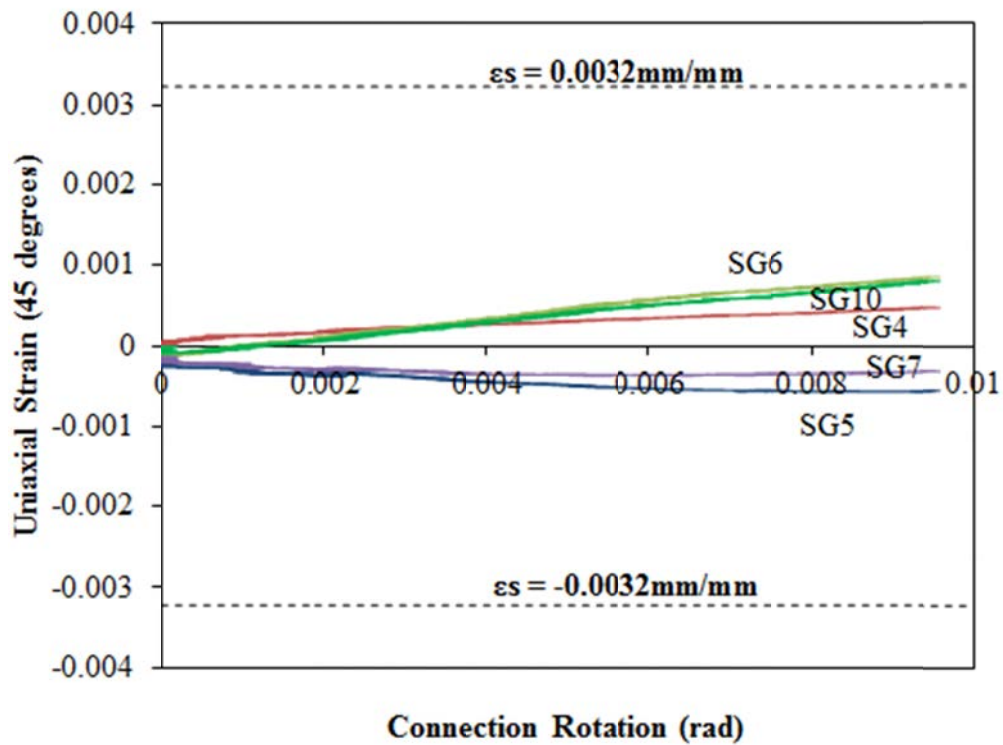


Figure D-68: Uniaxial Strain (45°) vs. Connection Rotation, Configuration 6

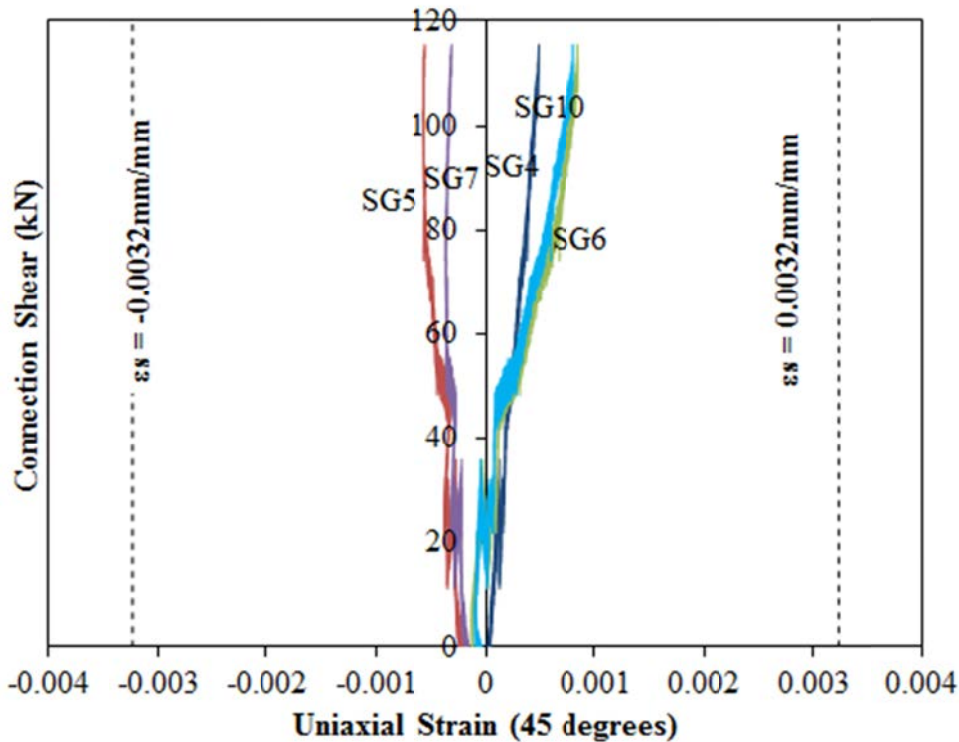


Figure D-69: Connection Shear vs. Uniaxial Strain (45°), Configuration 6

Yielding of Supporting Girder

Significant deformation occurred in the web and top flange of the girder during the test. Rotation of the shear tab caused compressive stresses to develop along the centre line of the girder web, as well as tension stresses along the underside of the flange. Bulging of the girder web on the opposite side of the shear tab and depression of the top flange above the shear tab was significant as Figure D-70 shows yielding of the girder web at the edge of the shear tab. Strain gauges were placed on the supporting girder to measure the extent of this deformation and the data can be seen in Figures D-71 and D-72. SG13 and SG14 were placed on top of the girder flange on the shear tab side and plain side, respectively (see Figure D-64). Compression yielding at SG13 occurred at 0.007 radian rotation. SG15 was placed vertically on the girder web opposite the base of the shear tab. Yielding occurred very early (0.00165 radians). Figure D-73 shows the relative rotation of the girder web with respect to the girder flange. Since the shear tab did not undergo plastic deformation, this can be computed using the shear tab rotation and the girder flange rotation. Measurements were taken from inclinometers placed on the top of the girder flange and the shear tab face. This rotation becomes significant after approximately 30 kN.



Figure D-70: Yielding of Girder Web at Shear Tab Edge, Configuration 6

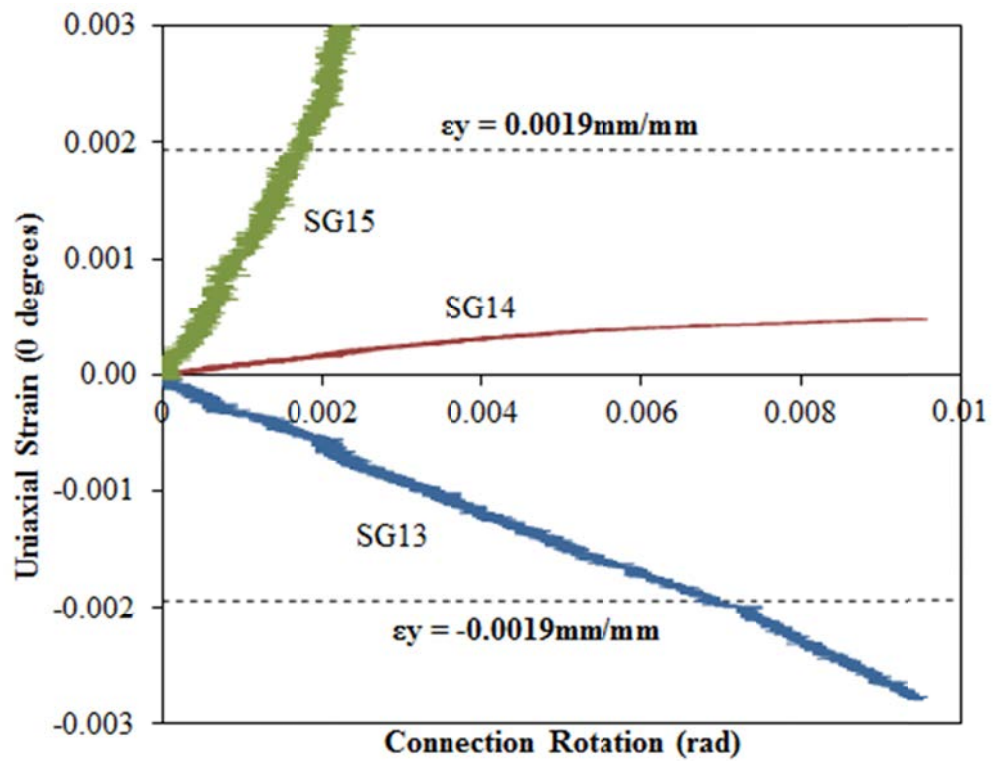


Figure 71: Girder Strain vs. Connection Rotation, Configuration 6

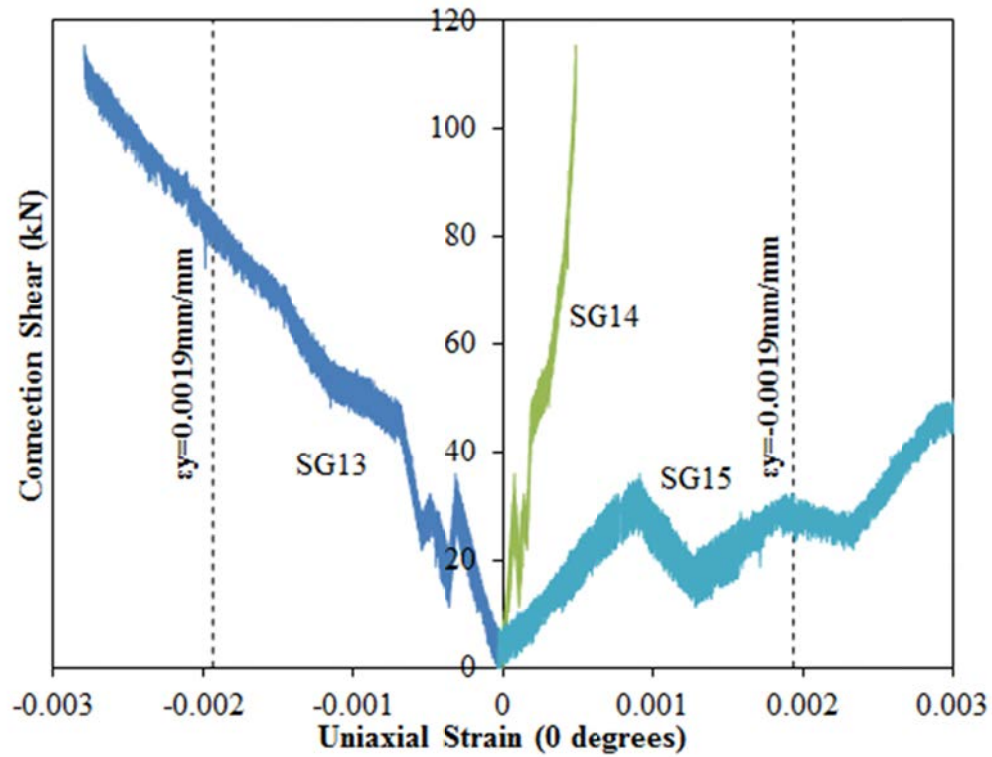


Figure 72: Connection Shear vs. Girder Strain, Configuration 6

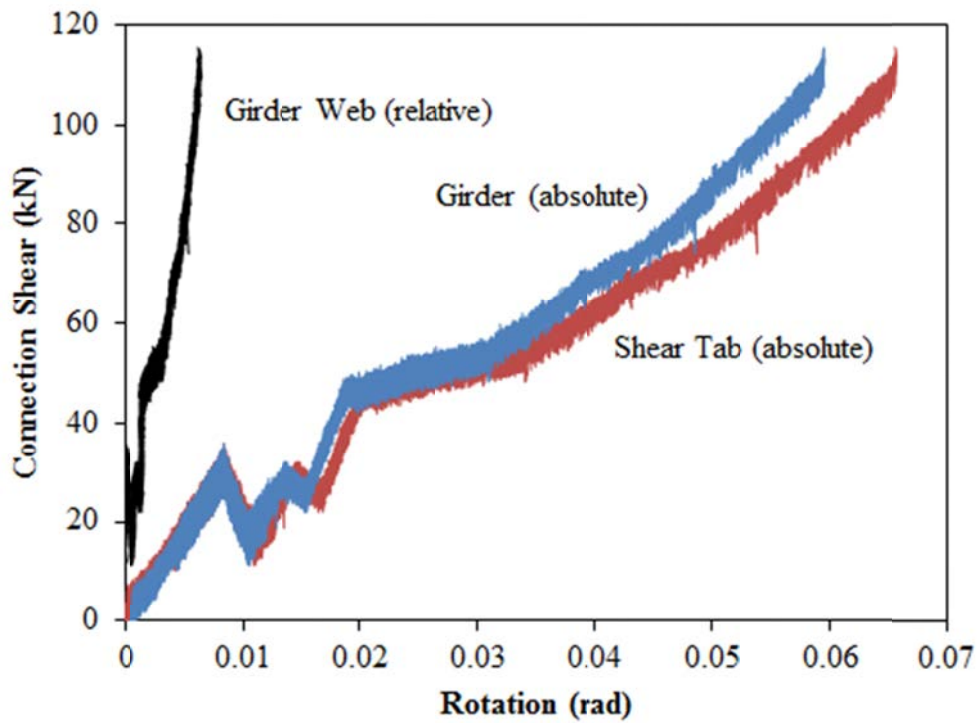


Figure D-73: Connection Shear vs. Relative Girder Web Rotation, Configuration 6

Bearing

Before the test ended due to malfunction of lab equipment, slight bearing deformation was measured. Since this deformation was very small, the rotation and deflection of the shear tab was compared with that of the beam to determine when deformation began. Inclinometers and string potentiometers were attached to the bottom of the beam and the face of the shear tab to measure rotation and deflection, respectively. Figures D-75 and D-76 show the relative rotation and deflection of the bolt group within the shear tab and beam. The relative bearing deflection is seen to be constant for the duration of the test, eventually reaching 0.5mm. Relative bearing rotation begins at approximately 0.0051 radians and the corresponding stiffness decrease can be seen on the Shear Rotation Curve (see Rotation History). Figure D-74 shows a developing tension field in the beam web due to this bearing.



Figure D-74: Tension Field on Beam Web, End of Test, Configuration 6

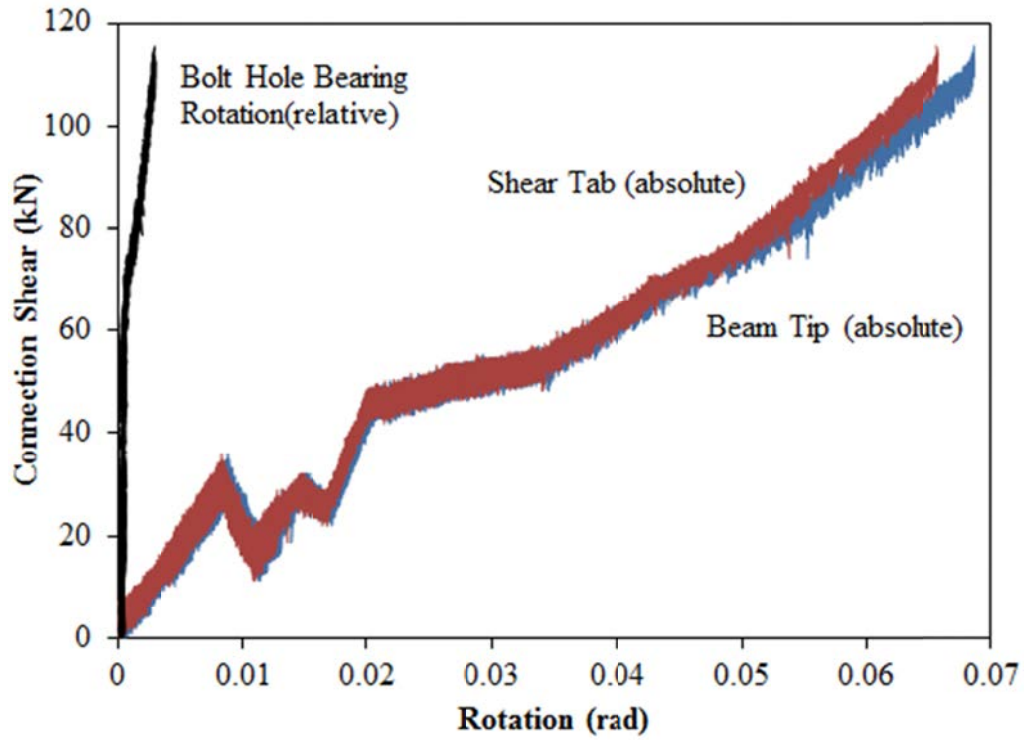


Figure D-75: Connection Shear vs. Relative Bearing Rotation, Configuration 6

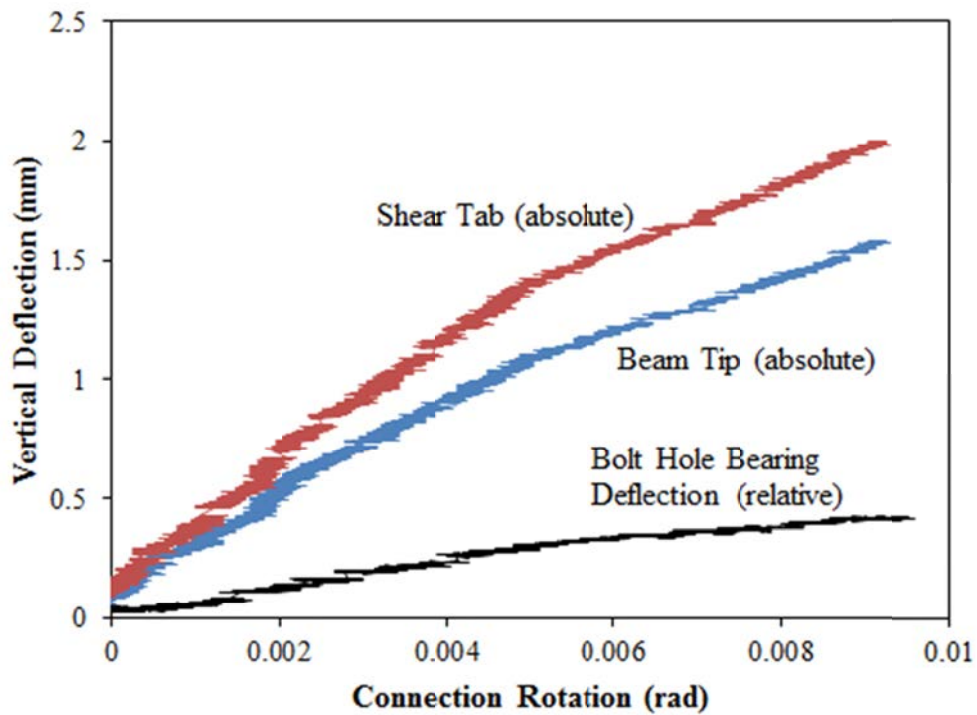


Figure 76: Relative Bearing Deflection vs. Connection Rotation, Configuration 6

EXTENDED SHEAR TAB CONNECTION EXPERIMENTAL STUDY

TEST SUMMARY OF CONFIGURATION 7

Specimen ID	CONFIGURATION 7
Key Words	Shear Tab, Extended Configuration; Flexible Support Condition; Beam to Girder;
Test Location	Structures Lab, Macdonald Engineering Building, McGill University
Test Date	June 28, 2013
Investigators	Colin A. Rogers, Dimitrios G. Lignos, Jacob W. Hertz
Main References	AISC Steel Construction Manual, 13th & 14th Editions; CISC Handbook of Steel Construction, 10th Edition
Sponsors	ADF Group Inc., DPHV and NSERC

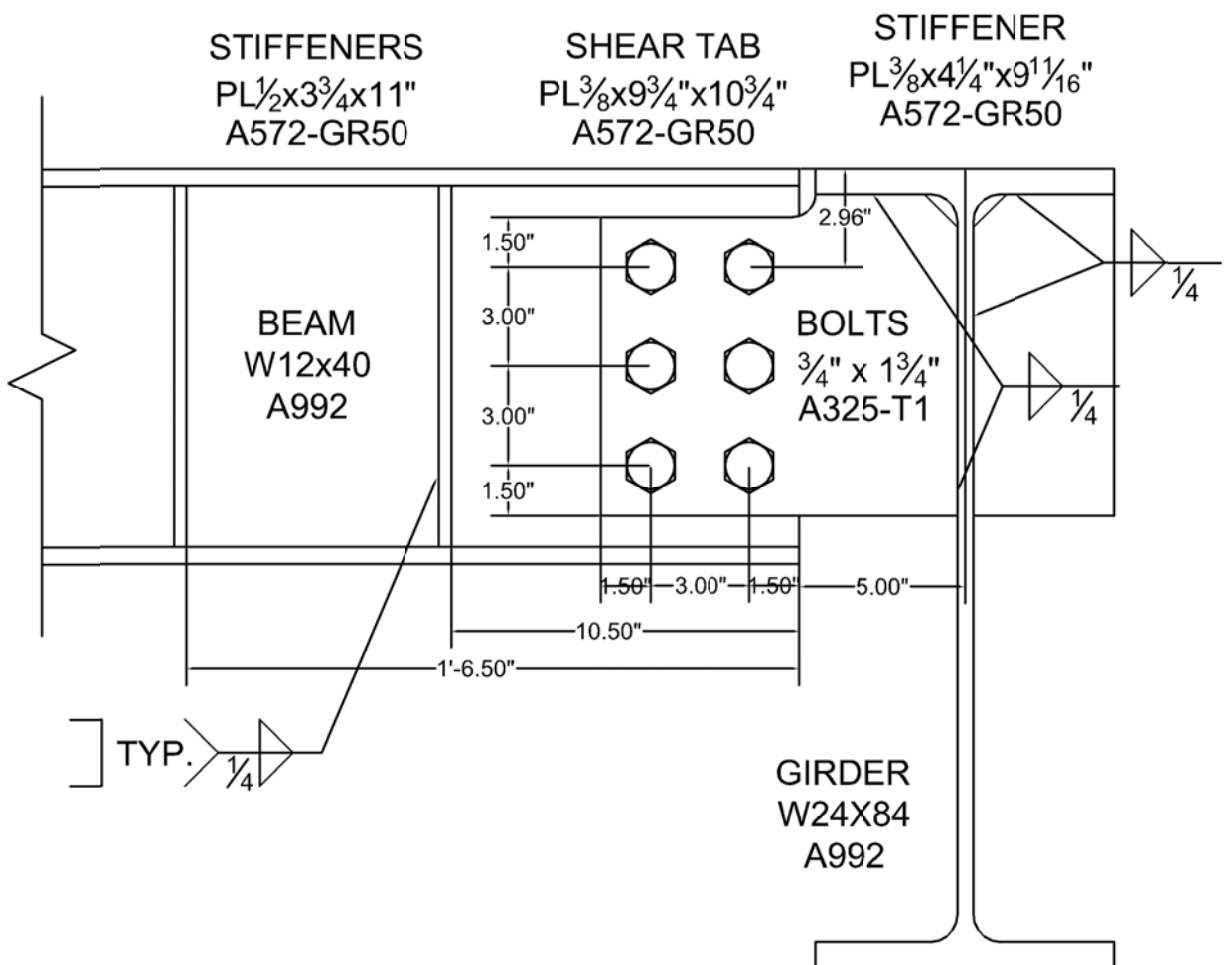


Figure D-77: Connection Details, Configuration 7

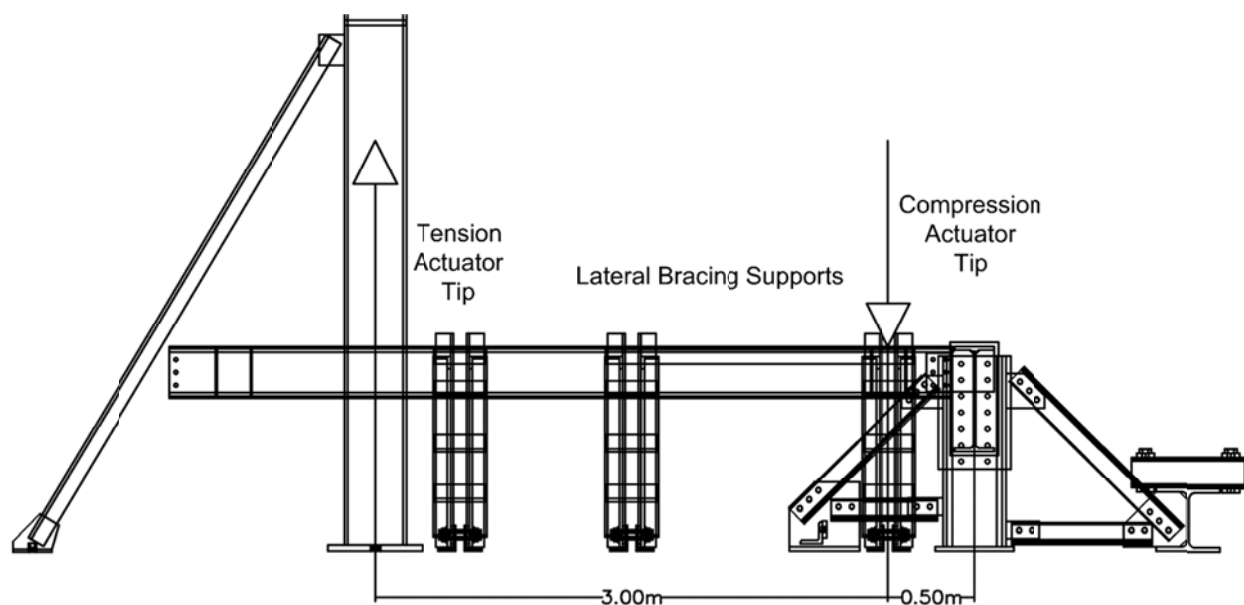
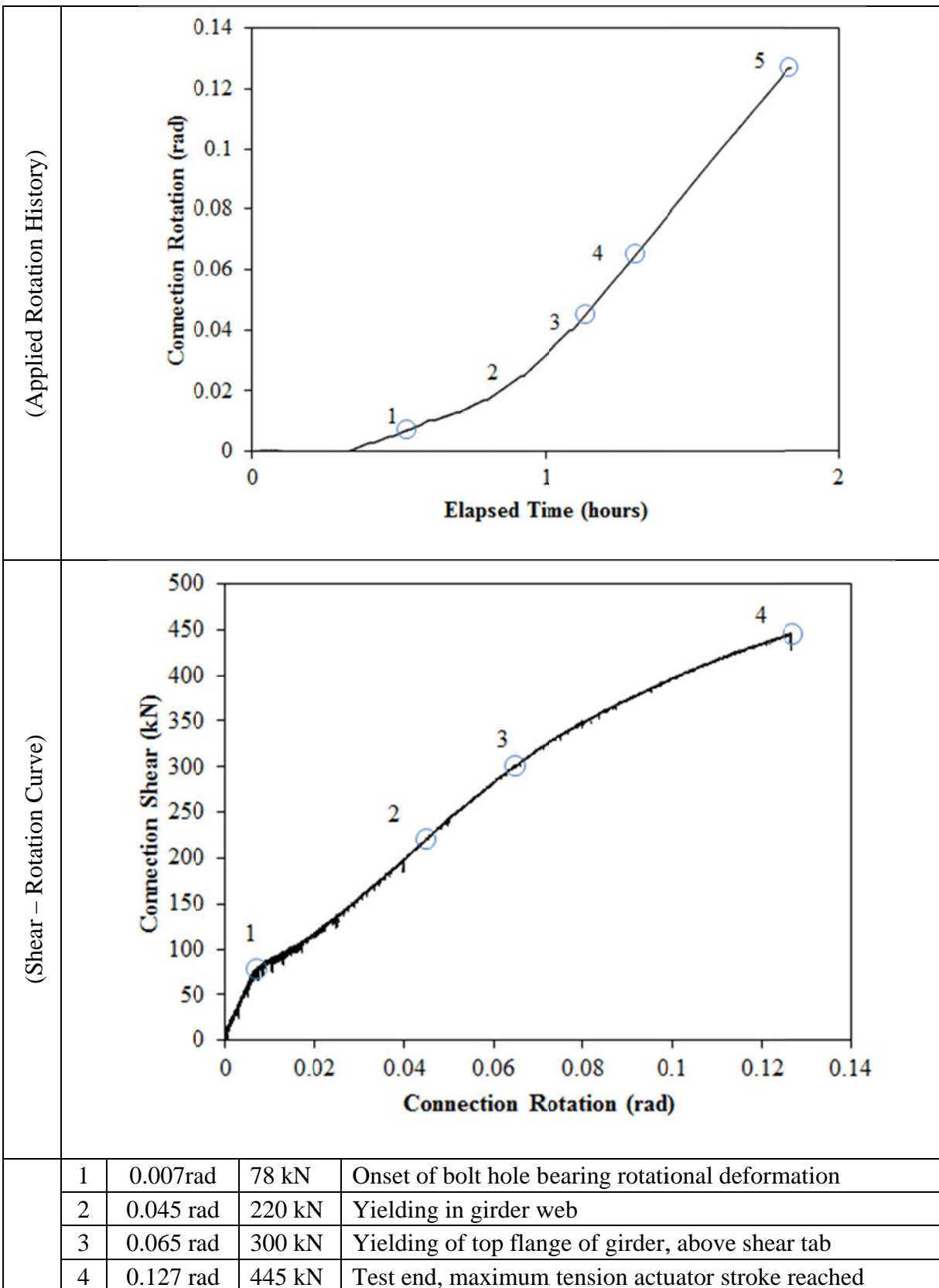


Figure 78: Test Setup, Configuration 7

MATERIAL PROPERTIES AND SPECIMEN DETAILS

Member	Size	Grade	Yield Stress (MPa)		Ultimate Stress (MPa)	
			Mill Cert.	Coupon	Mill Cert.	Coupon
Beam	W12x40	A992	367	Flange:376 Web:414	485	Flange:492 Web:511
Beam Stiffeners	PL1/2"x3 3/4"	A572-GR50	-	-	-	-
Girder	W24x84	A992	387	-	498	-
Shear Tab	PL3/8"x9 3/4"	A572-GR50	452	456	531	525
Girder Stiffener	PL3/8"x4 1/4"	A572-GR50	367	Flange:376 Web:414	485	Flange:492 Web:511
Bolts	3/4" x 1 3/4"	A325-T1	3 rows of 2 bolts; 3" spacing, 1 1/2" end distance; snug tight; one washer per bolt; 13/16" bolt holes;			
Welding Procedure Specification	Electrode Classification E70					
	Welding Procedure <i>Shop Welding:</i> FCAW-G (flux-cored arc welding with gas shielding) <ul style="list-style-type: none">Fillet Weld, Shear Tab and Stiffener to Girder"C" Weld, Beam Stiffeners					
Boundary Condition	Tension Actuator Capacity: 268kN tension, 495kN compression; Stroke: 254mm; Displacement controlled					
	Compressive Actuator Capacity: 8018 kN tension, 11414kN compression; Stroke: 305mm; Displacement controlled					
	Lateral Bracing System Top and bottom flange out of plane movement restrained by ball and socket rods fixed to frame tensioned to strong floor					

ROTATION HISTORY AND KEY EXPERIMENTAL OBSERVATIONS



RESISTANCE SUMMARY

Limit State	Design Check	Predicted	Observed
Girder Yielding	-	-	220 kN
Combined Shear and Flexural Yielding	AISC Manual, 14 th Ed; Part 10; Equation 10-5	298 kN	-
Bearing	AISC 14 th Ed, Part 10, Extended Shear Tabs, Design Check 1 & S16-09 Clause 13.12.1.2	392 kN	-

TEST OBSERVATIONS

Combined Shear and Flexural Yielding

Deformation within the tab was monitored using a combination of horizontal and inclined strain gauges organized as seen in Figure D-79. White wash was applied to the tab such that the yielding pattern could be observed. The deformed shear tab at the end of test can be seen in Figure D-80.

Horizontal strain gauges were placed on the top and bottom edges of the tab to record flexural strains and the results can be seen in Figure D-81 and D-82.

Strain gauges oriented to 45° were placed along the height of the tab to measure shear strains and the results can be seen in Figure D-83 and D-84. Shear yielding was only seen at the location of SG4 at 0.087 radian rotation.

Since yielding occurred only at two locations, it can be said that the shear tab behaved elastically for the test. Significant plastic deformation occurred solely in the supporting girder.

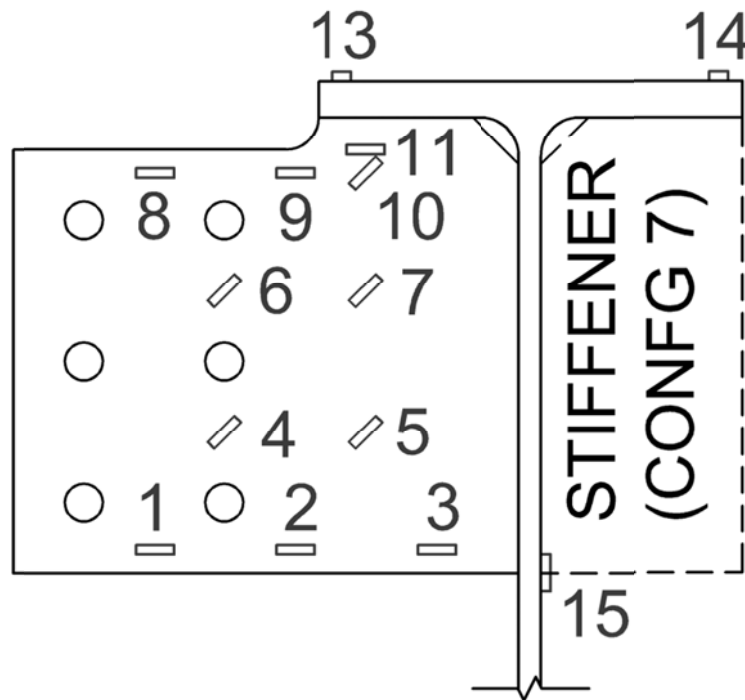


Figure D-79: Strain Gauge Layout, Configuration 7



Figure D-80: Shear Tab, End of Test, Configuration 7

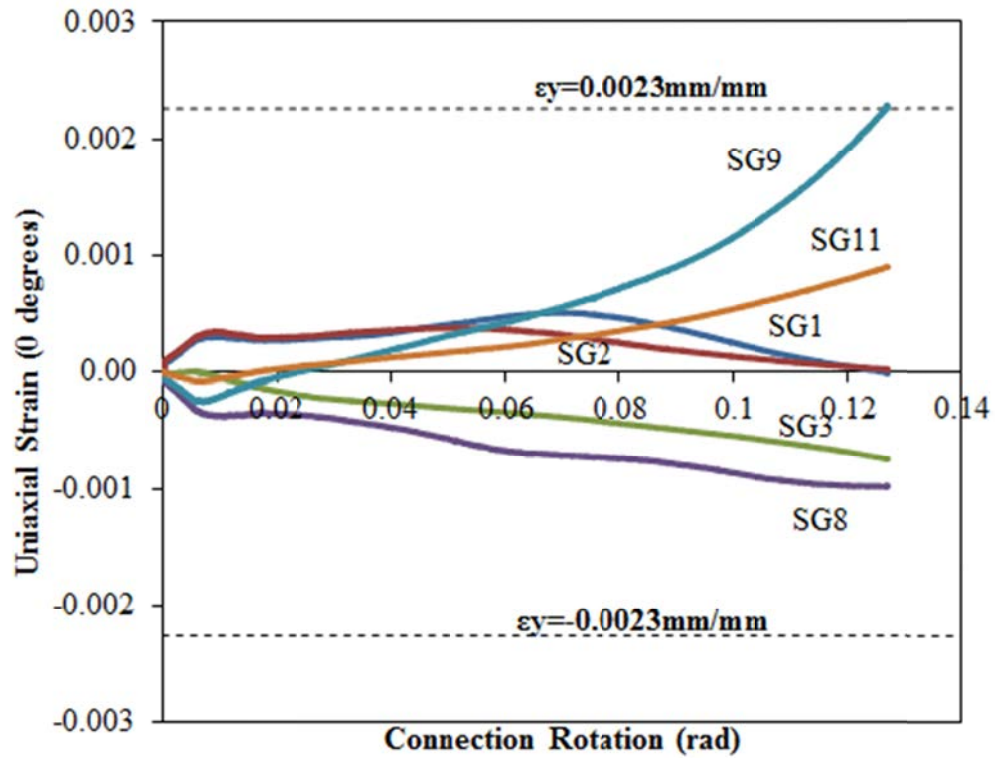


Figure D-81: Uniaxial Strain (0°) vs. Connection Rotation, Configuration 7

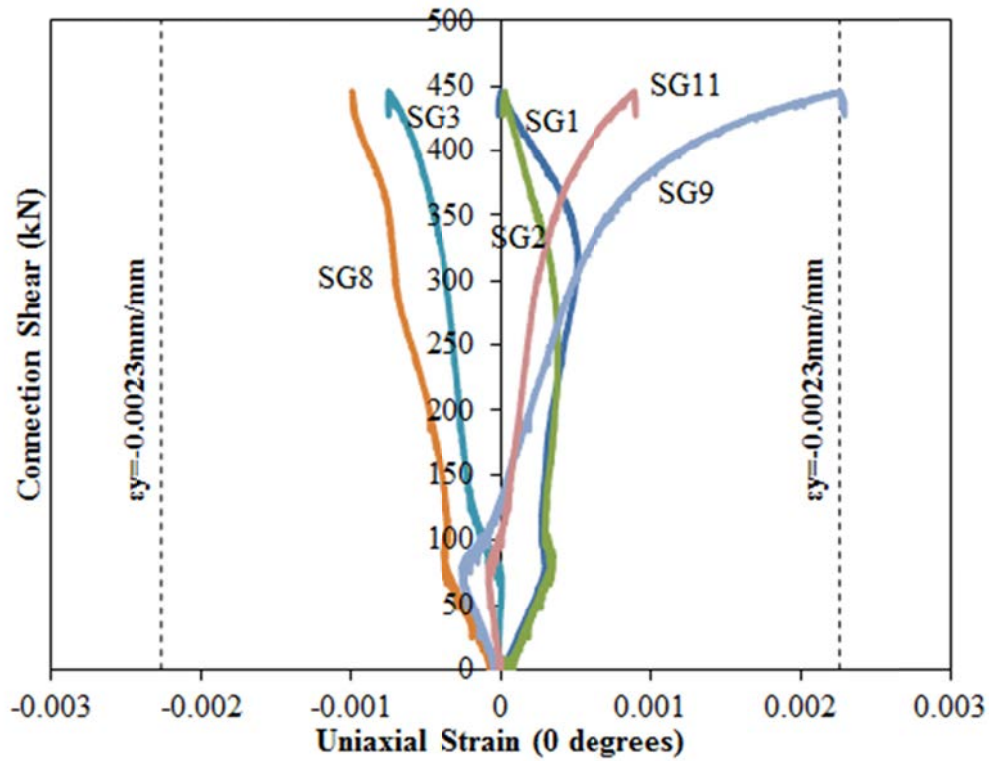


Figure D-82: Connection Shear vs. Uniaxial Strain (0°), Configuration 7

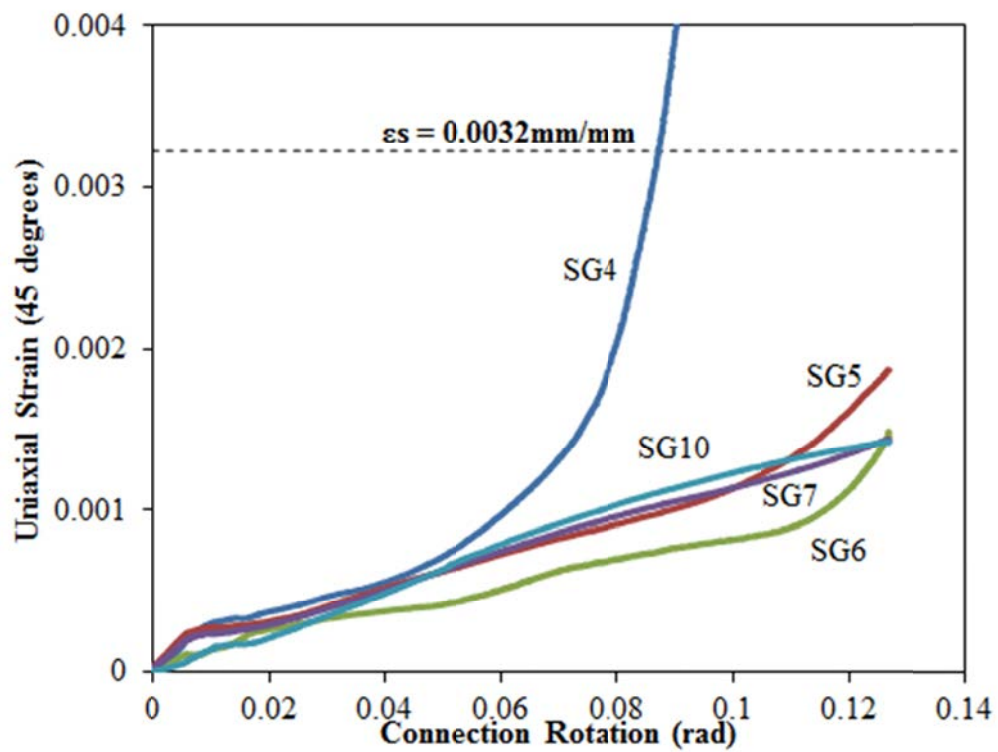


Figure D-83: Uniaxial Strain (45°) vs. Connection Rotation, Configuration 7

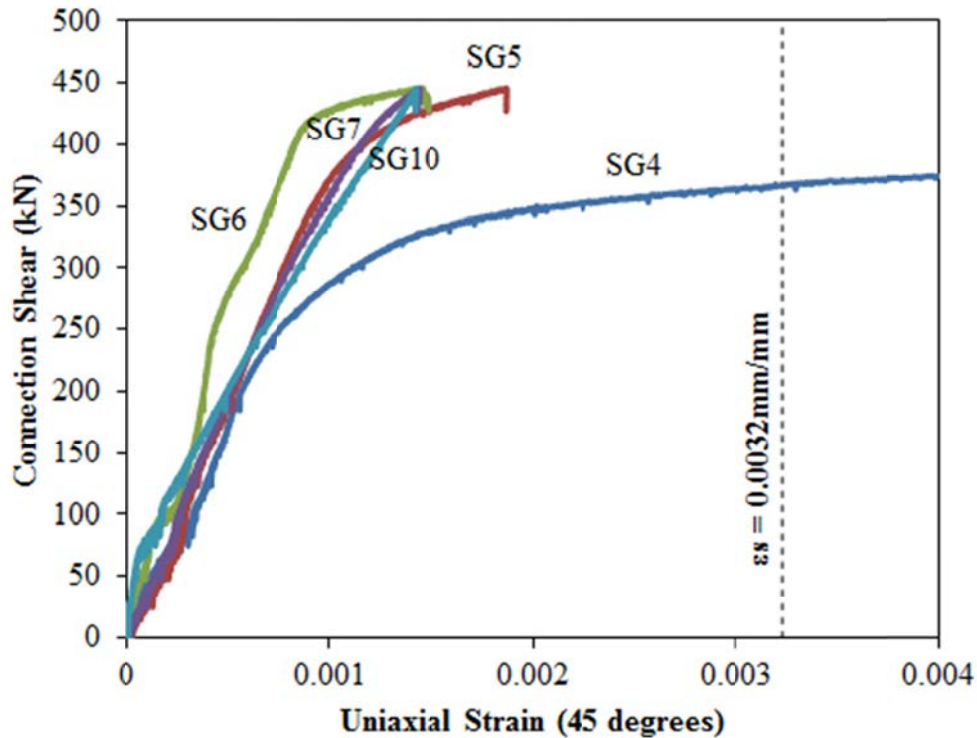


Figure D-84: Connection Shear vs. Uniaxial Strain (45°), Configuration 7

Yielding of Supporting Girder

Significant deformation occurred in the web and top flange of the girder during the test. Rotation of the shear tab caused compressive stresses to develop along the centre line of the girder web, as well as tension stresses along the underside of the flange. Bulging of the girder web on the opposite side of the shear tab and depression of the top flange above the shear tab was significant as Figure D-85 shows yielding of the girder web at the edge of the shear tab. Strain gauges were placed on the supporting girder to measure the extent of this deformation and the data can be seen in Figures D-86 and D-87. SG13 and SG14 were placed on top of the girder flange on the shear tab side and plain side, respectively (see Figure D-79). Compression yielding at SG13 occurred at 0.065 radian rotation. SG15 was placed vertically on the girder web opposite the base of the shear tab. Yielding occurred at 0.045 radians. Figure D-88 shows the relative rotation of the girder web with respect to the girder flange. Since the shear tab did not undergo plastic deformation, this can be computed using the shear tab rotation and the girder flange rotation. Measurements were taken from inclinometers placed on the top of the girder flange and the shear tab face. This rotation was seen to be insignificant for the duration of the test.

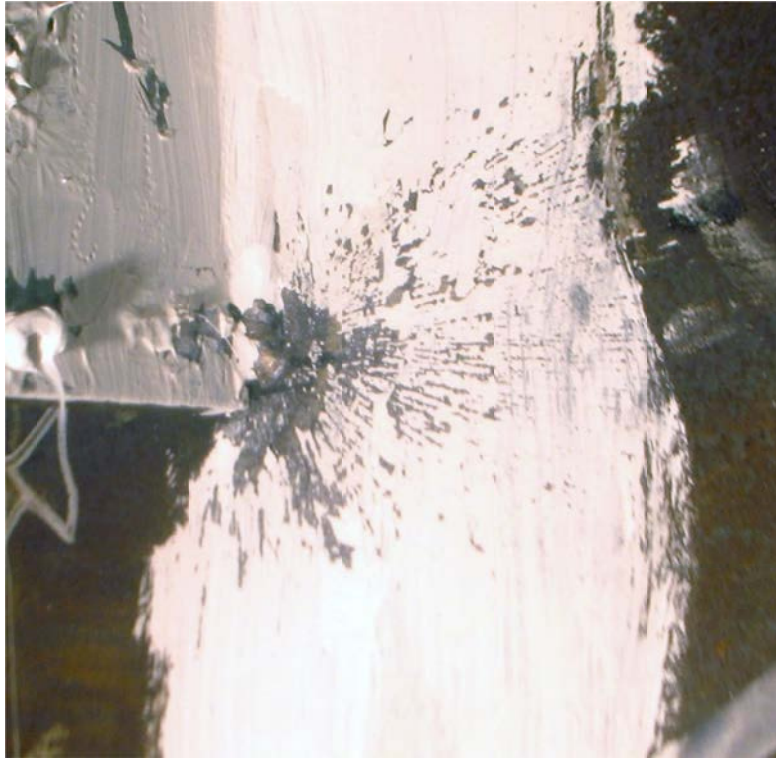


Figure D-85: Yielding of Girder Web at Shear Tab Edge, Configuration 7

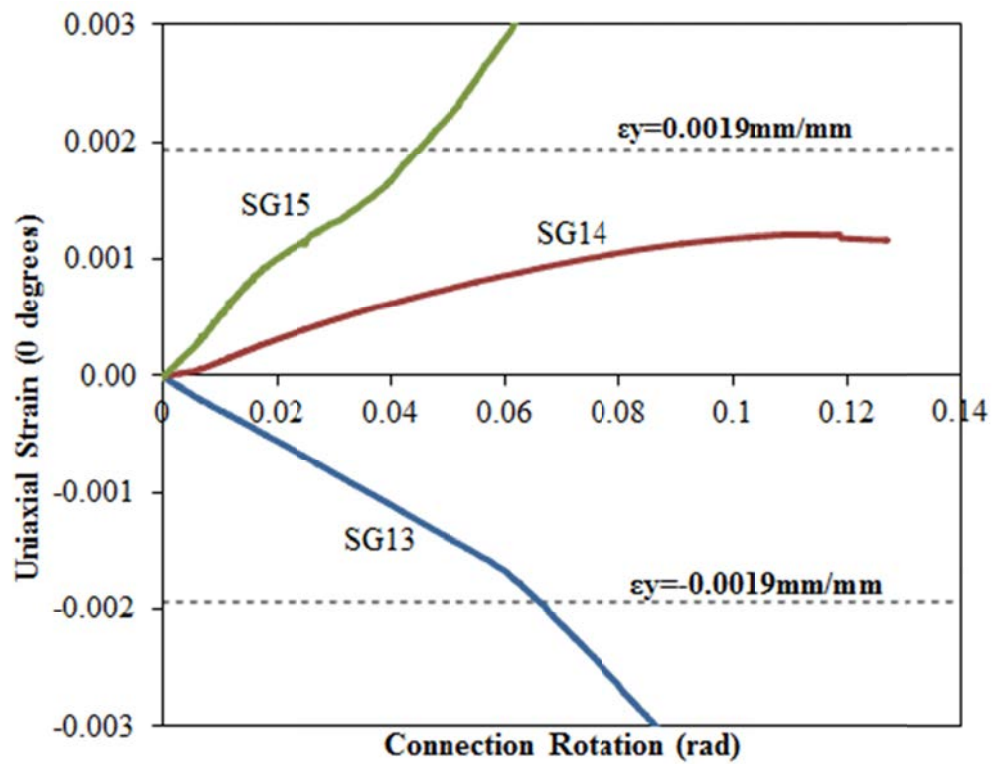


Figure D-86: Girder Strain vs. Connection Rotation, Configuration 7

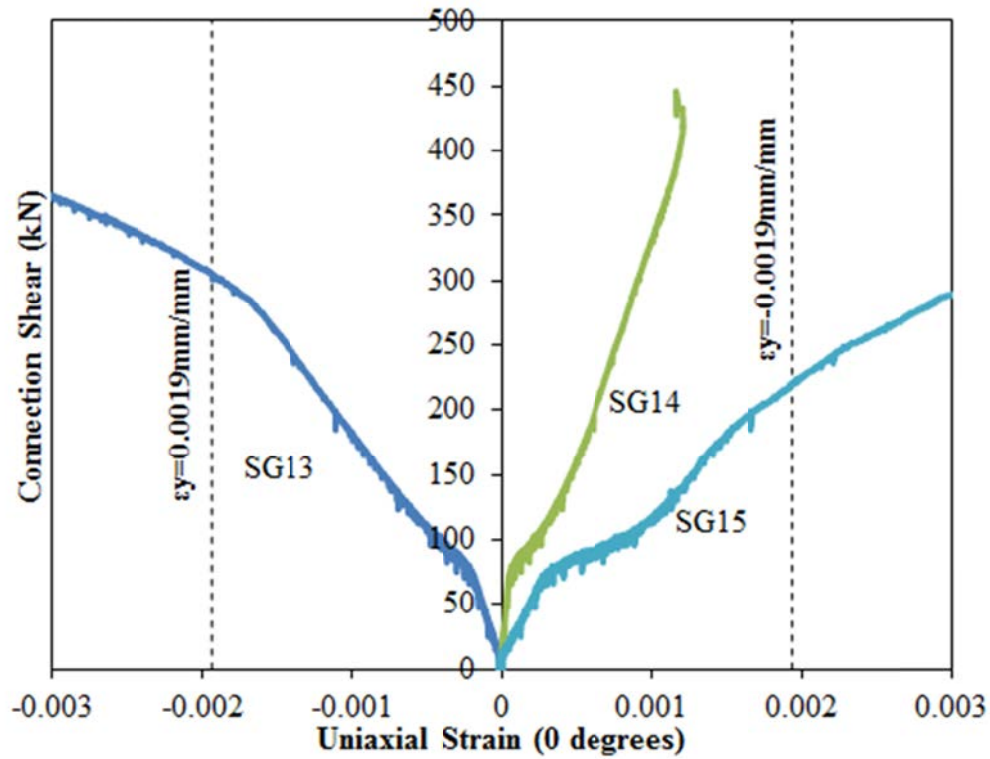


Figure D-87: Connection Shear vs. Girder Strain, Configuration 7

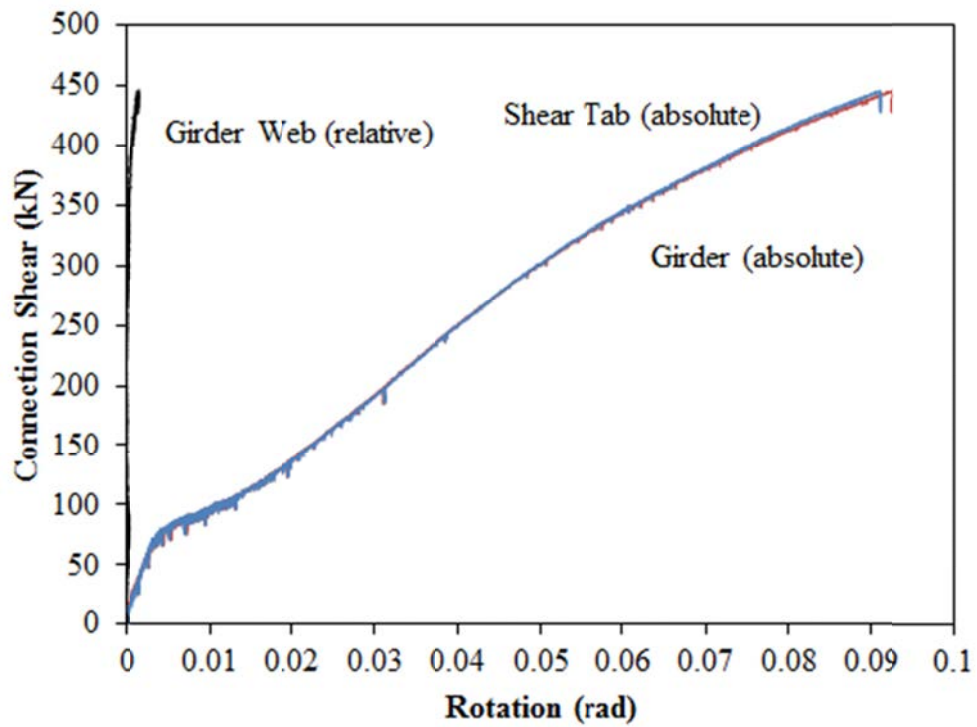


Figure D-88: Connection Shear vs. Relative Girder Web Rotation, Configuration 7

Bolt Bearing

Substantial bolt hole bearing deformation was seen in the web of the supported beam. Inclinometers and string potentiometers were attached to the bottom of the beam and the face of the shear tab to measure rotation and deflection, respectively. Figures D-90 and D-91 show the relative rotation and deflection of the bolt group within the shear tab and beam. The relative bearing deflection remained zero until 0.023 radian rotation where it began to increase. The vertical bolt hole bearing deflection could not be computed due to malfunction of the string potentiometer attached to the beam tip. The relative bearing rotation of the bolt group began to increase after 69 kN connection shear. The corresponding stiffness decrease can be seen on the Shear Rotation Curve (see Rotation History). Figure D-89 shows a developed tension field in the beam web due to this bearing. Figure D-92 shows the deformed bolt holes within the supported beam at the end of test.



Figure D-89: Tension Field on Beam Web, End of Test, Configuration 7

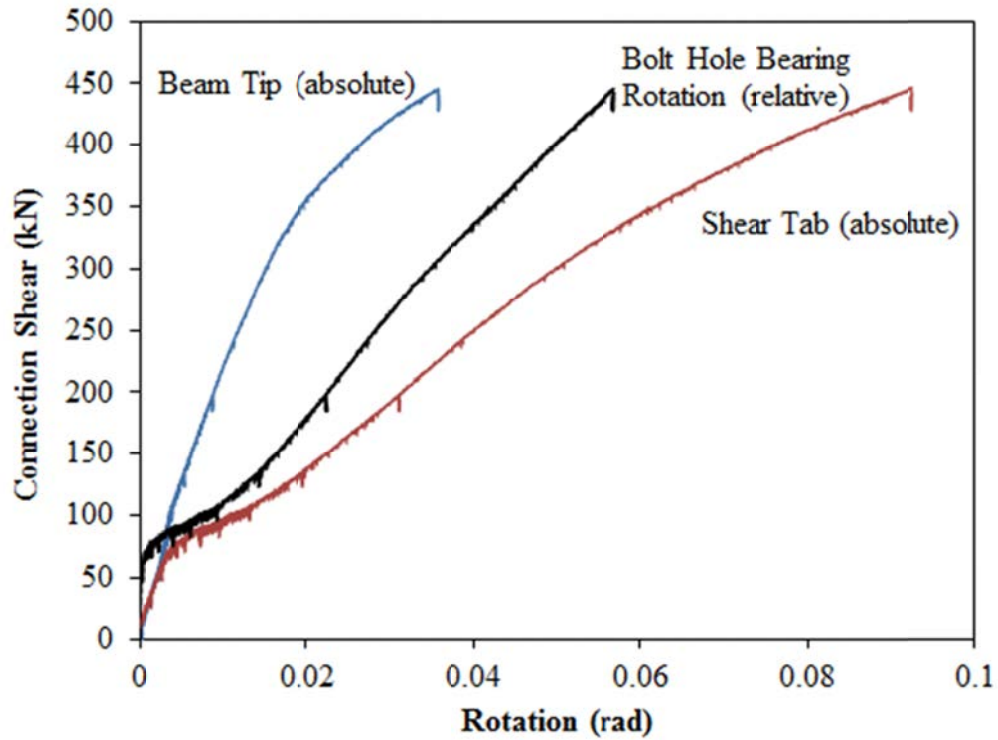


Figure D-90: Connection Shear vs. Relative Bearing Rotation, Configuration 7

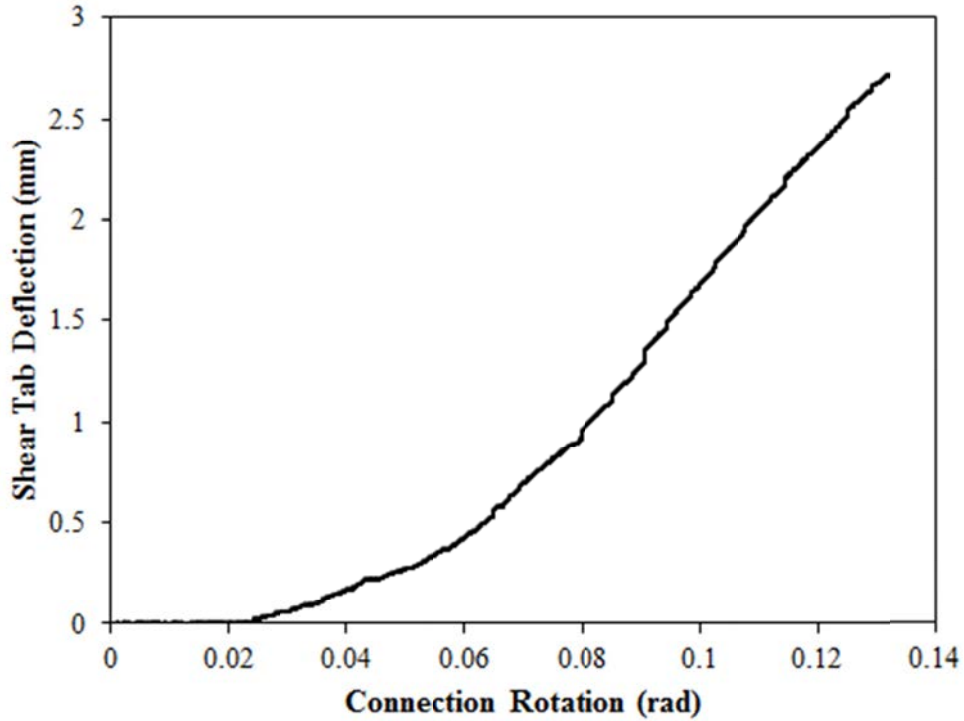


Figure D-91: Bearing Deflection vs. Connection Rotation, Configuration 7



Figure D-92: Beam Bolt Hole Bearing Deformation, Configuration7

EXTENDED SHEAR TAB CONNECTION EXPERIMENTAL STUDY

TEST SUMMARY OF CONFIGURATION 8

Specimen ID	CONFIGURATION 8
Key Words	Shear Tab, Extended Configuration; Flexible Support Condition; Beam to Girder;
Test Location	Structures Lab, Macdonald Engineering Building, McGill University
Test Date	July 4, 2013
Investigators	Colin A. Rogers, Dimitrios G. Lignos, Jacob W. Hertz
Main References	AISC Steel Construction Manual, 13th & 14th Editions; CISC Handbook of Steel Construction, 10th Edition
Sponsors	ADF Group Inc., DPHV and NSERC

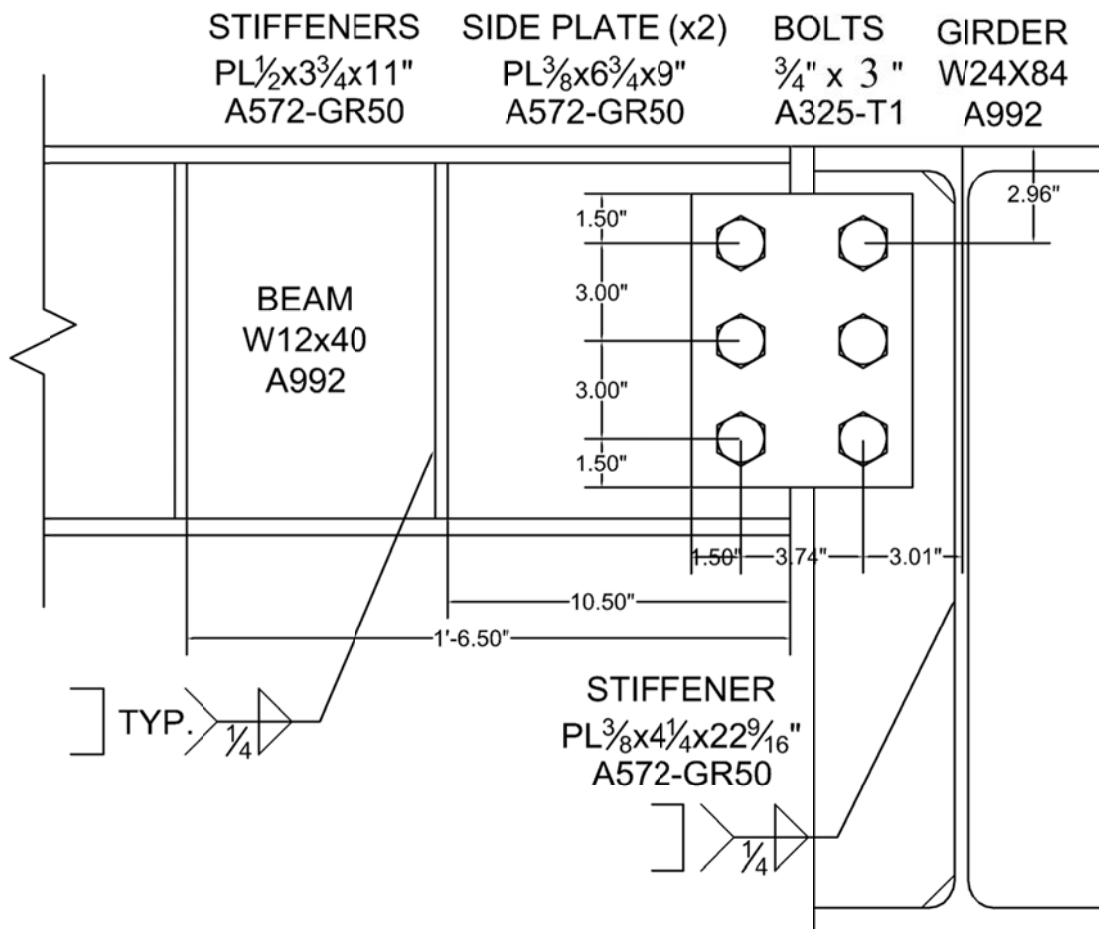


Figure D-93: Connection Details, Configuration 8

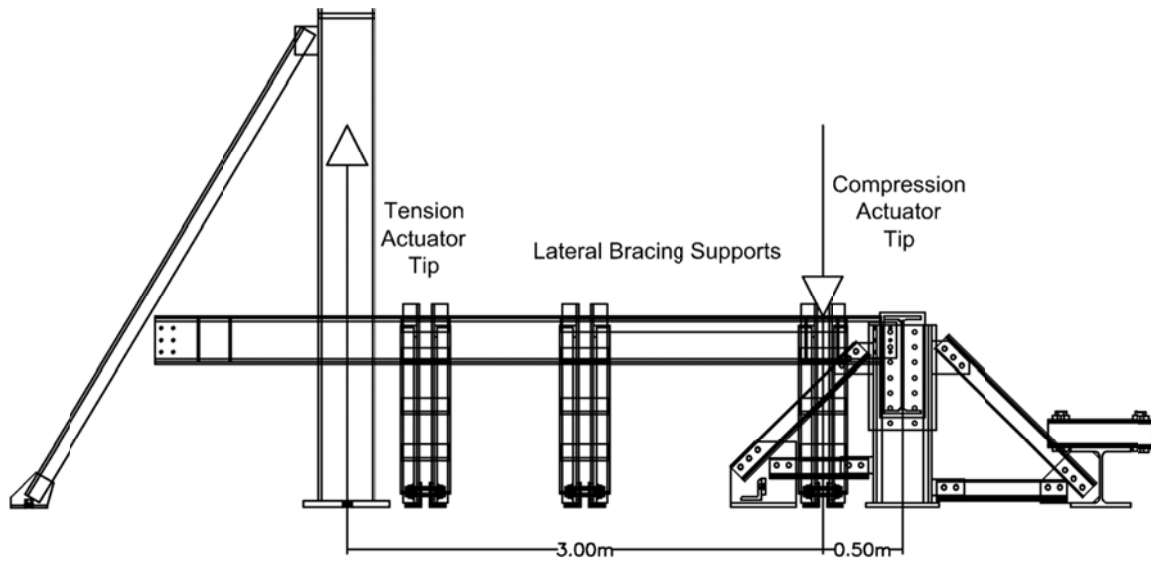
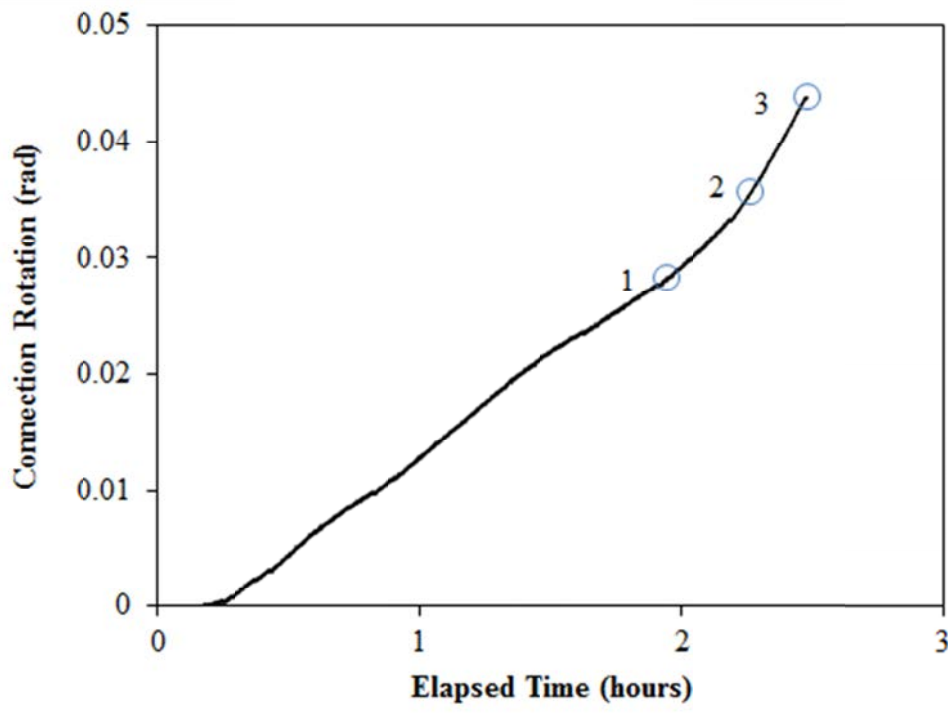
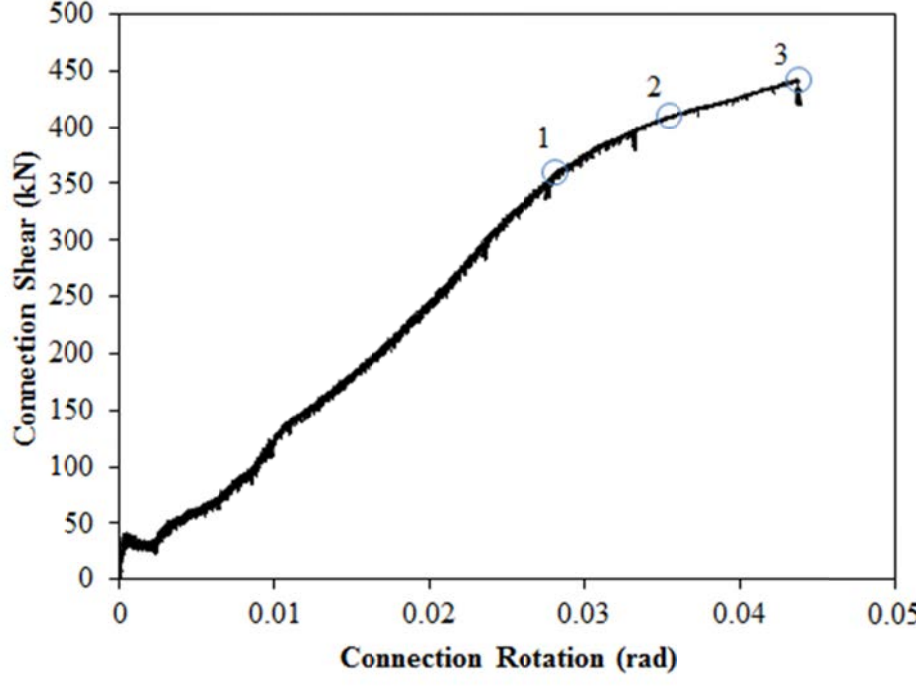


Figure D-94: Test Setup, Configuration 8

MATERIAL PROPERTIES AND SPECIMEN DETAILS

Member	Size	Grade	Yield Stress (MPa)		Ultimate Stress (MPa)	
			Mill Cert.	Coupon	Mill Cert.	Coupon
Beam	W12x40	A992	367	Flange:376 Web:414	485	Flange:492 Web:511
Beam Stiffeners	PL1/2"x3 3/4"	A572-GR50	-	-	-	-
Girder	W24x84	A992	387	-	498	-
Shear Tab	PL3/8"x4 1/4"	A572-GR50	452	456	531	525
Side Plates (x2)	PL3/8"x6 3/4"	A572-GR50	452	456	531	525
Bolts	3/4" x 3"	A325-T1	3 rows of 1 bolt within beam and shear tab; 3" spacing, 1 1/2" end distance; snug tight; one washer per bolt; 13/16" bolt holes;			
Welding Procedure Specification	Electrode Classification E70					
	Welding Procedure <i>Shop Welding:</i> FCAW-G (flux-cored arc welding with gas shielding) <ul style="list-style-type: none">Fillet Weld, Shear Tab to Column"C" Weld, Beam Stiffeners					
Boundary Condition	Tension Actuator Capacity: 268kN tension, 495kN compression; Stroke: 254mm; Displacement controlled					
	Compressive Actuator Capacity: 8018 kN tension, 11414kN compression; Stroke: 305mm; Displacement controlled					
	Lateral Bracing System Top and bottom flange out of plane movement restrained by ball and socket rods fixed to frame tensioned to strong floor					

ROTATION HISTORY AND KEY EXPERIMENTAL OBSERVATIONS

(Applied Rotation History)				
(Shear – Rotation Curve)				
	1	0.028 rad	360 kN	Significant rotational bolt hole bearing deformation in stiffener
	2	0.036 rad	410 kN	Bottom flange of beam begins to bear on stiffener
	3	0.043 rad	442 kN	Test end

Note: The variation in stiffness seen during the first 0.002 radians of rotation is due to adjustment of the displacement rates of both tension and compression actuators to achieve the desired stiffness. Once this stiffness value was reached, the ratio of rates was held constant for the remainder of the test.

RESISTANCE SUMMARY

Limit State	Design Check	Predicted	Observed
Bolt Bearing	S16-09 Clause 13.12.12.1.2 a)	202 kN	360 kN

TEST OBSERVATIONS

Combined Shear and Flexural Yielding

Deformation within the side plates and stiffener was monitored using a combination of horizontal and inclined strain gauges organized as seen in Figure D-95. White wash was applied to the side plates, beam web and stiffener such that the yielding pattern could be observed. The deformed condition at the end of test can be seen in Figure D-96.

Horizontal strain gauges were placed on the top and bottom of the side plates and stiffener to record flexural strains and the results can be seen in Figure D-97 and D-98. Flexural yielding was not seen in the side plates or stiffener during the test.

Strain gauges oriented to 45° were placed along the height of the side plates and stiffener to measure shear strains and the results can be seen in Figure D-99 and D-100. Shear yielding was only seen underneath the line of bolts in the stiffener (SG10) at 0.025 radian rotation.

The side plates were seen to behave elastically for the duration of the test. The limit state of combined shear and flexural yielding is not applicable.

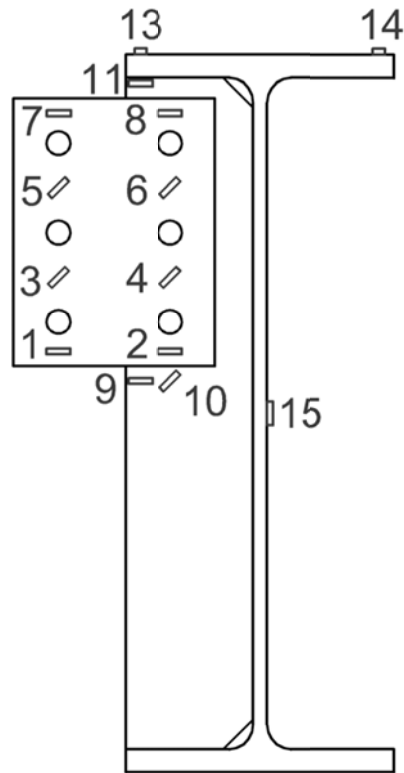


Figure D-95: Strain Gauge Layout, Configuration 8



Figure D-96: Deformed Condition, End of Test, Configuration 8

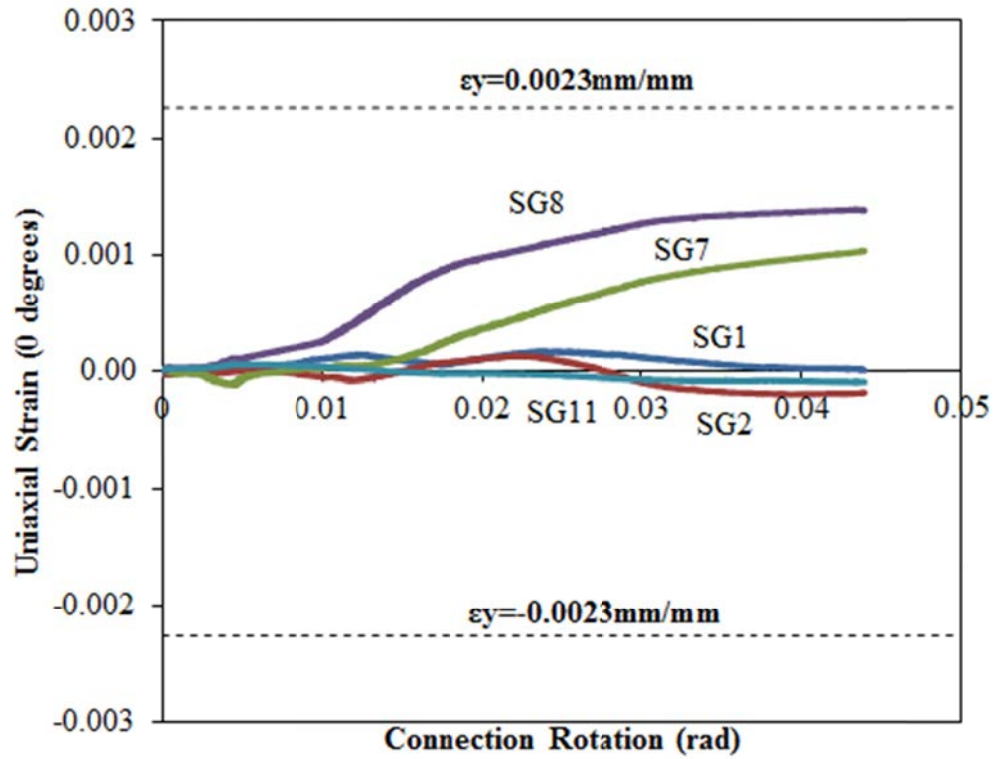


Figure D-97: Uniaxial Strain (0°) vs. Connection Rotation, Configuration 8

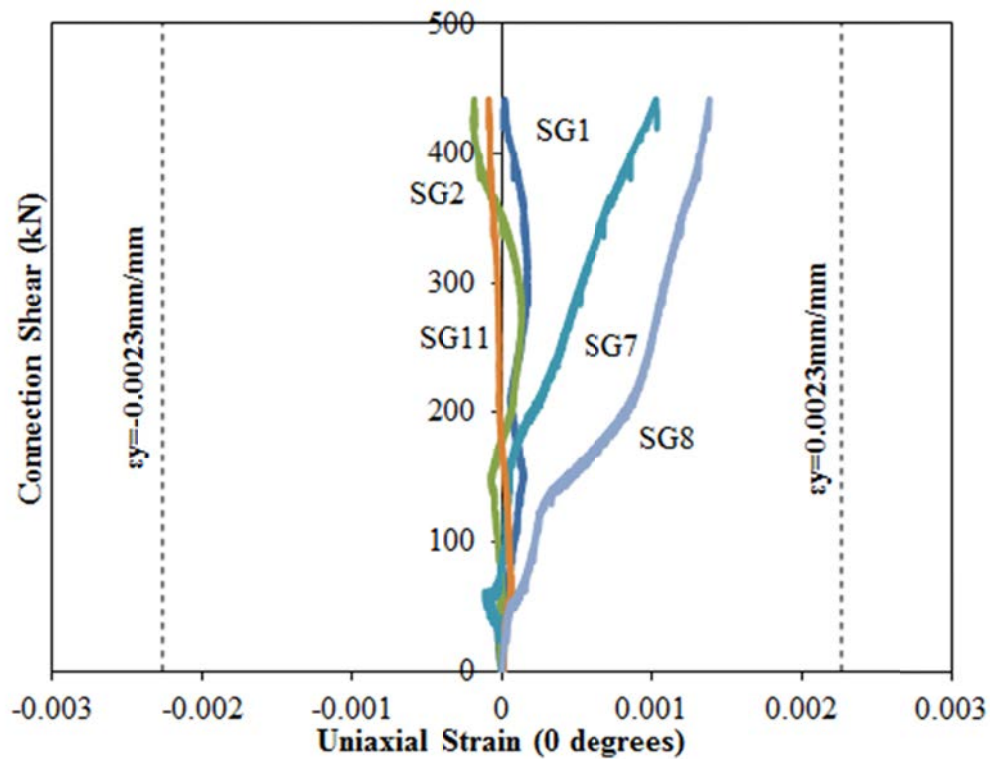


Figure D-98: Connection Shear vs. Uniaxial Strain (0°), Configuration 8

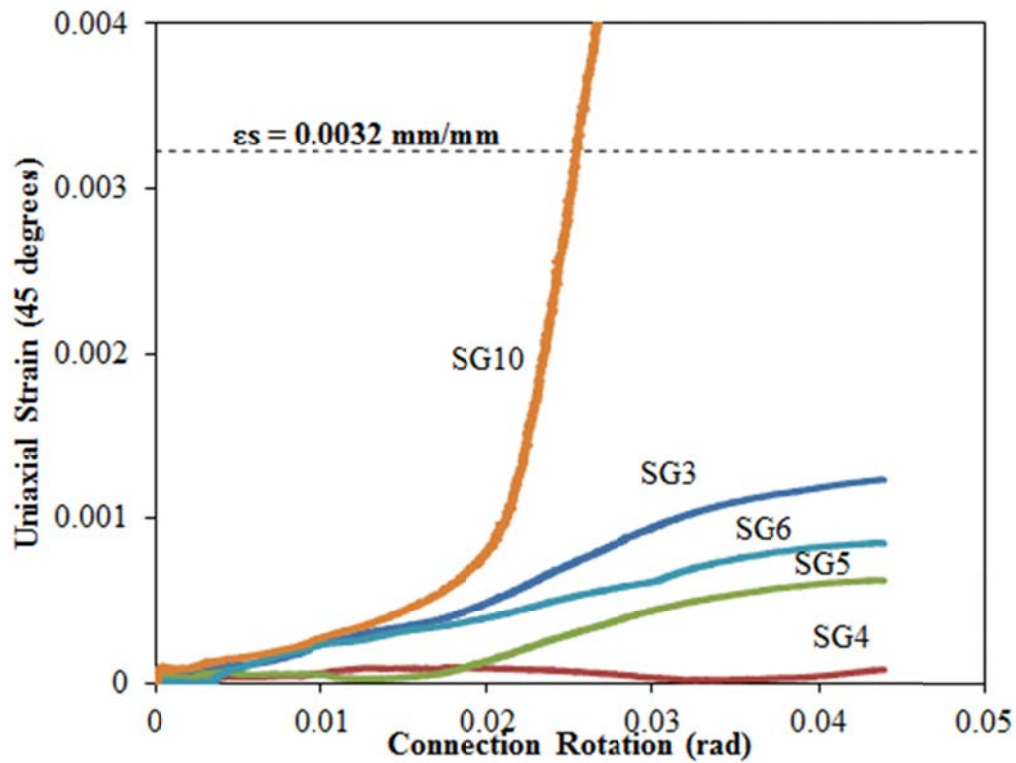


Figure D-99: Uniaxial Strain (45°) vs. Connection Rotation, Configuration 8

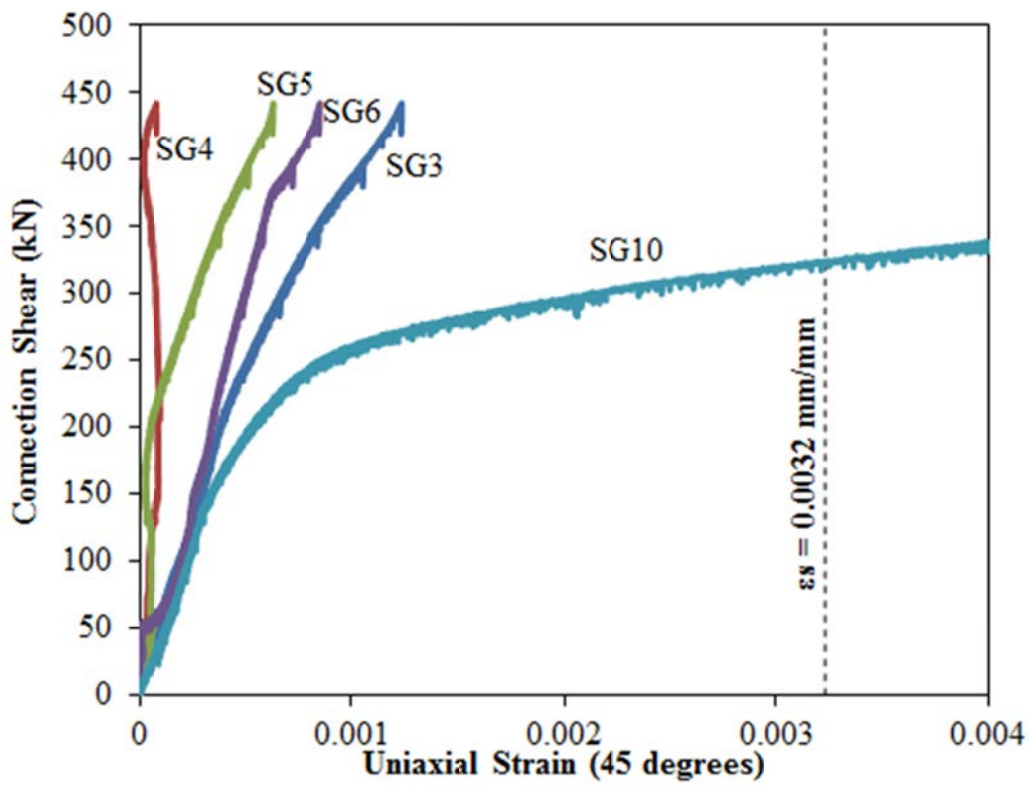


Figure D-100: Connection Shear vs. Uniaxial Strain (45°), Configuration 8

Bolt Bearing

Bearing deformation was seen both in the bolt holes located inside the supported beam as well as those inside the stiffener. The deformation in the beam holes was mostly vertical and that within the stiffener was rotational. Inclinoimeters and string potentiometers were attached to the bottom of the beam and the face of the shear tab to measure rotation and deflection, respectively (see Figure D-101).

Figures D-102 and D-103 show the relative rotation of the bolt group within the stiffener and beam, respectively. That within the stiffener was seen to be much greater than the beam. The rotational bearing stiffness within the stiffener decreases after approximately 360 kN and this can also be seen on the Shear – Rotation Curve (see Rotation History).

The vertical deformation within the beam bolt holes can be seen in Figure D-104. The deformation was seen to increase over the duration of the test at a constant rate.

The global stiffness of the connection began to decrease simultaneously with the decrease in rotational stiffener bearing stiffness. Thus, the experimental bearing failure connection load was seen to be 410 kN. At this point, the stiffness had decrease substantially and the bottom of the beam flange began to bear on the stiffener. This contact can be seen in Figure D-105.

The extent of bolt hole deformation in both the beam and the stiffener can be seen in Figure D-106. The vertical deformation within the beam caused a tension field to develop and this can be seen in Figure D-107.

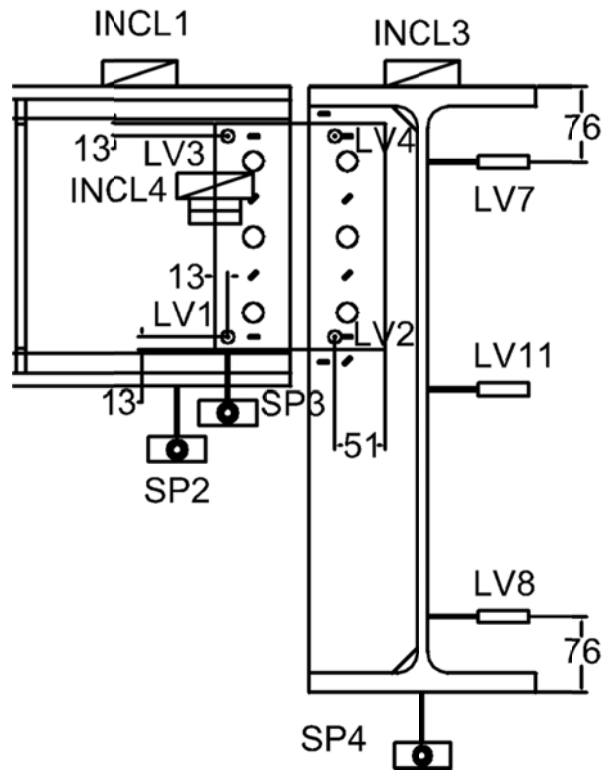


Figure D-101: Instrumentation Layout, Configuration 8

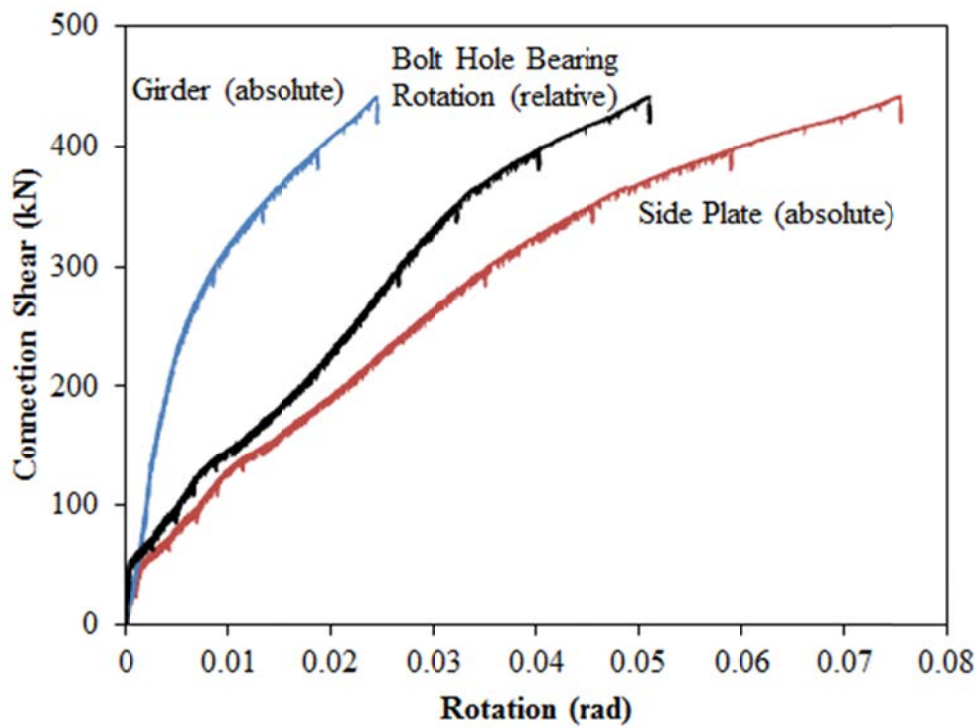


Figure D-102: Connection Shear vs. Stiffener Bolt Bearing Rotation, Configuration 8

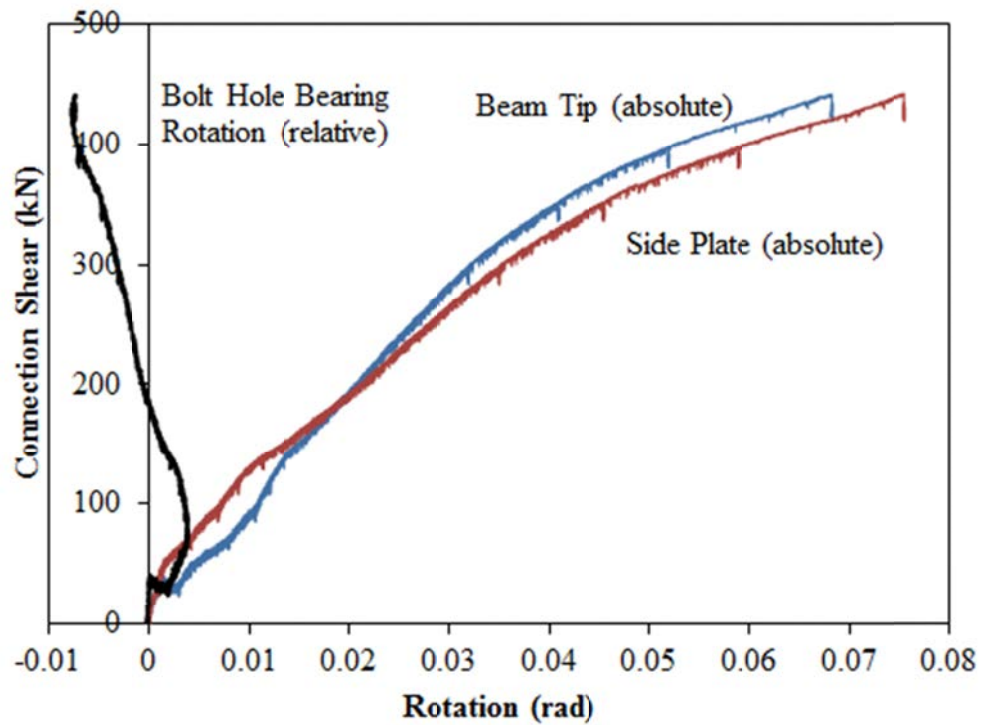


Figure D-103: Connection Shear vs. Beam Bolt Bearing Rotation, Configuration 8

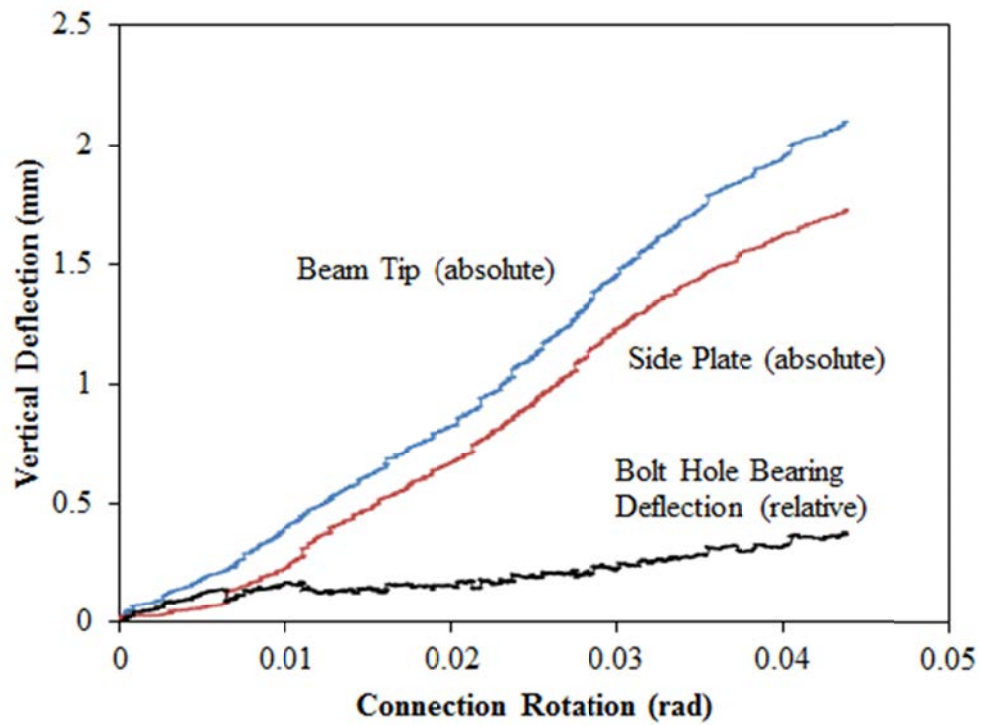


Figure D-104: Relative Beam Bearing Deflection vs. Connection Rotation, Configuration 8



Figure D-105: Bearing Deformation in Girder Stiffener, End of Test, Configuration 8

Beam



Stiffener



Figure 106: Deformed Bolt Holes, Beam and Stiffener, Configuration 8



Figure D-107: Tension Field on Beam Web, End of Test, Configuration 8

Yielding of Supporting Girder

Strain gauges were placed on the supporting girder to measure the extent of deformation during the test. The data can be seen in Figures D-109 and D-110. SG13 and SG14 were placed on top of the girder flange on the shear tab side and plain side, respectively (see Figure D-96). SG15 was placed on the beam web, opposite the stiffener (see Figure D-96).

The girder was seen to behave elastically for the test. A sharp increase in strain on the girder web (SG15) can be seen at 0.018 radians and again at 0.039 radians. The first spike could be due to bolt slipping. The second was most likely due to the bottom beam flange bearing on the stiffener, causing axial stresses on the stiffener which were transferred to the girder web.

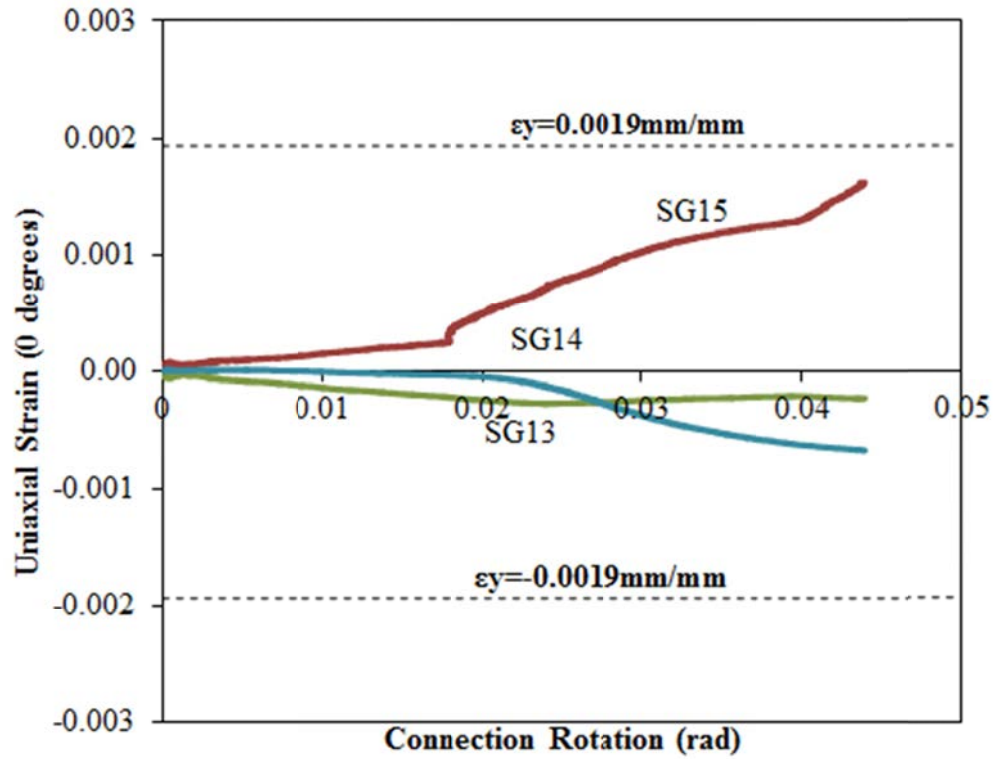


Figure D-108: Girder Strain vs. Connection Rotation, Configuration 8

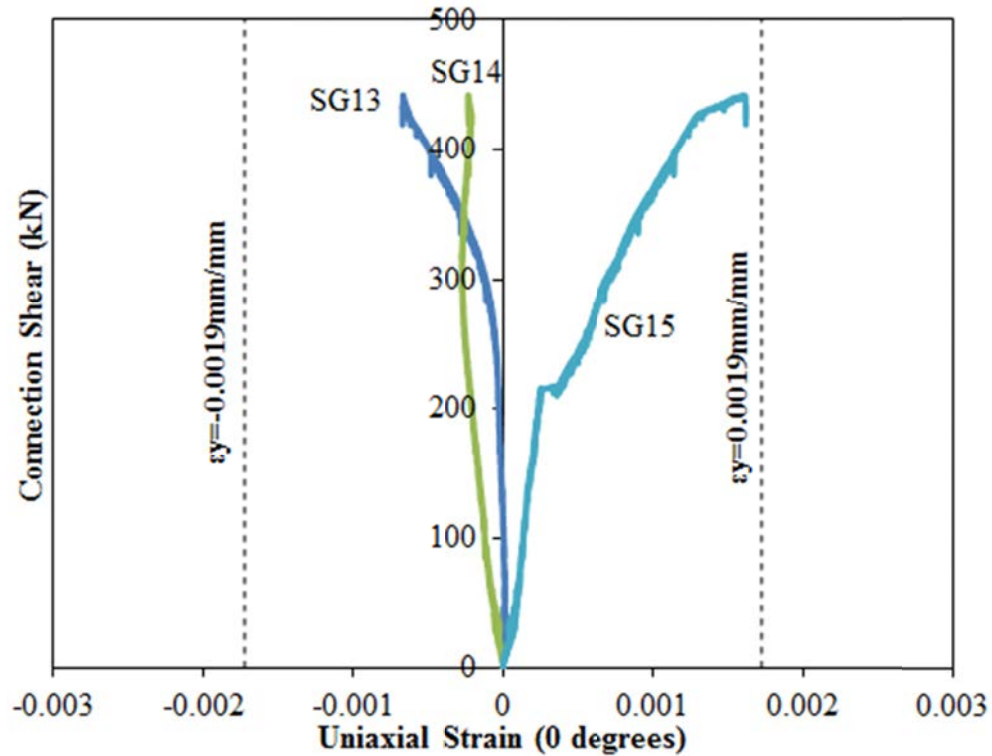


Figure D-109: Connection Shear vs. Girder Strain, Configuration 8

TEST SUMMARY OF CONFIGURATION 9

STIFFENERS
PL $\frac{1}{2}$ x3 $\frac{3}{4}$ x11"
A572-GR50

SHEAR TAB
PL $\frac{3}{8}$ x9 $\frac{7}{16}$ "x13 $\frac{11}{16}$ "
A572-GR50

GIRDER
W30x173
A992

BEAM
W12x40
A992

BOLTS
 $\frac{3}{4}$ " x 1 $\frac{3}{4}$ "
A325-T1

1.50"
3.00"
3.00"
1.50"

2.96"

1.50" 3.00" 1.50" 8.00"

9.50"

1'-1.50"

TYP. $\frac{1}{4}$ "

D - 96

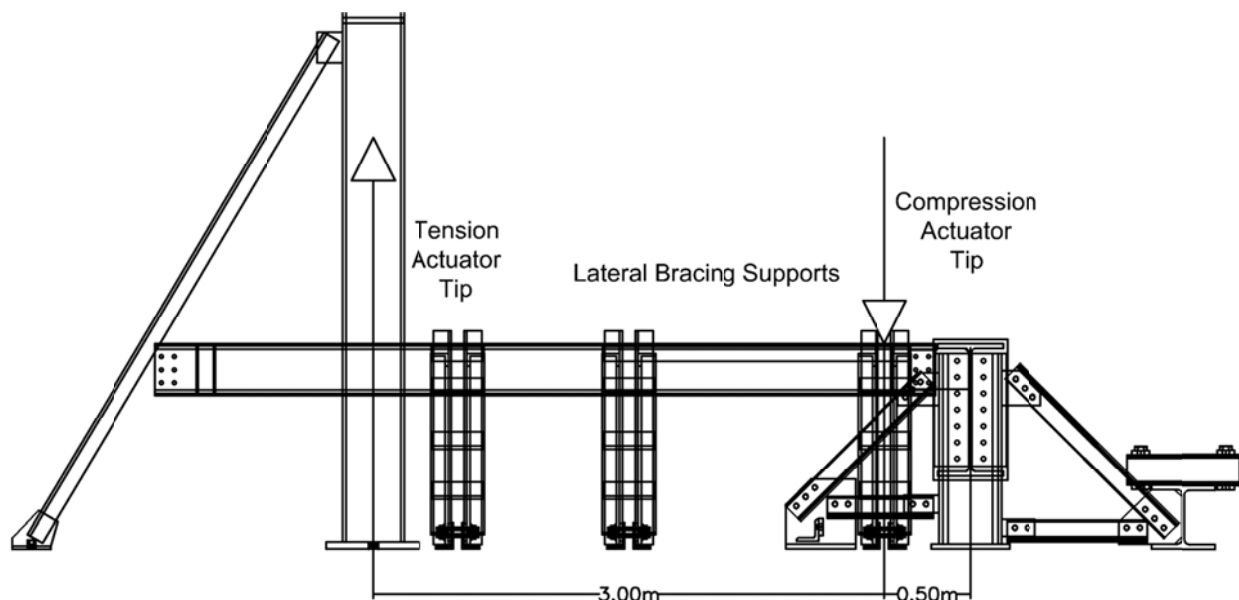
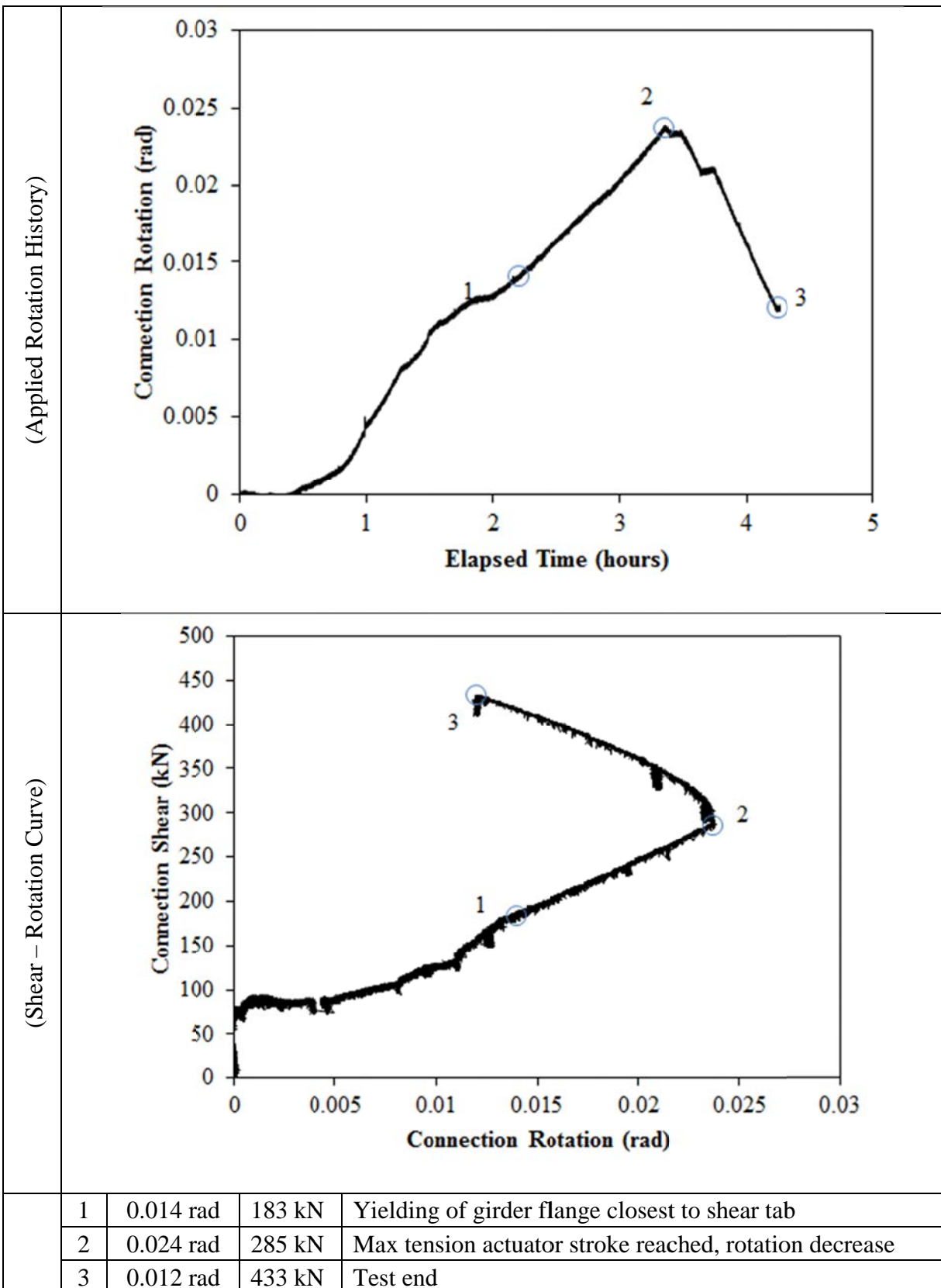


Figure D-111: Test Setup, Configuration 9

MATERIAL PROPERTIES AND SPECIMEN DETAILS

Member	Size	Grade	Yield Stress (MPa)		Ultimate Stress (MPa)	
			Mill Cert.	Coupon	Mill Cert.	Coupon
Beam	W12x40	A992	367	Flange:376 Web:414	485	Flange:492 Web:511
Beam Stiffeners	PL1/2"x3 3/4"	A572-GR50	-	-	-	-
Girder	W30x173	A992	390	-	515	-
Shear Tab	PL3/8"x9 7/16"	A572-GR50	452	456	531	525
Bolts	3/4" x 1 3/4"	A325-T1	3 rows of 2 bolts; 3" spacing, 1 1/2" end distance; snug tight; one washer per bolt; 13/16" bolt holes;			
Welding Procedure Specification	Electrode Classification E70					
	Welding Procedure <i>Shop Welding:</i> FCAW-G (flux-cored arc welding with gas shielding) <ul style="list-style-type: none">Fillet Weld, Shear Tab and Stiffener to Girder"C" Weld, Beam Stiffeners					
Boundary Condition	Tension Actuator Capacity: 268kN tension, 495kN compression; Stroke: 254mm; Displacement controlled					
	Compressive Actuator Capacity: 8018 kN tension, 11414kN compression; Stroke: 305mm; Displacement controlled					
	Lateral Bracing System Top and bottom flange out of plane movement restrained by ball and socket rods fixed to frame tensioned to strong floor					

ROTATION HISTORY AND KEY EXPERIMENTAL OBSERVATIONS



Note: The variation in stiffness seen during the first 0.0135 radians of rotation is due to adjustment of the displacement rates of both tension and compression actuators to achieve the desired stiffness. Once this stiffness value was reached, the ratio of rates was held constant for the remainder of the test.

Note: After 0.024 radians of rotation, the maximum stroke for the tension actuator was reached. The tension actuator displacement was held constant from this point onward while the compressive actuator displacement continued to be increased. The result was decreasing rotation with increasing shear.

RESISTANCE SUMMARY

Limit State	Design Check	Predicted	Observed
Girder Yielding	-	-	183 kN
Bolt Bearing	AISC 14 th Ed, Part 10, Extended Shear Tabs, Design Check 1 & S16-09 Clause 13.12.1.2	278 kN	-
Combined Shear and Flexural Yielding	AISC Manual, 14 th Ed; Part 10; Equation 10-5	202 kN	

TEST OBSERVATIONS

Combined Shear and Flexural Yielding

Deformation within the tab was monitored using a combination of horizontal and inclined strain gauges organized as seen in Figure D-112. White wash was applied to the tab such that the yielding pattern could be observed. The deformed shear tab at the end of test can be seen in Figure D-113.

Horizontal strain gauges were placed on the top and bottom edges of the tab to record flexural strains and the results can be seen in Figure D-114 and D-115. Tension yielding was seen at 0.021radian rotation at the location of SG15.

Strain gauges oriented to 45° were placed along the height of the tab to measure shear strains and the results can be seen in Figure D-116 and D-117. Shear yielding was not seen during the test.

Combined shear and flexural yielding did not occur for this test.

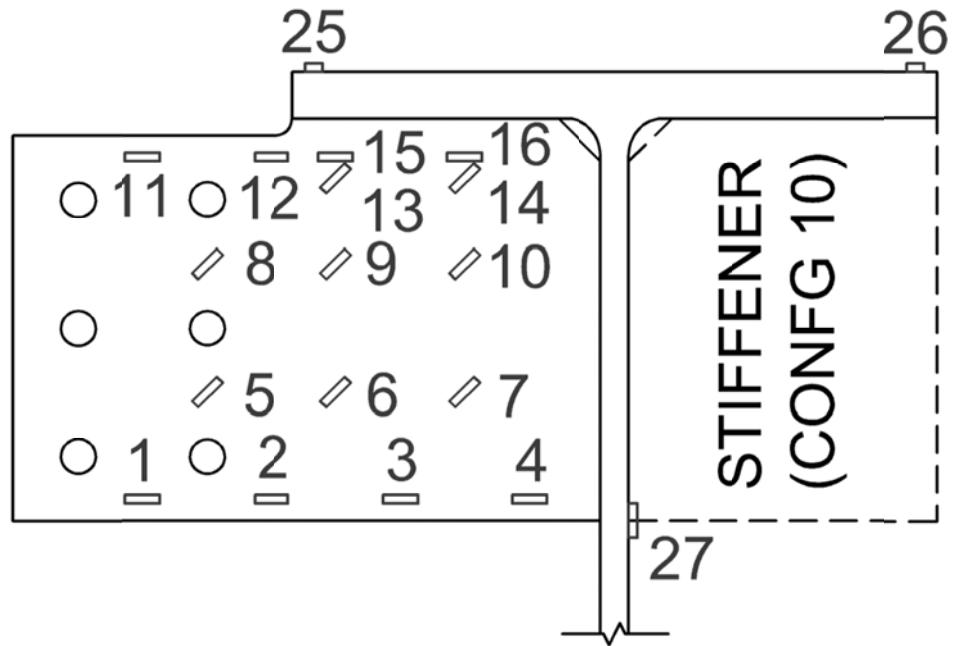


Figure D-112: Strain Gauge Layout, Configuration 9



Figure D-113: Shear Tab, End of Test, Configuration 9

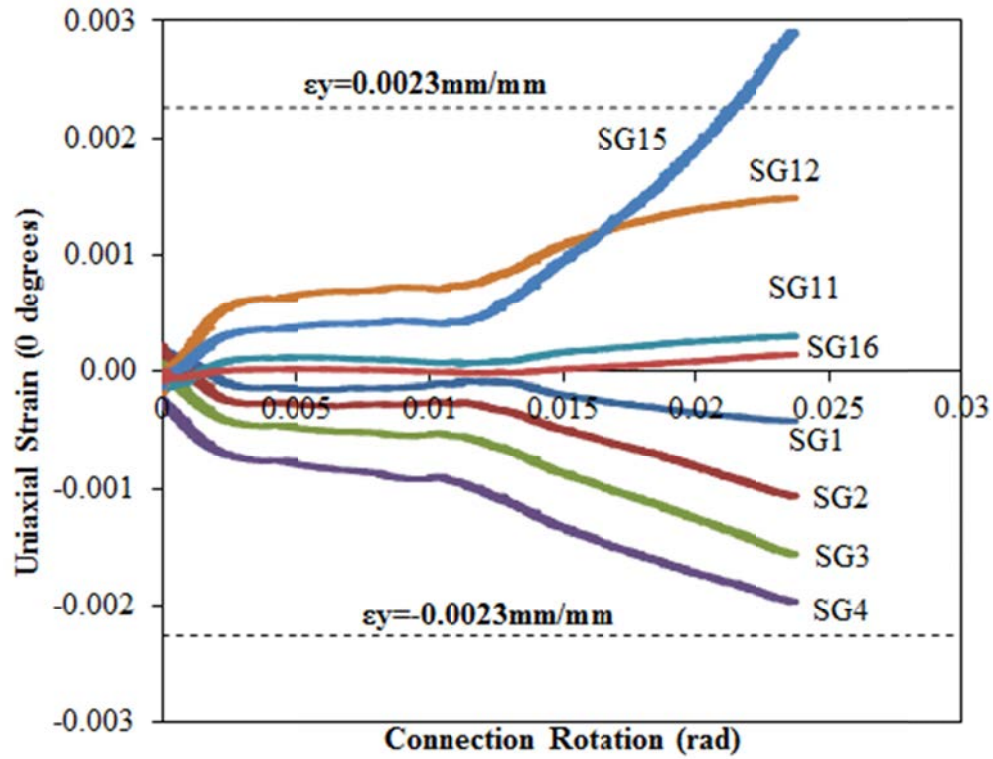


Figure D-114: Uniaxial Strain (0°) vs. Connection Rotation, Configuration 9

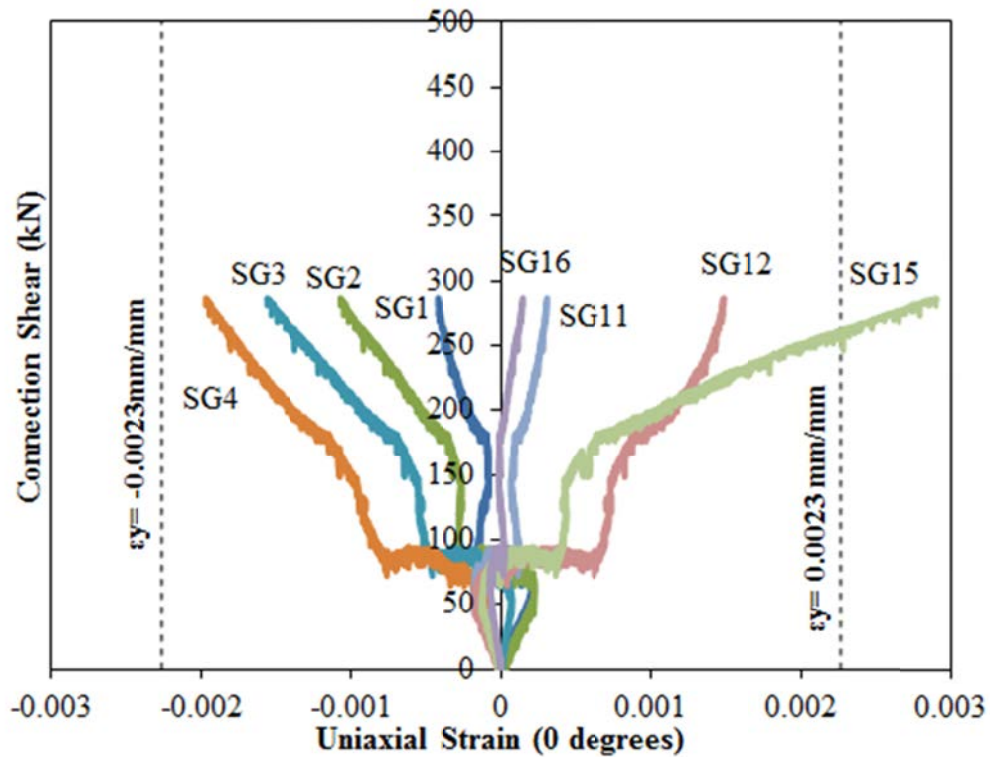


Figure D-115: Connection Shear vs. Uniaxial Strain (0°), Configuration 9

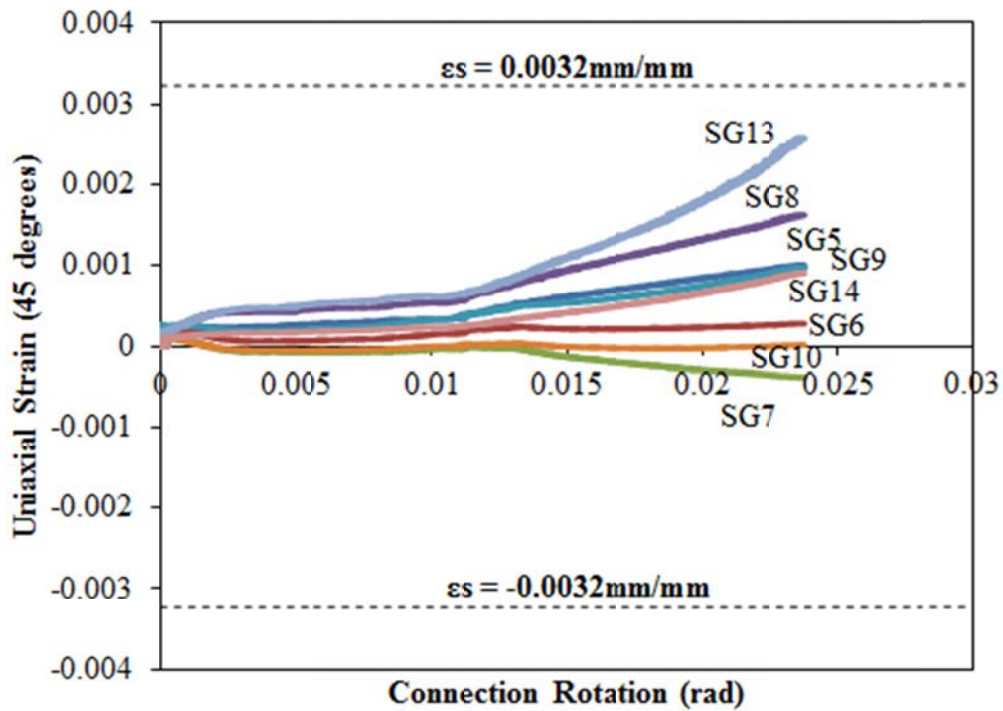


Figure D-116: Uniaxial Strain (45°) vs. Connection Rotation, Configuration 9

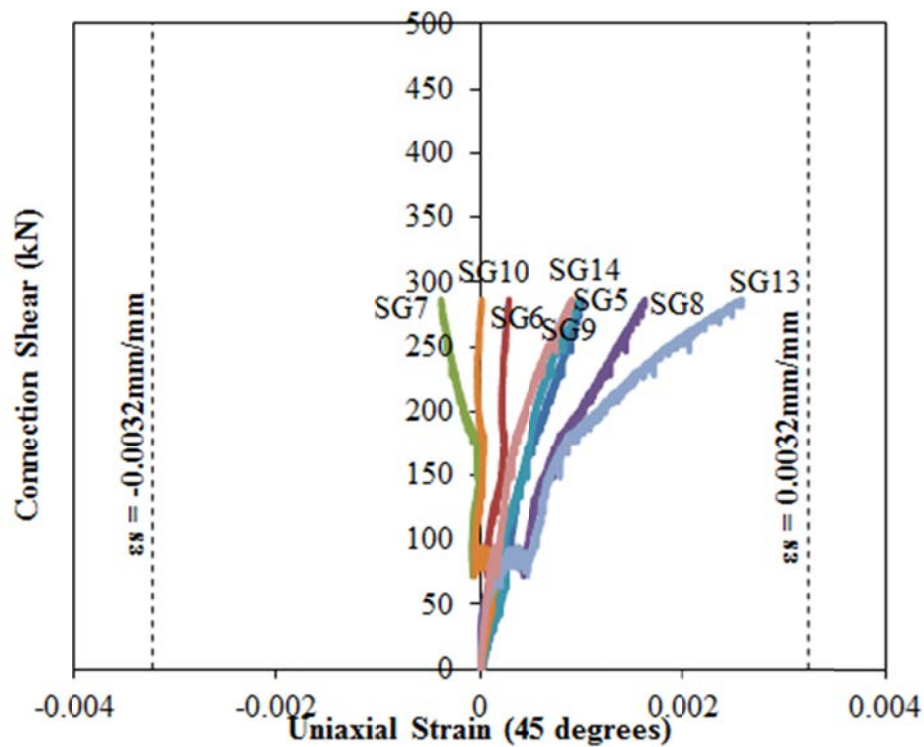


Figure D-117: Connection Shear vs. Uniaxial Strain (45°), Configuration 9

Yielding of Supporting Girder

Significant plastic deformation occurred in the web and top flange of the girder during the test. Rotation of the shear tab caused compressive stresses to develop along the centre line of the girder web, as well as tension stresses along the underside of the flange. Bulging of the girder web on the opposite side of the shear tab and depression of the top flange above the shear tab was significant. Figure D-118 shows the extent of yielding of the girder web at the edge of the shear tab.

Strain gauges were placed on the supporting girder to measure the extent of this deformation and the data can be seen in Figures D-121 and D-122. SG25 and SG26 were placed on top of the girder flange on the shear tab side and plain side, respectively (see Figure D-112). Compression yielding at SG25 occurred at 0.014 radian rotation. SG27 was placed vertically on the girder web opposite the base of the shear tab.

A combination of inclinometers and LVDTs were used to measure the extent of girder web bulging. An inclinometer (INC3) was placed on top of the girder flange and LVDTs 11 and 7 were placed on the back side of the girder web (see Figure D-119). The girder web rotation was computed using the two LVDT measurements and the distance in between. This was compared with the top flange rotation to see the relative web rotation and this is shown. This relative rotation was found to be negligible.

Since plastic behaviour is only supposed to occur inside the shear tab and supported beam, it can be said that the girders elastic limit was reached when the top flange began to behave plastically. This occurred at 0.014 radians.



Figure D-118: Yielding of Girder Web at Shear Tab Edge, Configuration 9

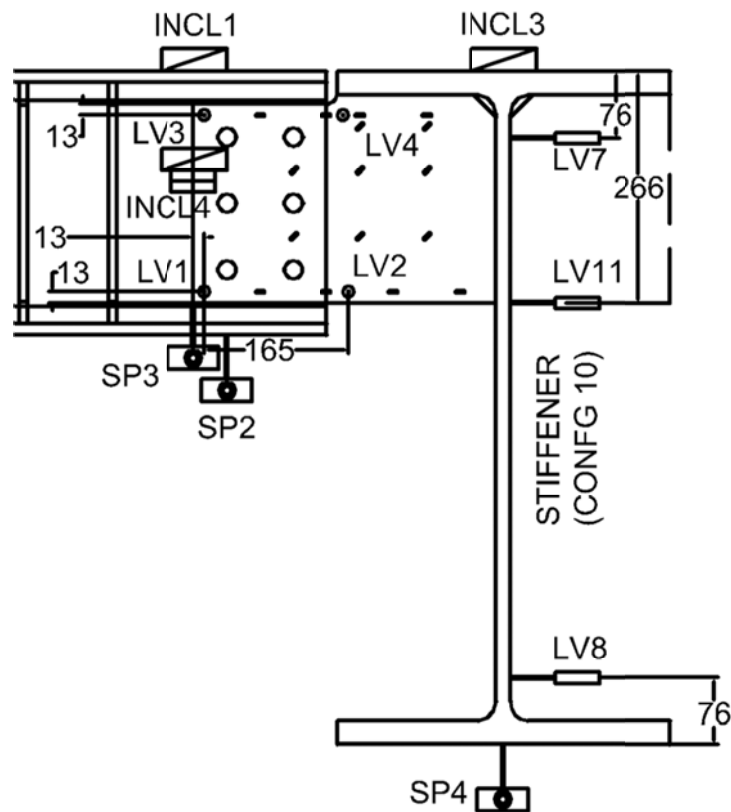


Figure D-119: Instrumentation Details, Configuration 9

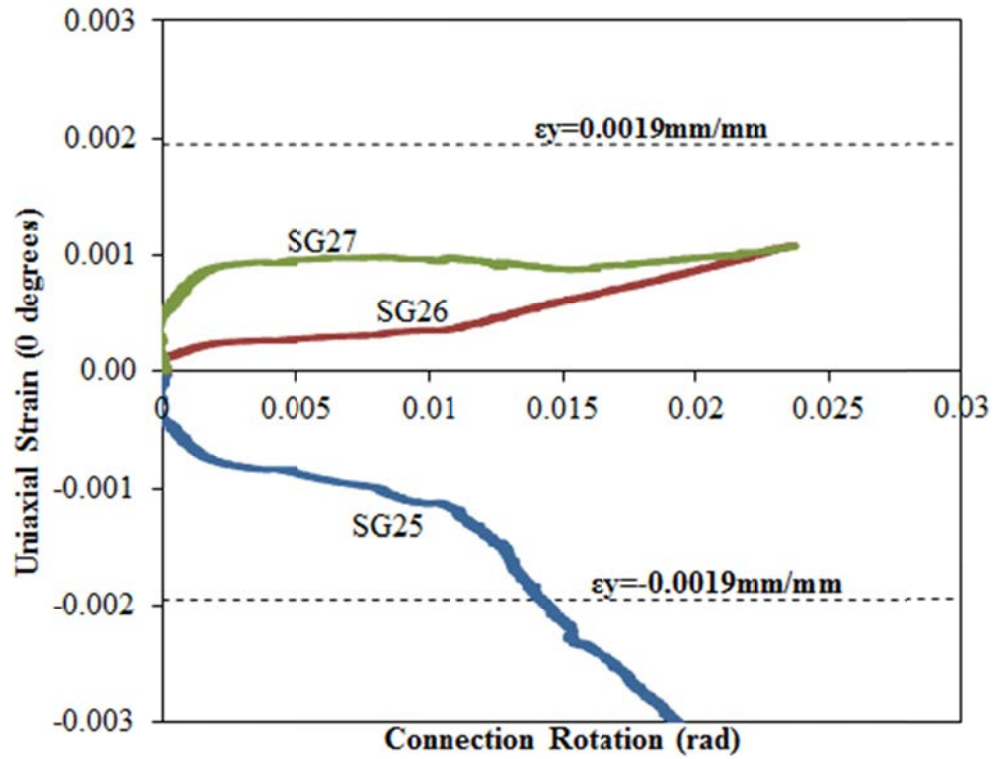


Figure D-120: Girder Strain vs. Connection Rotation, Configuration 9

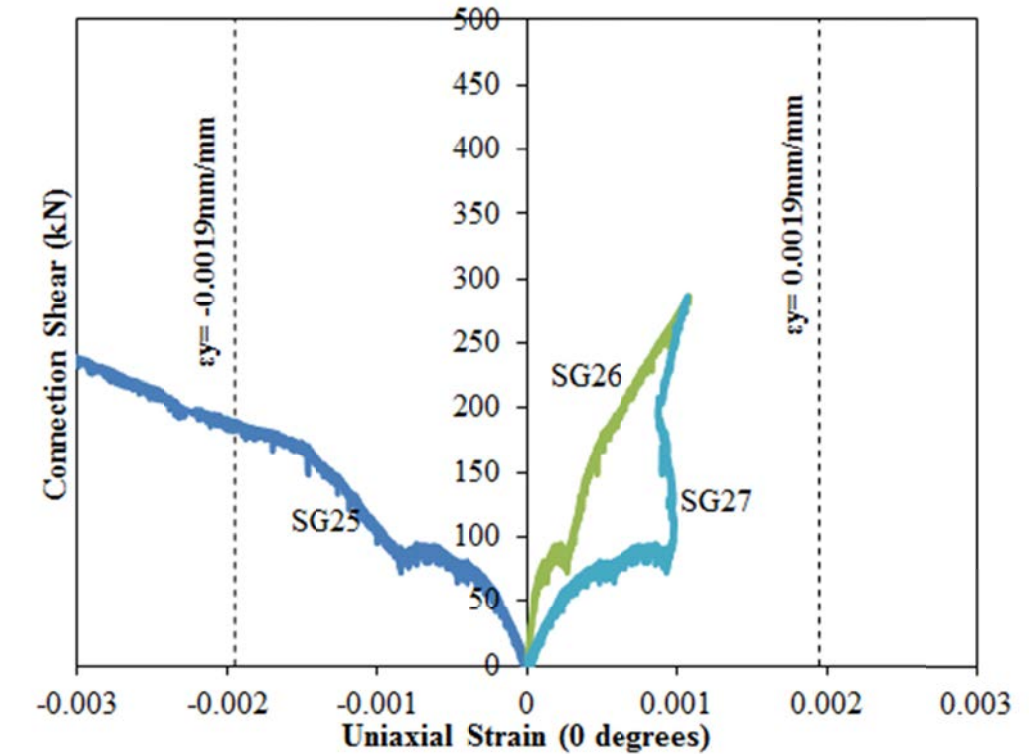


Figure D-121: Connection Shear vs. Girder Strain, Configuration 9

Bearing

Slight rotational bearing deformation was seen during the test. Inclinometers and string potentiometers were attached to the bottom of the beam and the face of the shear tab to measure rotation and deflection, respectively (see Figure D-119). The bearing deformation was computed as the difference in rotation or vertical deflection between the shear tab and the supported beam.

Figures D-123 shows the relative bolt hole bearing rotation within the beam. The relative bearing deflection was seen to be insignificant. The relative bearing rotation increased constantly over the test reaching a maximum value of 0.014 radians. It should be noted that until a 180 kN connection load, the global stiffness was being adjusted. The rotation values before this point were ignored.

Since the rotational and vertical bearing stiffness was constant, it can be said that the limit state of bearing failure is not applicable. The tension field on the beam web can be seen in Figure D-122.

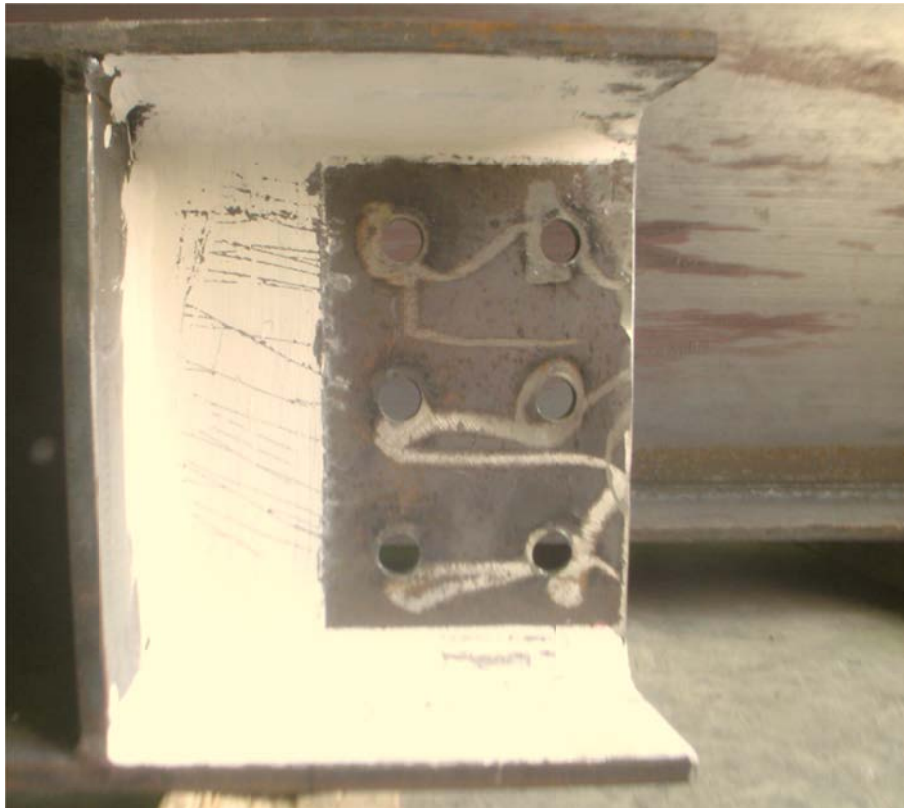


Figure D-122: Tension Field on Beam Web, End of Test, Configuration 9

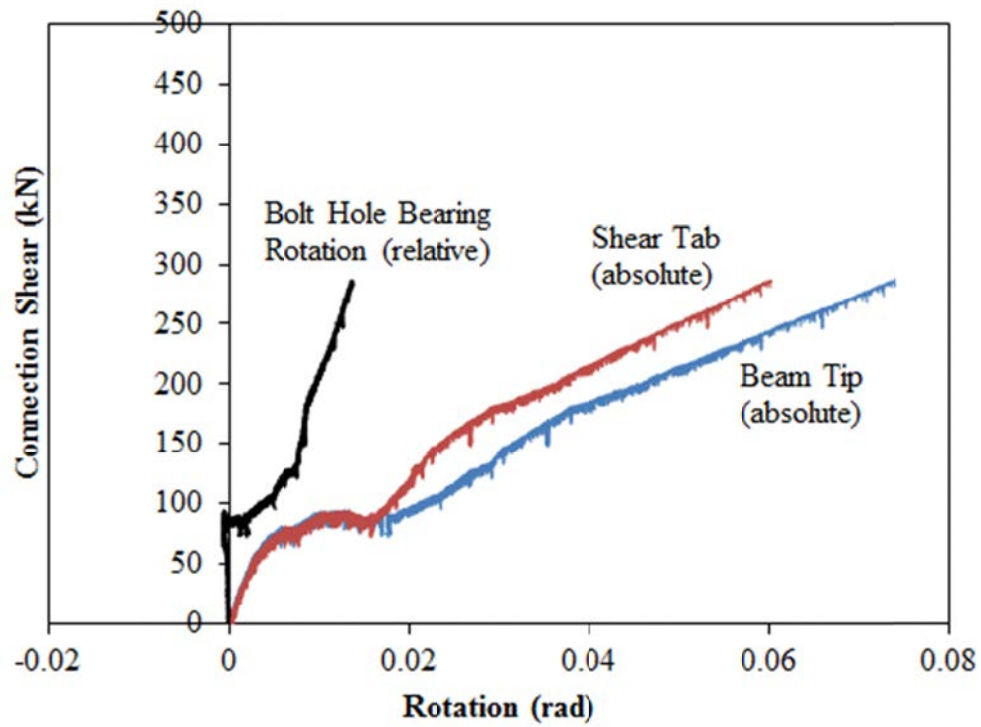


Figure D-123: Connection Shear vs. Relative Bearing Rotation, Configuration 9

EXTENDED SHEAR TAB CONNECTION EXPERIMENTAL STUDY

TEST SUMMARY OF CONFIGURATION 10

Specimen ID	CONFIGURATION 10
Key Words	Shear Tab, Extended Configuration; Flexible Support Condition; Beam to Girder;
Test Location	Structures Lab, Macdonald Engineering Building, McGill University
Test Date	July 10, 2013
Investigators	Colin A. Rogers, Dimitrios G. Lignos, Jacob W. Hertz
Main References	AISC Steel Construction Manual, 13th & 14th Editions; CISC Handbook of Steel Construction, 10th Edition
Sponsors	ADF Group Inc., DPHV and NSERC

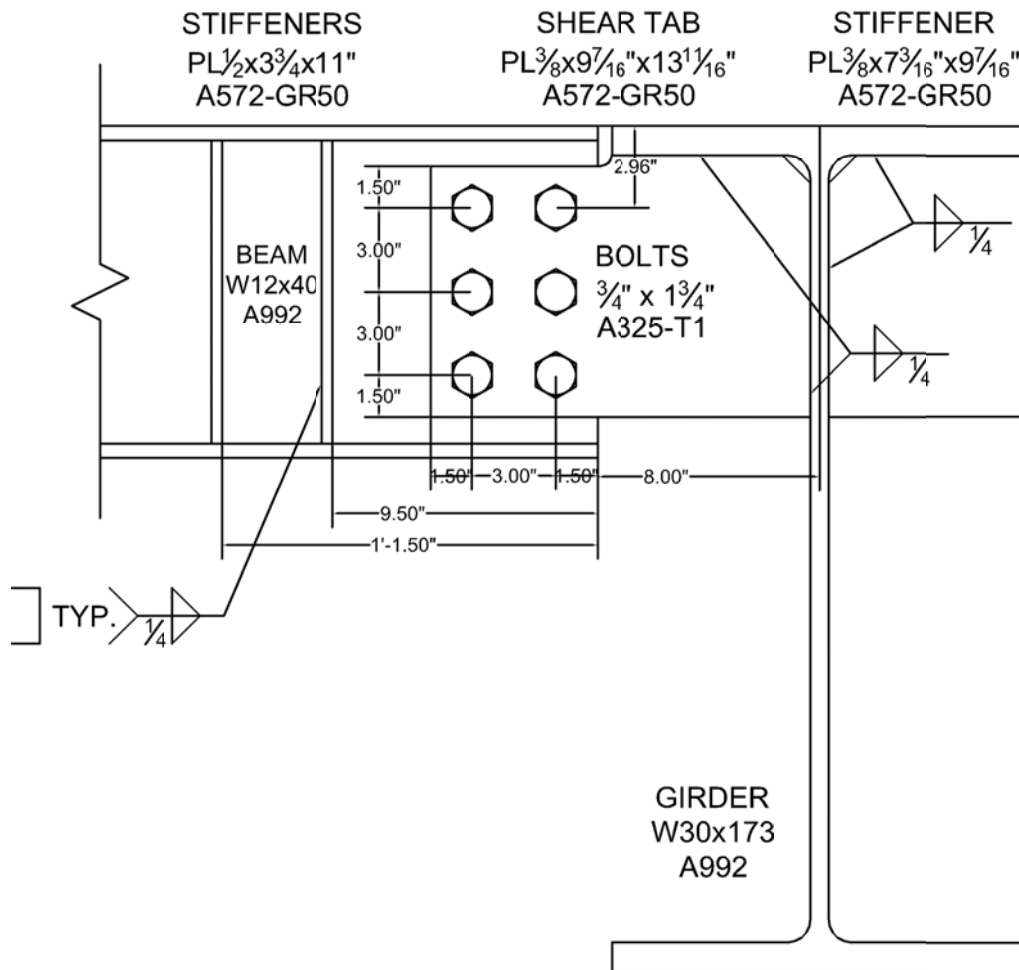


Figure D-124: Connection Details, Configuration 10

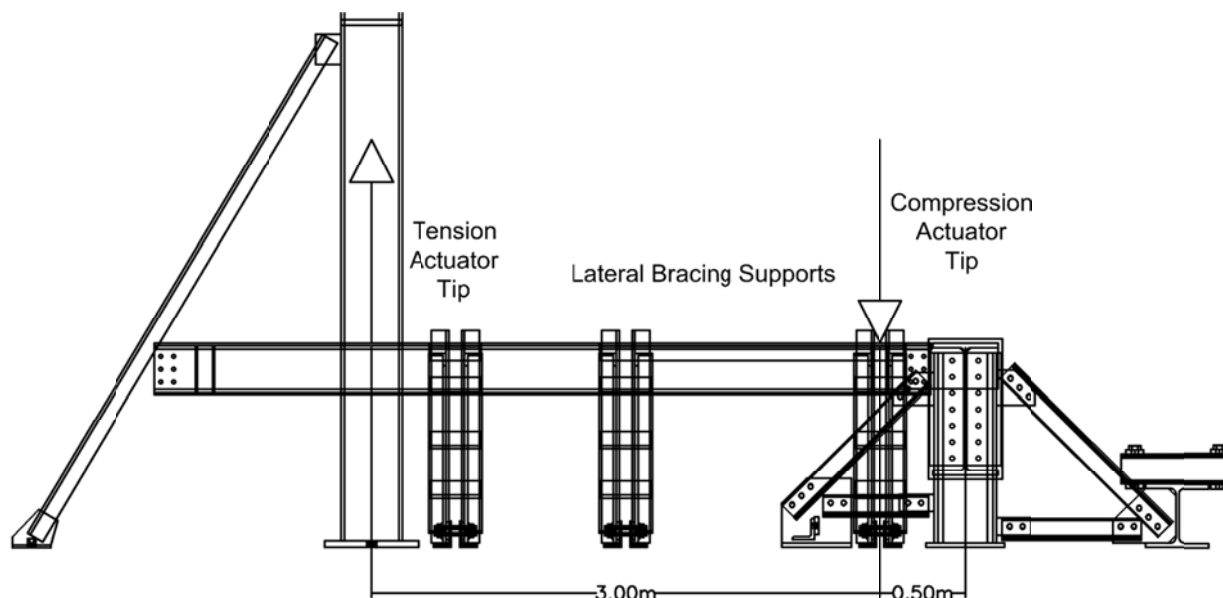
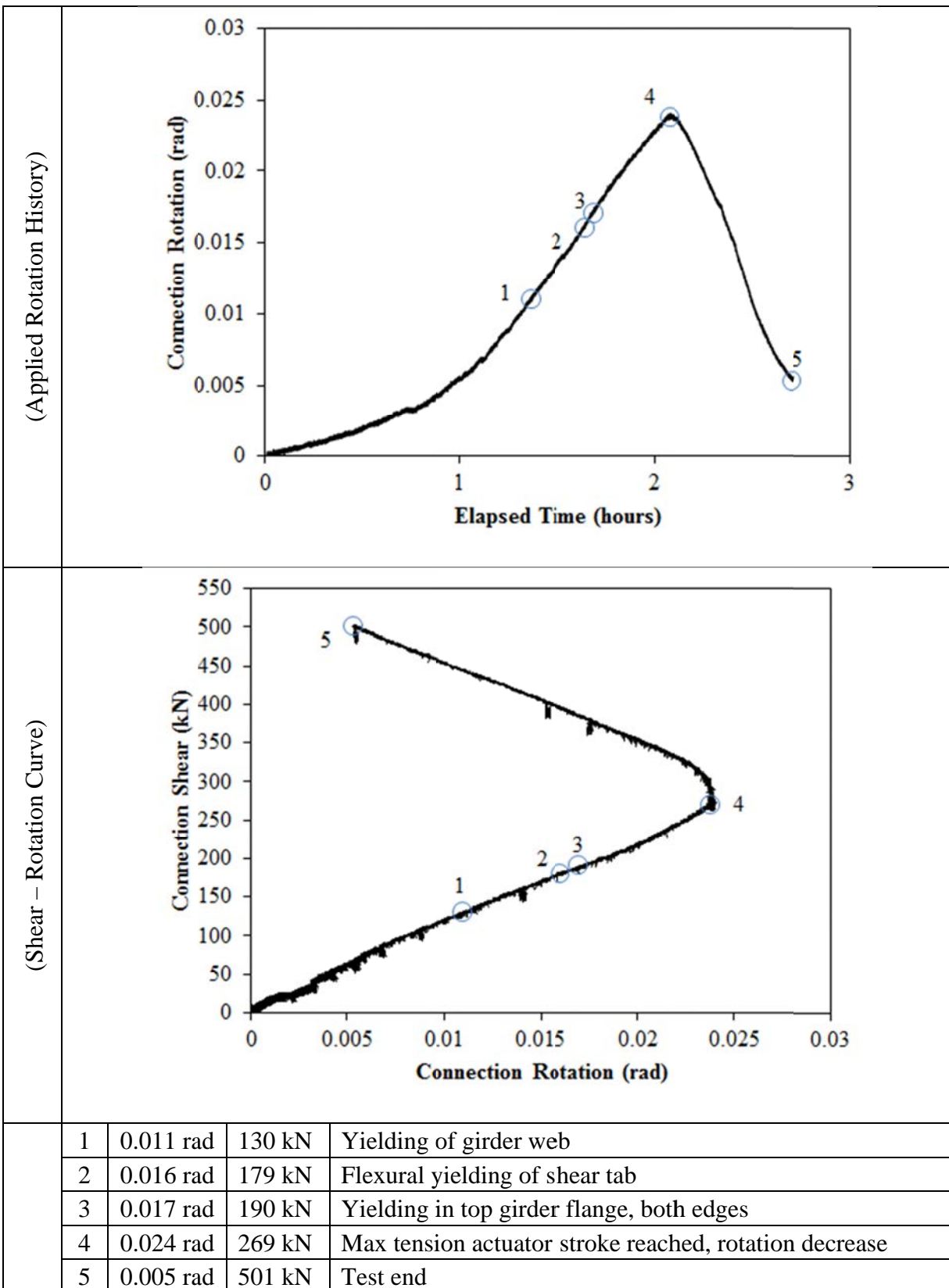


Figure D-125: Test Setup, Configuration 10

MATERIAL PROPERTIES AND SPECIMEN DETAILS

Member	Size	Grade	Yield Stress (MPa)		Ultimate Stress (MPa)	
			Mill Cert.	Coupon	Mill Cert.	Coupon
Beam	W12x40	A992	367	Flange:376 Web:414	485	Flange:492 Web:511
Beam Stiffeners	PL1/2"x3 3/4"	A572-GR50	-	-	-	-
Girder	W30x173	A992	390	-	515	-
Shear Tab	PL3/8"x9 7/16"	A572-GR50	452	456	531	525
Girder Stiffener	PL3/8"x7 3/16"	A572-GR50	452	456	531	525
Bolts	3/4" x 1 3/4"	A325-T1	3 rows of 2 bolts; 3" spacing, 1 1/2" end distance; snug tight; one washer per bolt; 13/16" bolt holes;			
Welding Procedure Specification	Electrode Classification E70					
	Welding Procedure <i>Shop Welding:</i> FCAW-G (flux-cored arc welding with gas shielding) <ul style="list-style-type: none">Fillet Weld, Shear Tab and Stiffener to Girder"C" Weld, Beam Stiffeners					
Boundary Condition	Tension Actuator Capacity: 268kN tension, 495kN compression; Stroke: 254mm; Displacement controlled					
	Compressive Actuator Capacity: 8018 kN tension, 11414kN compression; Stroke: 305mm; Displacement controlled					
	Lateral Bracing System Top and bottom flange out of plane movement restrained by ball and socket rods fixed to frame tensioned to strong floor					

ROTATION HISTORY AND KEY EXPERIMENTAL OBSERVATIONS



Note: The variation in stiffness seen during the first 0.0034 radians of rotation is due to adjustment of the displacement rates of both tension and compression actuators to achieve the desired stiffness. Once this stiffness value was reached, the ratio of rates was held constant for the remainder of the test.

Note: After 0.024 radians of rotation, the maximum stroke for the tension actuator was reached. The tension actuator displacement was held constant from this point onward while the compressive actuator displacement continued to be increased. The result was decreasing connection rotation with increasing connection shear.

RESISTANCE SUMMARY

Limit State	Design Check	Predicted	Observed
Girder Yielding	-	-	130 kN
Flexural Yielding (Gross Section)	AISC 14 th Ed, Gross Plate Bending	235 kN	179 kN
Bolt Bearing	AISC 14 th Ed, Part 10, Extended Shear Tabs, Design Check 1 & S16-09 Clause 13.12.1.2	315 kN	-

TEST OBSERVATIONS

Combined Shear and Flexural Yielding

Deformation within the tab was monitored using a combination of horizontal and inclined strain gauges organized as seen in Figure D-126. White wash was applied to the tab such that the yielding pattern could be observed. The deformed shear tab at the end of test can be seen in Figure D-127.

Horizontal strain gauges were placed on the top and bottom edges of the tab to record flexural strains and the results can be seen in Figure D-128 and D-129. Tension yielding at was first seen the location of SG12 and compression yielding at the location of SG4 occurred simultaneously at 0.016 radians.

Strain gauges oriented to 45° were placed along the height of the tab to measure shear strains and the results can be seen in Figure D-130 and D-131. Shear yielding was not seen during the test.

Since both the top and bottom edges began to behave plastically after 0.016 radians, it can be said that flexural yielding had occurred.

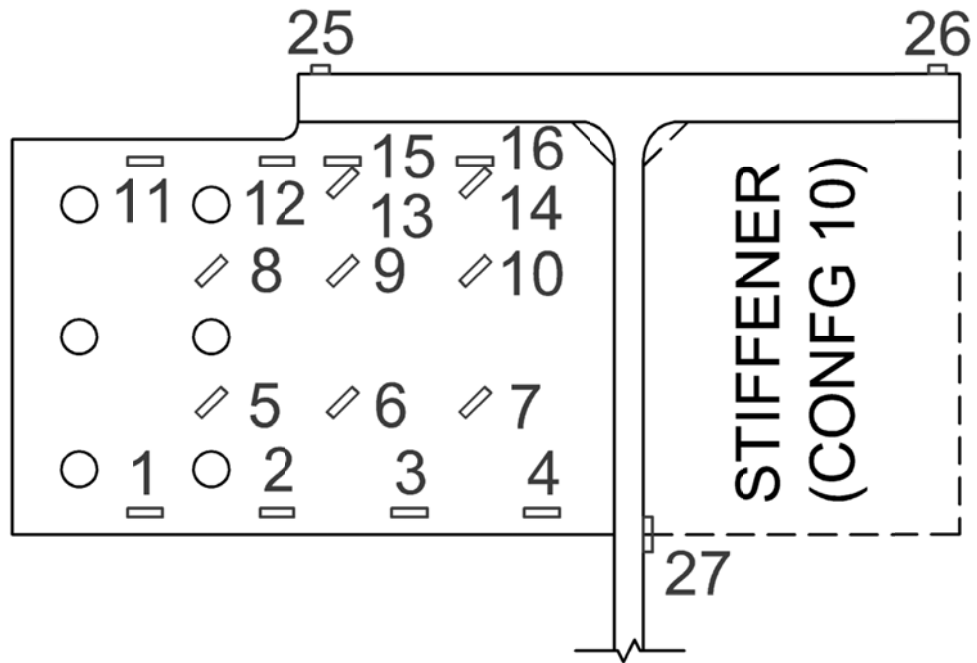


Figure D-126: Strain Gauge Layout, Configuration 10



Figure D-127: Shear Tab, End of Test, Configuration 10

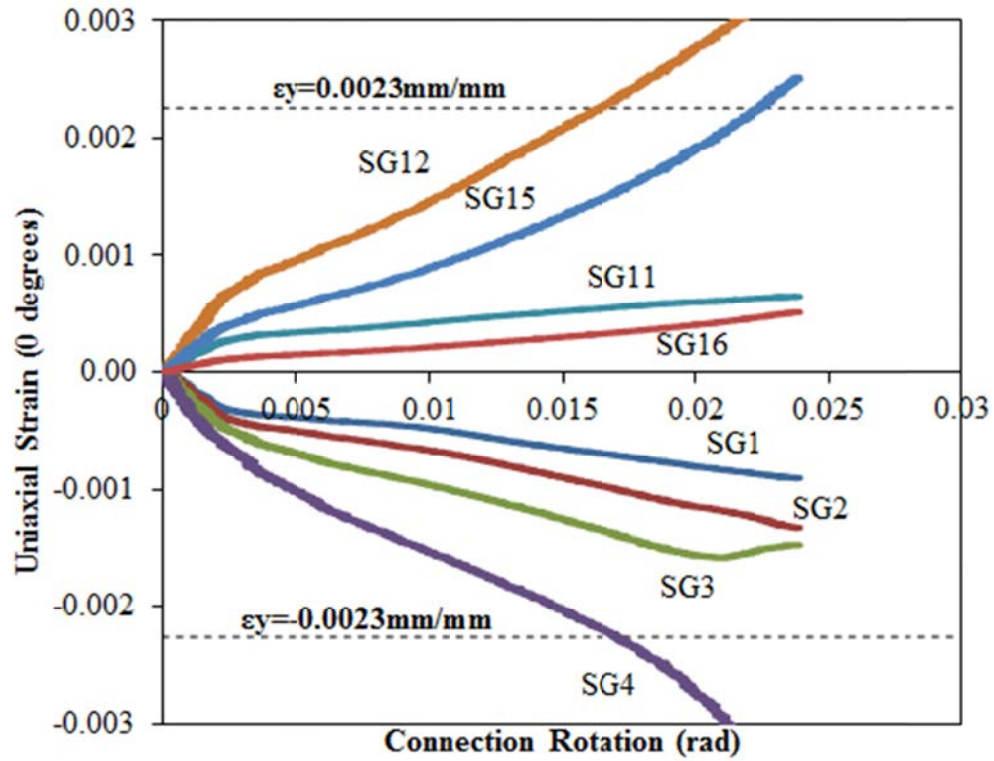


Figure D-128: Uniaxial Strain (0°) vs. Connection Rotation, Configuration 10

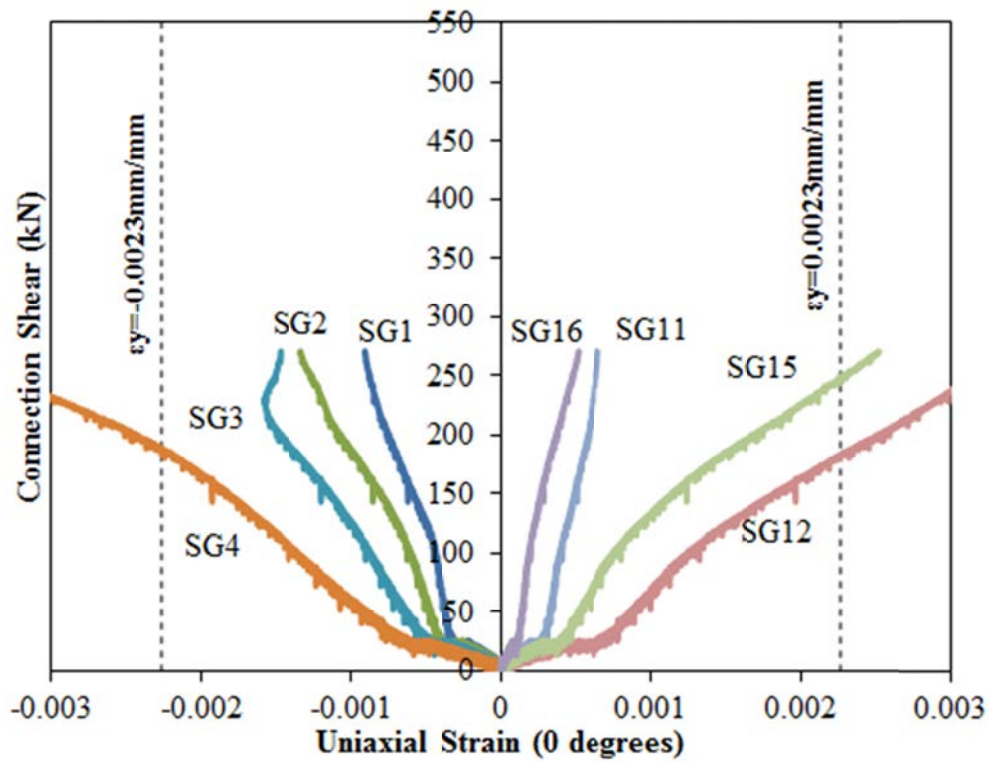


Figure D-129: Connection Shear vs. Uniaxial Strain (0°), Configuration 10

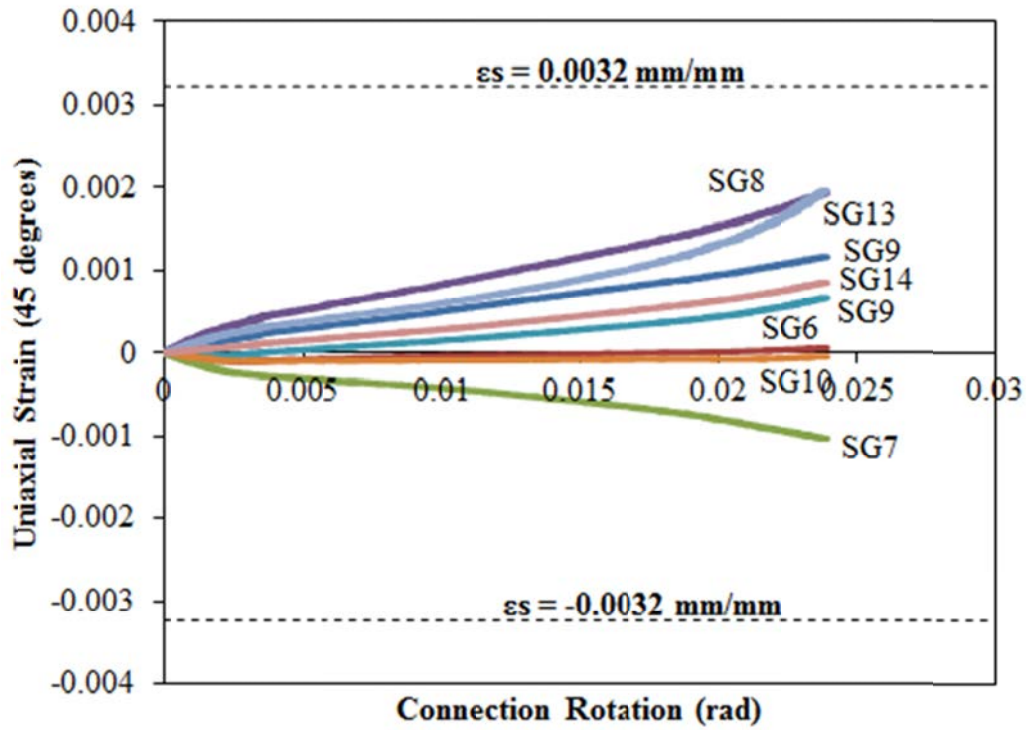


Figure D-130: Uniaxial Strain (45°) vs. Connection Rotation, Configuration 10

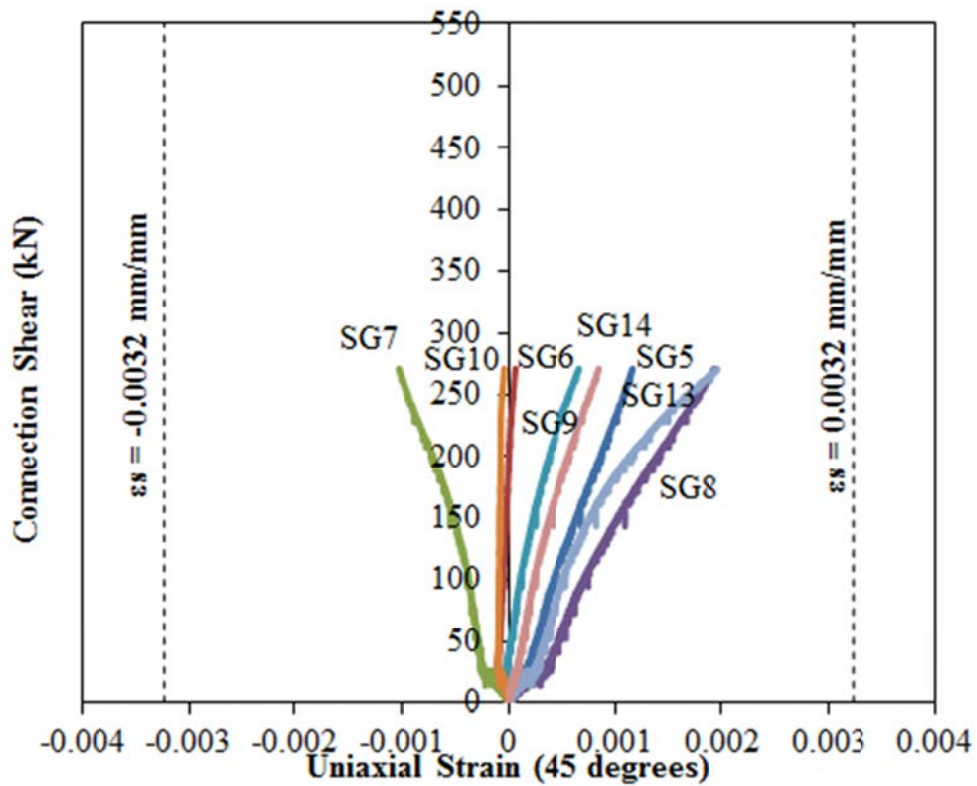


Figure D-131: Connection Shear vs. Uniaxial Strain (45°), Configuration 10

Yielding of Supporting Girder

Significant plastic deformation occurred in the web and top flange of the girder during the test. Rotation of the shear tab caused compressive stresses to develop along the centre line of the girder web, as well as tension stresses along the underside of the flange. Bulging of the girder web on the opposite side of the shear tab and depression of the top flange above the shear tab was significant. Figure D-132 shows the extent of yielding of the girder web at the edge of the shear tab.

Strain gauges were placed on the supporting girder to measure the extent of this deformation and the data can be seen in Figures D-133 and D-134. SG27 was placed vertically on the girder web opposite the base of the shear tab (see Figure D-129) and yielding was seen at 0.011 radians. SG25 and SG26 were placed on top of the girder flange on the shear tab side and plain side, respectively. Compression yielding and tension yielding of the edges of the top flange (SG25 and SG26) occurred simultaneously at 0.017 radian rotation.

A combination of inclinometers and LVDTs were used to measure the extent of girder web deformation. An inclinometer (INC3) was placed on top of the girder flange and LVDTs 11 and 7 were placed on the back side of the girder web (see Figure D-136). The girder web rotation was computed using the two LVDT measurements and the distance in between. This was compared with the top flange rotation to see the relative web rotation. This relative rotation was insignificant.

Since plastic behaviour is only supposed to occur inside the shear tab and supported beam, it can be said that the girders elastic limit occurred when the top flange began to behave plastically. This occurred at 0.011 radians.

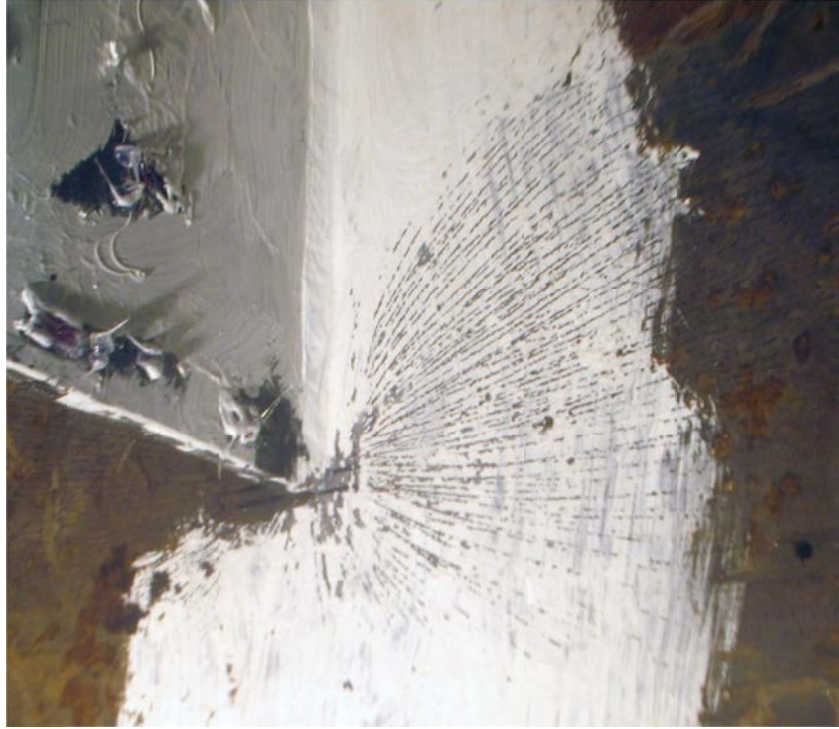


Figure D-132: Yielding of Girder Web at Shear Tab Edge, Configuration 10

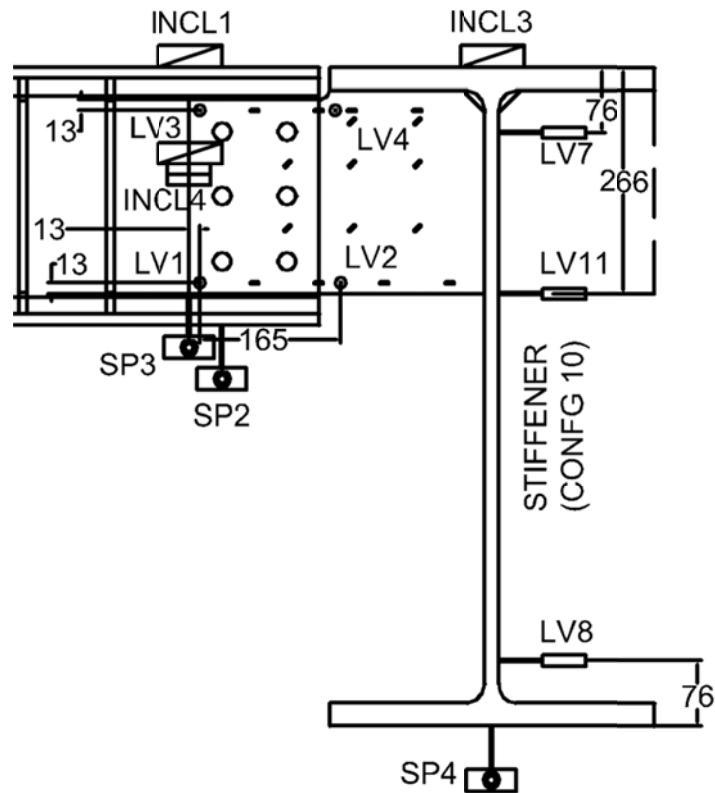


Figure D-133: Instrumentation Details, Configuration 10

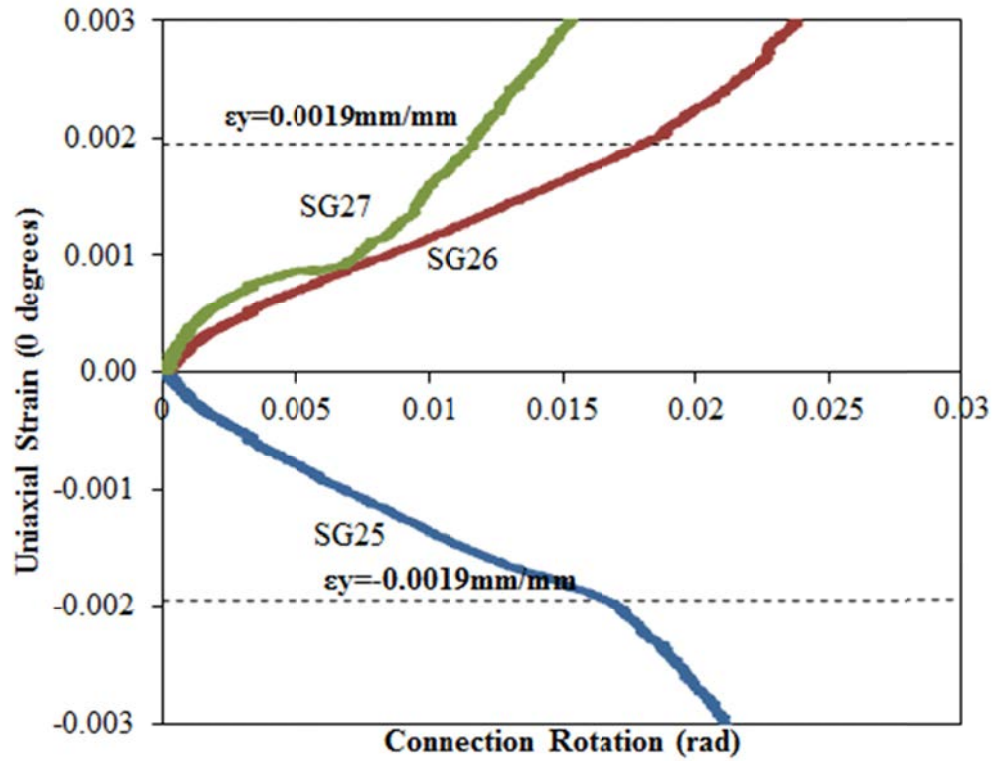


Figure D-134: Girder Strain vs. Connection Rotation, Configuration 10

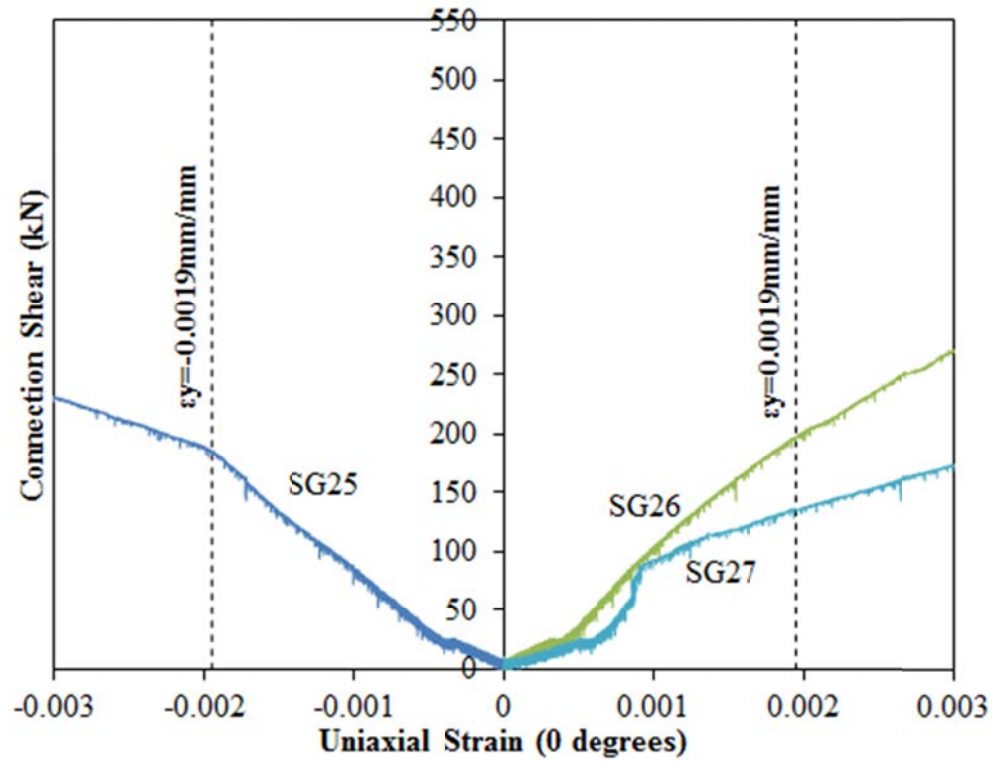


Figure D-135: Connection Shear vs. Girder Strain, Configuration 10

Bolt Bearing

Slight rotational bearing deformation was seen during the test. Inclinometers and string potentiometers were attached to the bottom of the beam and the face of the shear tab to measure rotation and deflection, respectively (see Figure D-133). The bearing deformation was computed as the difference in rotation or vertical deflection between the shear tab and the supported beam.

Figure D-137 shows the relative bolt bearing rotation within the shear tab and beam. The relative bearing deflection was seen to be insignificant and is not shown. The relative bearing rotation increased constantly over the test reaching a maximum value of 0.016 radians.

Since the rotational and vertical bearing stiffness was constant, it can be said that the limit state of bearing failure is not applicable. The tension field on the beam web can be seen in Figure D-136.



Figure D-136: Tension Field on Beam Web, End of Test, Configuration 10

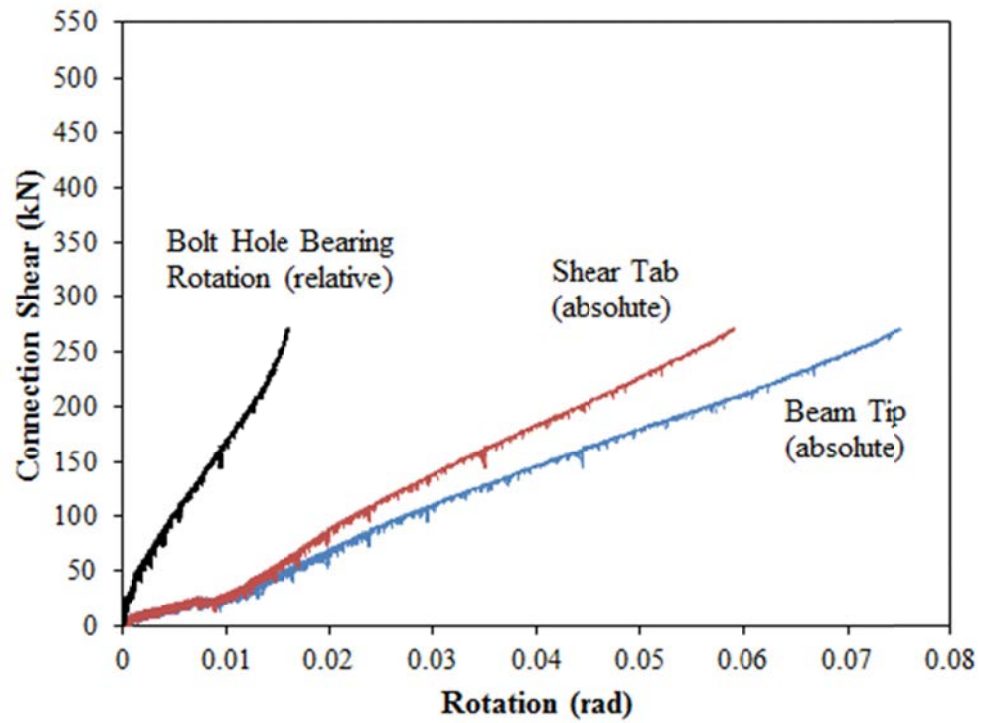


Figure D-137: Connection Shear vs. Relative Bearing Rotation, Configuration 10

EXTENDED SHEAR TAB CONNECTION EXPERIMENTAL STUDY

TEST SUMMARY OF CONFIGURATION 11

Specimen ID	CONFIGURATION 11
Key Words	Shear Tab, Extended Configuration; Flexible Support Condition; Beam to Girder;
Test Location	Structures Lab, Macdonald Engineering Building, McGill University
Test Date	July 15, 2013
Investigators	Colin A. Rogers, Dimitrios G. Lignos, Jacob W. Hertz
Main References	AISC Steel Construction Manual, 13th & 14th Editions; CISC Handbook of Steel Construction, 10th Edition
Sponsors	ADF Group Inc., DPHV and NSERC

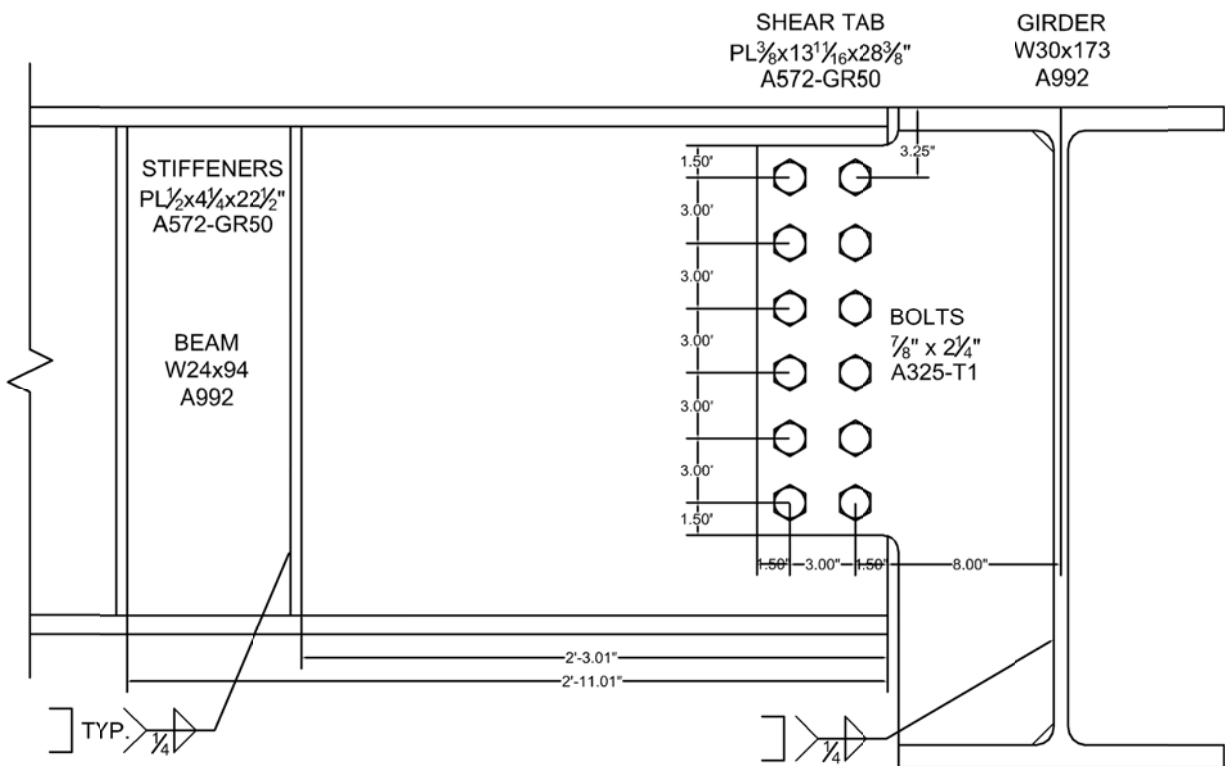


Figure D-138: Connection Details, Configuration 11

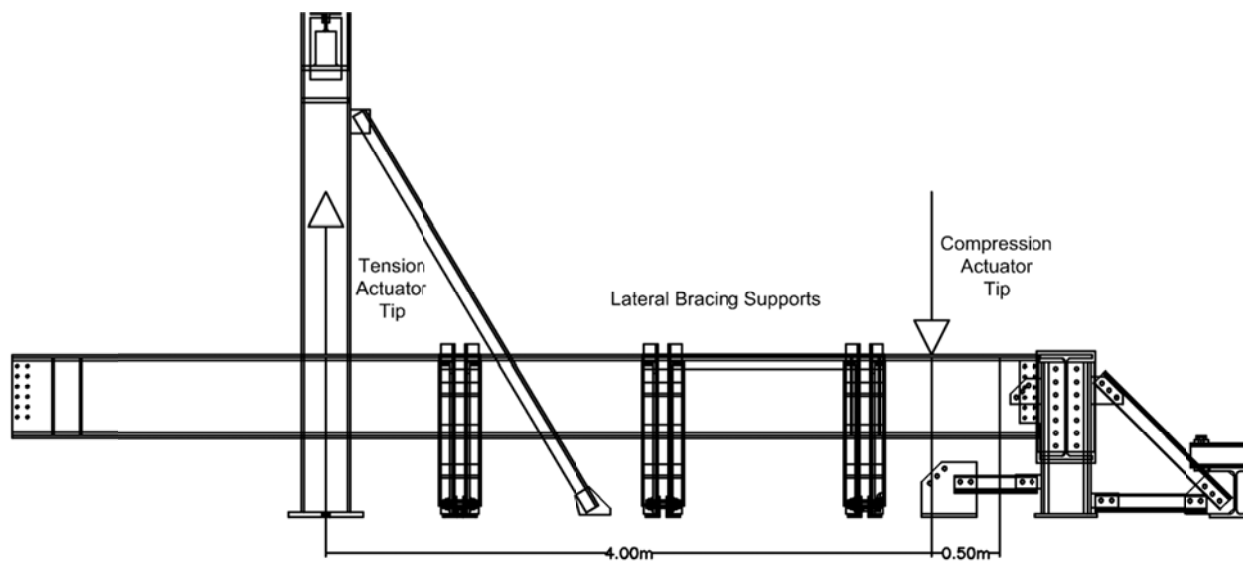
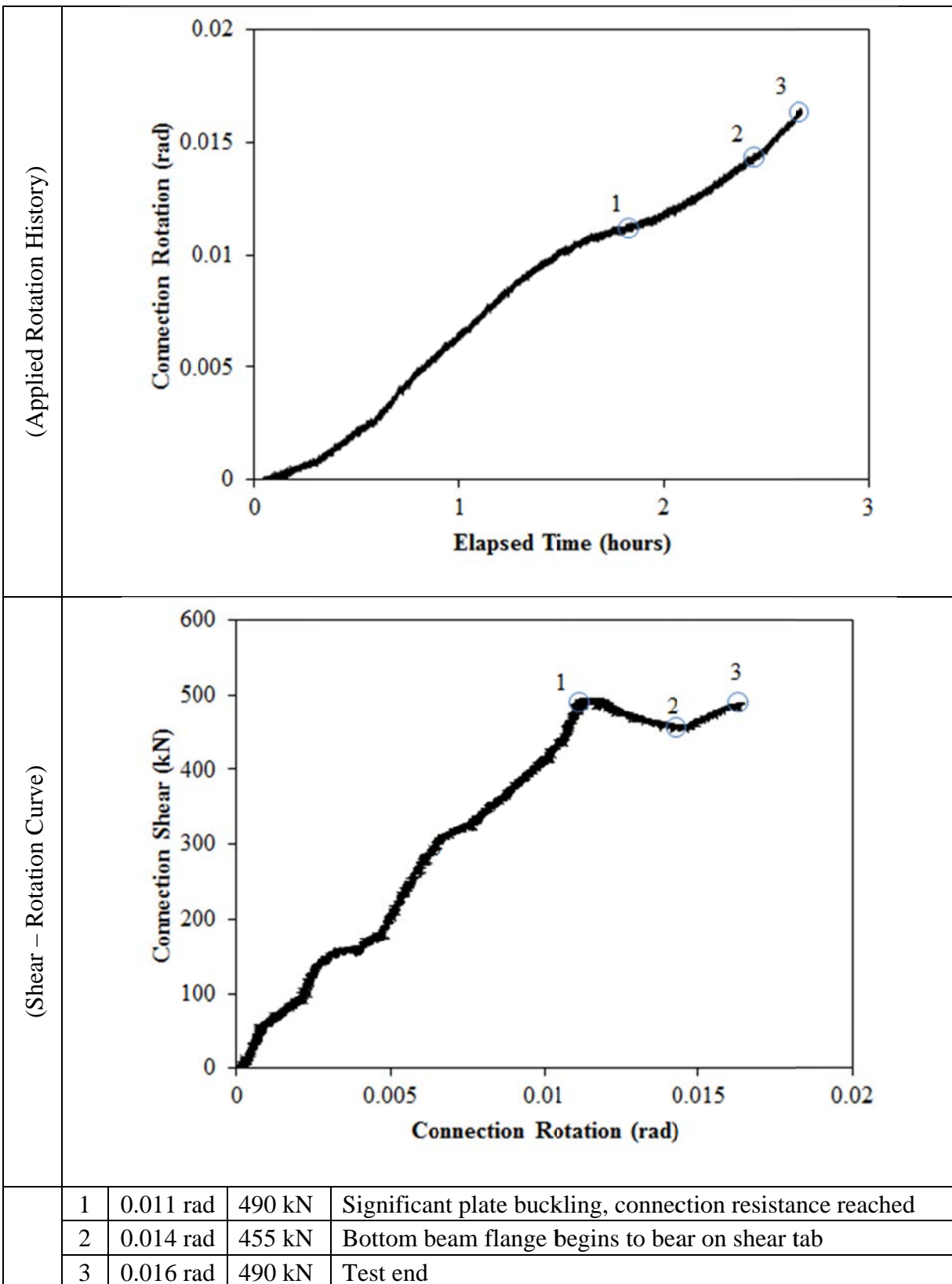


Figure D-139: Test Setup, Configuration 11

MATERIAL PROPERTIES AND SPECIMEN DETAILS

Member	Size	Grade	Yield Stress (MPa)		Ultimate Stress (MPa)	
			Mill Cert.	Coupon	Mill Cert.	Coupon
Beam	W24x94	A992	383	Flange:390 Web:448	507	Flange:513 Web:539
Beam Stiffeners	PL1/2"x4 1/4"	A572-GR50	-	-	-	-
Girder	W30x173	A992	390	-	515	-
Shear Tab	PL3/8"x13 11/16"	A572-GR50	452	456	531	525
Bolts	7/8" x 2 1/4"	A325-T1	6 rows of 2 bolts; 3" spacing, 1 1/2" end distance; snug tight; one washer per bolt; 15/16" bolt holes;			
Welding Procedure Specification	Electrode Classification E70					
	Welding Procedure <i>Shop Welding:</i> FCAW-G (flux-cored arc welding with gas shielding) <ul style="list-style-type: none">Fillet Weld, Shear Tab to Girder"C" Weld, Beam Stiffeners					
Boundary Condition	Tension Actuator Capacity: 268kN tension, 495kN compression; Stroke: 254mm; Displacement controlled					
	Compressive Actuator Capacity: 8018 kN tension, 11414kN compression; Stroke: 305mm; Displacement controlled					
	Lateral Bracing System Top and bottom flange out of plane movement restrained by ball and socket rods fixed to frame tensioned to strong floor					

ROTATION HISTORY AND KEY EXPERIMENTAL OBSERVATIONS



Note: The variation in stiffness seen during the first 0.008 radians of rotation is due to adjustment of the displacement rates of both tension and compression actuators to achieve the desired stiffness. Once this stiffness value was reached, the ratio of rates was held constant for the remainder of the test.

RESISTANCE SUMMARY

Limit State	Design Check	Predicted	Observed
Plate Buckling (biaxial)	-	-	490 kN
Combined Shear and Flexural Yielding	AISC Manual, 14 th Ed; Part 10; Equation 10-5	739 kN	-

TEST OBSERVATIONS

Plate Buckling (Two Directional)

The portion on the shear tab to the bottom right of the bolt group buckled outwards during the test. An LVDT (see Figure D-140) placed at this region measured a sharp increase in the out-of-plane displacement rate at approximately 0.01 radians (see Figure D-141). The connection shear reached a maximum value of 490 kN at 0.011 radians (see Shear Rotation Curve, Rotation History). This can be attributed to this plate buckling mechanism. Afterwards, the connection load stabilized and then started to decrease. At 0.0146 radians, the bottom beam flange began to bear on the vertical edge of the shear tab and the test was ended soon after. Figure D-142 shows the buckled shear tab neck after the test.

The AISC Manual includes provisions for one-directional plate buckling of the unsupported shear tab length. For this configuration, this length would be less than 2 inches so this limit state was ignored. The failure mode encountered is most likely the result of buckling along the bottom edge of the shear tab due to compressive forces from flexure on the tab in addition to shear forces acting thru the vertical edge of the tab under the neck. The resistance was measured as 490 kN.

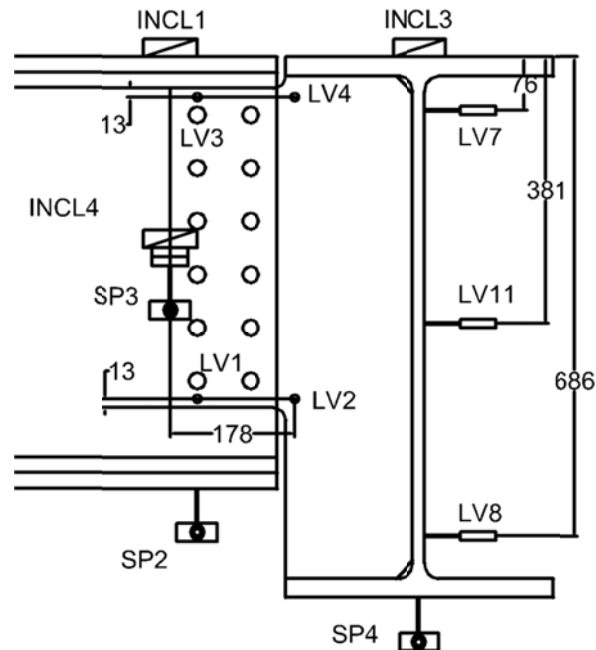


Figure D-140: Out of Plane LVDT Layout, Configuration 11

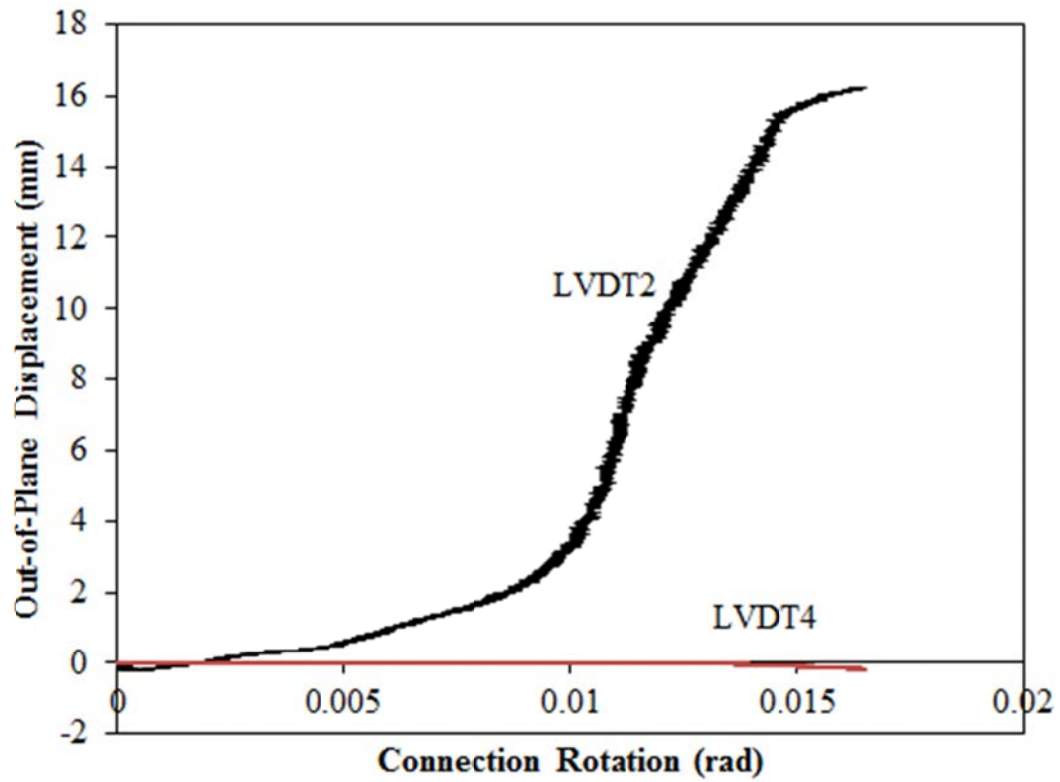


Figure D-141: Out-of-Plane Buckling Displacement vs. Rotation, Configuration 11



Figure D-142: Buckled Shear Tab Neck, Various Angles, Configuration 11

Combined Shear and Flexural Yielding

Deformation within the tab was monitored using a combination of horizontal and inclined strain gauges organized as seen in Figure D-143. White wash was applied to the tab such that the yielding pattern could be observed. The face of the shear tab at the end of test can be seen in Figure D-144.

Horizontal strain gauges were placed on the top and bottom edges of the tab to record flexural strains and the results can be seen in Figure D-145 and D-146. Flexural yielding was not seen in this test. SG2 was located directly on the buckled portion of the tab. As the buckling increased, the strain became positive.

Strain gauges oriented to 45° were placed along the height of the tab to measure shear strains and the results can be seen in Figure D-147 and D-148. Shear yielding was seen at the locations of SG4 at 0.011 radians, SG11 at 0.013 radians and SG9 at 0.015 radians. Yielding at SG4 can be attributed to the plate buckling mechanism forming.

The predicted shear and flexural yielding resistance is calculated under the assumption that the entire cross section of the shear tab ($3/8'' \times 18''$) undergoes shear and flexural yielding. Shear yielding was isolated between bolt holes and at the buckling region and flexural yielding did not occur. Therefore, the limit state of combined shear and flexural yielding does not govern for the connection resistance.

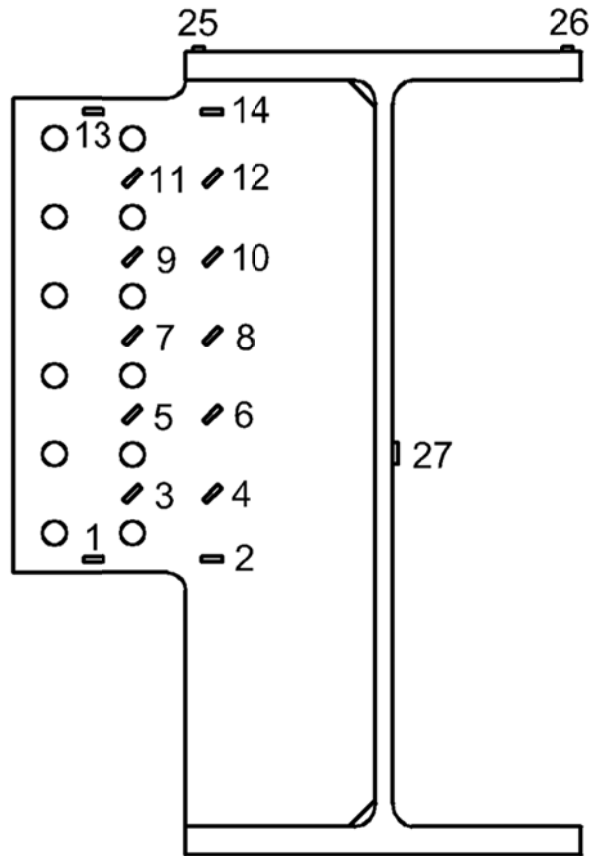


Figure D-143: Strain Gauge Layout, Configuration 11



Figure D-144: Deformed Shear Tab, End of Test, Configuration 11

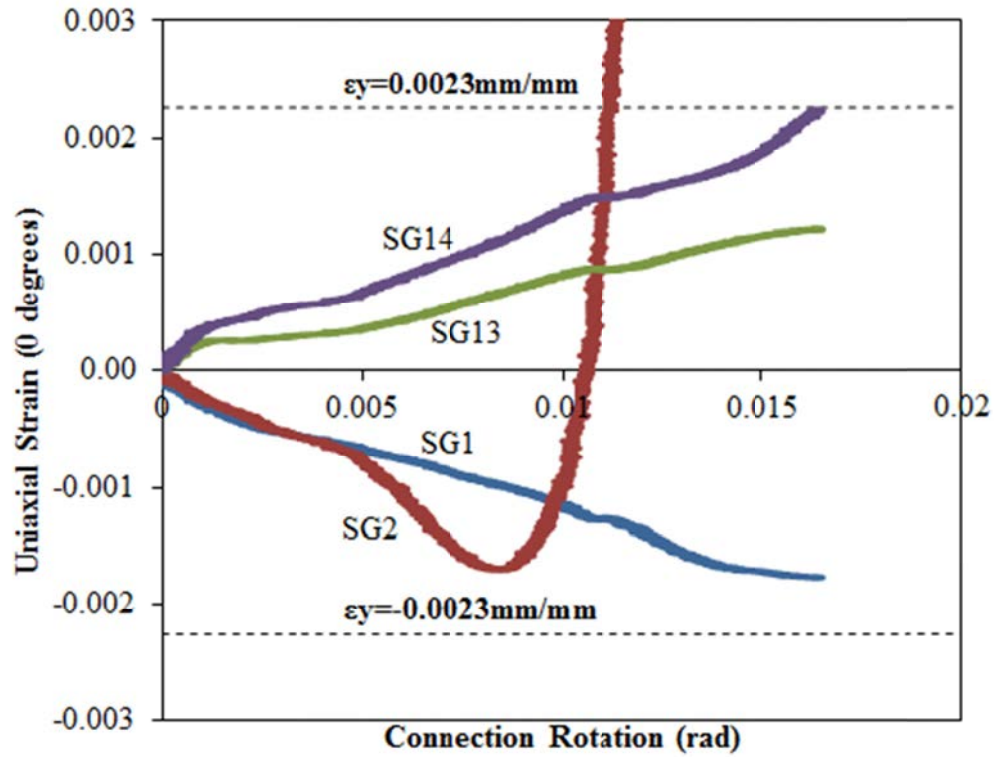


Figure D-145: Uniaxial Strain (0°) vs. Connection Rotation, Configuration 11

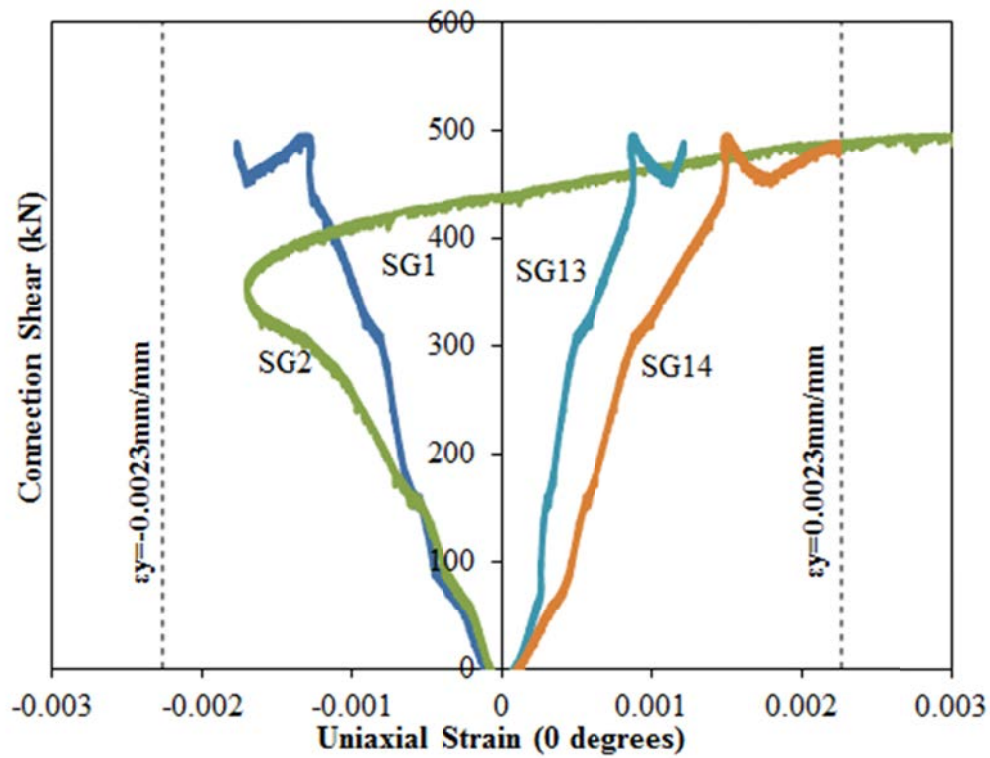


Figure D-146: Connection Shear vs. Uniaxial Strain (0°), Configuration 11

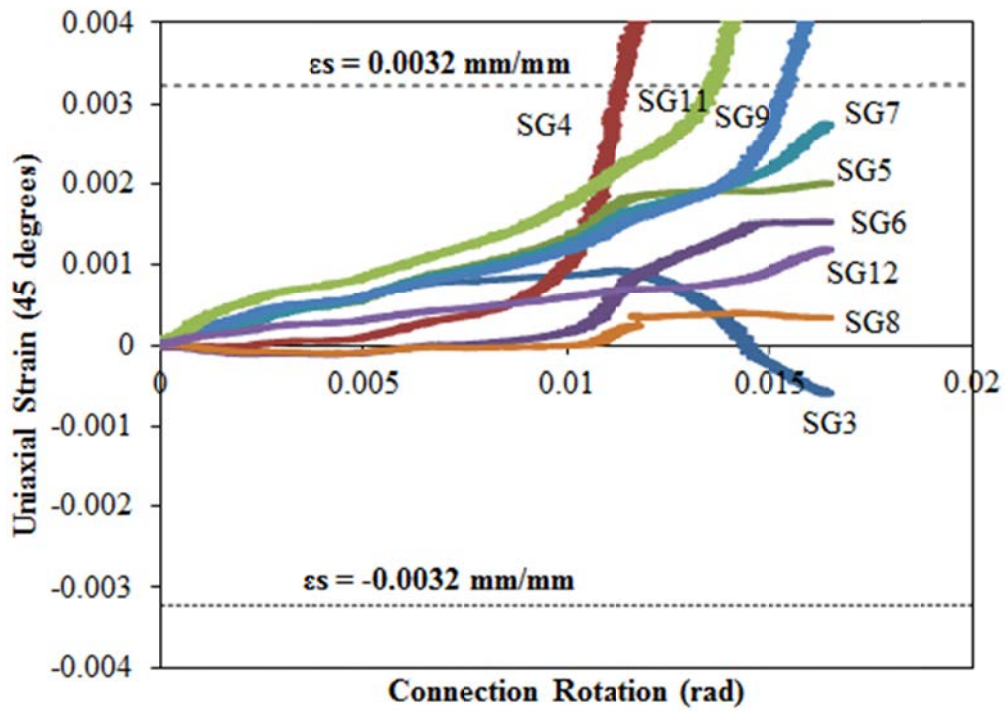


Figure D-147: Uniaxial Strain (45°) vs. Connection Rotation, Configuration 11

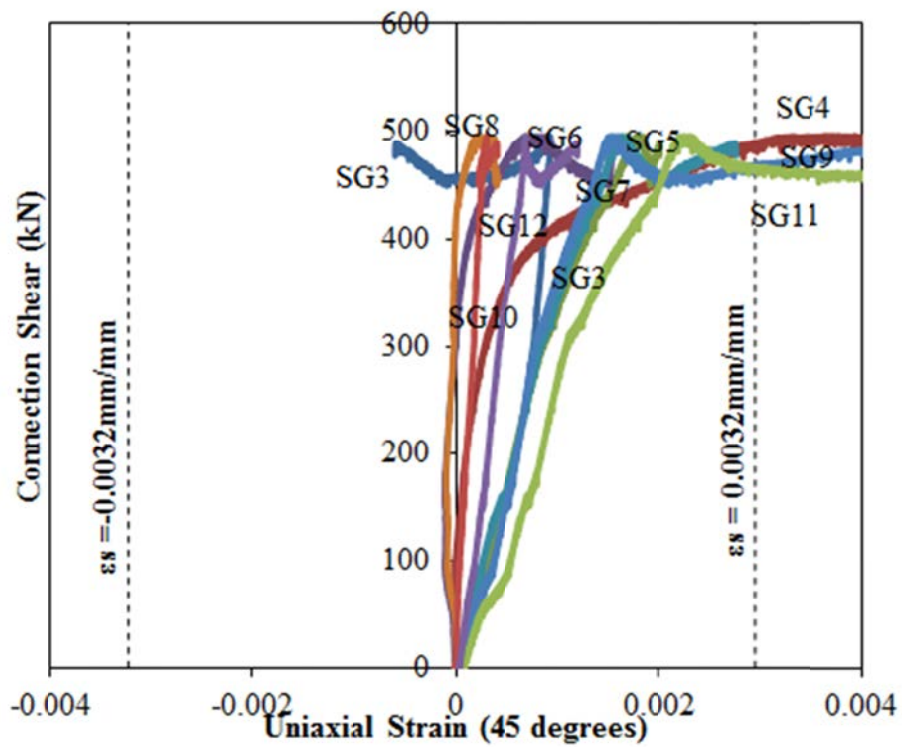


Figure D-148: Connection Shear vs. Uniaxial Strain (45°), Configuration 11

EXTENDED SHEAR TAB CONNECTION EXPERIMENTAL STUDY

TEST SUMMARY OF CONFIGURATION 12

Specimen ID	CONFIGURATION 12
Key Words	Shear Tab, Extended Configuration; Flexible Support Condition; Beam to Girder;
Test Location	Structures Lab, Macdonald Engineering Building, McGill University
Test Date	July 17, 2013
Investigators	Colin A. Rogers, Dimitrios G. Lignos, Jacob W. Hertz
Main References	AISC Steel Construction Manual, 13th & 14th Editions; CISC Handbook of Steel Construction, 10th Edition
Sponsors	ADF Group Inc., DPHV and NSERC

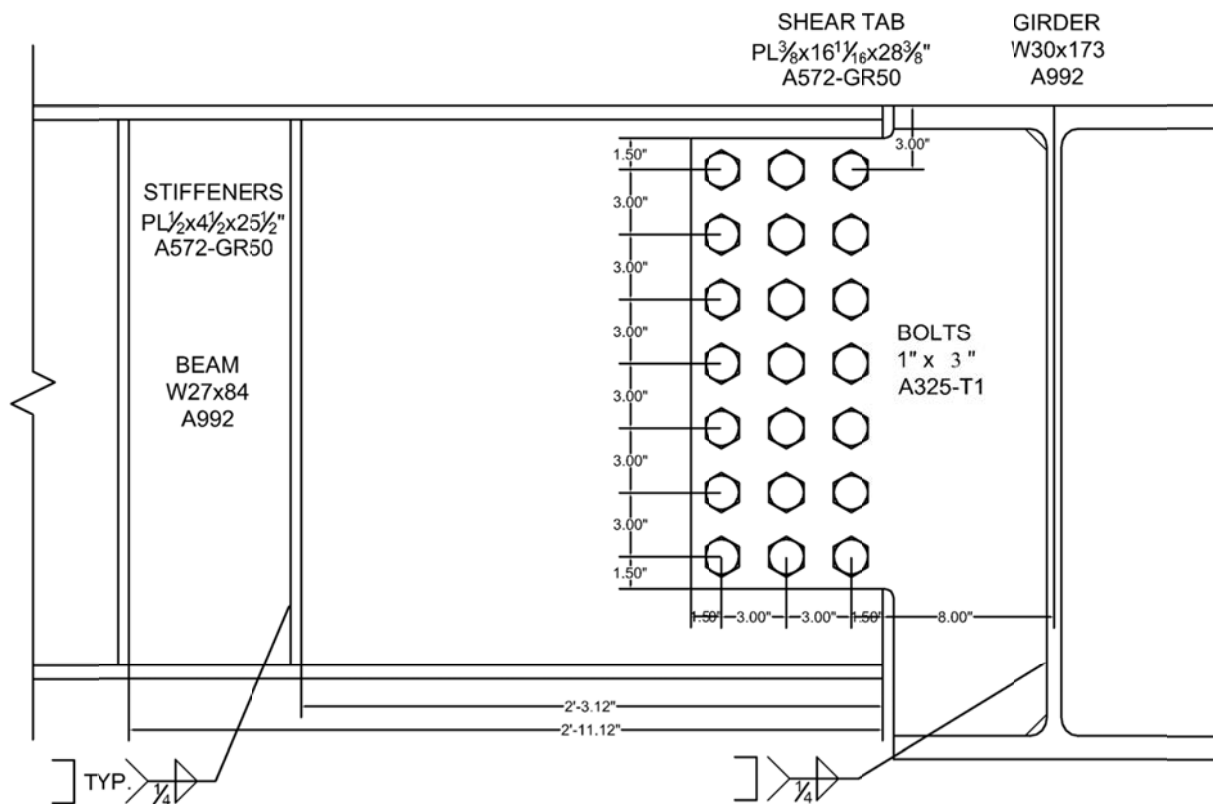


Figure D-149: Connection Details, Configuration 12

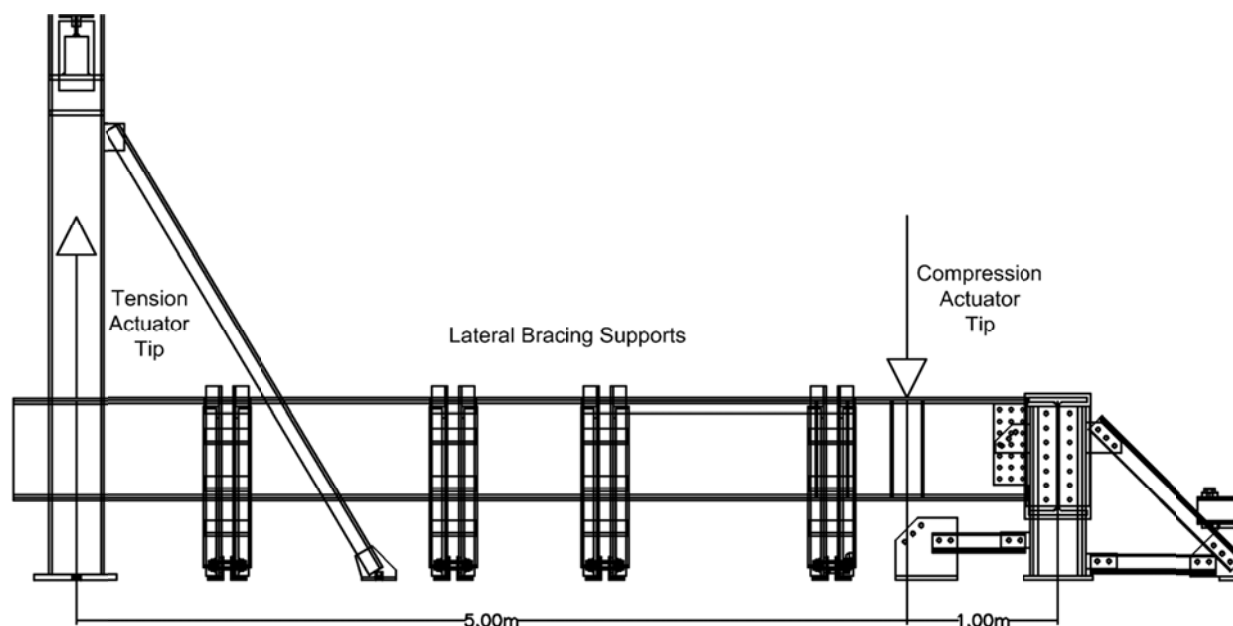
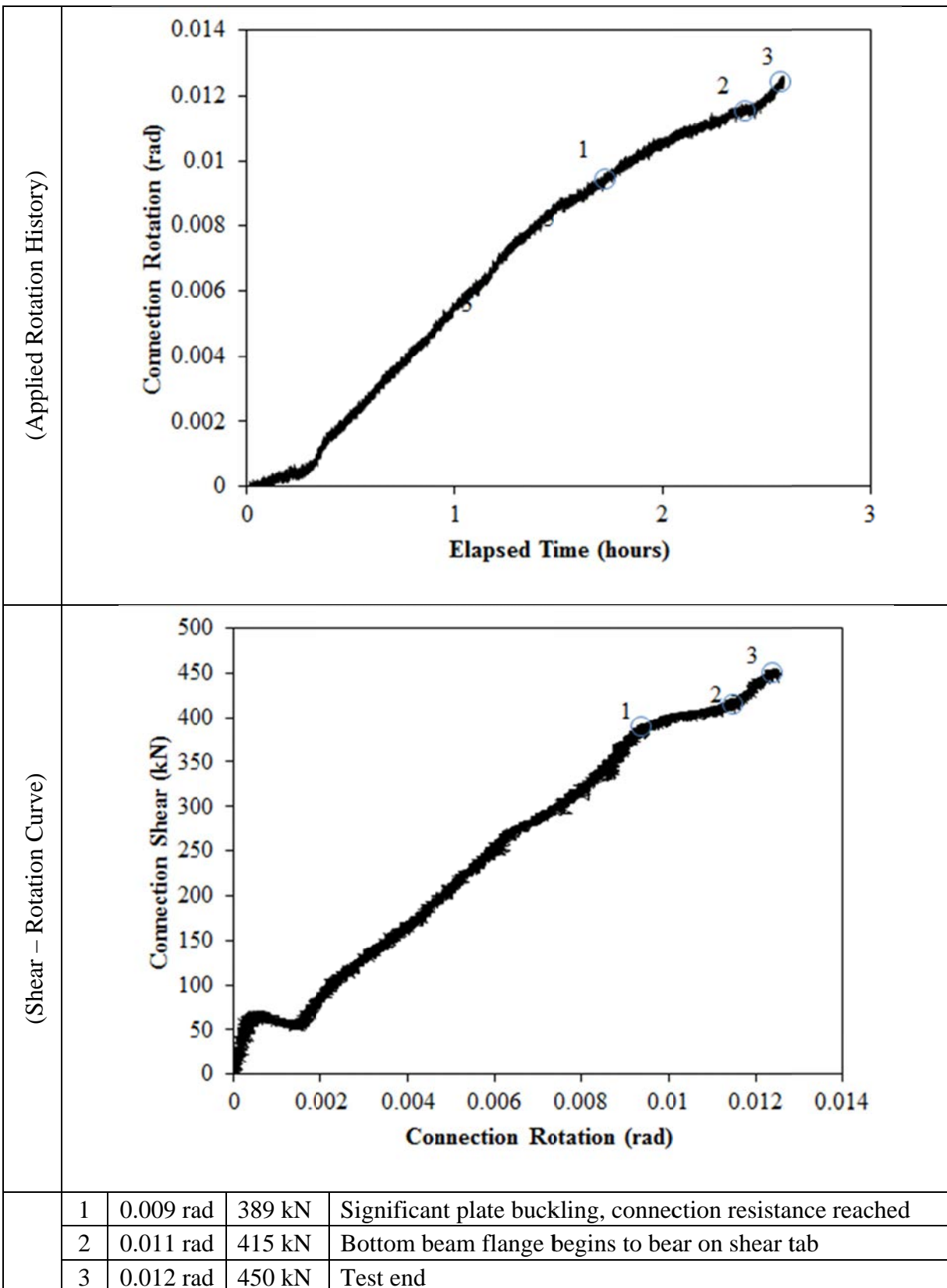


Figure D-150: Test Setup, Configuration 12

MATERIAL PROPERTIES AND SPECIMEN DETAILS

Member	Size	Grade	Yield Stress (MPa)		Ultimate Stress (MPa)	
			Mill Cert.	Coupon	Mill Cert.	Coupon
Beam	W27x84	A992	400	Flange:371 Web:405	520	Flange:503 Web:511
Beam Stiffeners	PL1/2"x4 1/2"	A572-GR50	-	-	-	-
Girder	W30x173	A992	390	-	515	-
Shear Tab	PL3/8"x16 11/16"	A572-GR50	452	456	531	525
Bolts	1" x 3"	A325-T1	7 rows of 3 bolts; 3" spacing, 1 1/2" end distance; snug tight; one washer per bolt; 1 1/16" bolt holes;			
Welding Procedure Specification	Electrode Classification E70					
	Welding Procedure <i>Shop Welding:</i> FCAW-G (flux-cored arc welding with gas shielding) <ul style="list-style-type: none">Fillet Weld, Shear Tab to Girder"C" Weld, Beam Stiffeners					
Boundary Condition	Tension Actuator Capacity: 268kN tension, 495kN compression; Stroke: 254mm; Displacement controlled					
	Compressive Actuator Capacity: 8018 kN tension, 11414kN compression; Stroke: 305mm; Displacement controlled					
	Lateral Bracing System Top and bottom flange out of plane movement restrained by ball and socket rods fixed to frame tensioned to strong floor					

ROTATION HISTORY AND KEY EXPERIMENTAL OBSERVATIONS



Note: The variation in stiffness seen during the first 0.003 radians of rotation is due to adjustment of the displacement rates of both tension and compression actuators to achieve the desired stiffness. Once this stiffness value was reached, the ratio of rates was held constant for the remainder of the test.

RESISTANCE SUMMARY

Limit State	Design Check	Predicted	Observed
Plate Buckling (two directional)	-	-	389 kN
Combined Shear and Flexural Yielding	AISC Manual, 14 th Ed; Part 10; Equation 10-5	943 kN	-

TEST OBSERVATIONS

Plate Buckling (Two Directional)

The portion on the shear tab to the bottom right of the bolt group buckled outwards during the test. An LVDT (see Figure D-151) placed at this region measured a sharp increase in the out-of-plane displacement rate at approximately 0.009 radians (see Figure D-152). At 0.011 radian rotation and 389 kN connection shear, the connection stiffness decreased sharply (see Shear Rotation Curve, Rotation History). This can be attributed to this plate buckling mechanism. Afterwards, the connection load continued to increase with a constant stiffness until 0.012 radians. At this point the bottom beam flange began to bear on the vertical edge of the shear tab and the test was ended soon after. Figure D-153 shows the buckled shear tab neck after the test.

The AISC Manual includes provisions for one-directional plate buckling of the unsupported shear tab length. For this configuration, this length would be less than 2 inches so this limit state was ignored. The failure mode encountered is most likely the result of buckling along the bottom edge of the shear tab due to compressive forces from flexure on the tab in addition to shear forces acting thru the vertical edge of the tab under the neck.

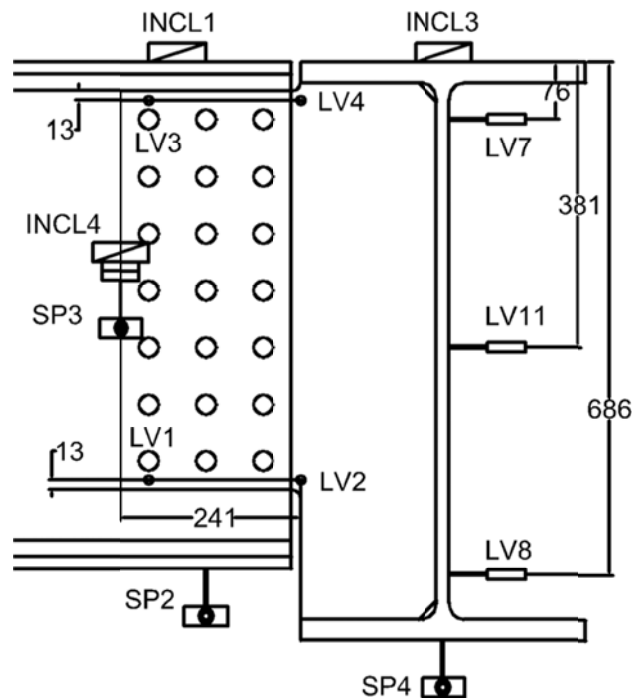


Figure D-151: Out of Plane LVDT Layout, Configuration 12

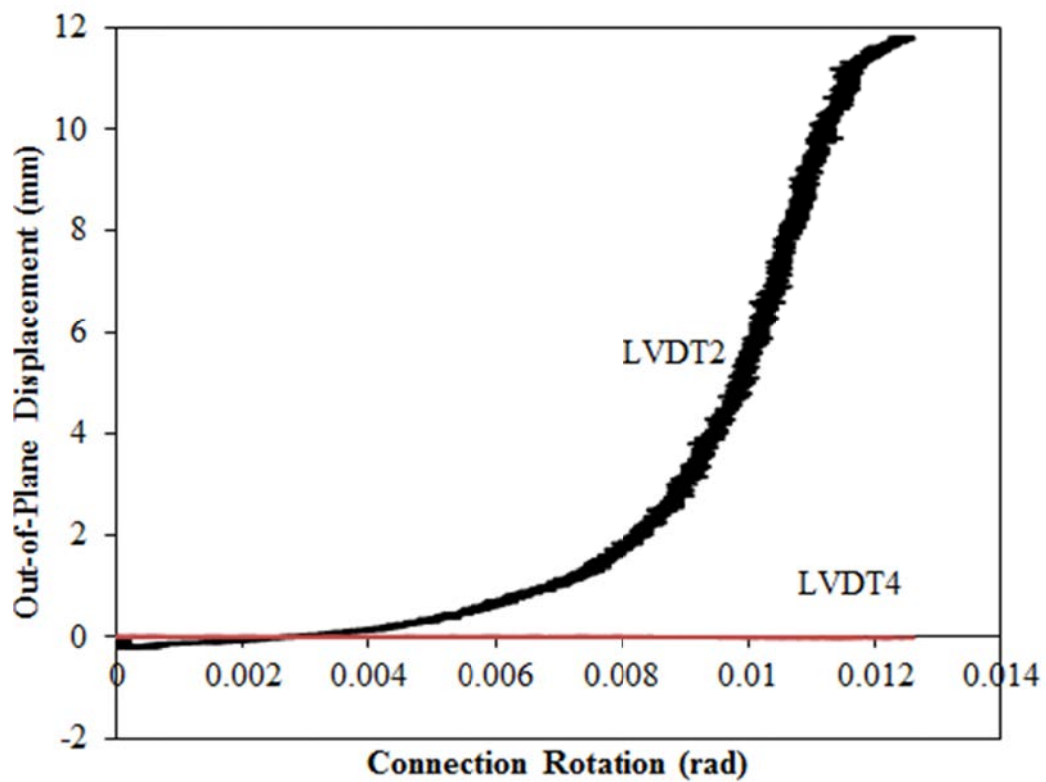


Figure D-152: Out-of-Plane Buckling Displacement vs. Rotation, Configuration 12

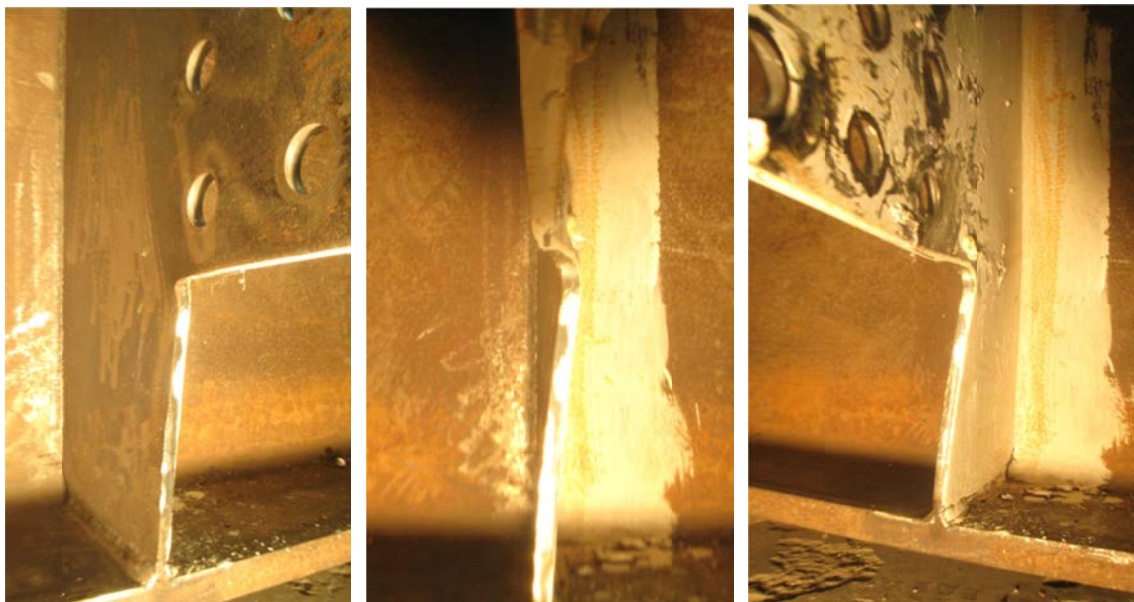


Figure D-153: Buckled Shear Tab Neck, Various Angles, Configuration 12

Combined Shear and Flexural Yielding

Deformation within the tab was monitored using a combination of horizontal and inclined strain gauges organized as seen in Figure D-154. White wash was applied to the tab such that the yielding pattern could be observed. The face of the shear tab at the end of test can be seen in Figure D-155.

Horizontal strain gauges were placed on the top and bottom edges of the tab to record flexural strains and the results can be seen in Figure D-156 and D-157. Tension yielding was seen at SG16 at 0.01 radian rotation. SG2 was located directly on the buckled portion of the tab. As the buckling increased, the strain became positive and eventually yielded in tension at 0.009 radians.

Strain gauges oriented to 45° were placed along the height of the tab to measure shear strains and the results can be seen in Figure D-158 and D-159. Shear yielding was seen at the locations of SG4 at 0.010 radians. Yielding at SG4 can be attributed to the plate buckling mechanism forming.

The predicted shear and flexural yielding resistance is calculated under the assumption that the entire cross section of the shear tab ($3/8'' \times 21''$) undergoes shear and flexural yielding. Shear yielding was strictly located near the buckled portion of the shear tab and flexural yielding was only seen in the top neck of the tab. Therefore, the limit state of combined shear and flexural yielding does not govern for the connection resistance.

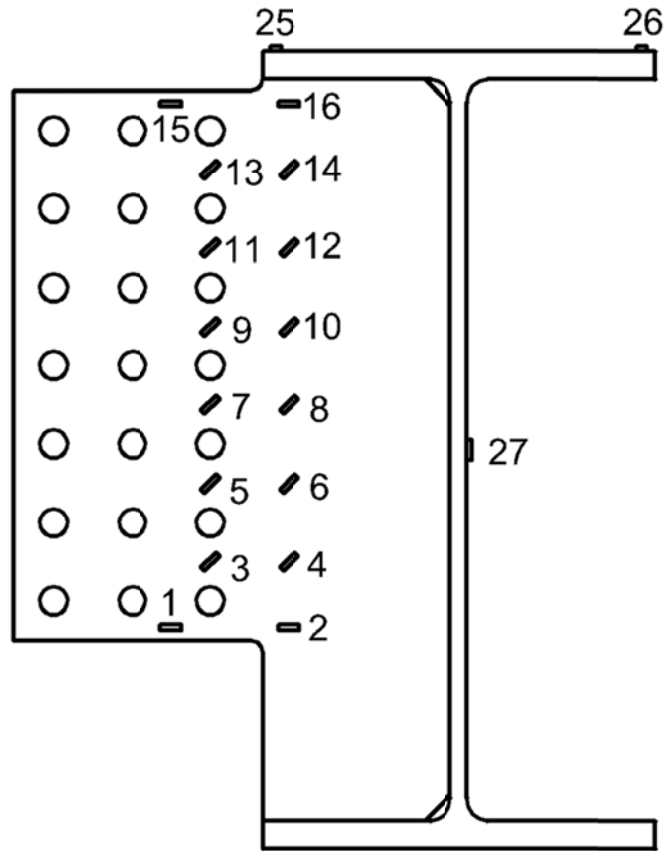


Figure D-154: Strain Gauge Layout, Configuration 12

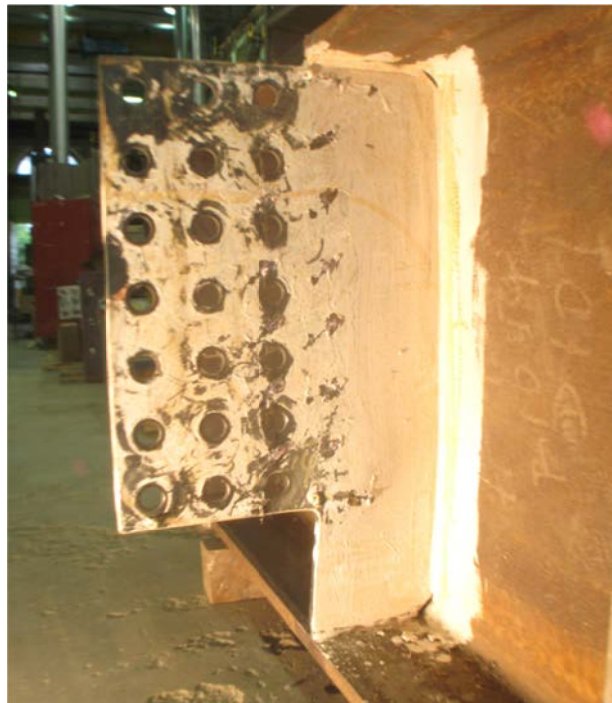


Figure D-155: Deformed Shear Tab, End of Test, Configuration 12

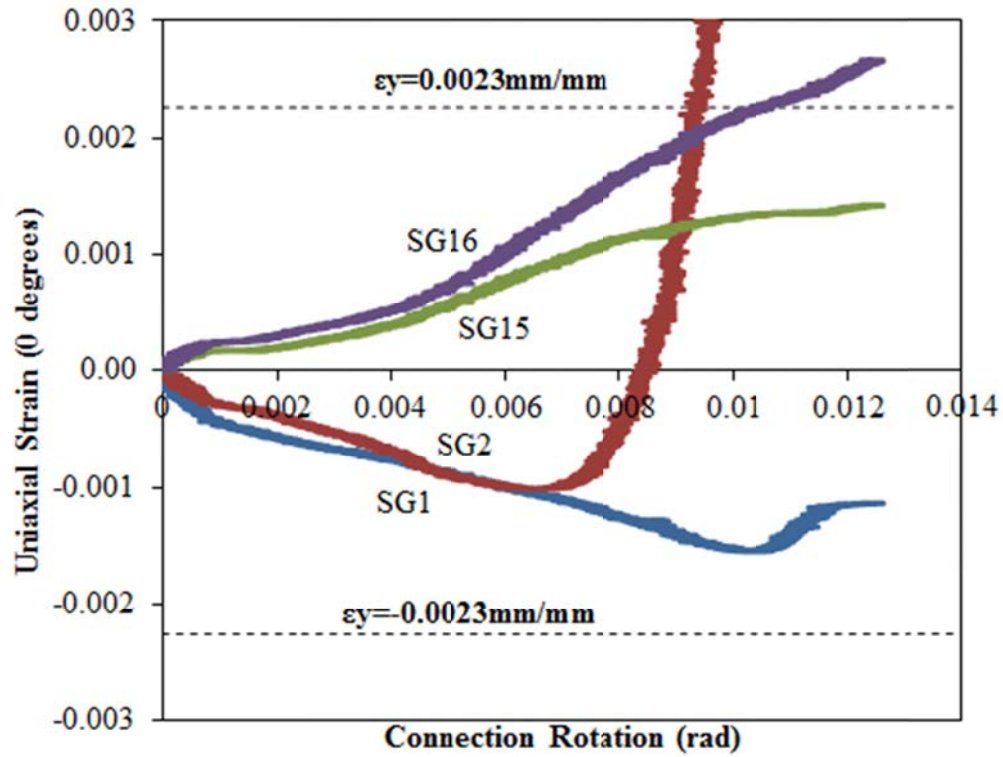


Figure D-156: Uniaxial Strain (0°) vs. Connection Rotation, Configuration 12

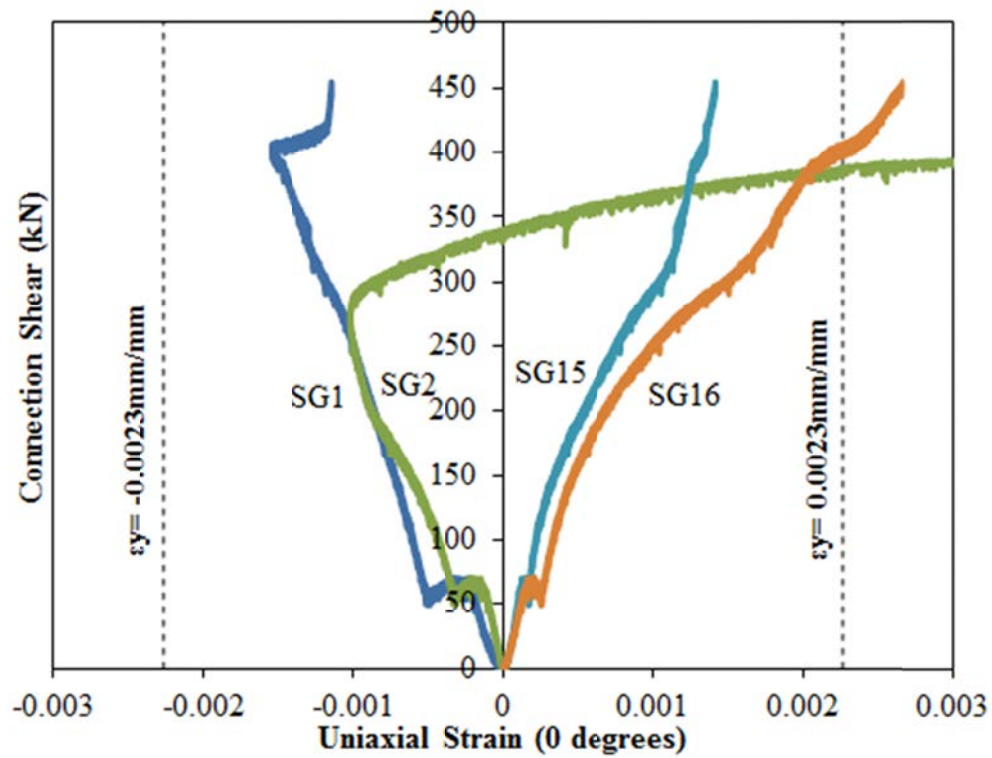


Figure D-157: Connection Shear vs. Uniaxial Strain (0°), Configuration 12

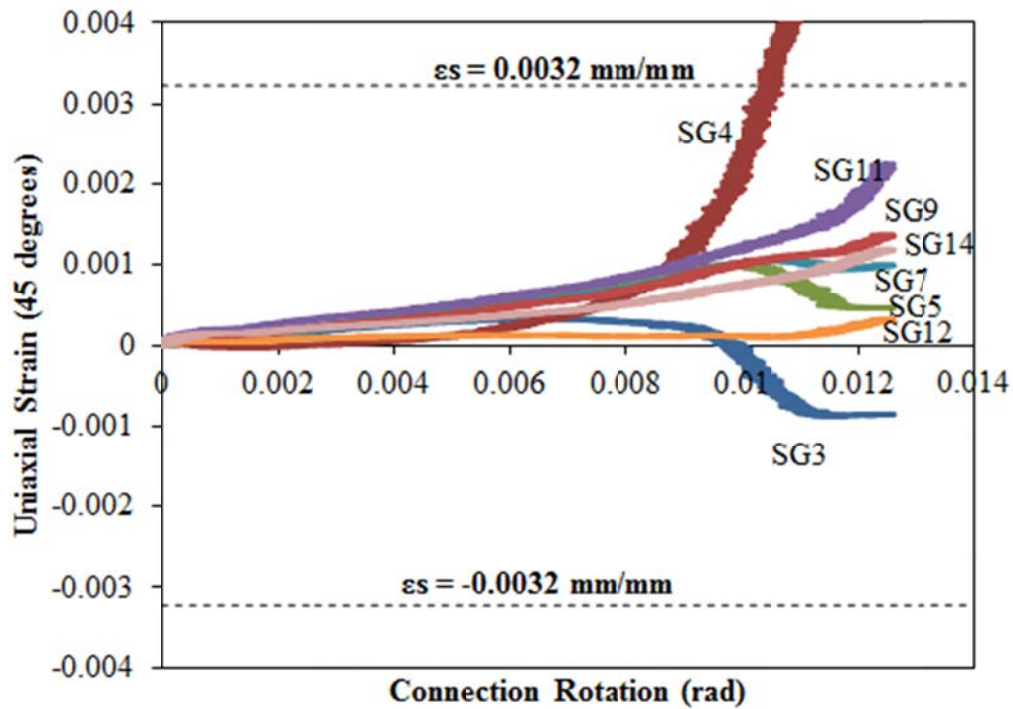


Figure D-158: Uniaxial Strain (45°) vs. Connection Rotation, Configuration 12

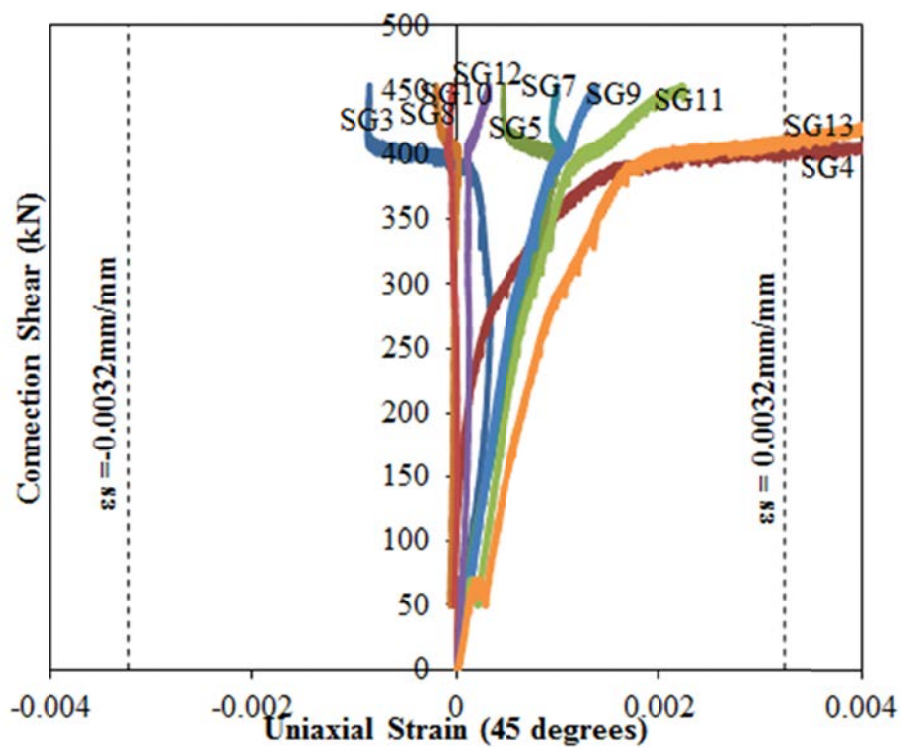


Figure D-159: Connection Shear vs. Uniaxial Strain (45°), Configuration 12